School of Molecular and Life Sciences

Synthesis and Application of Distally-Bridged Chiral Resorcinarenes as Enantioselective Membrane Carriers

Daniel Aquila Tan

This thesis is presented for the Degree of
Doctor of Philosophy
of
Curtin University

October 2018

Declaration

To the best of my knowledge and belief this thesis contains no material previously published by any other person except where due acknowledgment has been made. This thesis contains no material which has been accepted for the award of any other degree or diploma in any university.

Signature: ....*Daniel*........................

Date: ...31/10/2018....

Abstract

The aim of this project is to synthesise and investigate potential enantioselective membrane carriers for the enantioseparation of racemic drugs. Tetramethoxy-resorcinarene is a potential enantioselective membrane carrier because it possesses a chiral cavity. This project proposes to enhance the binding of the tetramethoxy-resorcinarene by partial enclosure of the cavity via synthetic installation of a crown ether bridge that spans from distal positions over the cavity of the resorcinarene. In the synthesis, a key intermediary product was a distally-functionalised tetramethoxy-resorcinarene, since it would prevent proximal-bridging and pave the way for the bridge to selectively attach at distal positions of the resorcinarene.

The first strategy towards the distally-functionalised tetramethoxyresorcinarene aimed to spatially enforce distal selectivity on the resorcinarene through the direct attachment of a rigid bridge of identical length to the resorcinarene. A calixarene was chosen to serve as the rigid bridge due to its similar dimensions to the resorcinarene, as well as the existing literature methods to readily produce a distally-functionalised calixarene. Imine linkages were chosen to link the rigid bridge to the resorcinarene because the reactions to form these are reversible and would reduce the possibility of oligomeric products. The synthesis of both tetraaldehyde- and tetraamino- resorcinarene precursors were both accomplished in three steps from the starting resorcinarene, according to literature procedures. The corresponding distal dialdehyde- and diamino-calixarene rigid-bridges were respectively synthesised in two and five steps from tetrahydroxycalixarene. The imine coupling of both the resorcinarenes with their corresponding calixarene rigid bridges was investigated. The results were however lacking in success, giving ambiguous and inconclusive ^{1}H NMR spectra. Considering these unpromising results, together with the effort required in synthesising the resorcinarene and calixarene precursors, this strategy was deemed to be impractical and was abandoned.

The second strategy towards the distally-functionalised tetramethoxyresorcinarene precursor was a partially-selective lithiation of the aromatic ring followed by quenching, as was described in the literature for an octamethoxyresorcinarene. In order to apply this lithiation to the tetramethoxyresorcinarene, the phenols were first protected with benzyloxy and methoxymethyl groups. Under the lithiation conditions,

the benzyloxyresorcinarene appeared to decompose, while the methoxymethylresorcinarene yielded the entire range of partially-functionalised products with no selectivity. As a proof of concept, the tetramethoxyresorcinarene was *O*-alkylated with ethoxy groups, then subjected to the lithation delivering the distally-functionalised product in 36% yield, after separation from starting material. These results suggest that the selective lithiation is not widely applicable being only successful for alkoxyresorcinarenes with an alkyl group that is similar to a methyl.

The third strategy towards the distally-functionalised precursor was through direct, partially-selective protection of the tetramethoxyresorcinarene phenols. The reaction with TBDMS-Cl and potassium *tert*-butoxide in tetrahydrofuran successfully delivered the distally-functionalised resorcinarene in a best yield of 31%. All other partially-protected resorcinarenes were also produced and these were readily isolated and characterised. Furthermore, this reaction was scalable, and through this simple single-step reaction, the key intermediary product of a distally-functionalised resorcinarene was produced in gram-quantities. Due to the instability of the TBDMS protecting groups, the TBDMS groups were replaced with benzyloxy groups via two additional high-yielding steps.

With gram-quantities of the key intermediary product, the distal-bridging of the tetramethoxyresorcinarene was a success. Three sizes of the distally-bridged crown resorcinarenes were synthesised in good yields ranging from 49-70%. Removal of the benzyloxy protecting groups was accomplished in quantitative yield to furnish the target dihydroxy crown 5-7 resorcinarene products in a total of five steps from the starting resorcinarene. All six of these crown resorcinarenes were characterised by NMR, and some by X-ray crystallographic methods. To investigate these crown resorcinarenes as enantioselective membrane carriers, camphorsulfonate diastereomers were made and separated for all three derivatives, enabling the crown resorcinarenes to be obtained as single enantiomers. In total, twelve distally-bridged crown resorcinarenes in three different sizes (crown 5-7), and in three different types (dibenzyloxy, dihydroxy, dicamphorsulfonate) were synthesised and characterised.

The twelve distally-bridged crown resorcinarenes, together with three synthesised bis-crown 5-7 resorcinarenes, were investigated as membrane carriers for salbutamol. The membrane transport experiments found that all crown resorcinarenes were enhancing

the transport of salbutamol to varying degrees. However, all of these crown resorcinarenes were transporting salbutamol at a low rate. To examine the possibility of enantioselective transport, single enantiomers of one of the best membrane carriers were obtained from the hydrolysis of the respective camphorsulfonate diastereomers. Membrane transport of salbutamol by these single enantiomers unfortunately showed no enantioselectivity according to chiral HPLC analysis. Nevertheless, this work offers a proof of concept, being the first demonstration of salbutamol transport across a membrane mediated by a membrane carrier. Optimisation of the chiral resorcinarene and membrane transport conditions may provide the breakthrough of an enantioselective membrane carrier.

Some of the work in this thesis has been published in the following:

Tan, D. A.; Mocerino, M., in *Calixarenes and Beyond*, Neri, P.; Sessler, J. L.; Wang, M.-X., Eds. Springer International Publishing: Cham, 2016; pp 235-253.
DOI: 10.1007/978-3-319-31867-7_10

Tan, D. A.; Mocerino, M., *J Incl Phenom Macrocycl Chem* **2018**, *91* (1), 71-80.
DOI: 10.1007/s10847-018-0802-4

Acknowledgements

Table of Contents

Abbreviations

Ar	Aryl
Bn	Benzyl
BuLi	Butyllithium
DCM	Dichloromethane
DEPT	Distortionless enhancement by polarisation transfer
DMF	*N,N*-dimethylformamide
DMSO	Dimethylsulfoxide
eq	Equivalents
EtOAc	Ethyl acetate
HSQC	Hetronuclear single quantum correlation
HMBC	Hetronuclear multiple bond correlation
HPLC	High performance liquid chromatography
HRMS	High resolution mass spectrometry
IR	Infrared
KOtBu	Potassium *tert*-buoxide
MeCN	Acetonitrile
MeOH	Methanol
mp	Melting point
NBS	*N*-bromosuccinimide
NMR	Nuclear magnetic resonance
Ph	Phenyl
ppm	Parts per million
Pr	Propyl
R_f	Retention factor
RT	Room temperature
TBDMS	*tert*-Butyldimethylsilyl
TBDPS	*tert*-Butyldiphenylsilyl
TEA	Triethylamine
THF	Tetrahydrofuran
TLC	Thin layer chromatography
TsO	Toluenesulfonate
UV	Ultra violet

1 Introduction

Some of the content presented in this chapter has been published in a peer reviewed book cited below:

Chiral molecules are molecules that have mirror images that are not superimposable. The different mirror images of chiral molecules are known as enantiomers and an equimolar mixture of enantiomers is known as a racemic mixture. The potential for the undesired enantiomer of a chiral molecule to cause harm is well known.[1,2] This is of concern wherever chiral organic molecules are made to interact with living organisms, whether in agriculture, fragrances, cosmetics or medicine. Medicines are particularly important, because of their common widespread use, dependence, and the potential risk to human lives. Chiral drugs consisted of 40-50% of the drugs marketed around 2013.[1] Furthermore, newly-approved chiral drugs are a majority, accounting for 73% of globally-approved drugs between 2001-2010.[3] The issue of racemic mixtures of chiral drugs came to the spotlight in the infamous case of thalidomide where pregnant women in the 1950s were administered a racemic mixture of the drug to relieve their morning sickness. Tragically, the (*S*) enantiomer of thalidomide caused major deformations in the infants, which resulted in many of their deaths as well as many handicapped survivors.[4] This example clearly illustrates the issue: one enantiomer produces the therapeutic effect, but the other enantiomer impacts the body differently in a manner which may be undesirable. Some drugs today have undesirable enantiomers, but are still administered as racemic mixtures.[1] This is because the side-effects due to the undesirable enantiomer are not as serious and are often overlooked, but are nevertheless a nuisance. Therefore, removal of the undesirable enantiomer of

these drugs could remove the undesirable side-effects, and also halve the dosage. This would improve the quality of the therapeutic treatment for the many patients taking the drug.

The issue of negative side effects is not universal for all chiral drugs, since some chiral drugs are still being approved as racemic mixtures. In some cases, the advantage of a single enantiomer drug over a racemic mixture is unclear, or that both enantiomers contribute to the therapeutic effect.[1] This is evident in the selection of common racemic drugs listed in **Table 1.1**.[1, 5-7]

Table 1.1 A selection of common and current racemic drugs.

Name	Application	(*S*) enantiomer	(*R*) enantiomer
Salbutamol[8-10]	Treatment of asthma	Associated with pro-inflammaotry effects	Relaxes airway muscles
Fluoxetine[5]	Anti-depressant	More potent than (*R*)	Metabolised faster
Citalopram[5]	Anti-depressant	More potent than (*R*)*	Possible antagonist of (*S*)
Venlafaxine[5]	Anti-depressant	Both enantiomers are useful	
Sotalol[1]	Treatment of abnormal heart rhythms	Both enantiomers are useful	
Propanolol[1]	Treatment of abnormal heart rhythms	Both enantiomers are useful	
Ketamine[1]	Anaesthetic and analgesic	More potent than (*R*)*	Associated with hallucinogenic effects

*Single enantiomer commercially available

In fact the infamous thalidomide, being racemized in the body,[11] has been approved by the U.S. Food and Drug Administration for the treatment of leprosy.[12] Therefore, the potential risks of racemic mixtures of chiral drugs is case-dependent, and requires individual consideration. Nevertheless, statistics from Agranat et al. have shown that of the 73% of globally-approved chiral drugs, 87% were approved as single enantiomers.[3] This demonstrates that there is a strong preference for enantio-pure drugs, and that there are already existing methods for obtaining drugs in single enantiomers on industrial scales. But the fact that some common drugs, with enantiomer-induced side-effects, are still sold today as racemic mixtures indicates a need for improvement – the need for these drugs to be industrially-obtained as single enantiomers.

1.1 Asymmetric synthesis and chiral resolution

A single enantiomer of a desired chiral molecule could be obtained by extraction from nature. However, this requires that the molecule, is available in nature in substantial concentrations, and can be extracted in an industrially-viable process. This is often not the case, hence synthetic methods have been employed. There are two main methods to producing chiral molecules as a single enantiomer: asymmetric synthesis and chiral resolution. Asymmetric synthesis is the synthesis of a chiral molecule as a single enantiomer. Enantio-pure molecules may be obtained from nature for use as precursors, but the necessary transformations also need to preserve chirality. Asymmetric synthesis can also be performed on achiral starting materials which are more readily available, albeit a longer synthetic process. A well-known example of this is the asymmetric synthesis of menthol, developed by Noyori, who was awarded the 2001 Nobel Prize in Chemistry in recognition of his work. Alternatively, chiral resolution is the separation of enantiomers obtained from a racemic product of regular symmetric synthesis. The suitability of either method is dependent on a number of factors including, the properties of the molecule, its application, its synthesis, its ability to be scaled up for the industry, and the associated costs. The advantage of asymmetric synthesis is that only the desired enantiomer is formed, so there is no wastage. However, the fact that only a few chiral molecules have been synthesised by asymmetric methods on industrial scales illustrates the difficulty.[13] It may be more feasible to resolve a racemic mixture from a regular symmetric synthetic process, or perhaps from a natural product if available. If there was a requirement for both

enantiomers, chiral resolution of a racemic mixture would be applicable. Otherwise, the undesired enantiomer could be discarded if it is cheap, or may be possibly converted to the desired enantiomer, by establishing a dynamic equilibrium between the enantiomers via a catalytic entity.[14] All in all, both methods require a chiral entity to accomplish enantiopurity of a chiral molecule. This may give rise to beneficiary overlaps between the two methods, which are both useful for obtaining enantiopurity, given the uniqueness of chiral molecules. This project aims to contribute to the method of chiral resolution. The methods of chiral resolution can be classified into the following categories: diastereomeric resolution, crystallisation resolution, kinetic resolution, capillary electrophoresis, chromatography, and membrane-based separation.[15]

1.1.1 Resolution of diastereomers

The difficulty in chiral resolution arises from the enantiomers having the same physical properties. However, enantiomers can be converted into diastereomers which have different solubility and other physical properties which result from the existence of multiple chiral centres within the same molecule. The difference in the physical properties of diastereomers could enable easier separation by conventional crystallisation or chromatography. Separation of diastereomers from enantiomers can be thought of in three steps: (1) conversion of the enantiomers to diastereomers by attachment of a chiral moiety to the enantiomeric mixture, (2) separation of the diastereomers, (3) removal of the chiral moiety from the separated diastereomers to recover the pure enantiomers. The key factor to the separation of enantiomers via diastereomers is the chiral moiety; the chiral moiety may be expensive, difficult to determine, and needs to be enantio-pure and removable.[15] Although diastereomers have different properties, they are still isomers and hence their physical properties may be similar, causing difficulty in their separation. The difference in diastereomers is affected by the chiral moiety they are made from, so a chiral moiety that would render a significant difference in the resulting diastereomers needs to be determined. This determination may be difficult because it is typically done through experimental screening. Nevertheless, these issues have been resolved in some cases, enabling chiral resolution by diastereomeric crystallisation of some drugs at industrial scales. An example of this is (*S*)-naproxen, a common anti-inflammatory drug, that is industrially

resolved in >95% ee through the enantioselective formation of an insoluble diasteromic salt with *N*-alkylglucamine serving as the chiral moiety.[16]

1.1.2 Crystallisation resolution

Crystallisation resolution is the selective crystallisation of an enantiomer from a racemic solution. Since its discovery by Pasteur in 1848[17] the concept has been used to resolve enantiomers from small to large scales. In this method, the enantiomers in a racemic mixture become separated by aggregating into enantio-pure crystals. This is able to occur because the enantio-pure crystals make up conglomerates which are overall racemic, thus the overall racemic character is preserved. Selective crystallisation of an enantiomer can then be effected by introducing a seed crystal of the desired enantiomer which causes the respective enantio-pure crystals in the conglomerates to crystallise out of solution.[18] Though this method of chiral resolution is simple and economical, its widespread application to chiral molecules is limited since only 5-10% of chiral molecules are able to form crystalline conglomerates.[15]

1.1.3 Kinetic resolution

Kinetic resolution separates enantiomers by exploiting the different reaction rates of the enantiomers with a chiral catalyst. Of a racemic mixture, one enantiomer has a favourable orientation with the chiral catalyst and reacts, while the other enantiomer should remain unreacted. Complete conversion of a racemic mixture into a single enantiomer can be achieved by dynamic kinetic resolution. In this method, a racemisation equilibrium is established between the two enantiomers by a suitable process such as by catalysis, or heating. With the racemisation equilibrium in place, the desired enantiomer is reacted through a chiral catalyst, producing an enantio-pure product (**Scheme 1.1**). This causes the undesired enantiomer to be racemised through a shift in the equilibrium, and the resultant desired enantiomer then reacts with the chiral catalyst.[14] Theoretically, the end result is that the entire racemic reactant is converted into an enantio-pure product. In situations where the chiral catalyst is not entirely enantioselective, it is critical for the racemisation process to be rapid to avoid the formation of product of the undesired enantiomer. The chiral catalyst may be a chemical or an enzyme catalyst. Although enzymes have been shown to be fairly versatile chiral catalysts, with high resolving efficiencies, the main drawbacks are that enzyme modification techniques are lacking, and that enzymes are susceptible to degradation.[14] Therefore, it is necessary for the chiral catalyst and the racemisation

process to be compatible. Kinetic resolutions are possible on industrial scales, but industrial applications are currently very limited and a work in progress.[19, 20]

Chiral
catalyst
Reactant (*S*) ⟶ Product (*S*)

Racemisation

Reactant (*R*)
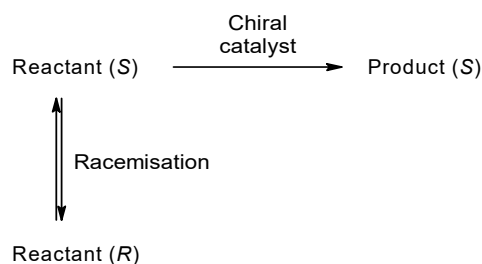
Scheme 1.1 Schematic illustrating chiral resolution through dynamic kinetic resolution.

Microbial systems have been known to use enzymes to entirely convert a racemic mixture, to the desired enantiomer.[14] This occurs because the enzyme is able to selectively react with the undesired enantiomer, converting it to the desired enantiomer. There is no need to establish an equilibrium between the enantiomers, and no overall transformation of functional groups in this process. Therefore, this is simply a deracemization of a racemic mixture, and is similar to dynamic kinetic resolution, but more convenient. This method is in its infancy, and the limitations associated with the use of enzymes need to be dealt with.

1.1.4   Chromatography

Chromatography is a well-established and general method for separating mixtures of compounds. The application of chiral molecules to stationary phases is also well-established, and has enabled the resolution of most racemic mixtures to be achieved with the generality of this method. As a result, chromatography is the most common technique used for chiral resolution. However, at industrial scales, chromatography often becomes expensive and inefficient, with a discontinuous operation.[15] Nevertheless, these obstacles have been overcomed to an extent that has allowed chromatography to be a common method for resolving enantiomers at industrial scales.

Simulated moving bed (SMB) chromatography is a well-established method to resolve enantiomers at industrial scales. Since the first multi-tonne SMB was installed in 1997, the technology has improved and expanded, with several installations currently operating around the world.[21] Escitalopram (the *S*-enantiomer of Citaloplam) is one such drug to be resolved by this method. The principle of separation of the moving bed in SMB is that the racemic mixture is loaded at the mid-point of a column that has the 'stationary' phase moving in the opposite direction to the mobile phase. The faster

eluting enantiomer is carried along with the mobile phase, and collected, while the slower eluting enantiomer is carried along with the 'stationary' phase, and collected. This enables enantiomers, which would closely-elute by regular elution chromatography, to be completely separated by moving bed chromatography. In practice, the principle of the moving bed is simulated (SMB) by continuously loading the racemic mixture onto the middle of a series of columns which are connected in series in a closed cycle. The stationary phase of these columns remains stationary, but the opposite motion of the stationary phase relative to the mobile phase is simulated by continuously moving the input of the racemic mixture as well as the two collection points of the separated enantiomers, in a motion that is opposite to the direction of the mobile phase. Advantages of these over regular HPLC are that a racemic mixture can be continuously resolved, and that the solvents can be recycled, once the analytes have been recovered. Currently, the main drawbacks of SMBs are: the requirement of a mathematical model for the design, optimisation and control of SMBs with the need for improvement of this process; the need for better chiral stationary phases with higher capacity; the need for solvent usage and energy consumption to be reduced; and the need to address other environmental concerns.

Supercritical fluid chromatography (SFC) is another chromatographic method that has been demonstrated to separate enantiomers, with potential industrial applications. SFC uses the same standard columns as HPLC, but makes use of supercritical carbon dioxide as the mobile phase. Supercritical carbon dioxide has liquid-like densities and dissolving capabilities, while also having gas-like viscosities and diffusion properties, thus making it an advantageous mobile phase. With SFC, resolution times could be faster, the solvation power of the mobile phase could be adjusted by adjusting the pressure of carbon dioxide, and a reduction of organic solvent usage would be certain.[21] However, the adoption of SFC has been hindered by a number of problems, including safety and cost issues associated with the temperature and pressure required to obtain supercritical carbon dioxide. Furthermore, there may be solubility issues, since carbon dioxide is relatively non-polar. Nevertheless, these issues are being resolved, and SFC is already being utilised in industry.[22-24] There is a current effort to resolve some issues of SMB by incorporation of SFC.[21-24]

1.1.5   Capillary electrophoresis

Chiral resolution by capillary electrophoresis has been proposed as an alternative to liquid chromatography because of the potential to increase separation efficiency, reduce analysis time, lower the amounts of mobile phase and buffers required, and the possible use of a wide variety of chiral mobile phase additives.[25] Research into capillary electrophoresis is largely in development, with the intention of it being an analytical tool rather than for large scale separation.

1.1.6 Membrane-base separation

The principle of membranes for separation is most commonly encountered as a simple separation of solids from a liquid by filtration through a membrane. The membrane only allows liquid to pass through, thus separation is based on the size of the particles. This principle of membrane-based separation has been expanded for potential separation based on a variety of other properties, including chirality, through the development of different membranes.[15, 26] To conveniently enable a variety of membranes to be used, membrane-based separations are often performed in apparatus as illustrated in **Figure 1.1**. Two aqueous phases are separated by an organic phase which serves as a membrane. The organic phase could be a plasticiser in a supported liquid membrane, or a solvent in bulk liquid membrane. Membranes could be designed to be selective alone, or could contain a chiral agent. Membrane agents are molecules which permanently reside in the membrane, while the mixture to be separated is loaded in the source aqueous phase. Separation would be performed by the membrane agent which should selectively allow passage of a component of the mixture, from the source aqueous phase, through the organic membrane, to the receiving aqueous phase. Eventually an equilibrium between the source and receiving phases will be reached. Therefore, equilibrium principles apply, and further separation can be achieved by driving the equilibrium forward through establishing a concentration or pH gradient across the source and receiving phases. Membrane-based separation is not as well-established as chromatography, but there is a great potential for this method, due to its simple operating mechanism that offers many advantages such as: being low cost, energy saving, environmentally friendly, high capacity, continuous operation, easy to maintain, operate and to scale up to industrial scales.[15] For these merits, this project aims to utilise membrane-based separation for the chiral resolution of racemic mixtures, ultimately at industrial scales, through the employment of enantioselective membrane agents. However, the design and synthesis of an appropriate

enantioselective membrane agent is the main obstacle. Though it may not be a requirement,[27] it is thought that a potential enantioselective membrane agent should possess a cavity that is chiral and able to achieve an appropriately weak binding so that the guest molecule can be carried across the membrane and released.[28]
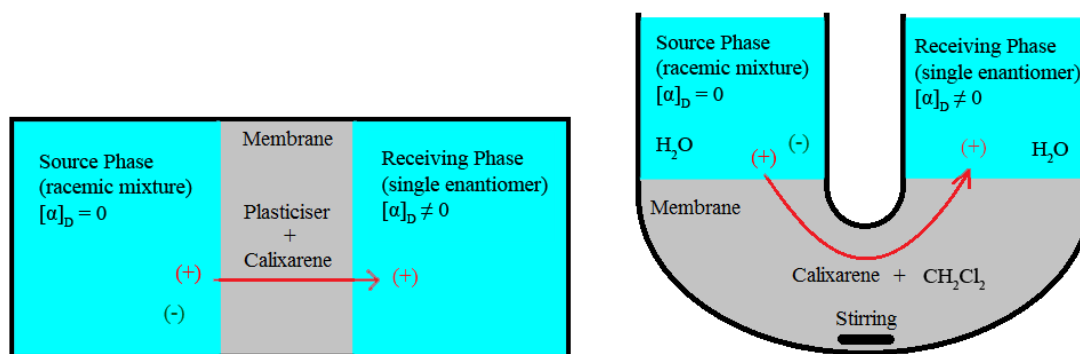
Figure 1.1 Chiral resolution via enantioselective calixarene transport agent in supported liquid membrane or U-shaped bulk liquid membrane apparatus. Image from Tan and Mocerino.[29]

1.2 Cavity molecules as chiral selectors

1.2.1 Cyclodextrins

Cyclodextrins are bowl-shaped macrocycles that are made up of glucose subunits, and can be simply obtained by the enzymatic conversion of starch.[30] The cyclodextrin bowl has a hydrophobic cavity which is able to contain a variety of different molecules as widely reported in the literature.[31-38] The chiral cavity of cyclodextrins has been employed as the stationary phase or additive in SMB chromatography,[39] gas chromatography, HPLC, capillary electrophoresis and capillary zone electrophoresis for the chiral resolution of a variety of natural products.[40] Cyclodextrins are commonly available, and have advantageous properties such as being water soluble, relatively non-toxic, stable in solution, non-UV absorbing, and ionisable.[25, 41] For these reasons, cyclodextrins have been most commonly researched as chiral selectors for capillary electrophoresis. An example of this is the carboxy methyl-β-cyclodextrin used by Li and co-workers to resolve enantiomers of salbutamol and sotalol.[42] As shown in their results (**Figure 1.2**), four analytes were resolved from each other, and further resolution of enantiomers of each analyte was also shown. The enantiomers of salbutamol and sotalol were completely resolved, while chiral resolution of the other two analytes, 2-amino-1-phenyl-ethanol and 1-(4-methoxyphenyl)-2-(methylamino)ethanol, was incomplete. β-Cyclodextrin was also tested, but showed

significantly inferior enantioseparation compared to the carboxy methyl counterpart. Further analysis provided evidence that the negatively-charged carboxylate groups of carboxy methyl-β-cyclodextrin were providing stronger interactions via electrostatic interactions and hydrogen bonding with the analyte guests resulting in better chiral recognition.
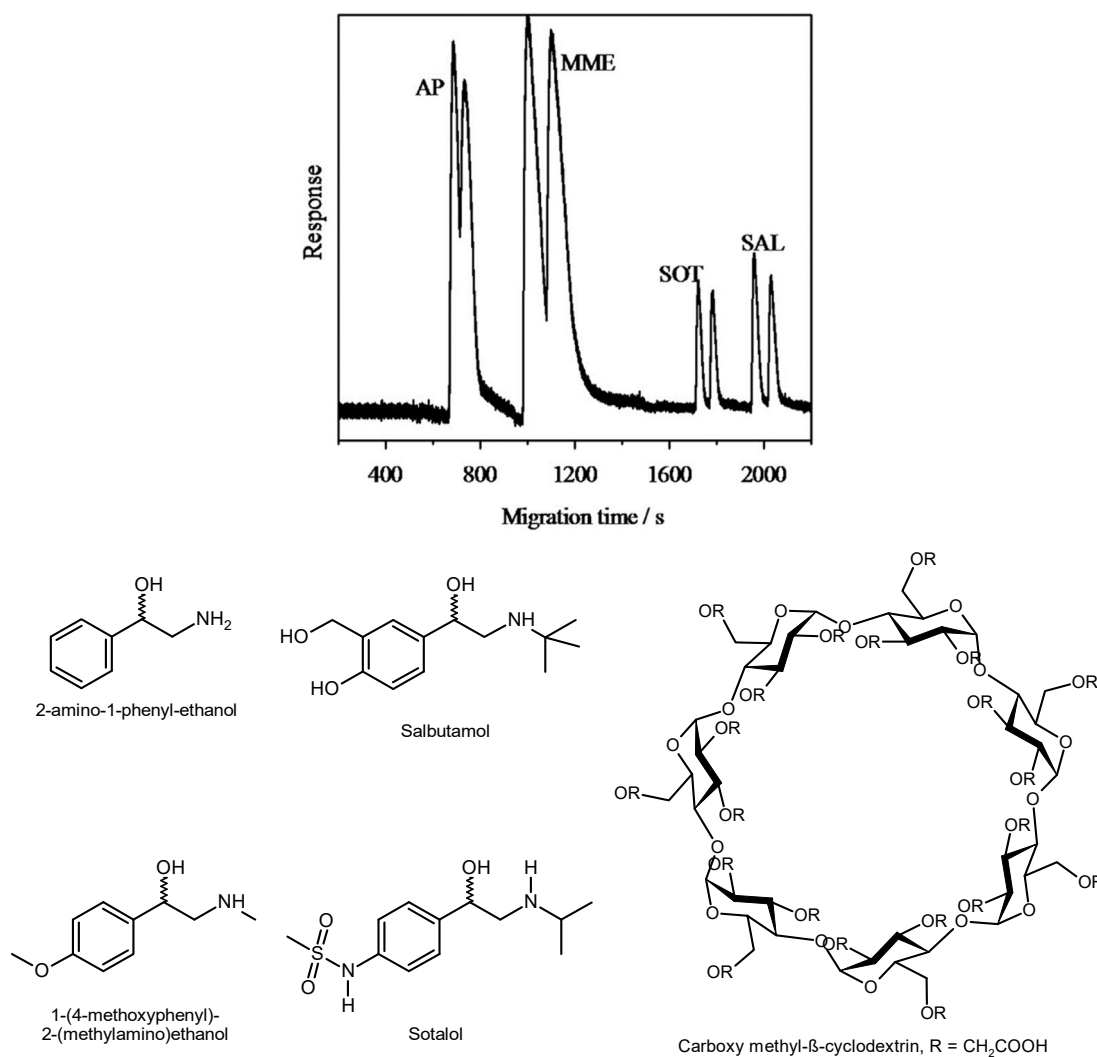
Figure 1.2   Separation of four analytes and their enantiomers via carboxy methyl-β-cyclodextrin in capillary electrophoresis. Image from Li et al.[42]

Given the success of cyclodextrins as chiral resolving agents, and the advantages of membrane-based separation, the potential of cyclodextrins to acts as an enantioselective transport agents have been investigated by Stancu et al.[43] A heptakis (2,3,6-tri-o-acetyl)-β-cyclodextrin membrane carrier was shown to transport tryptophan, phenylalanine, tyrosine and their respective methyl esters across a bulk liquid membrane. The most successful transport was for tryptophan and phenylalanine

methyl esters which were transported in over 75% yield during a 24 hour period. This was most likely due to the complementary structure, together with the increased hydrophobicity of the two amino acids. However, in all experiments, the cyclodextrin showed poor enantioselectivity, transporting significant amounts of both enantiomers. The best enantioselectivity of 16% ee was recorded for phenylalanine.
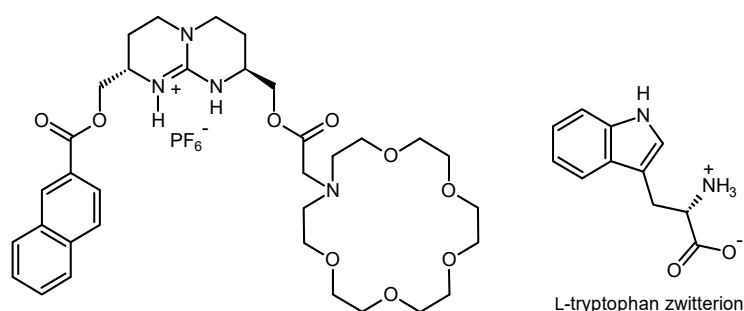
1.2.2 Crown ethers

Crown ethers are macrocyclic molecules made up of ethylene glycol subunits. The oxygen atoms of a crown ether are available hydrogen bond acceptors, enabling the cavity inside the ring of a crown ether to participate in binding interactions of smaller guest species. Although the parent structure of a crown ether renders an achiral cavity, functional groups about the ring of a crown ether can be arranged in a manner that imparts chirality to the cavity. A chiral crown ether as such has been utilised by Steffeck et al., for the chiral resolution of racemic mixtures of secondary amine drugs by HPLC.[44] The crown ether used was either enantiomer of (18-crown-6)-2,3,11,12-tetracarboxylic acid, which was immobilised onto the silica gel stationary phase by covalent bonds (**Figure 1.3**). The crown ether was believed to cause retention of the secondary amines by hydrogen bonding of the hydrogen atoms of the amine to the crown ether oxygen atoms, as well as electrostatic attraction between the protonated amine to the carboxylate of the crown ether stationary phase. The different affinities of the enantiomers toward the chiral crown ether stationary phase led to different retention of the enantiomers that was sufficient for their resolution.
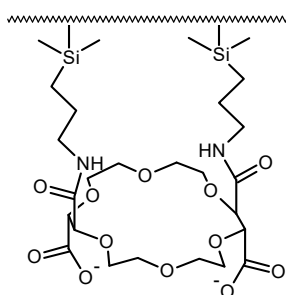
Figure 1.3   Chiral crown ether stationary phase for chiral resolution of secondary amines by HPLC.[44]

Crown ethers have also been a part of enantioselective membrane transport agents. Using a U-shaped apparatus (**Figure 1.1**), Breccia et al. showed that their crown-guanidinium membrane carrier (**Figure 1.4**) was able to efficiently transport 1.2 % of zwitterionic tryptophan amino acid over a short period of 1.5 hours, with up to 80% ee

for the L-enantiomer.[45] The enantioselectivity of the carrier was enabled by its chiral structure, effected by the specific orientations of the aza-crown ether and the naphthalene substituents on the bicyclic guanidinium moiety. Through molecular dynamics studies, the guanidinium moiety of the carrier was shown to hydrogen bond with the carboxylate group of the zwitterionic L-tryptophan, whilst the ammonium group of the amino acid was bound in the cavity of the aza-crown ether through alternating hydrogen bonds to the ether oxygen atoms. The naphthalene group of the carrier was envisioned to interact with the side chain of the amino acid. However, it was reported to be slightly oscillating in solution at room temperature, indicating that it was largely not participating in the binding and recognition of the amino acid.


Figure 1.4 Aza-crown ether guanidinium efficiently transported the L-tryptophan zwitterion in up to 80% ee.[45]

1.2.3 Calixarenes

The versatile ability of calixarene derivatives to act as hosts for a variety of smaller guest species as well as membrane transport has been widely demonstrated in the literature.[28, 46-52] This is because calixarenes are relatively large bowl-shaped molecules that are readily synthesised and functionalised. **Figure 1.5** illustrates a range of conformations calixarenes and their derivatives may adopt. Calixarenes may interconvert between conformations if not rigidly held together by steric forces, hydrogen bonding or by other intramolecular interactions.[53] As depicted in **Figure 1.6**, only a calixarene in the cone confirmation is bowl-shaped and possesses a cavity. A calixarene in the cone confirmation has a narrower (bottom) rim as well as a wider (upper) rim. The wider rim of a calixarene may be selectively and variously functionalised to enable the calixarene cavity to engage in a range of interactions with smaller guest molecules. This range of interactions can be adjusted to be charged or neutral, and may lead to the cavity being selective for a particular type of guest molecule, depending on the configuration and the type of functional groups on the wider rim.
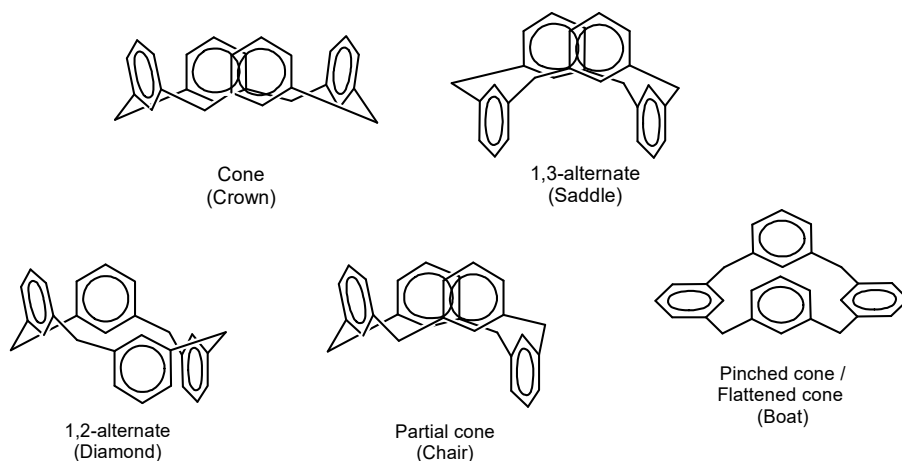
Figure 1.5 Some conformations of calixarenes.[54] Resorcinarene terminology in parentheses.[55]
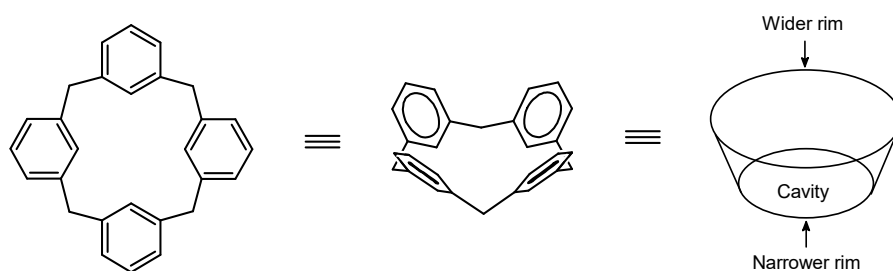

Figure 1.6 Calixarenes are bowl-shaped molecules possessing a cavity.

An example that illustrates the influence of functional groups on the binding of calixarenes is the membrane transport studies by Adhikari et al.[28] Knowing that certain calixarenes are able to bind choline and tetraalkylammonium molecules, a potential application of this principle to membrane carriers was investigated. The investigation aimed to utilise the choline functional group to act as a 'handle' to facilitate binding between a particular calixarene host, and a fluorophore guest. A choline handle was attached to various fluorophore molecules, which were tested as guests to be transported across a liquid membrane by a couple of known choline-binding calixarenes acting as experimental membrane carriers. The highest transport of 11% was achieved with tetraphosphonic acid calixarene as carrier for the FITC-choline guest (**Figure 1.7**), over a period of 200 hours.

Tetraphosphonic acid calixarene host
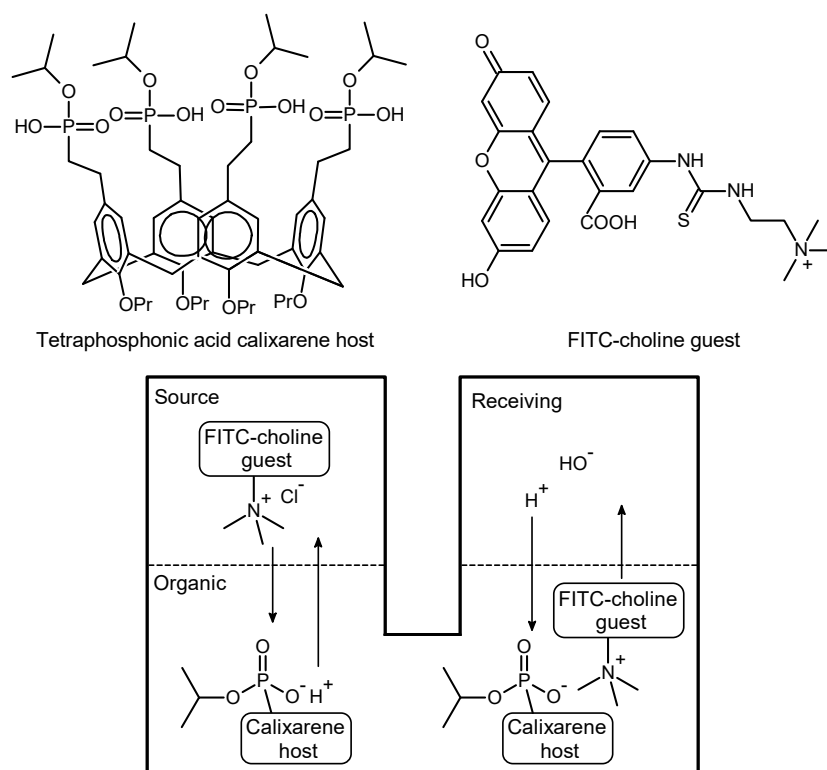
FITC-choline guest

Figure 1.7 The membrane transport of the FITC-choline guest was facilitated by maintaining a charge balance through exchange of H^+ to and from the tetraphosphonic acid calixarene.[28]
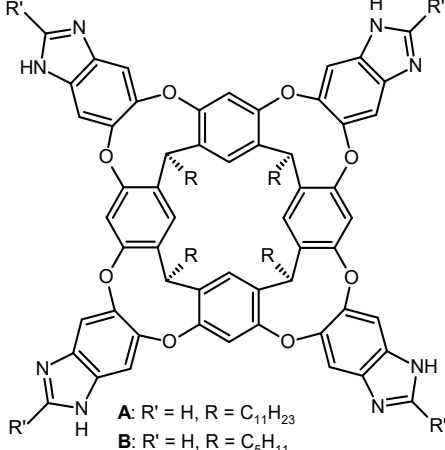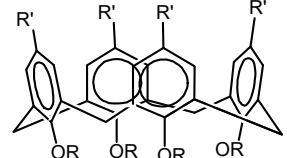
The binding was mainly effected by the ionic attractions between the negatively charged tetraphosphates of the calixarene, and the positively charged ammonium of the guest. Transport of the guest was facilitated by maintenance of charge balance through an exchange of a H^+ from a phosphonic acid of the calixarene host with the source and receiving phases. Since this main interaction occurred at the wider rim of the calixarene, the electron-rich calixarene cavity may have also been able to hold the ammonium guest via a cation-π attraction as depicted in **Figure 1.8**.
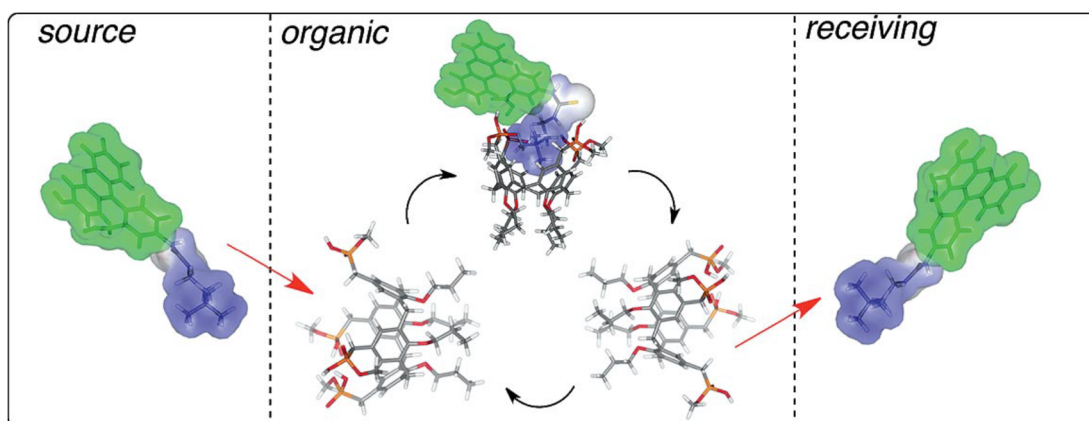
Figure 1.8 Binding and releasing of the FITC-choline guest by the tetraphosphonic acid calixarene membrane carrier. Reprinted with permission from Adhikari et al., *Eur. J. Org. Chem.* **2014,** *2014* (14), 2972-2979 (graphical abstract). Copyright John Wiley & Sons 2014.[28]

15

However, the resorcinarene cavitands (**A-C**, **Table 1.2**) that were also known for binding choline moieties exhibited no transport ability. These resorcinarene cavitands showed good binding by preliminary NMR studies, which were a contrast to the successful calixarene membrane carrier, which appeared to be a weak binder during NMR tests. Indeed, the resorcinarene cavitands which appeared to be strong binders, simply extracted the guests out of the source phase, never to be released again to either of the aqueous phases. This demonstrates the importance for a calixarene to have the appropriately weak binding for the guest, to be a successful membrane carrier. The appropriate weak binding may be obtained by adjustment of the functional groups present on the calixarene.

Table 1.2   The appropriately weak binding of a calixarene host is crucial to its success as a membrane carrier.[28]

| Calixarene Host | A: R' = H, R = C₁₁H₂₃ | D: calix[4]arene, R' = *t*Bu, R = CH₂COOH |

Calixarene Host	A: R' = H, R = $C_{11}H_{23}$ B: R' = H, R = C_5H_{11} C: R' = CH_2COOEt, R = $C_{11}H_{23}$	D: calix[4]arene, R' = *t*Bu, R = CH_2COOH E: calix[6]arene, R' = *t*Bu, R = CH_2COOH F: calix[4]arene, R' = $CH_2PO_2(OH)O^iPr$, R = *n*Pr
NMR	Strong binding	Weak binding
Transport	No	Yes

Looking to their end goal of the delivery of drugs through cell walls by endocytosis, Adhikari et al. have extended their membrane transport studies by replacing the FITC portion of the guest, with drug molecules such as tryptophan, acetaminophen, ibuprofen, dimethylresveratrol and bentiromide.[52] Moreover, different binding moieties, other than choline, in the form of ionisable amine moieties in unaltered neurotransmitters such as dopamine and serotonin were also tested as guests. Calixarenes **D** and **F** were shown to transport all of the aforementioned guests to varying degrees as highlighted in **Table 1.3**.

Table 1.3 Transport of drug-choline conjugates and neurotransmitters via calixarenes **D** and **F**. Experiments were conducted with varying pH of the receiving phase; the best results are highlighted here.[52]

Guest	Guest in source phase (mM)	Guest transported (%)		
		Background	Calixarene D	Calixarene F
Tryptophan-choline	0.5	6.83 [a]	63.36 [a]	43.13 [a]
Acetaminophen-choline	0.5	0.75 [a] 0.72 [n]	4.47 [a]	2.07 [n]
Ibuprofen-choline	0.5	9.05 [a][n]	27.02 [a]	50.38 [a]
Dimethylresveratrol-choline	0.5	1.57 [a]	4.08 [a]	5.34 [a]
Bentiromide-choline	0.5	2.05 [a] 1.23 [n]	11.68 [a]	8.66 [n]
Dopamine	5.0	1.86 [a] 2.04 [n]	3.72 [a]	45.04 [n]
Serotonin	5.0	0.00 [n]	6.98 [n]	29.50 [n]

[a] The receiving phase was acidic. [n] The receiving phase was neutral. Transport experiments were conducted over a 72 hour period.

The position of the functional groups at the wider rim of a calixarene can enable the calixarene to act as a selective membrane carrier for a particular molecule. An example of this is the work by Duggan and co-workers who have demonstrated selective membrane transport of fructose from a mixture with glucose, mediated by cavitand boronic acids.[56] Boronic acids are known for the ability to selectively transport carbohydrates across lipid membranes, while cavitands are known to be conformationally-rigid calixarenes. Therefore, cavitands with boronic acids would present prime candidates as membrane carriers for carbohydrates. The synthesis of mono-, proximal-, distal-, tri-, and tetra- cavitand boronic acids was accomplished, and the five cavitands were tested for the potential to selectively transport fructose over glucose through a solid supported liquid membrane. The results (**Table 1.4**) show that all five cavitand boronic acids were selective membrane carriers for fructose. In particular, the distal cavitand boronic acid showed the best selectivity, while its proximal isomer showed increased transport for both fructose and glucose. This observation clearly shows that the rate and selectivity of the transport was impacted by the positioning of the boronic acids about the wide rim of the cavitand. The increase in glucose transport was thought to be due to the glucose being able to form two ester

linkages between the boronic acids at the proximal positions of the cavitand, while at the distal positions, the two boronic acids would be too far apart, preventing the glucose from forming the two ester linkages. This rationale would also explain the marked increase in transport of the two sugars by the tri bronic acid derivative.

Table 1.4   Selective membrane transport of fructose from a mixture with glucose, mediated by various cavitand boronic acids.[56]
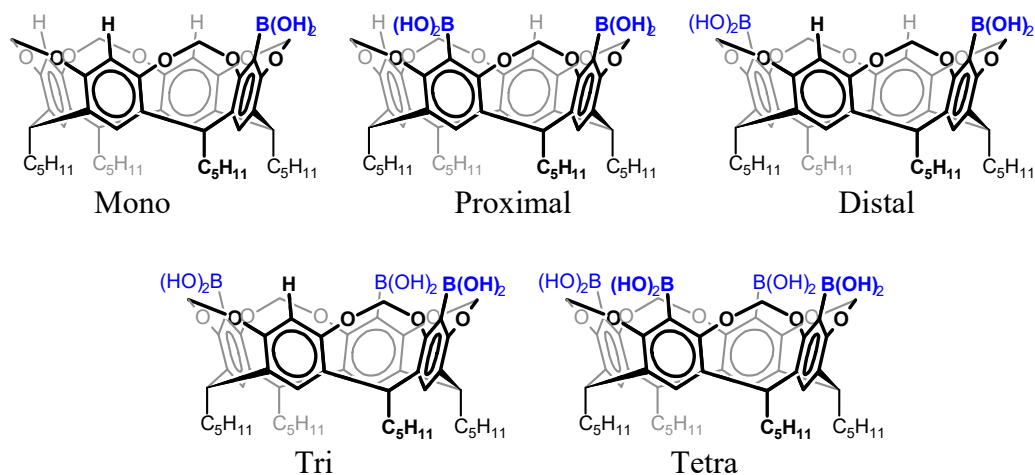

Cavitand boronic acid	Transport yield % over 5 hours		Ratio
	Fructose	Glucose	
Mono	0.029	0.004	6.5
Proximal	0.038	0.004	10.6
Distal	0.054	0.013	4.2
Tri	0.164	0.029	5.7
Tetra	0.105	0.016	6.4

The effect of the size of the calix[n]arene on the transport of tryptophan methyl ester across a liquid membrane was studied by Oshima et al.[57] Of the carboxymethyleneoxy derivatives of tetramer, hexamer, and octamer of *p-tert*-octylcalix[n]arene, the best transport rate was recorded with the hexamer (**Figure 1.9**), followed by the octamer, while the tetramer showed essentially no transport. With the calix[6]arene derivative, quantitative transport of the tryptophan methyl ester was achieved under a pH gradient. The success of the calix[6]arene over other sizes was attributed to the C_6-symmetrical structure which enabled a complementary tripodal hydrogen bonding of the protonated amino group of the tryptophan methyl ester with the six carboxylic acids of the narrower rim of the calix[6]arene. It was thought that the remainder of the tryptophan

methyl ester was binding within the hydrophobic cavity of the calix[6]arene. The transport of phenylalanine methyl ester, tyrosine methyl ester, and tryptophan by this calix[6]arene derivative was also studied. Phenylalanine methyl ester transported similarly to tryptophan methyl ester, but the free tryptophan amino acid showed neglible transport. These results indicate that the hydrophobicity of the guests was critical for their transport by the calix[6]arene.
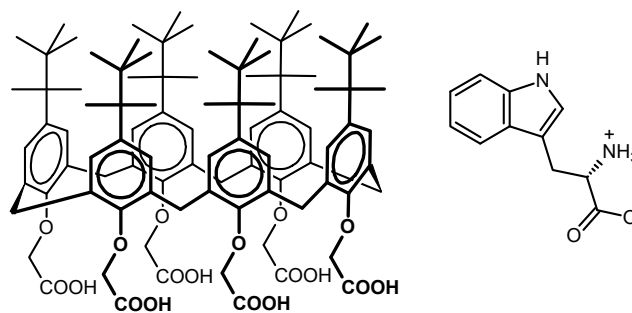
Figure 1.9 Structure of the *p-tert*-octyl carboxylic acid calix[6]arene membrane carrier for tryptophan methyl ester guest.[57]

One of the relatively few examples of a calixarene being tested as a membrane carrier for chiral resolution is the work by Durmaz and Sirit et al. In their three publications, non-chiral *p-tert*-butylcalixarene was distally-*O*-alkylated at the narrower rim with enantio-pure α-hydroxy amide,[49] aminonaphthol,[50] aminoalcohol[58] moieties. A total of sixteen calixarene derivates were prepared and tested as enantioselective membrane carriers in a U-tube apparatus, for the methyl esters of phenylalanine, phenylglycine, and tryptophan. The best result was achieved with amino alcohol calixarene (**Figure 1.10**), which transported phenylalaine methyl ester in the highest recorded transport flux with 52% ee. The best ee of 53% was recorded with another amino alcohol calixarene for tryptophan methyl ester, but had a far lower transport flux of 3% of the best result. All calixarene derivatives tested generally had a significantly lower transport flux for the tryptophan methy ester compared to the other amino acid methyl esters. It was thought that the enantioselectivity was the result of hydrogen bonding, π-π stacking binding interactions, and structural rigidity or flexibility between the host and guest.
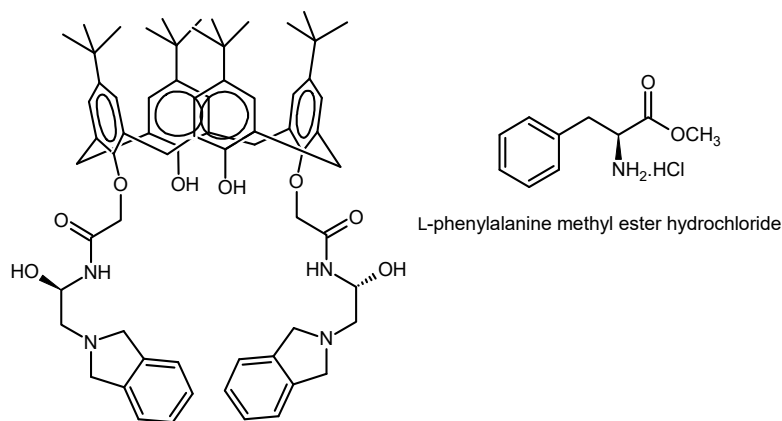
Figure 1.10   The amino alcohol calixarene derivative which transported L-phenylalanine methyl ester in 52% ee.[58]

L-phenylalanine methyl ester hydrochloride

The calixarenes, in the enantioseparation experiments by Durmaz and Sirit et al., were simply functioning as a scaffold for the chiral moieties. However, since a key feature of a calixarene is its cavity, this project aims to achieve enantioselective transport through the use of the cavity of the calixarene. A few other studies have shown that the chiral cavities of some calixarenes can achieve some chiral recognition.[59, 60] However, the key requirement is to obtain a calixarene with the appropriate a chiral cavity.

1.2.4   Chiral resorcinarenes

Resorcinarenes are a subclass of calixarenes. Compared to calixarenes, resorcinarenes, derived from resorcinol subunits, tend to have more functionality at the wider rim. If the configuration of the functional groups at the wider rim is chiral, then the cavity is chiral (axially chiral), and so the resorcinarene has the potential to be an enantioselective host for chiral guest molecules. Axial chirality arises when one or more moieties are arranged about a molecule either in a clockwise or anticlockwise fashion, and thus the molecule does not need to have a chiral centre. Calixarenes with chiral cavities are known, but the specific arrangement required often complicates their synthesis.[61, 62]

The first enantioselective synthesis of an axially-chiral resorcinarene was reported by Heaney and co-workers in 1999. Starting with a Mannich reaction between octaphenol resorcinarene and the (*R*) enantiomer of an α-methylbenzylamine derivative, tetrakis(dihydro-1,3-benzoxazine) resorcinarene was produced in 77% yield, with very high distereoselectivity (**Scheme 1.2**).[63] The key to the diastereoselectivity of this reaction was due to the particular arrangement of the benzoxazine groups around the

resorcinarene. This was caused by the formation of four hydrogen bonds between the phenols and the oxygen of the benzoxazine group on the neighbouring aromatic ring, together with the steric interactions of the chiral amines. The crystalline tetrakis(dihydro-1,3-benzoxazine) resorcinarene product was stable over long periods of time, however the diastereoselectivity would be lost when placed in solution with a trace amount of acid. The acid would cause the benzoxazine ring to open, and re-form; and on reformation, there are two possible *ortho* phenols to react with, hence leading to loss of diastereoselectivity.[64] Therefore, preservation of the diastereoselectivity was achieved by methylating the other *ortho* phenol of the tetrakis(dihydro-1,3-benzoxazine) resorcinarene. With the diastereoselectivity secured, the benzoxazine ring was opened by simply refluxing in formic acid. Finally, reduction of the α-methylbenzylamine chiral moiety converted the diastereomerically-pure resorcinarene to its pure enantiomer.[63]
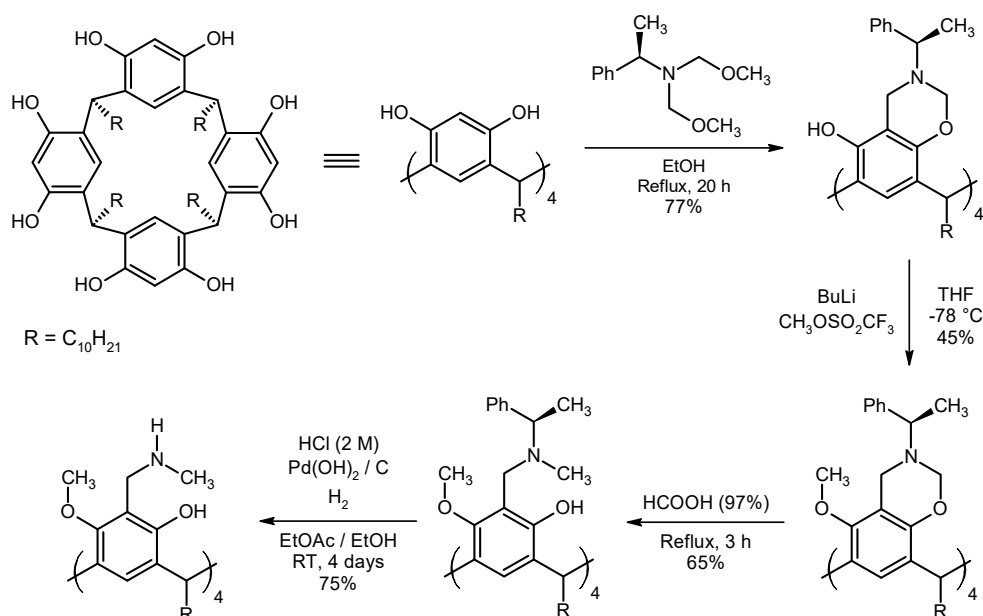
Scheme 1.2. Enantioselective synthesis of an axially-chiral resorcinarene via diastereoselective Mannich reaction.[63]

In 2000, McIldowie and co-workers synthesised an axially-chiral tetramethoxyresorcinarene in a single step from starting subunits (**Scheme 1.3**).[65] Borontrifluoride, a strong Lewis acid, facilitated the cyclisation of the aldehyde and 3-methoxyphenol subunits, to regioselectively construct the axially-chiral resorcinarene in high yields, as a racemic mixture. Out of the many possible regioisomers, the axially-chiral regioisomer was essentially the only product. The particular regioisomer obtained enabled four hydrogen bonds to be formed between phenols and methoxy

groups at the wider rim, causing the resorcinarene to adopt the cone conformation. Assembly of the resorcinarene could also be accomplished with long-chain aliphatic aldehydes, thus increasing its solubility in organic solvents.[65] Furthermore, separation of the axially-chiral resorcinarene enantiomers from the resultant racemic mixture has been accomplished by Buckley et al. in good yields, through diasteromic separation.[66] In this procedure, the four phenols of the resorcinarene enantiomers were converted to camphorsulfonates to give the resorcinarene as a diasteromic mixture. Separation of the diastereomers of tetracamphorsulfonate resorcinarene was then achieved by column chromatography, and hydrolysis of all camphorsulfonates from each diastereomer afforded the enantiomerically-pure axially-chiral tetramethoxy-resorcinarene.
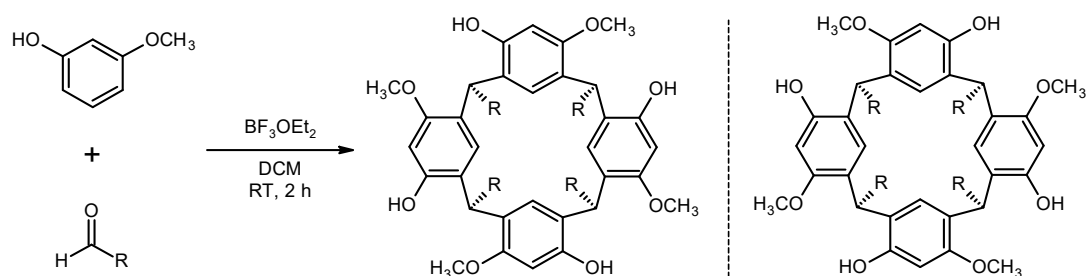

Scheme 1.3 One-step synthesis of an axially-chiral resorcinarene.[65]

Therefore, this tetramethoxyresorcinarene appears to have the key features of a potential enantioselective membrane carrier, which this project aims to investigate. However, the major remaining obstacle is that the cavity of the tetramethoxy-resorcinarene is likely too open and has not enough binding interactions for the guest to be retained during transport. This work proposes to bind guests inside the cavity of tetramethoxyresorcinarene by partially-enclosing the cavity through installation of a bridge over the wider rim from distal aromatic rings.

1.3 Bridged calixarenes

Calixarenes that are distally-bridged on the narrower rim are common in the literature.[67-71] The crown ether bridged calixarene synthesised by Ungaro and co-workers in 1995 is one of many examples.[48] Selective distal functionalisation of a calixarene on the narrower rim was first achieved by treating tetrahydroxycalixarene with 1.1 equivalents of potassium carbonate base with an octyl halide (**Scheme 1.4**). Simple alkylation of the remaining two distal phenols by pentaethylene glycol ditosylate furnished the crown ether-bridged calixarene in the 1,3-alternate

conformation. The calixarene crown ether was then shown to be a membrane transport agent selective for caesium ions over sodium ions. Such a system has been utilised by the U.S. Department of Energy to remove caesium ions from more than 11 million litres of radioactive waste.[72, 73]

$R = (CH_2)_7CH_3$
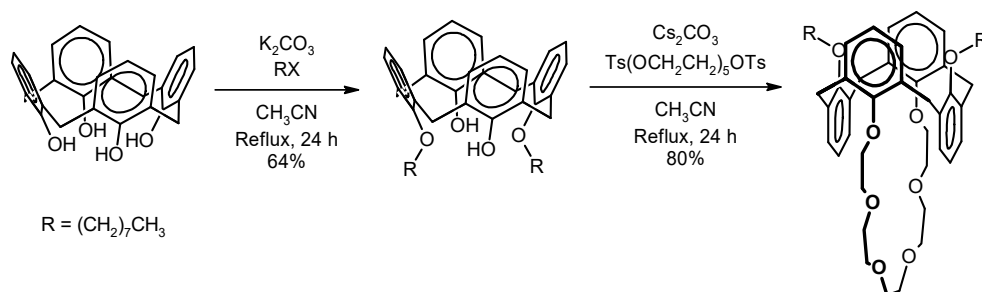
Scheme 1.4 Selective distal bridging of calixarene at the narrower rim.

Distal selectivity is a key requirement for selective distal-bridging of calixarenes. The simple two-step procedure developed by Ungaro and co-workers has been responsible for the many narrow-rim, distally-bridged calixarenes reported in the literature. The mechanism of the distal selectivity of the phenol alkylation is illustrated in **Scheme 1.5**. After the first phenol is alkylated, the distal phenol is most favourable for subsequent deprotonation because the resultant phenoxide is stabilised by two hydrogen bonds formed from the two phenols on adjacent aromatic rings. Therefore, the second alkylation occurs on the distal phenol.[74]
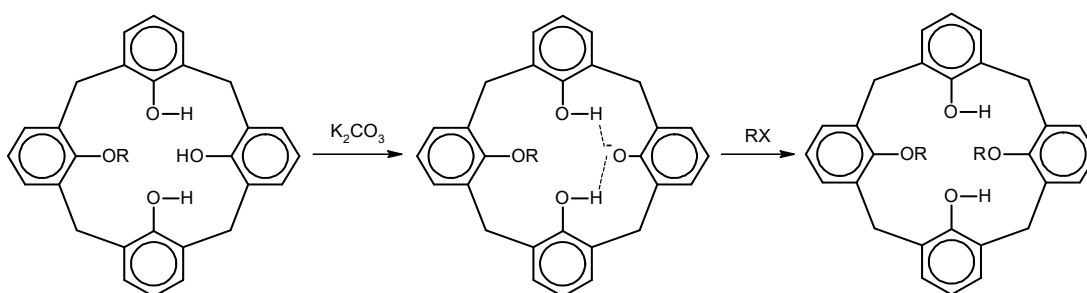

Scheme 1.5 Mechanism of the selective distal alkylation of tetraphenol calixarene at the narrower rim.

This mechanism of distal selectivity is only applicable to the narrower rim of calixarenes where the hydrogen bonding stabilisation is enabled by the phenols being in proximity to each other. Therefore, the popular method for distal bridging calixarenes does not directly apply to the wider rim of calixarenes. Unfortunately, a bridge at the narrower rim in the cone conformation does not make use of the cavity, which is a key attribute of a calixarene. Generally, the calixarene portion in these

23

narrow-rim bridged calixarenes simply serves as a scaffold. Nevertheless, distal bridging over the wider rim has been accomplished by transferring the distal selectivity from the narrower rim to the wider rim via the stronger para-activating effect of the remaining two phenols, as reported in the literature.[74-76]

The first characterisation of calixarenes with a distal bridge at the wider rim was reported by Böhmer and co-workers in 1988.[77] In their pioneering work, distally-bridged calixarenes were synthesised by the TiCl$_4$-catalysed Friedel-Crafts alkylation of α,ω-(*p*-hydroxyphenyl)alkanes with bis(bromomethyl)phenols (**Scheme 1.6**). TiCl$_4$ was thought to also act as a template for the cyclisation. Calixarenes with various aliphatic bridge lengths were synthesised, but with lower yields. Calixarenes with bridges of eight carbons and longer were observed to be in the cone conformation, but shorter bridges resulted in the cone conformation becoming pinched. The cyclisation reaction with a shorter bridge of four carbons was not successful.
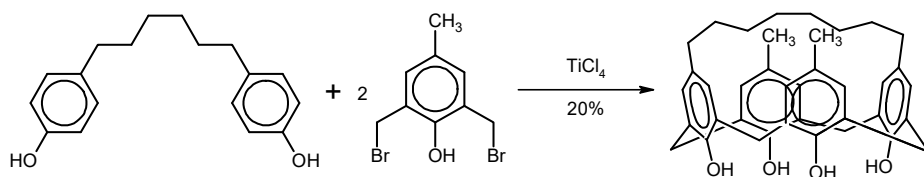
Scheme 1.6 Pioneering synthesis of distally-bridged calixarene by Böhmer and co-workers.[77]

To study the effect of the bridge length and rigidity on the synthesis of a distally-bridged calixarene, Zeng et al. have tried various diacid chlorides to form diester linkages with a distal-diol calixarene (**Scheme 1.7**).[78] Each experiment was conducted at dilute concentrations and produced multiple products which were separated by column chromatography into three main fractions. The yields of the three fractions of the various trials are shown in (**Table 1.5**). At these conditions, it is evident that the longer bridge with an eight-carbon chain gives the highest proportion of distally-bridged calixarene. This could be attributed to the increasing flexibility of the longer chain,[78] and perhaps the reduction of strain on the calixarene cone conformation. It is also evident that that the distally-bridged calixarene was the predominant product for all tests, except for the teraphthalate, which may have suffered from steric strain / hindrance due to its rigidity. The reactions were also attempted at higher concentrations, producing a greater proportion of calixarene oligomer products, as well as trace amounts of shorter-bridged calixarene dimers. Thus as expected, a higher

24

concentration of the reactants increases the chance of intermolecular reactions between calixarenes at the expense of intramolecular reactions within calixarenes.
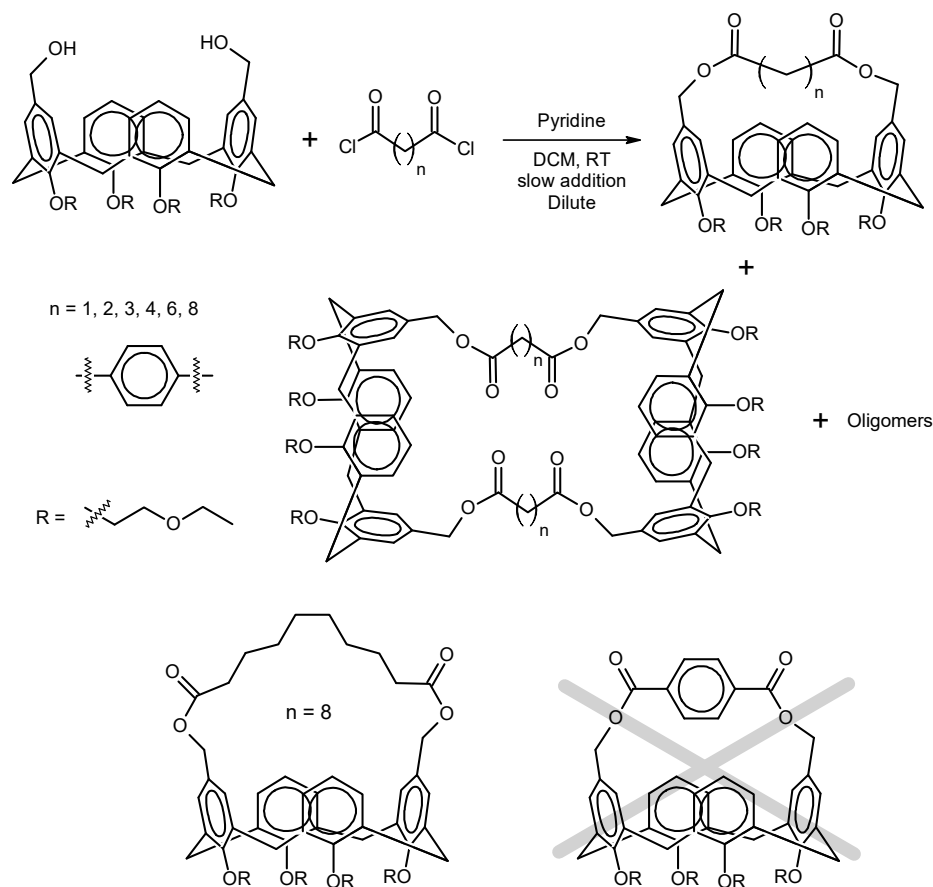
Scheme 1.7 Synthesis of distally-bridged calixarenes via diester linkages. Experiments to explore the impact of bridge length and rigidity.[78]

Table 1.5 Yields of the three main fractions from various calixarene bridging experiments.

Bridge	Yield determined by HPLC (%)		
n	Distally-bridged calixarene	Calixarene dimer	Calixarene oligomer mixture
1	55.6	0	41.0
2	39.8	17.4	42.8
3	41.3	23.7	35.0
4	42.2	25.5	32.3
6	66.5	0	33.5
8	82.2	0	17.8
phenyl	0	34.5 [a]	45.4 [a]

[a] isolated yield (not determined by HPLC)

In a related reaction, Cacciapaglia and co-workers constructed a distally-bridged calixarene with acetal linkages (**Scheme 1.8**).[79] The outcome of this reaction was also

25

similar to Zheng et al. in that the reaction produced multiple calixarene products which were separated by column chromatography into three main fractions: distally-bridged calixarene, calixarene dimer and calixarene oligomer mixture. This work was part of an investigation into the synthesis of dynamic 'living' polymers which could be manipulated by concentration, to selectively give a particular product or oligomer at equilibrium. In this case, it was envisioned that the creation of a dynamic family of cyclic calixarene oligomers linked by formaldehyde acetals would be enabled by the reversible formation of the acetal linkages of the calixarene products upon the addition of a catalytic amount of acid. However, when a catalytic amount of trifluoroacetic acid was added to all three acetal calixarene fractions, a distally-bridged ether calixarene formed instead. This was thought to proceed via a benzylic carbocation on the calixarene that could be formed by the acid-catalysed cleavage of one of the acetal bonds. The resultant hemiacetal and stabilised *p*-propoxy benzyl carbocation would then react in an intramolecular reaction, eliminating formaldehyde and forming the unreactive distal ether bridge. This mechanism would explain the observation that all acetal calixarenes, regardless of the type of acetal linkage, resulted in the same distal ether bridge when treated with acid.
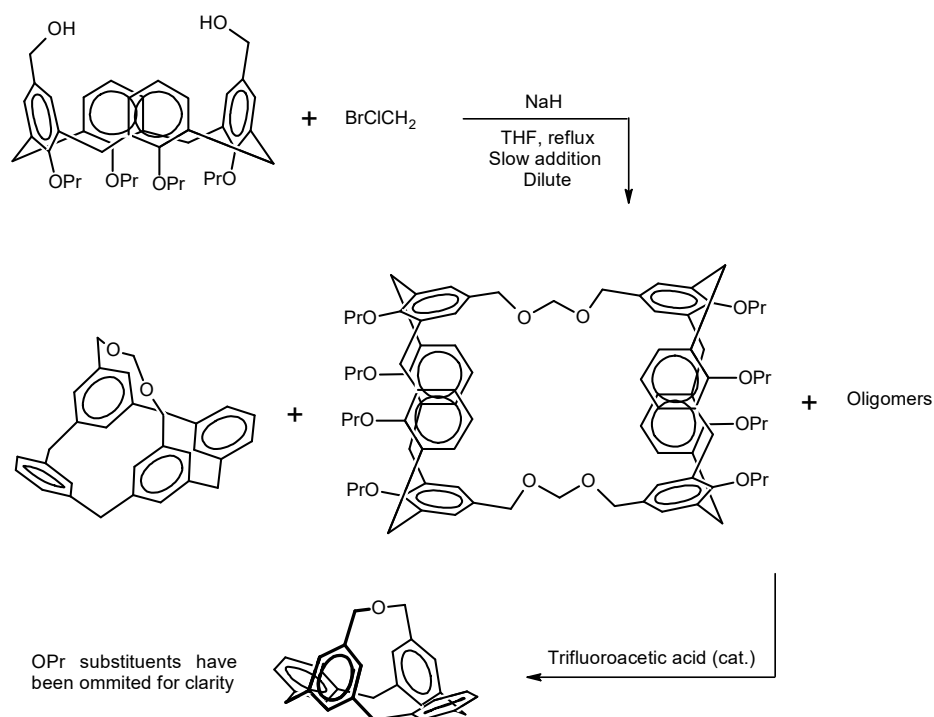
Scheme 1.8 Synthesis of acetal-bridged calixarenes and their decomposition into distally-bridged ether calixarene upon treatment with acid.[79]

A very similar calixarene with the short distal ether bridge has also been synthesised by Arduini et al. in 30% yield, beginning from the same distal diol calixarene (**Scheme 1.9**).[80] The ^{1}H NMR spectrum of the product provided evidence that the ether-bridged calixarene was rigid, adopting a highly-distorted flattened-cone conformation. The protons of the aromatic rings involved in the bridge appeared at a significantly lower chemical shift ($\sim\delta$ 5.7), which suggested their shielding by the un-bridged proximal aromatic rings. The intermolecular bridging product, a calixarene pair linked by two acetal bridges, was also produced, but as a minor product. Interestingly, the intermolecular reaction could be favoured by reacting the distal diol calixarene with a distal dichloromethyl calixarene with caesium hydroxide as base, to give the calixarene pair product in 50% yield.
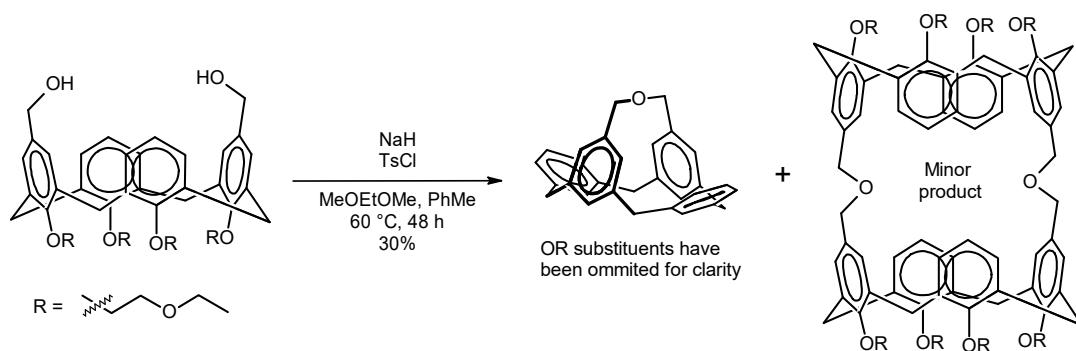
Scheme 1.9 Synthesis of distal ether bridged calixarene.[80]

The intramolecular bridging on the wider rim of the calixarenes was further studied by Arduini et al. with a McMurry reductive coupling between the formyl groups of various formyl calixarenes (**Scheme 1.10**).[81] The reductive coupling of distal diformylcalixarene afforded a distally-bridged calixarene with a diol bridge, after 5 hours, which could be further reduced to an alkene after 16 hours. A similar result was also reported by Lhoták and Shinkai in separate work.[82] Arduini et al. also explored the possibility for the coupling to occur between formyl groups on proximal aromatic rings of tri and tetraformylcalixarenes. With both these calixarenes, only the distal formyl groups showed coupling, while the remaining formyl groups were reduced to methyl groups.
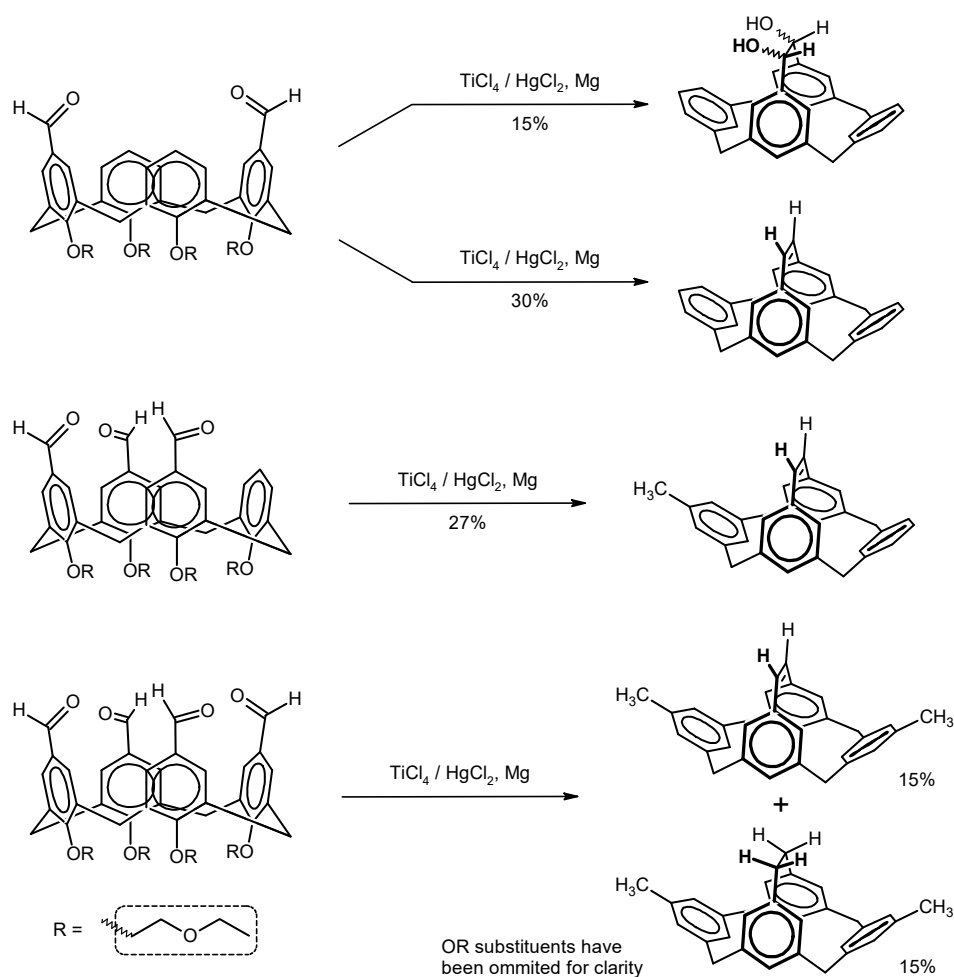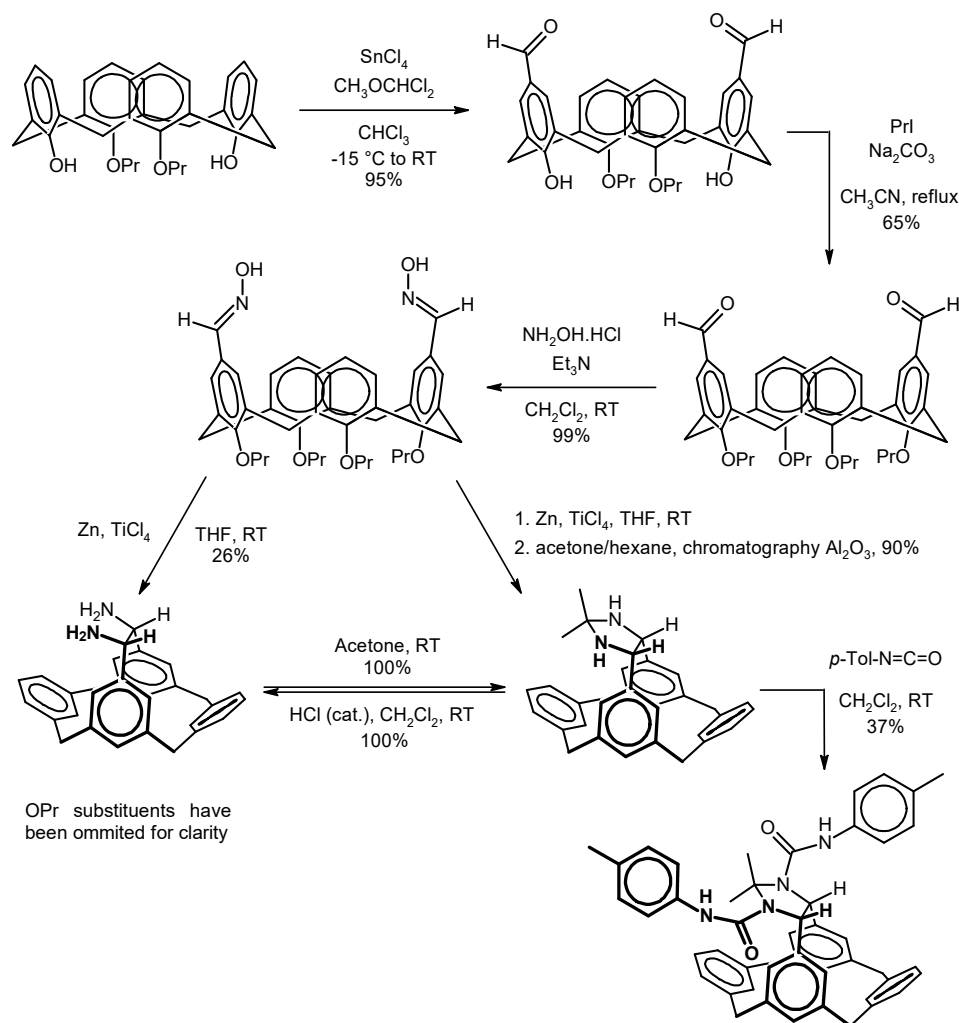
Scheme 1.10 Distal bridging of formyl calixarenes via intramolecular McMurry reductive coupling.[81]

Another calixarene with a short distal bridge is the siloxane-bridged calixarene synthesised by Hudrlik et al.[83] The synthesis of this calixarene was accomplished in four steps, as described in **Scheme 1.11**. The distal selectivity on the wider rim of the calixarene was obtained through a selective bromine to lithium exchange, followed by quenching with methanol, as described by Larsen and Jørgensen.[84]
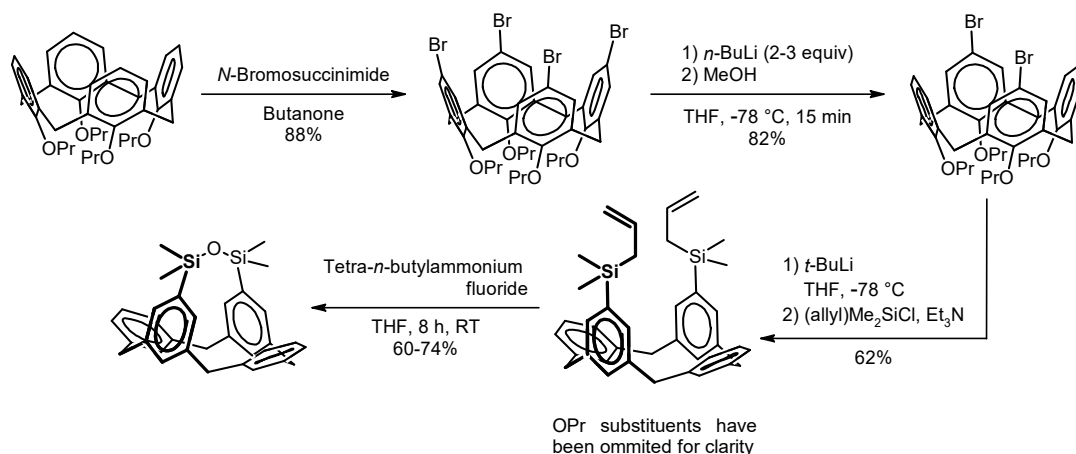
Scheme 1.11 Synthesis of distally-bridged siloxane calixarene.[83]

In another example, Zajícová et al. reported a distally-bridged calixarene obtained from the reductive coupling of a distal dialdoxime calixarene (**Scheme 1.12**).[75] The distal selectivity of the starting dialdoxime calixarene was obtained by the stronger para-directing effect of distal phenols at the narrower rim. The reductive coupling afforded the diamine product in a rather low yield of 26%, which was attributed to decomposition of the product under aerobic conditions. However, it was discovered that the product easily formed a stable aminal with acetone. Therefore, immediate chromatography of the diamine product with acetone afforded the aminal of the distally-bridged diamine calixarene in 90% yield. The scope of the reductive coupling was investigated with a number of dialoximine calixarene derivatives with various substituents at both rims of the calixarene, as well as a calixarene in the 1,3-alternate conformation (**Figure 1.11**). In all these other cases, no distally-bridged calixarene was detected, alluding to the sensitivity of the reductive coupling to the conformation of the starting dialoximine calixarene. A crystal structure of an amide derivative of the distally-bridged calixarene showed that the short bridge, of two carbons, forced the supporting aromatic rings to be bent into the cavity, causing the calixarene to take the pinched cone conformation.

Scheme 1.12 Distal bridging of dialdoxime calixarene via reductive coupling.[75]
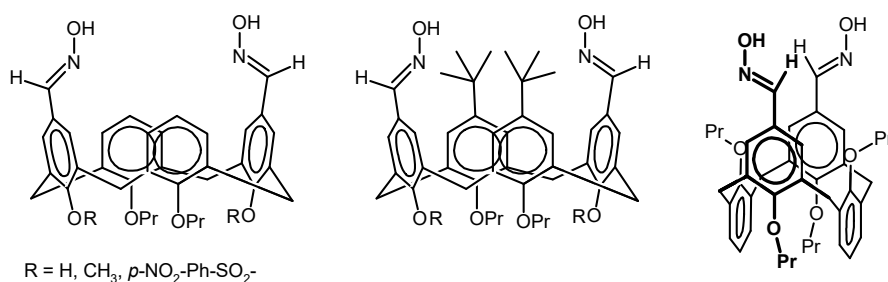
Figure 1.11 Reductive coupling with other dialdoxime calixarene derivatives failed to give the distally-bridged product.[75]

While investigating the synthesis of phenanthrene calixarenes via photochemical cyclisation, Barton[85] synthesised a distally-bridged calixarene with a cyclobutane bridge (**Scheme 1.13**). The photolysis of tetra-stilbene calixarene produced a highly complex mixture of cyclisation products including the distally-bridged cyclobutane calixarene, which was isolated in 1% yield by HPLC. Deducing that the bridging does not occur on the proximal aromatic rings, Hüggenberg et al. attempted the same

photochemical cyclisation on proximal di-stilbene calixarene.[86] As anticipated, the proximal di-phenanthrene calixarene was produced as three diastereomers in 67% yield, without any bridged calixarene. It is interesting that the bridging only occurred on the distal aromatic rings, rather than on proximal.
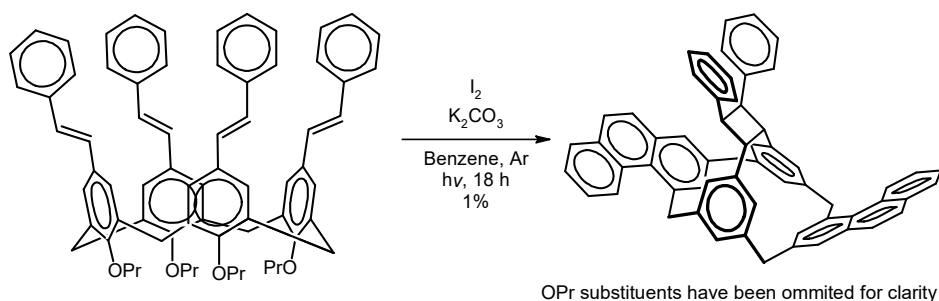
Scheme 1.13 Photochemical [2+2] cycloaddition of tetra-stilbene calixarene to give distal cyclobutane-bridged diphenanthrene calixarene.[85]

Liu et al., while exploring the synthesis of cage-like compounds, reported another unexpected distal bridging of calixarenes by intramolecular coupling.[87] The aim was to couple two tetraalkynylcalixarenes via a reversible intermolecular zirconocene coupling to form a cage-like structure. However, the intramolecular coupling was prevalent, and a two-carbon distally bridged calixarene formed instead (**Scheme 1.14**).
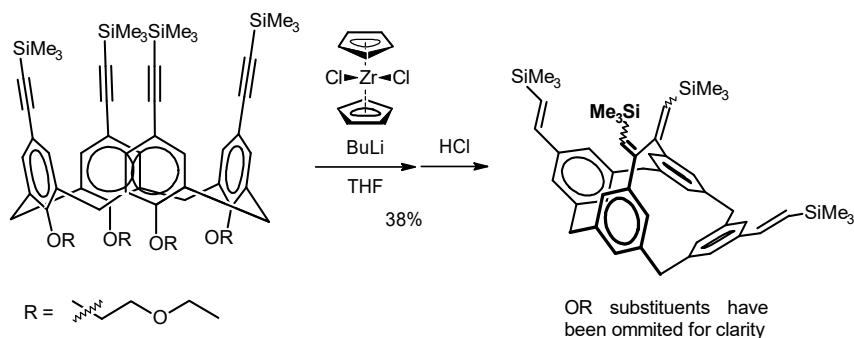
Scheme 1.14 Zirconocene coupling of tetraalkynylcalixarene leads to distal bridging of calixarene.[87]

A distally bridged calixarene with the shortest possible bridge has been synthesised by Struck et al.[88] The distal methylene-bridged calixarene was reported to be exclusively formed by the reaction shown in **Scheme 1.15**. The 'collapsed' cone conformation of the product was evident by signals at δ 5.6 in the ^{1}H NMR spectrum. These signals were attributed to the protons of the bridging aromatic ring, which had become shielded by the neighbouring non-bridging aromatic rings.
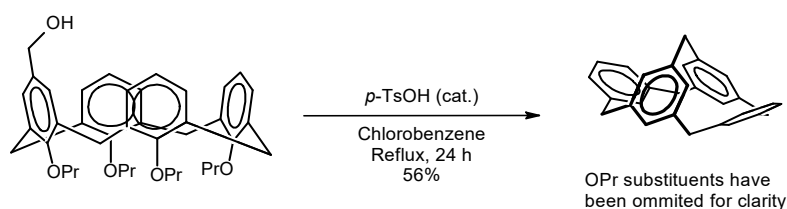
Scheme 1.15 Synthesis of distal methylene bridged calixarene.[88]

It is noteworthy from the preceding examples that it is possible to span across the wider rim of the calixarene with short bridges. This is possible because the calixarene in the cone conformation is not entirely rigid, despite the steric bulk of the four substituents on the narrower rim. In such a scenario, the cone calixarene oscillates between two pinched cone conformers, enabling the calixarene to adopt a highly-distorted, pinched cone conformation where the pair of distal aromatic rings involved in bridging are pinched close enough together to form the short bridge. The vibrational motion also allows the other pair of unbridged distal aromatic rings to be forced outwards from the cavity.

Seeing the potential utilisation of this phenomenon, Düker and co-workers have experimented with the synthesis of tetrathiafulvene bridges across the wider rim of calixarenes for the construction of redox-active molecular architectures.[89] Their aims were to attach the tetrathiafulvene bridges on the proximal or distal aromatic rings of a calixarene and their results are summarised in **Scheme 1.16**. Dual tetrathiafulvene bridges on proximal aromatic rings of the calixarene were synthesised in good yields, however bridging the tetrathiafulvene across distal aromatic rings was unsuccessful for calixarene derivatives in both the 1,3-alternate and cone conformations. The lack of success may be due to the conditions used as the bridging reactions were carried out at room temperature. Under these conditions, there may not be sufficient oscillation energy to bring the distal rings close enough to be bridged. Interestingly, when the propanitrile groups were relocated along the length of the tetrathiafulvene, the distal bridging was possible, although a calixarene dimer was also produced (**Scheme 1.17**). It is notable that the distal bridging was accomplished along the length of tetrathiafulvene, being a rigid, planar molecule of a fixed length. This may suggest that tetrathiafulvene is the same length as the diameter of the wider rim of a calixarene in the cone conformation.
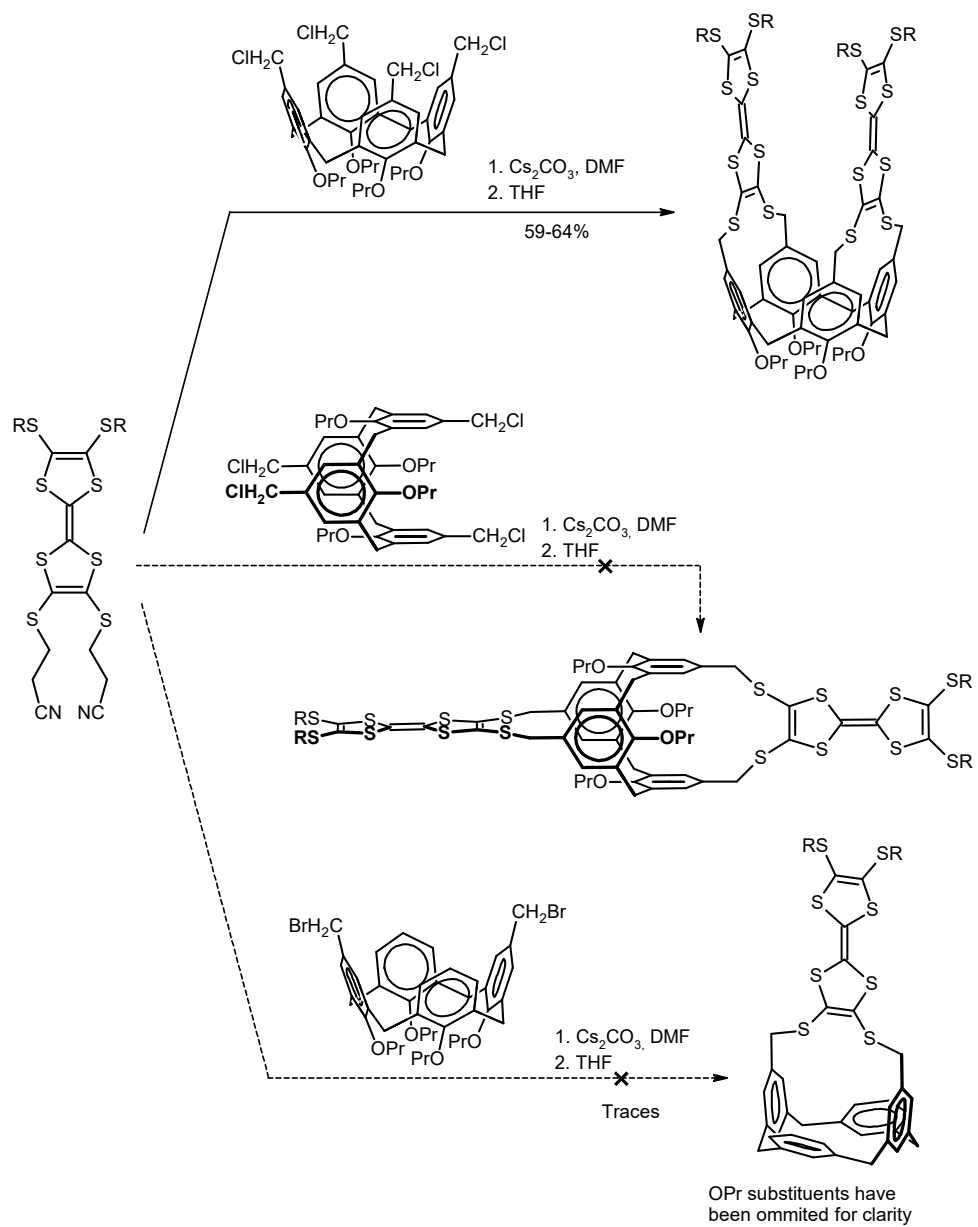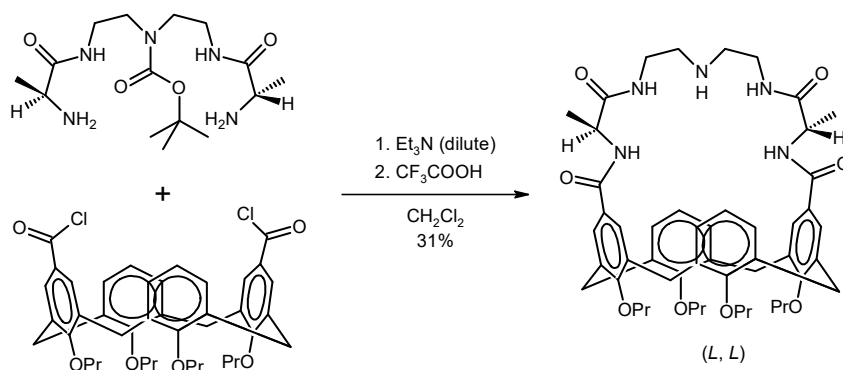
**Scheme 1.16** Synthesis of bridged calixarenes with tetrathiafulvene derivatives.[89]
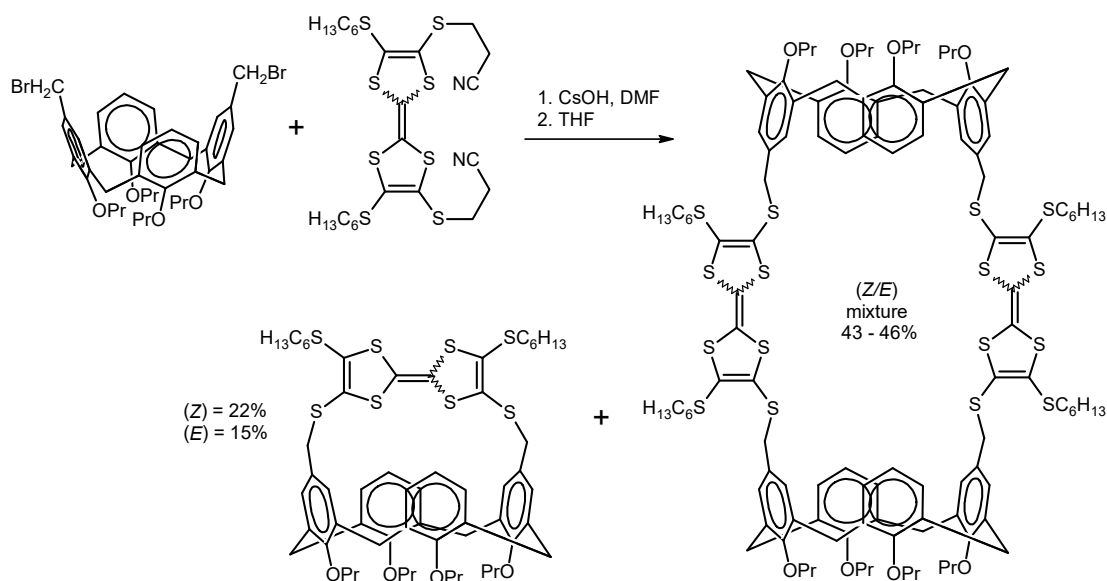
Scheme 1.17 Distal bridging of calixarene with tetrathiafulvene.[89]

The potential application of calixarenes to function as biomimetic receptors has led Casnati et al. to design distally-bridged calixarenes with peptide bridges. The aim was to use the hydrophobic cavity of the calixarene in conjunction with the hydrogen bonding of the peptide bridge to enable binding of guest molecules. Starting with a distally-functionalised diacid chloride calixarene, the cavity of the calixarene was bridged over by two alanine residues linked together by a nitrogen atom (**Scheme 1.18**).[90] The distally-bridged *N*-linked peptidocalixarene was shown to bind D-Ala-D-Ala (**Figure 1.12**), thus mimicking the mode of binding of the vancomycin group of antibiotics. Studies indicated that a proton transfer from the carboxylic acid group of the guest to the amino group of the calixarene pseudopeptide bridge generated a salt which was thought to be the key binding interaction, besides the hydrogen bonding between NH and CO groups. It was speculated that the hydrophobic calixarene cavity may have hosted the methyl group of the non-terminal alanine residue.[91]

Scheme 1.18 Synthesis of distally-bridged (L, L) peptidocalixarene.[90]
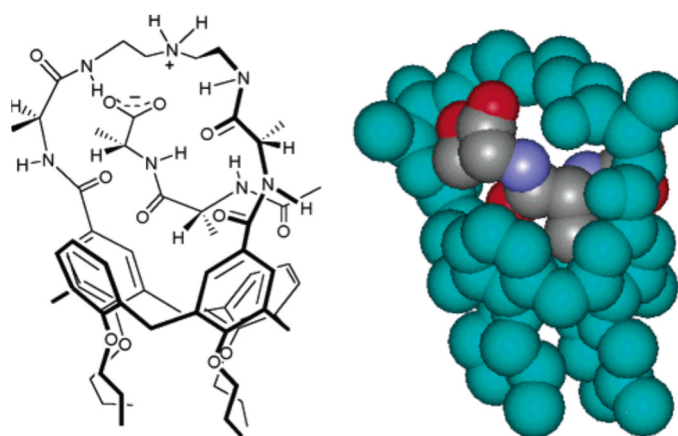
Figure 1.12   Distally-bridged peptidocalixarene mimics the mode of binding of vancomycin antibiotics by binding D-Ala-D-Ala by the suggested binding mechanism. Reprinted with permission from Casnati et al, *Acc. Chem. Res.* **2003**, *36* (4), 246-254. Copyright American Chemical Society 2003.[91]

However, some peptidocalixarenes are poor receptors due to intramolecular hydrogen bonding between amino acid residues within the molecule. This is caused by the peptidocalixarene being conformationally flexible. Therefore, to increase conformational rigidity, Sansone et al. have placed a rigid aromatic spacer between the two amino acid residues in a distally-bridged peptidocalixarene that adopted a pinched cone conformation (**Scheme 1.19**).[92] This peptidocalixarene was shown to bind anionic guests, having the best affinity for benzoate. From investigations, it appeared again that a proton transfer had occurred, and that the resultant carboxylate anion was electrostatically attracted to the amide protons of the bridge of the peptidocalixarene (**Figure 1.13**). π-π Stacking between the aromatic rings also appeared to contribute to the binding.[91]
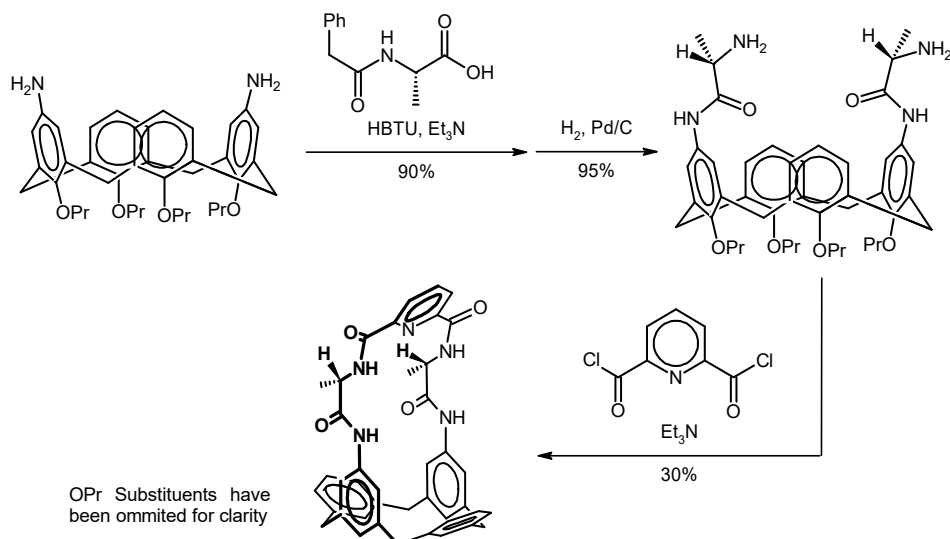
Scheme 1.19 Synthesis of distally-bridged peptidocalixarene linked with a rigid aromatic spacer.[92]
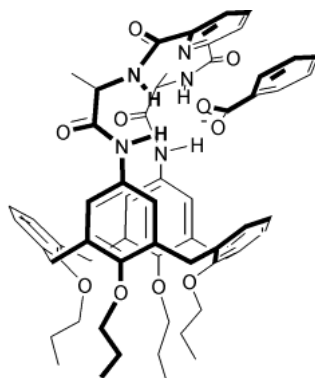
Figure 1.13 Proposed binding of benzoate by distally-bridged peptidocalixarene. Reprinted with permission from Casnati et al, *Acc. Chem. Res.* **2003**, *36* (4), 246-254. Copyright American Chemical Society 2003.[91]

Distal bridging of calixarenes has also been performed on resorcinarenes. An interesting example is the thiocrown resorcinarenes synthesised by Konishi et al. by the bridging of distal dibromoresorcinarene with 2-mercaptoethyl ether, propane-1,3-dithiol, and ethane-1,2-dithiol (**Scheme 1.20**).[93] The octahydroxy thiacrown resorcinarene product was reportedly difficult to purify, hence the conversion to octaacetates for characterisation. Despite the various bridge lengths, all the thiocrown resorcinarenes were determined to be in the pinched cone conformation, by analysis of the ^{1}H-NMR chemical shifts and molecular modelling. The bridging was also attempted with rigid dithiols such as 2,6-dimercaptomethylpyridine or *m*-xylylenedithiol, but to no success. The distal dibromoresorcinarene starting material was obtained by the careful, direct bromination of octahydroxyresorcinarene with

limited *N*-bromosuccinimide. Though this bromination reaction is simple, it was not completely selective for the distal product, since 9 % of the obtained product was proximal dibromoresorcinarene.[94]

OAc substituents have been ommited for clarity
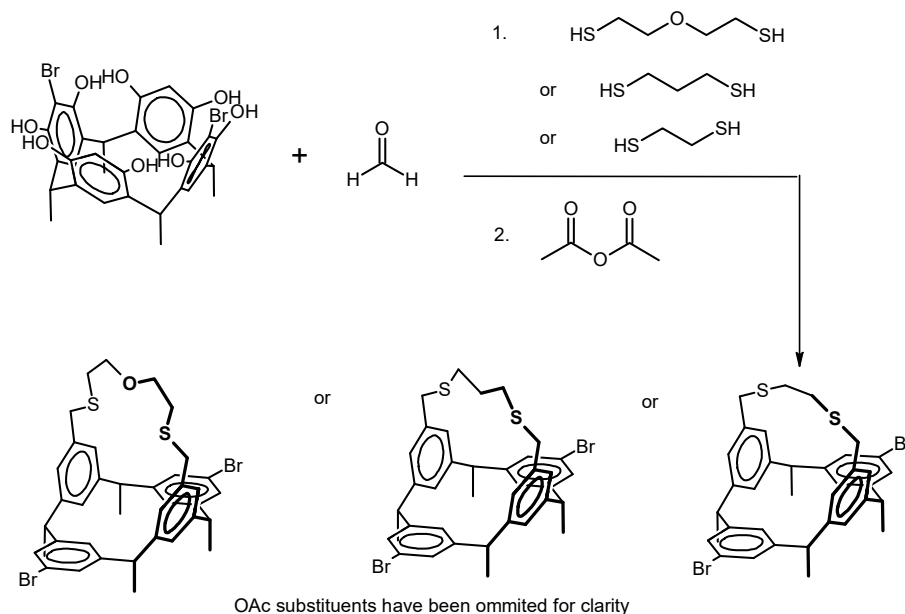
Scheme 1.20 Synthesis of distally-bridged thiacrown resorcinarenes with three bridges of varying length. OAc substituents have been omitted for clarity[93]

Shivanyuk et al. had developed a method for regioselectively obtaining the starting distal tetratosylate resorcinarene from the reaction of octahydroxyresorcinarene with triethylamine followed by four equivalents of tosyl chloride in dry acetonitrile (**Scheme 1.21**).[95, 96] Selectivity was likely to due to the observed precipitate which formed when the triethylamine was added to the resorcinarene. Addition of the sulfonylating agent to the precipitate needed to be performed quickly and followed by rapid stirring of the reaction mixture to avoid the formation of complicated mixtures.

R = *p*-toluene, 53%
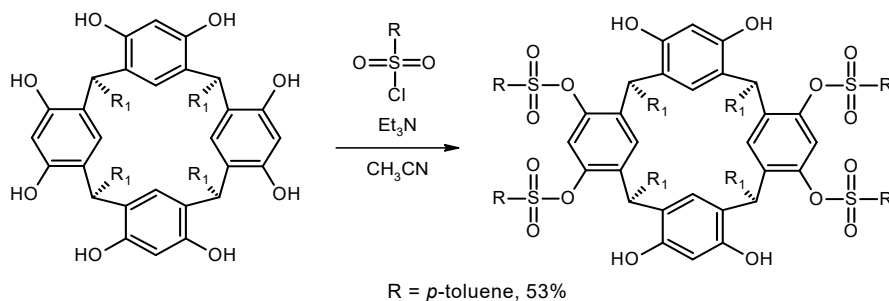
Scheme 1.21 Mechanism of selective distal tetrasulfonylation of octaphenol resorcinarene.[93, 94]

By this method, other distally-bridged resorcinarenes have been synthesized by Shivanyuk et al. who used aliphatic diamines to bridge distal tetratosylate resorcinarenes by the formation of benzoxazine linkages from a Mannich condensation with formaldehyde (**Scheme 1.22**).[97] The cavity of the crown ether-bridged resorcinarene was actually chiral due to the positions of the two benzoxazine linkages. However, no attempt was made to separate the enantiomers. The impact of a shorter bridge on the distal-bridging Mannich condensation was also investigated. Based on the conformation from the crystal structures of the previous chiral benzoxazine resorcinarenes, bridging should not be possible with shorter diamines. Contrary to expectation, the distal bridging was accomplished with ethylene diamine, but the shorter bridge forced the benzoxazine linkages to form on the phenols that were closer together, producing the other possible regioisomer which is not chiral. Both these distally-bridged resorcinarene regioisomers took on the boat conformation.
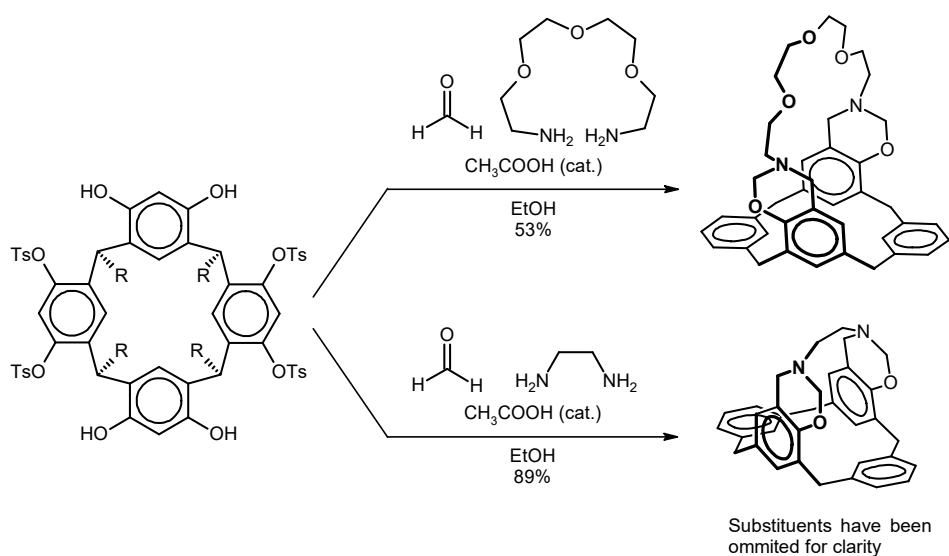
Scheme 1.22 Synthesis of axially-chiral distally-bridged tetratosylate resorcinarene via benzoxazine linkages. Substituents have been omitted for clarity.[97]
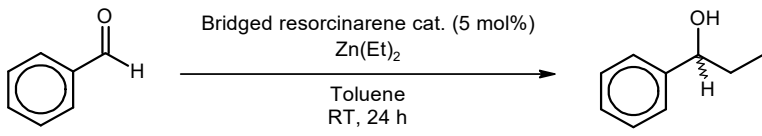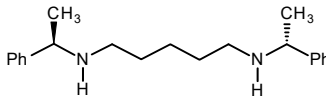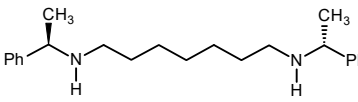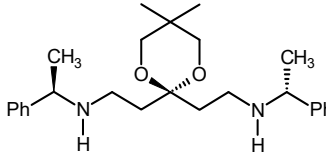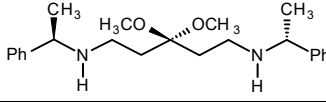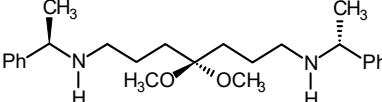
In similar work, the Mannich condensation was also used by Arnott et al. to distally-bridge tetratosylate resorcinarene with various diamines in good yields of 47-80% (**Scheme 1.23**).[98] Various derivatives of these distally-bridged resorcinarenes were then tested for potential to act as enantioselective asymmetric catalysts for the alkylation of benzaldehyde with dimethyl zinc (**Table 1.6**).[99, 100] Addition of functionality to the bridge, in the form of a dioxane and dimethoxy acetals, was explored for potential coordination to zinc. The different acetals caused a reversal in enantioselectivity. Modifications such as changing the tosylate to smaller mesylate

groups, or to ester groups resulted in a reversal of enantioselectivity as well. Lengthening, or functionalising the bridge with a dimethoxy acetal also reversed the enantioselectivity. These reversals of enantioselecitivity were indicative that the modifications were causing a significant change in conformation of the bridged resorcinarene. Moreover, it appears that the longer alkyl chains, despite being on the narrower rim, had an influence on the cavity, which resulted in the increased the enantioselectivity. In all tests, the ability of the bridged resorcinarene for enantioselective catalysis was limited to about 50% ee. Arnott et al. have suggested a hypothetic mechanism based on Noyori's model to explain this limitation.[100]
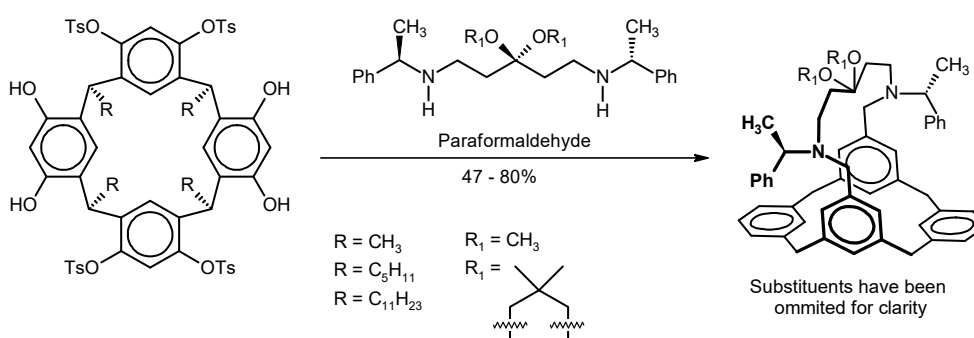
Scheme 1.23 Distal bridging of tetratosylate resorcinarene.[98]

Table 1.6 Studies into the potential enantioselective alkylation of benzaldehyde with diethylzinc in the presence of distally-bridged resorcinarene derivatives.[96, 97]

Bridge	R	Tetraphenol substituent	Yield	ee %	R/S
	CH$_3$	Toluenesulfonate	91	12	R
	C$_5$H$_{11}$	Toluenesulfonate	94	41	R
	C$_{11}$H$_{23}$	Toluenesulfonate	99	52	R
	CH$_3$	Methanesulfonate	84	5	S
	CH$_3$	Triisopropyl-benzenesulfonate	73	14	R
	CH$_3$	OAcetate	75	12	S
	CH$_3$	OToluene	79	20	S
	CH$_3$	Carbamazepine ester	99	49	S
	CH$_3$	Toluenesulfonate	41	19	S
	CH$_3$	Toluenesulfonate	85	34	R
	CH$_3$	Toluenesulfonate	85	51	S
	CH$_3$	Toluenesulfonate	3	21	S

In almost all the examples presented so far in this review, the distal-bridging of calixarenes at the wider rim has been accomplished on calixarenes that have already been distally functionalised. However, if bridging were to be performed on a non-distally-functionalised calixarene with four equally-reactive subunits, multiple bridged-calixarene products are possible. Reinhoudt and co-workers have demonstrated this with flexible crown ether bridges on a cavitand.[101] In this work, a cavitand with four equally-reactive phenol subunits was treated with 1.2 equivalents of pentaethyleneglycol ditosylate to give three differently-bridged crowncavitand

products (**Scheme 1.24**). The bridging reaction was performed with various solvents and bases, and the yields of each crowncavitand are shown in Table 1.7. It is evident that the proximally-bridged crowncavitand can be selectively produced in 33% yield, but with a significant amount of unreacted starting cavitand. The distally-bridged crowncavitand could only be obtained in trace yields of 2-3 % as part of a mixture of all three crowncavitands products. This example with a cavitand suggests that directly bridging a resorcinarene containing four equally-reactive subunits, with a flexible bridge, would produce either a proximally-bridged calixarene, or a mixture of bridged calixarene products.
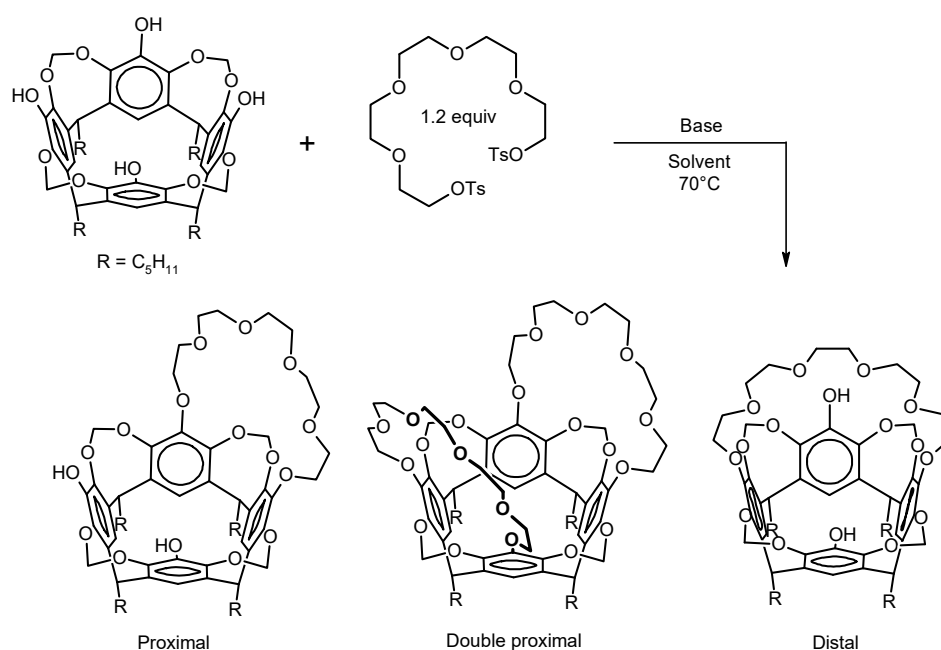
Scheme 1.24 Bridging of tetrol cavitand with pentaethyleneglycol ditosylate to form three different crowncavitand products.[101]

Table 1.7   Reaction with various solvents and bases, and the yields of each crowncavitand product.

Solvent	Base	Yield (%)			
		Starting cavitand	Proximal	Double proximal	Distal
DMF	NaH	21	33	0	0
DMF	Na$_2$CO$_3$	22	18	0	0
DMF	K$_2$CO$_3$	22	2	8	2
DMF	Cs$_2$CO$_3$	40	2	10	2
CH$_3$CN	NaH	3	13	0	3

Bridging calixarenes on the wider rim with crown ethers has also been explored by Nissinen and co-workers in their synthesis of tetramethoxyresorcinarene crown ethers.[102] Tetramethoxyresorcinarene was treated with caesium carbonate base for 15 minutes, followed by 2 equivalents of the tetraethylene glycol ditosylate to produce proximally-bridged bis-crown tetramethoxyresorcinarene in 31 % yield (**Scheme 1.25**). When the deprotonation time with caesium carbonate was extended to 60 minutes, the bis-crown tetramethoxyresorcinarene was produced in 10% yield along with the proximally-bridged mono-crown by-product in 13% yield.[103] Both the mono-crown and this bis-crown tetramethoxyresorcinarenes adopted the boat conformation. The bis-crown tetramethoxyresorcinarene was shown to bind potassium, rubidium, caesium, and silver ions.[104-106] The binding of silver ions was reversible, and was utilised to deliver silver ions to bacteria resulting in cell death and an anti-bacterial effect.[105] The mono-crown tetramethoxyresorcinarene, having a larger cavity, was not able to bind alkali metal cations. Nevertheless, the mono-crown was an optimal host for an acetylcholine (neurotransmitter) guest, binding through interactions between the crown ether with the ammonium portion, as well as hydrogen bonding between the two phenols with the acetate group of the guest. The distal mono-crown tetramethoxy-resorcinarene was not reported, signalling a tendency for flexible bridges to form on proximal aromatic rings of a calixarene with equally-reactive subunits.
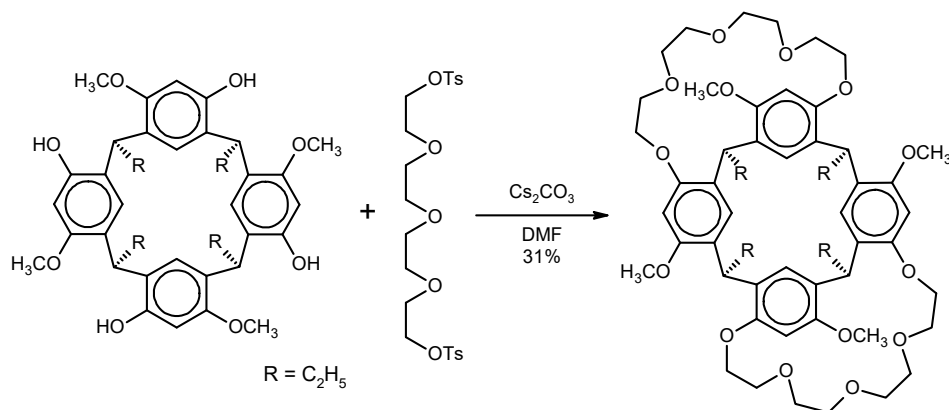
Scheme 1.25 Synthesis of proximally-bridged crown ether tetramethoxyresorcinarenes.[102]

1.4   Outlook and research objectives

Calixarenes have been well studied and have proven to be suitable for industrial applications. However, axially-chiral calixarenes and resorcinarenes in particular, despite having potential for enantiorecognition, remain relatively unexplored. Although multiple methods for distally-bridging calixarenes and resorcinarenes exist in the literature, these methods are not applicable to the entire range of diverse calixarene derivatives. Furthermore, achieving selective distal bridging can be challenging, and the aforementioned example has shown that this is particularly true for the tetramethoxyresorcinarene – proximal bridging seems to be favoured. **Scheme 1.26** outlines the three main strategies for achieving distal-bridging of the tetramethoxyresorcinarene. In particular, a distally-functionalised resorcinarene would serve as a key intermediate that would enable the distal-bridging to proceed smoothly.
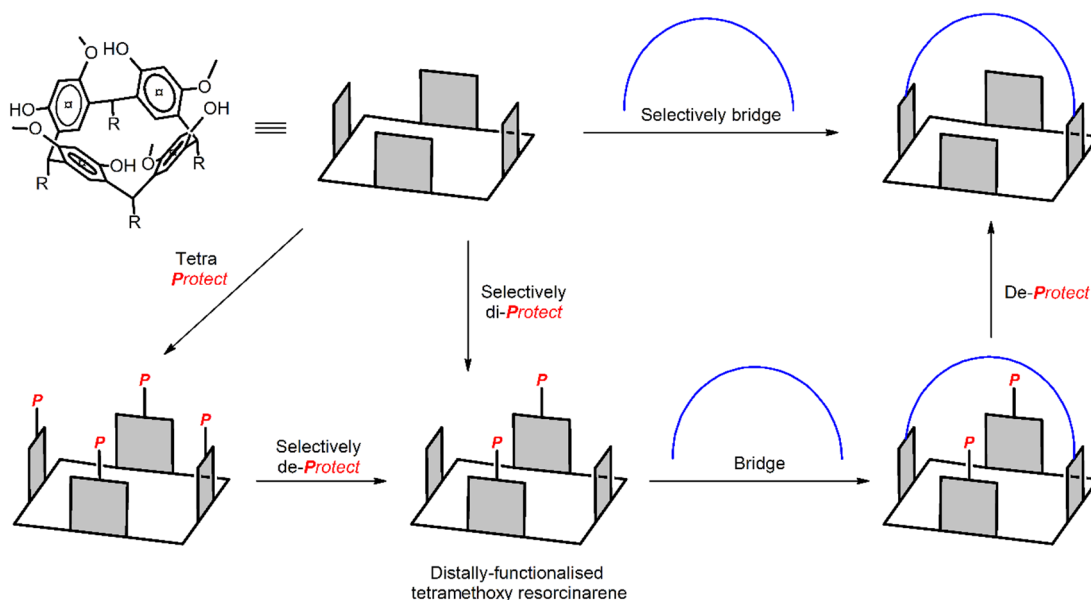
Scheme 1.26 The three main routes to achieving distal-bridging of tetramethoxyresorcinarene.

The synthesis of this key intermediate was explored in preliminary work involving multiple strategies.[107] A selective deprotection approach was investigated by partial hydrolysis of tetramethanesulfonate- and tetrabenzoate- derivatives of the tetramethoxyresorcinarene using 2 equivalents of sodium hydroxide (**Scheme 1.27**). However, the hydrolysis reactions delivered the partially-hydrolysed products in a non-selective manner.
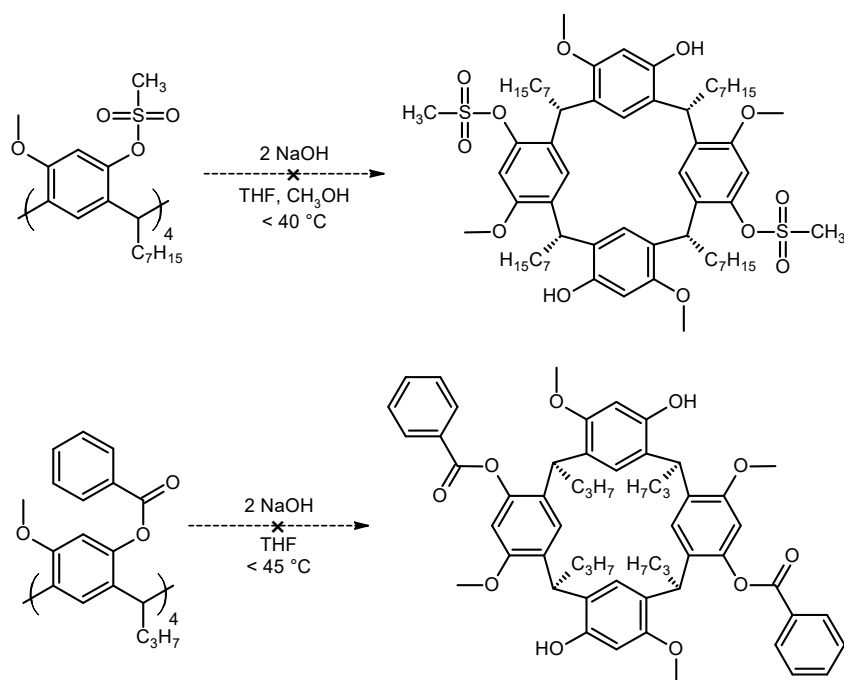
Scheme 1.27 Attempted distal functionalisation of tetramethoxyresorcinarene by selective hydrolysis.

The selective deprotection was also attempted on the tetrabenzoate resorcinarene using DIBAL, a sterically bulky reducing agent (**Scheme 1.28**). In these reactions, 4 to 22 equivalents of DIBAL were used, producing asymmetrical resorcinarenes without the target C_2-symmetrical distally-functionalised resorcinarene.
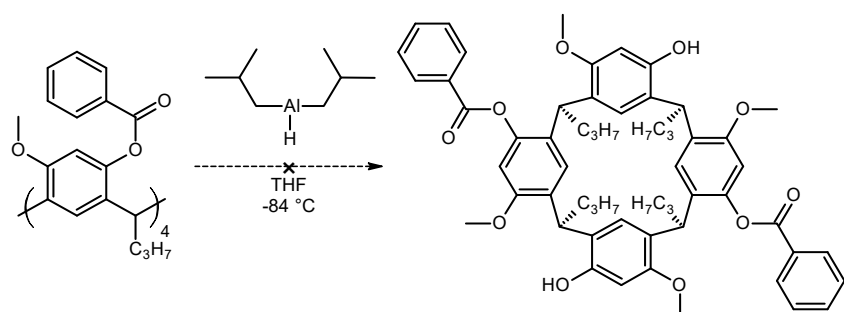

Scheme 1.28 Attempted distal functionalisation of tetramethoxyresorcinarene by selective reduction.

Other than selective deprotection, another approach investigated in this preliminary work was distal functionalisation by selective bromine-lithium exchange, as reported for calixarenes[84] and cavitands.[108-110] A prerequisite to this approach is the bromination of the *ortho* position of the tetramethoxyresorcinarene. However, direct bromination with *N*-bromosuccinimide (NBS) or bromine, respectively gave a mixture of incompletely brominated or unknown products (**Scheme 1.29**).

44
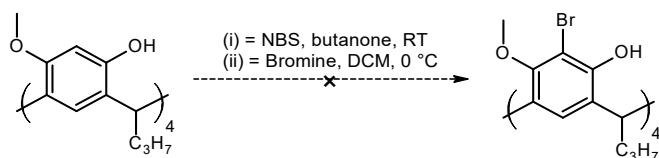
Scheme 1.29 Attempted bromination of tetramethoxyresorcinarene.

The bromination was also attempted on a *O*-protected tetramethoxyresorcinarene via lithiation with butyllithium then quenching with NBS (**Scheme 1.30**) in a similar procedure to the literature.[111] However, the reaction produced a complex mixture. ^{1}H NMR spectroscopy of D_2O quenching studies indicated that the butyllithium was causing decomposition of the protecting group as well as the resorcinarene.
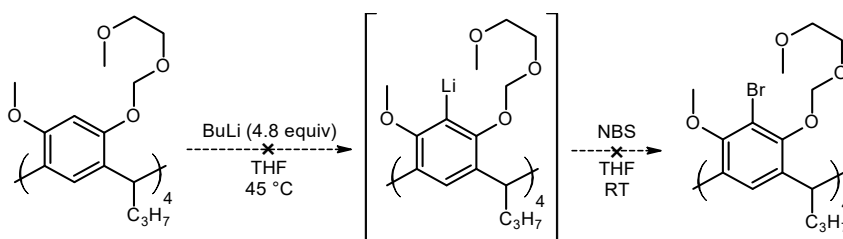
Scheme 1.30 Attempted bromination of *O*-protected tetramethoxyresorcinarene.

From these preliminary investigations, the uniqueness of the tetramethoxy-resorcinarene has been realised. It seems that the synthesis of a distally-functionalised tetramethoxyresorcinarene requires a new procedure that is unknown to the literature.

Therefore, the objective of this project is to continue the development of the practical synthesis of a distally-functionalised tetramethoxyresorcinarene, with the aim of distal-bridging. Crown ethers would be appropriate candidates for the bridge, due to their well-known ability to act as hydrogen-bond acceptors, and their availability in various lengths. If successful, the distally-bridged crown resorcinarene can then be investigated as a potential enantioselective membrane carrier for the chiral resolution of certain racemic drugs.

2 Distal functionalisation of resorcinarene by a calixarene rigid bridge

A method to achieve direct distal-functionalisation of the tetramethoxyresorcinarene is through attachment of a rigid bridge of the appropriate length. This would be a molecule which is rigid and has exactly the same length as the diameter of the resorcinarene wider rim. The idea is that such a rigid bridge would directly attach to the resorcinarene at the distal positions, with the rigidity and length of the bridge being key to giving distal selectivity. This idea is illustrated in **Scheme 2.1** where the tetramethoxyresorcinarene has been simplified into four grey squares which represent the four equally-reactive aromatic ring subunits (A in **Scheme 2.1**). In principle, direct attachment of the rigid bridge to the resorcinarene would give intermediate (B) where one end of the rigid bridge has attached to the resorcinarene. The other end of the rigid bridge would be spatially prevented from approaching proximal positions, unlike flexible bridges[102, 103] or the standard protecting groups.[107] Thus, the attachment of the other end of the rigid bridge should occur at the distal position of the resorcinarene, leading to selective formation of product (C). The remaining two aromatic rings of product (C) could be protected to give product (D), then the rigid bridge could be cleaved, like a protecting group, to give product (E) which would be the key intermediate of a distally-functionalised resorcinarene. As discussed in **Scheme 1.26**, a distally-functionalised resorcinarene is a key intermediate because it would be able to accept any bridge to furnish the desired distally-bridged resorcinarene, product (F).
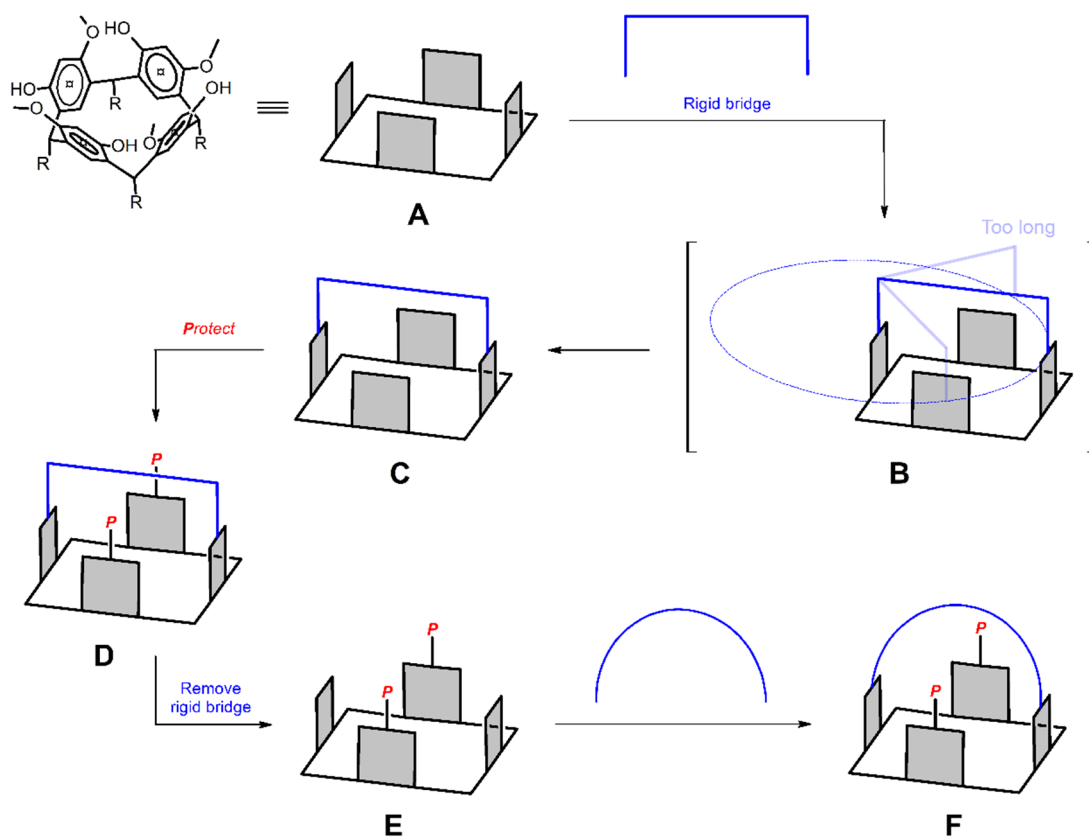
Scheme 2.1 Illustration of the distal bridging of tetramethoxyresorcinarene by a rigid bridge.

The preceeding examples, by Zheng et al. (**Scheme 1.7**) and Düker et al. (**Scheme 1.16** and **Scheme 1.17**) show that the length of the bridge affects the proportion of the variously-bridged calixarene products. Therefore, the ideal rigid bridge needs to be a molecule that is of the same length as the wider rim of the resorcinarene. A molecule that has the same dimensions as the resorcinarene would be another calixarene in the cone conformation. There are multiple methods documented in the literature for distally-functionalising calixarenes.[112] For these reasons, a distally-functionalised calixarene would ideally serve as the rigid bridge for the resorcinarene. Furthermore, though the rigid bridge idea is novel for distally-functionalising a calixarene, the feasibility of the calixarene rigid bridge idea has been demonstrated in the literature by the formation of hemicarcerands. Hemicarcerands were first synthesised by Cram and co-workers by linking two calixarenes together at the wider rim to give a cage-like calixarene dimer (hence the carcerand naming, to incarcerate).[113-121] **Scheme 2.2** provides a few examples of the synthesis of carcerands and hemicarcerands in the literature. A di-imine linkage between the two bowls is proposed, because examples in the literature have shown that the formation of hemicarcerands by di-imine linkages is high-yielding and reversible, preventing the formation of oligomeric bridging by-

47

products.[113, 114] Moreover, imine linkages can be cleaved by hydrolysis, enabling the calixarene rigid bridge to be removed. These examples in the literature with calixarenes, should be applicable to the tetramethoxyresorcinarene since it has the same macrocyclic calixarene skeleton.
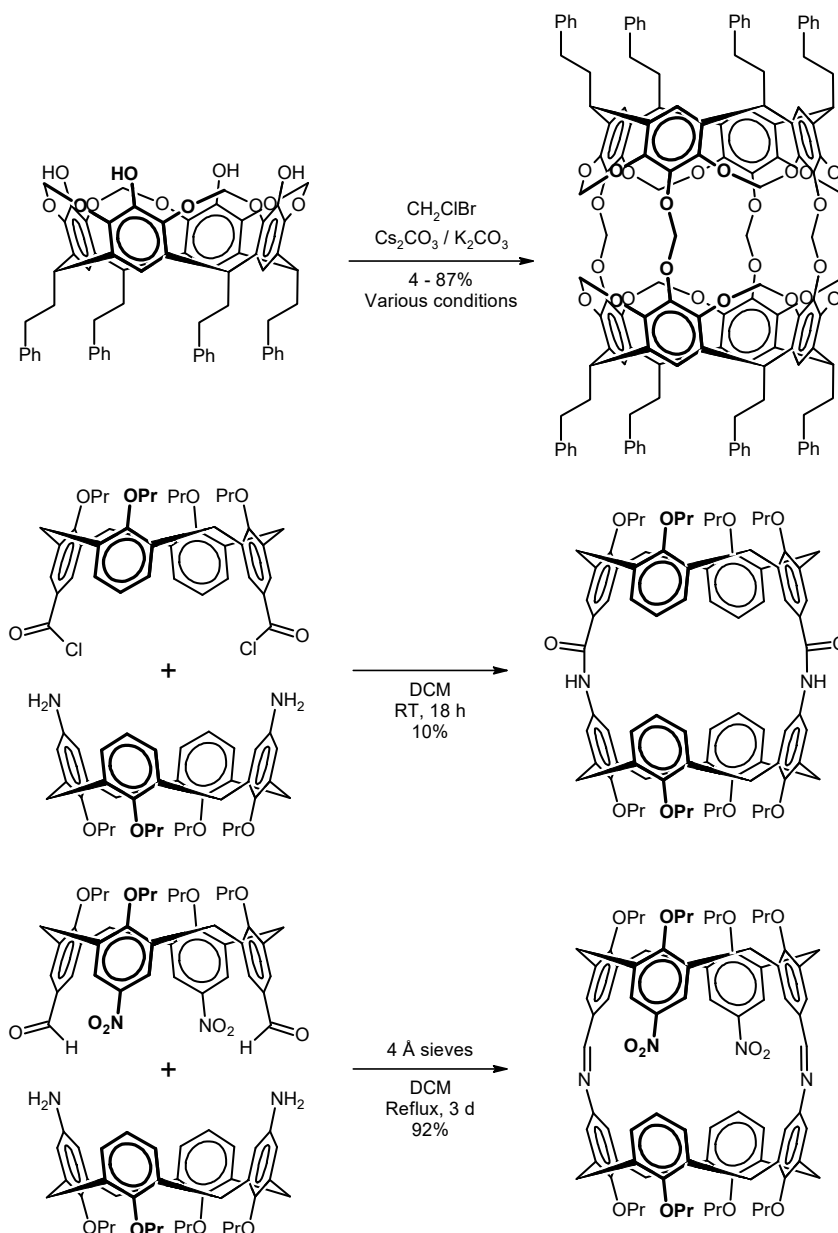
Scheme 2.2 Examples of the synthesis of carcerands / hemicarcerands in the literature.[113, 118, 119, 122]

To experimentally prepare for this strategy, amine or aldehyde groups first need to be installed onto the tetramethoxyresorcinarene, as well as the respective calixarene (**Scheme 2.3**). The wider rim of the tetramethoxyresorcinarene has potentially two positions for functionalisation – the phenol and the *ortho* carbon of the aromatic ring. The amine and aldehyde groups should ideally be directly installed onto the bowls,

with minimal or no spacer atoms in between, to maintain the dimensions of the bowls for the selective distal coupling.
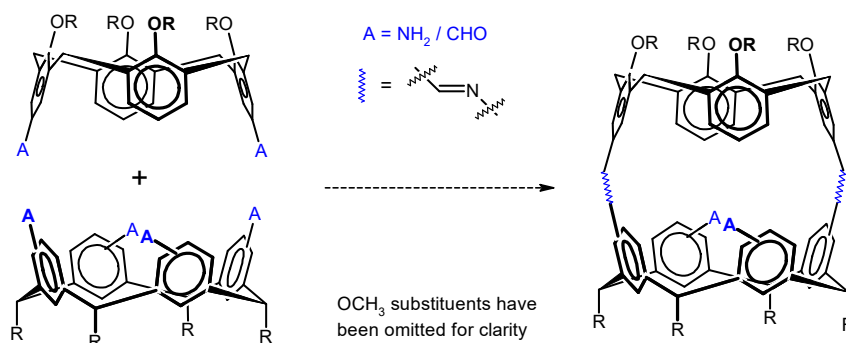
Scheme 2.3   Amine and aldehyde resorcinarene and calixarene starting materials required for the rigid bridge strategy.

The functionalisation of the tetramethoxyresorcinarene is detailed in the first two sections: **Section 2.1** describes functionalisation at the *ortho* position, while **Section 2.2** describes the functionalisation of the phenolic position. The synthesis of a relevant calixarene rigid bridge, and the investigations into its coupling to the tetramethoxyresorcinarene is covered in **Sections 2.3** and **2.4**.

2.1   Functionalisation of the ortho position of the resorcinarene

The most direct method to install amines and aldehydes onto the resorcinarene is by electrophilic aromatic substitution on the activated aromatic carbon that is *ortho* to the phenol and methoxy groups. In principle, this can be achieved by nitration of tetramethoxyresorcinarene **(1)** followed by reduction of the nitro group to give the amine, or by direct formylation to give the aldehyde (**Scheme 2.4**).
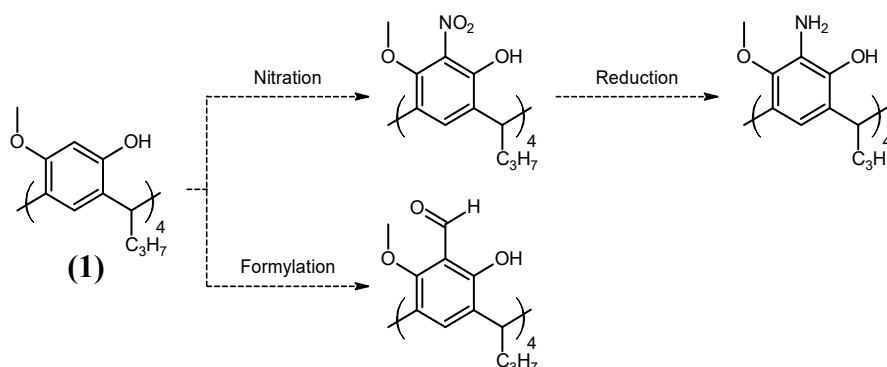
Scheme 2.4   Possible installation of nitro or aldehyde groups on the *ortho* position of resorcinarene **(1)**.

2.1.1 Nitration

The nitration of calixarenes has been well-documented in the literature.[127, 135-137] However, the nitration of resorcinarenes has been scarcely reported, which is rather surprising for a theoretically simple reaction. The tetranitro octahydroxyresorcinarene has been reported in the literature, but was synthesised from pre-nitrated resorcinol subunits, rather than by nitration of the resorcinarene macrocycle.[123-125] Tetramethoxy-resorcinarene should be readily nitrated at the *ortho* position, since it is activated for electrophilic aromatic substitution by the electron-donating hydroxy and methoxy groups. Therefore, the nitration of the starting resorcinarene **(1)** was investigated, first with concentrated nitric acid and glacial acetic acid, with dichloromethane as the solvent (**Scheme 2.5**). With the nitrating agent in vast excess (75-100 eq), the reaction was conducted at various conditions from 0°C to room temperature, and from 40 minutes to 6 hours, but the outcome of these experiments yielded essentially the same complex mixture apparent by TLC and ^{1}H NMR spectroscopy. In the ^{1}H NMR spectra of these reactions, the group of peaks at 6.5 and 8 ppm, representing the two aromatic protons, were consistently integrating in a 1:1 ratio, which was a clear indicator that the substitution of one of the aromatic protons was not occurring at all. Furthermore, the appearance of peaks at 11 ppm were likely indicators of the presence of phenols hydrogen-bonded to nitro groups, but the appearance of apparent doublet of doublets around 6.1 ppm was unexpected and puzzling.
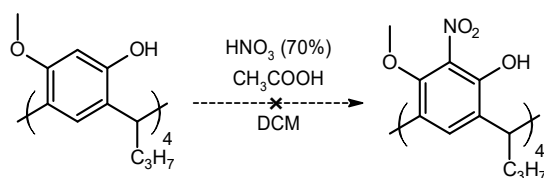
Scheme 2.5   Investigation into the nitration of the *ortho* position of resorcinarene **(1)**.

The nitration was also conducted at milder conditions using nitric acid on silica,[126] but the outcome appeared to be essentially the same. After subjecting some of the crude mixture to column chromatography, one of the products was isolated. The chromatographed product was recrystallised from chloroform-MeOH to form slightly-yellow crystals. The ^{1}H NMR spectrum of the recrystallised product, shown in **Figure 2.1**, indicated it to be a pure material, with peaks reminiscent of a C$_4$-symmetrical resorcinarene. However, the absence of the benzylic triplet around 4.3 ppm, and the appearance of a triplet at 2.9 ppm was the main inconsistency with a resorcinarene.

50
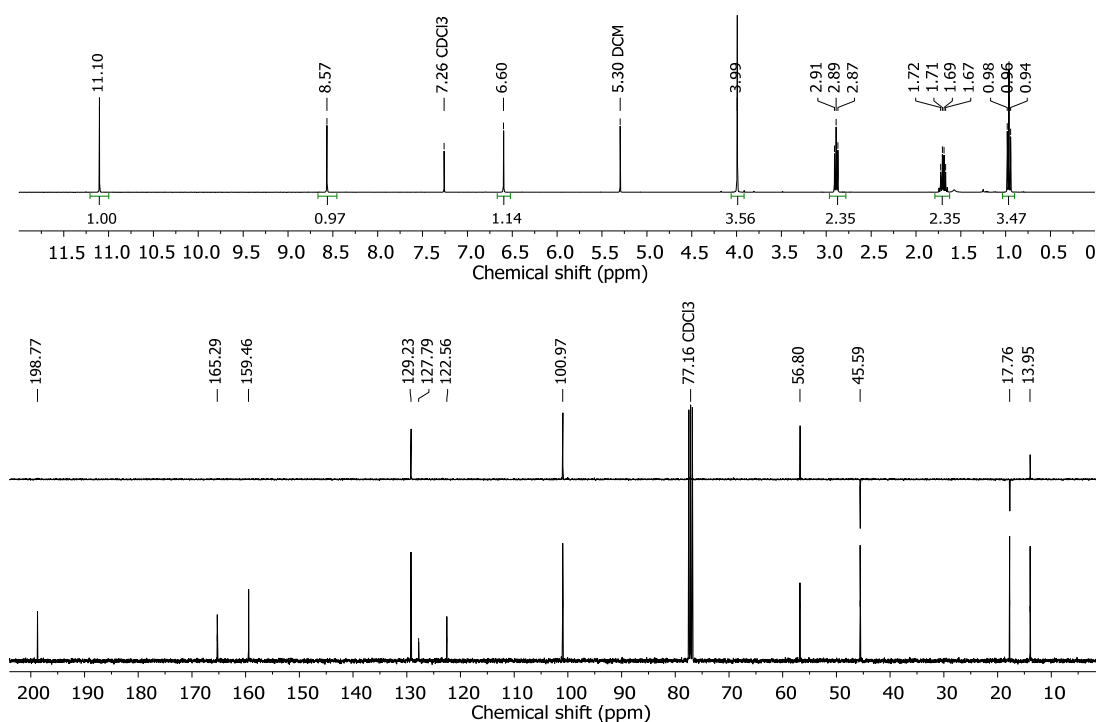
Figure 2.1　NMR spectra of the unknown resorcinarene nitration product recorded in CDCl₃: ¹H spectrum (top), DEPT-135 and ¹³C spectra (bottom).

Other notable differences in the ¹H NMR spectrum was the appearance of a peak at 11.1 ppm, and the downfield shift of one of the aromatic peaks to 8.6 ppm, both of which may suggest the presence of a hydrogen-bonded phenol and a nitro group. The absence of the benzylic methine was also evident on the ¹³C NMR and DEPT-135 spectra which recorded no CH peak around the usual 33 ppm. The appearance of a peak at 199 ppm indicated the presence of a carbonyl group. The IR spectrum confirmed the presence of a hydroxy group, however no characteristic carbonyl peak was recorded around 1700 cm⁻¹. Perhaps the carbonyl was in conjugation with the aromatic ring, and has overlapped with C=C peaks around 1600 cm⁻¹. Based on the NMR and IR data, two isomeric structures (**Figure 2.2**) for the unknown product were proposed. Further evidence supporting the proposed product was provided by HRMS which recorded a main peak corresponding to its mass. A search of the literature shows that these are not known compounds.
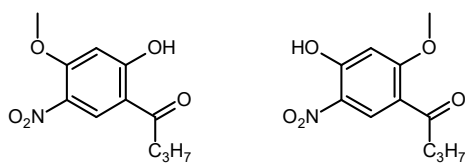
Figure 2.2　Proposed structures for the unknown resorcinarene nitration product.

51

This theoretically-simple nitration of an activated aromatic ring has yielded some unexpected and confusing results. Hence a more thorough search of the literature was performed. A search of the literature for "resorcinarene nitration" yielded only one match which appears to confirm the suspicion that the nitration of resorcinarenes is in fact a far more difficult and complex process than one would expect. In this literature work, Botta and co-workers were investigating the complexation of highly-reactive NO$^+$ in the cavities of resorcinarenes.[127] It was discovered that when a greater excess of NO$^+$ was used, the resorcinarene unexpectedly reacted to form two new products. These products were fully characterised and were revealed to be products from the ring-opening of the resorcinarene macrocycle caused by the insertion of a nitro group on one of the aromatic rings (**Scheme 2.6**). Simulation by computational methods provided substantial evidence that these products were formed by an *ipso* electrophilic addition of NO$^+$ on the resorcinarene macrocycle, which was catalysed by another complexed NO$^+$.
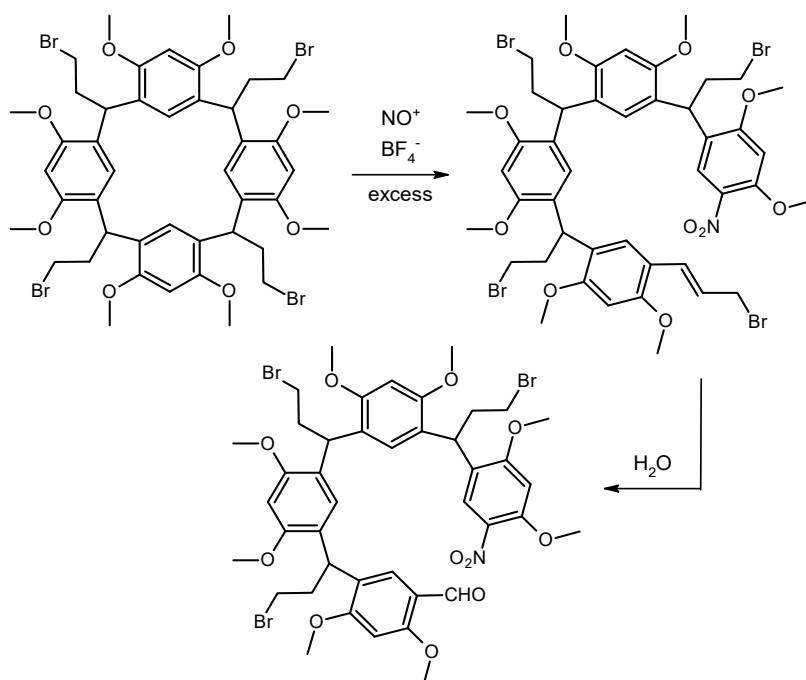
Scheme 2.6 Unexpected ring-opening of the resorcinarene macrocycle via *ipso* electrophilic attack by NO$^+$.[127]

Therefore, the results obtained from the nitration of tetramethoxyresorcinarene seem to confirm the work by Botta and co-workers. Both of the proposed isomers in **Figure 2.2** could possibly be formed by a similar mechanism as proposed by them, where the resorcinarene macrocycle could open and fragment through *ipso* electrophilic addition

by NO_2^+ (**Scheme 2.7**). The resultant benzylic alcohol could become oxidised by the nitric acid to give a ketone conjugated with the aromatic ring.

Further investigation is required to develop these preliminary results into a more conclusive outcome of the nitration of tetramethoxyresorcinarene. The nitration reaction needs to be repeated, followed by careful chromatographic separation of the products. The isolated products would need to be fully characterised, with a crystal structure being ideal. However, regarding the investigation into the direct functionalisation of the resorcinarene *ortho* position, there is much evidence to show that this nitration reaction has delivered a completely different outcome than desired. Therefore, regarding this investigation, the direct nitration of the resorcinarene was abandoned.
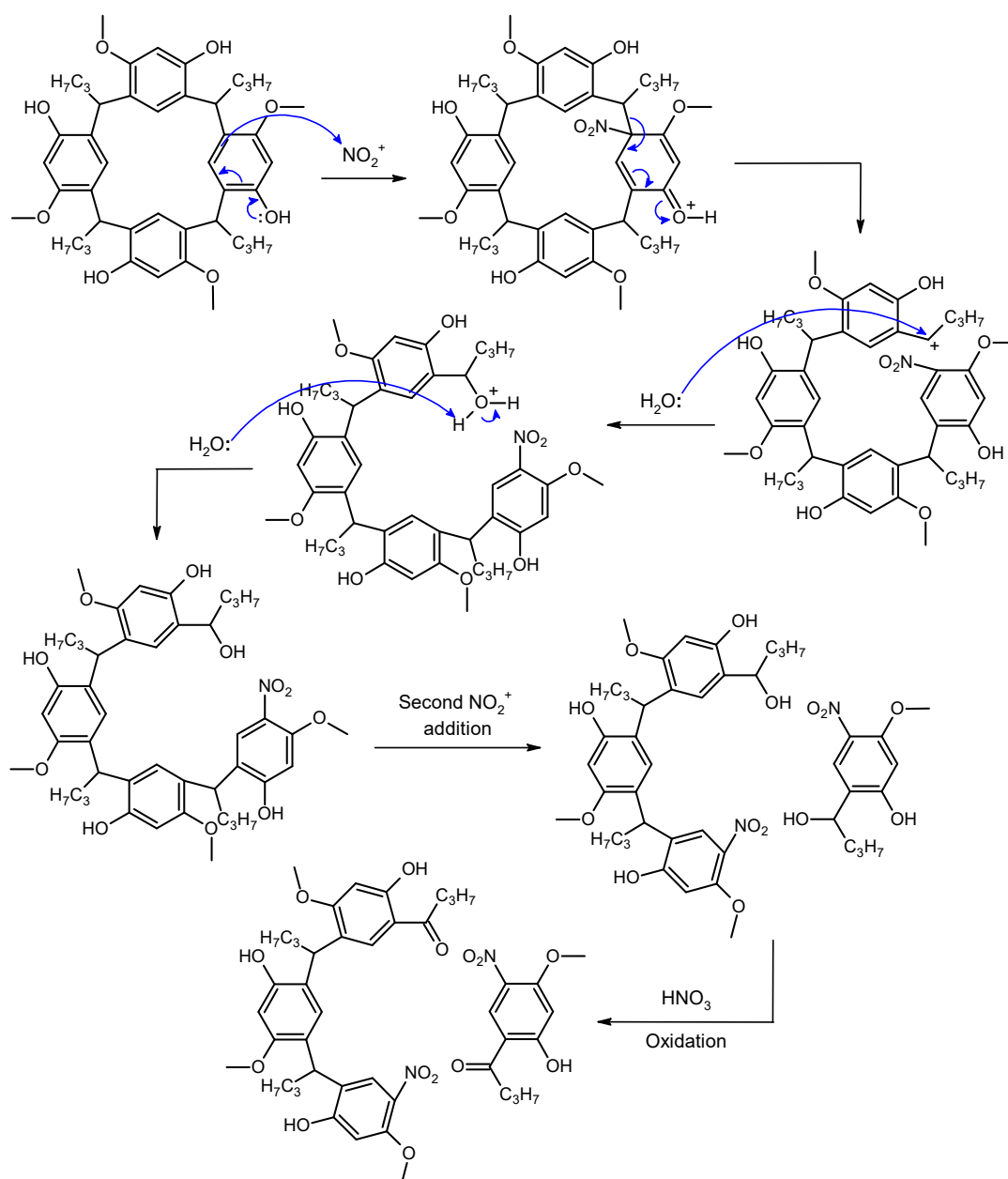
Scheme 2.7 Proposed mechanism for the ring-opening of the resorcinarene **(1)** macrocycle by *ipso* nitration.

2.1.2 Attempted synthesis of *ortho*-formylated resorcinarene

2.1.3 Rieche formylation

The next part of the investigation focuses on installing aldehyde groups on the *ortho* position of the tetramethoxyresorcinarene. Di-*O*-alkylated calixarenes have been conveniently formylated in high yields through the Rieche formylation which involves the generation of an electrophile from the activation of 1,1-dichloromethyl methyl ether with tin(IV) chloride.[69, 128] Under these conditions, only the two non-*O*-alkylated aromatic rings of the calixarene were formylated. Nevertheless, tetra *O*-alkylated calixarenes have been formylated by a similar procedure, albeit in a lower yield.[80]

These examples indicate that the Rieche formylation is more successful on calixarenes with aromatic rings activated with a hydroxy substituent. According to this rationale, tetramethoxyresorcinarene **(1)**, should readily undergo formylation at the *ortho* position since it is activated by both hydroxy and methoxy substituents.
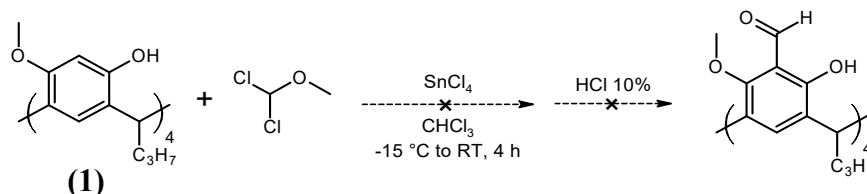
Scheme 2.8 Attempted formylation of tetramethoxyresorcinarene under Rieche conditions.

Tetramethoxyresorcinarene **(1)** was reacted under Rieche formylation conditions (**Scheme 2.8**), as per the literature, to give a brown-black crude product which had a ^{1}H NMR spectrum showing the resorcinarene signals as broad humps. A hydrogen-bonded phenol was clearly visible as a single peak at 11.38 ppm; this was confirmed by its disappearance upon addition of D$_2$O. A broad group of signals at 10.25 ppm were indicative of the presence of the formyl group. This may suggest that the formylation of the resorcinarene had proceeded, but not to completion. However, the broad humps of resorcinarene signals together with the black colour of the crude product suggests some decomposition of the resorcinarene may have occurred. Moreover, the TLC was a complete streak, thus preventing any chromatographic separation. In face of these results, it was decided to focus efforts on a different formylation method.

2.1.4 Duff formylation

The other method in the literature for the formylation of calixarenes is by the Duff formylation. By this method, calixarenes[129] as well as resorcinarenes[130] have been formylated. The Duff fomylation of octahydroxyresorcinarene was accomplished in 48% yield by Szumna and co-workers using hexamethylenetetramine in trifluoroacetic acid via microwave irradiation.[130]
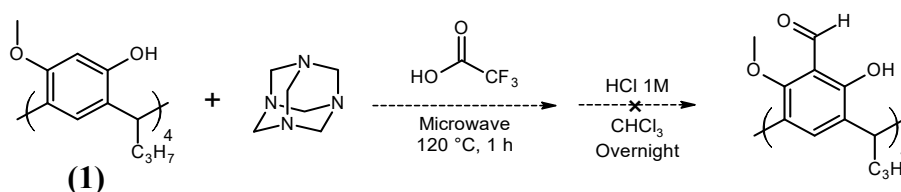
Scheme 2.9 Attempted formylation of tetramethoxyresorcinarene under Duff conditions.

Reaction of tetramethoxyresorcinarene (1) under the same conditions (Scheme 2.9) as described by Szumna and co-workers,[130] gave a crude product of mass that was double the theoretical yield, and appeared to be a complex mixture by ^{1}H NMR spectroscopy. The TLC of the crude mixture, though slightly streaked, indicated absence of the starting resorcinarene (1), and two major product spots at higher R_f, other than baseline material. In preparation for chromatography, the baseline material was removed by filtering the crude product through a plug of silica. However, in this process, 70% of the mass was lost. Nevertheless, TLC confirmed the presence of the two remaining product spots, with most of the baseline material being removed. To isolate the two product spots, a portion of the remaining material after the silica plug was subjected to preparative TLC. The preparative TLC was highly streaked when visualised under UV, but under ambient light, three yellow bands were apparent. These were collected as separate fractions, but totalled to only 16% of the original mass that was applied to the preparative TLC. TLC of the fractions indicated that co-elution had persisted through each fraction. It seems that the chromatographic separation on the TLC did not carry through to the preparative TLC. This result, together with the low mass recovery may be due to decomposition of the material on the silica. The partially-separated compounds were analysed by ^{1}H NMR spectroscopy and showed multiple aldehyde signals for all products. The signals around 6.4 ppm associated with the *ortho* aromatic proton had a relatively lower integration compared to the signals of the other aromatic proton. This again may suggest that the formylation was occurring but not proceeding to completion. Given the unpromising results, particularly the suspected decomposition of the products on silica, it was decided to abandon the resorcinarene formylation. In their brief review of resorcinarene formaylation, Szumna and co-workers noted many unsuccessful attempts by other research groups to formylate resorcinarenes, observing that formylations of macrocyclic scaffolds are theoretically simple, but practically difficult.[130]

2.1.5 Mannich

Since direct installation of nitro and aldehyde groups onto the *ortho* position of resorcinarene (1) has been rather unsuccessful, the reported[131] functionalisation of this position with a Mannich base may provide an alternative strategy. A Mannich base on the *ortho* position of the resorcinarene could be quarternised into the amine salt, then substituted with an appropriate nucleophile by S_N2 substitution (Scheme 2.10).

Gutsche et al. has reported success with this idea with tetrahydroxycalixarenes, having substituted the dimethylamino group with various nucleophiles including azides and nitriles.[132] If this were applicable for tetramethoxyresorcinarene (1), then it would provide access to an amine or aldehyde group at the *ortho* position via full or partial reduction of the azide or nitrile.
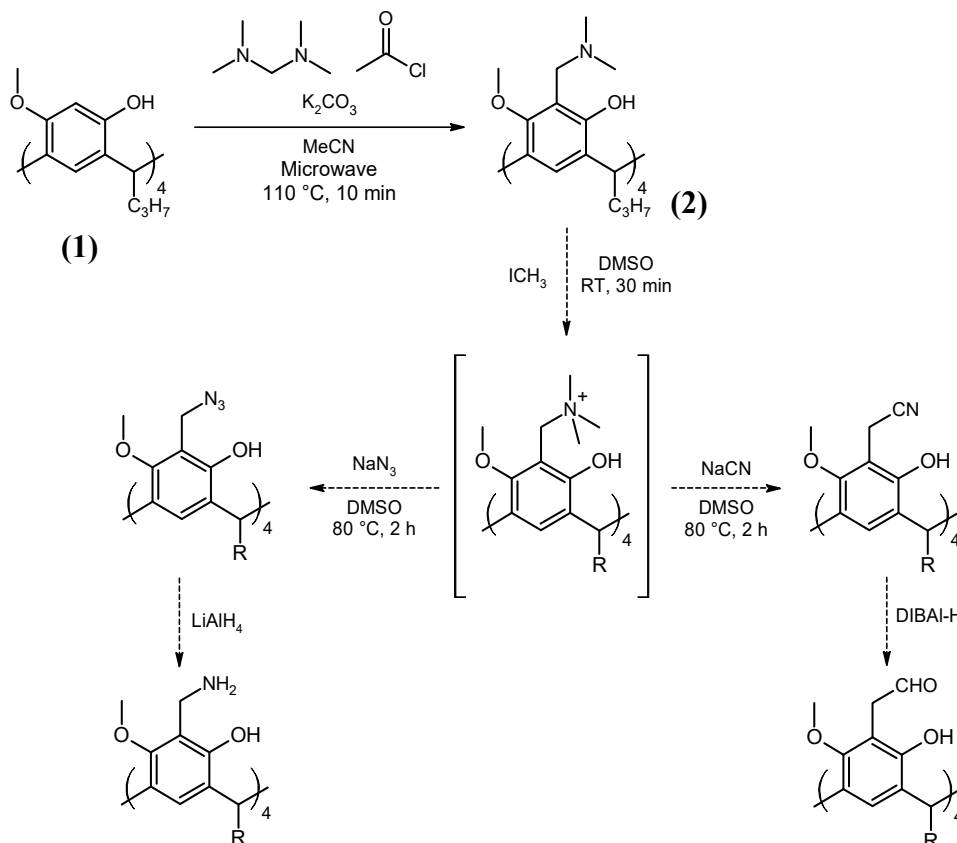
Scheme 2.10 Potential strategy for installing amines or aldehydes onto the *ortho* position of resorcinarene via nucleophilic substitution of the Mannich base.

After some experimentation and modification to the brief literature report,[131] the desired dimethylamine Mannich base resorcinarene (2) was afforded in good yield and purity using potassium carbonate, *N,N,N',N'*-tetramethylmethylenediamine and acetyl chloride in dry acetonitrile under microwave irradiation at 110°C for 10 minutes. The reported yield of 70% may actually be quantitative as apparent from a small-scale reaction. The rather difficult and inconsistent crystallisation of the product was the likely cause of the product loss. The successful electrophilic aromatic substitution of the *ortho* hydrogen with a Mannich base was confirmed by the dimethylamine peak at 2.21 ppm and 44.4 ppm on the respective ^{1}H and ^{13}C NMR spectra (**Appendix A – 1**). The ^{1}H NMR spectrum provided clear evidence that this was a substitution, in that only one aromatic hydrogen peak was present. The methylene between the aromatic

ring and the nitrogen appeared as an AB pair at 3.53 and 3.66 ppm in the ^{1}H spectrum, which correlated via HSQC spectroscopy, to the peak at 56.3 ppm in the DEPT-135 spectrum.

Investigations into the nucleophilic substitution by the quarternisation of the Mannich base of **(2)** via Gutsche and Nam's[132] procedure produced complex mixtures for both azide and nitrile nucleophiles. The Mannich base resorcinarene **(2)** was not entirely soluble in DMSO. The ^{1}H NMR spectra of the crude products showed that the resorcinarene signals had become broad humps. The TLC, being fairly streaked, suggested that unreacted resorcinarene **(2)** was present amongst multiple products. Therefore, there was no clear sign that any target product had been formed, and given the lack of success in these preliminary investigations, this route was abandoned.

2.2 Functionalisation of resorcinarene phenols

Since the functionalisation of the resorcinarene *ortho* position yielded no success, the investigation moved on to functionalisation of the resorcinarene phenols. A search of the literature provided a method for installing aldehyde or priamry amine groups onto the tetramethoxyresorcinarene by conversion of the phenols.[133] This however necessitates as longer synthetic procedure (**Scheme 2.11**) compared to direct nitration or formylation of the resorcinarene aromatic ring. In this synthetic procedure, the phenols of the tetramethoxyresorcinarene are converted to nitriles via a Buchwald-Hartwig cyanation of the triflated phenols. The reduction of the nitrile group on the resorcinarene provides access to the desired aldehydes or primary amines.
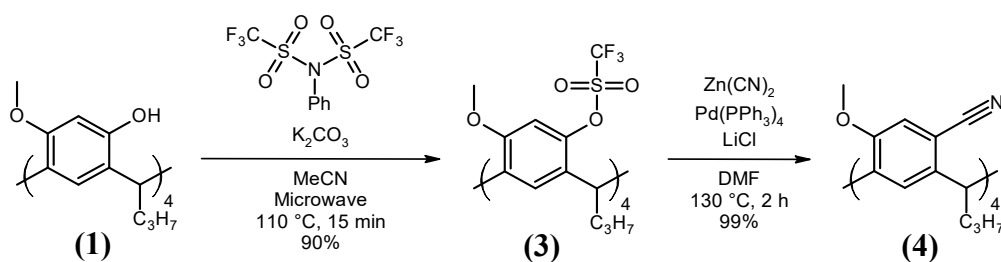
Scheme 2.11 Conversion of resorcinarene phenols to nitriles for subsequent reduction to aldehydes or primary amines.

The first step of this synthesis is the conversion of the phenols of tetramethoxy-resorcinarene **(1)** into trifluoromethanesulfonates. This conversion has been reported by Heaney and co-workers[134] who employed microwave irradiation to achieve a more rapid reaction. After some experimentation on the procedure, the desired trifluoromethanesulfonate resorcinarene was conveniently afforded in high yield and purity using potassium carbonate with *N*-phenylbis(trifluoromethanesulfonimide) in acetonitrile under microwave irradiation for 15 minutes at 110°C. It was discovered that the microwave reaction was best performed with a small amount of acetonitrile at high concentrations, since the bulk of the target product conveniently crystallises directly from the reaction mixture. This does not necessitate the usual work up procedure, because the product can be directly filtered from the reaction mixture, washed with water to remove the potassium carbonate, then oven-dried. By this method, some target product remains dissolved in the acetonitrile mother liquor, but a yield of 90% is achieved. Complete recovery of the product from the acetonitile mother liquor is difficult and may not be worthwhile. Another advantage to this method is the ability to perform a large-scale reaction with up to 2.6 grams of resorcinarene **(1)** in the limitations of a relatively small microwave vial. Evidence that the desired trifluoromethanesulfonate resorcinarene **(3)** was obtained was provided by the ^{13}C NMR spectrum which showed a quartet at 118.7 ppm which is attributed to the carbon of the trifluoromethyl group (**Appendix A − 3**). A recently published alternative synthetic procedure employing triflic anhydride and pyridine in dichloromethane may be more convenient since it offers essentially quantitative yield without the need for formal purification.[135]

With substantial quantities of the trifluoromethanesulfonate **(3)** prepared, the Buchwald-Hartwig cyanation was then conducted using zinc cyanide and lithium chloride with tetrakistriphenylphosphine palladium in dimethylfomamide, following the procedure by Mattay and co-workers.[133] From initial attempts, it was discovered that special attention needs to be taken to ensure that the lithium chloride was anhydrous, and that the tetrakistriphenylphosphine palladium catalyst was properly active. To counter these issues, prior to the reaction, the lithium chloride, together with the solid reactants were placed in the reaction flask and dried in the oven overnight. Moreover, the palladium catalyst was carefully stored in a Schlenk flask under nitrogen. With these countermeasures in place, the cyanation of **(3)** proceeded

smoothly and was completed within 2 hours, according to TLC monitoring. After column chromatography, the target nitrile resorcinarene **(4)** was recovered in an excellent yield of 99%, confirming the literature. The nitrile group in resorcinarene **(4)** was confirmed by the C≡N stretch in the IR spectrum, as well as a peak at 118 ppm in the ^{13}C NMR spectrum which could be distinguished from the quarternary aromatic carbon peaks by HMBC spectroscopy (**Appendix A – 4**).

With the nitrile resorcinarene **(4)** prepared, Mattay and co-workers have shown that, on a small scale, the *iso*-butyl derivative of the nitrile resorcinarene could be partially reduced by DIBAL-H to give the aldehyde, or fully reduced to the primary amine by lithium aluminium hydride to give the primary amine (**Scheme 2.12**).[133]
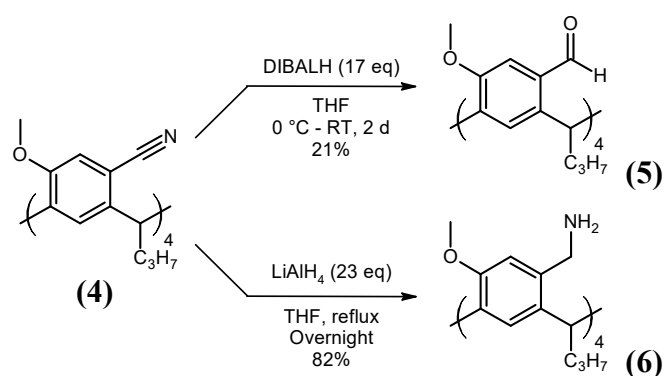
Scheme 2.12 Reduction of nitrile resorcinarene to aldehydes or primary amines.

The reduction of nitrile resorcinarene **(4)** by DIBAL-H in diethyl ether followed by quenching with sodium potassium tartrate as per the procedure by Mattay and co-workers gave a low yield of target aldehyde resorcinarene **(5)**. A potential source of product loss was during the quenching of the DIBAL-H at the end of the reaction, which turns the reaction mixture into a gelatinous white precipitate which was difficult to dissolve. The gel likely ensnares some of the product preventing it from being extracted by organic solvents. It was realised that the formation of the gel could be avoided by quenching with an excess of dilute hydrochloric acid, followed by prolonged stirring. The amount of crude product afforded from this method suggested a good yield, with a TLC that indicated only baseline material other than the desired product. Filtration through a plug of silica afforded the target target aldehyde resorcinarene **(5)** in excellent purity, as shown by ^{1}H NMR spectroscopy, which clearly evidenced the aldehyde with a peak at 10.3 ppm (**Appendix A – 6**). The aldehyde was further confirmed on the ^{13}C NMR spectrum with a peak at 191 ppm, as well as on the

IR spectrum with a C=O stretch and the disappearance of the C≡N stretch. However, the amount of target product (21%) afforded after filtration through a plug of silica was much lower than the crude material. A Mićović[136, 137] work up and also a basic work up of the DIBAL-H reaction were also attempted, but no desired product was recovered.

Regarding the reduction of the nitrile resorcinarene to give the primary amine, the procedure by Mattay and co-workers employed lithium aluminium hyride in ether followed by work up with sodium potassium tartrate. However, nitrile resorcinarene (4), under these conditions, gave a low yield of incompletely reduced tetranitrile resorcinarene products, as indicated by the many small peaks on the ^{1}H NMR spectrum, as well as a small nitrile peak on the IR spectrum. Attempts to reduce the nitrile groups by hydrogenation with Raney Nickel and hydrazine returned only the starting nitrile resorcinarene (4). In the literature, nitrile calixarenes have been easily reduced to the corresponding amines by borane.[138] Applying the borane procedure to nitrile resorcinarene (4) yielded the target product as indicated by the ^{1}H NMR spectrum, but with broad peaks. Attempts to purify the product by recrystallisation and acid/base reprecipitation were of no effect. Therefore, attention was returned to reduction by lithium aluminium hydride. Changing the work up from sodium potassium tartrate to the Mićović[136, 137] work up, with washing of the aluminium salts with dichloromethane, drastically improved the yields. However, the ^{1}H NMR and IR spectra indicated that the reduction had still not proceeded to completion. Therefore, the material was subject to reduction reaction again at the same conditions. The small peaks on the ^{1}H NMR spectrum of the product were significantly less, indicating that the reaction had proceeded further, but still not to completion. During the experimentation, it was realised that the target amine resorcinarene (6) was not very soluble in ether, but completely soluble in tetrahydrofuran. Therefore, the reduction using lithium aluminium hydride was performed in tetrahydrofuran at reflux overnight. After a Mićović work up, the target amine resorcinarene (6) was furnished in good yields without needing further purification. Amine resorcinarene (6) was fully characterised, with the amine group being confirmed by a N-H stretch in the IR spectrum. The methylene of the primary amine appeared on the ^{1}H NMR spectrum as an AB pair at 3.54 and 3.79 ppm, while in the DEPT-135 spectrum the peak at 43.8 ppm was attributed to it (**Appendix A – 6**).

2.3 Coupling of tetraaminoresorcinarene with dialdehydecalixarene

With sufficient quantities of tetramethoxyresorcinarene furnished with both aldehyde and amine functional groups, the next step was to synthesise a distal aldehyde or amine calixarene to serve as the rigid bridge.

The most convenient synthesis of a calixarene, that is distally-functionalised at the wider rim with either an aldehyde or amine, is distal aldehyde calixarene **(9)**. This calixarene can be synthesised by the procedure by Bonini et al.,[128] as outlined in **Scheme 2.13**. According to this literature procedure, the distal two hydroxy groups of starting tetrahydroxycalixarene **(7)** were propylated to decrease the para-activating effect of the distal two aromatic rings, while also keeping the calixarene in a fairly rigid cone conformation.[139] The dipropoxy-calixarene **(8)** was confirmed by a triplet and multiplet in the aliphatic region of the ^{1}H NMR spectrum, while in the aromatic region, there was a doubling of signals due to the change from C_4 to C_2 symmetry (**Appendix A – 7**). Formylation of the remaining two OH-activated aromatic rings of the dipropoxycalixarene **(8)** under Rieche conditions conveniently furnished the distal aldehyde calixarene **(9)** in quantitative yield, which was confirmed by the C=O stretch in the IR spectrum, and a ^{1}H NMR spectrum which matched the literature (**Appendix A – 8**).
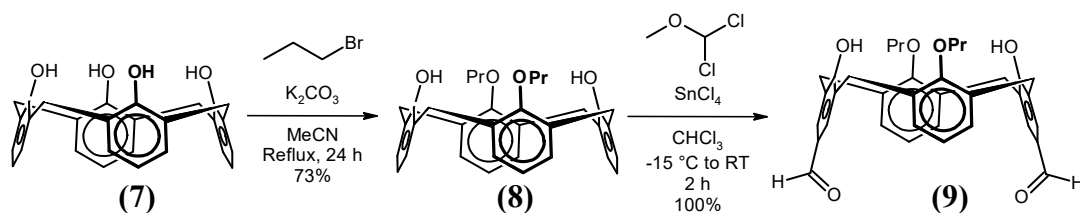
Scheme 2.13 Synthesis of a distal dialdehyde calixarene.

With a distal dialdehyde calixarene prepared, the coupling of tetraaamino-resorcinarene **(6)** and **(9)** by imine linkages was investigated (**Scheme 2.14**). A preliminary reaction at a dilution of 1 mg/mL using molecular sieves while refluxing in dichlormethane, at similar conditions to the literature,[113] gave an ^{1}H NMR spectrum with broad humps, which was inconclusive. Therefore, to enable monitoring of the reaction by ^{1}H NMR spectroscopy, a small scale reaction was conducted in an NMR tube in CDCl$_3$.
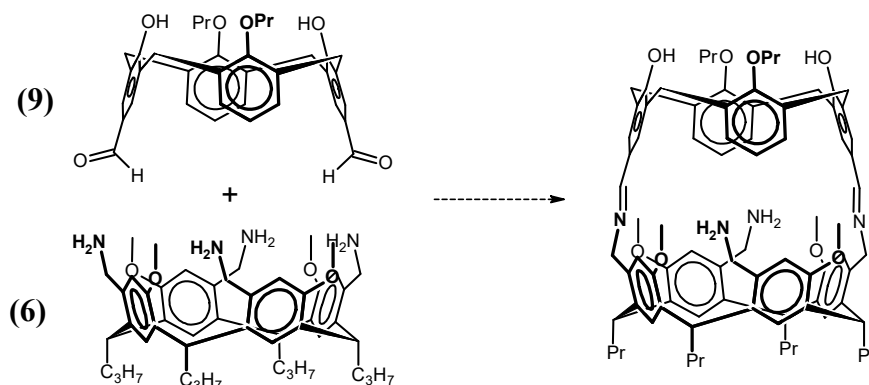
Scheme 2.14 Investigation into the coupling of tetraaminoresorcinarene **(6)** with dialdehyde calixarene **(9)**.

Immediately after the two were combined, the starting dialdehyde calixarene **(9)** was clearly evident on the ^{1}H NMR spectrum, but the tetraaminoresorcinarene **(6)** was essentially not observed, other than two broad lumps in the hydrocarbon region. Excess tetraaminoresorcinarene **(6)** was added to the NMR solution, and after overnight, the dialdehyde **(9)** peaks which had been sharp became broad humps on the ^{1}H NMR spectrum, while the tetraamine **(6)**, being in excess, was clearly visible. Of note was the disappearance of the calixarene aldehyde peak, as well the appearance of two tiny bumps at 8.26 and 8.69 ppm, which may correspond to the imine and phenol of the product(s). A more concentrated NMR solution of **(6)** and **(9)** in a 1:1 ratio yielded similar results where signals associated with an imine were present on NMR spectra, but were tiny or broad. In light of these inconclusive results, it was decided to explore the imine coupling in a different manner by swapping the the aldehyde groups from the calixarene to the resorcinarene, and vice-versa for the amine groups.

2.4 Coupling of tetraaldehyderesorcinarene with diaminocalixarene

The goal for the next part of the investigation was to synthesise a distal diamino-calixarene to act as a rigid bridge, instead of a dialdehyde calixarene. A distal diamino-calixarene could be prepared through multiple methods.

2.4.1 Diaminocalixarene method 1

The same synthetic strategy for dialdehyde calixarene (9) would provide the most convenient path to obtaining a distal diaminocalixarene (**Scheme 2.15**).
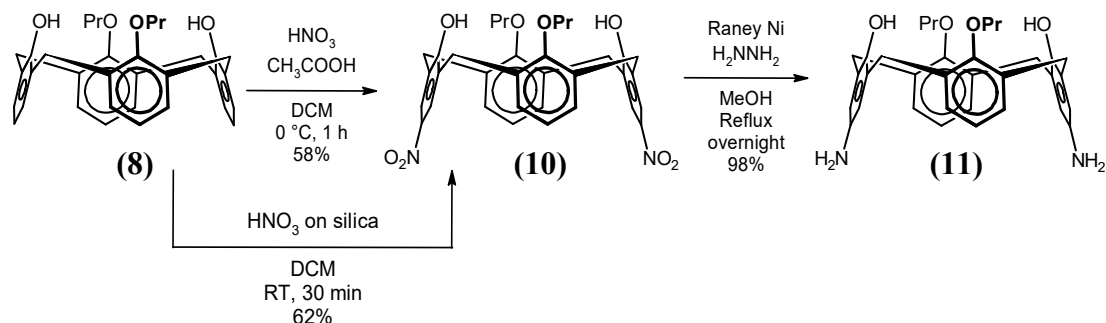
Scheme 2.15 Synthesis of distal diaminocalixarene (11).

The nitration of dipropoxycalixarene (8) has been documented by Struck et al. using sodium nitrate and a catalytic amount of lanthanum nitrate hexahydrate in concentrated hydrochloric acid, to give dinitrodipropoxycalixarene (10) in 56% yield after column chromatography.[113] However, due to the availability of reagents, the nitration using concentrated nitric acid and glacial acetic acid was preferred. The nitration under these conditions has been reported in the literature by Liang et al., but no experimental procedure was provided.[140] Nevertheless, based on similar nitration procedures in the literature,[141, 142] dinitrodipropoxycalixarene (10) was successfully synthesised in 58% yield using nitric acid and glacial acetic acid in dichloromethane. The ^{1}H NMR spectrum showed a downfield shift of a singlet in the aromatic region, which indicated the presence of the electron-widthdrawing nitro group (**Appendix A – 9**). The ^{1}H NMR spectrum and melting point were consistent with Struck's data. An alternative nitration procedure utilising nitric acid on silica[126] also successfully deliverered calixarene (10) in similar yield. Compared to using nitric acid and acetic acid, this procedure was more convenient in that the silica could simply be filtered off from the reaction mixture, and the filtrate concentrated for chromatography.

The nitro groups of calixarene (10) were then reduced by Raney nickel and hydrazine monohydrate to furnish the diamino calixene (11) according to the procedure by Struck et al.[113] The ^{1}H NMR spectrum of the product obtained after work up appeared fairly pure. The signal in the aromatic region had shifted upfield from 8.0 to 6.5 ppm, evidencing the conversion of the nitro group to the electron-donating amine group (**Appendix A – 9**). The ^{1}H NMR spectrum was identical to the literature.[113]

The diaminocalixarene **(11)** however, appeared as a light-red solid, which was an unexpected colour for such a compound. Nevertheless, the imine coupling of this material with tetraformylresorcinarene **(5)** was attempted under the conditions reported by Struck et al. (**Scheme 2.16**). Mini-work ups of the reaction mixture were taken and analysed by ^{1}H NMR spectroscopy. The spectra indicated the presence of the tetraformylresorcinarene **(5)**, but the signals for the diaminocalixarene **(11)** were unclear, appearing to have broadened.
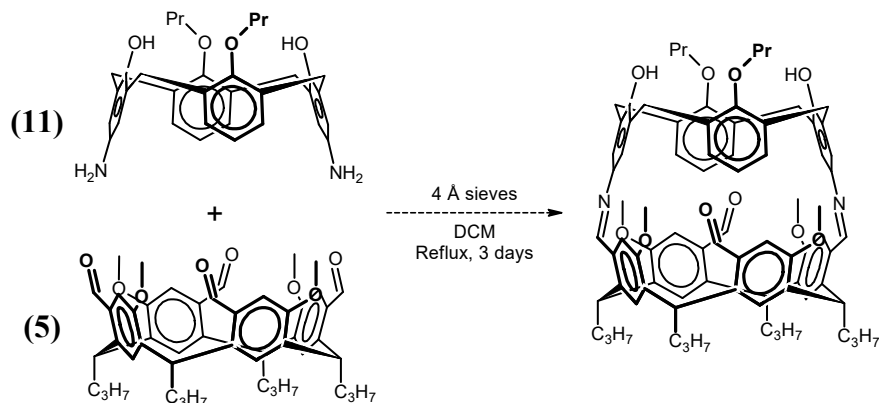
Scheme 2.16 Attempted imine coupling of diaminocalixarene **(11)** and tetraformylresorcinarene **(5)**.

Monitoring of the coupling reaction in CDCl$_3$ at room temperature by ^{1}H NMR spectroscopy confirmed the gradual broadening of the diaminocalixarene **(11)** signals, while the signals for the tetraformylresorcinarene **(5)** were essentially intact. This provided clear evidence that the diaminocalixarene **(11)** was at fault. In fact, the ^{1}H NMR spectrum of a sample of **(11)** that had been kept in storage for nine months had shown significant peak broadening, which was indicative of decomposition. Even the ^{1}H NMR spectrum of freshly prepared **(11)** exhibited slight peak broadening and integration discrepancy. These observations, together with the unexpected red colour, agree with the reasoning made by Struck et al. that the instability of diaminocalixarene **(11)** was due to the decomposition of the aminophenols to quinone systems.[113] Struck et al. also reported lower yields for the imine coupling reactions involving **(11)**, suspecting that the acidic phenolic protons were interfering with the imine coupling. Therefore, it appears necessary to protect the phenol groups of the diaminocalixarene.

2.4.2 Diaminocalixarene method 2

Diaminotetrapropoxycalixarene has been reported in the literature by the synthetic procedure in **Scheme 2.17**.[143, 144] The downside of this method is that it is not high-yielding and efficient, because the distal nitration of tetrapropoxycalixarene produces multiple products that have to be separated by column chromatography. A search of the literature does not present any other procedure for obtaining the diaminotetrapropoxycalixarene.
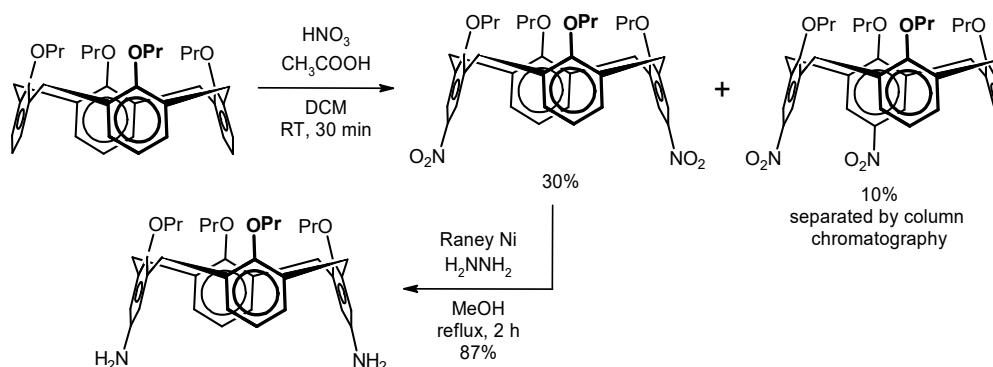
Scheme 2.17 Literature synthetic procedure for diaminotetrapropoxycalixarene.[143, 144]

The logical method to overcome the nitration selectivity issues is to synthesise dinitro-calixarene **(10)**, then alkylate the remaining distal nitrophenols (**Scheme 2.18**).
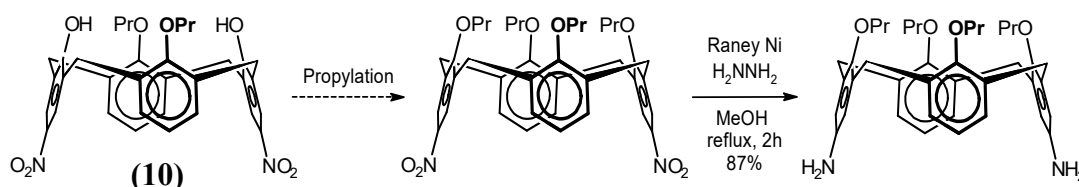
Scheme 2.18 Theoretical alternative route to diaminotetrapropoxycalixarene.

This may seem trivial at first glance, but a search of similar calixarene alkylation reactions in the literature reveals that the calixarene flips conformation during alkylation to give calixarene products in the partial cone / 1,3-alternate conformations.[145-148] The alkylation of calixarene phenols on the narrower rim has been shown to be affected by the metal cation of the base, the alkyl halide, and the solvent.[149] Considering this, the alkylation of dinitrocalixarene **(10)** was attempted under various other conditions (**Table 2.1**).

Table 2.1 Alkylation of dinitrodipropoxycalixarene **(10)** under various conditions. Comparison of outcomes from this investigation to the literature.
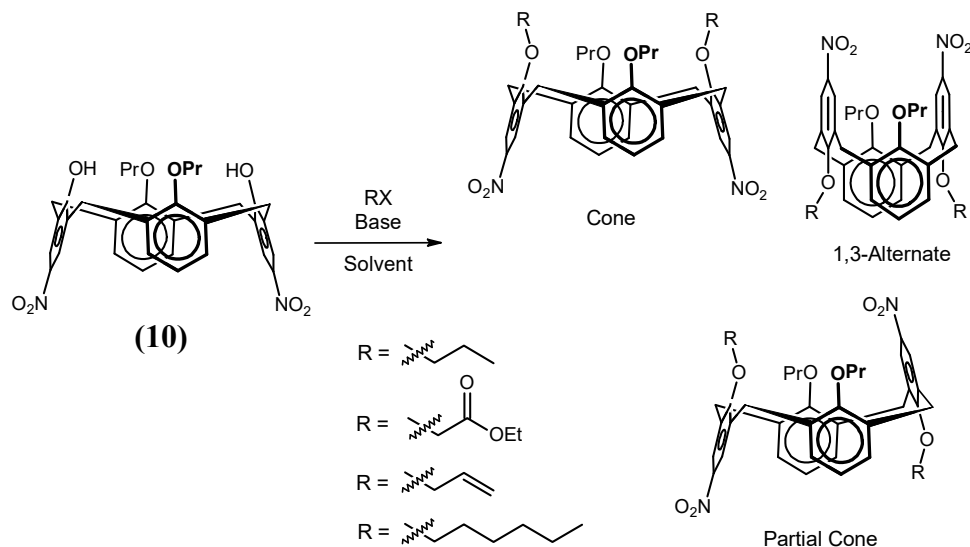
RX	Base	Solvent	Outcome
I⌐∿∿ (iodopropane)	K$_2$CO$_3$	MeCN	Cone + partial cone
	NaH	DMF	No reaction
	Na$_2$CO$_3$	MeCN	Cone + partial cone + unknown
	Cs$_2$CO$_3$	DMF	1,3-alt (26%) + Partial cone (67%)[145]
Br∿CO-OEt (ethyl bromoacetate)	Na$_2$CO$_3$	MeCN	Cone **(12)** (41%)
			+ partial cone **(13)** (23%)
	K$_2$CO$_3$	MeCN	Partial cone (44%)[146]
Br∿∿ (allyl bromide)	NaH	DMF	No reaction
	K$_2$CO$_3$	MeCN	Cone **(14)** (5%)
			+ partial cone **(15)** (24%)
			+ 1,3-alt **(16)** (21%)
I∿∿∿∿	Cs$_2$CO$_3$	DMF	1,3-alt (17%) + Partial cone (70%)[148]

In the propylation reactions, the calixarene conformations in the crude product were determined based on literature ^{1}H NMR spectra of the known compounds.[144, 145] Dinitrocalixarene **(10)** did not react with iodopropane and sodium hydride presumably due to the rather poor nucleophilicity of the nitro phenoxide, which may instead allow the iodopropane to undergo elimination by sodium hydride to give propene gas.

The alkylation of dinitrocalixarene (10) was also attempted with other alkylating agents. In the literature, the tetra-alkylation of *p-tert*-butylcalixarene with ethyl bromoacetate by sodium carbonate in acetone was reported to give the tetra-alkylated calixarene product with retention of the cone conformation.[149] Based on this, dinitrocalixarene (10) was alkylated with ethyl bromoacetate under similar reaction conditions as the literature, but gave two calixarene products. These were separated by preparative TLC and identified to be the di-alkylated calixarene in both the cone (12) (41%) and partial cone (13) (23%) conformations. The alkylation with ethylbromo acetate was confirmed by the ester carbonyl group being evident in both conformers by the C=O stretch in both IR spectra, as well as the peaks at about 169 ppm in both ^{13}C NMR spectra. The partial cone conformer (13) was differentiated from the cone conformer (12) by additional peaks in the NMR spectra, which are attributed to the loss of C_2 symmetry (**Appendix A – 9**). The cone conformer (12) was easily identified by the single AB pair in the ^{1}H NMR spectrum, which represented the methylene bridges of the calixarene macrocycle. The partial cone conformer (13) has been described by Regayeg et al.,[146] but the cone conformer (12) appears to be unknown to the literature.

Dinitrocalixarene (10) was also alkylated with allyl bromide, since allyl bromide cannot readily eliminate to form propene gas under alkaline conditions. It was surprising that no reaction was observed by TLC and ^{1}H NMR when dinitrocalixarene (10) was treated with excess sodium hydride and allyl bromide. However, with potassium carbonate, the reaction with allyl bromide produced multiple products, which were isolated by preparative TLC and identified to be cone (14) (5%), partial cone (15) (24%), and 1,3-alternate (16) (21%) conformers of the diallylcalixarene. The allyl group was confirmed in each conformer by the multiplets around 5.5-6.5 ppm in the ^{1}H NMR spectra, together with the CH_2 peaks at 117 ppm in the DEPT-135 spectra (**Appendix A – 13**). Applying the same rotational symmetry rationale on the NMR spectra, the partial cone could be identified from the other two C_2-symmetrical conformers. In the ^{1}H NMR spectrum, the AB pair characteristic to the cone conformer enabled it to be distinguished from the 1,3-alternate conformer. A search of the literature reveals that none of the three conformers are known, with the closest match being a calixarene in the 1,3-alternate conformation, having *p-tert*-butyl groups on the propoxy aromatic rings.[150]

In the ^{1}H NMR spectra of the partial cones **(13)** and **(15)**, the six aromatic protons on the two equivalent propoxy aromatic rings appear as three signals integrating for two protons each (**Figure 2.3**). They appear as a doublet of doublets, a triplet, and an unresolved doublet of doublets (designated as a multiplet). The opposite orientations of the adjacent nitro aromatic rings of the partial cone causes the protons *meta* to the propoxy group to be non-equivalent. The signals for these *meta* protons appear as a doublet of doublets because there is *ortho* and *meta* coupling between the non-equivalent protons on the ring. The signal for the proton *para* to the propoxy group appears as a triplet which could be considered as a doublet of doublets with coincidentally identical coupling constants from the two non-equivalent *meta* protons.
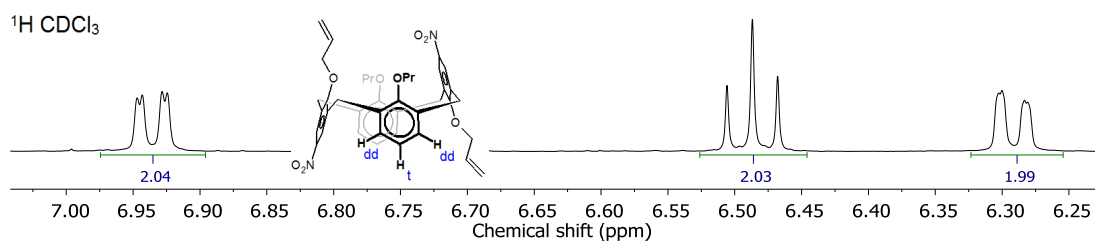
Figure 2.3 The ^{1}H NMR spectrum of the parital cone calixarene **(15)** showing the aromatic protons on the propoxy aromatic rings which are splitting each other due to their non-equivalence.

However, for the cone calixarenes with greater symmetry, one would expect the aromatic protons on the propoxy aromatic rings to appear as a doublet and a triplet in the ^{1}H NMR spectrum. In the ^{1}H NMR spectra of the cone calixarenes **(12)** and **(14)**, a doublet was present, however the expected triplet appeared as a doublet of doublets (**Figure 2.4**). Since the only other signal that was split was the expected doublet, this doublet of doublets was unexpected. Perhaps it was due to conformational effects of the calixarene, hence the ^{1}H NMR spectrum of **(12)** was recorded at 50°C. However, at this elevated temperature, instead of coalescing to a triplet, the doublet of doublets became better-resolved. The possibility of a solvent effect was probed by recording the ^{1}H NMR spectrum in acetone-d_6 instead of CDCl$_3$, however the doublet of doublets was still apparent. The appearance of these doublet of doublets was surprising and could not be explained.
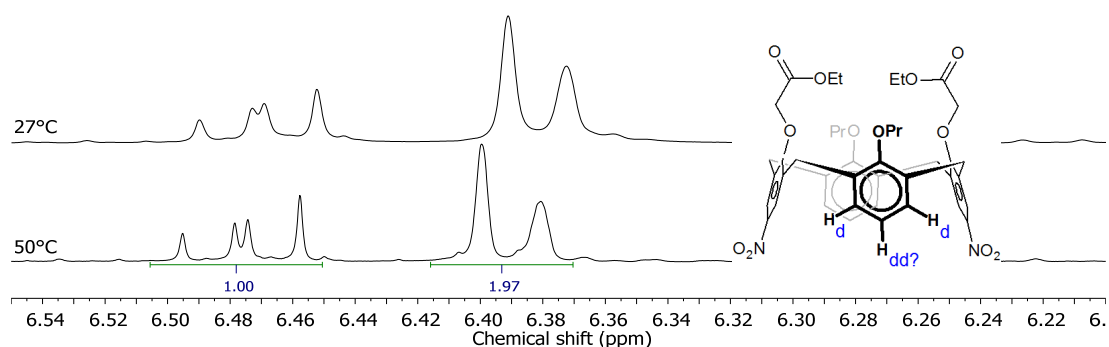
Figure 2.4 The ^{1}H NMR spectrum of cone calixarene **(12)** recorded in CDCl$_3$ showing the aromatic protons on the propoxy aromatic rings which surprisingly appear as a doublet and a doublet of doublets.

From this investigation (**Table 2.1**), the alkylation of dinitrocalixarene **(10)** under various conditions produced mixtures of conformers where the cone conformation of the calixarene was never fully retained. This result confirms the trend in the literature. Unfortunately, this apparently simple strategy, does not readily provide a tetra-alkylated distal diaminocalixarene in the cone conformation, as required for the imine coupling reaction.

2.4.3 Diaminocalixarene method 3

The previous methods for synthesising a distally-functionalised calixarene relied on the selective distal alkylation of the phenols on the narrow rim for distal selectivity. As discovered from the previous attempt, the issue with this method, is that alkylation of the remaining two hydroxy groups affects the conformation of the calixarene, causing conformers other than the desired cone conformer to be produced. This issue could be circumvented by tetra-alkylating the calixarene phenols, then employing a selective bromine-lithium exchange,[84] which is another well-documented method for distally-functionalising the wider rim of calixarenes. The application of this method for this purpose utilises the bromine as protecting groups, which enables the selective nitration of the remaining distal two aromatic rings (**Scheme 2.19**). However, the nitration and subsequent reduction to the amine is unknown to the literature for the particular dibromocalixarene. Similar work in the literature suggests that the entire synthetic strategy should be fairly high-yielding and convenient.[84, 143, 144, 151-154]
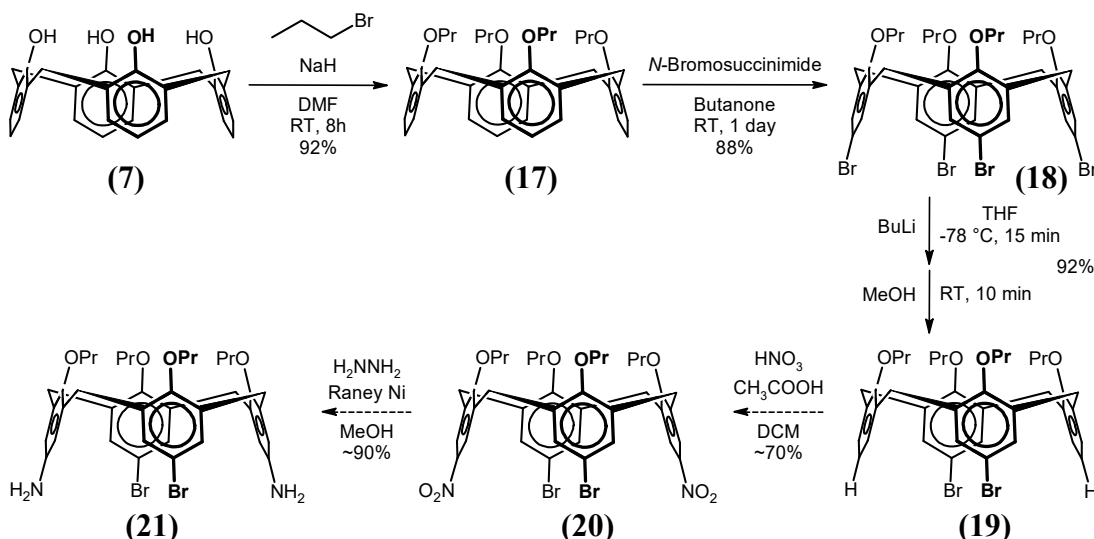
Scheme 2.19 Proposed synthetic strategy for diaminotetrapropoxycalixarene. Yields are based on literature examples.[84, 143, 144, 151-154]

To prepare for the selective bromine-lithium exchange, the starting tetrahydroxy-calixarene **(7)** was first tetrapropylated to permanently protect the hydroxy groups, and to also lock the calixarene in the cone conformation.[139] Under the standard literature conditions described by Mendez-Arroyo et al,[151] issues with complete propylation of the calixarene were encountered, despite using excess base and alkylating agent. It was often the case that the reaction appeared to be completed by TLC, but upon work up and trituation, ^{1}H NMR analysis clearly showed that starting calixarene was still present. The propylation was only completed when the material was subjected to reaction again. The best yield obtained of 78% was significantly lower than the 92% yield reported by Mendez-Arroyo et al. The propylation was confirmed by the appearance of a triplet and a multiplet in the aliphatic region of the ^{1}H NMR spectrum (**Appendix A – 18**). A sharp AB pair (δ 3.15 and 4.46) of the methylene groups of the macrocycle confirmed the locking of calixarene **(17)** in the cone conformation.

Next, tetrabromination of **(17)** with *N*-bromosuccinimide in butanone conveniently furnished **(18)** in near quantitative yield. A single singlet in the aromatic region of the ^{1}H NMR spectrum confirmed that complete bromination was achieved (**Appendix A – 18**). The selective bromine-lithium exchange was then performed on tetrabromocalixarene **(18)** according to the procedure by Larsen and Jørgensen[84] to give the dibromocalixarene **(19)** in the expected yield of 93%. The use of sufficient butyllithium is imperative to the selectivity of the dilithiation reaction. For this reason, a slight excess (2.5 eq) of butyllithium was used. This did not have an impact on the reaction outcome, which agrees with the observation by Larsen and Jørgensen. The

distal debromination was confirmed by the appearance of an additional apparent singlet in the aromatic region of the ^{1}H NMR spectrum, integrating for two hydrogens (**Appendix A – 19**).

The nitration of the distal dibromocalixarene **(19)** should be selective for the non-brominated distal aromatic rings to give calixarene **(20)**. Up till this stage, all calixarenes synthesised were known compounds, with their synthesis being well described in the literature. However, dibromodinitrocalixarene **(20)** is not a known compound, and its synthesis was in fact more challenging than anticipated. In the literature, the nitration of *O*-alkylated and non-*O*-alkylated calixarenes has been reported,[144, 152-154] but none of the usual procedures for nitrating calixarenes appeared to give the target product (**Table 2.2**). After much experimentation, the target product was achieved by nitration using 'claycop' (copper nitrate on clay)[155] in the presence of a few drops of anhydrous nitric acid. Nitration by this method appeared to be capricious, with the ^{1}H NMR spectrum of the crude product from some reactions showing a complex mixture of products without the target product. Purification by chromatography was necessary to remove other unknown calixarene by-products, which were likely responsible for the relatively low yield of 21%. The dibromodinitro-calixarene **(20)** was evidenced by the two singlets of equal integration in the aromatic region of the ^{1}H NMR spectrum (**Appendix A – 19**).

Table 2.2. Nitration of dibromocalixarene **(19)** under various nitration conditions.
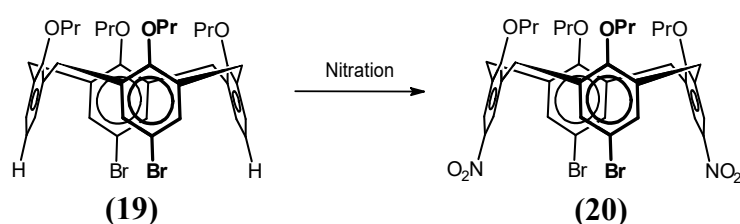
Nitrating agent	Acid	Solvent	Outcome
HNO$_3$ (70%)	CH$_3$COOH	DCM	No reaction
HNO$_3$ (100%)	CH$_3$COOH	DCM	Complex mixture
KNO$_3$	CF$_3$COOH	DCM	Mixture
KNO$_3$	AlCl$_3$	DCM	Decomposition
HNO$_3$	Silica	DCM	No reaction
Cu(NO$_3$)$_2$ + HNO$_3$ (100%)	Montmorillonite clay	DCM	Target product **(20)** (21%) + unknown by-products

Finally, the reduction of the nitro groups by Raney Nickel and hydrazine[143] proceeded smoothly to furnish the pure diaminotetrapropoxycalixarene (21) after work up (Scheme 2.20). The success of the reduction was apparent by the appearance of a broad amine peak in the ^{1}H NMR spectrum, and the replacement of the signal at 7.63 with one at 5.98 ppm which evidences the switch from an electron-withdrawing nitro to an electron-donating amine (Appendix A – 20).
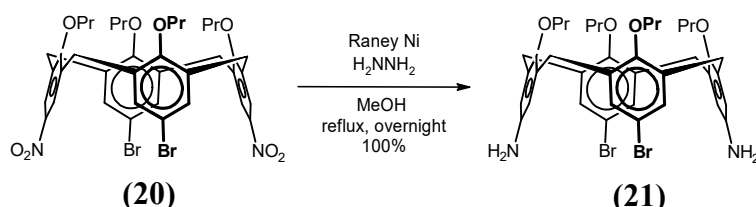
Scheme 2.20 Reduction of dinitrocalixarene (20) to give diaminocalixarene (21).

With a sufficient quantity of the diaminocalixarene (21) prepared, its imine coupling with tetraaldehyde resorcinarene (5) was then investigated (Scheme 2.21) at a dilution of 1 mg/mL under similar conditions to the literature.[113] The reaction mixture appeared as a yellow colour, characteristic of an aromatic Schiff base, but the ^{1}H NMR spectrum of a portion of the reaction mixture showed that the peaks associated with the diamino-calixarene (21) had all become broad humps, while the peaks of the tetraaldehyde-resorcinarene (5) were clearly intact. To gain more insight, the same reaction was conducted in an NMR tube to allow monitoring of the reaction by ^{1}H NMR spectroscopy. The ^{1}H NMR spectra indicated that, upon mixing of tetraaldehyde (5) and diamino (21), the same phenomenon was occurring rapidly within 30 minutes. In the hope that the reversible imine linkages would rearrange to form the desired product, portions of the NMR solution were diluted many times, but to no effect.
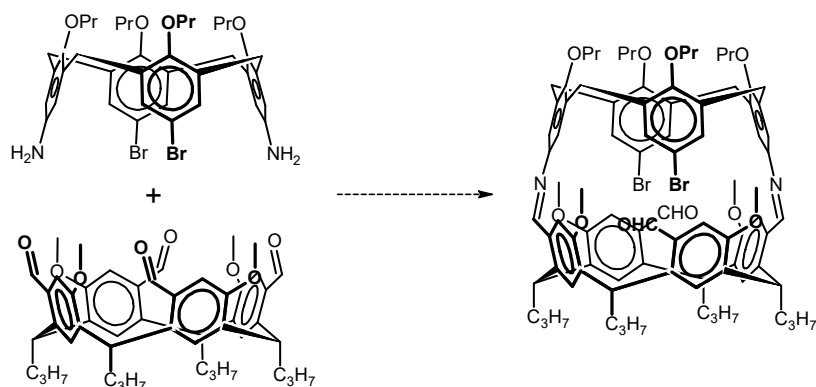
Scheme 2.21 Investigation into the coupling of tetraaldehyde resorcinarene (5) with diaminocalixarene (21).

As a simple test, aniline was added to a solution of tetraaldehyderesorcinarene **(5)** in CDCl$_3$. After 20 minutes, the ^{1}H NMR spectrum recorded an absence of starting resorcinarene and an appearance of the expected imine, as represented by the peak at 8.9 ppm. However, in the reaction between **(5)** and **(21)**, no imine peak was definitively observed in any of the ^{1}H NMR spectra. Perhaps steric hinderance, particularly in regards to the bromine atoms, may have impeded the coupling of the calixarene and resorcinarene in the envisaged manner.

From the overall investigations into the calixarene rigid bridge strategy, the target resorcinarene-calixarene imine was never definitively observed, with the data being inconclusive. The signals for both the amine calixarene and amine resorcinarene appeared to broaden in the ^{1}H NMR spectra of their respective coupling reactions, while the signals of the corresponding aldehyde appeared to be intact. This has not been understood, although it signals that the fault lies with the amine coupling partner.

A possible reason for the lack of success may be the conformations of the calixarene and resorcinarene. In general, solid state crystal structures demonstrate that the calixarenes would most likely be in the cone conformation, while the resorcinarenes would likely adopt the boat conformation. However, this reaction was in solution, not in the solid state, hence there would be conformational mobility of both the calixarene and resorcinarene which should permit their coupling. Nevertheless, despite the conformational mobility in solution, the calixarene and resorcinarene would still gravitate to their preferred conformations, and this may prevent the ideal fit required for the envisioned coupling. Moreover, steric hinderance may have also played a role by impeding the coupling between the calixarene and resorcinarene.

All in all, taking into consideration the significant effort to synthesise the aldehyde and amino resorcinarenes and calixarenes for this coupling step, together the lack of progress, the decision was made to entirely abandon this strategy of a calixarene rigid bridge to focus efforts on more promising strategies.

2.5 Experimental

2.5.1 General methods

NMR spectra were recorded on a Bruker UltraShield Avance 400 spectrometer (400 MHz for ^{1}H, 100 MHz for ^{13}C). All chemical shifts were reported in parts per million (ppm). NMR spectra were calibrated to their respective solvents:[156] chloroform-*d* (CDCl$_3$, δ 7.26 ppm; ^{13}C, δ 77.16 ppm); DMSO-d$_6$ (CD$_3$SOCD$_3$, δ 2.50 ppm; ^{13}C, δ 39.52 ppm); acetone-d$_6$ (CD$_3$COCD$_3$, δ 2.05 ppm; ^{13}C, δ 29.84 ppm). Multiplicity was assigned as follows: s = singlet, d = doublet, t = triplet, q = quartet, sxt = sextet, br = broad.

A PureSolv MD5 solvent purification system from Innovative Technology Incorporated was used for the purification and drying of the following solvents: tetrahydrofuran, dimethylformamide, acetonitrile, diethyl ether, dichloromethane. Reactions were subjected to microwave irradiation in a Biotage Initiator+ (0 – 400 W, 2.45 GHz). IR spectra were acquired on a Perkin Elmer Spectrum 100 with ATR attachment and a scan range from 650 – 4000 cm^{-1}. Melting points were determined using an Electrothermal IA9300 melting point apparatus. For melting points where the solvent of crystallisation was not quoted, the solvent was removed under reduced pressure, and the product was not crystallised. Solvents were removed under reduced pressure by vaporisation using a Buchi R-114 rotavapor. A Javac Shark^{TM} high vacuum pump was used to remove trace solvents from solid samples. Elemental composition of samples was analysed via Perkin Elmer 2400 Series II CHNS/O. Optical rotations were measured on a Rudolph Research Analytical Autopol I automatic polarimeter.

Sodium hydride in oil was washed twice with petroleum spirits prior to use.

Thin layer chromatography was performed using 200 μm silica gel F-254 aluminium-backed sheets. Preparative TLC was performed using 20×20 cm, 1000 μm thick silica gel F-254 glass-backed plates. UV light (254 nm) was used to visualise TLC plates. Column chromatography was performed using 40-63 μm silica gel.

Heated Electro spray ionisation – high resolution mass spectrometry (HESI-HRMS). The HRMS was determined by Dr. Frankie Busetti at Edith Cowan University. A Thermo Scientific Q-Exactive Orbitrap mass spectrometer (Thermo

75

Fisher Scientific Corporation, Waltham, USA) was employed for high accuracy mass determination of the compounds. Stock solutions were prepared by dissolving 1 mg of compound into 1 mL of DCM. Solutions were diluted down to 10 ng/μL in MeOH containing 0.1% formic acid and infused at 3 μL/min into the mass spectrometer using a built-in syringe pump. Full calibration of the LTQ Orbitrap XL in the 70-3000 *m/z* range was conducted prior to each measurement with the positive and negative ion calibration solutions provided by Thermo Scientific (Australia). Optical lenses were optimised with the positive calibration solution prior to each batch of samples. For increased mass accuracy on the Q-Exactive Orbitrap mass spectrometer, a plasticizer interfering peak present in the background (*n*-butyl benzenesulfonamide, $C_6H_5SO_2NH(CH_2)_3CH_3$, $[M+H]^+=214.0896$ *m/z*), was used for the lock mass function. The screening analysis was conducted operating the Q-Exactive Orbitrap mass spectrometer in full-scan mode from 70-1000 *m/z* with a mass resolution of 70.000 (@ 200 *m/z*). When necessary, samples were also analysed operating the Q-Exactive Orbitrap mass spectrometer in $HRMS^2$ mode, where the mass spectrometer was forced to isolate the parent compound in the first quadrupole, fragment it in the HCD cell and then scan for the product ions in the Orbitrap mass analyser. A mass resolution of 17.500 (@ 200 *m/z*) was used for the fragmentation experiments. The possibility for NH_4^+ adducts was confirmed by running a MS/MS on the adducts for a few samples. For substance identification the deviation of the measured mass (i.e. parent compound and fragments) was compared against the theoretical mass (< 2 ppm, relative error). To confirm elemental composition, the measured isotope pattern was also compared with that obtained from isotopic simulation. Data was processed using the Xcalibur QualBrowser software.

2.5.2 Functionalisation of the ortho position of the resorcinarene

2.5.2.1 $1^4,3^6,5^6,7^6$-tetrahydroxy-$1^6,3^4,5^4,7^4$-tetramethoxy-2,4,6,8-tetrapropylresorcin[4]arene (1)
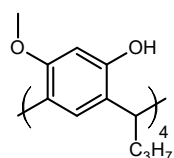
Resorcinarene **(1)** was synthesised according to the procedure by McIldowie et al.[65] To a mixture of 3-methoxyphenol (30.1 g, 0.243 mol), butanal (22 mL, 17.6 g, 0.245 mol) and dichloromethane (550 mL) was added boron trifluoride etherate (90 mL, 104 g, 0.729 mol) while in an ice bath under nitrogen. The solution turned from orange-yellow to dark red. The ice bath was removed and the reaction mixture was allowed to warm to room temperature over

about 20 minutes. After 2 hours at room temperature, the reaction mixture was quenched by adding water (400 mL), producing some white fumes and slight warming. The organic layer was separated, and the solvent was removed under reduced pressure to give a foamy brown solid as the crude product. The crude product was triturated with methanol (~200 mL) to give the product **(1)** as a white powder (36.9 g, 85%): mp 256-259 °C (lit.[131] 257-258 °C); IR 3400 cm^{-1} (OH phenol); ^{1}H NMR (CDCl$_3$) δ 0.97 (t, J = 7.4 Hz, 12 H, CH$_2$C*H*$_3$), 1.30 (apparent sxt, 8 H, C*H*$_2$CH$_3$), 2.18 (apparent q, 8 H, C*H*$_2$CH), 3.83 (s, 12 H, OC*H*$_3$), 4.30 (t, J = 7.9 Hz, 4 H, C*H*CH$_2$), 7.23 and 6.34 (2s, 2 × 4 H, Ar*H*), 7.50 (s, 4 H, O*H*).

2.5.2.2 Attempted Rieche formylation of resorcinarene (1)

The procedure by Bonini et al was applied.[128] To a solution of resorcinarene **(1)** (0.258 g, 0.362 mmol) in chloroform was added 1,1-dichloromethyl methyl ether (0.18 mL, 1.23 mmol) followed by tin(IV) chloride (0.86 mL, 1.48 mmol) while in a brine-liquid nitrogen bath at -20 °C under nitrogen. Upon warming to room temperature, the reaction mixture became somewhat cloudy red-brown with a dark precipitate. The reaction mixture gradually became opaque dark brown and then opaque black over 5 h. The reaction was then quenched with HCl (20 mL, 10%), and a black precipitate was observed. The solids were mostly dissolved after an hour of stirring and sonicating. The opaque dark red-brown organic layer was separated and the aqueous layer was extracted with dichloromethane (3 × 20 mL). The combined organic extracts were washed with water (3 × 20 mL), dried (MgSO$_4$) and solvent removed under reduced pressure to afford the crude product as a black-brown solid (0.346 g), which appeared as a complex mixture by ^{1}H NMR. TLC of the crude product was a complete streak.

2.5.2.3 Attempted Duff formylation of resorcinarene (1)

The procedure by Szumna and co-workers was applied to resorcinarene **(1)**.[130] Resorcinarene **(1)** (0.205 g, 0.288 mmol) and hexamethylenetetramine (0.288 g, 2.05 mmol) were combined in a vial with stirrer bar, followed by trifluoroacetic acid (2 mL). The vial was capped and shaken vigourously till the solids were largely dissolved to produce a clear dark red solution. The reaction mixture was then subjected to microwave irradiation at 120 °C for 1 h. The resultant dark yellow-brown mixture was added to HCl (15 mL, 1 M) and CHCl$_3$ (15 mL) and stirred rapidly overnight at room temperature. The layers were then separated and the aqueous layer was extracted with

dichloromethane (6 × 15 mL). The combined organic extracts were dried (MgSO$_4$), filtered, and solvent removed under reduced pressure to afford the crude product as a dark orange oil (0.462 g). The crude product was filtered through a plug of silica using EtOAc (30 mL), and the solvent was removed under reduced pressure to give a dark yellow oil (0.137 g). A portion (0.055 g) of the material after the silica plug was subjected to preparative TLC (EtOAc – petroleum spirits 30:70). Three fractions were collected, which in total were 9 mg. TLC indicated incomplete separation. ^{1}H NMR spectroscopy of the fractions could not identify any compounds.

2.5.2.4 $1^4,3^6,5^6,7^6$-tetrahydroxy-$1^6,3^4,5^4,7^4$-tetramethoxy-$1^5,3^5,5^5,7^5$-tetra(dimethylaminomethylene)-2,4,6,8-tetrapropylresorcin[4]arene (2)
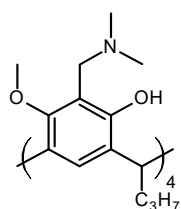
This resorcinarene was synthesised based on the report by Buckley et al.[131] To a mixture of potassium carbonate (0.82 g, 5.95 mmol), anhydrous acetonitrile (1 mL) and N,N,N',N'-tetramethylmethylenediamine (0.57 mL, 4.21 mmol) was carefully added acetyl chloride (0.30 mL, 4.21 mmol) with rapidly stirring in an ice bath. The resultant white slurry was stirred for 5 minutes under nitrogen. Resorcinarene (1) (0.50 g, 0.706 mmol) was then added, together with anhydrous acetonitrile (2 mL). The resultant white slurry was subject to microwave irradiation for 10 minutes at 110°C. The clear orange mixture was then filtered though cotton wool to remove potassium carbonate, and more acetonitrile was added. The filtrate was heated until boiling, and then water and triethylamine were added to precipitate the product. After allowing the mixture to cool to room temperature, filtration of the mixture afforded the previously unreported compound (2) as a white solid (0.46 g, 70%): mp 221-222 °C; IR 3066 cm^{-1} (OH); ^{1}H NMR (CDCl$_3$) δ 0.90 (t, J = 7.3 Hz, 12 H, CH$_2$CH_3), 1.25-1.43 (m, 8 H, CH_2CH$_3$), 1.70-1.83 (m, 4 H, CH_2CH), 1.85-1.96 (m, 4 H, CH_2CH), 2.21 (s, 24 H, NCH_3), 3.41 (s, 12 H, OCH_3), 3.53, 3.66 (AB, 2 × 4 H, J = 13.7 Hz, ArCH_2N), 4.49 (t, J = 7.5 Hz, 4 H, CHCH$_2$), 6.73 (s, 4 H, ArH); ^{13}C NMR (CDCl$_3$) δ **14.4 (CH$_2$CH$_3$), 21.5 (CH$_2$CH$_3$), 35.7 (CHCH$_2$), 38.3** (CH$_2$CH)**, 44.4 (NCH$_3$), 56.3 (br,** ArCH$_2$N)**, 61.2 (OCH$_3$), 113.7 (C, Ar), 125.7 (br, CH, Ar), 127.5, 127.9, 154.2, 154.4 (C, Ar).** Found: C, 70.19; H, 8.90; N, 5.78; C$_{56}$H$_{84}$N$_4$O$_8$.H$_2$O; requires C, 70.11; H, 9.04%; N, 5.84%.

2.5.2.5 Attempted quarternisation and nucleophilic substitution of (2)

The basis for this synthesis was the procedure by Gutsche and Nam.[132] To a suspension of partially-dissolved resorcinarene **(2)** (0.0513 g, 0.0545 mmol) in DMSO-d_6 was added iodomethane (0.0227 mL, 0.0518 g, 0.365 mmol) in an NMR tube. After 40 minutes of periodic mixing at room temperature, sodium cyanide (0.030 g, 0.612 mmol) was added, turning the cloudy reaction mixture a darker yellow colour. The reaction was then heated at 80 °C. After 3 hours, ^{1}H NMR spectroscopy of the reaction mixture indicated broadening of resorcinarene signals with many peaks. After 3 days, ^{1}H NMR spectroscopy indicated that the resorcinarene signals had become broader.

2.5.3 Functionalisation of resorcinarene phenols

2.5.3.1 $1^4,3^6,5^6,7^6$-tetratrifluoromethanesulfonyl-$1^6,3^4,5^4,7^4$-tetramethoxy-2,4,6,8-tetrapropylresorcin[4]arene (3)
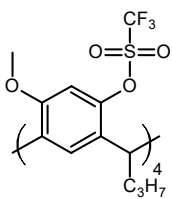
This synthesis was based on the procedure by Heaney and co-workers.[134] Resorcinarene **(1)** (2.64 g, 3.70 mmol), potassium carbonate (3.16 g, 22.86 mmol), N-phenylbis-(trifluoromethanesulfonimide) (9.08 g, 5.41 mmol) and anhydrous acetonitrile (8 mL) were combined in the respective order. The reaction mixture was then subject to microwave irradiation at 110 °C for 15 minutes. The reaction mixture was allowed to cool to room temperature, then filtered to collect the white crystals which were washed with acetonitrile (25 mL), followed by plenty of water. After drying in the oven (120 °C), the pure, previously unreported product **(3)** was obtained as white crystals (4.12 g, 90%): mp 129 °C (MeCN); ^{1}H NMR (CDCl$_3$) δ 0.93 (t, J = 7.3 Hz, 12 H, CH$_2$CH_3), 1.33 (apparent sxt, 8 H, CH_2CH$_3$), 1.72-1.96 (m, 8 H, CH_2CH), 3.68 (s, 12 H, OCH_3), 4.50 (t, J = 7.5 Hz, 4 H, CHCH$_2$), 6.61 and 6.77 (s, 2 × 4 H, ArH); ^{13}C NMR (CDCl$_3$) δ 14.10 (CH$_2$$CH_3$), 21.0 ($CH_2CH_3$), 36.0 ($CHCH_2$), 37.1 ($CH_2$CH), 55.5 (O$CH_3$), 103.5 ($C$H, Ar), 118.7 (q, J = 319.8 Hz, CF$_3$), 126.8 (CH, Ar), 127.8, 132.0 (C, Ar), 147.0, 156.2 (C, Ar). Found: C, 46.29; H, 4.05; C$_{48}$H$_{52}$F$_{12}$O$_{16}$S$_4$; requires C, 46.45; H, 4.22%.

2.5.3.2 $1^4,3^6,5^6,7^6$- tetramethoxy-$1^6,3^4,5^4,7^4$-tetranitrile -2,4,6,8-tetrapropylresorcin[4]arene (4)

This synthesis was adapted from the procedure by Mattay and co-workers.[133] Tetratriflate resorcinarene **(3)** (4.12 g, 3.32 mmol), zinc cyanide (3.14 g, 26.8 mmol) and oven-dried lithium chloride (1.95 g, 46.0 mmol) were combined with stirrer bar and placed in an oven at 120 °C overnight. The flask with reagents was taken out of the oven and cooled under a stream of nitrogen. Anhydrous dimethylformamide (43 mL) was then added, and the mixture was de-oxygenated by freeze-pump-thaw procedure three times before adding dark orange tetrakistriphenylphosphine palladium(0) (0.784 g, 0.678 mmol), then de-oxygenated again twice after. The cloudy bright yellow mixture was then heated at 130 °C under nitrogen. After about 5 minutes of heating, the reaction mixture appeared to turn cloudy colourless. Then after 1 hour, the reaction mixture appeared to become cloudy yellow-orange. After 2 hours, the cloudy dark yellow reaction mixture was allowed to cool, then dichloromethane and sodium hydrogencarbonate solution were added to the reaction mixture, and the layers were allowed to settle before separation. The dark yellow organic layer was separated, and the aqueous layer was extracted twice with dichloromethane. The solvent was removed under reduced pressure from the combined organic extracts to give a white-brown solid (4.38 g) as the crude product. Purification by column chromatography (EtOAc – DCM 1:99 to 5:95) afforded the pure, previously unreported compound **(4)** as a white solid (2.47 g, 99%): mp 300 °C; IR 2223 cm^{-1} (C≡N); ^{1}H NMR (CDCl$_3$) δ 0.97 (t, J = 7.3 Hz, 12 H, CH$_2$CH_3), 1.27-1.43 (m, 8 H, CH_2CH$_3$), 1.82-2.01 (m, 8 H, CH_2CH), 3.77 (s, 12 H, OCH_3), 4.66 (t, J = 7.5 Hz, 4 H, CHCH$_2$), 6.80, 6.93 (2s, 2 × 4 H, ArH); ^{13}C NMR (CDCl$_3$) δ 14.2 (CH$_2$CH$_3$), 20.9 (CH$_2$CH$_3$), 37.3 (CHCH$_2$), 40.4 (CH$_2$CH), 56.1 (OCH$_3$), 112.1 (C, Ar), 114.1 (CH, Ar), 118.0 (CN), 125.7 (CH, Ar), 138.1, 139.7, 155.6 (C, Ar). Found: C, 76.64; H, 6.86; N, 7.32; C$_{48}$H$_{52}$N$_4$O$_4$; requires C, 76.98; H, 7.00; N, 7.48%.

2.5.3.3 $1^4,3^6,5^6,7^6$-tetraformyl-$1^6,3^4,5^4,7^4$-tetramethoxy-2,4,6,8-tetrapropylresorcin[4]arene (5)

This synthesis was based on the procedure by Mattay and co-workers.[133] To a cloudy colourless mixture of resorcinarene (4) (0.111 g, 0.148 mmol) in anhydrous tetrahydrofuran (8 mL), was added dropwise DIBAL-H in toluene (2.5 mL, 1.02 M, 2.55 mmol), while in an ice bath, with stirring under nitrogen. The cloudy colourless solution was stirred in the ice bath, allowing to warm to room temperature. After 2 days, the reaction mixture was quenched with dilute HCl (10 mL, 1 M) producing bubbles. With a few drops of dilute HCl, the mixture turned into a white gel; bubbling and heat produced. With more dilute HCl and rapid stirring, the mixture became a cloudy slightly yellow solution. After stirring for 2 hours, the quenched reaction mixture was allowed to settle, forming two layers, which were separated. The bottom aqueous layer was extracted with dichloromethane (3 × 5 mL). The organic layers were combined, dried (MgSO$_4$) and solvent evaporated to give the crude product as a slightly yellow solid (0.121 g). The crude product was filtered through a short column of silica beginning with dichloromethane, then with (EtOAc – DCM 5:95) to give the pure, previously unreported product (5) (0.024 g, 21%) as a white solid: mp 190 °C; IR 1682 cm^{-1} (C=O); ^{1}H NMR (CDCl$_3$) δ 0.97 (t, J = 7.3 Hz, 12 H, CH$_2$CH_3), 1.30-1.47 (m, 8 H, CH_2CH$_3$), 1.89-2.04 (m, 8 H, CH_2CH), 3.71 (s, 12 H, OCH_3), 5.11 (t, J = 7.4 Hz, 4 H, CHCH$_2$), 6.95, 7.22 (2s, 2 × 4H, ArH), 10.30 (s, 4 H, CHO); ^{13}C NMR (CDCl$_3$) δ 14.3 (CH$_2$$CH_3$), 21.1 ($CH_2CH_3$), 36.8 ($CHCH_2$), 37.7 ($CH_2$CH), 55.7 (O$CH_3$), 109.6, 126.7 ($C$H, Ar), 132.8, 139.6, 140.1, 154.9, (C, Ar), 191.4 (CHO). HRMS (ESI): calcd. for C$_{48}$H$_{57}$O$_8$ as [M + H]$^+$ 761.4048; found 761.4044.

2.5.3.4 $1^4,3^6,5^6,7^6$-tetra(aminomethyl)-$1^6,3^4,5^4,7^4$-tetramethoxy-2,4,6,8-tetrapropylresorcin[4]arene (6)
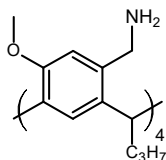
To a grey slurry of lithium aluminium hydride (0.355 g, 9.35 mmol) in anhydrous tetrahydrofuran (35 mL) was added resorcinarene (4) (0.302 g, 0.403 mmol) while stirring at room temperature. The resultant cloudy dark grey mixture was stirred at reflux under nitrogen overnight. Thereafter, the mixture was cooled in an ice bath, quenched by slowly adding water (0.355 mL), causing vigorous bubbling and fumes, followed by sodium hydroxide (0.355 mL, 15%), then more water (3 × 0.355 mL). After stirring at room temperature for 1 hour, the tetrahydrofuran was removed under reduced pressure. Dichloromethane (50 mL)

was added to the white residue with sonicating. The mixture was filtered, and the solvent was removed from the clear colourless filtrate to give the pure, previously unreported product **(6)** as a white solid (0.252 g, 82%): mp 207 °C (DCM); IR 3375 and 3280 (NH$_2$), 1194 cm^{-1} (C-N); ^{1}H NMR (CDCl$_3$) δ 0.94 (t, J = 7.4 Hz, 12 H, CH$_2$C*H$_3$*), 1.30-1.45 (m, 8 H, C*H$_2$*CH$_3$), 1.75-1.87, 1.87-2.00 (2m, 8 H, C*H$_2$*CH), 3.54, 3.79 (AB, 2 × 4 H, J = 13.7 Hz, C*H$_2$*N), 3.68 (s, 12 H, OC*H$_3$*), 4.37 (t, J = 7.3 Hz, 4 H, C*H*CH$_2$), 6.68 and 6.74 (s, 2 × 4 H, Ar*H*); ^{13}C NMR (CDCl$_3$) δ 14.5 (*C*H$_2$CH$_3$), 21.4 (*C*H$_2$CH$_3$), 37.9 (*C*HCH$_2$), 38.1 (*C*H$_2$CH), 43.8 (*C*H$_2$N), 55.4 (O*C*H$_3$), 110.7, 126.3 (*C*H, Ar), 131.7, 134.8, 140.0, 154.7 (*C*, Ar). HRMS (ESI): calcd. for C$_{48}$H$_{69}$N$_4$O$_4$ as [M + H]$^+$ 765.5313; found 765.5284.

2.5.4   Dialdehydecalixarene

2.5.4.1   25,26,27,28-Tetrahydroxycalixarene (7)

25,26,27,28-Tetrahydroxycalixarene **(7)** was prepared by a literature procedure.[157]

2.5.4.2   25,27-Dihydroxy-26,28-di-*n*-propoxycalixarene (8)
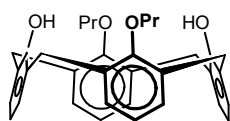
This calixarene was prepared according to literature.[128] To a mixture of calixarene **(7)** (1.99 g, 4.70 mmol) and potassium carbonate (0.731 g, 5.29 mmol) in acetonitrile (100 mL) was added 1-bromopropane (3.4 mL, 37.43 mmol). The resultant slightly cloudy white mixture was stirred at reflux open to air for 24 hours. The reaction was allowed to cool to room temperature. The solvent was removed under reduced pressure and dichloromethane (30 mL) was added to the residue. The cloudy white organic layer was washed with HCl (3 × 30 mL, 10%), dried (MgSO$_4$), and solvent removed (evaporated) to give a white, slightly yellow solid (2.20 g). The solid was recrystallised from chloroform-methanol to give pure **(8)** as white crystals (1.74 g, 73%): mp 260-263 °C (lit.[69] 268-270 °C); IR 3290 cm^{-1} (OH phenol); ^{1}H NMR (CDCl$_3$) δ 1.32 (t, J = 7.4 Hz, 6 H, CH$_2$C*H$_3$*), 2.08 (apparent sxt, 4 H, C*H$_2$*CH$_3$), 3.38, 4.33 (AB, J = 12.9 Hz, 2 × 4 H, ArC*H$_2$*Ar), 3.99 (t, J = 6.3 Hz, 4 H, OC*H$_2$*), 6.65 (t, J = 7.5 Hz, 2 H, Ar*H*), 6.75 (t, J = 7.6 Hz, 2 H, Ar*H*), 6.93 (d, J = 7.6 Hz, 4 H, Ar*H*), 7.06 (d, J = 7.5 Hz, 4 H, Ar*H*), 8.29 (s, 2 H, O*H*).

2.5.4.3 5,17-Diformyl-25,27-dihydroxy-26,28-di-*n*-propoxycalixarene (9)
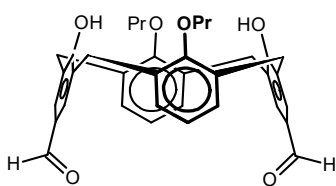
This calixarene was prepared according to literature.[128] To a solution of calixarene **(8)** (1.02 g, 2.01 mmol) in chloroform (50 mL) was added 1,1-dichloromethyl methyl ether (0.48 mL, 0.61 g, 5.3 mmol), followed by tin(IV) chloride (2.35 mL, 5.23 g, 20.9 mmol) while at -15°C under nitrogen. The reaction mixture immediately turned red, then quickly became pink with a precipitate. The reaction mixture was allowed to warm to room temperature, then stirred at room temperature under nitrogen for 2 hours. During this time, the reaction mixture turned from light-pink to dark pink then to purple. The reaction was then quenched with HCl (15 mL, 10%), then stirred till all solids dissolved. The resultant layers were separated, and the aqueous phase was extracted with dichloromethane (3 × 15 mL). The combined organic extracts were washed with water (3 × 20 mL) dried ($CaCl_2$) and the solvent removed under reduced pressure to afford pure **(9)** as an off-white solid (1.13 g, 100%): mp. 320-321 °C (CHCl$_3$/MeOH) (lit.[69] >320 °C); IR 1670 (C=O), 3159 cm^{-1} (OH phenol); ^{1}H NMR (CDCl$_3$) δ 1.33 (t, J = 7.4 Hz, 6 H, CH$_2$C*H*$_3$), 2.09 (apparent sxt, 4 H, C*H*$_2$CH$_3$), 3.51, 4.31 (AB, J = 13.1 Hz, 2 × 4 H, ArC*H*$_2$Ar), 4.02 (t, J = 6.2 Hz, 4 H, OC*H*$_2$), 6.80 (t, J = 7.6 Hz, 2 H, Ar*H*), 6.97 (d, J = 7.6 Hz, 4 H, Ar*H*), 7.64 (s, 4 H, Ar*H*), 9.25 (s, 2 H, O*H*), 9.79 (s, 2 H, C*H*O).

2.5.5 Diaminocalixarene method 1

2.5.5.1 5,17-Dinitro-26,28-dipropoxycalixarene (10)
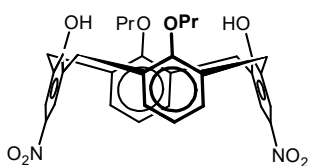
To a colourless mixture of calixarene **(8)** (1.00 g, 1.96 mmol) in glacial acetic acid (12 mL) and dichloromethane (10 mL) was added nitric acid (3 mL, 70%) while in an ice bath. The mixture was stirred in the ice bath open to air, and suddenly turned black after a couple of seconds, then to a dark yellow-green colour within a minute. After 30 minutes, the reaction mixture was diluted with water (30 mL). The layers were separated, and the organic layer was washed with water (3 × 20 mL), dried ($MgSO_4$) and solvent removed under reduced pressure to give a dark orange solid as the crude product. The crude product was purified by column chromatography (DCM – petroleum spirits 7:3 to 9:1) to give pure **(10)** as a yellow-white solid (0.680 g, 58%): mp 320-345 °C dec (lit.[113] >320 °C dec); IR 3086 cm^{-1} (OH phenol); ^{1}H NMR (CDCl$_3$) δ 1.33 (t, J = 7.4 Hz, 6 H, CH$_2$C*H*$_3$), 2.09 (apparent sxt, 4 H, C*H*$_2$CH$_3$), 3.51, 4.30 (AB, J = 13.2 Hz, 2 × 4 H,

ArCH_2Ar), 4.02 (t, J = 6.2 Hz, 4 H, OCH_2), 6.85 (t, J = 7.4 Hz, 2 H, ArH), 7.00 (d, J = 7.6 Hz, 4 H, ArH), 8.04 (s, 4 H, ArH), 9.45 (s, 2 H, OH).

2.5.5.2 Preparation of nitric acid on silica

Nitric acid on silica (16-20%) was prepared according to a literature procedure.[126] Nitric acid (47 mL, 8 M) and silica gel (20 g) were combined to give a slurry which was stirred at room temperature for 2 hours. The slurry was then filtered and allowed to air-dry for 40 minutes.

2.5.5.3 5,17-Dinitro-26,28-dipropoxycalixarene (10) via nitric acid on silica

Calixarene (8) (0.337 g, 0.663 mmol), nitric acid on silica (1.33 g, ~16%, 0.213 g, 3.39 mmol) and dichloromethane (12 mL) were combined and stirred at room temperature open to air. The white mixture turned light yellow within seconds. After 30 minutes, the reaction mixture was filtered with dichloromethane washing, and the solvent was evaporated from the filtrate to give a yellow solid as the crude product. Purification by column chromatography (DCM – petroleum spirits 7:3 – 9:1) afforded pure (10) white, slightly yellow solid (0.242 g, 61%).

2.5.5.4 5,17-Diamino-26,28-dipropoxycalixarene (11)
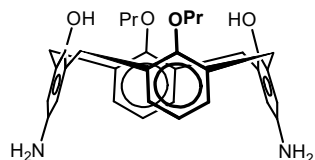
The synthesis was performed according to the procedure by Struck et al.[113] To a yellow slurry of (10) (0.100 g, 0.167 mmol) and hydrazine monohydrate (0.374 mL) in methanol (25 mL) was added a spatula tip (~0.1 g wet slurry) of Raney nickel. Then, the mixture was heated at reflux with rapid stirring, overnight. However, TLC of the reaction mixture thereafter indicated remaining starting material. So more hydrazine monohydrate (0.374 mL) and Raney nickel (~0.1 g wet slurry) was added to the reaction mixture, and reflux continued. TLC after about 6 hours indicated completion of the reaction. The cloudy dark green mixture was allowed to cool to room temperature, then filtered through celite. The solvent of the yellow filtrate was removed under reduced pressure, and the yellowish residue was dissolved in dichloromethane (10 mL), instantly turning the yellow solution to a peach, light-red colour. The organic solution was washed with NaHCO$_3$ solution (3 × 5 mL), dried (MgSO$_4$), and solvent evaporated to give fairly-pure (11) as a light-red solid (0.088 g, 98%): ^{1}H NMR (CDCl$_3$) δ 1.28 (t, J = 7.4 Hz, 6 H, CH_2CH$_3$), 2.06 (apparent sxt, 4 H, CH_2CH$_3$), 3.25, 4.31 (AB, J = 12.9 Hz, 2 × 4 H, ArCH_2Ar), 3.95 (t, J = 6.4 Hz, 4 H,

OCH_2), 6.46 (s, 4 H, ArH), 6.75 (t, J = 7.5 Hz, 2 H, ArH), 6.93 (d, J = 7.5 Hz, 4 H, ArH), 7.64 (s, 2 H, OH).

2.5.6 Diaminocalixarene method 2

2.5.6.1 Propylation of calixarene (10) by potassium carbonate and MeCN

Dinitrodipropoxycalixarene **(10)** (0.207 g, 0.346 mmol), potassium carbonate (0.643 g, 4.65 mmol), acetonitrile (10 mL) and 1-bromopropane were combined and the yellow reaction mixture was heated at reflux under nitrogen for 12 days. During this time, cumulative amounts of sodium iodide (0.434 g, 2.90 mmol), 1-bromopropane (2.2 mL, 2.98 g, 24.2 mmol), then iodopropane (1.6 mL, 2.79 g, 16.4 mmol) were added to the reaction mixture, while the acetonitrile was also refilled. After this, the acetonitrile was evaporated, and the residue was dissolved in dichloromethane and water. The layers were separated, and the aqueous layer was extracted with dichloromethane (2 × 10 mL). The yellow-coloured combined organic extracts were dried (MgSO$_4$) and solvent removed under reduced pressure to give a dark yellow solid (0.253 g) as the crude product. The ^{1}H NMR spectrum of the crude product shows it to be a mixture of cone[144] and partial cone[145] propylated products, according to literature data.

2.5.6.2 Attempted propylation of calixarene (10) by sodium hydride and DMF

Dinitrodipropoxycalixarene **(10)** (0.201 g, 0.336 mmol), dissolved in anhydrous dimethylformamide (12 mL) was added to washed sodium hydride (0.345 g, 60% in oil, 0.207 g, 8.63 mmol) and a couple of crystals of imidazole, and the resultant cloudy yellow mixture was stirred under nitrogen at room temperature for 30 minutes. 1-Iodopropane (0.400 mL, 0.697 g, 4.10 mmol) was added, and the reaction mixture was stirred overnight at the same conditions. Thereafter, the reaction mixture had turned cloudy brown-yellow, and it was quenched with water producing bubbling. After stirring at room temperature for 30 minutes, the solvent was removed under reduced pressure. The residue was taken up in water and extracted with dichloromethane (3 × 20 mL). The combined organic extracts were washed with brine, dried (MgSO$_4$), and solvent removed under reduced pressure to give a yellow-brown solid (0.188 g) as the crude product. The ^{1}H NMR spectrum of the crude product showed it to be the starting calixarene **(10)**, essentially intact.

2.5.6.3 Propylation of calixarene (10) by sodium carbonate and MeCN

Dinitrodipropoxycalixarene **(10)** (0.188 g, 0.314 mmol), sodium carbonate (0.289 g, 2.73 mmol), acetonitrile (10 mL) and iodopropane (0.368 mL, 0.641 g, 3.77 mmol) were combined, and the brown reaction mixture was heated at reflux over 4 days. The acetonitrile was then evaporated from the reaction mixture, and the residue was extracted with dichloromethane (3 × 10 mL) and dilute HCl (10 mL, 1 M). The combined dark brown organic extracts were dried (MgSO$_4$) and solvent removed under reduced pressure to give a brown oily residue (0.199 g) as crude product. The ^{1}H NMR spectrum of the crude product indicated the absence of starting calixarene **(10)**, with cone, partial cone and an unknown product.

2.5.6.4 Attempted allylation of calixarene (10) with sodium hydride and DMF

Dinitrodipropoxycalixarene **(10)** (0.101 g, 0.169 mmol), dissolved in anhydrous dimethylformamide (10 mL) was added to washed sodium hydride (0.549 g, 60% in oil, 0.329 g, 13.7 mmol) and a couple of crystals of imidazole, and the resultant cloudy yellow mixture was stirred under nitrogen at room temperature for 30 minutes. The reaction mixture was then cooled in an ice bath, and allyl bromide (0.087 mL, 0.122 g, 1.01 mmol) was added. The reaction mixture was then allowed to warm to room temperature, and then stirred overnight under nitrogen. After, TLC of the reaction mixture showed only starting calixarene. Therefore, more allyl bromide (0.217 mL, 0.303 g, 2.51 mmol) was added to the reaction while in an ice bath. The reaction was then stirred over another night at room temperature under nitrogen. Thereafter, the reaction mixture was a yellow-brown with white precipitate. TLC of the reaction still only showed starting calixarene. After stirring for a total of three days, the reaction mixture was a highly-coloured yellow, and was quenched with methanol, producing bubbling. Dilute HCl (80 mL, 1 M) was added causing the mixture to lose its yellow colour. The mixture was further diluted with water, stirred for a few mins, then filtered. The collected solid was dissolved in dichloromethane, washed with dilute HCl (20 mL, 1 M), dried (MgSO$_4$), filtered, and solvent removed under reduced pressure to give a light-brown solid (0.104 g), which was indicated by ^{1}H NMR spectroscopy to be the starting calixarene **(10)**, essentially intact.

2.5.6.5 Attempted synthesis of cone 5,17-dinitro-26,28-di((ethoxycarbonyl)methoxy)-25,27-dipropoxycalixarene (12)

Dinitrodipropoxycalixarene **(10)** (0.074 g, 0.124 mmol), sodium carbonate (0.125 g, 1.18 mmol), acetonitrile (7 mL) and ethyl bromoacetate (0.055 mL, 0.083 g, 0.496 mmol) were combined to give a cloudy pale-yellow mixture, which was heated at reflux under nitrogen for up to 5 days (or 67 h). The acetonitrile was boiled off. The residue was extracted with HCl (10 mL, 1 M) and dichloromethane (3 × 10 mL). The combined organic extracts were dried (MgSO₄) and solvent removed under reduced pressure to give a yellow solid with crystals (0.123 g) as crude mixture. The crude mixture was separated by preparative TLC (DCM 100%) to give, in elution order: partial cone calixarene **(13)** as a white solid (0.022 g, 23%), and previously unreported cone calixarene **(12)** as a white solid (0.039 g, 41%).
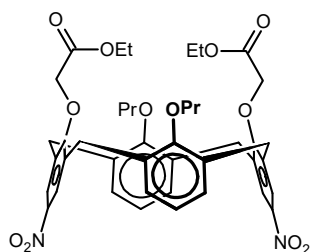
Cone calixarene **(12)**: mp 159-195 °C; IR 1732 and 1754 cm^{-1} (C=O ester); ^{1}H NMR (CDCl₃) δ 1.03 (t, J = 7.4 Hz, 6 H, CH₂CH₂CH_3), 1.29 (t, J = 7.1 Hz, 6 H, OCH₂CH_3), 1.89 (apparent sxt, 4 H, CH₂CH_2CH₃), 3.35, 4.69 (AB, J = 13.9 Hz, 2 × 4 H, ArCH_2Ar), 3.79 (t, J = 7.2 Hz, 4 H, OCH_2CH₂), 4.22 (q, J = 7.1 Hz, 4 H, OCH_2CH₃), 4.83 (s, 4 H, OCH_2C=O), 6.38 (d, J = 7.5 Hz, 4 H, ArH), 6.47 (dd, J = 6.7, 1.6 Hz, 2 H, ArH), 7.83 (s, 4 H, ArH); ^{13}C NMR (CDCl₃) δ 10.6 (CH₂CH₃), 14.3 (OCH₂CH₃), 23.3 (CH₂CH₂CH₃), 31.5 (ArCH₂Ar), 61.1 (OCH₂CH₂), 70.9 (OCH₂CH₃), 77.4 (OCH₂C=O), 123.3, 124.3, 128.6 (CH, Ar), 132.7, 137.2, 143.0, 155.7, 161.8 (C, Ar), 169.2 (C=O); HRMS (ESI): calcd. for C₄₂H₄₇N₂O₁₂ as [M + H]$^+$ 771.3124; found 771.3112.
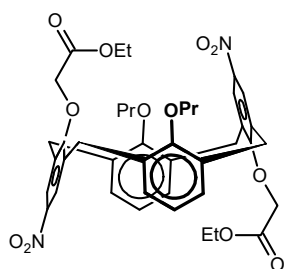
Partial cone calixarene **(13)**: mp 60-80 °C; IR 1732 and 1753 cm^{-1} (C=O ester); ^{1}H NMR (CDCl₃) δ 1.10 (t, J = 7.4 Hz, 6 H, CH₂CH_3), 1.21 (t, J = 7.1 Hz, 3 H, OCH₂CH_3), 1.38 (t, J = 7.2 Hz, 3 H, OCH₂CH_3), 1.88-1.99 (m, 4 H, CH₂CH_2CH₃), 3.30, 4.34 (AB, J = 14.3 Hz, 2 × 2 H, ArCH_2Ar), 3.59-3.69 (m, 2 H, OCH_2CH₂), 3.80, 3.90 (overlapped AB, J = 13.3 Hz, 2 × 2 H, ArCH_2Ar), 3.76-3.85 (overlapped m, 2 H, OCH_2CH₂), 3.89, 4.55 (2s, 2 × 2 H, OCH_2C=O), 4.02 (q, J = 7.1 Hz, 2 H, OCH_2CH₃), 4.34 (q, J = 7.1 Hz, 2 H, OCH_2CH₃), 6.29 (m, 2 H, ArH), 6.52 (t, J = 7.6 Hz, 2 H, ArH), 7.08 (dd, J = 7.6, 1.4 Hz, 2 H, ArH), 8.01 and 8.25 (2s, 2 × 2 H, ArH), ^{13}C NMR (CDCl₃) δ 10.8 (CH₂CH₃), 14.0, 14.4 (OCH₂CH₃), 23.8

(CH$_2$CH$_2$CH$_3$), 31.8, 35.2 (ArCH$_2$Ar), 60.8, 61.7 (OCH$_2$CH$_3$), 67.6, 70.7 (OCH$_2$C=O), 76.8 (OCH$_2$CH$_2$), 122.9, 124.7, 126.0, 129.1, 129.4 (CH, Ar), 130.9, 132.2, 135.3, 137.2, 142.5, 142.7, 155.8, 161.0, 162.1 (C, Ar), 168.6, 169.5 (C=O); HRMS (ESI): calcd. for C$_{42}$H$_{47}$N$_2$O$_{12}$ as [M + H]$^+$ 771.3124; found 771.3102.

2.5.6.6 Attempted synthesis of cone 5,17-dinitro-26,28-diallyl-25,27-dipropoxycalixarene (14)

To a dark brown slurry of dinitrodipropoxycalixarene (10) (0.101 g, 0.169 mmol), potassium carbonate (0.229 g, 1.66 mmol) and allyl bromide (1.5 mL, 2.10 g, 17.3 mmol) was added acetonitrile (5 mL) to give a yellow-brown cloudy mixture, which was heated at reflux under nitrogen for 3 days. Thereafter, the solvent had evaporated to dryness, and TLC showed absence of starting calixarene. The residue was extracted with dichloromethane (3 × 10 mL) and HCl (20 mL, 1 M). The combined organic extracts were dried (MgSO$_4$), filtered, and solvent removed under reduced pressure to give a light-brown oily solid (0.130 g) as crude mixture. Completion of the phenol allylation reaction was verified by the lack of disappearance of signals when a drop of D$_2$O as added to the NMR solution of the crude mixture. The crude mixture was separated by preparative TLC (DCM – petroleum spirits 80:20) to give, in elution order previously unreported products: partial cone calixarene (15) as an off-white solid (0.027 g, 24%), cone calixarene (14) as an orange solid (0.006 g, 5%), and 1,3-alternate calixarene (16) as a white-yellow solid (0.024 g, 21%).
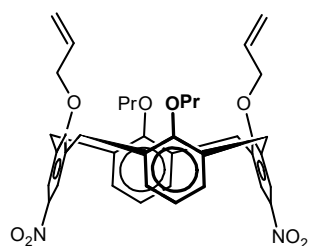
Cone calixarene (14): ^{1}H NMR (CDCl$_3$) (impure, only relevant signals quoted) δ 1.07 (t, J = 7.4 Hz, 6 H, CH$_2$CH$_3$), 1.81-2.00 (m, 4 H, CH$_2$CH$_3$), 3.29, 4.45 (AB, J = 13.6 Hz, 2 × 4 H, ArCH$_2$Ar), 3.75 (t, J = 7.1 Hz, 4 H, OCH$_2$CH$_2$), 4.70 (d, J = 6.6 Hz, 4 H, OCH$_2$CH), 5.14-5.24 (m, 4 H, CH=CH$_2$), 6.28-6.39 (overlapped m, 2 H, CH=CH$_2$), 6.31 (d, J = 7.6 Hz, 4 H, ArH), 6.41 (dd, J = 6.8 or 1.4 Hz, 2 H, ArH), 7.89 (s, 4 H, ArH); ^{13}C NMR (CDCl$_3$) δ 10.8 (CH$_3$), 23.6 (CH$_2$CH$_3$), 31.4 (ArCH$_2$Ar), 76.4 (OCH$_2$CH)), 77.4 (OCH$_2$CH$_2$), 118.6 (C=CH$_2$), 123.0, 124.2, 128.3 (CH, Ar), 132.5 (C, Ar), 134.6 (CH=CH$_2$), 138.2, 142.8, 155.7, 162.5 (C, Ar); HRMS (ESI): calcd. for C$_{40}$H$_{43}$N$_2$O$_8$ as [M + H]$^+$ 679.3014; found 679.2998.
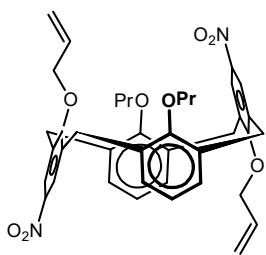
Partial cone calixarene (15): mp 182-184 °C; ^{1}H NMR (CDCl$_3$) δ 1.10 (t, J = 7.4 Hz, 6 H, CH$_2$CH_3), 1.85-2.03 (m, 4 H, CH_2CH$_3$), 3.21, 4.11 (AB, J = 13.7 Hz, 2 × 2 H, ArCH_2Ar), 3.55-3.65 (overlapped m, 2 H, OCH_2CH), 3.65, 3.80 (overlapped AB, J = 12.9 Hz, 2 × 2 H, ArCH_2Ar), 3.75-3.85 (overlapped m, 2 H, OCH_2CH), 4.03 (dt, J = 6.5, 1.2 Hz, 2 H, OCH_2CH), 4.44 (dt, J = 5.2, 1.6 Hz, 2 H, OCH_2CH), 4.82-4.96, 5.33-5.48 (2m, 2 × 2 H, CH=CH_2), 5.73 (ddt, J = 16.8, 10.3, 6.5 Hz, 1 H, CH=CH$_2$), 6.15 (ddt, J = 17.1, 10.4, 5.1 Hz, 1H, CH=CH$_2$), 6.29 (m, 2 H, ArH), 6.49 (t, J = 7.6 Hz, 2 H, ArH), 6.94 (dd, J = 7.6, 1.5 Hz, 2 H, ArH), 8.02, 8.25 (2s, 2 × 2 H, ArH); ^{13}C NMR (CDCl$_3$) δ 10.9 (CH$_2$$CH_3$), 23.9 ($CH_2CH_3$), 31.1, 35.8 (Ar$CH_2$Ar), 73.8, 75.1 (O$CH_2$CH), 76.8 (O$CH_2CH_2$), 117.1, 117.9 (C=$CH_2$), 122.3, 124.4, 126.1, 129.1, 130.1 (CH, Ar), 131.0, 132.0 (C, Ar), 133.3, 134.6 (CH=CH$_2$), 135.5, 138.4, 142.5, 142.8, 155.7, 162.19, 162.21 (C, Ar) (note some signals are coincident); HRMS (ESI): calcd. for C$_{40}$H$_{46}$N$_3$O$_8$ as [M + NH$_4$]$^+$ 696.3279; found 696.3272 (main peak); and calcd. for C$_{40}$H$_{43}$N$_2$O$_8$ as [M + H]$^+$ 679.3014; found 679.3011.

1,3-alternate calixarene (16): mp 192-205 °C (THF/MeOH); ^{1}H NMR (CDCl$_3$) δ 0.99 (t, J = 7.5 Hz, 6 H, CH$_2$CH_3), 1.79 (apparent sxt, 4 H, CH_2CH$_3$), 3.60, 3.72 overlap (AB, J = 14.2 Hz, 2 × 4 H, ArCH_2Ar), 3.70 (overlapped t, J = 7.4 Hz, 4 H, OCH_2CH$_2$), 4.21 (dt, J = 4.9, 1.6 Hz, 4 H, OCH_2CH), 5.14-5.28 (m, 4 H, CH=CH_2), 5.93 (ddt, J = 17.1, 10.6, 4.9 Hz, 2 H, CH=CH$_2$), 6.69 (t, J = 7.5 Hz, 2 H, ArH), 6.98 (d, J = 7.5 Hz, 4 H, ArH), 7.95 (s, 4 H, ArH); ^{13}C NMR (CDCl$_3$) δ 10.4 (CH$_2$$CH_3$), 23.7 ($CH_2CH_3$), 36.5 (Ar$CH_2$Ar), 72.6 (O$CH_2$CH), 74.1 (O$CH_2CH_2$), 117.3 (C=$CH_2$), 122.2, 125.7, 131.2 ($C$H, Ar), 132.4 ($C$, Ar), 133.1 ($C$H=CH$_2$), 135.13, 142.1, 156.3, 161.3 (C, Ar); HRMS (ESI): calcd. for C$_{40}$H$_{43}$N$_2$O$_8$ as [M + H]$^+$ 679.3014; found 679.2992.
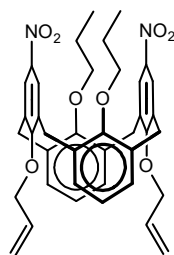
2.5.7 Diaminocalixarene method 3

2.5.7.1 25,26,27,28-Tetrapropoxycalixarene (17)
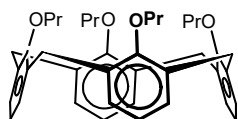
The calixarene was prepared as described by Mendez-Arroyo et al.[151] Calixarene (7) (1.01 g, 2.37 mmol) was added to a mixture of washed sodium hydride (1.25 g, 60% in oil, 0.75 g, 31.3 mmol) and a few of crystals of imidazole in anhydrous dimethylformamide (50 mL), and the resultant off-white slurry was stirred under nitrogen at room temperature for 30 minutes. Then, 1-bromopropane (1.75 mL, 2.40 g, 19.3 mmol) was added to the slurry, and the reaction mixture was stirred under nitrogen at room temperature overnight. The reaction mixture was then quenched with methanol (5 mL) producing bubbles. The solvent was removed under reduced pressure and the residue was dissolved in dichloromethane (40 mL) and dilute HCl (40 mL, 1 M). The layers were separated, and the aqueous layer was extracted a further two times with dichloromethane (30 mL). The combined cloudy yellow organic extracts were dried ($MgSO_4$), and solvent removed under reduced pressure to give a yellow solid residue. The yellow solid was triturated with methanol (20 mL) to give pure (17) an off-white solid (1.09 g, 78%), mp 183-194 °C (lit.[158] 197-199 °C); ^{1}H NMR ($CDCl_3$) δ 0.99 (t, J = 7.5 Hz, 12 H, CH_2CH_3), 1.92 (apparent sxt, 8 H, CH_2CH_3), 3.15, 4.46 (AB, J = 13.3 Hz, 2 × 4 H, $ArCH_2Ar$), 3.85 (t, J = 7.5 Hz, 8 H, OCH_2), 6.52-6.64 (m, 12 H ArH).

2.5.7.2 5,11,17,23-Tetrabromo-25,26,27,28-tetrapropoxycalixarene (18)
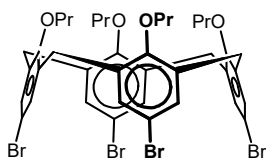
The calixarene was prepared as described in literature.[151] To a slightly yellow solution of (17) (0.86 g, 1.46 mmol) partially dissolved in butanone (10 mL) was added light-yellow N-bromosuccinimide (1.68 g, 9.44 mmol). The resultant mixture was dark yellow with a white precipitate, which warmed slightly, and within 7 minutes became clear yellow. After stirring under nitrogen at room temperature for 24 hours, the reaction was stopped by the addition of sodium hydrogensulfite solution (2 mL, 40%), turning the mixture cloudy with ppt and slight warming. The quenched reaction mixture was stirred for 10 minutes, then extracted with dichloromethane (3 × 20 mL) and dilute HCl (20 mL, 1 M). The combined yellow-coloured organic extracts were dried ($MgSO_4$) and solvent removed to give a white-yellow solid. The white-yellow solid was triturated with methanol (10 mL), then washed with ethanol (3 × 4 mL) to give pure (18) as an off-white solid (1.30 g, 98%): mp 272-279 °C (lit.[84] 280-282 °C); ^{1}H

NMR (CDCl$_3$) δ 0.97 (t, J = 7.5 Hz, 12 H, CH$_2$CH_3), 1.87 (apparent sxt, 8 H, CH_2CH$_3$), 3.08, 4.35 (AB, J = 13.4 Hz, 2 × 4 H, ArCH_2Ar), 3.80 (t, J = 7.6 Hz, 8 H, OCH_2), 6.80 (s, 8 H ArH).

2.5.7.3   5,17-Dibromo-25,26,27,28-tetrapropoxycalixarene (19)
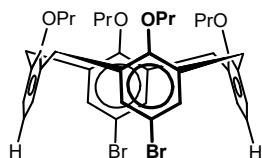
The bromine-lithium exchange reaction was conducted according to literature procedures.[84, 151] To a clear light-yellow solution of calixarene **(18)** (0.422 g, 0.465 mmol) in anhydrous tetrahydrofuran (5 mL) was rapidly added butyllithium (1.2 mL, ~1.6 M, 1.9 mmol) with rapid stirring while under nitrogen at -84 °C. The solution immediately turned dark orange and was stirred for 15 minutes at the same conditions. The reaction mixture was quenched with methanol (0.50 mL) and stirred for 10 minutes at the same conditions. The reaction mixture was then extracted with dichloromethane (3 × 10 mL) and dilute HCl (10 mL, 1 M). The organic extracts were combined, dried (MgSO$_4$) and solvent removed under reduced pressure to give an off-white, yellowish crystalline solid as the crude product. The crude product was triturated with methanol to give **(19)** as a white, slightly-yellowish solid (0.325 g, 93%): mp 220-238 °C (lit.[84] 243-245 °C); ^{1}H NMR (CDCl$_3$) δ 0.99 (t, J = 7.5 Hz, 6 H, CH$_2$CH_3), 1.00 (t, J = 7.5 Hz, 6 H, CH$_2$CH_3), 1.84-1.98 (m, 8 H, CH_2CH$_3$), 3.12, 4.41 (AB, J = 13.4 Hz, 2 × 4 H, ArCH_2Ar), 3.82 (t, J = 7.5 Hz, 4 H, OCH_2), 3.84 (t, J = 7.5 Hz, 4 H, OCH_2), 6.64 (apparent s, 6 H ArH), 6.78 (s, 4 H ArH).

2.5.7.4   Preparation of anhydrous nitric acid

Preparation of anhydrous nitric acid: concentrated sulfuric acid (32 mL, 98%) was added to potassium nitrate (23 g, 0.23 mol) to give a clear colourless solution, which was distilled to give anhydrous nitric acid (12.4 g, 86%) as a yellow liquid.

2.5.7.5   5,17-Dibromo-22,23-dinitro-25,26,27,28-tetrapropoxycalixarene (20)
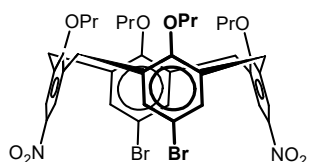
To a mixture of calixarene **(19)** (0.069 g, 0.0919 mmol), claycop (0.109 g) and acetic anhydride (0.276 mL, 0.299 g, 2.92 mmol) in dichloromethane (4 mL) was added fuming anhydrous HNO$_3$ (1 drop) while stirring at room temperature, immediately darkening the reaction mixture. After 20 minutes stirring at room temperature open to air, the reaction was monitored by TLC, and more anhydrous HNO$_3$ (2 drops) was added as necessary. Once the reaction was complete, the turquoise-green reaction mixture was

filtered, and the filtrate was washed with water (7 mL), turning yellow. The organic extract was dried (MgSO$_4$) and solvent evaporated to give a yellow solid (0.092 g) as crude product. The crude product was purified by preparative TLC (toluene) to give pure, previously unreported product **(20)** as a mainly colourless solid (0.016 g, 21%), which could be recyrstallised to give off-white needles: 273-274 °C (CHCl$_3$/MeOH); ^{1}H NMR (CDCl$_3$) δ 0.99 (t, J = 7.5 Hz, 6 H, CH$_2$C*H$_3$*), 1.00 (t, J = 7.5 Hz, 6 H, CH$_2$C*H$_3$*), 1.80-1.98 (m, 8 H, C*H$_2$*CH$_3$), 3.25, 4.44 (AB, J = 13.7 Hz, 2 × 4 H, ArC*H$_2$*Ar), 3.79 (t, J = 7.5 Hz, 4 H, OC*H$_2$*), 3.98 (t, J = 7.6 Hz, 4 H, OC*H$_2$*), 6.76 (s, 4 H Ar*H*), 7.63 (s, 4 H Ar*H*); ^{13}C NMR (CDCl$_3$) δ 10.2, 10.4 (CH$_2$*C*H$_3$), 23.3, 23.4 (*C*H$_2$CH$_3$), 31.1 (Ar*C*H$_2$Ar), 77.5, 77.6 (O*C*H$_2$), 115.9 (*C*, Ar), 124.0, 131.5 (*C*H, Ar), 135.7, 136.2, 142.8, 155.3, 162.3 (*C*, Ar). Found: C, 57.28; H, 5.27; N, 3.34; C$_{40}$H$_{44}$Br$_2$N$_2$O$_8$; requires C, 57.15; H, 5.28; N, 3.33%.

2.5.7.6 5,17-Diamino-22,23-dibromo-25,26,27,28-tetrapropoxycalixarene (21)
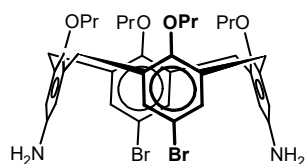
The procedure by Timmerman et al. served as a guide.[143] To a mixture of calixarene **(20)** (0.106 g, 0.126 mmol), and hydrazine monohydrate (0.54 mL) in methanol was added a spatula tip (~ 0.1 g wet slurry) of Raney nickel, immediately producing small bubbles. The mixture was heated at reflux under nitrogen overnight. The reaction was monitored by TLC, and more Raney nickel and hydrazine monohydrate were added as necessary. Once the reaction has been completed, the reaction mixture was filtered through celite with methanol rinsing, and the solvent was removed under reduced pressure from the filtrate. The residue which was dissolved in dichloromethane (20 mL) and washed with NaHCO$_3$ (3 × 20 mL, 5%). The organic layer was dried (MgSO$_4$) and solvent removed under reduced pressure to give pure, previously unreported product **(21)** as a yellow glassy amorphous solid (0.099 g, ~100%) which could not be crystallised: ^{1}H NMR (CDCl$_3$) δ 0.97 (t, J = 7.4 Hz, 6 H, CH$_2$C*H$_3$*), 0.98 (t, J = 7.4 Hz, 6 H, CH$_2$C*H$_3$*), 1.78-1.97 (m, 8 H, C*H$_2$*CH$_3$), 3.01, 4.34 (AB, J = 13.4 Hz, 2 × 4 H, ArC*H$_2$*Ar), 3.32 (br s, 4 H, N*H$_2$*), 3.74 (t, J = 7.5 Hz, 4 H, OC*H$_2$*), 3.82 (t, J = 7.6 Hz, 4 H, OC*H$_2$*), 5.98 (s, 4 H Ar*H*), 6.87 (s, 4 H Ar*H*); ^{13}C NMR (CDCl$_3$) δ 10.3, 10.5 (CH$_2$*C*H$_3$), 23.2 (*C*H$_2$CH$_3$), 31.0 (Ar*C*H$_2$Ar), 76.88, 76.91 (O*C*H$_2$), 114.6, 116.0, 130.8, 134.8, 137.5, 140.7, 149.7, 156.1 (Ar) (note some signals are coincident).

3 Distal functionalisation of resorcinarene by selective lithiation

The work presented in this chapter has been published in a peer reviewed journal cited below:

In this chapter, another strategy towards the key intermediary product of a distally-functionalised tetramethoxyresorcinarene (**Scheme 1.26**) is explored. In the literature, there exists a few procedures for distally-functionalising resorcinarenes. In the method by Shivanyuk et al.,[93, 94] a distally-functionalised resorcinarene was directly obtained in 53% yield through regioselective tetratosylation of octahydroxyresorcinarene (**Scheme 1.21**). However, this method excludes the tetramethoxyresorcinarene because four of the hydroxy groups have already been alkylated. Aside from this work, in the literature there is one other main strategy for distally-functionalising a resorcinarene – that is by selective lithiation (**Scheme 3.1**) as reported by Arnott and co-workers.[111]
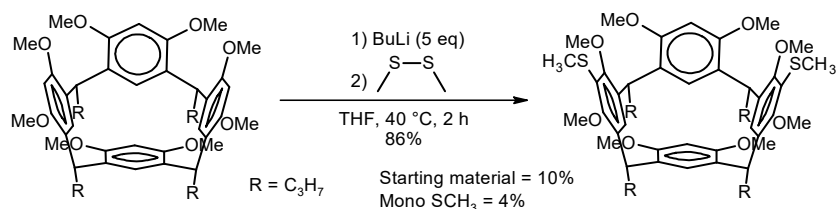
Scheme 3.1 Partially selective distal functionalisation at the wider rim of octamethoxyresorcinarene.

This direct lithiation method is similar to the selective bromine-lithium exchange by Larsen and Jørgensen on calixarenes (**Scheme 1.11**),[84] as well as by Sherburn and co-workers on cavitands.[108-110] But in contrast, the lithiation by Arnott and co-workers is not a bromine–lithium exchange, and thus does not require a brominated resorcinarene.

93

In this direct lithiation method, octamethoxyresorcinarene was lithiated using butyllithium, then quenched with dimethyldisulfide to give a thioether, which enabled elucidation of the result by ^{1}H NMR spectroscopy of the crude mixture. The lithation under various conditions was investigated with variation of the reaction solvent, number of equivalents of butyllithium, lithiation time and temperature. Using five equivalents of butyllithium in THF at a temperature of 40 °C for 2 hours, the best yield of 86% for the distal product was achieved, albeit the presence of unreacted starting material and mono product. The lithation under these optimal conditions was also demonstrated to work with other electrophiles, such as carbon dioxide, to give useful functional groups, while still retaining a good yield for the distal product. It was hypothesised that the distal selectivity was the result of the randomly-lithiated species equilibrating to the distally-lithiated intermediate which was presumably the most thermodynamically stable.[111]

The first step to prepare tetramethoxyresorcinarene for the lithiation is to protect all four hydroxy groups with a protecting group that would be stable under the lithation conditions (**Scheme 3.2**).
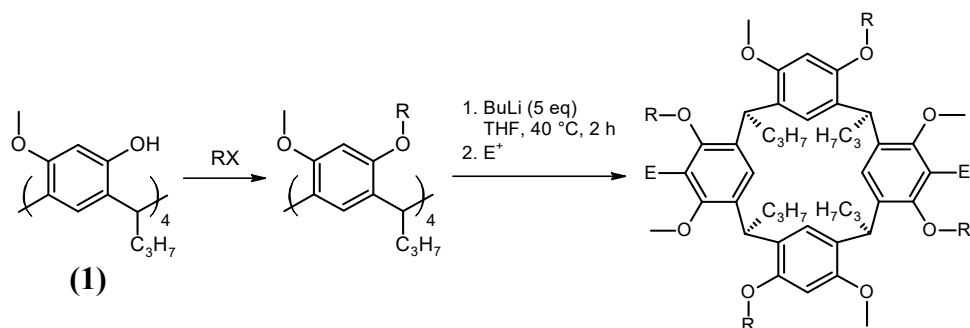
Scheme 3.2 Investigation into the distal-lithiation of various *O*-protected resorcinarene derivatives.

3.1 Benzyl ether

The protecting group first chosen was the benzyl ether. Benzyl ethers are known to be fairly robust, pH stable, and are usually only cleavable by reduction to return the alcohol. Furthermore, benzyl bromide is relatively safe to use and was readily available. Reaction of the starting resorcinarene **(1)** with benzyl bromide, sodium hydride and tetrahydrofuran furnished the desired tetrabenzyloxyresorcinarene **(22)** in a good yield and purity after recrystallisation (**Scheme 3.3**). Evidence of the benzyl ether was provided by NMR spectroscopy, which showed the benzylic protons as an

AB pattern at 4.70 and 4.94 ppm on the ^{1}H NMR spectrum, while the benzylic carbon appeared on the ^{13}C NMR spectrum at 71.1 ppm (**Appendix A – 21**).
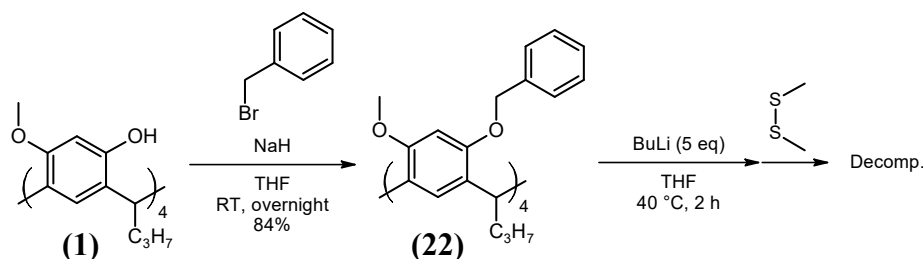
Scheme 3.3 Protection of resorcinarene phenols with benzyl ethers and attempted distal lithiation.

With tetrabenzyloxyresorcinarene **(22)** in hand, the lithiation was then performed according to the same conditions as described by Arnott and co-workers, with quenching with dimethyldisulfide. Unfortunately, TLC did not show any well-defined spots and the ^{1}H NMR spectrum of the quenched reaction mixture indicated the resorcinarene peaks as broad humps, with multiple methoxy and aromatic signals. The benzyl ether was still apparent by a broad hump from 6.7 to 7.7 ppm. This complex mixture suggests that the benzyl ether was not as robust as thought. A protecting group that would be more stable under the strongly basic lithiation conditions may perhaps provide success.

3.2 Methoxymethyl ether

The methoxy methyl (MOM) protecting group, when functionalised to a phenol, is known to direct lithiation to the *ortho* position of the aromatic ring.[159, 160] MOM protecting groups can be easily removed by acid-catalysed hydrolysis. Therefore, the MOM protecting group is an ideal candidate for this application. However, the main issue is the safety of methoxymethyl halides,[161] which is required for synthesising the MOM ether of the phenol. Nevertheless, the reaction of **(1)** with methoxymethyl bromide under standard sodium hydride / THF conditions afforded the target product **(23)** in excellent purity in quantitative yield without any formal purification (**Scheme 3.4**). NMR spectroscopy confirmed the MOM ether resorcinarene by an additional methoxy peak appearing on both ^{1}H and ^{13}C spectra (**Appendix A – 22**). The acetal was evidenced by the AB at 4.84 and 4.73 ppm on the ^{1}H spectrum, as well as the CH$_2$ peak at 95.8 ppm on the DEPT-135 spectrum.
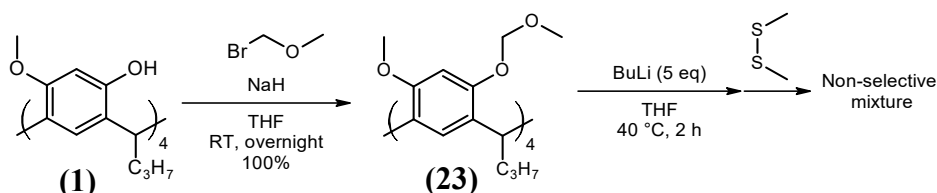
Scheme 3.4 Protection of resorcinarene phenols with methoxymethyl ethers and attempted distal lithiation.

The lithiation was performed on resorcinarene **(23)** as per the literature, but yielded a complex mixture of six compounds as indicated by TLC ($R_{f(EtOAc/Petrol\ 4:6)}$) = 0.71, 0.63, 0.48, 0.38, 0.31, 0. 19, **Figure 3.1**). Doubling the amount of butyllithium from five to ten equivalents also produced the same result, but with the least retained spot on TLC becoming darker. The crude products from the reactions with five and ten equivalents were combined, and the six compounds were separated sufficiently by preparative TLC to enable identification of each compound by ^{1}H NMR spectroscopy. The structures of the six compounds were tentatively assigned by analysis of their ^{1}H NMR spectra, based principally on symmetry and integration data. The ^{1}H NMR data suggested that the six compounds obtained were the five possible products plus the starting material (**Scheme 3.5**). The ^{1}H NMR data (**Appendix A – 23**), together with the isolated yields and assignments are summarised in **Table 3.1**.
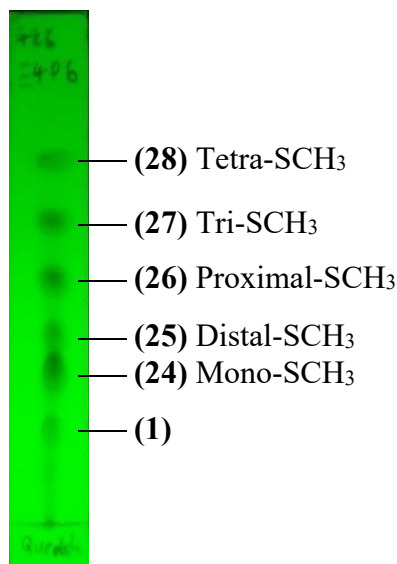
Figure 3.1 TLC ($R_{f(EtOAc/Petrol\ 4:6)}$) of the quenched reaction mixture from the lithiation of **(23)** with 10 equivalents of butyllithium.

96
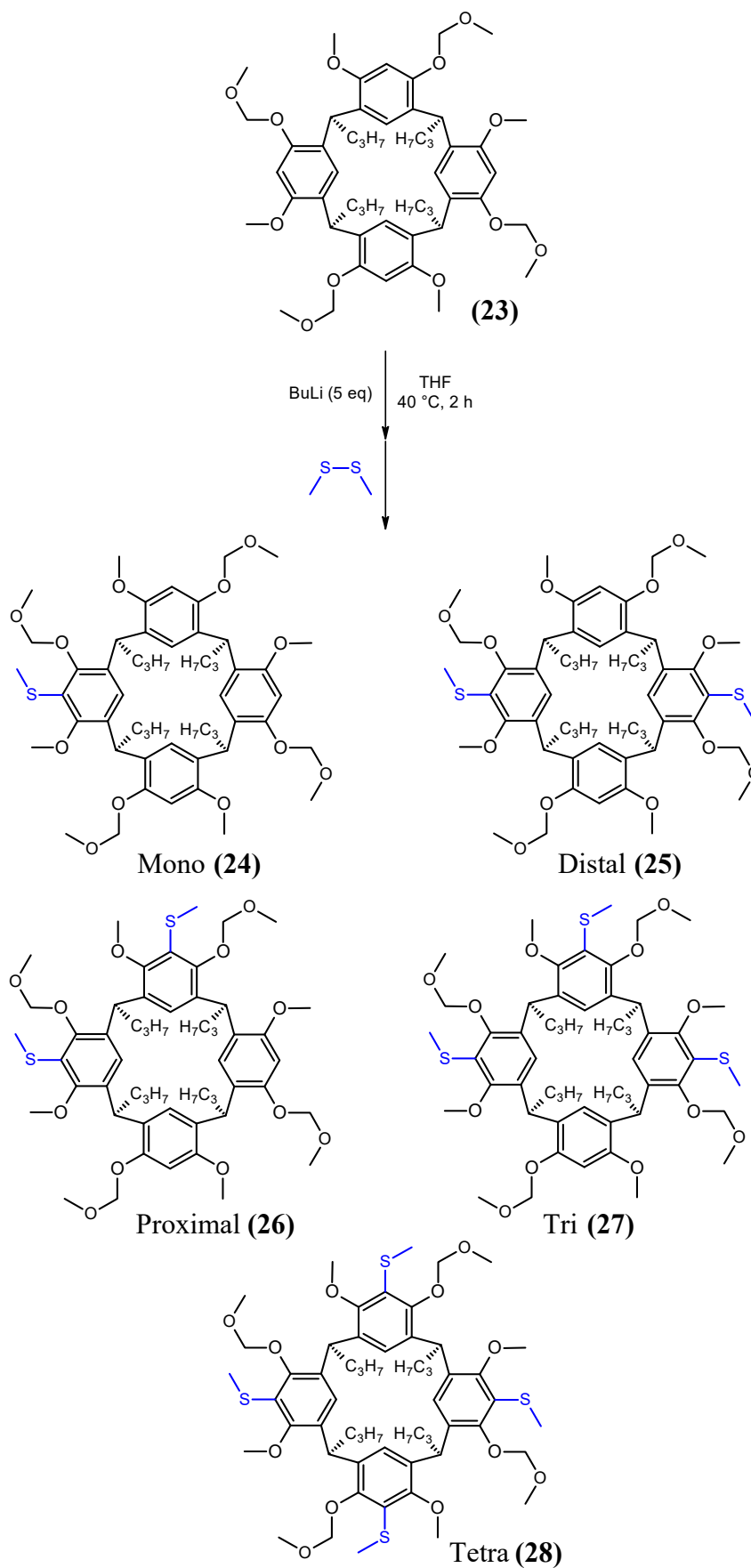
Scheme 3.5 Lithiation of MOM resorcinarene produces the five possible SCH_3 resorcinarene products.

Table 3.1 Summary of key ^{1}H NMR spectroscopic data of SCH$_3$ resorcinarene products recorded in CDCl$_3$. Chemical shifts are listed in ppm. R$_f$ (EtOAc/Petrol 4:6).

R$_f$	SCH$_3$	ArH	SCH$_3$ resorcinarene	Symmetry	Isolated yield (%)
0.71	2.34	6.68	Tetra **(28)**	C$_4$	0.9
0.63	2.28, 2.43*	6.35, 6.38, 6.42, 6.93, 6.95	Tri **(27)**	C$_s$	3.6
0.48	2.32, 2.39	6.46, 6.49, 6.53, 6.55, 6.77, 6.78	Proximal **(26)**	C$_s$	8.1
0.38	2.42	6.38, 6.44, 6.94	Distal **(25)**	C$_2$	4.4[#]
0.31	2.37	6.48, 6.49, 6.51, 6.59, 6.63, 6.69, 6.70	Mono **(24)**	C$_s$	27.5[#]
0.19	None	6.36, 7.25	**(1)**	C$_4$	14.6

*Coincidental peaks, integration is double
[#]The yields for distal di-SCH$_3$ resorcinarene and mono-SCH$_3$ are not accurate, since both were not completely separated.

The signals in the ^{1}H NMR spectra, which provided clear indicators for assigning the products were the SCH$_3$ and the aromatic signals. The distal product **(25)**, having C$_2$ rotational symmetry, would have half the peaks compared to its asymmetrical proximal isomer **(26)**. The appearance of many peaks indicated an absence of rotational symmetry in the product. These asymmetrical products – tri **(27)**, proximal **(26)**, and mono **(24)** – could be distinguished from each other by the number of ArH and SCH$_3$ signals. For example, tri **(27)**, having three SCH$_3$ replacing three ArH, would have three less ArH from the original eight, which would result in five ArH peaks. Therefore, based on the number and integration of these signals, together with symmetry considerations, the particular SCH$_3$ resorcinarene product could be assigned for each spectrum. For all isolated products, the retention of the MOM protecting group through the lithiation was confirmed by the pairs of AB doublets around 4.2-5.2 ppm and the corresponding extra methoxy singlet in all ^{1}H NMR spectra.

It is clear from the results that distal di-SMe resorcinarene is not the main product. In efforts to optimise the yield for the target distal product, the lithiation was attempted under milder conditions, at room temperature overnight, but only returned unreacted starting resorcinarene. The lithiation was also attempted with *sec*-butyllithium, a stronger base, but yielded similar results as with butyllithium. From the results, it is clear that the lithiation of resorcinarene methoxymethyl ether **(23)** is not a viable

method for obtaining a distally-functionalised resorcinarene due to the lack of selectivity and difficulty of separation.

3.3 Ethyl ether

Finally, for the purpose of simply testing the applicability of the lithation procedure on this particular tetramethoxyresorcinarene, the ethyl ether was chosen. The ethyl ether would not be readily cleavable to recover the phenol and has no functional value. Furthermore, as the methyl and ethyl groups are of similar size, and chirality influence would be minimal. However, it was for this similarity that the ethyl ether was chosen; to liken the resorcinarene to the literature octamethoxyresorcinarene, while retaining its characteristic C_4 symmetry.

The tetraethylation of resorcinarene **(1)** under standard sodium hydride / THF conditions did not proceed to completion despite using up to 30 equivalents of iodoethane and subjecting the mixture to reaction again. However, changing the reaction solvent to dimethylformamide conveniently furnished the target product **(29)** in good yield and purity (**Scheme 3.6**). The ethoxy group was confirmed by ^{1}H NMR spectroscopy as a multiplet overlapped with the methoxy singlet, and an additional triplet in the hydrocarbon region (**Appendix A – 25**). The methyleneoxy carbon was accounted for on the DEPT-135 spectrum by the CH_2 peak at 64.9 ppm.
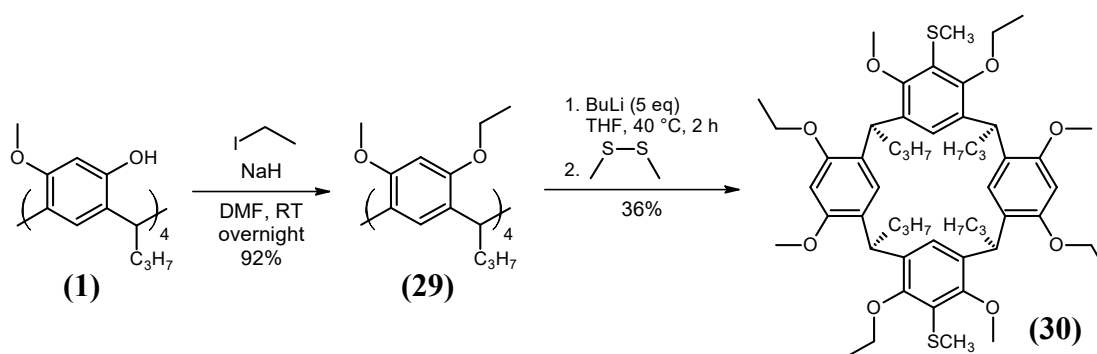
Scheme 3.6 Ethylation of resorcinarene phenols and subsequent distal lithiation.

The ethoxy derivative **(29)** was then subjected to the same lithiation procedure to give a single product along with unreacted starting resorcinarene, as indicated by TLC. The product was successfully separated by column chromatography to afford the target product **(30)** in yield of 36%. ^{1}H NMR spectroscopy of the pure product conclusively showed a C_2-symmetrical resorcinarene product with a single SCH_3 peak at 2.42 ppm and three peaks in the aromatic region with the same integration (**Appendix A – 26**).

The correct number of peaks for target product **(30)** was present on the ^{13}C NMR spectrum, with the SCH$_3$ peak being identified as the peak at 18.3 ppm according to HSQC spectroscopy. Therefore, this experiment with the ethoxy functionalised resorcinarene proved that the lithiation for octamethoxyresorcinarene was applicable to this chiral resorcinarene. However, from this limited investigation it is apparent that the phenols needed to be alkylated with a group with close likeness to a methoxy group.

The selective distal lithiation of three novel C$_4$ symmetric *O*-substituted derivatives of tetramethoxyresorcinarene was investigated. These included the benzyloxy, the MOM and the ethoxy derivatives of tetramethoxyresorcinarene. Lithiation, followed by quenching with dimethyldisulfide gave very different results for the three derivatives. The benzyloxy derivative gave a complex mixture that could not be resolved. The lithiation on the MOM ether resorcinarene **(23)** gave a mixture of the five possible products, as well as unreacted starting resorcinarene. Separation of the five products was not complete, but the isolated compounds were sufficiently pure for tentative characterisation. The most abundant product was the mono-SMe **(24)** which was recovered in approximately 28% yield, while the distal-SMe **(25)** was recovered in a minor yield of about 4%. The lithiation with ethoxyresorcinarene **(29)** selectively produced the distal-SMe product **(30)** in 36%, after separation of unreacted starting resorcinarene. This served as a proof of concept that the selective distal lithiation was applicable to C$_4$ symmetric tetramethoxyresorcinarene, albeit with an *O*-substituent with close similarity to a methoxy. Perhaps the tetrahydroxy functionality of the distal-SMe resorcinarene **(30)** could be restored by selective removal of the methoxy groups to hydroxy groups. The reaction conditions to accomplish this selective demethylation has been reported for calixcrowns[48] and may be a worthwhile future investigation. In conclusion, these results suggest that the selective distal lithiation is not very robust, with the distal selectivity being dramatically affected by the *O*-substituents on the resorcinarene.

3.4 Experimental

3.4.1 General reaction procedure for *O*-alkylation of resorcinarene (1)

Resorcinarene **(1)** (1 eq) was added to a mixture of washed sodium hydride (10-20 eq, 60% in oil) and a couple of crystals of imidazole in anhydrous tetrahydrofuran, and the resultant mixture was stirred under nitrogen at room temperature for 30 minutes. To this white slurry was added the relavent alkyl halide (10-20 eq), and the cloudy white reaction mixture was stirred overnight at room temperature, under nitrogen. The work up and purification is specific for each resorcinarene derivative.

3.4.1.1 $1^4,3^6,5^6,7^6$-tetrabenzyloxy-$1^6,3^4,5^4,7^4$-tetramethoxy-2,4,6,8-tetrapropylresorcin[4]arene (22)
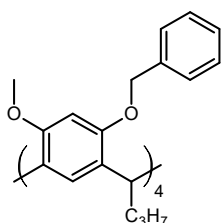
The general reaction procedure was applied with resorcinarene **(1)** (0.50 g, 0.703 mmol), sodium hydride (1.07 g, 60% in oil, 0.64 g, 26.8 mmol), anhydrous tetrahydrofuran (25 mL), and benzyl bromide (1.69 mL, 1.21 g, 14.0 mmol). After stirring overnight, the reaction mixture was cooled in an ice bath and carefully quenched with water, producing bubbles. More water was added, and the solvents were removed under reduced pressure (rotavap up to 65°C). The yellow residue was dissolved in dichloromethane, and the organic layer was washed with water, separated and evaporated to give the crude product as a yellow crystalline solid (0.88 g). The crude product was dissolved in minimum dichloromethane; then methanol was added so that the product remained dissolved. The yellow solution was gently boiled to remove dichloromethane. At a certain point, white crystals formed in the solution, and the mixture was immediately taken off the heat and allowed to cool to room temperature. More methanol was added, and **(22)** was collected by vacuum filtration as white crystals (0.64 g, 84%): mp 188-189 °C (DCM/MeOH); ^{1}H NMR (CDCl$_3$) δ 0.91 (t, J = 7.3 Hz, 12 H, CH$_2$CH_3), 1.31 (apparent sxt, 8 H, CH_2CH$_3$), 1.79-1.96 (m, 8 H, CH_2CH), 3.40 (s, 12 H, OCH_3), 4.59 (t, J = 7.4 Hz, 4 H, CHCH$_2$), 4.70, 4.95 (AB, J = 11.3 Hz, 8 H, OCH_2), 6.37, 6.71 (s, 2 × 4 H, ArH), 7.20-7.35 (overlapped with CDCl$_3$, m, ArH); ^{13}C NMR (CDCl$_3$) δ 14.5 (CH$_2$$CH_3$), 21.6 ($CH_2CH_3$), 35.9 ($CHCH_2$), 37.1 ($CH_2$CH), 55.6 (O$CH_3$), 71.1 (O$CH_2$), 97.8, 126.4 ($C$H, Ar), 126.5 ($C$, Ar), 127.5, 127.6, 128.3 (CH, Ar), 137.9, 155.2, 155.8 (C, Ar) (note some signals are coincident). Found: C, 80.58; H, 7.69; C$_{72}$H$_{80}$O$_8$; requires C, 80.56; H, 7.51%.

3.4.1.2 $1^4,3^6,5^6,7^6$-tetramethoxymethyl-$1^6,3^4,5^4,7^4$-tetramethoxy-2,4,6,8-tetrapropylresorcin[4]arene (23)

The general reaction procedure was applied with resorcinarene **(1)** (1.00 g, 1.40 mmol), sodium hydride (0.68 g, 60% in oil, 0.409 g, 17.0 mmol), anhydrous tetrahydrofuran (8 mL), and bromomethyl methyl ether (0.345 mL, 1.76 g, 14.1 mmol). After stirring overnight, the reaction mixture was then quenched with methanol (2 mL) till bubbling ceased, and was then stirred for 45 minutes at room temperature. The solvent was removed under reduced pressure, and the residue was dissolved in dichloromethane (30 mL) and dilute sodium hydroxide solution (20 mL, 1 M) to give a cloudy light yellow organic layer and a clearer dark yellow aq layer. The layers were separated, and the aqueous layer was extracted with dichloromethane (10 mL) to give a clear colourless extract. The combined cloudy organic extracts were dried (MgSO$_4$), and solvent removed under reduced pressure to give pure **(23)** as a beige-coloured solid (1.36 g, ~100%): mp 149-150 °C (CHCl$_3$/MeOH); ^{1}H NMR (CDCl$_3$) δ 0.92 (t, J = 7.3 Hz, 12 H, CH$_2$C*H$_3$*), 1.35 (apparent sxt, 8 H, C*H$_2$*CH$_3$), 1.82 (apparent q, 8 H, C*H$_2$*CH), 3.34 and 3.63 (2s, 2 × 12 H, OC*H$_3$*), 4.51 (t, J = 7.5 Hz, 4 H, C*H*CH$_2$), 4.73, 4.85 (AB, 8 H, J = 6.4 Hz, OC*H$_2$*O), 6.48, 6.66 (s, 2 × 4 H, Ar*H*); ^{13}C NMR (CDCl$_3$) δ 14.4 (CH$_2$*C*H$_3$), 21.3 (*C*H$_2$CH$_3$), 35.3 (*C*H$_2$CH), 37.4 (*C*HCH$_2$), 55.7, 55.8 (O*C*H$_3$), 95.8 (O*C*H$_2$O), 100.1, 126.1 (*C*H, Ar), 127.0, 127.5, 153.6, 155.6 (*C*, Ar). Found: C, 70.16; H, 8.19; C$_{52}$H$_{72}$O$_{12}$; requires C, 70.24; H, 8.16%.

3.4.1.3 $1^4,3^6,5^6,7^6$-tetraethoxy-$1^6,3^4,5^4,7^4$-tetramethoxy-2,4,6,8-tetrapropylresorcin[4]arene (29)

The general reaction procedure was applied with resorcinarene **(1)** (0.101 g, 0.142 mmol), sodium hydride (0.103 g, 60% in oil, 0.062 g, 2.58 mmol), anhydrous dimethylformamide (25 mL), and iodoethane (0.168 mL, 0.328 g, 2.10 mmol). After stirring overnight, the cloudy reaction mixture was quenched with water, producing bubbles. Then water (50 mL) was added, the white precipitate was filtered, and washed with more water. The filtered white precipitate was washed off the funnel with dichloromethane, and the solvent was removed under reduced pressure. The resultant residue was placed in an oven (140°C) for 5 minutes to remove water, and furnish pure **(29)** as a white solid (0.106 g, 92%): mp 206-208 °C (EtOAc); ^{1}H NMR (CDCl$_3$) δ 0.93 (t, J = 7.3 Hz, 12 H, CH$_2$CH$_2$C*H$_3$*), 1.18 (t, J = 7.0 Hz, 12 H, OCH$_2$C*H$_3$*), 1.37 (m, 8 H, C*H$_2$*CH$_3$), 1.82 (apparent q, 8 H,

CH_2CH), 3.59 (s, 12 H, ArOCH_3), 3.60-3.69 and 3.85-3.98 (2m, 2 × 4 H, OCH_2CH$_3$), 4.51 (t, J = 7.5 Hz, 4 H, CHCH$_2$), 6.29, 6.63 (s, 2 × 4 H, ArH); ^{13}C NMR (CDCl$_3$) δ 14.5, 15.0 (CH$_2$$CH_3$), 21.3 ($CH_2CH_3$), 35.2 ($CHCH_2$), 37.2 ($CH_2$CH), 55.9 (O$CH_3$), 64.9 (O$CH_2$), 98.1, 126.1 ($C$H, Ar), 126.6, 126.8, 155.3, 155.7 (C, Ar). Found: C, 75.66; H, 9.11; C$_{72}$H$_{80}$O$_8$; requires C, 75.69; H, 8.80%.
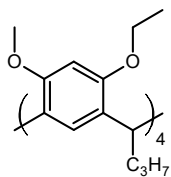
3.4.2 Distal lithiation

3.4.2.1 Attempted synthesis of 1^4,3^6,5^6,7^6-tetrabenzyloxy-1^6,3^4,5^4,7^4-tetramethoxy-1^5,5^5-di(methylthio)-2,4,6,8-tetrapropylresorcin[4]arene by selective distal lithiation

The synthesis was performed according to the procedure by Arnott et al.[111] To a clear colourless solution of resorcinarene benzyl ether **(22)** (0.050 g, 0.0503 mmol) in anhydrous tetrahydrofuran (5 mL) at room temperature was added butyllithium (0.16 mL, 1.6 M, 0.256 mmol). The clear colourless solution immediately turned bright yellow, then dark yellow, then orange, then dark orange. The reaction mixture was stirred at 40 °C under nitrogen for 2 h. Upon heating, the reaction mixture became very dark opaque brown, eventually turning black after 10 minutes at 40 °C. At the end of 2 hours, the reaction mixture appeared to be opaque dark brown, perhaps not as black. The reaction mixture was then quenched by the addition of dimethyl disulfide (45 μL, 0.50 mmol), rapidly turning clear light yellow. The quenched reaction mixture was then stirred at 40 °C under nitrogen for 3 h. The solvent was evaporated to give a dark reddish solid. TLC indicated multiple streaked spots around the baseline that were of significantly lower R$_f$ compared to the starting resorcinarene. ^{1}H NMR showed the resorcinarene signals as broad humps, indicating decomposition of the resorcinarene.

3.4.2.2 Synthesis of 1^4,3^6,5^6,7^6-tetramethoxy-1^6,3^4,5^4,7^4-tetramethoxymethyl-1^5,5^5-di(methylthio)-2,4,6,8-tetrapropylresorcin[4]arene by selective distal lithiation

The synthesis was performed based on the procedure by Arnott et al.[111] To a clear colourless solution of resorcinarene methoxymethyl ether **(23)** (0.0497 g, 0.0559 mmol) in anhydrous tetrahydrofuran (5 mL) at 40 °C was added dropwise butyllithium (0.18 mL, 1.6 M, 0.288 mmol). The clear slightly yellow solution rapidly turned clear dark yellow. The reaction mixture was allowed to stir at 40 °C under nitrogen for 2 hours, appearing to be the same throughout. The reaction mixture was quenched by the addition of dimethyldisulfide (0.053 mL, 0.589 mmol), and was stirred under nitrogen, at 40 °C for 20 minutes. The tetrahydrofuran solvent was then removed under

reduced pressure to give a slightly yellow solid, which appeared as a mixture of resorcinarenes by ^{1}H NMR spectroscopy, and of at least five compounds by TLC. The synthesis was repeated at the same scale (0.046 g, 0.052 mmol) with double the amount of butyllithium (0.33 mL, 1.6 M, 0.528 mmol, 10 eq), giving a similar crude product with a sixth spot clearly visible by TLC. The two crude products were combined (0.093 g) and subjected to preparative TLC (EtOAc – petroleum spirits 40:60). Compounds were sufficiently separated to be clearly identified by ^{1}H NMR spectroscopy as: tetra-SCH$_3$ **(28)** (0.001 g, 0.9%), tri-SCH$_3$ **(27)** (0.004 g, 3.6%), proximal-SCH$_3$ **(26)** (0.009 g, 8.1%), distal-SCH$_3$ **(25)** (0.005 g, 4.4%), mono-SCH$_3$ **(24)** (0.028 g, 27.5%), and starting resorcinarene **(1)** (0.014 g, 14.6%).
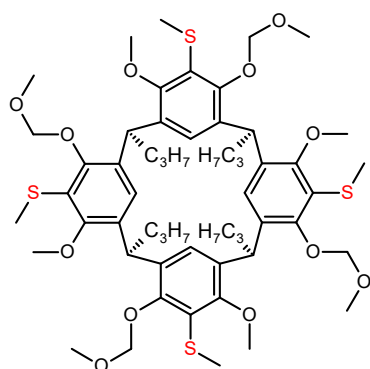
Tetra-SCH$_3$ resorcinarene **(28)**: ^{1}H NMR (only relevant signals quoted, CDCl$_3$) δ 0.92 (t, J = 7.3 Hz, 12 H, CH$_2$CH_3), 1.27-1.38 (m, 8 H, CH_2CH$_3$), 1.76-1.91 (m, 8 H, CH_2CH), 2.34 (s, 12 H, SCH_3), 3.55, 3.64 (2s, 2 × 12 H, OCH_3), 4.63 (t, J = 7.5 Hz, 4 H, CHCH$_2$), 4.89, 5.04 (AB, J = 4.8 Hz, 8 H, OCH_2O), 6.68 (s, 4 H, ArH).
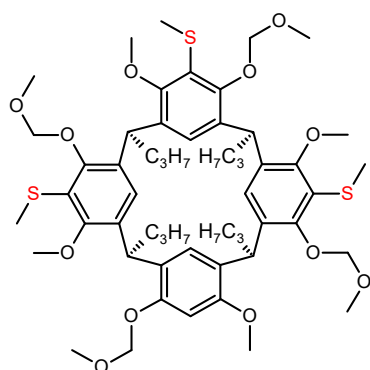
Tri-SCH$_3$ resorcinarene **(27)**: ^{1}H NMR (only relevant signals quoted, CDCl$_3$) δ 0.77-1.02 (m, 12 H, CH$_2$CH_3), 1.19-1.48 (m, 8 H, CH_2CH$_3$), 1.59-1.97 (m, 8 H, CH_2CH), 2.28, 2.43 (2s, 3 H, 6 H, SCH_3), 3.25, 3.36, 3.45, 3.54, 3.64, 3.65, 3.80, 3.85 (8s, 8 × 3 H, OCH_3), 4.20, 4.63 (AB, J = 4.7 Hz, OCH_2O), 4.46-4.56, 4.54-4.62 (m, 2 × 2 H, CHCH$_2$), 4.85, 4.90 (AB, J = 6.7 Hz,

2 H, OCH_2O), 5.00 (d, J = 4.7 Hz, 1 H, OCH_2O), 5.05 (d, J = 4.7 Hz, 1 H, OCH_2O), 5.17 (d, J = 4.7 Hz, 1 H, OCH_2O), 5.19 (d, J = 4.7 Hz, 1 H, OCH_2O), 6.35, 6.38, 6.42, 6.93, 6.95 (5s, 5 × 1 H, ArH).
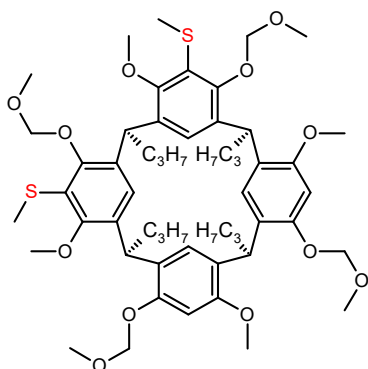
Proximal-SCH₃ resorcinarene **(26)**: ^{1}H NMR (only relevant signals quoted, CDCl₃) δ 0.87-0.98 (m, 12 H, CH₂C*H₃*), 1.23-1.45 (m, 8 H, C*H₂*CH₃), 1.73-1.92 (m, 8 H, C*H₂*CH), 2.32, 2.39 (2s, 2 × 3 H, SC*H₃*), 3.31, 3.44, 3.49, 3.58, 3.65, 3.69 (6s, 3 H, 3 H, 6 H, 6 H, 3 H, 3 H, OC*H₃*), 4.37 (d, *J* = 4.4 Hz, 1 H, OC*H₂*O), 4.45-4.61 (m, 4 H, C*H*CH₂), 4.70 (d, *J* = 5.0 Hz, 1 H, OC*H₂*O), 4.85 (d, *J* = 4.5 Hz, 1 H, OC*H₂*O), 4.90-4.99 (m, 3 H, OC*H₂*O), 5.04 (s, 2 H, OC*H₂*O), 6.46, 6.49, 6.53, 6.55, 6.77, 6.78 (6s, 6 × 1 H, Ar*H*).
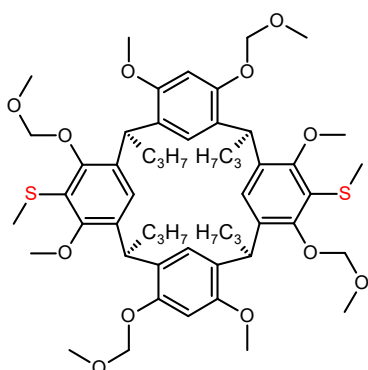
Distal-SCH₃ resorcinarene **(25)**: ^{1}H NMR (only relevant signals quoted, CDCl₃) δ 0.91 (t, *J* = 6.7 Hz, 6 H, CH₂C*H₃*), 0.94 (t, *J* = 6.8 Hz, 6 H, CH₂C*H₃*), 1.19-1.50 (m, 8 H, C*H₂*CH₃), 1.72-1.97 (m, 8 H, C*H₂*CH), 2.42 (s, 6 H, SC*H₃*), 3.18, 3.55, 3.65, 3.80 (4s, 4 × 6 H, OC*H₃*), 4.45-4.56 (m, 4 H, C*H*CH₂), 4.58, 4.73 (AB, *J* = 6.7 Hz, 4 H, OC*H₂*O), 4.96, 5.13 (AB, *J* = 4.7 Hz, 4 H, OC*H₂*O), 6.38, 6.44, 6.94 (3s, 3 × 2 H).
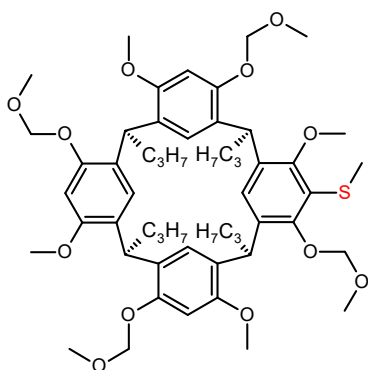
Mono-SCH₃ resorcinarene **(24)**: ^{1}H NMR (only relevant signals quoted, CDCl₃) δ 0.85-1.00 (m, 12 H, CH₂C*H₃*), 1.27-1.49 (m, 8 H, C*H₂*CH₃), 1.72-1.93 (m, 8 H, C*H₂*CH), 2.37 (s, 3 H, SC*H₃*), 3.29, 3.32, 3.40, 3.54, 3.59, 3.62, 3.63, 3.65 (8s, 8 × 3 H, OC*H₃*), 4.46-4.59 (m, 5 H, C*H*CH₂ + OC*H₂*O), 4.71 (d, *J* = 6.4 Hz, 1 H, OC*H₂*O), 4.76 (d, *J* = 6.4 Hz, 1 H, OC*H₂*O), 4.83 (d, *J* = 6.4 Hz, 1 H, OC*H₂*O), 4.87 (d, *J* = 6.4 Hz, 1 H, OC*H₂*O), 4.94 (d, *J* = 6.4 Hz, 1 H, OC*H₂*O), 4.96 (d, *J* = 6.4 Hz, 1 H, OC*H₂*O), 4.99 (d, *J* = 6.4 Hz, 1 H, OC*H₂*O), 6.48, 6.49, 6.51, 6.59, 6.63, 6.69, 6.70 (7s, 7 × 1 H, Ar*H*).

3.4.2.3 Synthesis of $1^4,3^6,5^6,7^6$-tetraethoxy-$1^6,3^4,5^4,7^4$-tetramethoxy-$1^5,5^5$-di(methylthio)-2,4,6,8-tetrapropylresorcin[4]arene (30)
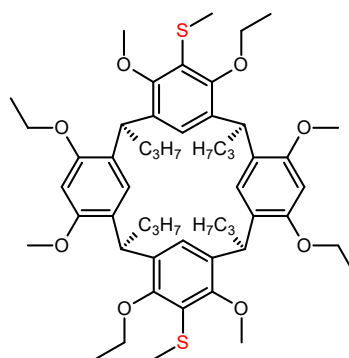
Synthesis was performed according to the procedure by Arnott et al.[111] To a clear colourless solution of resorcinarene ethyl ether **(29)** (0.050 g, 0.061 mmol) in anhydrous tetrahydrofuran (5 mL) at 40 °C was added dropwise butyllithium (0.19 mL, 1.6 M, 0.30 mmol). The clear colourless solution rapidly turned yellow. The reaction mixture was allowed to stir at 40 °C under nitrogen for 2 hours, becoming almost clear colourless after 1 h. The clear colourless reaction mixture was quenched by the addition of dimethyldisulfide (55 µL, 0.61 mmol), and was stirred under nitrogen, at 40 °C for 20 minutes. The tetrahydrofuran solvent was removed under reduced pressure from the reaction mixture to give the crude product as a white to off-white solid which turned light-brownish yellow on prolonged exposure to air. The crude product was subjected to column chromatography (EtOAc – petroleum spirits 20:80) to afford pure **(30)** as a clear colourless glassy solid (0.020 g, 36%): mp 155 °C (CHCl₃/MeOH); ^{1}H NMR (CDCl₃) δ 0.86-0.97 (m, 12 H, CH₂CH_3), 1.05 (t, $J = 7.0$ Hz, 6 H, OCH₂CH_3), 1.21-1.52 (m, 8 H, CH₂CH_2CH₃), 1.36 (t, $J = 7.0$ Hz, 6 H, OCH₂CH_3), 1.65-1.94 (m, 8 H, CHCH_2), 2.42 (s, 6 H, SCH_3), 3.43-3.58 (m, 2 H, OCH_2), 3.51 (s, 6 H, OCH_3), 3.71-3.83 (m, 2 H, OCH_2), 3.76 (s, 6 H, OCH_3), 3.83-3.95, 4.02-4.14 (2m, 2 × 2 H, OCH_2), 4.41-4.56 (m, 4 H, CHCH₂), 6.22, 6.36, 6.87 (s, 3 × 2H, ArH); ^{13}C NMR (CDCl₃) δ 14.35, 14.37, 15.0, 16.0 (CH₂CH₃), 18.3 (SCH₃), 21.51, 21.54 (CH₂CH₃), 36.66, 36.69 (CHCH₂), 37.6, 37.8 (CH₂CH), 55.3, 60.7 (OCH₃), 64.4, 68.8 (OCH₂), 97.4 (CH, Ar), 123.0, 124.2, 124.4 (C, Ar), 125.9, 126.6 (CH, Ar), 135.6, 135.8, 155.8, 156.0, 156.3, 156.9 (C, Ar). Found: C, 70.75; H, 8.41; $C_{54}H_{76}O_8S_2$ requires C, 70.70; H, 8.35%.

4 Direct distal functionalisation of resorcinarene phenols

In this chapter, another strategy for synthesising the key intermediate of a distally-functionalised tetramethoxyresorcinarene is reported. As illustrated in **Scheme 1.26**, a distally-functionalised resorcinarene is a key intermediate because it enables the resorcinarene to be distally-bridged. The aim of this strategy is to directly distally-functionalise the resorcinarene via protection of the phenols. In previous work[107] outlined in **Scheme 4.1**, this was investigated by treating starting heptyl resorcinarene **(31)** with two equivalents of butyllithium to give a resultant precipitate mixture to which was added *tert*-butyldimethylsilyl chloride (TBDMS-Cl).
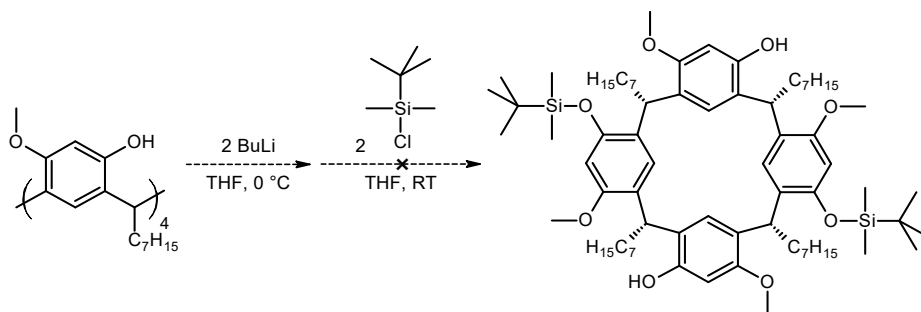
Scheme 4.1   Previous investigation into the direct silylation of resorcinarene phenols.[107]

A resorcinarene product was recovered in about 13% yield after partial chromatographic separation from unreacted starting resorcinarene. The resorcinarene product, having two SiCH$_3$ signals in both ^{1}H and ^{13}C NMR spectra, was initially thought to be the proximal di-TBDMS resorcinarene which would possess no rotational symmetry.[107] However, a closer look at the integration of the ^{1}H NMR spectrum clearly showed that each silicone-methyl peak had a relative integration of three hydrogens, and the *tert*-butyl peak was integrating for nine hydrogens. This integration pattern strongly suggested that the product was the mono-TBDMS resorcinarene, and this was indeed later confirmed by further work, including an NMR study which is discussed in the next section. Reaction with up to ten equivalents of butyllithium and TBDMS-Cl with propyl resorcinarene **(1)** still gave the about same proportion of mono-TBDMS product to starting resorcinarene as indicated by the integration in the ^{1}H NMR spectra of the crude mixtures (**Table 4.1**). No additional products were definitively observed in any of the TLC or ^{1}H NMR spectra of the crude mixtures. Interestingly, this lack of reaction appears to contradict a similar butyllithium reaction protocol employed by Heaney and co-workers for the

tetracamphorsulfonylation of tetramethoxyresorcinarene.[66] Nevertheless, the limited ability of the resorcinarene to react may be due to the small lithium cation of the butyllithium strongly coordinating to the phenoxide anions of the resorcinarene, forming a tight ion-pair which results in their decreased solubility and nucleophilicity. Therefore, potassium *tert*-butoxide was investigated as the base.

Table 4.1 Silylation of resorcinarenes via butyllithium. *Yields were calculated based on approximated ^{1}H NMR integration of the crude mixtures.

R = C$_3$H$_7$ **(1)**
R = C$_7$H$_{15}$ **(31)**
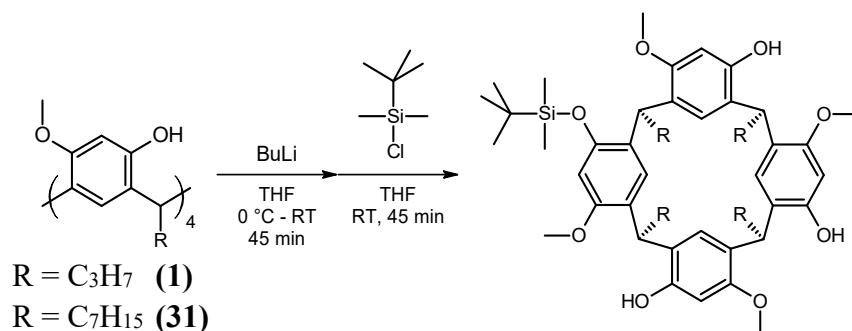
Starting resorcinarene	Eq of BuLi/TBDMS-Cl	Yield %*	
		Mono	Unreacted starting resorcinarene
(31)	2	26	74
(31)	3	28	72
(1)	2	22	78
(1)	10.7	29	71

4.1 Silylation with potassium *tert*-butoxide as base

4.1.1 TBDMS (*tert*-butyldimethylsilyl)

With potassium *tert*-butoxide as the base, a small-scale test of the silylation reaction with TBDMS-Cl in tetrahydrofuran gave a promising TLC. Despite the multiple products, the suspected target distal product spot seemed darker than the rest, with all products having good chromatographic separation. Therefore, the crude mixture was chromatographed, and complete separation of all products was achieved. The separated compounds were identified by NMR spectroscopy (**Appendix A – 28**) to be tri- (12%) **(35)**, distal di- (31%) **(34)**, proximal di- (15%) **(33)**, and mono- (28%) **(32)** TBDMS products, as well as starting resorcinarene (10%) **(1)** (**Scheme 4.2**).
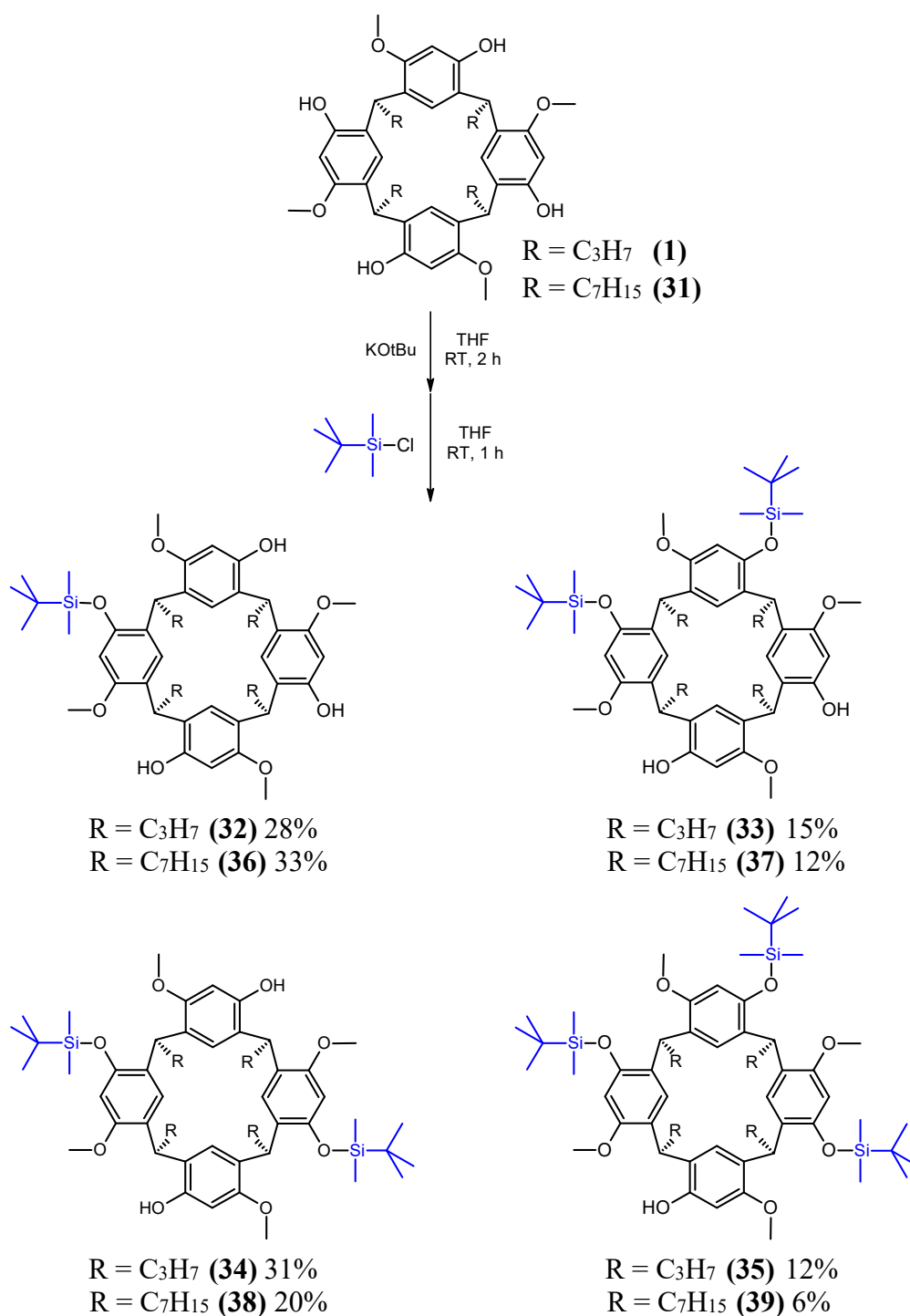
Scheme 4.2 *O*-Substitution of tetramethoxyresorcinarenes **(1)** and **(31)** with two equivalents of TBDMS-Cl and potassium *tert*-butoxide in THF.

A key indicator enabling identification of the products by NMR spectrsocopy was the rotational symmetry of the products, which was evident in the number of peaks in the NMR spectra. Compared to the starting resorcinarene, there are many more peaks in the NMR spectra of the products, which was a result of a loss of the C_4 rotational symmetry. A clear indicator of the rotational symmetry of the resorcinarene products was the methoxy groups. For products where there was no rotational symmetry – tri,

proximal, and mono – the four methoxy groups appear as four separate peaks in both ^{1}H and ^{13}C NMR spectra. This rotational symmetry rationale enables determination of the number of substituted phenols in a resorcinarene product by the number of SiC or *tert*-butyl peaks in the ^{13}C NMR spectrum. However, the distally-subsituted resorcinarene product, due to its unique C$_2$ symmetry, can be distinguished from the other products by a halving of all peaks. This can be observed in the list of key signals of the NMR spectra for the TBDMS resorcinarene products (**Table 4.2**). The ^{1}H NMR integrations of the silyl methyl groups and *tert*-butyl groups of the TBDMS substituents agree with the resorcinarene substitution as determined by rotational symmetry arguements.

Table 4.2   Summary of key NMR spectroscopic data of TBDMS resorcinarene products recorded in CDCl$_3$ (**Appendix A – 28**). Chemical shifts are listed in ppm. R$_f$ (EtOAc/Petrol 4:6).

R$_f$	Si(CH$_3$)$_2$		SiC	SiC(CH$_3$)$_3$		OCH$_3$		TBDMS resorcinarene
	^{1}H	^{13}C	^{13}C	^{1}H	^{13}C	^{1}H	^{13}C	
0.87	-0.10, 0.07, 0.15, 0.19, 0.26, 0.28	-4.28, -4.35, -4.1, -4.0, -3.7, -3.4	18.2, 18.39, 18.40	0.84, 1.04, 1.02	25.86, 25.93, 26.0	3.46, 3.51, 3.70, 3.79	54.8, 55.3, 55.5, 55.7	Tri **(35)**
0.76	0.31	-3.7	18.5	1.08	26.0	3.54, 3.87	55.3, 55.8	Distal **(34)**
0.63	-0.27, 0.04, 0.28, 0.31	-4.6, -4.1, -3.8, -3.5	18.3, 18.5	0.85, 1.07	25.9, 26.1	3.47, 3.70, 3.75, 3.87	54.9, 55.1, 55.6, 56.0	Proximal **(33)**
0.31	0.26, 0.29	-4.0, -3.5	18.6	1.06	26.1	3.59, 3.78, 3.857, 3.863	55.4, 55.9, 55.99, 56.04	Mono **(32)**

It is important to keep in mind the diastereotopic effects on the *O*-substituents due to the influence of the chirality of the resorcinarene. Initially, the NMR spectra for mono-TBDMS resorcinarene **(32)** was misinterpreted as being proximal-TBDMS resorcinarene **(33)** due to the two silicon-methyl singlets, which were assumed to represent two non-equivalent TBDMS groups. However, synthesis and characterisation of tri, distal, proximal and mono TBDMS resorcinarenes has proven

that each non-equivalent TBDMS group gives rise to two silicon methyl peaks. This phenomenon is general and was also evident for other resorcinarene derivatives previously reported. An exception was the distal-TBDMS, which gave only one silicon-methyl signal in CDCl₃, however this was a solvent effect, since the phenomenon was again apparent when the NMR spectrum was recorded in acetone-d₆ (**Figure 4.2**). This phenomenon was due to the silicon-methyl groups being diasteretopic, and therefore non-equivalent. Despite being able to freely rotate, the two methyl groups are diastereotopic due to the influence of the chiral centre of the resorcinarene. The potential contribution of restricted rotation of the TBDMS group was investigated by recording the ¹H NMR spectrum at elevated temperatures. If restricted rotation played a role in the non-equivalence of the silicon-methyl groups, then the corresponding two singlets would coalesce when the NMR spectrum is recorded at a higher temperature. The ¹H NMR spectrum of distal-TBDMS resorcinarene **(34)** was recorded in DMSO-d₆ at room temperature, and also at 77 °C (**Figure 4.1**). The spectra demonstrate a rather minor shift of the silicon-methyl singlets, which suggests that restricted rotation was not the principle cause, and that the non-equivalence of the silicon-methyl groups was mainly due to the methyl groups being diastereotopic.
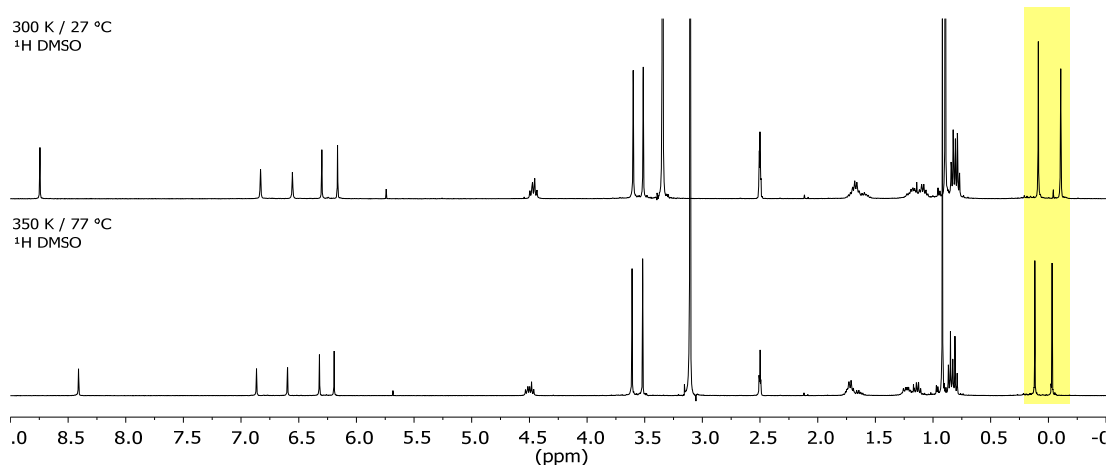
Figure 4.1   ¹H NMR study into the possibility of restricted rotation of the TBDMS groups of distal-TBDMS resorcinarene **(34)**. The upper spectrum was recorded at RT, while the bottom spectrum at 77°C.

In another initially baffling phenomenon, the ¹H NMR, recorded for distal-TBDMS resorcinarene **(34)** in CDCl₃, gave a rather bizarre and misleading spectrum where all peaks associated with the resorcinarene were very broad, except for the triplet of the methyl on the end of the propyl chain (**Figure 4.2**). However, when the ¹H NMR was

recorded in DMSO-d_6 or acetone-d_6, all the resorcinarene peaks sharpened to clearly show the distal-TBDMS resorcinarene **(34)** in good purity. Generally, peak broadening in NMR spectra is the result of slow oscillation of the atoms of the molecule. Therefore, the broad peaks in this case suggests that the oscillation of the resorcinarene conformation was slowed down in CDCl$_3$. The unusual solvent effect of the CDCl$_3$ is also evident in the fact that the silicon-methyl groups appears as a single peak rather than two peaks in both ^{1}H and ^{13}C NMR spectra recorded in CDCl$_3$.
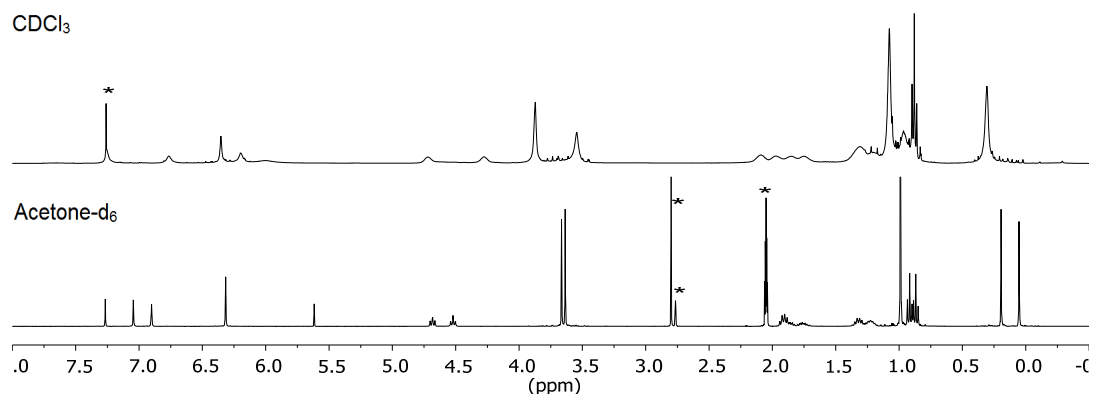
Figure 4.2 ^{1}H NMR spectra of distal-TBDMS resorcinarene **(34)** recorded in CDCl$_3$ (upper spectrum), and in acetone-d_6 (lower spectrum). *Denotes solvent peaks.

In the ^{1}H NMR spectra, it is notable that the signals for the resorcinarene benzylic methine for some of these TBDMS products have noticeably shifted downfield (**Figure 4.3**). The downfield shift of these peaks points to a de-shielding of the benzylic hydogens of the resorcinarene skeleton. These benzylic hydrogens are most likely de-shielded by diamagnetic anisotropy of an adjacent aromatic ring. This is where the magnetic field generated by the circulating π electrons of an aromatic ring causes the surrounding magnetic field to be non-uniform, resulting in de-shielding of nearby protons that are in planar alignment with the aromatic ring. This de-shielding effect is usually only observed for protons which are directly connected to an aromatic ring, however for some of these resorcinarenes, the benzylic protons appear to be de-shielded as well. This could happen by an adjacent aromatic ring being bent outwards till it comes into alignment with the benzylic proton. The extent of outward bending of the resorcinarene aromatic rings is due to the number and type of *O*-substituents, as evident in their crystal structures shown in **Figure 4.6**. It can be observed in **Figure 4.3** that the downfield shift of the benzylic methine signal is greater for the mono-TBDMS **(32)** than the tri-TBDMS **(35)** resorcinarene. Perhaps the aromatic rings for

112

the tri-TBDMS **(35)** have been flattened out too much such that it is no longer in planar alignment with the benzylic hydrogen.
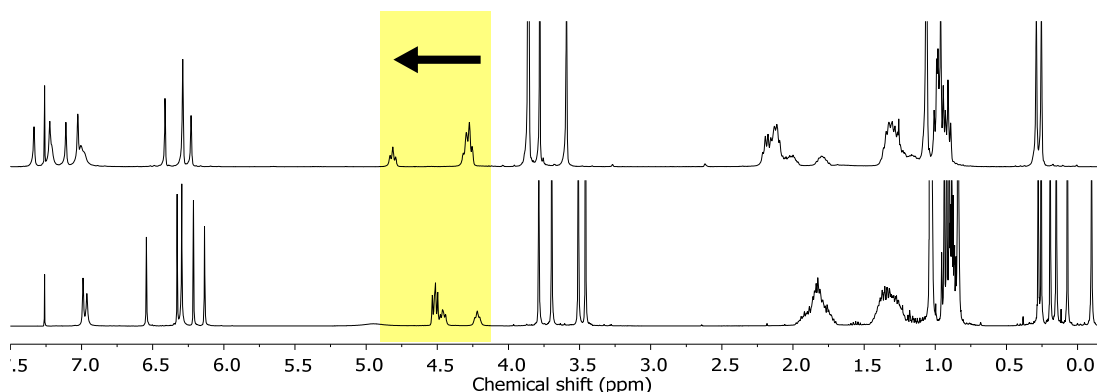
Figure 4.3   ^{1}H NMR spectra of mono-TBDMS **(32)** (top) and tri-TBDMS **(35)** (bottom) illustrating the downfield shift of the resorcinarene benzylic methine peak.

With the resorcinarene products definitively identified by NMR spectroscopy, it was encouraging that the distal target product was obtained in 31% yield, the highest-yielding product. Although 31% yield is relatively low, the key intermediate of a distally-functionalised chiral resorcinarene was delivered in a single-step, in practical amounts by a simple reaction. The starting resorcinarene **(1)** for this reaction can be easily synthesised in bulk, enabling scaling-up of the reaction. The work involved in this reaction was significantly less compared to that of the other strategies that have been explored and have returned overall unsuccessful results. Taking all these factors into consideration, this relatively low-yielding reaction becomes an attractive pathway to explore. To optimise the yield of the target distal product, and to determine the effect of the reaction conditions, the resorcinarene silylation reaction with TBDMS was explored with variation to the: reaction solvent, base, and length of the resorcinarene alkyl chain.

Since mono-TBDMS resorcinarene **(32)** was yielded in 28%, being the second-most abundant product, the number of equivalents of potassium *tert*-butoxide and TBDMS-Cl were increased from two to three, with the aim of converting more mono to distal. With three equivalents, the reaction in tetrahydrofuran gave a crude mixture with a TLC that indicated a faint spot for the target distal product, while two spots at higher R_f were significantly darker (**Figure 4.4**). This suggests that the distal product was reacting more readily and being converted to the tri. The impact of the reaction solvent was briefly explored by repeating the reaction, with three equivalents, in

113

dimethylformamide; the resultant TLC indicated that the target distal product was a minor product. The same reaction in acetonitrile mostly returned starting resorcinarene.
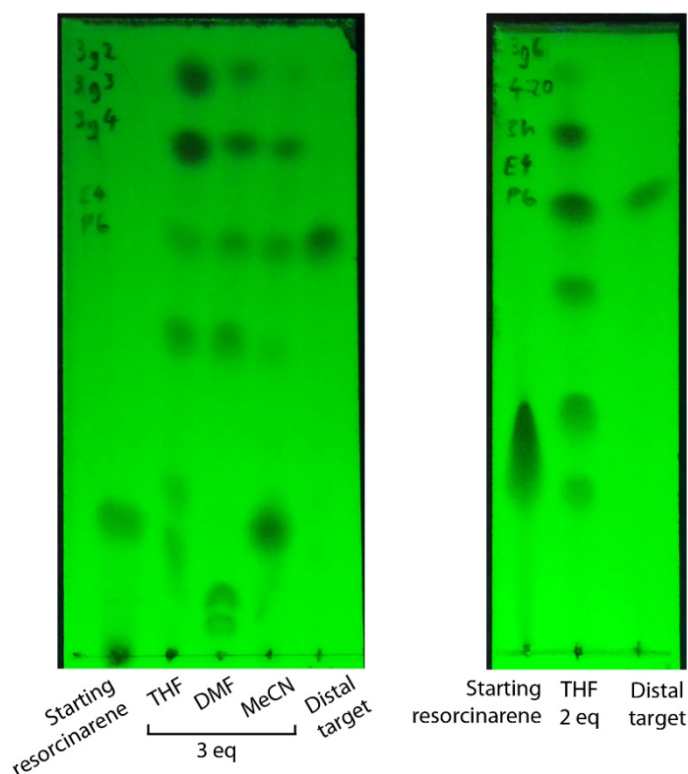
Figure 4.4 TLC analysis of various silylation reaction conditions of resorcinarene **(1)** with potassium *tert*-butoxide as base and TBDMS-Cl. Two equivalents of the base and TBDMS-Cl gives the best selectivity for distal target product **(34)**.

Therefore, from this brief investigation, the reaction in tetrahydrofuran with two equivalents of base and silylating agent appears to provide the best conditions for yielding the target distal product against other products. Further investigation of the reaction conditions with sodium hydride as base did not give a better yield of the distal product. The isolated yields of this reaction are reported in **Table 4.3**.

Table 4.3 *O*-Substitution of resorcinarenes **(1)** and **(31)** with TBDMS and various bases in THF.

Starting resorcinarene	Base (eq)	% Yield				
		Starting resorcinarene	Mono	Proximal	Distal	Tri
(1)	KOtBu (2.1)	10	28	15	31	12
(1)	NaH (2.0)	18	37	12	23	7
(31)*	KOtBu (2.0)	22	33	12	20	6
(31)*	KOtBu (3.0)	19	21	17	13	27

*Average of two experiments

114

To test if the alkyl chain of the resorcinarene had an impact on the yields of the products, heptyl resorcinarene (31) was subjected to the silylation reaction under the best conditions as determined for propyl resorcinarene (1). The silylation of heptyl resorcinarene (31) under these conditions produced a mixture of products which were separated by preparative TLC. Employing the same rotational symmetry interpretation of the NMR spectra (**Appendix A – 34**), the products were identifed to be the tri- (39), distal di- (38), proximal di- (37) and mono- (36) TBDMS resorcinarene products (**Table 4.4**).

Table 4.4   Summary of key NMR spectroscopic data of TBDMS heptyl resorcinarene products recorded in CDCl$_3$ (**Appendix A – 34**). Chemical shifts are listed in ppm. R$_f$ (EtOAc/Petrol 3:7).

R$_f$	Si(CH$_3$)$_2$		SiC	SiC(*CH$_3$*)$_3$		OCH$_3$		TBDMS resorcinarene
	^{1}H	^{13}C	^{13}C	^{1}H	^{13}C	^{1}H	^{13}C	
0.77	-0.12, 0.05, 0.13, 0.18, 0.24, 0.26,	-4.4, -4.3, -4.1, -4.0, -3.7, -3.4	18.2, 18.4	0.82, 1.01, 1.02	25.9, 25.9, 26.0	3.42, 3.48, 3.68, 3.77	54.8, 55.3, 55.5, 55.7	Tri (39)
0.68	0.30	-3.8	18.5	1.08	26.0	3.53, 3.87	55.3, 55.9	Distal (38)
0.50	-0.31, 0.01, 0.25, 0.29	-4.6, -4.2, -3.8, -3.5	18.3, 18.5	0.82, 1.05	25.9, 26.1	3.44, 3.68, 3.73, 3.88	54.8, 55.1, 55.6, 56.0	Proximal (37)
0.25	0.24, 0.29	-4.0, -3.5	18.6	1.06	26.1	3.58, 3.78, 3.85, 3.86	55.4, 55.9, 55.97, 56.05	Mono (36)

The reaction of the heptyl resorcinarene (31) with two equivalents of potassium *tert*-butoxide and TBDMS-Cl, afforded inferior selectivity for the distal product (38) compared to that of the propyl resorcinarene (1). Nevertheless, with the heptyl resorcinarene, the distal product was delivered in a greater yield than the tri (39) and the proximal (37) products, but not the mono (36) product (**Table 4.3**). Therefore, with the aim to convert more mono to distal, the equivalents of potassium *tert*-butoxide and TBDMS-Cl were increased from two to three. However, with three equivalents, the

distal product became the least abundant, with tri becoming the major product. This appears to be the same result for the propyl resorcinarene (**Figure 4.4**), the distal product was being converted to the tri product more readily than the mono and proximal products, thus suggesting that the distal product was the most reactive.

During attempts to crystallise the heptyl products, it was discovered that the products were decomposing in chloroform solution, though it had been pre-treated with potassium carbonate. It appears that the silyl ethers of the longer-chain resorcinarenes were more labile. The instability of the silyl ethers was especially evident for the proximal-TBDMS resorcinarene **(37)**, where satisfactory NMR spectra could not be readily acquired. The ^{1}H NMR spectrum of a solution of **(37)** in potassium carbonate-treated CDCl$_3$ confirmed the product in good purity, albeit a small silanol peak at 0.10 ppm. After leaving this solution at ambient conditions overnight, the ^{1}H NMR spectrum (**Figure 4.5**) showed a small amount of mono-TBDMS **(36)**, which was clearly evidenced by the methoxy peaks.
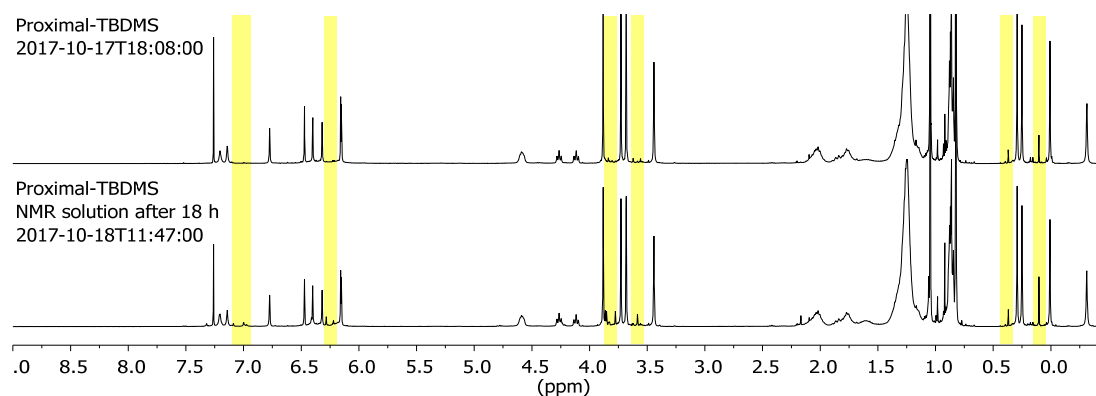
Figure 4.5 ^{1}H NMR spectra of a solution of proximal-TBDMS resorcinarene **(37)** in CDCl$_3$ shows some decomposition to the mono-TBDMS resorcinarene **(36)** after leaving overnight at RT.

After recording the NMR spectra of proximal-TBDMS **(37)** in CDCl$_3$, the CDCl$_3$ was evaporated, and the slightly-hydrolysed product was dissolved in acetone-d$_6$ to test its stability in a different solvent. After two weeks, it was clear that the proximal product was very slowly hydrolysing in the acetone-d$_6$. This observed lability was surprising as it seems unlikely that the longer alkyl chain could be the cause. This apparent lability was not further investigated since efforts were focused on advancing the main investigation. In summary, the silylation of the heptyl resorcinarene **(31)** with TBDMS-Cl, afforded inferior selectivity for the distal product, compared to the propyl resorcinarene **(1)**, as well as more labile products which were prone to decomposition.

Crystals suitable for single crystal X-ray diffraction analysis were obtained for all TBDMS resorcinarene derivatives (**Table 4.5**). The structures were determined by A/Prof. Chiara Massera from the University of Parma, Italy.

Table 4.5   Crystallisation solvents for single crystals of TBDMS resorcinarene derivatives for X-ray diffraction analysis.

Resorcinarene	Crystallisation solvent
Mono-TBDMS **(32)**	DCM-MeOH
Prox-TBDMS **(33)**	MeCN
Distal-TBDMS **(34)**	THF-MeOH
Tri-TBDMS **(35)**	Chloroform-MeOH

Analysis of these single crystals by X-ray diffraction confirmed the NMR assignment of the TBDMS resorcinarene derivatives at the solid state (**Appendix B – 3**). These crystal structures, shown in **Figure 4.6**, clearly show the expected crown conformation of the resorcinarenes. As anticipated, the mono-TBDMS resorcinarene **(32)** has the most crown-like conformation due to the increased number of hydrogen bonds, as well as the lower steric bulk.

Mono-TBDMS **(32)**

Prox-TBDMS **(33)**

Distal-TBDMS **(34)**

Tri-TBDMS **(35)**
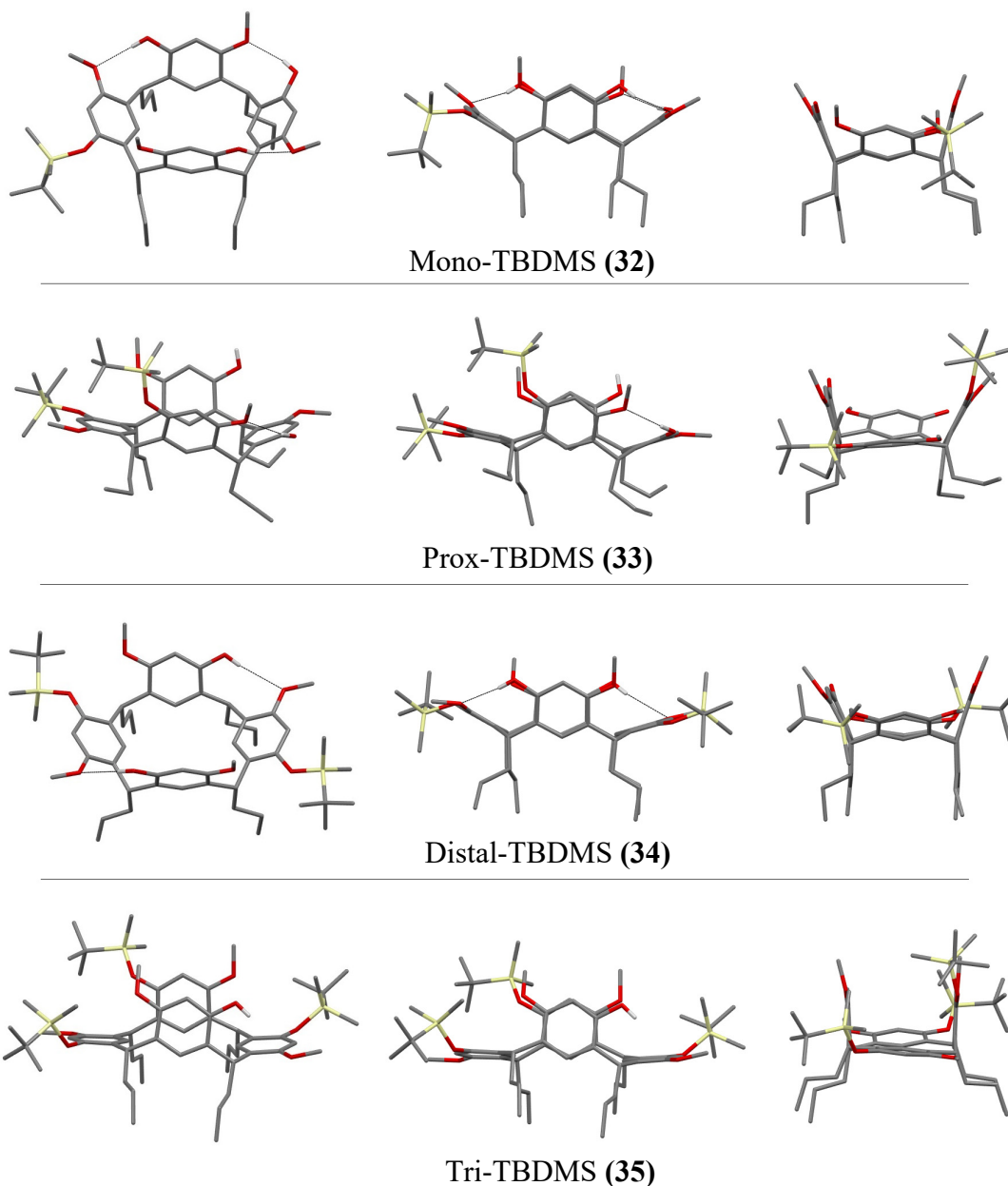
Figure 4.6   Crystal structures of TBDMS resorcinarenes. Colour code: C, grey; O, red; Si, yellow. Hydrogen atoms have been omitted for clarity. For ORTEP view see **Appendix B – 11**.

More substituents cause greater distortion of the resorcinarene crown conformation, generally in the form of a pinching of the crown conformation to a boat conformation. A boat conformation is where a distal pair of aromatic rings become flattened out, often due to the steric bulk of a substituent, causing the other distal pair of aromatic rings to be pinched together being roughly vertical and parallel to each other. Distal-TBDMS resorcinarene **(34)** has a fairly symmetrical crown conformation that is slightly pinched, while much asymmetric distortion is apparent for prox-TBDMS resorcinarene **(33)**. Of these partially-substituted resorcinarenes, the conformation of tri-TBDMS resorcinarene **(35)** was observed to be the most boat-like, owing to its

greater substitution. It is notable that even with one substituent, mono-TBDMS resorcinarene **(32)** begins to adopt the boat conformation. In this case, the aromatic ring bearing the substituent is being bent outwards due to the steric bulk of the TBDMS group, which in turn causes the distal aromatic ring to also be bent outwards, presumably to alleviate ring strain on the macrocycle. With the distal aromatic ring being extended outwards, it may become more reactive than the proximal pair of aromatic rings since it is now relatively sterically unhindered. Perhaps this boat conformation explains the observed selectivity for the distal-TBDMS resorcinarene product **(34)**.

Attempts to crystallise the TBDMS heptyl resorcinarene products tri- **(39)**, proximal-**(37)**, mono- **(36)** by slow diffusion of methanol into a solution of the product in chloroform, resulted in the colourless solutions turning to a yellow-orange colour. TLC showed multiple product spots, which were indicative of decomposition of the products. Of the TBDMS heptyl products, only distal **(38)** could be crystallised, while the other products formed glassy solids. The crystals of distal-TBDMS heptyl resorcinarene **(38)**, obtained from EtOAc-MeOH, were suitable for single crystal X-ray diffraction analysis (**Appendix B – 6**). The crystal structure (**Figure 4.7**), shows that the longer heptyl groups on the narrower rim do not have much impact on the conformation of the resorcinarene.
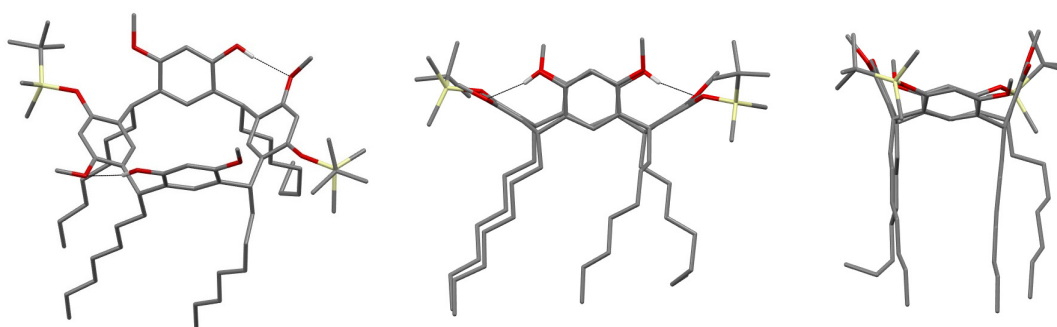
Figure 4.7   Crystal structure of TBDMS heptyl resorcinarene **(38)**. For ORTEP view see **Appendix B – 14**.

The crystal packing of the propyl resorcinarene derivatives generally follows that of the distal-TBDMS propyl **(34)**. The crystal packing of distal-TBDMS **(34)** is irregular compared to the heptyl **(38)** derivative (**Figure 4.8**). With the heptyl, the resorcinarenes are regularly arranged in a head-to-head / tail-to-tail packing along the *c*-axis direction. However, for the propyl resorcinarene, this head-to-head / tail-to-tail

packing alternates along the *b*-axis rather than being uniform as with the heptyl. This difference in packing is the result of the longer alkyl chains of the heptyl resorcinarene which make a uniform packing along the *b*-axis more favourable. This observation is consistent with the work by Nissinen and co-workers who reported the uniformed layered packing for bis-crown resorcinarenes with alkyl chains that were pentyl or longer.[106]
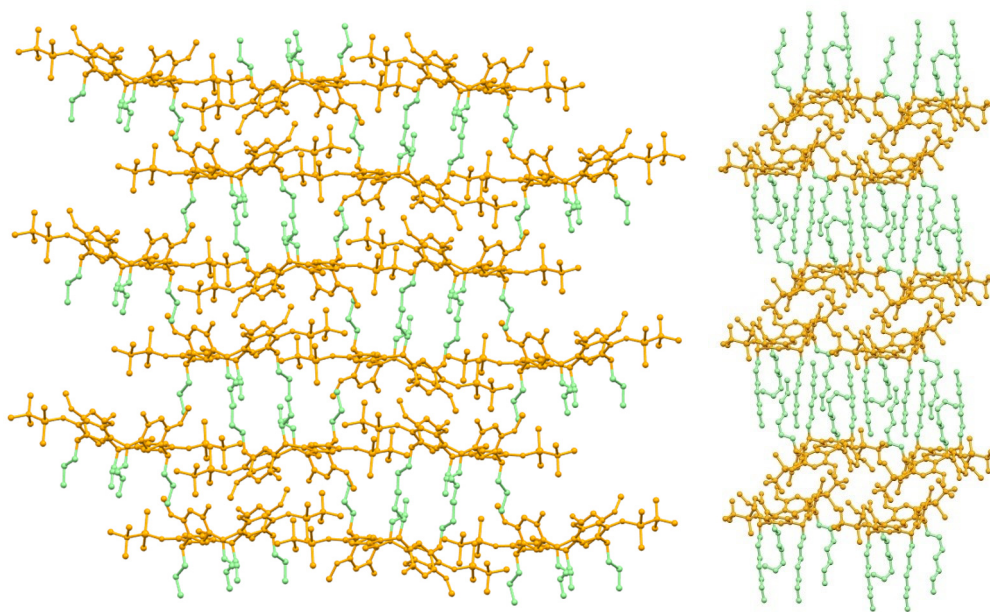
Figure 4.8   Crystal packing of the distal-TBDMS resorcinarenes: propyl **(34)** along the *a*-axis (left) and heptyl **(38)** along the *b*-axis (right). The tails and the heads of the resorcinarene molecules are represented in green and orange, respectively.

In the investigation so far, a set of optimum reaction conditions for the silylation of tetramethoxyresorcinarene has been determined. Next, the *O*-substitution of resorcinarene **(1)** with a few other bulky protecting groups was investigated, and where practicable, the products were separated by preparative TLC for characterisation and determination of the yield.

4.1.2   TBDPS (*tert*-butyldiphenylsilyl)

The silylation with TBDPS, was investigated because of its similarity to TBDMS, both being silyl protecting groups. TBDPS, however, having two phenyl groups instead of methyl groups, may perhaps have a greater steric bulk and thus increase the steric repulsion and favour the formation of the distal product. The silylation of resorcinarene **(1)** with two equivalents of potassium *tert*-butoxide and TBDPS-Cl in tetrahydrofuran produced three resorcinarene products, which were separated by preparative TLC. Characterisation by NMR spectroscopy (**Appendix A – 40**) revealed the products to

be the distal di- **(42)**, proximal di- **(41)** and mono- **(40)** TBDPS resorcinarene products (**Scheme 4.3**). A resorcinarene product, suspected to be tri-TBDPS resorcinarene **(43)**, was observed but had co-eluted and was not separated.
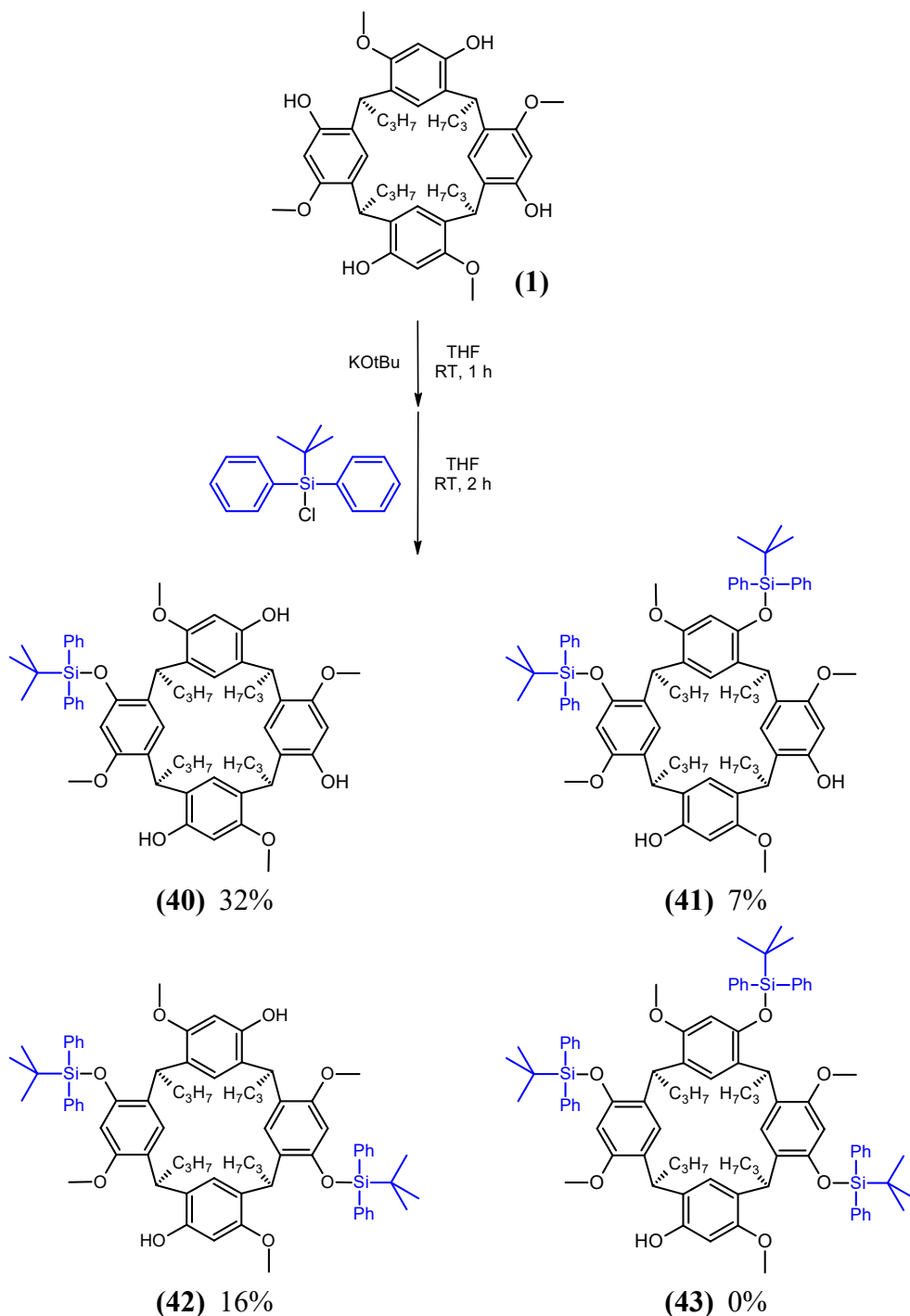
Scheme 4.3 *O*-Substitution of resorcinarene **(1)** with two equivalents of TBDPS-Cl and potassium *tert*-butoxide in THF.

In the NMR spectra, the signals from the phenyl groups of the TBDPS substituents could not be definitively distinguished from the aromatic signals from the resorcinarene macrocycle. The clear indicators of rotational symmetry were provided

by the signals from the silyl *tert*-butyl group and the methoxy groups (**Table 4.6**), thus enabling assignment of the TBDPS resorcinarenes by NMR spectroscopy as per the same rationale described for the TBDMS derivatives. Regarding proximal-TBDPS resorcinarene **(41)**, the signals in the aliphatic region of the ^{1}H NMR spectrum were broad and overlapping, hence making accurate assignment unclear. However, the correct number of peaks were present in the aliphatic region of the ^{13}C NMR spectrum, thus confirming **(41)** in good purity. It is notable that the peaks for the resorcinarene benzylic methine have shifted downfield as far as 5.1 ppm in some instances – a 1.0 ppm shift. Additionally, a non-resorcinarene product that eluted before the distal, was isolated. Comparison of the ^{1}H NMR spectrum of this product, with the literature,[162] determined it to be TBDPS-OH which most likely originated from the hydrolysis of unreacted TBDPS-Cl.

Table 4.6 Summary of key NMR spectroscopic data of TBDPS resorcinarene products recorded in CDCl$_3$ (**Appendix A – 40**). Chemical shifts are listed in ppm. R$_f$ (EtOAc/Petrol 4:6).

R$_f$	SiC	SiC(CH$_3$)$_3$		OCH$_3$		CHCH$_2$	TBDPS resorcinarene
	[13]C	[1]H	[13]C	[1]H	[13]C	[1]H	
0.76		0.79, 1.11, 1.18		2.80, 3.08, 3.15, 3.54		4.16, ^4.78, 5.03	Suspected tri (not separated from TBDPS-OH*)
0.61	19.8	1.20	26.7	3.17, 3.46	55.1, 55.5	4.18, 5.11	Distal **(42)**
0.47	19.2, 19.7	0.79, 1.16	26.4, 26.7	2.92, 2.97, 3.51, 3.88	54.3, 55.0, 55.1, 56.0	4.04, 4.34, 4.92, 5.12	Proximal **(41)**
0.29	19.8	1.19	26.8	3.11, 3.41, 3.76, 3.89	55.0, 55.7, 55.9, 56.1	4.13, 4.25, 4.34, 5.14	Mono **(40)**

^Integration is doubled
*TBDPS-OH was identified by comparison of the ^{1}H NMR spectrum to literature[162]

The isolated yields of the TBDPS resorcinarene products from the silylation reaction are listed in **Table 4.7**. With two equivalents of potassium *tert*-butoxide and TBDPS-Cl, the silylation did not proceed far, as starting resorcinarene and mono-TBDPS **(40)** were the main components, while no tri-TBDPS resorcinarene was detected.

Therefore, the number of equivalents of potassium *tert*-butoxide and TBDPS-Cl were increased from two to three. With three equivalents, there was significantly more resorcinarene silylation, and the distal-TBDPS **(42)** was afforded as the major product in 25% yield. An additional resorcinarene product that eluted before distal **(42)**, but co-eluted with the TBDPS-OH was also observed by ^{1}H NMR spectroscopy. The ^{1}H NMR spectrum of the co-eluted material (**Appendix A – 44**) showed that this was most likely the tri-TBDPS resorcinarene product (**Table 4.6**).

Table 4.7   *O*-Substitution of resorcinarene **(1)** with two and three equivalents of TBDPS and potassium *tert*-butoxide in THF.

KOtBu	% Yield				
	Starting resorcinarene	Mono	Proximal	Distal	Tri
2.0 eq	39	32	7	16	0
3.0 eq	Trace	12	9	25	~22*

*Not separated from TBDPS-OH; yield calculated based on approximated ^{1}H NMR integration.

The assignment of the reaction products mono-TBDPS **(40)** and distal-TBDPS **(42)** were confirmed at the solid state through X-ray diffraction analysis on single crystals (**Appendix B – 5**). Crystals of good quality were obtained for mono-TBDPS **(40)** by crystallisation from DCM-petroleum spirits, and also for distal-TBDPS **(42)** from chloroform-MeOH. As shown in **Figure 4.9**, the conformations of both mono-TBDPS **(40)** and distal-TBDPS **(42)** appear much like their TBDMS counterparts. The main difference is the aromatic rings bearing the substituents are slightly more flattened out, indicating a slightly greater steric bulk of TBDPS compared to the TBDMS groups. As a result, the crown conformation of the distal-TBDPS **(42)** is slightly more pinched compared to its TBDMS counterpart.
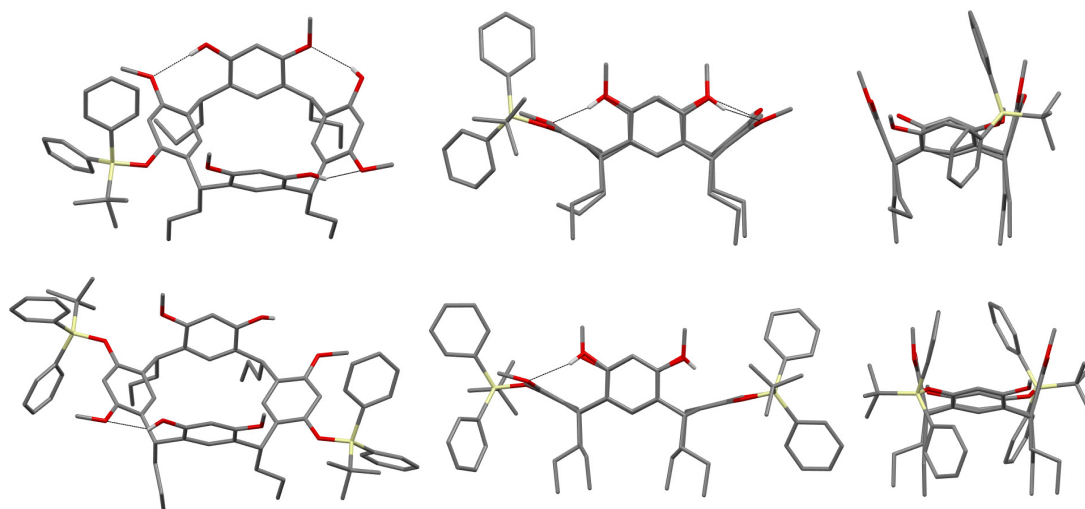
Figure 4.9 Crystal structures of mono-TBDPS **(40)** resorcinarene (top) and distal-TBDPS **(42)** resorcinarene (bottom). Colour code: C, grey; O, red; Si, yellow. Hydrogen atoms have been omitted for clarity. For ORTEP view see **Appendix B – 13**.

The investigation into the silylation of resorcinarene **(1)** with three equivalents of TBDPS-Cl and potassium *tert*-butoxide delivered the distal product in best yield of 25%. However, this is inferior compared to the silylation with TBDMS-Cl, which produces the distal product in a higher yield of 31%.

4.1.3 Benzyl ether

The selective *O*-substitution of resorcinarene **(1)** was further explored with benzyl ether protecting groups. Benzyl ethers were chosen because of their common availability and chemical stability but also, in this case, their difference from a silyl ether while retaining some steric bulk and compatibility with the reaction conditions. In **Section 3.1**, the tetrabenzyl derivative of resorcinarene **(1)** was prepared by treatment of excess base and benzyl bromide. This investigation aims to only use two equivalents of base and benzyl bromide to evaluate the possibility of partially-selective distal *O*-substitution. Therefore, the optimum set of reaction conditions with resorcinarene **(1)** and two equivalents of benzyl bromide and potassium *tert*-butoxide similarly produced multiple products, which were separated by preparative TLC. Analysis of the separated products by NMR spectroscopy (**Appendix A – 44**) identified them as mono- **(44)**, proximal di- **(45)**, distal di- **(46)**, tri- **(47)** and tetra- **(22)** benzyl ether resorcinarenes (**Scheme 4.4**).
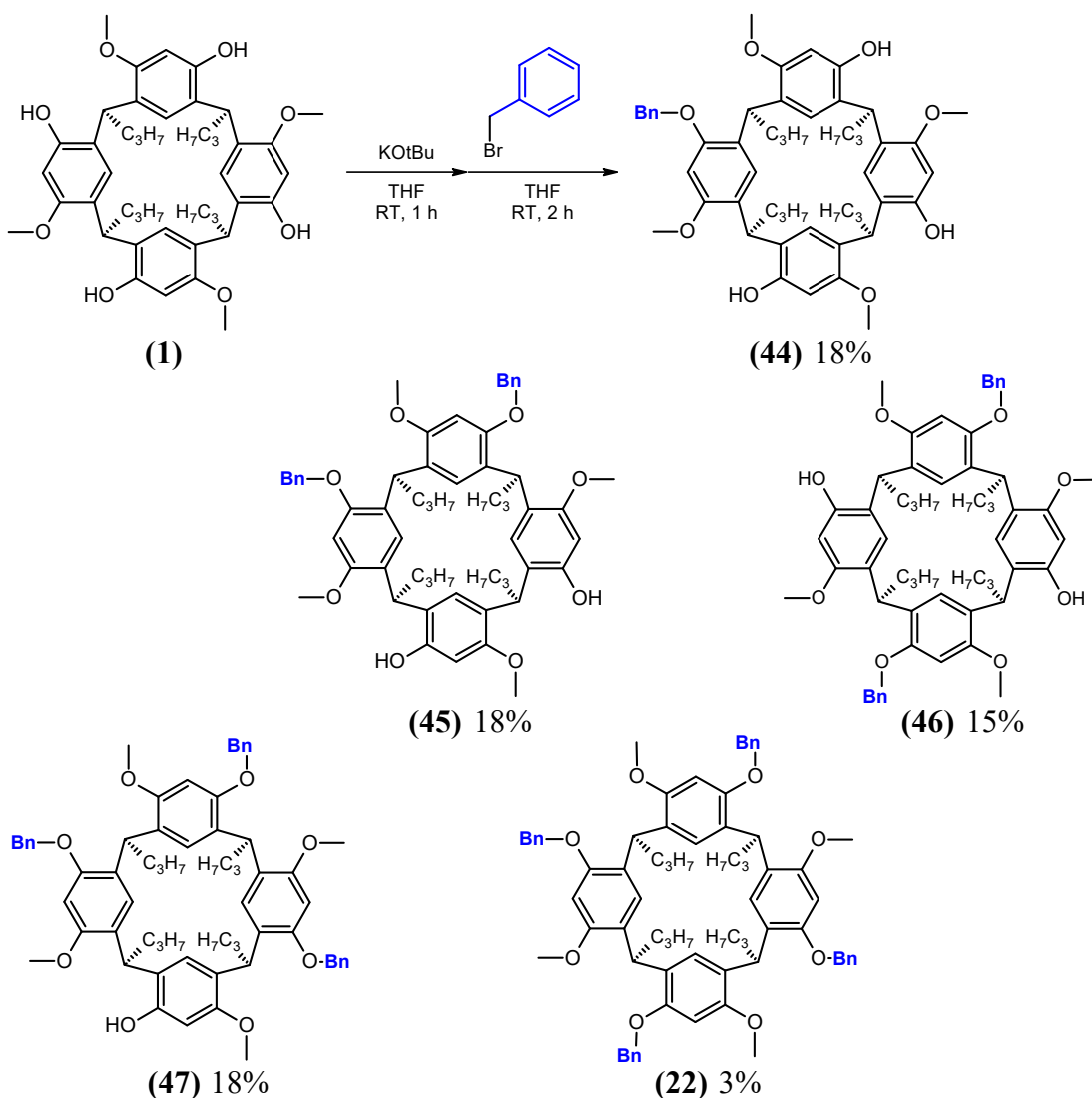
Scheme 4.4 *O*-Substitution of resorcinarene **(1)** with two equivalents of benzyl bromide and potassium *tert*-butoxide in THF. Yields are averages from two experiments.

As with the silyl ether resorcinarene derivatives, the same rotational symmetry interpretation provided the basis for identification of the benzyloxyresorcinarene products by NMR spectroscopy (**Table 4.8**). The number of benzylic methylene peaks around 71 ppm in the DEPT-135 spectra provided a clear indicator of the number of benzyl ether substituents on a resorcinarene. For products without symmetry – mono-OBn **(44)**, proximal-OBn **(45)** and tri-OBn **(47)** – the number benzylic methylene peaks equated to the number of benzyl ether substituents.

Table 4.8   Summary of key NMR spectroscopic data of benzyloxyresorcinarene products recorded in CDCl$_3$ (**Appendix A – 44**). Chemical shifts are listed in ppm. R$_f$ (EtOAc/Petrol 4:6).

R$_f$	PhCH$_2$O	OCH$_3$		C*H*CH$_2$	Benzyloxy resorcinarene
	^{13}C	^{1}H	^{13}C		
0.82	71.1	3.40	55.6	4.59	Tetra **(22)**
0.68	71.0, 71.1, 71.2	3.37, 3.41, 3.46, 3.79	55.4, 55.6, 56.0*	4.26, 4.56-4.64, 4.68-4.76	Tri **(47)**
0.52	71.1	3.48, 3.89	55.3, 56.1	4.21-4.42, 4.91-5.06	Distal **(46)**
0.38	71.0, 71.1	3.43, 3.47, 3.77, 3.84	55.3, 55.4, 55.9, 56.0	4.26, 4.30, 4.82-4.98	Proximal **(45)**
0.30	71.0	3.38, 3.80, 3.84, 3.85	55.2, 55.9, 56.0, 56.2	4.24-4.34, 5.00-5.06	Mono **(44)**

*HSQC shows two coincidental peaks

However, in the ^{1}H NMR spectra, the benzylic methylene group appears around 5 ppm as an AB pair, due to diastereotopic effects, which obscures and complicates the appearance of the peaks, particularly for asymmetrical proximal-OBn **(45)** and tri-OBn **(47)**. Oddly, for tri-OBn **(47)**, some of the AB peaks had shifted from 5.1 ppm as low as 4.43 ppm. To further obscure the AB peaks for proximal-OBn **(45)** and tri-OBn **(47)**, of some peaks of the benzylic methine resorcinarene macrocycle were shifted downfield to around 4.9 ppm, in a similar fashion that was observed for the silyl resorcinarene derivatives. The mingling and overlap of the peaks of the two different benzylic protons are apparent in the HSQC spectra shown in **Figure 4.10**. The HSQC spectrum of tri-OBn **(47)** also shows two coincidental methoxy peaks at 56.0 ppm in the ^{13}C NMR spectrum.
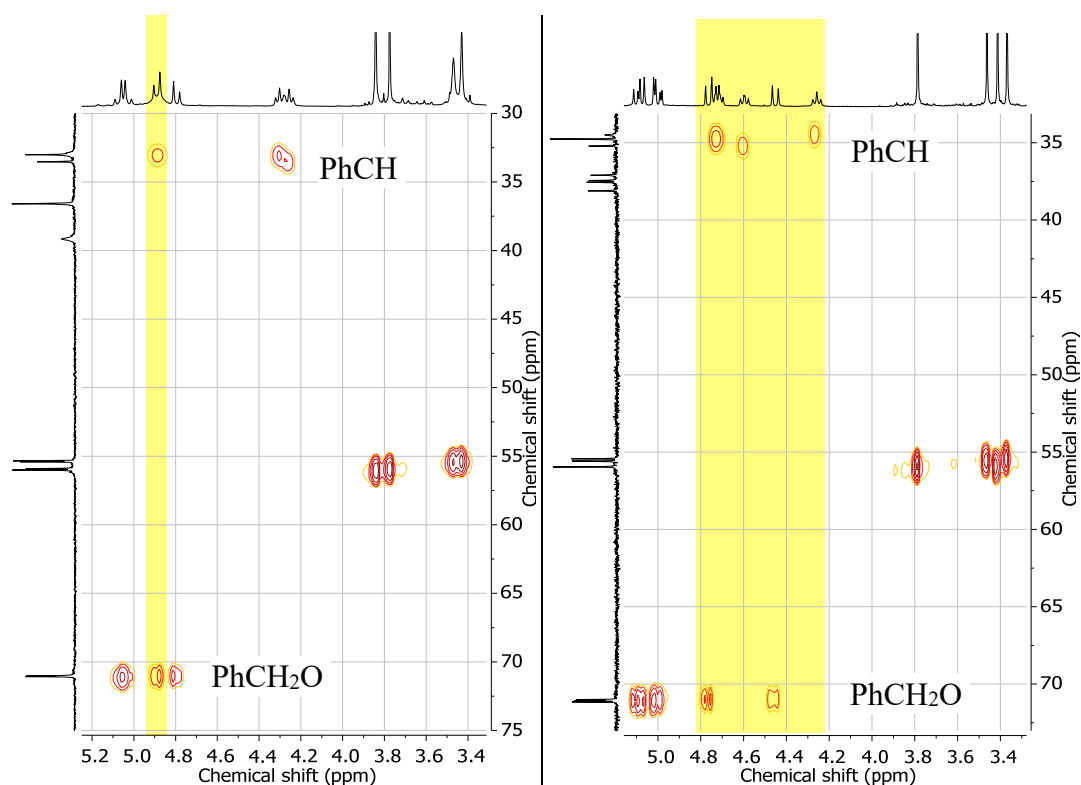
Figure 4.10   HSQC NMR spectra of proximal-OBn **(45)** (left) and tri-OBn **(47)** (right). The overlap of the peaks of benzylic methines and methylenes in the ^{1}H NMR spectra have been highlighted.

As shown in **Table 4.9**, the reaction with two equivalents of benzyl bromide and potassium *tert*-butoxide gave a rather inconsistent spread of product yields. The mono-OBn **(44)** and starting resorcinarene **(1)** could not be fully separated because of co-elution. Nevertheless, in both reactions with two equivalents, distal-OBn **(46)** was afforded in a yield of 15%, and was clearly not a major product.

Table 4.9   *O*-Substitution of resorcinarene **(1)** with two equivalents of benzyl bromide and potassium *tert*-butoxide in THF.

KOtBu	% Yield					
	Starting resorcinarene	Mono	Proximal	Distal	Tri	Tetra
2.0 eq	26*	25*	17	15	11	<1
2.0 eq	5^	11^	18	15	25	6

*Co-eluted and not separated; yield calculated based on approximated ^{1}H NMR integration
^Trace of the other material

Crystallisation of the proximal-OBn **(45)** and tri-OBn **(47)** products was not successful, with both forming brown glassy solids. Single crystals suitable for X-ray diffraction analysis could be obtained for distal-OBn **(46)** from chloroform-MeOH (**Appendix B – 6**). The crystal structure of distal-OBn **(46)**, shown in **Figure 4.11**,

confirms its assignment. The boat conformation is again apparent, but with slight distortion caused by the benzyl ether substituents.
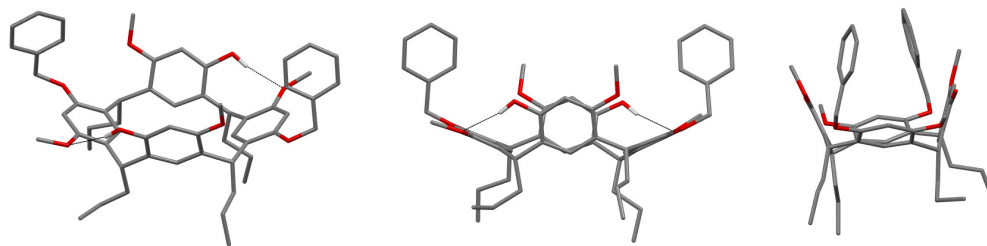
Figure 4.11 Crystal structure of distal-OBn **(46)** resorcinarene from three different angles. For ORTEP view see **Appendix B – 14**.

From the investigations of protecting groups, bases, reaction solvents, and a resorcinarene with a longer hydrocarbon chain, the original conditions with resorcinarene using potassium *tert*-butoxide and TBDMS-Cl in tetrahydrofuran still gave the best yield of the distally-functionalised resorcinarene. The reason for the observed selectivity for the distal product may be due to the increased reactivity of the distal aromatic ring which may be more exposed as the mono *O*-functionalised resorcinarene begins to adopt the boat conformation. Notably, in all cases, the chromatographic elution order was always the same: tri, distal, proximal, then mono. Under the original conditions, the reaction was scaled up (1 g), and the products were isolated in essentially the same yields as the small scale. In the chromatography of larger scale reactions (7 g), once the distal target product **(34)** had eluted, all remaining compounds were flushed out with EtOAc, and were thus unseparated. A reaction with 9.8 grams of starting resorcinarene **(1)** delivered the distal target product **(34)** in 31% yield, the same yield as the small scale. The starting resorcinarene could be conveniently recovered from the significant quantity of by-product mixture by subjecting it to TBDMS hydrolysis conditions as outlined in **Section 4.2.2**. This ability to conveniently convert the by-products back to starting resorcinarene is an advantage to the practicality of this synthesis as there is no large wastage of resorcinarene material.

4.2 Replacement of TBDMS protecting groups

Since the distal functionalisation of the chiral resorcinarene was accomplished in the form of distal-TBDMS resorcinarene **(34)**, the resorcinarene should be ready for distal bridging with a crown ether. However, initial attempts to bridge **(34)** with tetraethylene glycol ditosylate[163] according to the procedure by Nissinen et al.[103] gave a complex mixture. A search of the literature revealed that the conditions of caesium carbonate and dimethylformamide were in fact a proven method for deprotecting TBDMS-protected phenols.[164] Therefore, the TBDMS protecting groups needed to be replaced with a protecting group that is more base-stable.

4.2.1 Replacement of TBDMS protecting groups with methanesulfonates

The protecting group first chosen was the methanesulfonate. Methanesulfonates can be removed by base-catalysed hydrolysis, but should be stable under the conditions for bridging, since carbonate is a weak base. In previous work, tetra-protection of the starting resorcinarene was conveniently accomplished in high yields and in good purity.[107] The synthetic plan for the replacement of the silyl ether groups with methanesulfonates is outlined in **Scheme 4.5**. For the removal of the TBDMS protecting groups from resorcinarene **(48)**, hydrolysis by caesium carbonate and dimethylformamide at 90 °C was chosen. These reaction conditions, being the same conditions for the bridging reaction, were chosen to also test the stability of the methanesulfonate esters under the conditions for bridging. If the methanesulfonates were also hydrolysed together with the TBDMS groups, at this step, then the methanesulfonate groups would be also be unstable in the next step, under the reaction conditions for bridging, and thus would be an unsuitable protecting group.
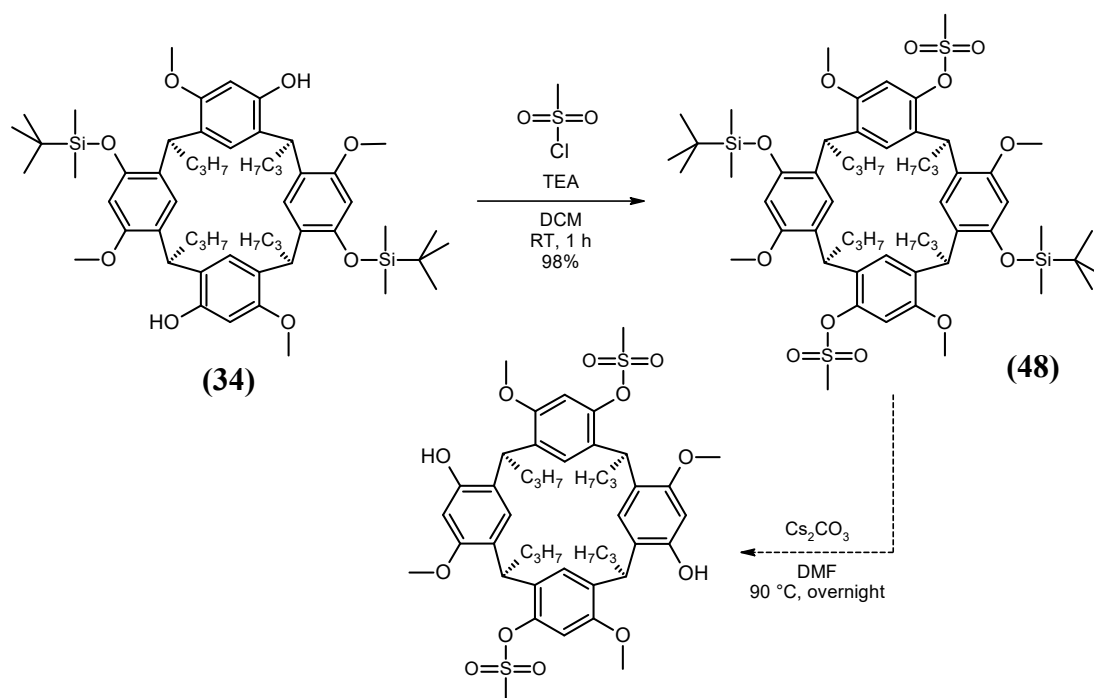
Scheme 4.5 Replacement of TBDMS protecting groups with methanesulfonates.

Resorcinarene **(34)** was subjected to the standard reaction conditions[107] of triethylamine and methanesulfonyl chloride to afford a product that had rather ambiguous NMR spectra. At first sight, the ^{1}H and ^{13}C NMR spectra (**Appendix A – 50**) indicated absence of the methyl of the methanesulfonate, thus suggesting starting material was obtained. However, TLC indicated a spot with R_f above the starting resorcinarene, and IR showed no OH stretch. An HRMS spectrum was obtained which recorded a main peak for the target product. Furthermore, single crystals of the product, which were obtained from chloroform-MeOH, were analysed by X-ray diffraction (**Appendix B – 7**). The crystal structure shown in **Figure 4.13** clearly evidenced the product as the target product **(48)**, which takes on a boat conformation that is similar to its precursor, distal-TBDMS resorcinarene **(34)**. On closer inspection of the NMR spectra, it was realised that the broad peak at 1.95 ppm on the ^{1}H spectrum gave an integration which did not fit in with the CH$_2$ multiplet it was partially-overlapped with. A closer look at this inconsistency by HSQC and DEPT-135 spectroscopy clearly showed that this broad peak was coupling to a carbon that was not a CH$_2$ (**Figure 4.12**); close inspection of the DEPT-135 spectrum, showed that the peak it was coupling to was partially-overlapped with the resorcinarene methine peak.

130
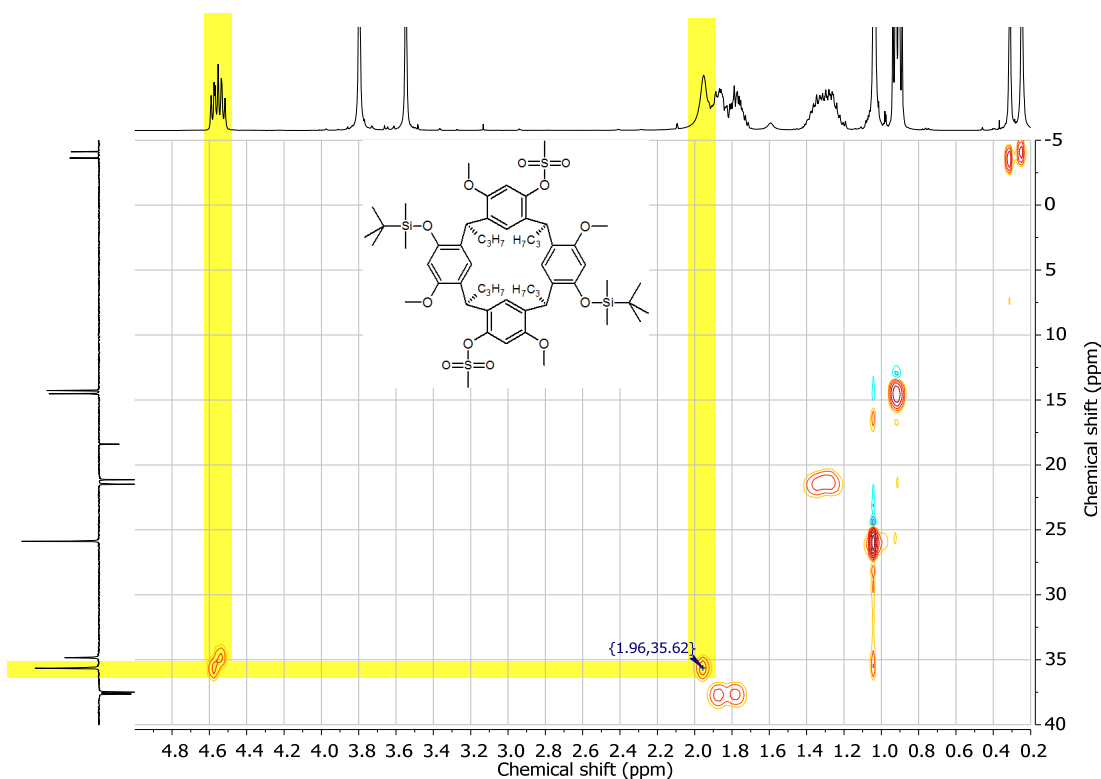
Figure 4.12 HSQC NMR spectrum of resorcinarene **(48)**. In the DEPT-135 spectrum, the peak for the methyl of the methanesulfonate is coincidental with the methine peak of the resorcinarene at 35.6 ppm.
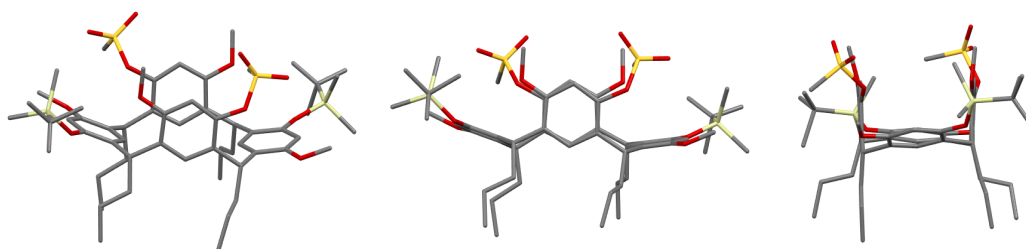
Figure 4.13 Crystal structure of resorcinarene **(48)**. Colour code: C, grey; O, red; Si, yellow; S, gold. Hydrogen atoms have been omitted for clarity. For ORTEP view see **Appendix B – 15**.

Resorcinarene **(48)** was then subjected to the caesium carbonate / DMF hydrolysis to give a mixture which appeared by TLC to have not starting resorcinarene, but three product spots. The ^{1}H NMR spectrum of the crude product showed no signals at low ppm, evidencing complete removal of the TBDMS groups. However, multiple peaks were present at ~2.7 ppm which suggested multiple methanesulfonate resorcinarene products. From these results, it was concluded that the methanesulfonate esters were also hydrolysing, but at a slower rate compared to the TBDMS groups. Therefore, the methanesulfonate protecting group was not sufficiently stable under the conditions for bridging, and a more base-stable protecting group is required.

4.2.2 Replacement of TBDMS protecting groups with benzyl ethers

The benzyl ether protecting group is pH stable and cleavable by hydrogenation, and is therefore a suitable candidate. The synthetic strategy would now be to benzylate the two distal phenols of (34), then hydrolyse the TBDMS groups to give a distal benzyl ether resorcinarene which would then be ready for bridging (**Scheme 4.6**).
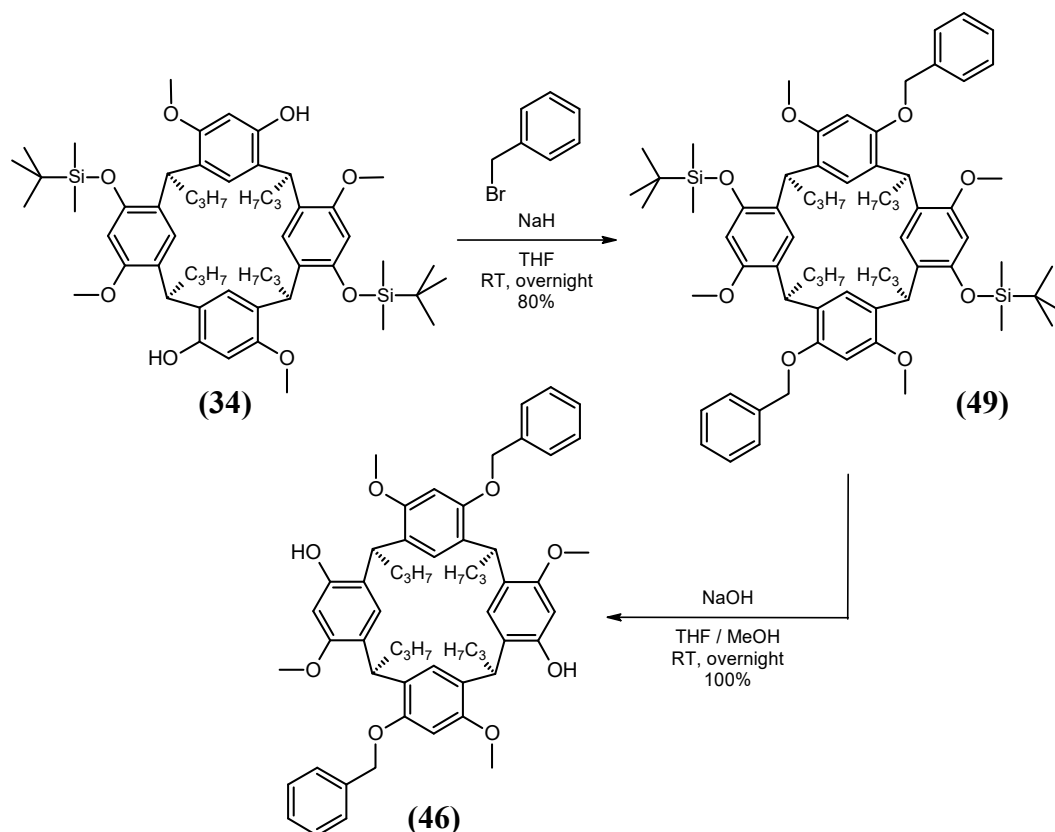
Scheme 4.6 Replacement of TBDMS protecting groups with benzyl ethers.

The benzylation on distal-TBDMS resorcinarene (34) was performed similarly to the general procedure described in **Section 3.4.1**. After removal of minor by-products by chromatography, the target distal-TBDMS distal-OBn resorcinarene product (49) was afforded in a good yield and confirmed by NMR spectroscopy (**Appendix A − 52**). The presence of the benzyl ether functional group was immediately apparent on the ^{13}C NMR spectrum by the single peak at 71.3 ppm, representing the benzylic carbon. The HSQC spectrum demonstrated that this peak was coupling to two peaks at 4.44 and 4.78 ppm on the ^{1}H NMR spectrum representing the diastereotopic benzylic protons, with the former peak appearing as a broad hump which overlapped with a benzylic methine peak of the resorcinarene. The retention of the TBDMS groups on the resorcinarene could be identified by two silicon-methyl signals at low chemical

shift on both the ^{1}H and ^{13}C NMR spectra. These signals, together with the two methoxy peaks on the ^{1}H NMR spectrum, confirmed the retention of C_2 symmetry of the resorcinarene; all four peaks had the same integration of six protons, and were broader than usual. However, on the ^{13}C NMR spectrum, only one methoxy peak was apparent rather than the anticipated two. HSQC showed that this peak was coupled to the two methoxy peaks on the ^{1}H NMR spectrum, therefore implying that the two anticipated methoxy peaks on the ^{13}C NMR spectrum were in fact coincidental in that one observed peak. The resorcinarene aromatic protons appeared as three broad peaks on the ^{1}H NMR spectrum at 6.33, 6.36, 7.07 ppm, rather than the expected four peaks. The fourth missing peak has probably overlapped with the two peaks at 6.33 and 6.36 ppm to give a total integration for six protons.

The structure assignment of distal-TBDMS distal-OBn resorcinarene **(49)** was confirmed at the solid state by X-ray diffraction analysis (**Appendix B – 7**) on single crystals that were readily obtained from slow evaporation from dichloromethane. As evident in the crystal structure (**Figure 4.14**), the resorcinarene takes on a boat conformation much similar to that of tri-TBDMS resorcinarene **(35)** (**Figure 4.6**) where the bulky TBDMS groups have pushed out a pair of distal aromatic rings till they are almost completely horizontal.
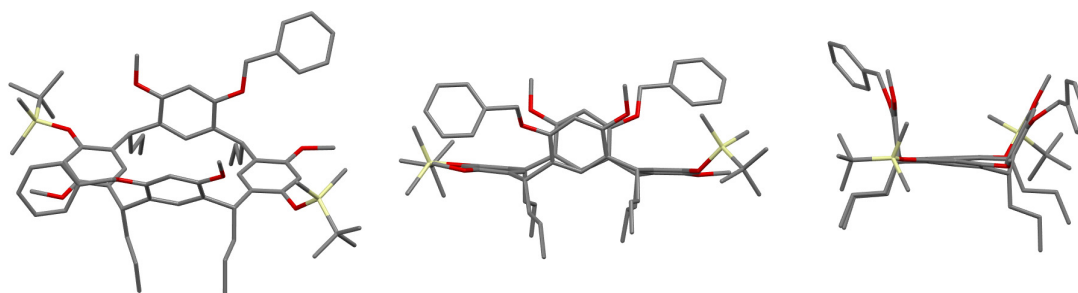
Figure 4.14   Crystal structure of resorcinarene **(49)**. Colour code: C, grey; O, red; Si, yellow.
Hydrogen atoms have been omitted for clarity. For ORTEP view see **Appendix B – 15**.

One of the minor by-products of the benzylation reaction isolated by chromatography, was indicated by ^{1}H NMR spectroscopy to be asymmetrical tri benzyl ether mono TBDMS resorcinarene, thus evidencing that a small amount of TBDMS hydrolysis was occurring. Running the benzylation at reflux produced the target product with significant amounts of by-products. Two of the by-products were isolated by preparative TLC, and were apparent by ^{1}H NMR spectroscopy to be the tri benzyl ether mono TBDMS resorcinarene as before, and also a di benzyl ether mono TBDMS mono

OH resorcinarene **(Figure 4.15)**. These by-products were likely caused by some hydrolysis of the TBDMS groups with sodium hydroxide,[165] which is produced when the sodium hydride reacts with water, especially during the quenching of the reaction with water. These by-products, although limited, are undesirable because they, necessitate chromatographic separation, and also reduce the yield of target product while wasting the distal-TBDMS resorcinarene **(34)**. In an effort to have a clean reaction without by-products, the benzylation reaction was investigated under various conditions which are summarised in **Table 4.10**.
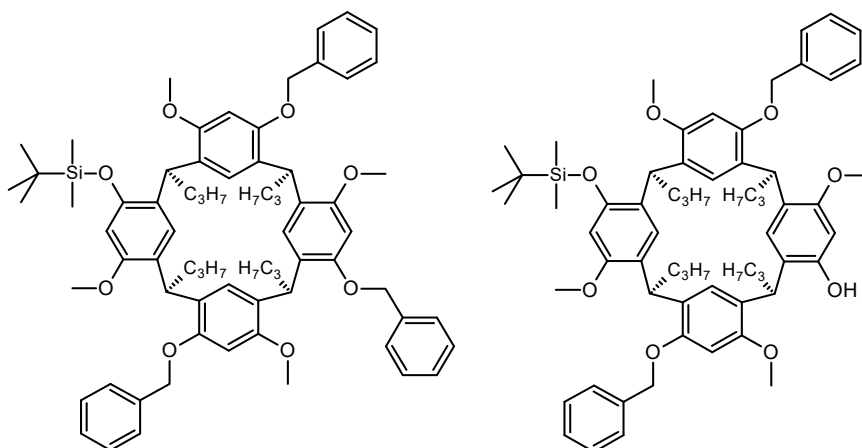
Figure 4.15 Suspected structures of two by-products from the benzylation of distal-TBDMS resorcinarene **(34)**.

Table 4.10 Benzylation of distal-TBDMS resorcinarene **(34)** under various reaction conditions.

Benzylation reaction conditions	Outcome
NaH, THF, RT, quench with water	Target product **(49)** with minor by-products
NaH, THF, reflux, quench with water	Significant by-products
NaH, THF, RT, quench with methanol	Many significant by-products
KOtBu, THF, RT	Tetrabenzyl ether resorcinarene **(22)** with no target product
Diisopropylethylamine, DCM, RT	No reaction
NaH, THF, RT, quench with HCl 10%	Target product **(49)** with minor by-products

When the sodium hydride was quenched with methanol instead of water, a mixture with a TLC which showed many compounds was produced; this was a far worse result compared with quenching with water. It seems that sodium methoxide is a better TBDMS hydrolysis agent compared to sodium hydroxide, most likely due to its increased solubility and nucleophilicity in tetrahydrofuran. Another strategy to avoid the TBDMS hydrolysis by-products is to perform the benzylation using potassium *tert*-butoxide in tetrahydrofuran, which are the same conditions for silylation. However, benzylation of **(34)** under these conditions produced tetrabenzyl ether resorcinarene **(22)** and no target product as confirmed by TLC and ^{1}H NMR spectroscopy. The benzylation was also attempted under similar conditions as the methanesulfonylation with a non-nucleophilic amine as base such as diisopropylethylamine, but no reaction was observed by TLC, and starting resorcinarene was recovered.

It was thought that the deprotection of the TBDMS ethers could be accomplished in the same pot, during the quenching of the benzylation reaction by quenching the sodium hydride with hydrochloric acid solution. This would avoid a separate reaction for the TBDMS deprotection, and could also lead to an easier purification without the need for column chromatography. Using hydrochloric acid to quench the sodium hydride, as well as to deprotect the TBDMS ethers, would also prevent reaction of the resultant phenols of **(49)** with the excess benzyl bromide.

When the benzylation reaction was quenched with hydrochloric acid (10%), TLC after 15 minutes, showed mainly diOBn diTBDMS resorcinarene **(49)**, but no de-silylated resorcinarene **(46)**. After stirring overnight, the TLC indicated the presence of resorcinarene **(46)**, with an intermediate spot, and a trace of precursor resorcinarene **(49)**. Therefore, to force the TBDMS hydrolysis to completion, concentrated hydrochloric acid (32%) was added and the quenched reaction mixture was heated at reflux. After 2 hours, TLC indicated that the reaction was complete. The TLC of the crude product showed that the target de-silylated resorcinarene **(46)** was the main product, but minor by-products were also present, suggesting that the benzylation was still not a clean reaction. Compared to the original water-quenching of the benzylation reaction, the chromatographic separation of this quenching with concentrated hydrochloric acid appears to be more difficult. Therefore, **Scheme 4.6** still provides the best synthetic path. Nonetheless, this investigation has shown that the TBDMS

ethers are fairly stable under acidic conditions. Thus, quenching the benzylation reaction with dilute hydrochloric acid would pose the least risk to unwanted TBDMS ether hydrolysis, and benzylation of the subsequent phenol. This benzylation reaction is scalable and was performed at a 4-gram scale to give a yield of 80% of the target resorcinarene **(49)**.

For the removal of the TBDMS protecting groups of **(49)**, the simple base-hydrolysis procedure by Davies et al.[165] was employed. After work up, a white solid was obtained which smelled like a silyl derivative. The ^{1}H NMR spectrum of this showed the target product **(46)** with two large impurity peaks at 0.11 and 0.93 ppm, indicating the impurity to be a TBDMS derivative, most likely *tert*-butyldimethylsilanol, the hydrolysis by-product. After some experimentation, it was discovered that the smell disappears after repeated addition of methanol and removal under reduced pressure. The ^{1}H NMR spectrum of the material after this treatment indicates that the peaks associated with the impurity are absent leaving the target product **(46)** in good purity. The suspected *tert*-butyldimethylsilanol impurity probably formed an azeotrope with methanol and was removed together with the methanol. This deprotection reaction was scalable with a 3.9-gram reaction yielding the target product **(46)** in 97%.

The success of the TBDMS removal was evidenced by the appearance of an OH stretch in the IR spectrum. The complete removal of the TBDMS protecting groups was indicated by the absence of peaks at low chemical shift in both ^{1}H and ^{13}C NMR spectra. The retention of the benzyl ether was clearly identified by the benzylic peak at 71.1 ppm in the ^{13}C NMR spectrum, as well as the AB pair at 5.10 and 5.14 ppm in the ^{1}H NMR spectrum. This, as well as the two prominent methoxy peaks in both the ^{1}H and ^{13}C NMR spectra confirm retention of C_2 symmetry. Moreover, the NMR spectra matched that of product **(46)** that was obtained from the direct benzylation of resorcinarene **(1)**.

In the work so far, the key intermediate of a distally-protected tetramethoxy-resorcinarene has been accomplished in the form of the distal-OBn resorcinarene **(46)**. The distal selectivity of this key compound was obtained by direct silylation of the starting resorcinarene. However, two additional synthetic steps were necessary, since the silyl groups of the distal-TBDMS resorcinarene **(34)** were unstable under the bridging reaction conditions. Nevertheless, the overall synthetic procedure to accomplish distal-OBn resorcinarene **(46)** is practical and has been demonstrated to work on a multi-gram scale. This key intermediate now enables the installation of a bridge over the resorcinarene cavity via *O*-alkylation of the remaining two resorcinarene hydroxy groups.

4.3 Experimental

4.3.1 X-ray crystallography

Crystal structures were determined by A/Prof. Chiara Massera from the University of Parma, Italy. Intensity data and cell parameters were recorded at 190(2) K on a Bruker ApexII diffractometer (MoKα radiation λ = 0.71073 Å) and at 298(2) K on a Bruker Smart Breeze at the University of Parma, or at 100(2) K at the ELETTRA Synchrotron Light Source (CNR Trieste, Basovizza, Trieste, Italy).

4.3.2 Phenol silylation of resorcinarenes via butyllithium

A representative procedure with 10.7 equivalents is given. To a solution of resorcinarene (0.225 g, 0.316 mmol, 1 eq) in anhydrous tetrahydrofuran (10 mL) was added butyllithium (2.5 mL, 1.35 M, 3.38 mmol, 10.7 eq) while at 0 °C under nitrogen. The resultant cloudy mixture with white precipitate was stirred at room temperature under nitrogen for 45 minutes. TBDMS-Cl (0.507 g, 3.36 mmol, 10.7 eq) was added with anhydrous tetrahydrofuran (~1 mL), and the reaction mixture was stirred at the same conditions for 45 minutes. During this time, the cloudy mixture became clear. The tetrahydrofuran was then removed under reduced pressure, and the residue was dissolved in ether and dilute HCl (1 M). The layers were separated, and the organic layer was washed with brine, dried (MgSO$_4$), filtered, and solvent removed under reduced pressure to give a yellow to orange-brown oil as the crude product. The ^{1}H NMR spectrum and TLC of the crude product indicated mostly starting material with some mono-TBDMS resorcinarene product.

4.3.3 General procedure for the distal phenol substitution of resorcinarenes via KOtBu and THF

To potassium *tert*-butoxide (2 eq) was added resorcinarene **(1)** or **(31)** (1 eq) with anhydrous tetrahydrofuran (5 mL) to give an initially cloudy pink mixture, which turned beige while stirring at room temperature under nitrogen for 45 minutes. The respective derivitising agent (2 eq) was then added to the mixture, rapidly turning it clear. After stirring at room temperature under nitrogen for 2 hours, the solvent was removed under reduced pressure to give a brown solid which was dissolved in dichloromethane and washed with dilute HCl (1 M). The aqueous layer was extracted with dichloromethane, and the combined organic extracts were dried (MgSO$_4$), filtered, and solvent removed under reduced pressure. The resultant crude solid was

subjected to preparative TLC to give the pure resorcinarenes. The beige products were recrystallised from the appropriate solvents to give white crystals for analysis.

4.3.3.1 $1^4,3^6,5^6,7^6$-tetrahydroxy-$1^6,3^4,5^4,7^4$-tetramethoxy-2,4,6,8-tetraheptylresorcin[4]arene (31)

Resorcinarene (31), that was synthesised in previous work[107] was used.

4.3.3.2 *tert*-Butyldimethylsilyl ether (TBDMS)

The general procedure was applied with potassium *tert*-butoxide (23.0 mg, 0.205 mmol, 2.06 eq), resorcinarene (1) (71.0 mg, 0.0996 mmol, 1.00 eq), anhydrous tetrahydrofuran (5 mL) and TBDMS-Cl (30.3 mg, 0.201 mmol, 2.02 eq) in petroleum spirits (0.1 mL) to give a mixture which was subjected to preparative TLC (EtOAc – petroleum spirits 40:60) to give pure, previously unreported resorcinarenes: tri (35) (13 mg, 12%), distal (34) (29 mg, 31%), proximal (33) (14 mg, 15%), mono (32) (23 mg, 28%) as beige solids as well as remaining resorcinarene (1) (7 mg, 10%) in respective elution order.
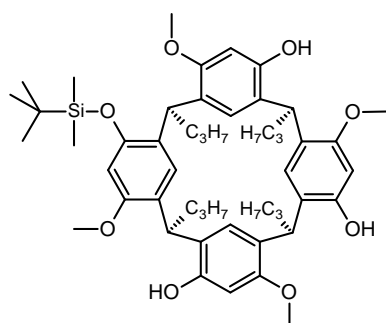
Mono-TBDMS resorcinarene (32): m.p. 255-256 °C (DCM/MeOH); IR 3420 cm^{-1} (OH phenol); ^{1}H NMR (CDCl$_3$) δ 0.26, 0.29 (2s, 2 × 3 H, Si(CH_3)$_2$), 0.87-1.03 (m, 12 H, CH$_2$CH_3), 1.06 (s, 9 H, SiC(CH_3)$_3$), 1.11-1.42 (m, 8 H, CH_2CH$_3$), 1.72-1.89, 1.93-2.08, 2.05-2.28 (3m, 1 H, 1 H, 6 H, CH_2CH), 3.59, 3.78, 3.857, 3.863 (4s, 4 × 3 H, OCH_3), 4.22-4.36 (m, 3 H, CHCH$_2$), 4.81 (t, *J* = 7.9 Hz, 1 H, CHCH$_2$), 6.23, 6.29, 6.41 (3s, 1 H, 2 H, 1 H, ArH), 6.99 (overlapped, br s, 2 H, OH), 7.03, 7.11 (2s, 2 × 1 H, ArH), 7.21 (overlapped, br s, 1 H, OH), 7.22, 7.33 (2s, 2 × 1 H, ArH); ^{13}C NMR (CDCl$_3$) δ -4.0, -3.5 (Si(CH_3)$_2$), 14.16, 14.20, 14.6 (CH$_2$CH_3), 18.6 (SiC(CH$_3$)$_3$), 21.05, 21.12, 21.14, 21.3 (CH$_2$CH$_3$), 26.1 (SiC(CH$_3$)$_3$), 32.5, 32.8, 32.9, 33.0 (CHCH$_2$), 36.0, 36.7, 37.1, 39.4 (CH$_2$CH), 55.4, 55.9, 56.0, 56.0 (OCH$_3$), 99.4, 99.6, 100.2, 101.7 (CH, Ar), 121.9, 123.1 (C, Ar), 123.3, 123.4 (CH, Ar), 124.2, 124.4, 125.1, 125.2 (C, Ar), 125.3, 126.8 (CH, Ar), 130.3, 151.8, 152.4, 152.8, 153.1, 153.40, 153.44, 154.3, 156.6 (C, Ar) (note some signals are coincident). Found: C, 72.46; H, 8.37; C$_{50}$H$_{70}$O$_8$Si; requires C, 72.60; H, 8.53%.
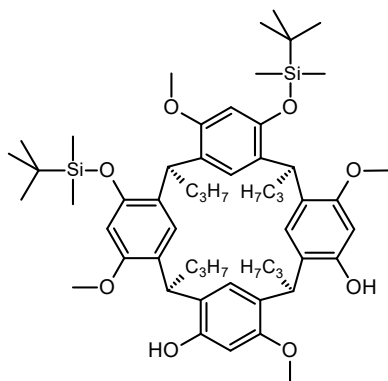
Proximal-TBDMS resorcinarene (33): m.p. 211 °C (MeCN); IR 3490 cm^{-1} (OH phenol); ^{1}H NMR (CDCl$_3$) δ -0.27, 0.04, 0.28, 0.31 (4s, 4 × 3 H, Si(C*H*$_3$)$_2$), 0.85 (s, 9 H, SiC(C*H*$_3$)$_3$), 0.85-0.94, 0.94-1.03 (2m, 2 × 6 H, CH$_2$C*H*$_3$), 1.07 (s, 9 H, SiC(C*H*$_3$)$_3$), 1.14-1.46 (m, 8 H, C*H*$_2$CH$_3$), 1.68-1.94, 1.97-2.13 (2m, 2 × 4 H, C*H*$_2$CH), 3.47, 3.70, 3.75, 3.87 (4s, 4 × 3 H, OC*H*$_3$), 4.18, 4.31 (2t, *J* = 7.4 Hz, 2 × 1 H, C*H*CH$_2$), 4.57-4.70 (m, 2 H, C*H*CH$_2$), 6.18, 6.19, 6.34, 6.45, 6.48, 6.82, 7.16, 7.23 (8s, 8 × 1 H, Ar*H*); ^{13}C NMR (CDCl$_3$) δ -4.6, -4.1, -3.8, -3.5 (Si(*C*H$_3$)$_2$), 14.28, 14.29, 14.6 (CH$_2$*C*H$_3$), 18.3, 18.5 (Si*C*(CH$_3$)$_3$, 21.1, 21.3, 21.6 (*C*H$_2$CH$_3$), 25.9, 26.1 (SiC(*C*H$_3$)$_3$), 33.0, 33.9 (*C*HCH$_2$), 34.4, 35.1 (br, CHCH$_2$), 36.4, 36.6 (*C*H$_2$CH), 38.9, 39.2 (br, *C*H$_2$CH), 54.9, 55.1, 55.6, 56.0 (O*C*H$_3$), 99.0, 100.1, 101.4, 102.5 (*C*H, Ar), 121.3, 123.1 (br), 124.3 (*C*, Ar), 124.7 (*C*H, Ar), 125.2 (*C*, Ar), 125.5 (br, *C*H, Ar), 125.6 (*C*, Ar), 125.7 (*C*H, Ar), 126.1 (*C*, Ar), 127.1 (*C*H, Ar), 128.7 (br), 151.2, 152.1, 152.7, 153.0, 153.5, 154.0, 154.7, 156.9 (*C*, Ar) (note some signals are coincident). Found: C, 71.49; H, 9.01; C$_{56}$H$_{84}$O$_8$Si$_2$; requires C, 71.44; H, 8.99%.
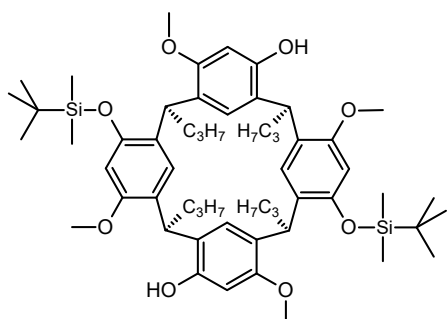
Distal-TBDMS resorcinarene (34): m.p. 236-237 °C (CHCl$_3$/MeOH); IR 3470 cm^{-1} (OH phenol); ^{1}H NMR (CDCl$_3$) δ 0.31 (br s, 12 H, Si(C*H*$_3$)$_2$), 0.88 (t, *J* = 7.3 Hz, 6 H, CH$_2$C*H*$_3$), 0.90-1.02 (m, 6 H, CH$_2$C*H*$_3$), 1.07-1.47 (m, 8 H, C*H*$_2$CH$_3$), 1.08 (br s, 18 H, SiC(C*H*$_3$)$_3$), 1.62-1.88, 1.70-1.97, 1.85-2.10, 1.93-2.30 (4m, 4 × 2 H, C*H*$_2$CH), 3.54, 3.87 (2br s, 2 × 6 H, OC*H*$_3$), 4.28, 4.72 (2 br s, 2 × 2 H, C*H*CH$_2$), 6.01, 6.20, 6.35, 6.76 (4br s, 4 × 2 H, Ar*H*), 7.25 (overlapped with CHCl$_3$, br s, 2 H, O*H*); ^{13}C NMR (CDCl$_3$) δ -3.7 (Si(*C*H$_3$)$_2$), 14.3, 14.5 (CH$_2$*C*H$_3$), 18.5 (Si*C*(CH$_3$)$_3$), 21.0, 21.4 (*C*H$_2$CH$_3$), 26.0 (SiC(*C*H$_3$)$_3$), 33.5 (*C*HCH$_2$), 36.9, 39.5 (*C*H$_2$CH), 55.3, 55.8 (O*C*H$_3$), 99.5, 101.1 (*C*H, Ar), 120.8, 123.6, 124.4 (*C*, Ar), 124.6, 127.5 (*C*H, Ar), 130.6, 151.8, 153.1, 153.4, 156.7 (*C*, Ar) (note some signals are coincident); ^{1}H NMR (DMSO-d$_6$) δ -0.11, 0.09 (2s, 2 × 6 H, Si(C*H*$_3$)$_2$), 0.79 (t, *J* = 7.3 Hz, 6 H, CH$_2$C*H*$_3$), 0.82 (t, *J* = 7.3 Hz, 6 H, CH$_2$C*H*$_3$), 0.89 (s, 18 H, SiC(C*H*$_3$)$_3$), 1.02-1.32 (m, 8 H, C*H*$_2$CH$_3$), 1.50-1.80 (m, 8 H, C*H*$_2$CH), 3.51, 3.60 (2s, 2 × 6 H, OC*H*$_3$), 4.39-4.53 (m, 4 H, C*H*CH$_2$), 6.16, 6.30, 6.55, 6.83 (4s, 4 ×

2 H, Ar*H*), 8.74 (s, 2 H, O*H*); ^{13}C NMR (20% CDCl$_3$ in DMSO-d$_6$) δ -4.9, -4.3 (Si(*C*H$_3$)$_2$), 13.9, 14.0 (CH$_2$*C*H$_3$), 17.7 (Si*C*(CH$_3$)$_3$), 20.7, 20.9 (*C*H$_2$CH$_3$), 25.4 (SiC(*C*H$_3$)$_3$), 33.8, 34.2 (*C*HCH$_2$), 37.4, 38.0 (*C*H$_2$CH), 54.6, 55.2 (O*C*H$_3$), 98.3, 102.0 (*C*H, Ar), 122.3, 122.6, 125.0, 125.3 (*C*, Ar), 125.6, 126.3 (*C*H, Ar), 150.9, 152.8, 154.6, 154.8 (*C*, Ar); ^{1}H NMR (Acetone-d$_6$) δ 0.05, 0.19 (2s, 2 × 6 H, Si(*C*H$_3$)$_2$), 0.87 (t, *J* = 7.4 Hz, 6 H, CH$_2$*C*H$_3$), 0.92 (t, *J* = 7.4 Hz, 6 H, CH$_2$*C*H$_3$), 0.99 (s, 18 H, SiC(*C*H$_3$)$_3$), 1.16-1.27, 1.27-1.40 (2m, 2 × 4 H, *C*H$_2$CH$_3$), 1.68-1.82, 1.82-1.98 (2m, 2 H, 6 H, *C*H$_2$CH), 3.64, 3.66 (2s, 2 × 6 H, O*C*H$_3$), 4.52 (t, *J* = 7.6 Hz, 2 H, *C*HCH$_2$), 4.68 (t, *J* = 7.7 Hz, 2 H, *C*HCH$_2$), 6.32, 6.90, 7.04 (3s, 4 H, 2 H, 2 H, Ar*H*), 7.27 (s, 2 H, O*H*); ^{13}C NMR (Acetone-d$_6$) δ -4.1, -3.7 (Si(*C*H$_3$)$_2$), 14.5, 14.6 (CH$_2$*C*H$_3$), 18.8 (Si*C*(CH$_3$)$_3$), 21.9, 22.2 (*C*H$_2$CH$_3$), 26.2 (SiC(*C*H$_3$)$_3$), 35.27, 35.30 (*C*HCH$_2$), 38.2, 39.5 (*C*H$_2$CH), 55.4, 56.1 (O*C*H$_3$), 99.6, 103.2 (*C*H, Ar), 123.6, 124.9, 126.1 (*C*, Ar), 126.6 (*C*H, Ar), 127.5 (*C*, Ar), 127.9 (*C*H, Ar), 152.7, 154.1, 155.9, 156.6 (*C*, Ar). HRMS (ESI): calcd. for C$_{56}$H$_{85}$O$_8$Si$_2$ as [M + H]$^+$ 941.5778; found 941.5781. Found: C, 71.05; H, 9.15; C$_{56}$H$_{84}$O$_8$Si$_2$; requires C, 71.44; H, 8.99%.
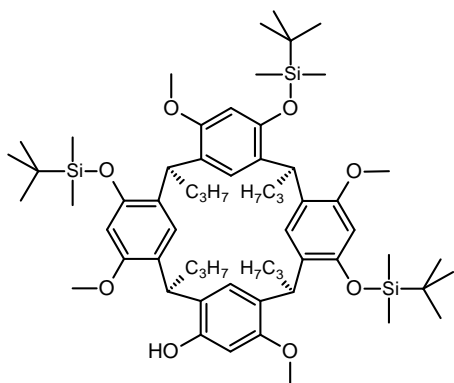
Tri-TBDMS resorcinarene (**35**): m.p. 261-262 °C (CHCl$_3$/MeOH); IR 3544 cm^{-1} (OH phenol); ^{1}H NMR (CDCl$_3$) δ -0.10, 0.07, 0.15, 0.19, 0.26, 0.28, (6s, 6 × 3 H, Si(*C*H$_3$)$_2$), 0.84-0.98 (m, 12 H, CH$_2$*C*H$_3$), 0.84, 1.04, 1.02 (3s, 3 × 9 H, SiC(*C*H$_3$)$_3$), 1.19-1.48 (m, 8 H, *C*H$_2$CH$_3$), 1.66-2.02 (m, 8 H, *C*H$_2$CH), 3.46, 3.51, 3.70, 3.79 (4s, 4 × 3 H, O*C*H$_3$), 4.22 (t, *J* = 6.7 Hz, 1 H, *C*HCH$_2$), 4.42-4.50, 4.48-4.56 (2m, 1 H, 2 H, *C*HCH$_2$), 6.14, 6.21 (2s, 2 × 1 H, Ar*H*), 6.30 (br s, 2 H, Ar*H*), 6.33, 6.54, 6.96, 6.99 (4s, 4 × 1 H, Ar*H*); ^{13}C NMR (CDCl$_3$) δ -4.3, -4.3, -4.1, -4.0, -3.7, -3.4 (Si(*C*H$_3$)$_2$), 14.37, 14.44, 14.5, 14.6 (CH$_2$*C*H$_3$), 18.2, 18.39, 18.40 (Si*C*(CH$_3$)$_3$), 21.2, 21.6, 21.6, 21.7 (*C*H$_2$CH$_3$), 25.86, 25.93, 26.0 (SiC(*C*H$_3$)$_3$), 34.7, 35.6, 36.00, 36.04 (*C*HCH$_2$), 37.2, 37.3, 37.70, 37.73 (*C*H$_2$CH), 54.8, 55.3, 55.5, 55.7 (O*C*H$_3$), 99.5, 101.4, 101.7, 103.0 (*C*H, Ar), 121.0, 123.5, 124.3, 124.5, 125.2 (*C*, Ar), 126.0, 126.2, 126.4 (*C*H, Ar), 127.4 (*C*CH, Ar), 127.7 (*C*H, Ar), 128.0, 129.6, 151.2, 152.1, 152.4, 154.2, 154.9, 155.8, 156.7 (*C*, Ar) (note some signals are coincident). Found: C, 70.51; H, 9.69; C$_{62}$H$_{98}$O$_8$Si$_3$; requires C, 70.54; H, 9.36%.

The procedure was repeated on a larger scale with resorcinarene **(1)** (1.24 g, 1.74 mmol, 1.00 eq), anhydrous tetrahydrofuran (50 mL), potassium *tert*-butoxide (0.390 g, 3.48 mmol, 2.00 eq), TBDMS-Cl (0.524 g, 3.47 mmol, 2.00 eq), and after column chromatography (EtOAc – petroleum spirits 5:95 to 40:60), gave pure resorcinarenes: tri **(35)** (0.267 g, 14%), distal **(34)** (0.403 g, 25%), proximal **(33)** (0.217 mg, 13%), mono **(32)** (0.356 g, 25%) as beige solids as well as remaining resorcinarene **(1)** (0.167 mg, 13%) in respective elution order.

The procedure was repeated on a larger scale with resorcinarene **(1)** (6.99 g, 9.80 mmol, 1.00 eq), anhydrous tetrahydrofuran (210 mL) potassium *tert*-butoxide (2.20 g, 19.6 mmol, 2.00 eq), TBDMS-Cl (2.97 g, 19.7 mmol, 2.01 eq), and after column chromatography (EtOAc – petroleum spirits 10:90 to 15:85), gave pure resorcinarenes tri **(35)** (1.73 g, 17%), and distal **(34)** (2.63 g, 28%) in respective elution order; the remaining compounds were not separated.

4.3.3.3 TBDMS with Sodium Hydride

Sodium hydride (60% in oil) was washed three times with petroleum spirits while under nitrogen in a schlenk flask. The residue petroleum spirits was evaporated under a stream of nitrogen. To the sodium hydride (10 mg, 0.417 mmol, 2.01 eq) was added resorcinarene **(1)** (148 mg, 0.208 mmol, 1.00 eq), a crystal of imidazole, and anhydrous tetrahydrofuran (5 mL) to produce a gently-bubbling, slightly-cloudy solution. After stirring for 30 minutes at room temperature under nitrogen, the solution gradually become completely cloudy white. Then, TBDMS-Cl (63 mg, 0.416 mmol, 2.00 eq) was added with anhydrous tetrahydrofuran (2 mL), and the cloudy white mixture was stirred overnight at room temperature under nitrogen, although TLC monitoring of the reaction mixture indicated that the reaction had finished within 3 hours. The reaction mixture was then filtered through a pad of silica and washed with EtOAc (10 mL). Removal of the solvent under reduced pressure gave the crude product as a yellowish solid (192 mg). About half the crude product (95 mg) was subjected to preparative TLC (EtOAc – petroleum spirits 35:65) to give pure resorcinarenes: tri **(35)** (8 mg, 7%), distal **(34)** (22 mg, 23%), proximal **(33)** (12 mg, 12%), mono **(32)** (31 mg, 37%) as beige solids as well as remaining starting resorcinarene **(1)** (13 mg, 18%) in respective order.

4.3.3.4 *tert*-Butyldiphenylsilyl ether (TBDPS)

The general procedure was applied with resorcinarene (**1**) (112 mg, 0.157 mmol, 1.00 eq)*,* anhydrous tetrahydrofuran (5 mL) potassium *tert*-butoxide (0.035 g, 0.312 mmol, 1.99 eq) and TBDPS-Cl (0.0817 mL, 86.4 mg, 0.3143 mmol, 2.00 eq)*,* the mixture was stirred overnight, concentrated, and half of the residue was then subjected to preparative TLC (EtOAc – petroleum spirits 30:70) to give pure, previously unreported resorcinarenes: distal (**42**) (15 mg, 16%), proximal (**41**) (6.8 mg, 7%), mono (**40**) (24 mg, 32%), and unreacted resorcinarene (**1**) (11 mg, 39%) in respective elution order.
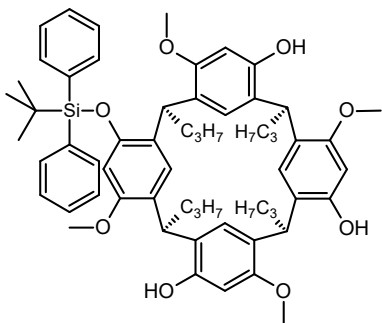
Mono-TBDPS resorcinarene (**40**): m.p. 260-261 °C (CHCl$_3$/MeOH); IR 3437 cm^{-1} (OH phenol); ^{1}H NMR (CDCl$_3$) δ 0.74-1.06 (m, 12 H, CH$_2$C*H*$_3$), 1.08-1.50 (m, 8 H, C*H*$_2$CH$_3$), 1.19 (s, 9 H, SiC(C*H*$_3$)$_3$), 1.82-1.97, 1.99-2.17, 2.17-2.32 (3m, 1 H, 5 H, 2 H, C*H*$_2$CH), 3.11, 3.41, 3.76, 3.89 (4s, 4 × 3 H, OC*H*$_3$), 4.13 (t, J = 7.7 Hz, 1 H, C*H*CH$_2$), 4.25 (t, J = 7.8 Hz, 1 H, C*H*CH$_2$), 4.34 (t, J = 7.8 Hz, 1 H, C*H*CH$_2$), 5.14 (t, J = 8.1 Hz, 1 H, C*H*CH$_2$), 5.86, 6.24, 6.43 (3s, 1 H, 2 H, 1 H, Ar*H*), 6.82 (br s, 1 H, O*H*), 7.00, 7.10 (2s, 2 H, 1 H, Ar*H*), 7.29-7.48 (m, 9 H, Ar*H, O*H*), 7.66-7.73, 7.74-7.84 (2m, 2 × 2H, Ar*H*); ^{13}C NMR (CDCl$_3$) δ 14.1, 14.2, 14.7 (CH$_2$*C*H$_3$), 19.8 (Si*C*(CH$_3$)$_3$), 20.9, 21.14, 21.15, 21.5 (*C*H$_2$CH$_3$), 26.8 (SiC(*C*H$_3$)$_3$), 32.5, 32.6, 32.8, 33.0 (*C*HCH$_2$), 35.7, 36.7, 37.1, 39.7 (*C*H$_2$CH), 55.0, 55.7, 55.9, 56.1 (O*C*H$_3$), 99.2, 99.2, 100.3, 102.8 (*C*H, Ar), 121.7, 122.9 (*C*, Ar), 122.9, 123.3 (*C*H, Ar), 124.1, 124.2, 125.0, 125.3 (*C*, Ar), 125.5 (*C*H, Ar), 125.5 (*C*, Ar), 126.8 , 127.88, 127.90 (*C*H, Ar), 129.6 (*C*, Ar), 129.9 (*C*H, Ar), 133.3, 133.5 (*C*, Ar), 135.70, 135.73 (*C*H, Ar), 151.5, 152.27, 152.31, 153.26, 153.33, 153.4, 154.4, 156.5 (*C*, Ar) (note some signals are coincident). Found: C, 75.53; H, 7.76; C$_{60}$H$_{74}$O$_8$Si; requires C, 75.75; H, 7.84%.
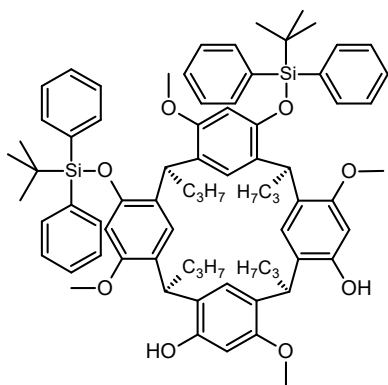
Proximal-TBDPS resorcinarene **(41)**: m.p. 137-138 °C (MeOH); IR 3455 cm^{-1} (OH phenol); ^{1}H NMR (CDCl$_3$) δ 0.79 (s, 9 H, SiC(CH_3)$_3$), 0.85-1.03 (m, 12 H, CH$_2$CH_3), 1.16 (s, 9 H, SiC(CH_3)$_3$), 1.23-1.52 (m, 8 H, CH_2CH$_3$), 1.67-1.78, 1.80-1.93, 1.94-2.22 (3m, 5 H, 2 H, 1 H, CH_2CH), 2.92, 2.97, 3.51, 3.88 (4s, 4 × 3 H, OCH_3), 4.04 (t, J = 7.6 Hz, 1 H, CHCH$_2$), 4.34 (t, J = 7.6 Hz, 1 H, CHCH$_2$), 4.88-4.98, 5.08-5.17 (2m, 2 × 1 H, CHCH$_2$), 5.68, 5.90, 6.29, 6.42, 6.65, 6.92 (6s, 6× 1 H, ArH), 7.05-7.14 (m, 4 H, ArH), 7.21-7.47 (overlapped with CHCl$_3$, m, 11 H, ArH), 7.63-7.74 (m, 5 H, ArH), 7.83-7.89 (m, 2 H, ArH); ^{13}C NMR (CDCl$_3$) δ 14.2, 14.26, 14.27, 14.8 (CH$_2$$CH_3$), 19.2, 19.7 (SiC(CH$_3$)$_3$), 21.0, 21.1, 21.3, 21.8 (CH$_2$CH$_3$), 26.4, 26.7 (SiC(CH$_3$)$_3$), 32.8, 33.70, 33.75 (br), 34.8 (CHCH$_2$), 36.3, 36.6, 39.8, 40.1 (CH$_2$CH), 54.3, 55.0, 55.1, 56.0 (OCH$_3$), 99.1, 100.3, 102.1, 102.6 (CH, Ar), 121.4, 123.3, 124.0 (C, Ar), 124.7, 125.2, 125.4 (CH, Ar), 125.4, 125.7 (C, Ar), 126.8 (CH, Ar), 126.9 (C, Ar), 127.70, 127.71, 127.9, 127.9, 129.56, 129.57, 129.79, 129.84 (CH, Ar), 133.0, 133.1, 134.32, 134.35 (C, Ar), 135.6, 135.68, 135.73, 135.75 (CH, Ar), 151.0, 152.0, 152.9, 153.0, 153.2, 153.5, 154.1, 157.0 (C, Ar) (note some signals are coincident). HRMS (ESI): calcd. for C$_{72}$H$_{92}$O$_8$Si$_2$ as [M]$^+$ 1188.6331; found 1188.6310.

Distal-TBDPS resorcinarene **(42)**: m.p. 270-271 °C (CHCl$_3$/MeOH); IR 3479 cm^{-1} (OH phenol); ^{1}H NMR (CDCl$_3$) δ 0.94 (t, J = 7.3 Hz, 6 H, CH$_2$CH_3), 0.95 (t, J = 7.3 Hz, 6 H, CH$_2$CH_3), 1.19-1.63 (m, 8 H, CH_2CH$_3$), 1.20 (s, 18 H, SiC(CH_3)$_3$), 1.80-1.93, 1.93-2.07, 2.07-2.20 (3m, 2 H, 4 H, 2 H, CH_2CH), 3.17, 3.46 (2s, 2 × 6 H, OCH_3), 4.18 (t, J = 7.5 Hz, 2 H, CHCH$_2$), 5.11 (t, J = 7.9 Hz, 2 H, CHCH$_2$), 5.90, 6.20, 6.30, 6.90 (4s, 4 × 2 H, ArH), 7.31-7.52 (m, 14 H, ArH, OH), 7.79 (d, J = 7.7 Hz, 8 H, ArH); ^{13}C NMR (CDCl$_3$) δ 14.2, 14.7 (CH$_2$$CH_3$), 19.8 (SiC(CH$_3$)$_3$), 21.0, 21.6 ($CH_2CH_3$), 26.7 (SiC($CH_3$)$_3$), 33.0, 33.1 ($CHCH_2$), 36.8, 40.0 ($CH_2$CH), 55.1, 55.5 (O$CH_3$), 99.0, 102.3 ($C$H, Ar), 120.6, 123.7 ($C$, Ar), 124.3 ($C$H, Ar), 124.3 ($C$, Ar), 127.3, 127.9, 127.9 (CH, Ar), 129.9 (C, Ar), 129.9, 130.0 (CH, Ar), 133.0, 133.7,
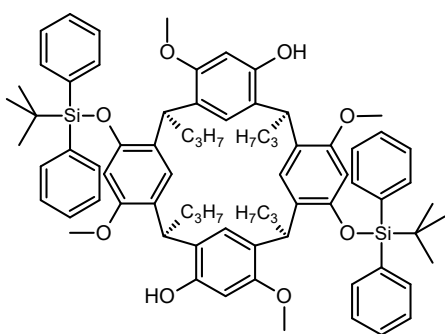
135.7, 135.8 (C*H*, Ar), 151.3, 152.4, 153.4, 156.7 (*C*, Ar). Found: C, 76.40; H, 8.06; $C_{76}H_{92}O_8Si_2$; requires C, 76.73; H, 7.79%.

4.3.3.5 Benzyl ether

The general procedure was applied with resorcinarene **(1)** (76 mg, 0.107 mmol, 1.00 eq), anhydrous tetrahydrofuran (6 mL) potassium *tert*-butoxide (24 mg, 0.214 mmol, 2.01 eq) and benzyl bromide (0.0254 mL, 36.5 mg, 0.213 mmol, 2.00 eq). After reaction overnight, the tetrahydrofuran solvent was evaporated, and the residue was filtered through a short plug of silica eluting with EtOAc. The EtOAc was evaporated, and the residue was subjected to preparative TLC (EtOAc – petroleum spirits 40:60) to give pure resorcinarenes: tetra **(22)** (6.5 mg, 6%), tri **(47)** (26 mg, 25%), distal **(46)** (14 mg, 15%), proximal **(45)** (17 mg, 18%), and mono **(44)** co-eluted with unreacted resorcinarene **(1)** in respective elution order. The co-eluted mono and starting resorcinarene was mostly separated by another preparative TLC (EtOAc – DCM 5:95) to give mono **(44)** (9 mg, 11%) and resorcinarene **(1)** (4 mg, 5%). Tri **(47)** and proximal **(45)** resorcinarenes formed brown oils which could not be crystallised. The ¹H NMR spectrum of the first-eluting product matched that of the tetra-OBn resorcinarene **(22)** which is described in **Section 3.4.1.1**. All other OBn resorcinarenes are previously unreported.
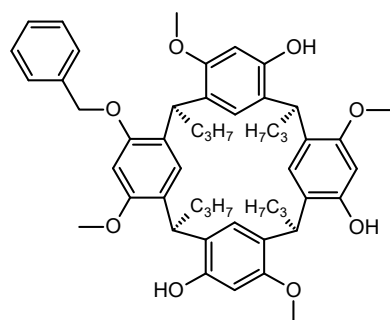
Mono-OBn resorcinarene **(44)**: mp 220-224 °C (MeCN); IR 3413 cm⁻¹ (OH phenol); ¹H NMR (only relevant signals quoted, CDCl₃) δ 0.85-1.03 (m, 12 H, CH₂C*H₃*), 1.15-1.38 (m, 8 H, C*H₂*CH₃), 1.92-2.02, 2.08-2.25 (2m, 2 H, 6 H, C*H₂*CH), 3.38, 3.80, 3.84, 3.85 (4s, 4 × 3 H, OC*H₃*), 4.24-4.34 (m, 3 H, C*H*CH₂), 5.00-5.06 (m, 1 H, C*H*CH₂), 5.01, 5.07 (AB, *J* = 12.0 Hz, 2 H, C*H₂*Ph), 6.21, 6.31, 6.38, 6.39 (4s, 4 × 1 H, Ar*H*), 7.09, 7.17 (2br s, 2 × 1 H, O*H*), 7.18, 7.19, 7.22 (3s, 3 × 1 H, Ar*H*), 7.24 (br s, 1 H, O*H*), 7.27-7.33, 7.34-7.41, 7.46-7.53 (3m, 2 H, 2 H, 2 H, Ar*H*); ¹³C NMR (only relevant signals quoted, CDCl₃) δ 14.1, 14.2, 14.3 (CH₂*C*H₃), 21.06, 21.09, 21.1, 21.2 (*C*H₂CH₃), 31.7, 32.86, 32.88, 33.0 (*C*HCH₂), 36.2, 36.5, 36.7, 39.0 (*C*H₂CH), 55.2, 55.9, 56.0, 56.2 (O*C*H₃), 71.0 (O*C*H₂Ph), 97.0, 99.5, 99.6, 100.1 (*C*H, Ar), 122.3 (*C*, Ar), 123.56 (*C*H, Ar), 123.64, 123.9, 124.5 (*C*, Ar), 124.7 (*C*H, Ar), 124.9, 125.1, 125.9 (*C*, Ar), 126.1, 127.0, 127.6, 128.6 (*C*H, Ar), 128.9, 138.0,

152.6, 152.9, 153.3, 153.4, 153.7, 154.1, 155.3, 156.2 (*C*, Ar) (note some signals are coincident). HRMS (ESI): calcd. for $C_{51}H_{63}O_8$ as $[M + H]^+$ 803.4517; found 803.4497.
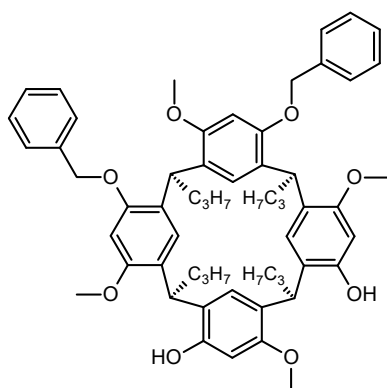
Proximal-OBn resorcinarene (45): IR 3447 cm^{-1} (OH phenol); ^{1}H NMR (CDCl$_3$) δ 0.84-1.02 (m, 12 H, CH$_2$C*H$_3$*), 1.12-1.42 (m, 8 H, C*H$_2$*CH$_3$), 1.77-2.01, 2.03-2.19 (2m, 2 × 4 H, C*H$_2$*CH), 3.43, 3.47, 3.77, 3.84 (4s, 4 × 3 H, OC*H$_3$*), 4.26 (t, *J* = 7.7 Hz, 1 H, C*H*CH$_2$), 4.30 (t, *J* = 7.7 Hz, 1 H, C*H*CH$_2$), 4.80, 4.89 (AB, *J* = 11.6 Hz, 2 H, C*H$_2$*Ph), 4.82-4.98 (m, 2 H, C*H*CH$_2$), 5.03, 5.07 (AB, *J* = 12.0 Hz, 2 H, C*H$_2$*Ph), 6.21, 6.34, 6.36, 6.42, 6.86, 7.04, 7.18 (7s, 7 × 1 H, Ar*H*), 7.26-7.33, 7.34-7.41, 7.46-7.53 (3m, 6 H, 3 H, 2 H, Ar*H*); ^{13}C NMR (CDCl$_3$) δ 14.2, 14.38, 14.40 (CH$_2$*C*H$_3$), 21.1 (*C*H$_2$CH$_3$), 33.1, 33.5 (*C*HCH$_2$), 36.6, 39.2 (br, *C*H$_2$CH), 55.3, 55.4, 55.9, 56.0 (O*C*H$_3$), 71.0, 71.1 (O*C*H$_2$Ph), 97.2, 97.4, 99.2, 100.0 (*C*H, Ar), 121.9, 124.3 (*C*, Ar), 124.4 (br, *C*H, Ar), 124.8, 125.1 (*C*, Ar), 125.2 (br, *C*H, Ar), 125.4 (*C*, Ar), 125.8 (*C*H, Ar), 127.1 (*C*, Ar), 127.1, 127.48, 127.52, 127.6, 128.4, 128.5 (*C*H, Ar), 137.7, 138.4, 152.4, 152.6, 153.8, 154.1, 154.9 (br), 155.4 (br), 155.8, 156.5 (*C*, Ar) (note some signals are coincident). HRMS (ESI): calcd. for $C_{58}H_{69}O_8$ as $[M + H]^+$ 893.4987; found 893.4913.
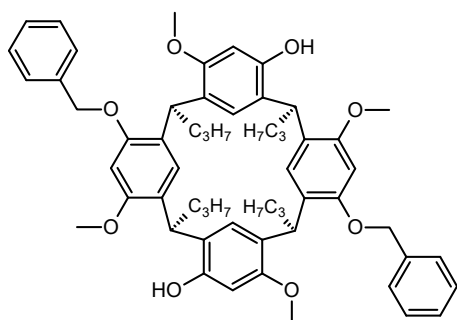
Distal-OBn resorcinarene (46): m.p. 202-203 °C (CHCl$_3$/MeOH); IR 3368 cm^{-1} (OH phenol); ^{1}H NMR (CDCl$_3$) δ 0.91 (t, *J* = 7.2 Hz, 6 H, CH$_2$C*H$_3$*), 0.99 (t, *J* = 7.2 Hz, 6 H, CH$_2$C*H$_3$*), 1.14-1.44 (m, 8 H, C*H$_2$*CH$_3$), 1.82-2.01, 2.03-2.23 (2m, 2 × 4 H, C*H$_2$*CH), 3.48, 3.89 (2s, 2 × 6 H, OC*H$_3$*), 4.21-4.42, 4.91-5.06 (2m, 2 × 2 H, C*H*CH$_2$), 5.10, 5.14 (AB, *J* = 12.1 Hz, 4 H, C*H$_2$*Ph), 6.22, 6.48, 7.04 (3s, 3 × 2 H, Ar*H*), 6.57 (br s, 2 H, ArO*H*), 7.28-7.37 (m, 4 H, Ar*H*), 7.41 (t, *J* = 7.4 Hz, 4 H, Ar*H*), 7.57 (d, *J* = 7.1 Hz, 4 H, Ar*H*); ^{13}C NMR (CDCl$_3$) δ 14.2, 14.3 (CH$_2$*C*H$_3$), 21.0, 21.1 (*C*H$_2$CH$_3$), 32.2, 33.1 (*C*HCH$_2$), 36.8, 39.5 (*C*H$_2$CH), 55.3, 56.1 (O*C*H$_3$), 71.1 (*C*H$_2$Ph), 96.9, 99.3 (*C*H, Ar), 121.3 (*C*, Ar), 124.1 (*C*H, Ar), 124.7, 124.9 (*C*, Ar), 127.0, 127.1, 127.6, 128.5 (*C*H, Ar), 129.2,

138.1, 153.2, 153.4, 155.1, 156.4 (*C*, Ar). Found: C, 77.67; H, 7.66; $C_{58}H_{68}O_8$; requires C, 78.00; H, 7.67%.
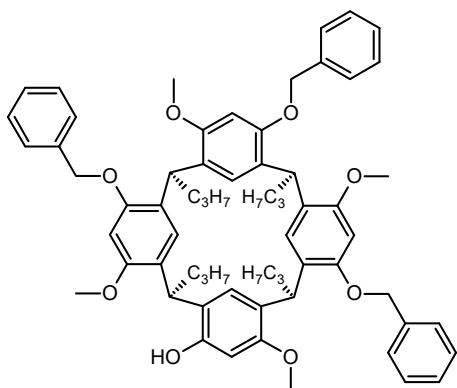
Tri-OBn resorcinarene (**47**): IR 3476cm^{-1} (O*H* phenol); ^{1}H NMR (CDCl$_3$) δ 0.81-1.01 (m, 12 H, CH$_2$C*H*$_3$), 1.18-1.48 (m, 8 H, C*H*$_2$CH$_3$), 1.74-2.06 (m, 8 H, C*H*$_2$CH), 3.37, 3.41, 3.46, 3.79 (4s, 4 × 3 H, OC*H*$_3$), 4.26 (t, *J* = 7.3 Hz, 1 H, C*H*CH$_2$), 4.45, 4.76 (AB, *J* = 11.2 Hz, 2 H, C*H*$_2$Ph), 4.56-4.64 (m, 1 H, C*H*CH$_2$), 4.68-4.76 (m, 2 H, C*H*CH$_2$), 4.99 (d, *J* = 11.8 Hz, 1 H, C*H*$_2$Ph), 5.00 (d, *J* = 11.8 Hz, 1 H, C*H*$_2$Ph), 5.08 (d, *J* = 11.8 Hz, 1 H, C*H*$_2$Ph), 5.10 (d, *J* = 11.8 Hz, 1 H, C*H*$_2$Ph), 6.19, 6.27, 6.39, 6.47, 6.50, 6.64, 7.03 (7s, 7 × 1 H, Ar*H*), 7.04-7.08 (m, 2 H, Ar*H*), 7.09 (s, 1 H, Ar*H*), 7.17-7.24, 7.27-7.42, 7.43-7.50 (3m, 3 H, 7 H, 4 H, Ar*H* + O*H*); ^{13}C NMR (CDCl$_3$) δ 14.3, 14.41, 14.45, 14.5 (CH$_2$*C*H$_3$), 21.1, 21.3, 21.4 (*C*H$_2$CH$_3$), 34.5, 34.8, 35.2 (*C*HCH$_2$), 37.1, 37.4, 37.5, 38.1 (*C*H$_2$CH), 55.4, 55.6, 56.0 (O*C*H$_3$), 71.0, 71.1, 71.2 (O*C*H$_2$Ph), 96.8, 97.6, 98.7, 99.4 (*C*H, Ar), 121.2, 124.3, 124.5, 125.3, 125.4 (*C*, Ar), 125.69, 125.73, 126.0, 127.28, 127.32 (*C*H, Ar), 127.35 (*C*, Ar), 127.5 (*C*H, Ar), 127.61 (*C*, Ar), 127.64, 127.7 (*C*H, Ar), 128.1 (*C*, Ar), 128.2, 128.50, 128.52 (*C*H, Ar), 128.9, 137.7, 138.0, 138.3, 152.5, 154.4, 154.7, 155.4, 155.6, 155.7, 156.1, 156.6 (*C*, Ar) (note some signals are coincident). HRMS (ESI): calcd. for $C_{65}H_{74}O_8$ as [M]$^+$ 982.5384; found 982.5373.

4.3.3.6 Heptyl TBDMS

General procedure with potassium *tert*-butoxide (21.9 mg, 0.195 mmol, 2.01 eq), resorcinarene (**31**) (92.5 g, 0.0987 mmol, 1.00 eq), anhydrous tetrahydrofuran (5 mL) and a solution of TBDMS-Cl in petroleum spirits (0.081 mL, 0.37 g/mL, 29.7 mg, 0.197 mmol) gave a mixture which was subjected to preparative TLC (EtOAc – petroleum spirits 30:70) to give pure, previously unreported resorcinarenes: tri (**39**) (7 mg, 6%), distal (**38**) (25 mg, 22%), proximal (**37**) (15 mg, 13%), mono (**36**) (34 mg, 33%) as colourless solids as well as remaining resorcinarene (**31**) (19 mg, 21%) in respective elution order. All products were colourless solids but, only distal (**38**) could be crystallised.

To assess repeatability, the same reaction was repeated at a similar scale to give: tri **(39)** (6%), distal **(38)** (19%), proximal **(37)** (12%), mono **(36)** (33%), starting resorcinarene **(31)** (23%).
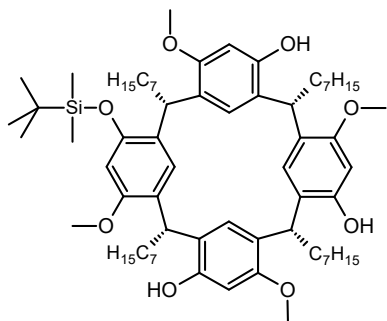
Mono-TBDMS heptyl **(36)**: IR 3434 cm^{-1} (OH phenol); ^{1}H NMR (CDCl$_3$) δ 0.24, 0.29 (2s, 2 × 3 H, Si(C*H*$_3$)$_2$), 0.80-0.95 (m, 12 H, CH$_2$C*H*$_3$), 1.06 (s, 9 H, SiC(C*H*$_3$)$_3$), 1.16-1.45 (m, 40 H, (C*H*$_2$)$_5$CH$_3$), 1.73-1.87, 1.91-2.26 (2m, 1 H, 7 H, C*H*$_2$CH), 3.58, 3.78, 3.85, 3.86 (4s, 4 × 3 H, OC*H*$_3$), 4.17-4.31 (m, 3 H, C*H*CH$_2$), 4.78 (t, J = 8.0 Hz, 1 H, C*H*CH$_2$), 6.22, 6.28, 6.41 (3s, 1 H, 2 H, 1 H, Ar*H*), 6.97 (overlapped, br s, 2 H, O*H*), 7.00, 7.09 (2s, 2 × 1 H, Ar*H*), 7.21 (overlapped, br s, 2 H, Ar*H* + O*H*), 7.32 (s, 1 H, Ar*H*); ^{13}C NMR (CDCl$_3$) δ -4.0, -3.5 (Si(*C*H$_3$)$_2$), 14.3 (CH$_2$*C*H$_3$), 18.6 (Si*C*(CH$_3$)$_3$), 22.8 (*C*H$_2$), 26.1 (SiC(*C*H$_3$)$_3$), 28.0, 28.1, 28.2, 28.3, 29.48, 29.50, 29.56, 29.57, 29.7, 29.9, 30.2, 32.02, 32.05, 32.1 (*C*H$_2$), 32.7, 33.1, 33.3, 33.4 (*C*HCH$_2$), 34.0, 34.7, 35.0, 37.2 (*C*H$_2$CH), 55.4, 55.9, 55.97, 56.05 (O*C*H$_3$), 99.4, 99.6, 100.2, 101.6 (*C*H, Ar), 121.9, 123.1 (*C*, Ar), 123.2, 123.4 (*C*H, Ar), 124.2, 124.5 (*C*, Ar), 125.2 (*C*H, Ar), 125.3, 125.4 (*C*, Ar), 126.7 (*C*H, Ar), 130.4, 151.8, 152.3, 152.8, 153.1, 153.4, 154.3, 156.6 (*C*, Ar) (note some signals are coincident); HRMS (ESI): calcd. for C$_{66}$H$_{103}$O$_8$Si as [M + H]$^+$ 1051.7417; found 1051.7410.
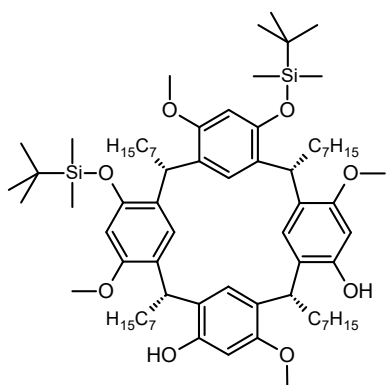
Proximal-TBDMS heptyl **(37)**: IR 3478 cm^{-1} (OH phenol); ^{1}H NMR (CDCl$_3$ Impure, only relevant signals quoted) δ -0.31, 0.01, 0.25, 0.29 (4s, 4 × 3 H, Si(C*H*$_3$)$_2$), 0.82 (s, 9 H, SiC(C*H*$_3$)$_3$), 0.84-0.92 (m, 12 H, CH$_2$C*H*$_3$), 1.05 (s, 9 H, SiC(C*H*$_3$)$_3$), 1.11-1.47 (m, 40 H, (C*H*$_2$)$_5$CH$_3$), 1.66-1.93, 1.93-2.16 (2m, 2 × 4 H, C*H*$_2$CH), 3.44, 3.68, 3.73, 3.88 (4s, 4 × 3 H, OC*H*$_3$), 4.11 (t, J = 7.6 Hz, 1 H, C*H*CH$_2$), 4.26 (t, J = 7.5 Hz, 1 H, C*H*CH$_2$), 4.52-4.66 (m, 2 H, C*H*CH$_2$), 6.15, 6.16 (overlapped 2s, 2 × 1 H, Ar*H*), 6.18 (br s, 1 H, O*H*), 6.32 (s, 1 H, Ar*H*), 6.40 (br s, 2 H, Ar*H* + O*H*), 6.47, 7.14, 7.20 (3s, 3 × 1 H, Ar*H*); ^{13}C NMR (CDCl$_3$) δ -4.6, -4.2, -3.8, -3.5 (Si(*C*H$_3$)$_2$), 14.25, 14.27, 14.29 (CH$_2$*C*H$_3$), 18.3, 18.5 (Si*C*(CH$_3$)$_3$), 22.80, 22.83, 22.9 (*C*H$_2$), 25.9, 26.1 (SiC(*C*H$_3$)$_3$), 28.02, 28.03, 28.2, 28.5, 29.4, 29.46, 29.49, 29.52, 29.85, 29.91, 29.93, 30.3, 32.06, 32.11, 32.2 (*C*H$_2$),

33.3 (CHCH2), 34.5 (CH2CH), 54.8, 55.1, 55.6, 56.0 (OCH3), 99.0, 100.1, 101.4, 102.5 (CH, Ar), 121.4, 123.1, 124.4 (C, Ar), 124.7, 125.3, 125.6 (CH, Ar), 125.7, 126.0, 127.1, 127.2, 128.8, 151.2, 152.1, 152.7, 153.0, 153.5, 154.0, 154.6, 156.9 (C, Ar) (note some signals are coincident); HRMS (ESI): calcd. for $C_{72}H_{117}O_8Si_2$ as $[M + H]^+$ 1165.8281; found 1165.8271.
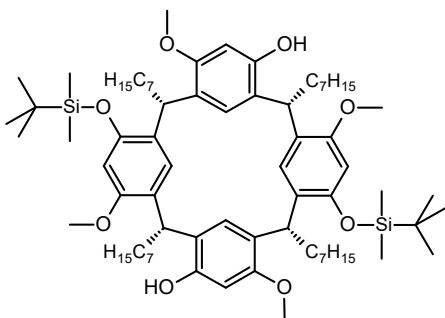
Distal-TBDMS heptyl **(38)**: mp 142 °C (EtOAc/MeOH); IR 3459 cm^{-1} (OH phenol); ^{1}H NMR (CDCl3) δ 0.30 (br s, 12 H, Si(CH3)2), 0.86 (t, J = 6.9 Hz, 12 H, CH2CH3), 1.08 (br s, 18 H, SiC(CH3)3), 1.15-1.45 (m, 40 H, (CH2)5CH3), 1.66-1.80, 1.78-1.90, 1.88-2.02, 2.00-2.18 (4m, 4 × 2 H, CH2CH), 3.53, 3.87 (2br s, 2 × 6 H, OCH3), 4.24, 4.69 (2 br s, 2 × 2 H, CHCH2), 5.77-6.11 (br s, 1 H, OH), 6.18, 6.35, 6.74, (3br s, 3 × 2 H, ArH), 7.25 (overlapped with CHCl3 br s, 2 H, ArH); ^{13}C NMR (CDCl3) δ -3.8 (Si(CH3)2), 14.3 (CH2CH3), 18.5 (br, SiC(CH3)3), 22.8 (CH2), 26.0 (SiC(CH3)3), 27.9, 28.4, 29.5, 29.9, 30.2, 32.1 (CH2), 33.8 (CHCH2), 34.7, 37.3 (CH2CH), 55.3, 55.9 (OCH3), 99.5, 101.2 (CH, Ar), 120.7, 123.7, 124.4 (C, Ar), 124.7, 127.4 (CH, Ar), 130.6, 151.8, 153.1, 153.3, 156.7 (C, Ar) (note some signals are coincident) ^{1}H NMR (Acetone-d6) δ 0.08, 0.21 (2s, 2 × 6 H, Si(CH3)2), 0.82-0.92 (m, 12 H, CH2CH3), 1.01 (s, 18 H, SiC(CH3)3), 1.12-1.45 (m, 40 H, (CH2)5CH3), 1.68-1.83, 1.84-2.01 (2m, 2 H, 6 H, CH2CH), 3.63, 3.68 (2s, 2 × 6 H, OCH3), 4.50 (t, J = 7.4 Hz, 2 H, CHCH2), 4.69 (t, J = 7.7 Hz, 2 H, CHCH2), 6.31, 6.33, 6.94, 7.03 (4s, 4 × 2 H, ArH), 7.24 (s, 2 H, OH); ^{13}C NMR (Acetone-d6) δ -4.0, -3.7 (Si(CH3)2), 14.416, 14.421 (CH2CH3), 18.8 (SiC(CH3)3), 23.36, 23.38 (CH2), 26.3 (SiC(CH3)3), 28.8, 29.1, 30.1, 30.2, 30.58, 30.62, 32.7, 32.8 (CH2), 35.4 (CHCH2), 35.9, 37.3 (CH2CH), 55.4, 56.1 (OCH3), 99.5, 103.1 (CH, Ar), 123.4, 124.8, 126.2 (C, Ar), 126.6 (CH, Ar), 127.7 (C, Ar), 127.9 (CH, Ar), 152.6, 154.0, 155.8, 156.6 (C, Ar) (note some signals are coincident); HRMS (ESI): calcd. for $C_{72}H_{117}O_8Si_2$ as $[M + H]^+$ 1165.8281; found 1165.8272.
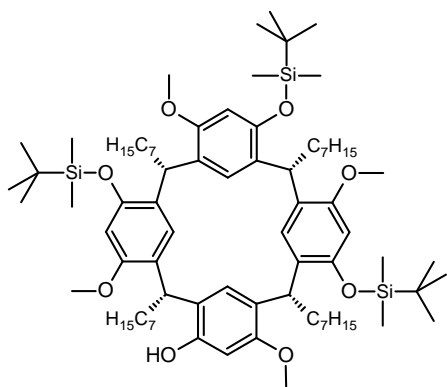
Tri-TBDMS resorcinarene heptyl (**39**): IR 3536 cm^{-1} (OH phenol); ^{1}H NMR (CDCl$_3$) δ -0.12, 0.05, 0.13, 0.18, 0.24, 0.26, (6s, 6 × 3 H, Si(C*H*$_3$)$_2$), 0.82 (s, 9 H, SiC(C*H*$_3$)$_3$), 0.82-0.89 (m, 12 H, CH$_2$C*H*$_3$), 1.01, 1.02 (2s, 2 × 9 H, SiC(C*H*$_3$)$_3$), 1.12-1.44 (m, 40 H, (C*H*$_2$)$_5$CH$_3$), 1.66-1.99 (m, 8 H, C*H*$_2$CH), 3.42, 3.48, 3.68, 3.77 (4s, 4 × 3 H, OC*H*$_3$), 4.10-4.24, 4.35-4.46, 4.44-4.52 (3m, 1 H, 1 H, 2 H, C*H*CH$_2$), 6.11, 6.19, 6.24 (br), 6.28, 6.31, 6.50, 6.95 (br), 6.97 (br), (8s, 8 × 1 H, Ar*H*); ^{13}C NMR (CDCl$_3$) δ -4.4, -4.3, -4.1, -4.0, -3.7, -3.4 (Si(CH$_3$)$_2$), 14.27, 14.29 (CH$_2$*C*H$_3$), 18.2, 18.4, (Si*C*(CH$_3$)$_3$), 22.8, 22.9 (*C*H$_2$), 25.87, 25.95, 26.0 (SiC(*C*H$_3$)$_3$), 28.1, 28.6, 28.7, 29.45, 29.47, 29.50, 29.53, 30.0, 30.1, 30.3, 32.17, 32.25, 34.7 (br) (*C*H$_2$), 34.8 (br, *C*HCH$_2$), 35.0 (br), 35.4 (*C*H$_2$), 35.8, 36.3 (*C*HCH$_2$), 54.8, 55.3, 55.5, 55.7 (O*C*H$_3$), 99.5, 101.3, 101.7, 103.0 (*C*H, Ar), 121.1, 123.5 (br), 124.3, 124.5, 125.2 (br) (*C*, Ar), 125.9, 126.2, 126.4 (br, *C*H, Ar), 127.6 (*C*, Ar), 127.7 (br, *C*H, Ar), 128.2 (br), 129.8 (br), 151.2, 151.3, 152.1, 152.4, 154.2, 154.9, 155.8, 156.7 (*C*, Ar) (note some signals are coincident); HRMS (ESI): calcd. for C$_{78}$H$_{131}$O$_8$Si$_3$ as [M + H]$^+$ 1279.9146; found 1279.9132.

4.3.4 Replacement of TBDMS protecting groups

4.3.4.1 1^4,5^6-di-*tert*-butyldimethylsilylether-3^6,7^6-dimethanesulfonyl-1^6,3^4,5^4,7^4-tetramethoxy-2,4,6,8-tetrapropylresorcin[4]arene (48)
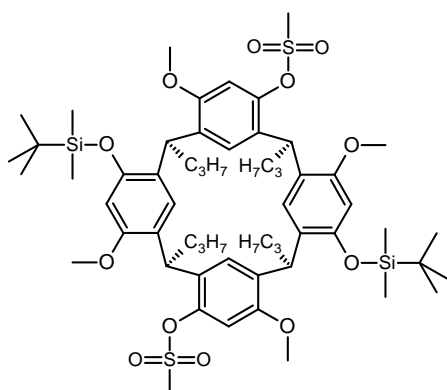
To a clear solution of resorcinarene (**34**) (0.127 g, 0.135 mmol) and triethylamine (0.226 mL, 0.164 g, 1.62 mmol) dissolved in dichloromethane (10 mL) was added methanesulfonyl chloride (0.084 mL, 0.124 g, 1.62 mmol), while in an ice bath. The resultant clear yellow solution was stirred at room temperature under nitrogen for 1 h. The reaction mixture was then washed with dilute HCl (15 mL, 1 M) and the aqueous layer was extracted with dichloromethane (3 × 5 mL). The combined organic extracts were dried (MgSO$_4$), filtered, and solvent removed under reduced pressure to give a yellow-white solid (0.155 g). A portion of the material (0.098 g) was triturated by heating with methanol, allowing to cool to room temperature, then filtering off the resultant yellow

150

solution from the pure, previously unreported product **(48)** which was collected as a white solid (0.078 g, 98%) then washed with methanol: mp 257-258 °C (CHCl$_3$/MeOH); ^{1}H NMR (CDCl$_3$) δ 0.25, 0.31 (2s, 2 × 6 H, Si(CH_3)$_2$), 0.91 (t, J = 7.3 Hz, 6 H, CH$_2$CH_3), 0.92 (t, J = 7.3 Hz, 6 H, CH$_2$CH_3), 1.04 (s, 18 H, SiC(CH_3)$_3$), 1.17-1.44 (m, 8 H, CH_2CH$_3$), 1.68-1.93 (m, 8 H, CH_2CH), 1.95 (br s, 6 H, SO$_2$CH_3), 3.55, 3.80 (2s, 2 × 6 H, OCH_3), 4.49-4.62 (m, 4 H, CHCH$_2$), 6.31 (br s, 2 H, ArH), 6.39 (s, 2 H, ArH), 6.85 (s, 2 H, ArH), 7.21 (br s, 2 H, ArH); ^{13}C NMR (CDCl$_3$) δ - 4.1, -3.6 (Si(CH$_3$)$_2$), 14.3, 14.5 (CH$_2$$CH_3$), 18.4 (Si$C$(CH$_3$)$_3$), 21.1, 21.5 ($CH_2CH_3$), 25.9 (SiC($CH_3$)$_3$), 34.8 ($CHCH_2$), 35.6, 35.7 ($CHCH_2$ + SO$_2$$CH_3$), 37.5, 37.6 ($CH_2$CH), 55.3, 55.6 (2 × O$CH_3$), 101.7, 103.2 ($C$H, Ar), 126.4, 126.7 ($C$, Ar), 126.8 ($C$H, Ar), 127.8, 130.2, 147.4, 151.9, 155.2, 155.6 (C, Ar) (note some signals are coincident). HRMS (ESI): calcd. for C$_{58}$H$_{89}$O$_{12}$S$_2$Si$_2$ as [M + H]$^+$ 1097.5328; found 1097.5296.

4.3.4.2 Attempted synthesis of 1^4,5^6-dimethanesulfonyl-1^6,3^4,5^4,7^4-tetramethoxy-2,4,6,8-tetrapropylresorcin[4]arene-3^6,7^6-diol

Slighlty impure resorcinarene **(48)** (57 mg, 0.052 mmol) was combined with caesium carbonate (62 mg, 0.19 mmol) and non-anhydrous dimethylformamide (4 mL), then heated at 90°C open to air, overnight. After overnight, the reaction mixture was a cloudy brown solution. The reaction mixture was diluted with water (80 mL) and filtered, but no solids were collected. Brine (20 mL) was added to the filtrate, and extracted with ether (3 × 15 mL). The combined ether extracts were washed with brine (10 mL), dried (MgSO$_4$), filtered, and solvent removed under reduced pressure to give a yellow oil which smelled like TBDMS-OH. Methanol (~15 mL) was added and removed under reduced pressure; after repeating a second time, a yellow-brown solid (0.041 g) was recovered. The material was then filtered through a plug of silica with EtOAc to give a yellow-brown solid (0.031 g). TLC and ^{1}H NMR analysis of the product indicated it to contain multiple methanesulfonate resorcinarene compounds.

4.3.4.3 $1^4,5^6$-dibenzyloxy-$3^6,7^6$-di-*tert*-butyldimethylsilylether-$1^6,3^4,5^4,7^4$-tetramethoxy-2,4,6,8-tetrapropylresorcin[4]arene (49)
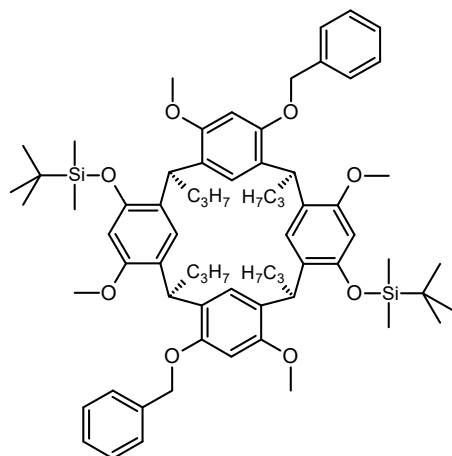
Resorcinarene **(34)** (4.07 g, 4.32 mmol) was added to a mixture of washed sodium hydride (1.81 g, 60% in oil, 1.09 g, 45.3 mmol) and a couple of crystals of imidazole in anhydrous tetrahydrofuran (150 mL), and the resultant mixture was stirred under nitrogen at room temperature for 10 minutes. To this off-white slurry was added benzyl bromide (5.2 mL, 7.48 g, 43.7 mmol), and the reaction mixture was stirred overnight at room temperature, under nitrogen. The reaction mixture was then cooled in an ice bath and carefully quenched with dilute HCl (1 M), producing bubbles. The solvents were removed under reduced pressure from the clear orange yellow solution, and the residue was dissolved in dichloromethane (70 mL) and water (70 mL). The layers were separated, and the the cloudy off-white aqueous layer was extracted with dichloromethane (20 mL). The combined organic layers were dried (MgSO4), filtered, and solvent removed under reduced pressure to give a yellow liquid residue. The residue was triturated with methanol to give a slightly yellow solid, which was further purified by column chromatography (DCM – petroleum spirits 50:50) to give pure, previously unreported product **(49)** as a white solid (3.86 g, 80%): mp 218-219 °C (DCM); ^{1}H NMR (CDCl3) δ 0.20, 0.32 (2s, 2 × 6 H, Si(CH_3)$_2$), 0.90-0.99 (m, 12 H, CH$_2$CH_3), 1.06 (s, 18 H, SiC(CH_3)$_3$), 1.24-1.54 (m, 8 H, CH_2CH$_3$), 1.77-1.99 (m, 8 H, CH_2CH), 3.38, 3.63 (2s, 2 × 6 H, OCH_3), 4.27-4.55 (m, 4 H, CH_2Ph and CHCH$_2$), 4.55-4.65 (m, 2 H, CHCH$_2$), 4.78 (br d, J = 10.7 Hz, 2 H, CH_2Ph), 6.18-6.50 (m, 6 H, ArH), 6.93-7.25 (m, 6 H, ArH), 7.27-7.37 (m, 6 H, ArH); ^{13}C NMR (CDCl3) δ -4.1, -3.4 (Si(CH$_3$)$_2$), 14.5, 14.6 (CH$_2$CH$_3$), 18.4 (SiC(CH$_3$)$_3$), 21.6, 21.8 (CH$_2$CH$_3$), 26.0 (SiC(CH$_3$)$_3$), 35.9, 36.6 (CHCH$_2$), 37.1 (CH$_2$CH), 55.4 (2 × OCH$_3$), 71.3 (CH$_2$Ph), 98.5, 101.9 (CH, Ar), 124.8 (C, Ar), 126.4, 126.8, 127.5, 128.2 (CH, Ar), 137.8, 151.3, 155.0, 155.7, 156.1 (C, Ar) (note some signals are coincident). Found: C, 75.01; H, 8.55; C$_{70}$H$_{96}$O$_8$Si$_2$ requires C, 74.95; H, 8.63%.

4.3.4.4 $1^4,5^6$-dibenzyloxy-$1^6,3^4,5^4,7^4$-tetramethoxy-2,4,6,8-tetrapropylresorcin[4]arene-$3^6,7^6$-diol (46)
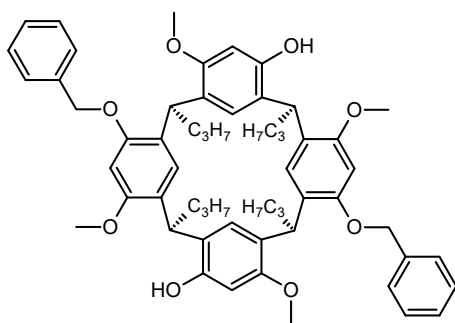
To a solution of **(49)** (3.86 g, 3.44 mmol) dissolved in tetrahydrofuran (30 mL) was added a solution of sodium hydroxide (1.48 g, 37.0 mmol) dissolved in methanol (20 mL). The slightly cloudy colourless reaction mixture was stirred at room temperature overnight under nitrogen. The solvent was removed under reduced pressure, and the residue dissolved in dichloromethane (50 mL) and dilute HCl (50 mL, 1 M). The layers were separated, and the aqueous layer was extracted with dichloromethane (50 mL). The combined cloudy organic extracts were dried (MgSO4), filtered, and solvent removed under reduced pressure to give a white solid which smelled like a silyl derivative (probably *tert*-butyldimethylsilanol). Methanol (20 mL) was added to the product, and then removed under reduced pressure; this process was repeated up to 10 times until the smell disappeared to give **(46)** as a white-beige solid (2.97 g, 97%). NMR data was consistent with **(46)** as described earlier.

153

5 Synthesis and investigation of crown resorcinarenes as enantioselective membrane carriers

The synthesis of distal-OBn resorcinarene **(46)** has provided the key intermediate that enables the installation of a bridge on distal positions of the resorcinarene (**Scheme 5.1**). The goal of the distal bridge is to partially-enclose the resorcinarene cavity to enable binding of smaller guest molecules through intermolecular interactions. Crown ethers were chosen as the bridge due to their well-known ability to act as hydrogen-bond acceptors. Their availability in various lengths, also enables the synthesis of various sizes of crown resorcinarenes, which would have different binding affinities for a guest molecule. The binding interactions and various sizes of the crown resorcinarenes are vital factors for their potential to act as enantioselective membrane carriers for chiral guest molecules.
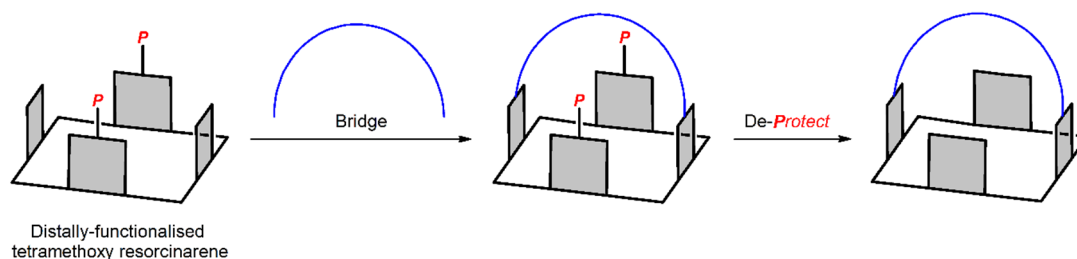
Scheme 5.1   Distal-OBn resorcinarene **(46)** enables the installation of a bridge on distal positions of the resorcinarene.

5.1   Synthesis of distal crown resorcinarenes

Distal-OBn resorcinarene **(46)** was reacted with 2.1 equivalents of tetra(ethylene glycol)-ditoluenesulfonate **(50)** with caesium carbonate in dimethylformamide, as per the procedure described by Nissinen and co-workers.[103] The reaction was successful with the target distally-bridged crown-5 resorcinarene product **(53)** being isolated in a yield of 26%. Since the tetra(ethylene glycol)ditoluenesulfonate **(50)** has two reactive sites, it is possible to form oligomers which would consist of multiple resorcinarenes intermolecularly-bridged by the tetraethylene glycol. With this in mind, the reaction was conducted at more dilute concentrations of 1 mg/mL, resulting in significantly improved yields of about 55%. When the reaction concentration was doubled to 2 mg/mL, the yield only decreased by about 5%. Therefore, at larger scales, the reaction was conducted at 2 mg/mL for the reason of minimising the volume of

dimethylformamide solvent, which becomes troublesome to remove at large volumes. After experimentation with various methods, it was found that large volumes (0.5 L) of dimethylformamide were most conveniently removed under high vacuum using a rotary evaporator. Resorcinarenes with crown-6 **(54)** and crown-7 **(55)** bridges were also synthesised through similar reaction conditions as summarised in **Table 5.1**. The use of alternative reaction solvents such as acetonitrile and acetone were also explored but resulted in significantly lower yields of the target product. Reaction using a carbonate base with a different cation, such as potassium carbonate, drastically decreased the yield, which could be due to the poorer solubility of potassium carbonate in dimethylformamide, however no unreacted starting resorcinarene was apparent by TLC. The caesium cation was possibly acting as a better template for the crown ether to facilitate its intramolecular coupling to the resorcinarene. In the literature, 15-crown-5 and 18-crown-6 have been demonstrated to bind caesium ions in dimethylformamide, with the latter forming a more stable complex.[166] This templating effect may explain the greater yields recorded for the crown-7 resorcinarene **(55)** which has a crown ether that is analogous to the 18-crown-6. In these investigations, slightly more (2.5 eq) ethylene glycol ditosylate was generally required to ensure complete reaction of the starting resorcinarene, as was monitored by TLC. The crude product was purified by column chromatography, with good chromatographic separation. The work up and purification of the crown-7 resorcinarene **(55)** was slightly more difficult, likely due to the greater hydrophilicity of the overall product. The phase separation during the work up was not as good, requiring more time to separate. Product **(55)** could be purified by filtering through a plug of silica, followed by trituration with methanol. However, a small amount of the product could not be recovered from the methanol filtrate, due to it having slight solubility in methanol. The trituration was not successful when performed immediately after the silica plug; this may be caused by trace residue solvents which enhance the solubility of the product in methanol.

Table 5.1 Investigation into the bridging of **(46)** with crown 5-7 ethers at various conditions.
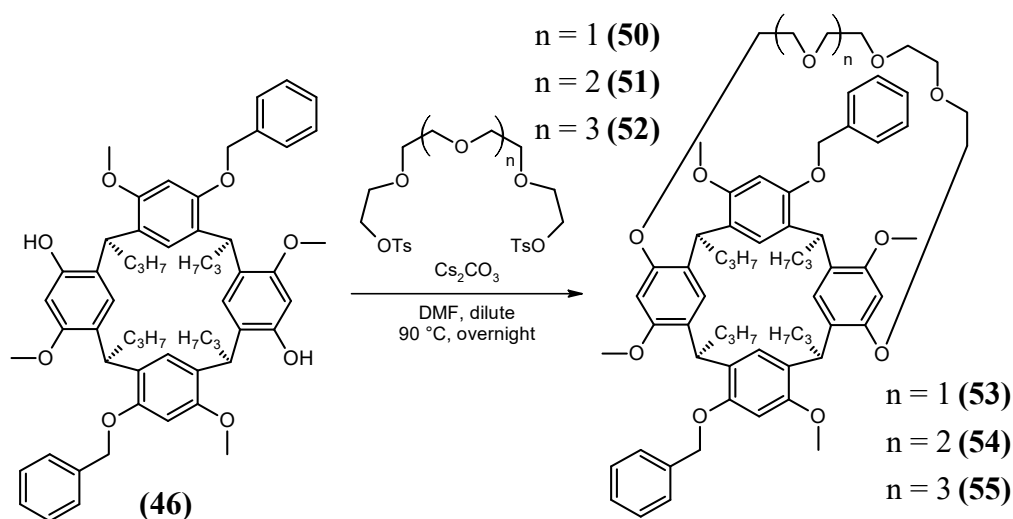
Resorcinarene crown	Ethylene glycol (2.5 eq)	Base	Solvent	Concentration of reaction mixture (mg/mL)	Yield (%)
(53)	Tetra- (n = 1)	Cs$_2$CO$_3$	DMF	4.2	26
		Cs$_2$CO$_3$	DMF	1	52-58
		Cs$_2$CO$_3$	DMF	2	48-50
(54)	Penta- (n = 2)	Cs$_2$CO$_3$	DMF	1	49-66
		Cs$_2$CO$_3$	DMF	2	36
		K$_2$CO$_3$	MeCN	1	20
		Cs$_2$CO$_3$	MeCN	1	40
		Cs$_2$CO$_3$	Acetone	1	38
(55)	Hexa- (n = 3)	Cs$_2$CO$_3$	DMF	1	50-51
		Cs$_2$CO$_3$	DMF	2	66-70
		Cs$_2$CO$_3$	DMF	3	61-62

The key evidence that the target dibenzyloxy crown resorcinarene products **(53)**, **(54)** and **(55)** were obtained was provided by NMR spectroscopy (**Appendix A – 56**). The retention of C$_2$ symmetry for all three products was confirmed by the two prominent methoxy peaks in both ^{1}H and ^{13}C spectra. The three resorcinarenes, despite having very similar NMR spectra, were all unambiguously distinguished by the number of peaks in the 71 ppm region of the ^{13}C NMR spectra. In this region, the oxygen-carbons of the newly-installed crown ether bridge were evident, having half the number of peaks due to the C$_2$ symmetry of the crown resorcinarene. A signal for the benzylic carbon of the benzyl ether is also present in this region, and was differentiated by HSQC spectroscopy. The crown ether bridge is also evident on the ^{1}H NMR spectrum,

but appeared as complicated overlapping multiplets, which roughly had the expected integration. The possibility that these crown resorcinarene products could be dimers from intermolecular bridging was refuted by the fact that there were no doubling of peaks in the ^{1}H NMR spectra as would be expected if two chiral resorcinarenes had combined. Nevertheless, for confirmation, dibenzyloxy crown-5 resorcinarene **(53)** was analysed by HRMS which recorded a main peak which corresponded to the mass of the intramolecularly bridged product. Furthermore, the dibenzyloxy crown resorcinarene products **(53)**, **(54)** and **(55)** were confirmed at the solid state by X-ray diffraction on single crystals (**Appendix B – 8**), respectively obtained from: DCM-petroleum spirits, THF-MeOH, and DCM-petroleum spirits. Overall, the crystal structures showed that these resorcinarene derivatives had a very similar basket shape (**Figure 5.1**).

| **(53)** | **(54)** | **(55)** |
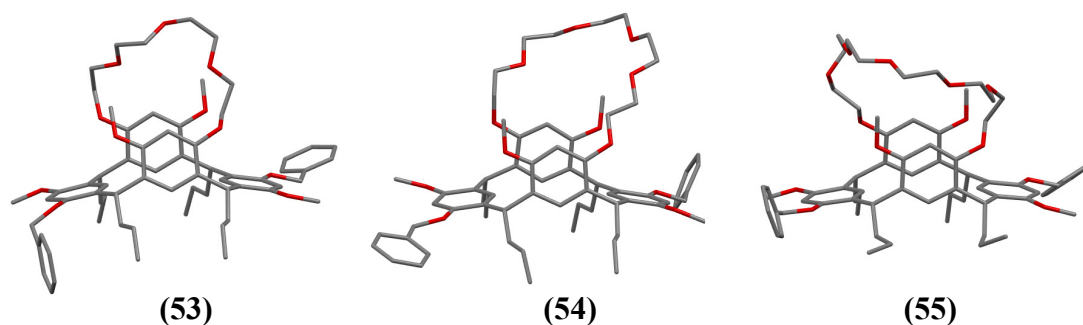
Figure 5.1   Overall view of crystal structures of benzyloxy crown resorcinarenes. For ORTEP view see **Appendix B – 16**.

The two distally-bridged aromatic rings are pinched together, causing the two other aromatic rings to be pushed outwards from the cavity. **Figure 5.2** shows that these aromatic rings bearing the benzyl ether groups, have been flattened out with an obtuse angle beyond horizontal for all three resorcinarenes. From this view, it is apparent that crown-6 resorcinarene **(54)** has a slightly distorted conformation compared to the other resorcinarenes, perhaps because of the odd number of ethylene glycol subunits in the crown-5 ether bridge.

(53)   **(54)**   **(55)**
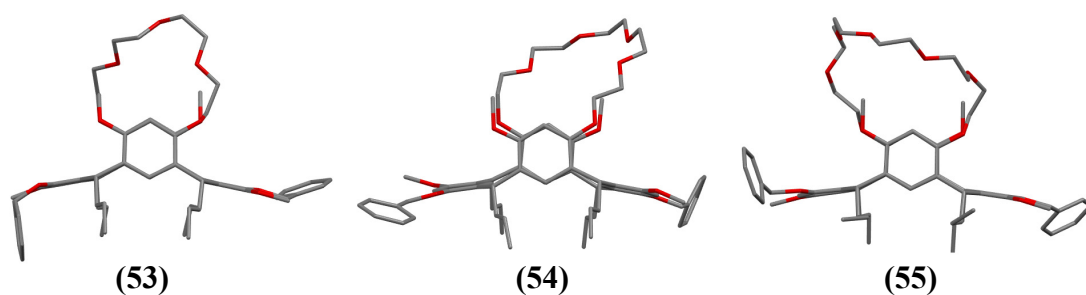
Figure 5.2   Crystal structures of benzyloxy crown resorcinarenes highlighting the obtuse angle of the benzyloxy aromatic rings.

As shown in **Figure 5.3**, all three benzyloxy crown resorcinarenes have different lengths of crown ethers, however they have all adopted essentially the same boat conformation, where the pair of bridged aromatic rings have been pinched together till they are vertical and parallel to each other. The overall shape of the resorcinarene cavity appears to be largely unaffected by the length of the crown ether bridge. The ability for the flexible crown ethers to fold is especially evident in these crystal structures of the crown resorcinarenes in the solid state. The crown ether bridge is folded to a greater extent for the crown-7 resorcinarene **(55)**. The flexibility of the crown ether renders the overall cavity of the crown resorcinarene to be more flexible and less well-defined. This could be a factor in the ability for the crown resorcinarene to contain guest molecules.
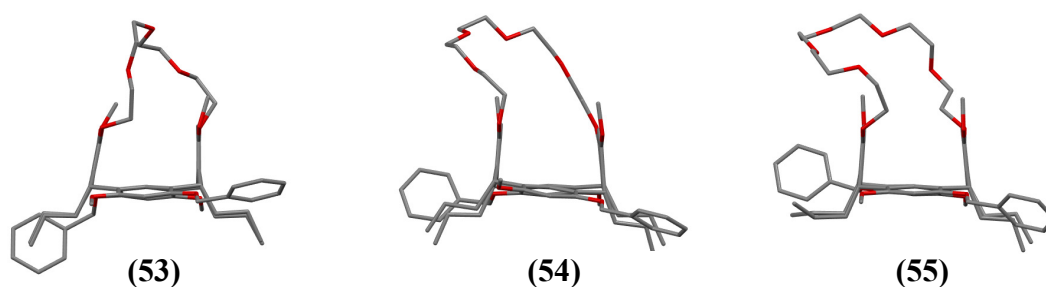
(53)   **(54)**   **(55)**

Figure 5.3   Crystal structures of benzyloxy crown resorcinarenes highlighting the cavity and boat conformation.

In the crystal structures of the three benzyloxy crown resorcinarenes – **(53)**, **(54)**, **(55)** – only **(55)** had a solvent molecule present in the crystal lattice. In the crystal structure of the crown-7 resorcinarene **(55)**, a molecule of dichloromethane from the crystallisation solvent has complexed within the crown ether bridge mainly through interactions between the oxygens of the crown ether and hydrogens of the dichloromethane (**Figure 5.4**). This confirms the ability for the crown ether to complex smaller molecules. However, since this was only observed for the crown resorcinarene derivative with the largest crown, this suggests that a longer crown ether bridge on the

158

resorcinarene may provide a better receptor. Nevertheless, these observations in the solid state are not an accurate representation of the solution state, but rather provide a general guide to the complexation in solution. These crown resorcinarenes will be applied in solution, where there should be greater flexibility of the resorcinarene boat conformation, which may increase the capacity of the cavity for the containment of smaller guest molecules.
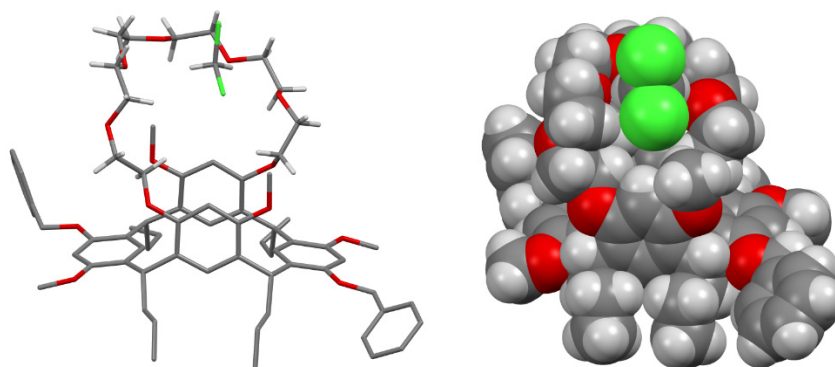
Figure 5.4   Crystal structure of benzyloxy crown-7 resorcinarene **(55)** demonstrating the complexation of dichloromethane in the crown ether bridge. A spacefill model is shown on the right.

Having accomplished the synthesis of distally-bridged crown resorcinarenes in three sizes, the examination of these products as potential membrane carriers for chiral drugs could commence. However, for the possibility of enantioselective transport, the crown resorcinarenes would need to be obtained as a single enantiomer. The plan for separating the enantiomers of the crown resorcinarene was to convert the enantiomers into diastereomers, separate the diastereomers, then remove the chiral moiety. Therefore, the attachment of a chiral moiety to the enantiomers of the crown resorcinarenes is required to convert them to diastereomers. As discussed in the next section, **Section 5.2**, this is most conveniently accomplished at this stage, the final stage of synthesis. A convenient method to attach a chiral moiety to the crown resorcinarenes would be to remove the benzyl ether protecting group, then attach the chiral moiety by esterification of the resultant phenol.

The first attempts to remove the benzyl ether groups by reduction using Pd/C with either hydrazine or hydrogen gas did not show any reaction by TLC. Work up of the reaction mixture and ^{1}H NMR spectroscopy of the resultant material confirmed only unreacted starting material. Therefore, a Birch-style reduction, using sodium metal and liquid ammonia, was employed. Under these harsher reduction conditions, the

debenzylation of the three crown resorcinarenes **(53)**, **(54)**, **(55)**, was completed in 30 minutes, and after work up, the respective target products **(56)**, **(57)**, **(58)** were afforded in good purity and in quantitative yield (**Scheme 5.2**). Poor phase separation in the DCM/water work up was again encountered with the crown-7 resorcinarene **(58)**. This was most likely due to its increased hydrophilicity. It was discovered that washing out the soluble salts with water, while collecting the water-insoluble product by filtration provided a more effective and convenient work up procedure.
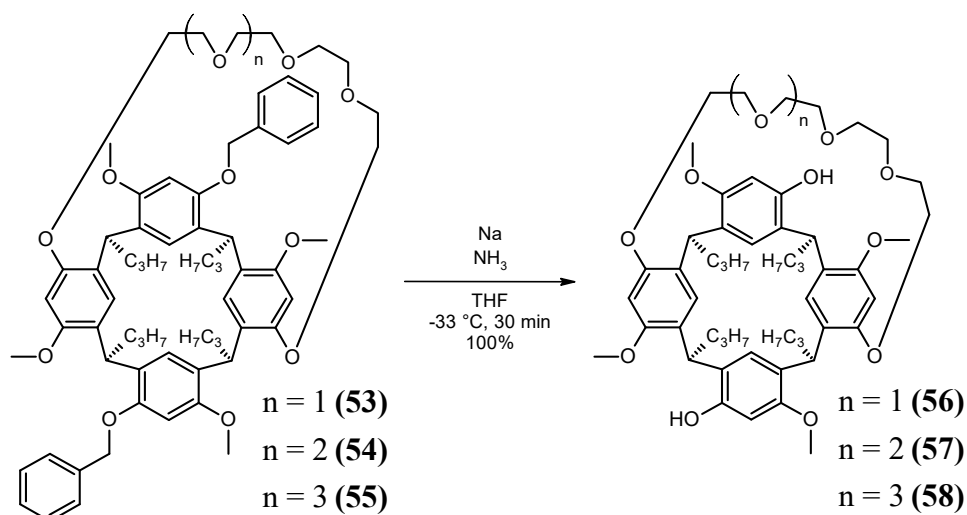
Scheme 5.2 Removal of benzyl ether protecting groups from crown resorcinarenes.

The complete removal of the benzyl ethers was clearly apparent on the ^{1}H NMR spectra (**Appendix A – 62**) for each of the crown resorcinarenes where the multiplets in the aromatic region associated with the benzyl ether were absent. In the aromatic region, there were only four singlets with the same integration, which represented the aromatic protons of the C_2-symmetrical resorcinarene macrocycle. The absence of the benzylic carbon peak at 71 ppm in the ^{13}C NMR spectra for the crown resorcinarenes provided further confirmation of the removal of the benzyl ethers.

In the ^{1}H NMR spectra of the three dihydroxy crown resorcinarenes, discreet multiplets ranging from 1.3-4.3 were apparent. These multiplets were indeed the methylenes of the crown ether bridge as confirmed on the HSQC spectrum (**Figure 5.5**), which showed them coupling to peaks at 70 ppm in the ^{13}C NMR spectrum. Although some of these multiplets were overlapped, it was evident on the HSQC spectra that the number of these methylene multiplets for the dihydroxy crown resorcinarenes **(56)**, **(57)**, **(58)** were eight, ten and twelve respectively. However in the ^{13}C NMR spectra, the number of peaks around 70 ppm for the crown ether methylenes

were half, as expected for a C₂-symmetrical resorcinarene. This non-equivalence of the protons of the crown ether bridge may have been a result of diastereotopicity, but not observed for the benzyloxy crown resorcinarenes.
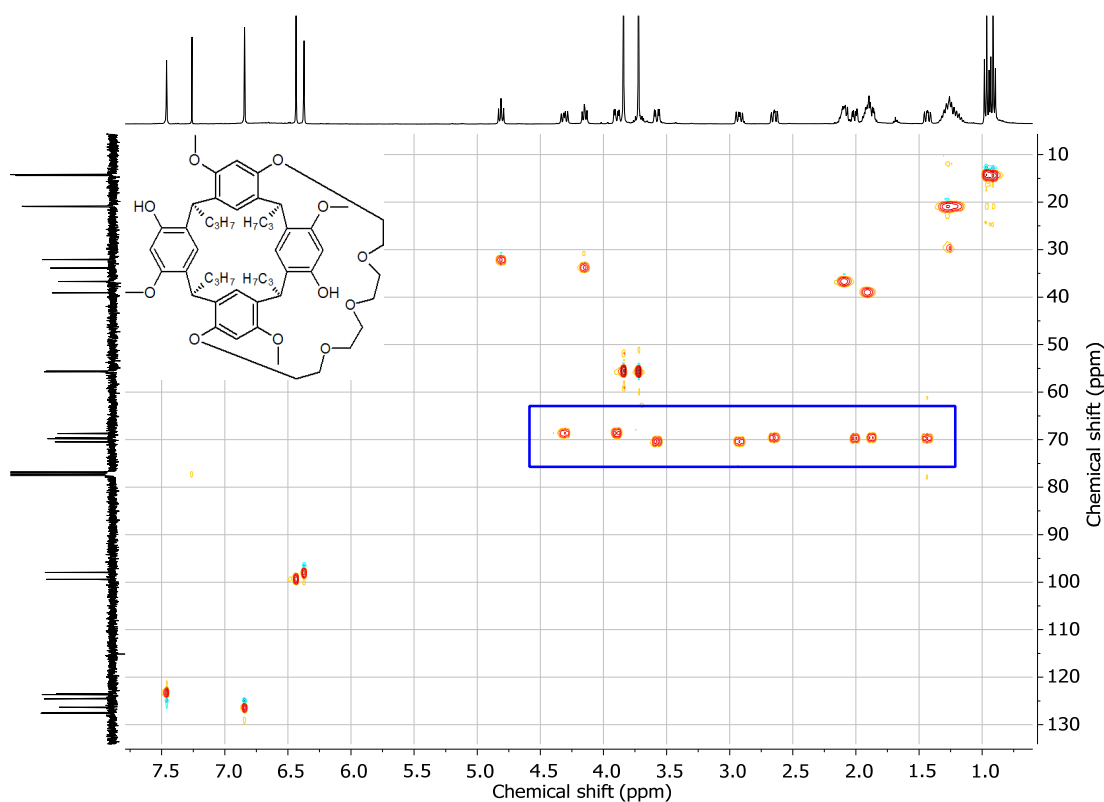
Figure 5.5 HSQC spectrum recorded in CDCl₃ of resorcinarene **(56)** demonstrating that the methylene peaks of the crown ether appear in the ¹H NMR spectrum as discreet multiplets over a wide chemical shift.

However, when the ¹H NMR spectra of the crown resorcinarenes were recorded in DMSO-d₆, the wide-ranging discreet multiplets became lumped together (**Figure 5.6**). Moreover, the two signals for the benzylic methine of the resorcinarene macrocycle have coalesced into one.
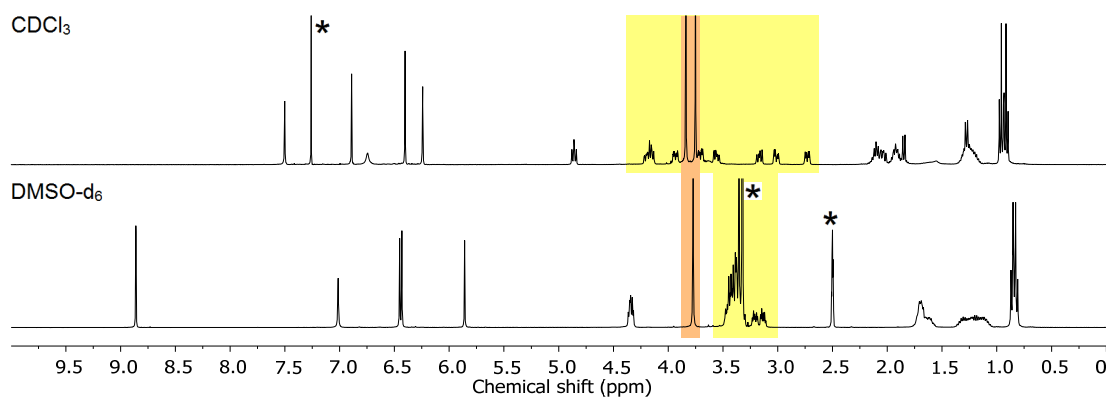
Figure 5.6 ¹H NMR spectra of resorcinarene **(56)** recorded in CDCl₃ (top) and DMSO-d₆ (bottom). The coalescing of the signals has been highlighted. *Denotes solvent peaks.

161

This indicates that the phenomenon of the wide-ranging multiplets was dependent on the solvent used to record the ^{1}H NMR spectrum. Unlike the benzyloxy counterparts, the dihydroxy crown resorcinarenes have two hydroxy groups which are able to from hydrogen bonds. In CDCl$_3$, these two hydroxy groups could form intramolecular hydrogen bonds to the oxygens of methoxy groups on proximal aromatic rings. Formation of these hydrogen bonds would increase rigidity of the overall crown resorcinarene, which may explain the appearance of the discreet multiplets in the ^{1}H NMR spectrum recorded in CDCl$_3$. However, in DMSO-d$_6$, a solvent which is able to accept hydrogen bonds, the intramolecular hydrogen bonds would be disrupted by the solvent, leading to greater flexibility and mobility of the crown resorcinarene. This could explain the lumping and coalescing of peaks in the ^{1}H NMR spectrum recorded in DMSO-d$_6$.

Single crystals of dihydroxy crown resorcinarene **(57)** were obtained from DCM-petroleum spirits. Analysis of the single crystals of **(57)** by X-ray diffraction confirmed the assignment at the solid state (**Appendix B – 9**). As evident in the crystal structure (**Figure 5.7**), the dihydroxy crown resorcinarene **(57)** has a similar basket shape to the dibenzyloxy counterpart. However, the dihydroxy crown resorcinarene appears to take on a more crown-like conformation where the non-bridged aromatic rings, have folded towards the cavity as a result of losing the steric bulk of the benzyl ether groups. This in turn causes the bridged aromatic rings to become slightly bent out of the cavity and are no longer vertical like in its benzyloxy precursor. Therefore, the cavity of the dihydroxy crown resorcinarene is wider in comparison to its benzyloxy precursor.
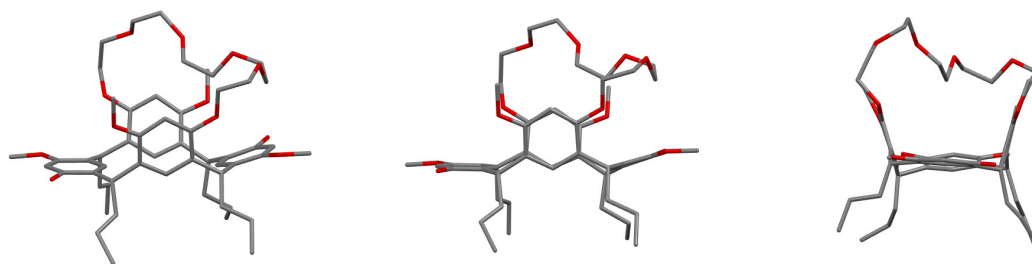
Figure 5.7   Crystal structure of dihydroxy crown-6 resorcinarene **(57)**. For ORTEP view see
                Appendix B – 17.

The crown ether bridge of the dihydroxy crown-6 resorcinarene **(57)** is also noticeably closer to the resorcinarene cavity, compared to its benzyloxy precursor **(54)**. This could be explained by the bending out of the bridged aromatic rings which pulls the crown ether bridge closer to the cavity, while the presence of free hydroxy groups would also

form intramolecular hydrogen bonds with the crown ether bridge. With the crown ether bridge being closer to the cavity, the spacefill models (**Figure 5.8**) of the solid-state crystal structure shows that half of the cavity has become sterically inaccessible. However, in solution, this may not necessarily be the case, as the crown ether bridge should be mobile and flexible in solution. In terms of overall flexibility of the cavity, the cavity of the dihydroxy resorcinarene **(57)** would likely be less flexible than its benzyloxy precursor **(54)**, due to the intramolecular hydrogen bonding.
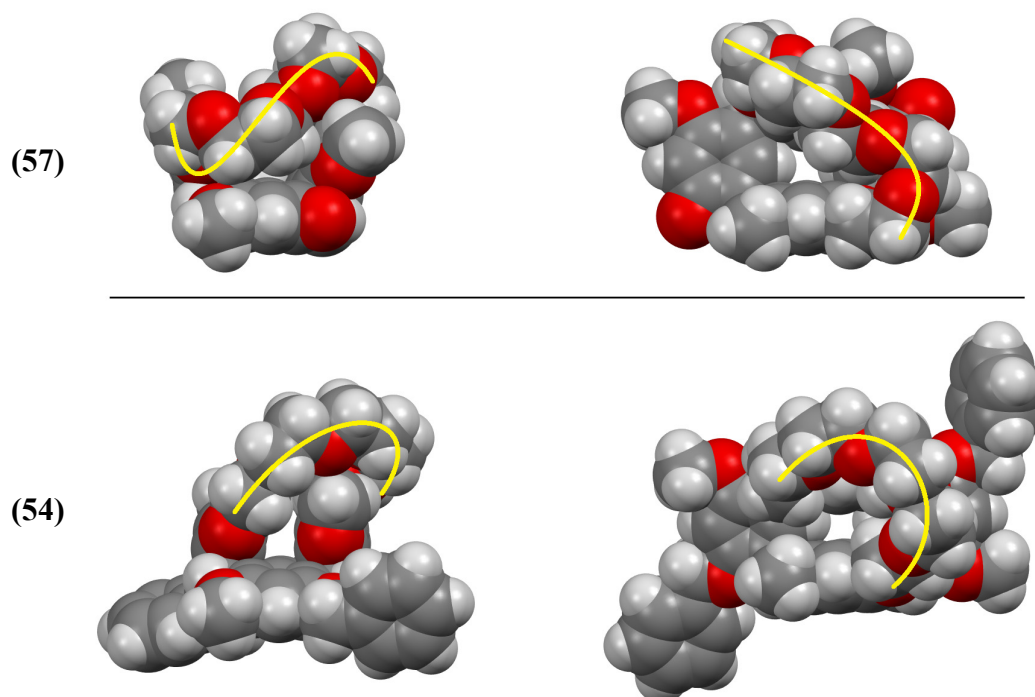
Figure 5.8   Side and top views in spacefilling mode of the dihydroxy crown-6 resorcinarene **(57)** (top) and dibenzyloxy crown-6 resorcianrene **(54)** (bottom) from their crystal structures. Outlined in yellow is the crown ether bridge which renders half of the cavity for **(57)** sterically inaccessible. Propyl chains have been omitted for clarity.

In the crystal structure of dihydroxy crown-6 resorcinarene **(57)**, water molecules were found to reside within the crystal lattice, with nothing being complexed within the resorcinarene cavity. The overall crystal packing was driven by hydrogen bonds between the free hydroxy group of the resorcinarene and the water molecules in the lattice. The resorcinarene molecules are connected through strong water-mediated hydrogen bonds involving the hydroxy groups O2B, whilst also directly interacting through O2D-H⋯O2D weak intermolecular bonds (**Figure 5.9**). The resorcinarene molecules are packed in a head-to-head / tail-to-tail manner that is similar to the other resorcinarene derivatives.
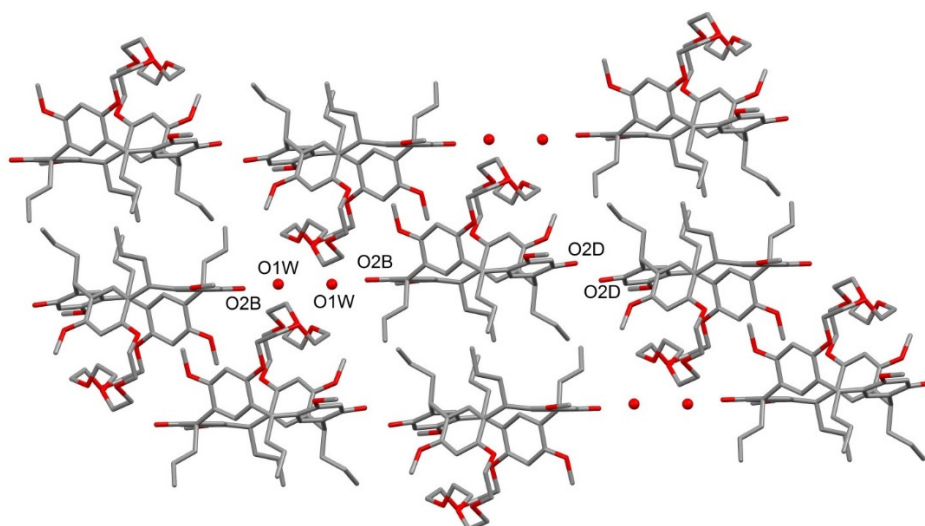
Figure 5.9 Crystal packing of dihydroxy crown-6 resorcinarene **(57)**. Hydrogen atoms have been omitted for clarity, and water molecules are represented as red spheres of arbitrary radius.

5.2 Diastereomic resolution of tetramethoxyresorcinarene

Having accomplished the synthesis of the distally-bridged resorcinarene products **(56)**, **(57)** and **(58)**, the investigation focused on obtaining these final products as their single enantiomers. The single resorcinarene enantiomers would enable enantioselective membrane transport to be examined.

Enantioseparation by diastereomic resolution requires the attachment of a chiral moiety, followed by separation of the diastereomers, then removal of the chiral moiety. Therefore, the chiral moiety needs to be attached by a cleavable link, such as an ester, to facilitate its removal once the diastereomers are resolved. With this requirement in mind, esterification of the phenols provides the most convenient linkage for the attachment and removal of a chiral moiety.

The chiral resolution of racemic tetramethoxyresorcinarene derivatives has been reported by Heaney and co-workers through conversion to camphorsulfonate diastereomers, which were separated by column chromatography.[66] Hydrolysis of the diastereomers, gave the separated enantiomers in overall yields of 12-41% (**Scheme 5.3**, **Table 5.2**, **Table 5.3**). In particular, the enantiomers of starting resorcinarene **(1)** were separated in an overall yield of 41% for the *S* enantiomer, and 18% for the *R* enantiomer. This significant discrepancy between the yields for the two enantiomers was attributed to the chromatographic process, since the NMR spectra of the crude material indicated formation of the diastereomers in equal proportions. However, in

one case (**Table 5.2**, reaction 2), diastereomers of tetracamphorsulfonates and tricamphorsulfonates were isolated in a 4:1:1:4 ratio, which suggested some enantiorecognition in the diastereomer formation, which may be due to steric bulk. It was also noted that diastereomers of resorcinarene derivatives with R groups bulkier than methyl on the $1^6,3^4,5^4,7^4$ alkyloxy positions of the resorcinarene were easier to separate (**Table 5.3**, reaction 2 & 3). However, with bulky alkoxy groups, the reaction did not proceed further than di-substitution, despite the use of excess camphorsulfonyl chloride (**Table 5.2** reaction 4 & 5). The incomplete tetra-substitution was again thought to be the result of the increased steric hindrance due to the bulky alkoxy groups. This result was perhaps unfortunate, since theoretically, more chiral moieties would amplify the diastereomic differences and improve diastereomer separation. Nevertheless, it is rather interesting that a proximally-functionalised resorcinarene was formed selectively from the various other possible products. Note, in the original paper, these compounds were assigned as distal however, close inspection of the NMR data suggests that the proximal dicamphorsulfonate regioisomers were obtained.

The absolute configurations for some of the single resorcinarene enantiomers were also determined by X-ray crystallography on the corresponding separated diastereomers.[66] The camphorsulfonate moiety, having a known absolute configuration, provided an internal reference that enabled the absolute configuration of the resorcinarene to be determined.[6] Therefore, the absolute configuration of the single resorcinarene enantiomer can be inferred from its corresponding diastereomer, however its designation will flip as the removal of the camphorsulfonate groups reverses the priority. In the work by Heaney and co-workers, the faster-eluting diastereomer always had a *R* absolute configuration, and a more positive specific rotation.
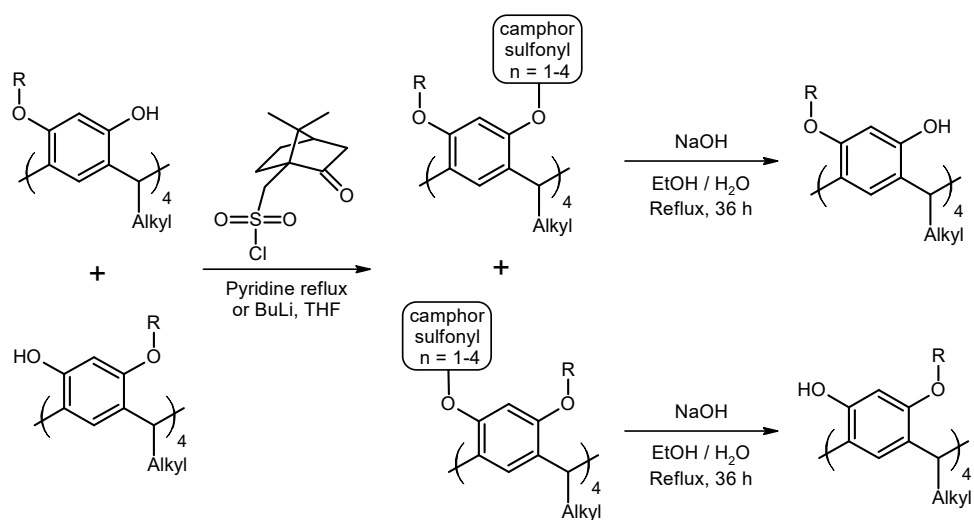
Scheme 5.3 Chiral resolution of axially-chiral resorcinarene derivatives by chromatographic separation of respective camphorsulfonate diastereomers, followed by hydrolysis of the corresponding diastereomer.[66]

Table 5.2   Synthesis of various camphorsulfonate resorcinarene diastereomers by pyridine reflux.[66]

		Diastereomer synthesis					Diastereomer hydrolysis	
Reaction	CS-Cl eq	Camphorsulfonate	Diastereomer AC	Alkyl	R	Yield (%)	Enantiomer AC	Yield (%)
1	8	Tetra	2*R*,4*R*,6*R*,8*R*	*n*-C$_3$H$_7$	CH$_3$	46	*S*	89
		Tetra	2*S*,4*S*,6*S*,8*S*	*n*-C$_3$H$_7$	CH$_3$	23	*R*	78
2	12	Tetra	2*R*,4*R*,6*R*,8*R*	*n*-C$_5$H$_{11}$	CH$_3$	23	*S*	65
		Tetra	2*S*,4*S*,6*S*,8*S*	*n*-C$_5$H$_{11}$	CH$_3$	5.5	*R*	64
		Tri	2*R*,4*R*,6*R*,8*S*	*n*-C$_5$H$_{11}$	CH$_3$	4.8		
		Tri	2*S*,4*S*,6*S*,8*R*	*n*-C$_5$H$_{11}$	CH$_3$	18		
3	8.1	Tetra	2*R*,4*R*,6*R*,8*R*	*n*-C$_7$H$_{15}$	CH$_3$	39	*S*	84
		Tetra	2*S*,4*S*,6*S*,8*S*	*n*-C$_7$H$_{15}$	CH$_3$	17	*R*	70
4	2	Tetra	2*R*,4*R*,6*R*,8*R*	*n*-C$_{11}$H$_{23}$	CH$_3$	38	*S*	79
		Tetra	2*S*,4*S*,6*S*,8*S*	*n*-C$_{11}$H$_{23}$	CH$_3$	20	*R*	60
5	3.9	Proximal*	2*R*,4*R*,6*S*,8*S*	*n*-C$_5$H$_{11}$	CH(CH$_3$)$_2$	34		
		Proximal	2*S*,4*S*,6*R*,8*R*	*n*-C$_5$H$_{11}$	CH(CH$_3$)$_2$	30		
6	12	Proximal	2*R*,4*R*,6*S*,8*S*	*n*-C$_5$H$_{11}$	*c*-C$_5$H$_9$	23		
		Proximal	2*S*,4*S*,6*R*,8*R*	*n*-C$_5$H$_{11}$	*c*-C$_5$H$_9$	23		

CS-Cl (Camphorsulfonyl chloride)   AC (Absolute configuration)   *Incorrectly assigned in the original paper

Table 5.3   Synthesis of various camphorsulfonate resorcinarene diastereomers by butyllithium/THF.[66]

			Diastereomer synthesis					Diastereomer hydrolysis	
Reaction	BuLi Eq	CS-Cl Eq	Camphorsulfonate	Diastereomer AC	Alkyl	R	Yield (%)	Enantiomer AC	Yield (%)
1	8.1	10.1	Tetra	2R,4R,6R,8R	n-C$_5$H$_{11}$	CH$_3$	33	S	65
			Tetra	2S,4S,6S,8S	n-C$_5$H$_{11}$	CH$_3$	33	R	64
2	2	2	Mono	2S,4R,6R,8R	n-C$_5$H$_{11}$	CH(CH$_3$)$_2$	25	S	89
			Mono	2R,4S,6S,8S	n-C$_5$H$_{11}$	CH(CH$_3$)$_2$	24	R	82
			Proximal*	2R,4R,6S,8S	n-C$_5$H$_{11}$	CH(CH$_3$)$_2$	8	S	82
			Proximal	2S,4S,6R,8R	n-C$_5$H$_{11}$	CH(CH$_3$)$_2$	8	R	83
3	2	2	Mono	2S,4R,6R,8R	n-C$_5$H$_{11}$	c-C$_5$H$_9$	23	S	75
			Mono	2R,4S,6S,8S	n-C$_5$H$_{11}$	c-C$_5$H$_9$	22	R	78
			Proximal	2R,4R,6S,8S	n-C$_5$H$_{11}$	c-C$_5$H$_9$	10	S	72
			Proximal	2S,4S,6R,8R	n-C$_5$H$_{11}$	c-C$_5$H$_9$	10	R	76
4	8.1	10.2	Proximal	2R,4R,6S,8S	n-C$_5$H$_{11}$	CH(CH$_3$)$_2$	41		
			Proximal	2S,4S,6R,8R	n-C$_5$H$_{11}$	CH(CH$_3$)$_2$	41		
5	8	10	Proximal	2R,4R,6S,8S	n-C$_5$H$_{11}$	c-C$_5$H$_9$	28		
			Proximal	2S,4S,6R,8R	n-C$_5$H$_{11}$	c-C$_5$H$_9$	28		
6	8	8	Tetra	2R,4R,6R,8R	n-CH$_2$CH(CH$_3$)$_2$	CH$_3$	26	S	80
			Tetra	2S,4S,6S,8S	n-CH$_2$CH(CH$_3$)$_2$	CH$_3$	24	R	74

Table 5.3 (continued)   Synthesis of various camphorsulfonate resorcinarene diastereomers by butyllithium/THF.[66]

			Diastereomer synthesis					Diastereomer hydrolysis	
Reaction	BuLi Eq	CS-Cl Eq	Camphorsulfonate	Diastereomer AC	Alkyl	R	Yield (%)	Enantiomer AC	Yield (%)
7	8	8	Tetra^R	2R,4R,6R,8R	n-CH$_2$CH(CH$_3$)$_2$	CH$_3$	36	R	78
			Tetra^R	2S,4S,6S,8S	n-CH$_2$CH(CH$_3$)$_2$	CH$_3$	35		
8	1.2	1.3	Mono	2S,4R,6R,8R	n-C$_5$H$_{11}$	CH$_3$	25		
			Mono	2R,4S,6S,8S	n-C$_5$H$_{11}$	CH$_3$	25		
			Proximal*	2R,4R,6S,8S	n-C$_5$H$_{11}$	CH$_3$	9	S	70
			Proximal	2S,4S,6R,8R	n-C$_5$H$_{11}$	CH$_3$	9	R	70

^{R} camphorsulfonate R enantiomer   CS-Cl (Camphorsulfonyl chloride)   AC (Absolute configuration)   *Incorrectly assigned in the original paper

To obtain single enantiomers of the crown resorcinarenes, it is possible to perform the diastereomic resolution on starting resorcinarene **(1)**, as demonstrated in the work by McIldowie and co-workers. However, the three steps to synthesise, separate, then cleave the diastereomers involves a significant amount of work, and thus the resultant enantio-pure material significantly increases in value. In view of this, it would be ideal to perform the three steps after all low-yielding steps, or at the end of synthesis. In the scheme to synthesise the crown resorcinarenes, there are three opportunities where the resorcinarene has free phenols to accommodate the attachment of a chiral moiety (**Scheme 5.4**).
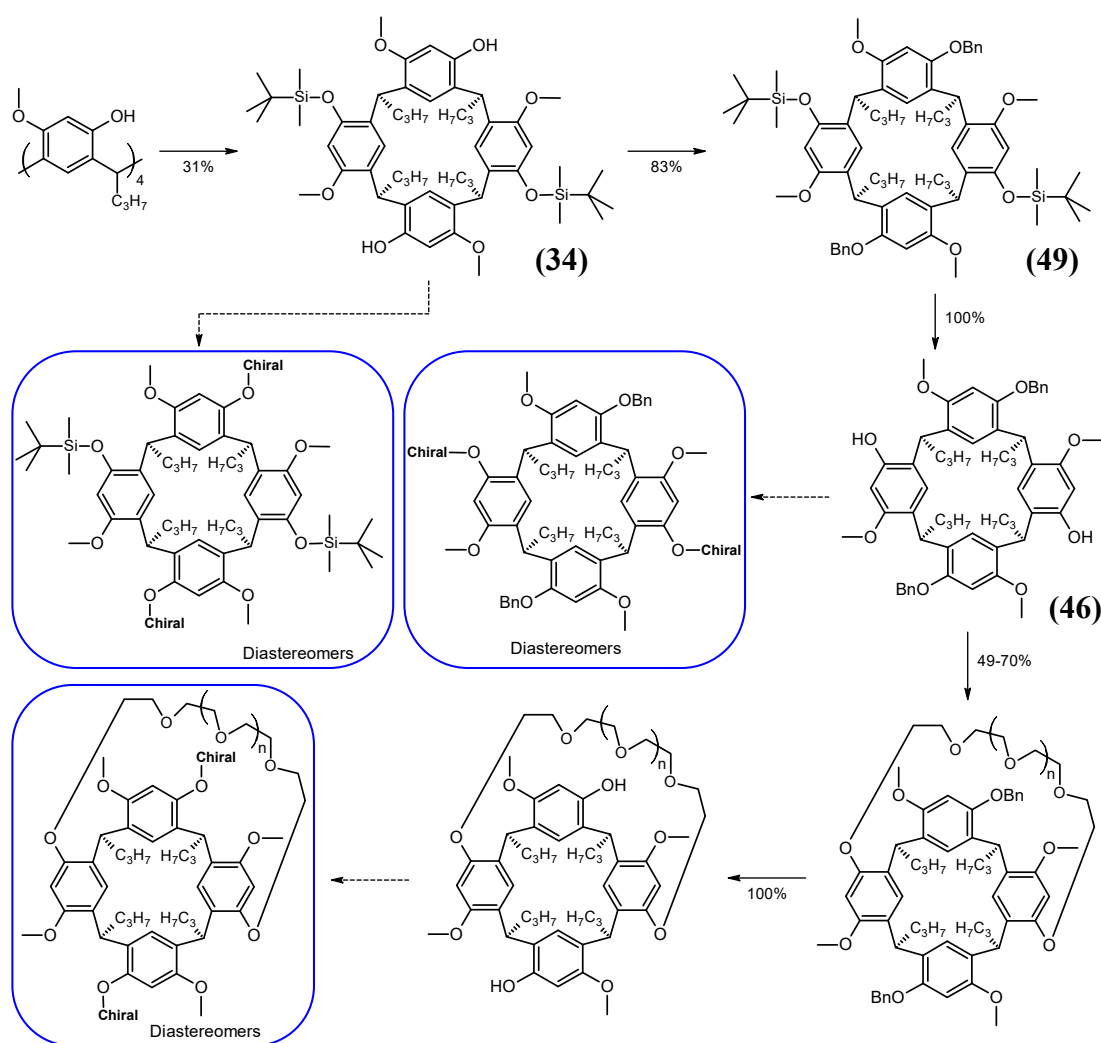
Scheme 5.4 Opportunities for making diastereomers via phenols during the synthesis of crown resorcinarenes for chiral resolution.

Separating the enantiomers at the end of synthesis would be advantageous if both enantiomers and diastereomers of the final product are required. However, a possible disadvantage would be if the yield from the three steps involved in the diastereomic

separation is low, because it would mean wastage of valuable product from the five-step synthesis. Considering these advantages and disadvantages, resolving the diastereomers of the crown resorcinarenes after the five-step synthesis, appears to be the most attractive option, and therefore this was investigated first. Moreover, since the diastereomers of the crown resorcinarenes will be synthesised, they would also be worth investigating as potential enantioselective membrane carriers.

5.2.1 Diastereomers of crown resorcinarenes

Camphorsulfonate diastereomers of the crown resorcinarenes were synthesised (**Table 5.4**) using the sulfonylation procedure in **Section 4.3.4.1** with camphorsulfonyl chloride and triethylamine. The reaction proceeded smoothly, with the ^{1}H NMR spectrum of the crude material clearly showing doubling of the key resorcinarene signals which provided strong evidence of the successful formation of the diastereomers. The ^{1}H NMR spectrum also indicated that the crude product was a fairly pure material, since no other resorcinarene peaks were apparent, other than the expected diastereomers. The yields for the isolated diastereomer mixture were often quantitative. To separate the diastereomers, preferential solubility in various solvents was investigated, but yielded no success. It was discovered from a TLC screen of various chromatographic solvent systems, that the chromatographic separation of the diastereomers was very close but could be achieved by developing the same TLC plate in MeOH-DCM (2:98) three times. Using this solvent system via preparative TLC, all resorcinarene diastereomer mixtures were successfully separated in sufficient quantities. The diastereomic separation for these crown resorcinarene derivatives appeared to be very similar, with separation for the crown-5 resorcinarene being slightly better, and the separation slightly worse for the crown-7 resorcinarene where a small amount of co-eluted diastereomers could not be separated.

Table 5.4 Preparation, yield and specific rotation of camphorsulfonate resorcinarene diastereomers.
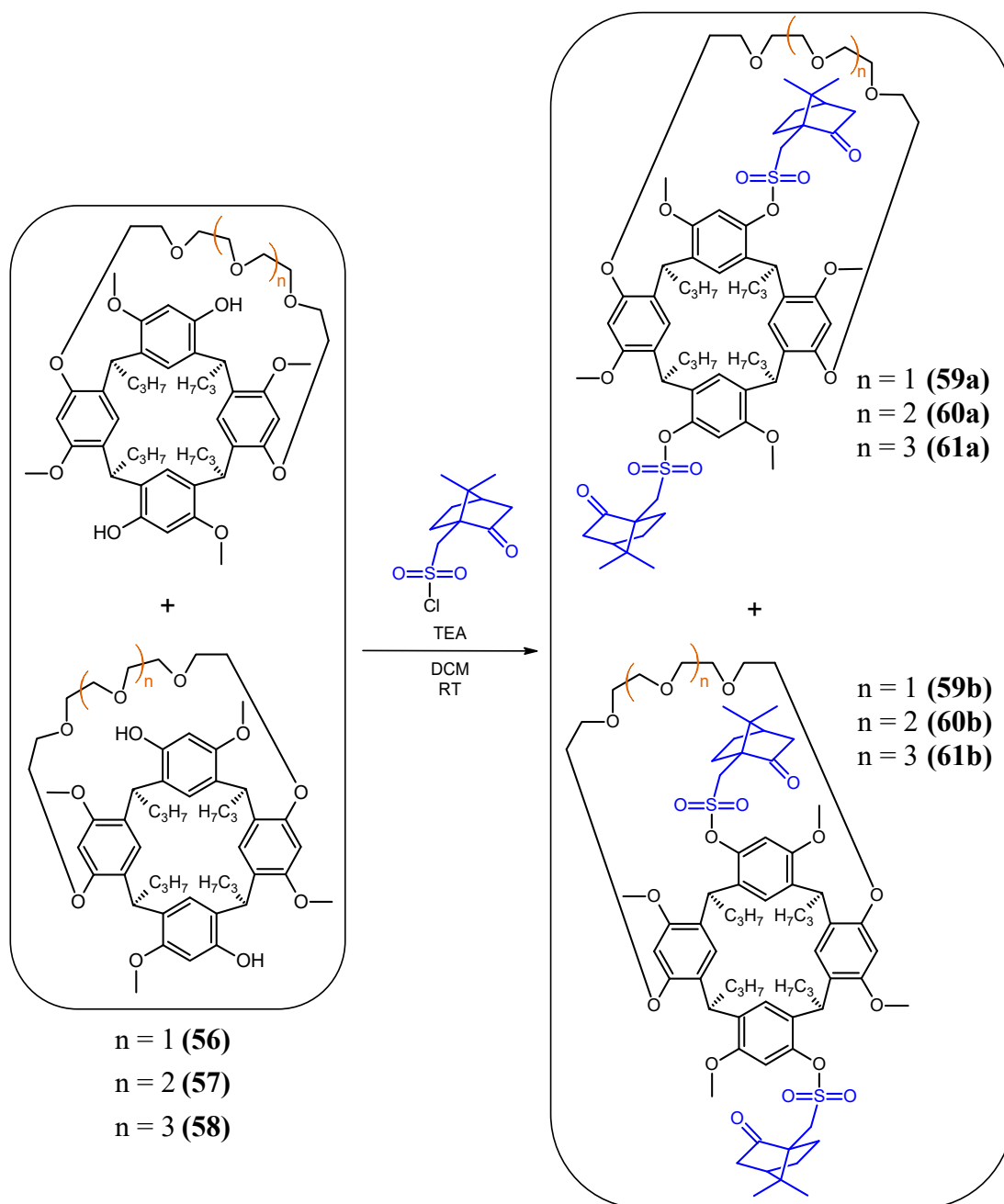
Resorcinarene	n	Yield	Specific rotation (c ~1.00)
(59a)	1	50%	+48.0°
(59b)	1	48%	-11.8°
(60a)	2	40%	+46.5°
(60b)	2	39%	-16.5°
(61a)	3	34%	+56.6
(61b)	3	22%	-22.1°

Confirmation of the attachment of the camphorsulfonate group to the resorcinarene was clearly provided by the C=O absorbance stretch in the IR spectrum. The separation of the diastereomers was unambiguously confirmed by the ^{1}H NMR spectra (**Figure 5.10**) which showed complete separation of the doubled peaks. The ^{13}C NMR spectra (**Appendix A – 72**) provided better evidence regarding the identity of the products; a peak around 214 ppm was recorded which is ascribed to the carbonyl carbon of the camphorsulfonate. The correct number of signals were observed in all ^{13}C NMR spectra for the separated diastereomers. The retention of the crown ether was represented by the signals around 70 ppm. The complicated overlapped multiplets of the camphorsulfonate moiety in the ^{1}H NMR spectra of the diastereomers were assigned by HSQC, DEPT-135 and ^{13}C NMR spectra. Analysis of the diastereomers by polarimetry showed that the first-eluting diastereomer always had a positive rotation, while the second-eluting diastereomer always had a negative rotation. This observation follows the trend observed by Heaney and co-workers for chiral tetramethoxyresorcinarenes.[66] An example of the specific rotation for a pair of separated diastereomers **(60a)** and **(60b)** was +46.5° and -16.5° respectively.
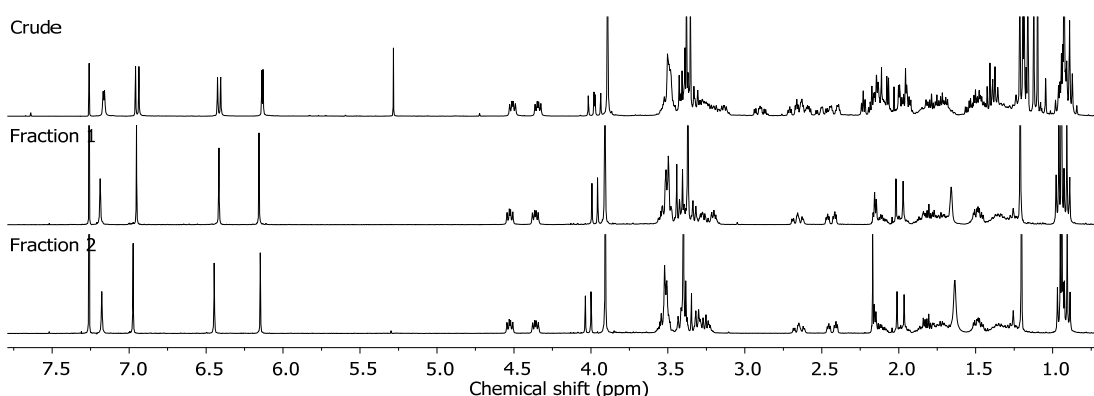
Figure 5.10   ^{1}H NMR spectra recorded in CDCl₃ of the diastereomeric mixture (top), first-eluting diastereomer **(60a)** (middle), and second-eluting diastereomer **(60b)** bottom.

The crystallisation of diastereomers **(60a)** and **(60b)** was examined but it was only possible to form crystals as a diastereomic mixture. Once the diastereomers were fully separated, crystallisation was no longer successful, with the separated diastereomers only forming oily, glassy solids. The diastereomeric mixture **(60a)** and **(60b)** was crystallised from ethanol, and the crystal structure was determined by X-ray diffraction on a single crystal (**Appendix B – 10**). The crystal structure (**Figure 5.11**) confirms the structure of the diastereomers, which adopt the boat conformation. The distal pair

of aromatic rings bearing the sterically-bulky camphorsulfonate groups have been flattened out near horizontal, in a similar manner to the tri-TBDMS resorcinarene (35).
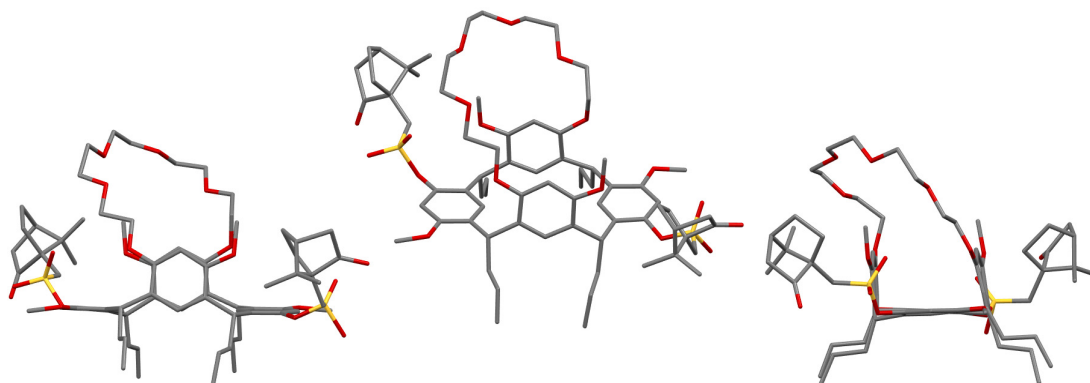
Figure 5.11   Crystal structure of a diastereomer of camphorsulfonate crown-6 resorcinarene **(60a)** or **(60b)**, obtained from a crystal of both diastereomers. Colour code: C, grey; O, red; S, gold. Hydrogen atoms have been omitted for clarity. For ORTEP view see **Appendix B – 18**.

The crystal packing of the diastereomeric mixture reveals that the two diastereomers have packed together in a manner that is complementary to the chirality of the resorcinarene. As shown in **Figure 5.12** the resorcinarenes do not pack head-to-head / tail-to-tail, but the two diastereomers interlock together via the camphorsulfonate substituents. The tendency for a diastereomer to pack in an interlocking, complementary manner with the other diastereomer, may be responsible for the difficulty in crystallising the separated diastereomers.
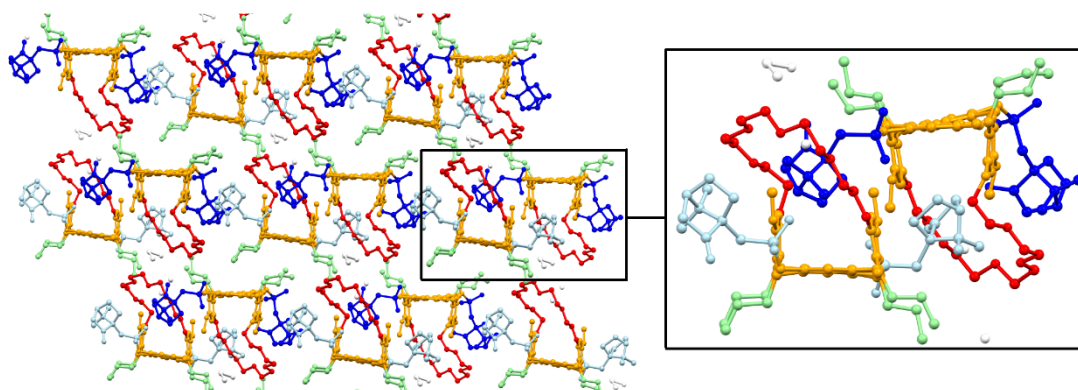
Figure 5.12   Crystal packing of resorcinarene diastereomers **(60a)** and **(60b)** crystallised from ethanol. Colour code: resorcinarene macrocycle, orange; crown ether, red; propyl tails, green; camphorsulfonate, dark-blue and light-blue for the two different diastereomers.

However, with a trace amount of the other diastereomer present from slightly co-eluted material, the crystallisation was difficult but was successful from diethyl ether. Perhaps the trace of the other diastereomer provided a complementary crystal packing which enabled a crystal of the diastereomeric mixture to form. This diastereomeric

crystal may have acted as a seed crystal which enabled the pure diastereomer to crystallise. These crystals of slightly co-eluted diastereomers **(60a)** and **(60b)**, obtained from ether, were analysed by X-ray crystallography to determine the absolute configuration of the separated camphorsulfonate resorcinarenes. Disappointingly, analysis of the crystals of **(60b)** revealed that both diastereomers were still present in the unit cell. The co-crystallisation of these diastereomers was rather surprising, since the co-crystallisation of covalent diastereomers is reportedly a rare occurrence.[167] An alternative method for the determination of the absolute configuration of chiral resorcinarenes has been reported by Neri and co-workers[168, 169] using electronic circular dicroism with comparison of the spectra with computational predictions. Samples of separated diastereomers **(59a)** and **(59b)** were sent to Neri's group for determination of absolute configuration, with results still outstanding. In lieu of these results, the absolute configuration of these crown resorcinarene camphorsulfonates has been tentatively assigned based on the similar work by McIldowie and co-workers,[66] who consistently recorded a *R* configuration and more positive specific rotation for the faster-eluting diastereomer.

Although the camphorsulfonylation reaction proceeded smoothly to give clean products in quantitative yield, the reaction was capricious, particularly on scaling up. A smooth reaction was indicated by a TLC showing the target diastereomers with minimal baseline. Moreover, the aromatic region of the ^{1}H NMR spectrum of the crude product clearly showed doubled resorcinarene peaks with an almost-flat baseline. Unsuccessful reactions could be distinguished by the appearance of spots near the baseline on TLC, as wells as lumps of peaks in the aromatic region of the ^{1}H NMR spectra. These observations point to the formation of undesirable material which results in significant reduction of the yield of the target diastereomers, therefore rendering the reaction unsuccessful. To recify this inconsistency on reaction scale-up, the triethylamine addition was performed with cooling of the reaction mixture in an ice bath, as well as decreasing the concentration of the reaction mixture; unfortunately these measures were of no effect. The reaction appeared to be the most reliable on a small 20 mg scale, which therefore necessitated multiple small-scale reactions to obtain the required quantities of diastereomers. For some reaction products, a small amount of impurity co-elutes with the diastereomeric mixture. This impurity was visible as small peaks in the aromatic region of the ^{1}H NMR spectrum, and appears to

be a resorcinarene-based by-product. Removal of this impurity was challenging but could be partially removed by repeatedly subjecting the material to preparative TLC with MeOH-toluene (5:95).

5.2.2 Diastereomers of synthetic intermediates of crown resorcinarene

Although the camphorsulfonate diastereomers of the crown resorcinarenes have been synthesised and separated, in hope of finding better diastereomic separation, the synthesis of diastereomers of intermediates during the crown resorcinarene synthesis was explored. Such resorcinarene diastereomers would not be considered as potential membrane carriers but would serve as a better method to synthesise single enantiomers of the crown resorcinarenes.

Making diastereomers of the distal-TBDMS resorcinarene **(34)** has the potential for the chiral moiety to also serve as the replacement protecting group for the TBDMS. This would be an advantage as it would integrate the diastereomer formation and hydrolysis into the synthetic procedure (**Scheme 5.5**), which would enable enantio-pure crown resorcinarenes to be synthesised without additional synthetic steps. Furthermore, it would also provide three possible intermediates at which the diastereomers could be separated. However, if a cleavable chiral moiety such as a camphorsulfonate were to function as a replacement protecting group for the TBDMS, it needs to be stable under the Cs_2CO_3/DMF conditions for bridging. This was a cause for concern since the methanesulfonate group was hydrolysing under these conditions (**Section 4.2.1**). Nevertheless, the camphorsulfonate group, being bulkier, may be more resilient to hydrolysis, and thus this was investigated.
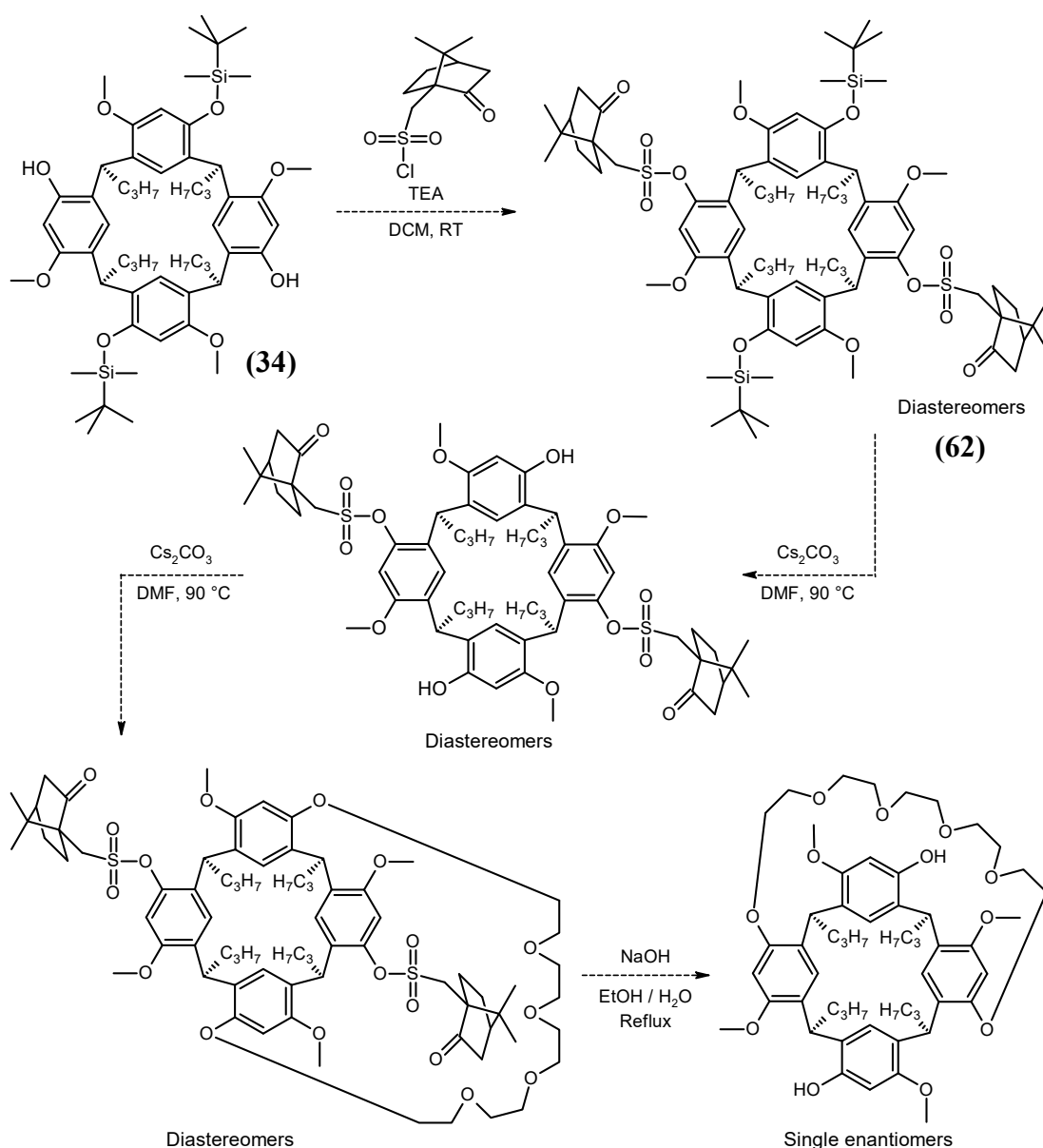
Scheme 5.5 Potential modification of the synthetic procedure where the chiral moiety could also function as the protecting group that replaces the TBDMS.

Distal-TBDMS resorcinarene **(34)** was subjected to the general camphorsulfonylation procedure. Despite using a vast excess of 16 equivalents of camphorsulfonyl chloride, the TLC of the reaction mixture still showed a spot of equal retention to the starting resorcinarene. Nevertheless, the reaction was worked up, and a crude product of at least four compounds by TLC was obtained. However, the ^{1}H NMR spectrum of the crude material showed no starting resorcinarene, but the key resorcinarene peaks were doubled which suggested the formation of diastereomers. The four UV-active spots were separated by preparative TLC, but only the highest-R_f spot contained the mixture of the resorcinarene diastereomers **(62)** in a combined yield of 50%, without the other impurities (**Appendix A – 86**). Experimentation of chromatographic solvent systems

yielded no separation of the purified diastereomer mixture **(62)**. Inspite of the low yield, difficult purification, and unsuccessful diastereomer separation, it was thought that purification and separation of the diastereomers may be easier after hydrolysis of the TBDMS protecting groups. Therefore, a crude diastreomeric mixture of **(62)** was subjected to hydrolysis via Cs_2CO_3/DMF to also test the stability of the camphorsulfonate esters under the conditions for bridging. The ^{1}H NMR of the hydrolysis crude product indicated removal of the TBDMS groups, but the resorcinarene signals appeared as a complex mixture. Unfortunately, this indicates that the camphorsulfonates, like the methanesulfonates (**Section 4.2.1**), were also hydrolysing under the Cs_2CO_3/DMF reaction conditions used for bridging. Consequently, the idea of forming camphorsulfonate diastereomers on distal-TBDMS resorcinarene **(34)**, then utilising the camphorsulfonate groups as protecting groups for the bridging reaction was proven to be unsuccessful on account of the low yield, unsuccessful diastereomer separation, and instability of the camphorsulfonate groups.

The final, and least attractive opportunity for making diastereomers in the synthetic scheme is to make diastereomers of the dibenzyloxyresorcinarene **(46)**. This is the least attractive opportunity because dibenzyloxyresorcinarene **(46)** is the precursor for the lower-yielding bridging reaction. Nevertheless, the potential for easier diastereomer separation was the motivation for investigating the synthesis of camphorsulfonates of this resorcinarene. Dibenzyloxyresorcinarene **(46)** was subjected to the general camphorsulfonylation procedure to give a crude mixture which was chromatographed by preparative TLC which delieved the purified diastereomers in a combined yield of 78%. The characteristic doubling of peaks in the ^{1}H NMR spectrum (**Appendix A – 87**) confirmed the successful synthesis and isolation of the diastereomers. Experimentation with chromatographic solvent systems unfortunately yielded no resolution of the diastereomers. Therefore, the formation of diastereomers on the crown resorcinarene final product, as was first investigated, provides the best method for the synthesis and separation of the resorcinarene diastereomers in sufficient quantities.

5.3 Synthesis of bis-crown resorcinarenes

Since bis-crown resorcinarenes can be simply synthesised by a single step procedure,[102, 103] bis-crown resorcinarene derivatives were also synthesised (**Figure 5.13**). These bis-crown resorcinarenes would be assessed as membrane carriers for comparison. Compared to the distally-bridged crown resorcinarenes, these bis crown resorcinarenes have a more open cavity, and thus are expected to be inferior membrane carriers.
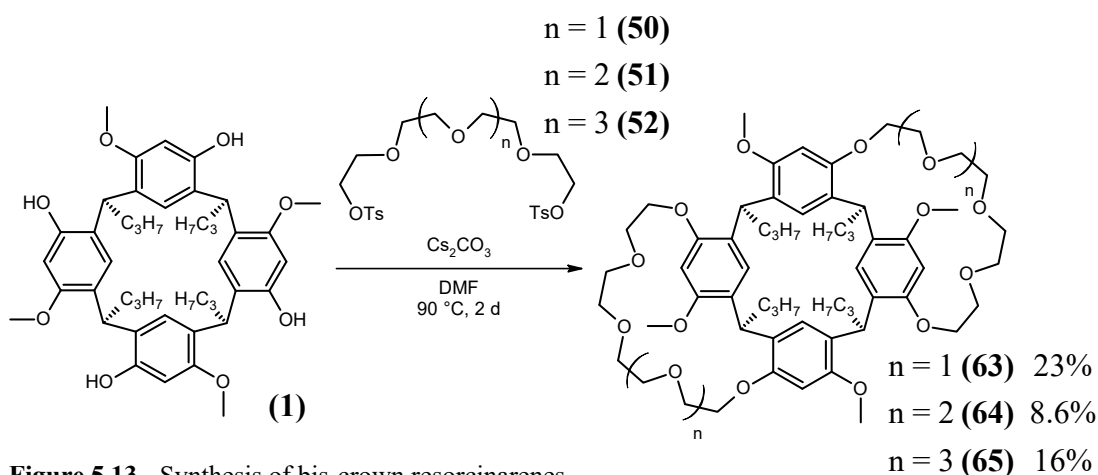
Figure 5.13 Synthesis of bis-crown resorcinarenes.

The successful synthesis of the target bis-crown resorcinarenes was demonstrated by the expected C_2 symmetry of the product. This was apparent by the doubling of the peaks in the aromatic region of the ^{1}H NMR spectrum (**Appendix A – 87**), from two to four, compared to the starting resorcinarene. The C_2 symmetry also rendered the two crown ether moieties to be equivalent, with the sixteen carbons for bis-crown-5 resorcinarene **(63)** appearing as eight CH_2 peaks around 70 ppm in the DEPT-135 spectrum.

5.4 Membrane transport experiments

Having accomplished the synthesis and separation of the camphorsulfonate diastereomers of crown 5-7 resorcinarenes in sufficient amounts, the investigation progressed to examining all synthesised crown resorcinarenes as membrane carriers for an appropriate chiral drug. The resorcinarene which demonstrates the greatest membrane transport will be obtained as single enantiomers via hydrolysis of the corresponding separated diastereomers. Then both single enantiomers would be examined as membrane carriers to determine if there was any enantioselectivity in the membrane transport. As discussed in **Section 1.1.6**, the membrane-based separation

technique was chosen for the many advantages such as its simplicity, low cost, continuous operation, industrial scalability, and applicability to calixarenes.

Since the membrane carrier is a crown resorcinarene, the guest racemic drug theoretically needs to have functional groups and a shape which would complement binding with the host resorcinarene crown. Regarding functional groups, aromatic rings are able to π-stack with other aromatic rings, as well as bind with ammonium species through electrostatic interactions. On the other hand, crown ethers are known to form hydrogen bonds through the multiple oxygen atoms which act as hydrogen bond acceptors. Based on this theoretical reasoning, a starting point for a racemic drug would be one with an ionisable amine group which could bind in the crown ether or in the electron-rich resorcinarene cavity. Additionally, having an aromatic ring would provide potential for π-stacking inside the resorcinarene cavity, while also enabling the transport rate of the drug to be monitored by UV-vis spectroscopy. Regarding shape, the racemic drug should not be bulky, but should be linear so that it can fit into the crown resorcinarene, which has a crown conformation. The chiral centre of the drug should also be fairly close to the functional groups that would bind with the resorcinarene to enable maximum chiral interaction between host and guest that should lead to chiral recognition.

In terms of structure and functional groups, salbutamol (**Figure 5.14**) may be a suitable racemic drug candidate for this membrane transport investigation. salbutamol is significant because it is the common drug used to treat asthma and chronic obstructive pulmonary diseases. It works by relaxing the constricted airway muscles, causing dilation of the airway, allowing the patient to breathe. *In vitro* studies of (*S*)-salbutamol suggest it produces pro-inflammatory effects,[8] as well as muscle-spasm effects which undermines the therapeutic muscle-relaxing effect of the (*R*) enantiomer.[9, 10] However, these advantages of enantio-pure (*R*)-salbutamol (Levosalbutamol) over racemic salbutamol has not been clearly evidenced in various clinical studies, which have yielded contradictory results. Some clinical studies have concluded that (*R*)-salbutamol provides no advantage in effectiveness and safety over racemic salbutamol,[170, 171] while others have suggested otherwise.[172, 173] This is due to the presence of many factors in a clinical setting and therefore the clinical advantages of (*R*)-salbutamol over racemic salbutamol is still being studied and debated. One

definitive factor limiting the use of (*R*)-salbutamol is the significantly greater cost compared to racemic salbutamol. In one clinical study, the total cost of treatment was $8003 with (*R*)-salbutamol, versus $5772 with racemic salbutamol, a 38% increase.[171] The additional expense is attributed to the additional steps required for enantioresolution, which is accomplished by the diastereomic crystallisation of an intermediate in the synthesis of (*R*)-salbutamol.[174]
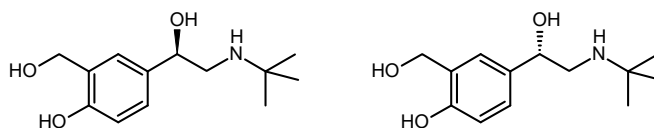
Figure 5.14 The structures of (*R*)-salbutamol (left) and (*S*)-salbutamol (right).

Studies regarding the diffusion of salbutamol across a membrane are present in the literature. Corrigan and co-workers have discovered that the diffusion of salbutamol sulfate can be enhanced by the application of an electric current across the membrane, with the quantity of salbutamol diffusing across being proportional to the current density applied.[175] In further work, Corrigan and co-workers have shown that salbutamol sulfate diffused through hydrophobic membranes at a slower rate compared to hydrophilic membranes.[176] The effect of the counter anion on the diffusion of salbutamol was briefly investigated by Patel et al.,[177] who showed that a hydrophobic anion (1-hydroxy-2-napthoic acid), instead of the standard hydrophilic sulfate anion, decreased the diffusion of salbutamol across a regenerated cellulose membrane. In spite of the examples in the literature, the membrane transport of salbutamol that is facilitated by a membrane carrier appears to be an unprecedented investigation.

The membrane transport of salbutamol was investigated through a bulk liquid dichloromethane membrane in a U-tube apparatus. UV-visible spectrometry was used to monitor the appearance of salbutamol in the receiving phase. In particular, the absorbance at 224 nm was monitored, since it provides a more accurate estimate of salbutamol at very low concentrations (<0.01 mg/mL),[178] which was the case for all experiments. Because of the many variables involved, much experimentation was required to develop a reliable method from the running of the transport experiments to the monitoring of the appearance of salbutamol by UV-visible spectrometry.
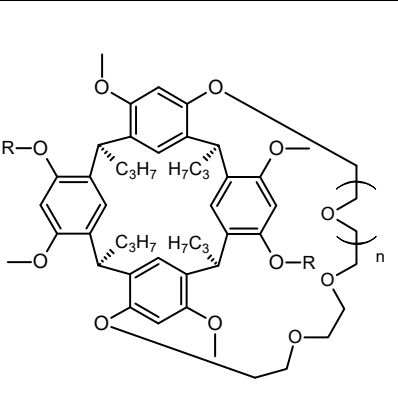
Preliminary investigations into some factors of the membrane transport of salbutamol indicated that:

- A blank membrane solvent of chloroform compared to dichloromethane exhibited a significantly faster rate of salbutamol self-transport, thus dichloromethane appears to be better membrane solvent.

- A source phase of 1 M HCl compared to water caused a significant increase of the salbutamol transport with resorcinarene **(57)** in dichloromethane. This observation confirms the initial assumption that the chloride salt is transported better than the more hydrophilic sulfate salt that the salbutamol comes in.

- U-tube glassware of slightly different dimensions (± 5 mm) may have an impact on the membrane transport, as suggested by some limited evidence.

- A receiving phase of 1 M HCl compared to water showed a slightly lower rate of transport with resorcinarene **(57)** in dichloromethane. This was an anticipated result because a HCl receiving phase already contains ions, and so it would receive ions less readily compared to a receiving phase that is pure water (empty of ions).

- Conducting the membrane transport experiments in a warm water bath to increase the rate of transport appears to give erratic results.

- Monitoring of the transport by conductivity gave erratic results. A consistent result could not be established in an experiment with a blank dichloromethane membrane and a 1 M HCl source phase. The erratic results were likely due to the passive diffusion of HCl through the dichloromethane membrane.

- Too much crown resorcinarene in the dichloromethane membrane caused it to precipitate over time, and float through to the top of the aqueous layers. A concentration of about 1.5 mg/mL of the crown resorcinarene appeared to be the ideal amount, however a little precipitation was still observed, particularly for dihydroxy crown-7 resorcinarene **(58)**.

These factors could be further investigated, however at this stage, a protocol that would give reasonably consistent results was required. After much experimentation, a protocol for the experiments was established using dichloromethane (20 mL) as the membrane solvent, with crown resorcinarene (~30 mg, 0.0277 mmol), salbutamol in 5 equivalents, a source phase of HCl (5 mL, 1 M), and a receiving phase of MilliQ water

(5 mL). With these conditions, the fifteen crown resorcinarene derivatives (**Table 5.5**) were monitored over a week for the ability to carry salbutamol hydrochloride across a bulk liquid dichloromethane membrane. The results of the investigation into the membrane transport of salbutamol with the resorcinarene derivatives are shown in **Figure 5.15** (**Appendix C – 1**). These results were an average of multiple replicate experiments. Comparison of the absorbance at 224 nm with a literature calibration curve[178] enabled approximation of the amount of salbutamol present in the receiving phase. With five equivalents of salbutamol to resorcinarene, the salbutamol in the receiving phase was very low; less than 0.1% of the salbutamol was transported after a week. The results would have a greater certainty if the salbutamol was transported in a greater amount. Therefore, to increase the amount of salbutamol transported to the receiving phase, all experiments were conducted with double the equivalents of salbutamol to resorcinarene. With 10 equivalents (**Appendix C – 17**), there was more salbutamol being transported as indicated by an increase in UV-vis absorbance (**Figure 5.16**), however the transport yield of salbutamol was still very low, still being less than 0.1% after a week. Moreover, after running the experiments with 10 equivalents of salbutamol for a week, a white precipitate appears at the source phase – membrane interface. This was also apparent for the blank dichloromethane membrane, leading to the conclusion that the salbutamol is slowly precipitating over time. Nevertheless, this precipitation was observed after a week and should not affect the results during the week.

Table 5.5   List of resorcinarenes investigated as membrane carriers for salbutamol hydrochloride.

	Crown-5 n = 1	Crown-6 n = 2	Crown-7 n = 3	
R = Bn	(53)	(54)	(55)	
R = H	(56)	(57)	(58)	
R = camphorSO$_2$	(59a)	(60a)	(61a)	
R = camphorSO$_2$	(59b)	(60b)	(61b)	
Bis-crown	(63)	(64)	(65)	

Parent resorcinarene (1) was also investigated.
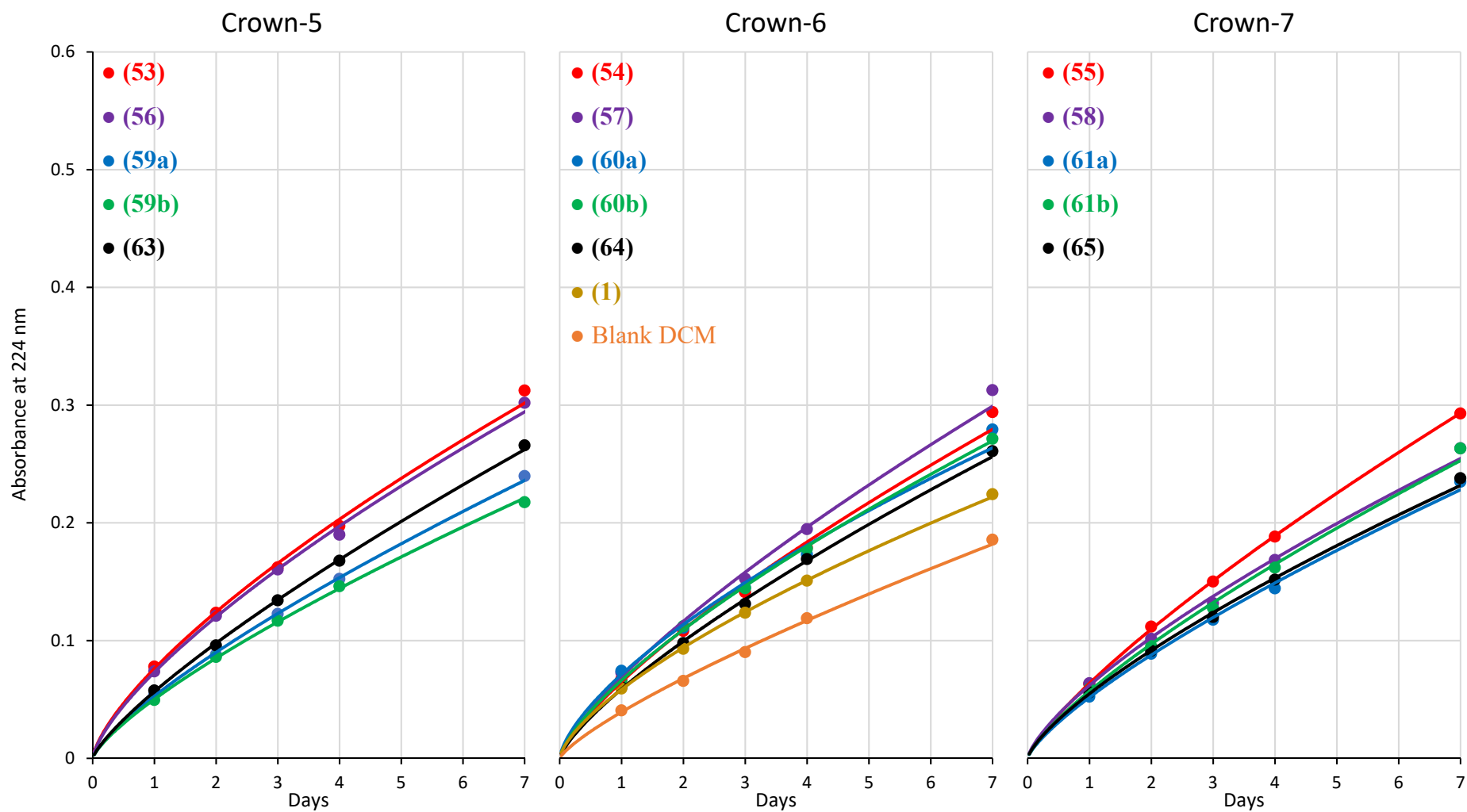
Figure 5.15 Comparison of resorcinarenes as membrane carriers with 5 equivalents of salbutamol hydrochloride. Averages of replicate experiments.
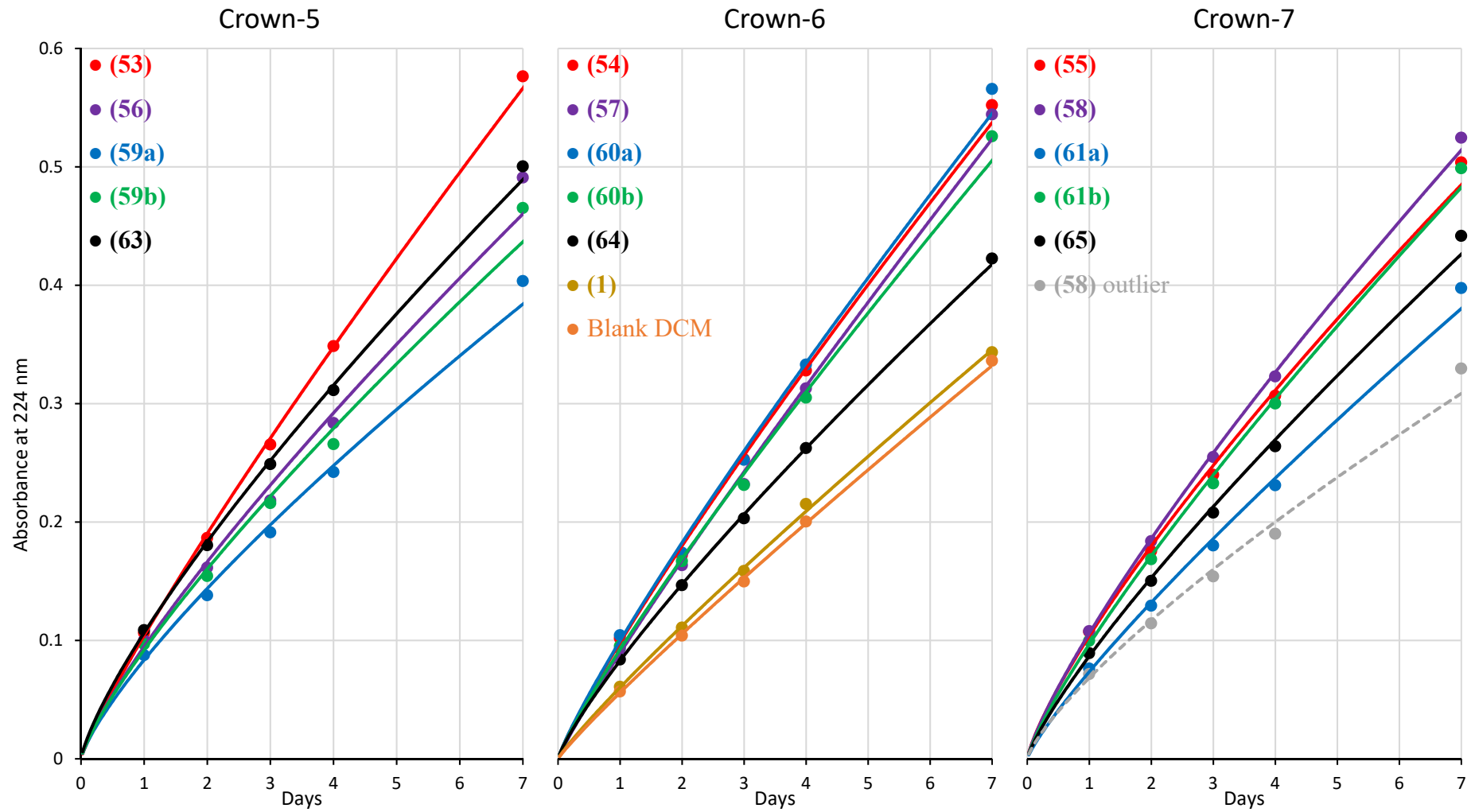
Figure 5.16   Comparison of resorcinarenes as membrane carriers with 10 equivalents of salbutamol hydrochloride. Averages of replicate experiments.

The UV-vis analysis of the receiving phases of the membrane transport experiments have shown that all crown resorcinarenes were enhancing the membrane transport of salbutamol to different extents compared to the blank dichloromethane control. Even the parent resorcinarene **(1)** appeared to be enhancing the salbutamol transport, albeit having a rather negligible enhancement, as expected. Across all the crown resorcinarenes, the best transporters generally appear to be the dibenzyl and dihydroxy crown resorcinarenes, followed by the camphorsulfonate diastereomers, then the bis-crown resorcinarenes. The bis-crown resorcinarenes were expected to be the poorest transporters because of their open cavities. The crown-5 resorcinarenes diastereomers **(59a)** and **(59b)** were an exception, being the worst transporters in their class. This may be due to the relatively small cavity of the crown-5 resorcinarene being obstructed by the bulky camphorsulfonate group. In terms of size, crown-6 resorcinarenes generally appeared to be better transporters, which may suggest that a resorcinarene with this crown offers a better fit for salbutamol. Generally, the transport between resorcinarene diastereomers appears to be noticeably different. In particular, the enhancement in transport appears to switch between crown-5 resorcinarenes **(59a)** and **(59b)** when the equivalents of salbutamol were changed from 5 to 10.

As shown in the preliminary membrane transport experiments, there were many variables involved in the setup, running, and analyses of these experiments. Considering this, together with the low level of salbutamol present, the uncertainties of these results are likely to be relatively high. Therefore, care was taken to identify and minimise unwanted variables. To assess the repeatability of the experiments, each experiment was replicated till consistent results were apparent. For most experiments, this was accomplished after two or three replicates, however, more variation was encountered for some experiments. These variations could be due to some undiscovered factor, or could be inherent to the particular resorcinarene derivative. For example, the experiment with resorcinarene **(58)** with 10 equivalents of salbutamol (**Figure 5.16**) produced a set of results which had a lower transport than with the blank dichloromethane. These were deemed to be outliers, which may have been caused by an undiscovered entity. All things considered, reasonably consistent results were obtained from these experiments, and these results provide a general, qualitative indicator of the trends.

Despite the uncertainties, a definitive observation in all these results is that a small amount of salbutamol was being transported across the membrane. Over an entire week, less than 0.1% of the salbutamol was transported by the membrane carrier as well as through passive diffusion. In comparison, Adhikari et al.,[28] reported the a best transport yield of 11% over 8.3 days for their system. This lack of transport of salbutamol by the crown resorcinarenes suggests that there was insufficient binding of the salbutamol to the resorcinarene. The salbutamol may have been carried across the membrane by weak association to the crown resorcinarene, rather than by being carried within its cavity. Perhaps the anticipated hydrogen bonding and π-stacking did not provide sufficient binding interactions needed for the binding and transportation of salbutamol. The examples of membrane carriers for organic molecules in the literature, mentioned in **Section 1.2.3**, often possess acid functionalities such as a carboxylic acid,[57] a phosphonic acid,[28, 52] or a boronic acid.[56] This is because the acid functionality facilitates stronger electrostatic binding interactions as well as maintaining charge balance by proton exchange. The inclusion of an acid functionality on the crown resorcinarene would be a next synthetic step in its investigation as a potential membrane carrier. On the other hand, the size of the resorcinarene cavity, its conformation, and the arrangement of the functional groups about the resorcinarene may not have provided a good fit for salbutamol. As a basic starting point, it was roughly speculated that salbutamol would bind within the cavity of the resorcinarene, however currently, no definitive evidence exists to determine if and how this would happen. Therefore, the binding of salbutamol with the resorcinarene needs to be investigated in a more informative way that would shed light to how the binding occurs. This information would enable more efficient design of the membrane transport experiment and the synthesis of a membrane carrier with a complimentary shape and functional-group arrangment.

5.4.1   NMR titrations of crown resorcinarenes with salbutamol sulfate

It would be ideal if the binding of the salbutamol and resorcinarene could be observed as a crystal structure, since that would provide a clear picture of the interaction. An attempt to obtain crystals of an inclusion complex was however, unsuccessful. Therefore, NMR spectroscopy, was utilised for the possibility to provide binding information, as well as a screening method for combinations of host and guest.

To probe the binding interactions of the dibenzyloxy and dihydroxy crown resorcinarenes with salbutamol, ^{1}H NMR titrations of the crown resorcinarenes with salbutamol sulfate were conducted in DMSO-d$_6$. In this titration, salbutamol sulfate was added in increments of up to 12 equivalents to a solution of the crown resorcinarene, while monitoring by ^{1}H NMR spectroscopy. The titration of dihydroxy crown-6 resorcinarene **(57)** at first glance appeared to demonstrate binding of the salbutamol and resorcinarene, as indicated by significant shifting of the salbutamol peaks in the ^{1}H NMR spectra (**Figure 5.17**).
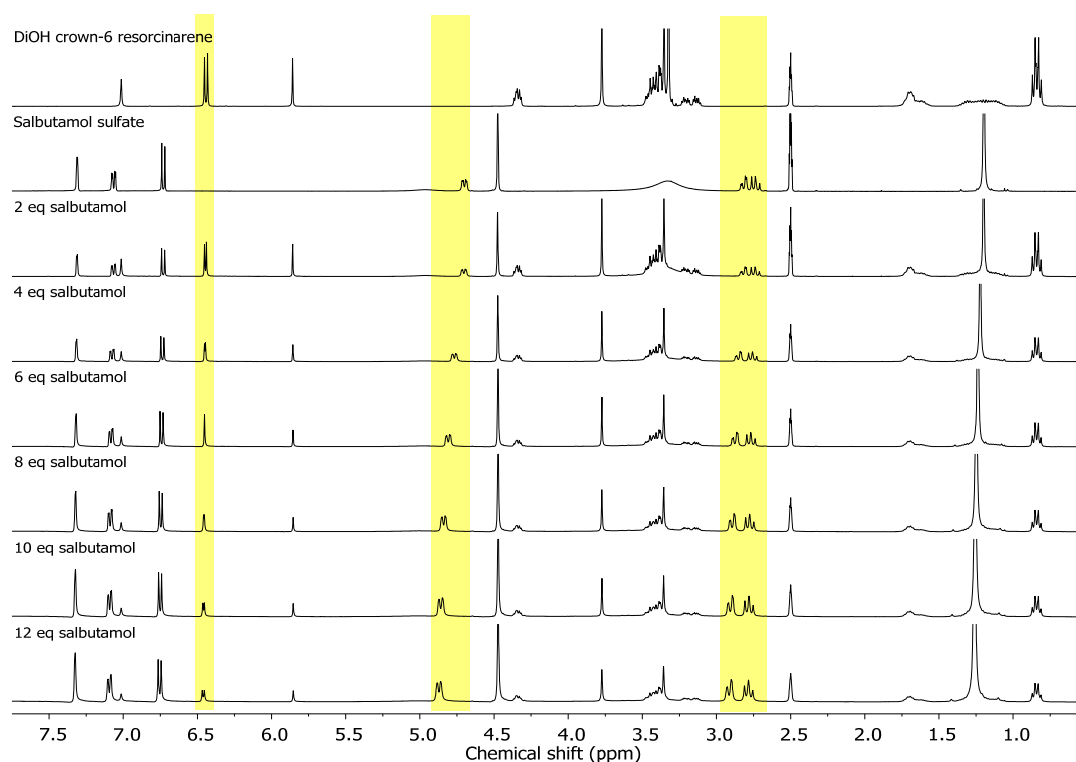
Figure 5.17   ^{1}H NMR spectra of the titration of dihydroxy crown-6 resorcinarene **(57)** with salbutamol sulfate in DMSO-d$_6$.

Initially, it was thought that this confirmed the result from the membrane transport experiments of resorcinarene **(57)** being one of the best salbutamol membrane carriers. However, in the titration spectra, the peaks of the resorcinarene were mostly unmoved. The resorcinarene peak with the greatest shift was the peak originally at 6.43 ppm, which shifted to 6.47 ppm after the addition of 12 equivalents of salbutamol sulfate (**Figure 5.18**). This shift of 0.04 ppm was a meager shift compared to the work by Adhikari et al. In their work, the best membrane carrier and guest combination produced a shift of about 0.1 ppm in the peaks of the calixarene host with 2 equivalents of the guest.[28]

188
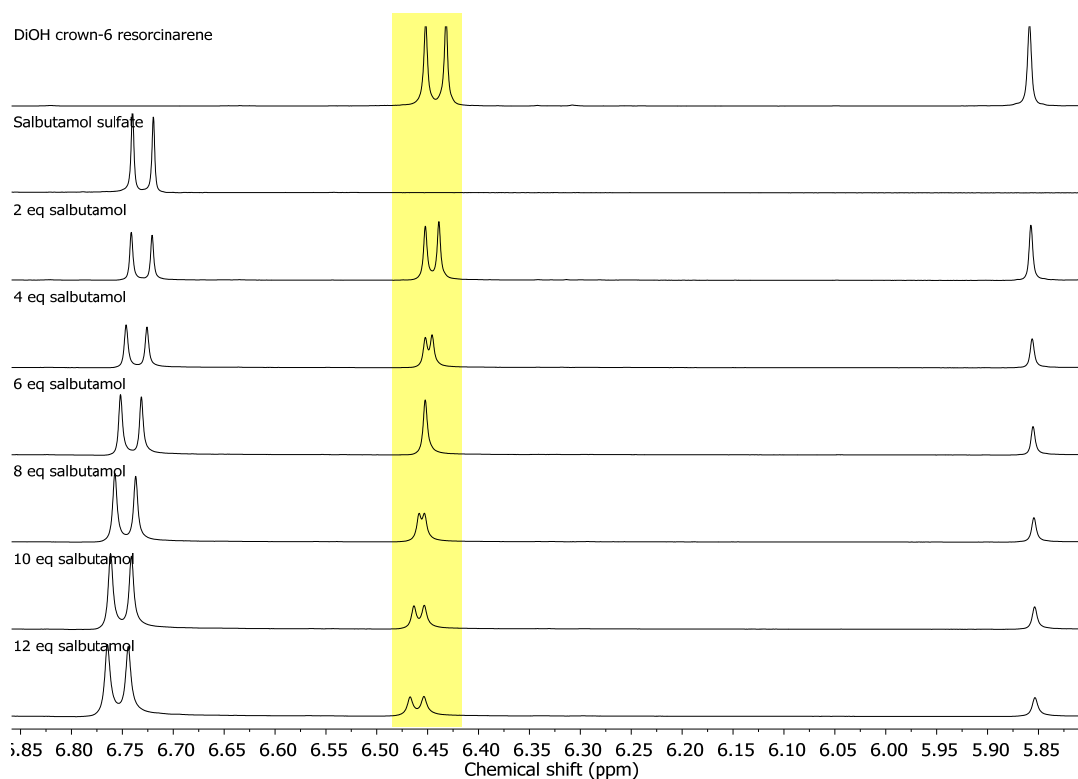
Figure 5.18   Expansion of the ^{1}H NMR titration shown in **Figure 5.17**. The resorcinarene peak with the greatest shift is highlighted.

The titrations of the crown-5 and crown-7 derivatives of the dihydroxyresorcinarenes yielded similar results (**Figure 5.19**). It was puzzling that significant shifts were consistently observed for the salbutamol peaks, while only a small shift was observed for the resorcinarene peak.
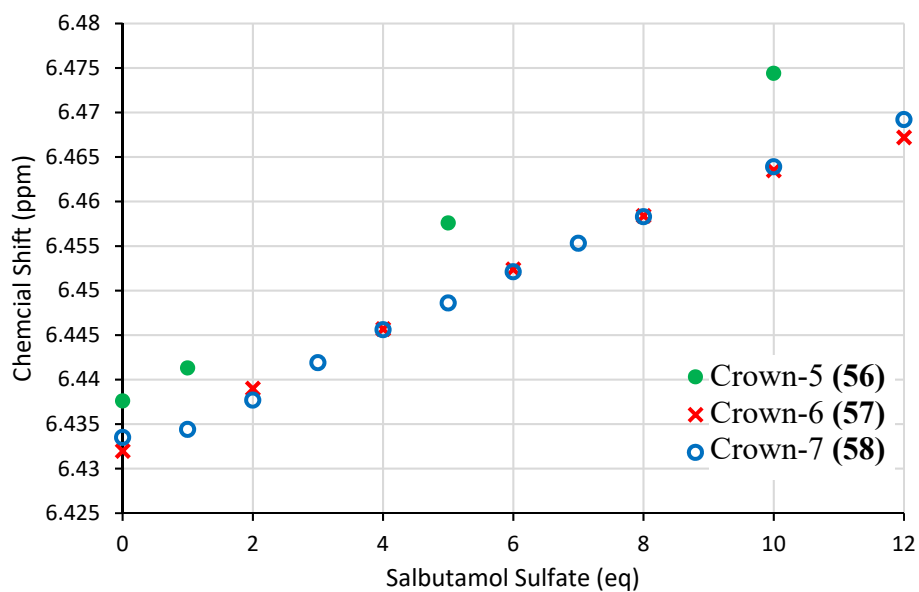
Figure 5.19   Comparison of the greatest-shifted resorcinarene peak from ^{1}H NMR titrations of salbutamol sulfate with dihydroxy crown 5-7 resorcinarenes in DMSO-d$_6$.

A search of the literature revealed a very helpful article by Thordarson[179] who cautions of the possibility for guests to aggregate in solution, and to examine this by performing trial titrations of the guest alone over a large range of concentrations. Therefore, the titration of salbutamol sulfate alone in DMSO-d_6 was performed, and the results (**Figure 5.20**) demonstrate that the salbutamol peaks were shifting with increasing concentration, confirming the suspicion of aggregation of salbutamol sulfate in solution. Therefore, the consistently observed shifts in the salbutamol peaks were an invalid indicator of the interaction of salbutamol with the resorcinarene. Nevertheless, the relatively small shift of the resorcinarene peak is still a valid indicator which shows a small interaction of the resorcinarene with salbutamol in dimethylsulfoxide.
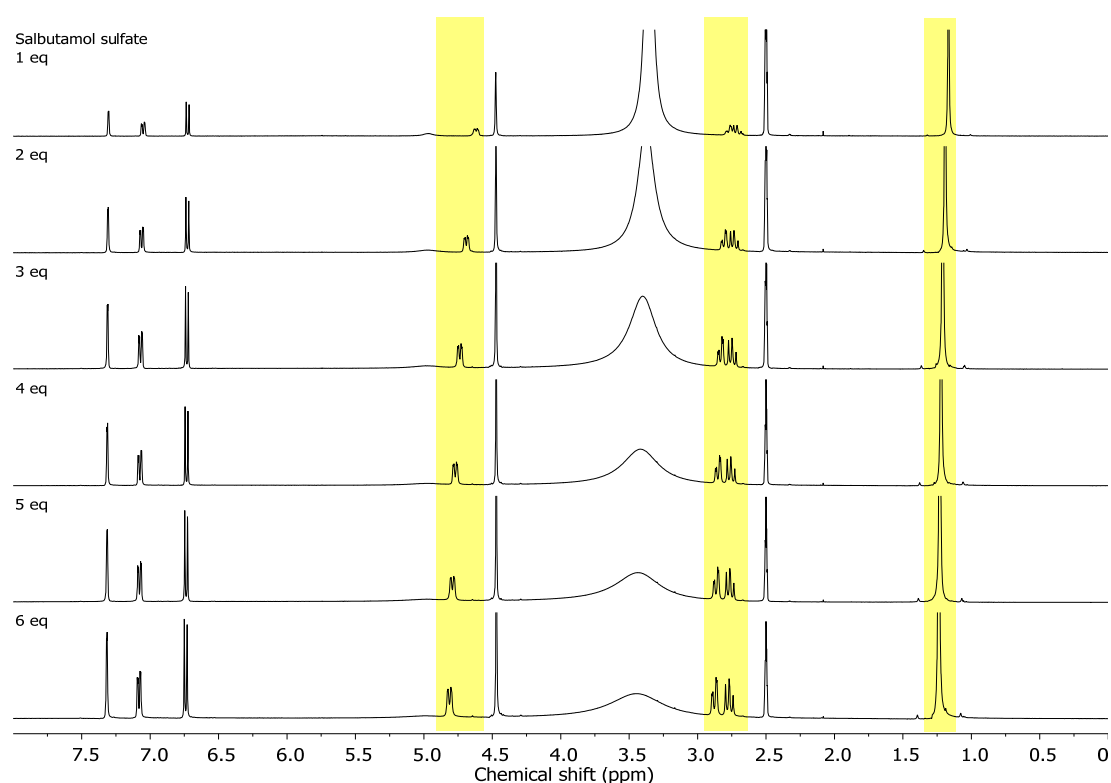
Figure 5.20 ^{1}H NMR spectra of the titration of salbutamol sulfate alone in DMSO-d_6.

^{1}H NMR titrations were also performed for dibenzyloxy crown 5-7 resorcinarenes **(53)**, **(54)**, **(55)** with salbutamol sulfate in DMSO-d_6. The usual shifts were observed for the salbutamol peaks, however the resorcinarene peaks remained completely unmoved even with up to 12 equivalents of salbutamol sulfate. The apparent lack of interaction in the ^{1}H NMR titration seems contradictory to the membrane transport results which shows similar salbutamol transport by both dibenzyloxy and dihydroxy derivatives of the crown resorcinarene. However, these ^{1}H NMR titrations, being conducted in DMSO-d_6, may not be an accurate representation of the membrane

190

transport process which was conducted in dichloromethane. Dimethylsulfoxide was used for these ^{1}H NMR titrations for the sake of solublility of the salbutamol sulfate. Unlike dichloromethane, dimethylsulfoxide is a coordinating solvent which may solvate the salbutamol and prevent its interaction with the resorcinarene. In fact, as shown in **Figure 5.6**, a change of the NMR solvent from CDCl$_3$ to DMSO-d$_6$ resulted in a significant difference in the ^{1}H NMR spectra of the dihydroxy crown resorcinarenes. The conformation of the resorcinarenes appears to be impacted by the solvent, and thus this may provide some supporting evidence for the hypothesis that the observed lack of binding in the ^{1}H NMR titrations could be due to the solvating effect of the dimethylsulfoxide solvent. Further NMR titration work is required to ascertain these suspicions.

5.4.2 Investigation of crown resorcinarenes as enantioselective membrane carriers for the chiral resolution of salbutamol

Although there was only less than 0.1 mg of salbutamol present in the receiving phase, this amount is sufficient for analysis by chiral HPLC to determine if there was any enantioselectivity in the salbutamol membrane transport. Of all the resorcinarenes examined as membrane carriers, the dihydroxy crown-6 resorcinarene **(57)** appears to be one of the best membrane carriers for salbutamol. Therefore, to examine if resorcinarene **(57)** could enantioselectively transport salbutamol, the enantiomers of resorcinarene **(57)** need to be separated. This could be achieved by simple base-catalysed hydrolysis of the sulfonate esters of the corresponding crown-6 resorcinarene diastereomers **(60a)** and **(60b)** which have already been separated. As per the procedure by McIldowie and co-workers,[66] the separated diastereomers **(60a)** and **(60b)** were both subjected to hydrolysis (**Scheme 5.6**), delivering the corresponding single enantiomers **(57a)** and **(57b)** in essentially quantitative yield in good purity after work up.
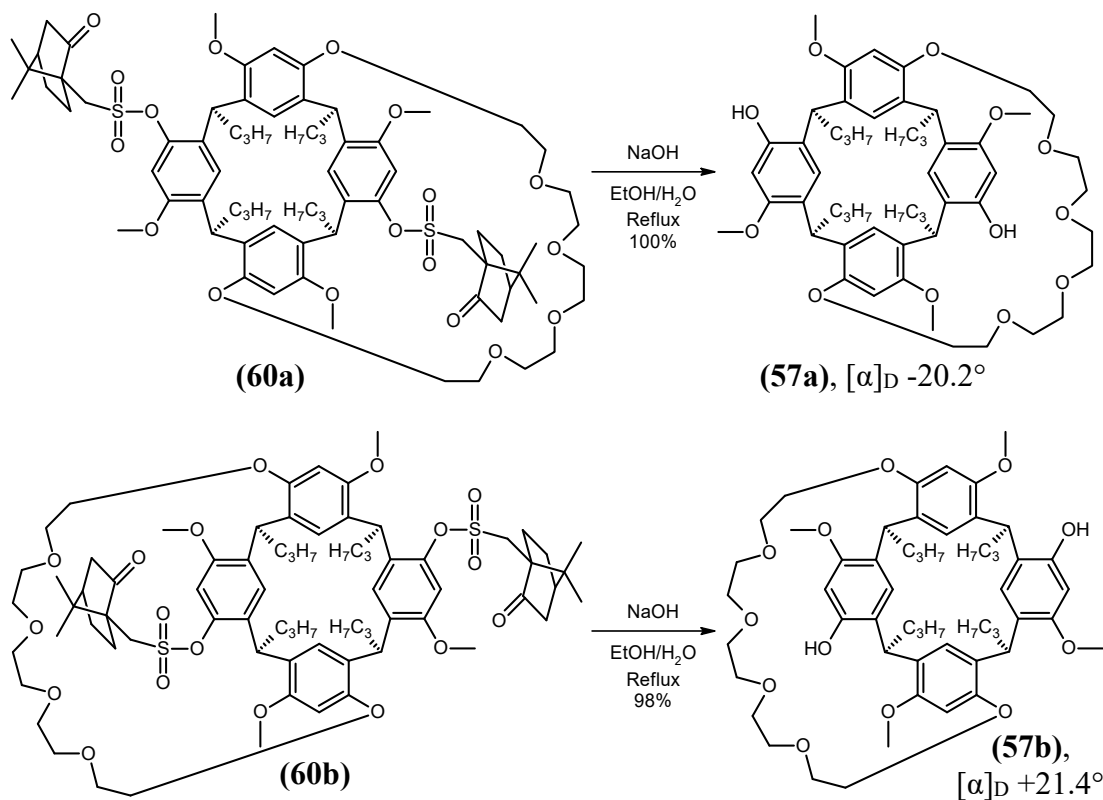
Scheme 5.6 Synthesis of single enantiomers of dihydroxy crown-6 resorcinarene **(57a)** and **(57b)** via hydrolysis of the separated diastereomers **(60a)** and **(60b)**.

The single enantiomers **(57a)** and **(57b)** were both confirmed by ^{1}H NMR spectroscopy, with both having identical spectra which matched the spectrum of racemic **(57)**. The two products were also confirmed to be enantiomers of each other with both giving opposite specific rotations of essentially the same magnitude.

The two single enantiomers **(57a)** and **(57b)** were then examined as enantioselective membrane carriers under the same conditions with 3.7 equivalents of salbutamol. After 5 days, the receiving phases were analysed by chiral HPLC, but unfortunately revealed equal proportions of both salbutamol enantiomers (**Figure 5.21**).
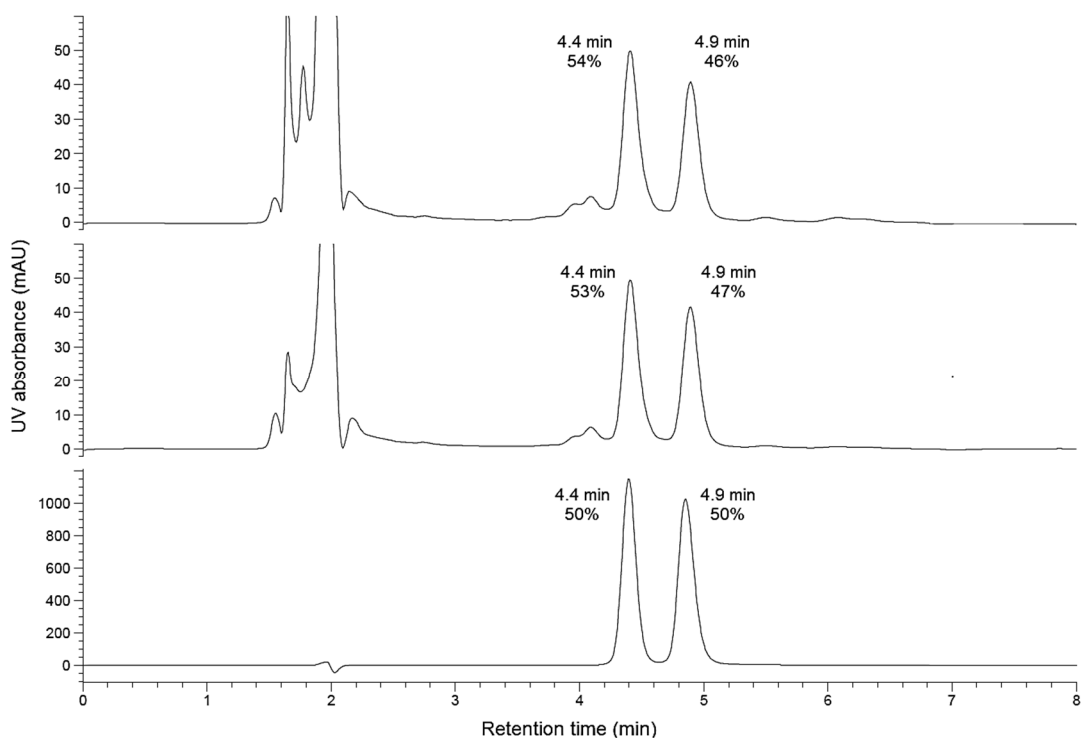
Figure 5.21   HPLC chromatograms of the receiving phases from the membrane transport of
salbutamol with resorcinarene single enantiomers **(57a)** (top) and **(57b)** (middle). The
bottom trace is of salbutamol sulfate for reference.

The six separated diastereomers, being optically active, were also examined as
enantioselective membrane carriers. The receiving phases from the earlier membrane
transport experiments with the separated diastereomers were analysed by chiral HPLC
but were also revealed to contain the salbutamol enantiomers in equal proportions. The
chromatograms for the membrane transport experiments with 10 equivalents of
salbutamol appeared to contain more baseline impurity peaks compared to the
experiments with 5 equivalents. Nevertheless, the chromatograms for both 5 and 10
equivalents of salbutamol demonstrated that there was no enantioselective transport
by any of the separated diastereomers. The lack of enantioselective membrane
transport by these enantio-pure chiral cavities **(57a)** and **(57b)**, including the six
diastereomers, may be due to the crown resorcinarene being too flexible, and thus able
to flex and accommodate both enantiomers. This lack of enantioselectivity may also
be due to the salbutamol associating on the outside of crown resorcinarene without
engaging with the chirality of the crown resorcinarene cavity.

In this chapter, the synthesis of distally-bridged crown 5-7 resorcinarenes from distally-functionalised resorcinarene **(46)** was described. Camphorsulfonate diastereomers of the three sizes of crown resorcinarenes were also synthesised and separated. Moreover, bis-crown 5-7 resorcinarenes were synthesised for comparison of their membrane transport capabilities. All fifteen of these crown resorcinarenes were then investigated as membrane carriers for salbutamol, with all of them exhibiting salbutamol transport to various degrees. Although, the transport yield of salbutamol for these crown resorcinarenes was very low, this was the first demonstration of a bulk liquid membrane carrier for salbutamol. This indicates that the binding interactions between the crown resorcinarenes and salbutamol were not sufficiently strong. Perhaps stronger interactions, such as electrostatic interactions via a carboxylic acid functionality on the resorcinarene, is needed. However, these functional groups that facilitate binding need to be located and arranged on the resorcinarene in a manner which provides a good fit for salbutamol. Therefore, the interaction of these crown resorcinarene derivatives with salbutamol was briefly investigated via NMR titrations, which suggested a small binding for the dihydroxy crown resorcinarenes. Despite the low transport yield, the enantioselective transport of salbutamol was investigated by performing the membrane transport with single enantiomers of one the best membrane carriers. Analysis of the receiving phase by chiral HPLC unfortunately indicated no separation of the salbutamol enantiomers. Perhaps the salbutamol did not bind to the resorcinarene in a way which was impacted by the chirality of the resorcinarene. Or perhaps the crown resorcinarene was conformationally too flexible and able to accommodate both salbutamol enantiomers.

5.5 Experimental

5.5.1 General procedure for the synthesis of poly(ethylene glycol) ditoluenesulfonates

The synthesis was performed according to the literature.[163] To a solution of poly(ethylene glycol) (1 eq) and *p*-toluenesulfonyl chloride (2 eq) dissolved in dichloromethane was added powdered potassium hydroxide (8 eq) in many small portions while in an ice bath. The potassium hydroxide was added over 30 minutes to keep the temperature of the reaction mixture below 5°C. The reaction mixture was then stirred at 0°C open to air for 3 hours. After, water was added to the reaction mixture, and the layers were separated. The aqueous layer was extracted twice with dichloromethane. The combined organic extracts were washed with water, dried (MgSO$_4$), filtered, and the solvent removed under reduced pressure to give the product as a mainly colourless oil.

5.5.1.1 Tetra(ethylene glycol)ditoluenesulfonate (50)
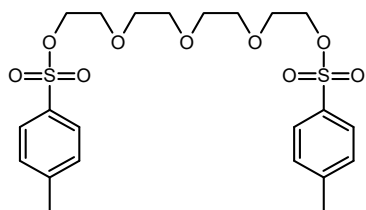
The general procedure was applied with tetra(ethylene glycol) (10.0 g, 0.0515 mol) and *p*-toluenesulfonyl chloride (19.5 g, 0.102 mol), dichloromethane (50 mL), and potassium hydroxide (23.4 g, 0.417 mol) to give **(50)** (16.1 g, 62%) as a mainly colourless oil: ^{1}H NMR (CDCl$_3$) δ 2.44 (s, 6 H, C*H*$_3$), 3.54-3.57 (m, 6 H, OC*H*$_2$), 3.63-3.74 (m, 6 H, OC*H*$_2$), 4.12-4.20 (m, 4 H, OC*H*$_2$), 7.31-7.36 (AA'BB', 4 H, Ar*H*), 7.76-7.82 (AA'BB', 4 H, Ar*H*).

5.5.1.2 Penta(ethylene glycol)ditoluenesulfonate (51)
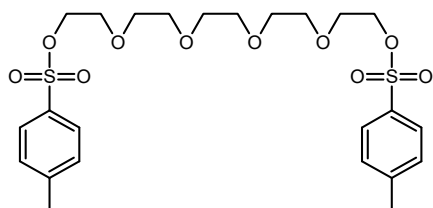
The general procedure was applied with penta(ethylene glycol) (5.01 g, 0.021 mol), toluenesulfonyl chloride (8.1 g, 0.043 mol), dichloromethane (25 mL) and potassium hydroxide (9.5 g, 0.169 mol) to give **(51)** (7.34 g, 64%) as a mainly colourless oil: ^{1}H NMR (CDCl$_3$) δ 2.44 (s, 6 H, C*H*$_3$), 3.58 (s, 6 H, OC*H*$_2$), 3.61-3.73 (m, 10 H, OC*H*$_2$), 3.13-4.18 (m, 4 H, OC*H*$_2$), 7.31-7.36 (AA'BB', 4 H, Ar*H*), 7.77-7.82 (AA'BB', 4 H, Ar*H*); ^{13}C NMR (CDCl$_3$) δ 21.8 (*C*H$_3$), 68.8, 69.4, 70.7, 70.7, 70.9 (O*C*H$_2$), 128.1, 130.0, 133.2, 144.9 (*C*, Ar).

5.5.1.3 Hexa(ethylene glycol)ditoluenesulfonate (52)
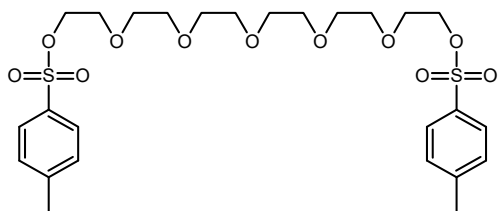
According to the procedure by Ouchi et al.,[180] to a solution of hexaethylene glycol (3.0 g, 0.011 mol) and sodium hydroxide (1.20 g, 0.03 mol) dissolved in water (50 mL) was added dropwise a solution of *p*-toluenesulfonyl chloride (3.78 g, 0.0198 mol) in tetrahydrofuran (50 mL), while keeping the temperature below 5°C in an ice bath. The reaction mixture was stirred at 0-5°C in an ice bath for 2 hours, then poured on to ice-cold water and extracted with dichloromethane (2 × 70 mL). The organic extracts were washed with water (2 × 70 mL), then with brine, dried (MgSO₄), filtered and solvent removed under reduced pressure to give a colourless, slightly yellow oil (2.26 g), which was shown to be the partially-reacted monotoluenesulfonate intermediate by NMR spectroscopy. Therefore, the monotoluenesulfonate intermediate was re-subjected to reaction using the general procedure as described earlier, using potassium hydroxide (1.22 g, 0.0217 mol) and *p*-toluenesulfonyl chloride (1.01 g, 0.0053 mol) in dichloromethane (30 mL). The presence of excess *p*-toluenesulfonyl chloride in the product was removed by filtration through silica, first with dichloromethane to elute the toluenesulfonyl chloride, then with EtOAc to elute **(52)** (2.28 g, 36%) in good purity: ^{1}H NMR (CDCl₃) δ 2.44 (s, 6 H, C*H₃*), 3.58 (s, 8 H, OC*H₂*), 3.61 (br s, 8 H, OC*H₂*), 3.66-3.71, 4.11-4.19 (2m, 2 × 4 H, OC*H₂*), 7.31-7.36 (AA'BB', 4 H, Ar*H*), 7.77-7.82 (AA'BB', 4 H, Ar*H*); ^{13}C NMR (CDCl₃) δ 21.8 (*C*H₃), 68.8, 69.4, 70.7, 70.7, 70.8, 70.9 (O*C*H₂), 128.1, 130.0, 133.2, 144.9 (*C*, Ar).

5.5.2 General procedure for the synthesis of crown resorcinarenes

To a clear solution of resorcinarene **(46)** (1 eq), caesium carbonate (8 eq) in anhydrous dimethylformamide was added poly(ethylene glycol) ditosylate (2.5 eq). The mainly clear colourless reaction mixture was heated at 90°C under nitrogen overnight. The dimethylformamide was removed under reduced pressure and dichloromethane was added to the residue. After washing with brine twice, the organic layer was dried (MgSO₄), filtered, and solvent removed under reduced pressure to give a dark brown residue as the crude product. The crude was purified by column chromatography to give the target product.

5.5.2.1 Dibenzyloxy crown-5 resorcinarene (53)
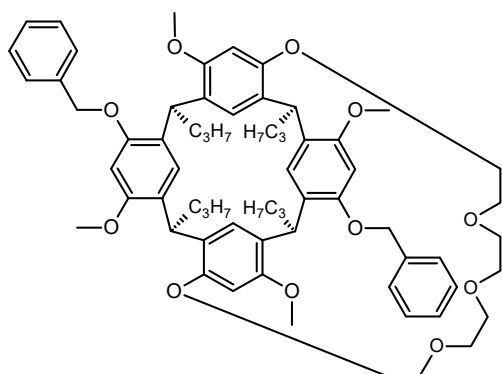
The general procedure for the synthesis of crown resorcinarenes was applied with resorcinarene **(46)** (1.03 g, 1.15 mmol), caesium carbonate (3.04 g, 9.33 mmol), anhydrous dimethylformamide (600 mL), and tetra(ethylene glycol) ditosylate **(50)** (0.975 mL, 1.21 g, 2.41 mmol). Column chromatography (EtOAc – DCM 2:8), afforded **(53)** as a slightly yellow solid (0.595 g, 49%). For analysis, the slightly yellow solid was recrystallised by diffusion from CHCl$_3$/MeOH to give the previously unreported product **(53)** as white plates and needles: mp 193 °C (CHCl$_3$/MeOH); ^{1}H NMR (CDCl$_3$) δ 0.896 (t, J = 7.3 Hz, 6 H, CH$_2$C*H*$_3$), 0.904 (t, J = 7.3 Hz, 6 H, CH$_2$C*H*$_3$), 1.16-1.53 (m, 8 H, C*H*$_2$CH$_3$), 1.69-2.04 (m, 8 H, C*H*$_2$CH), 3.13-3.32 (m, 8 H, C*H*$_2$O), 3.38-3.50 (m, 5 H, C*H*$_2$O), 3.44 (s, 6 H, OC*H*$_3$), 3.50-3.58 (m, 3 H, C*H*$_2$O), 3.86 (s, 6 H, OC*H*$_3$), 4.50-4.58, 4.64-4.73 (2m, 2 × 2 H, C*H*CH$_2$), 5.21 (s, 4 H, C*H*$_2$Ph), 6.20, 6.54, 6.56 (3s, 3 × 2 H, Ar*H*), 7.25 (overlapped with CHCl$_3$, s, 2 H, Ar*H*), 7.29-7.36 (m, 2 H, Ar*H*), 7.37-7.43 (m, 4 H, Ar*H*), 7.54-7.60 (m, 4 H, Ar*H*); ^{1}H NMR (DMSO-d$_6$) δ 0.81 (t, J = 7.3 Hz, 6 H), 0.83 (t, J = 7.3 Hz, 6 H), 1.01-1.23, 1.17-1.40 (2m, 2 × 4 H, C*H*$_2$CH$_3$), 1.55-1.88 (m, 8 H, C*H*$_2$CH), 3.07-3.21 (m, 4 H, OC*H*$_2$), 3.21-3.37 (overlapped with HDO, m, 10 H, OC*H*$_2$), 3.38 (s, 6 H, OC*H*$_3$), 3.38-3.56 (m, 6 H, OC*H*$_2$), 3.84 (s, 6 H, OC*H*$_3$), 4.33-4.44, 4.44-4.54 (2m, 2 × 2 H, C*H*CH$_2$), 5.23 (apparent s, 4 H, C*H*$_2$Ph), 5.99, 6.64, 6.73, 7.05 (4s, 2 × 2 H, Ar*H*), 7.30-7.37, 7.38-7.47, 7.51-7.59 (3m, 2 H, 4 H, 4 H, Ar*H*); ^{13}C NMR (CDCl$_3$) δ 14.4, 14.5 (CH$_2$*C*H$_3$), 21.3, 21.4 (*C*H$_2$CH$_3$), 35.2, 35.3 (*C*HCH$_2$), 37.5, 37.5 (*C*H$_2$CH), 55.3, 56.2 (O*C*H$_3$), 70.4, 70.6, 71.08 (O*C*H$_2$C), 71.14 (O*C*H$_2$Ph), 71.8 (O*C*H$_2$C), 97.5, 103.3 (*C*H, Ar), 125.3, 125.5 (*C*, Ar), 125.8, 126.7, 127.2, 127.6, 128.5 (*C*H, Ar), 129.0, 129.2, 138.4, 154.4, 155.0, 156.2, 157.2 (*C*, Ar). Found: C, 75.11; H, 7.54; C$_{66}$H$_{82}$O$_{11}$; requires C, 75.4; H, 7.86%. HRMS (ESI): calcd. for C$_{66}$H$_{83}$O$_{11}$H as [M + H]$^+$ 1051.5930; found 1051.5913.

5.5.2.2 Dibenzyloxy crown-6 resorcinarene (54)
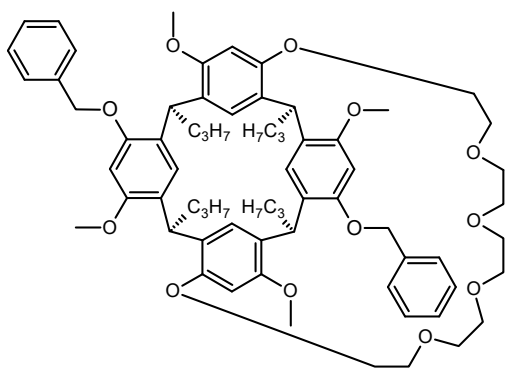
The general procedure for the synthesis of crown resorcinarenes was applied with **(46)** (0.503 g, 0.563 mmol), caesium carbonate (1.59 g, 4.88 mmol), anhydrous dimethylformamide (500 mL), and penta(ethylene glycol) ditosylate **(51)** (0.615 mL, 0.775 g, 1.42 mmol). Column chromatography (EtOAc – DCM 2:8) afforded the previously unreported product **(54)** (0.349 g, 57%) as a white solid: mp 181-182°C (CHCl$_3$/MeOH); ^{1}H NMR (CDCl$_3$) δ 0.90 (t, J = 7.2 Hz, 6 H, CH$_2$CH_3), 0.91 (t, J = 7.2 Hz, 6 H, CH$_2$CH_3), 1.15-1.54 (m, 8 H, CH_2CH$_3$), 1.66-2.02 (m, 8 H, CH_2CH), 3.17-3.33 (m, 6 H, CH_2O), 3.33-3.40 (m, 4 H, CH_2O) 3.41 (s, 6 H, OCH_3), 3.42-3.58 (m, 10 H, CH_2O), 3.86 (s, 6 H, OCH_3), 4.47-4.57, 4.63-4.73 (2m, 2 × 2 H, CHCH$_2$), 5.19, 5.22 (AB, J = 12.6 Hz, 4 H, CH_2Ph), 6.17, 6.43, 6.53, (3s, 3 × 2 H, ArH), 7.26 (overlapped with CHCl$_3$, 2 H, ArH), 7.32 (t, J = 7.3 Hz, 2 H, ArH), 7.40 (t, J = 7.4 Hz, 4 H, ArH), 7.57 (d, J = 7.3 Hz, 4 H, ArH); ^{1}H NMR (DMSO-d$_6$) δ 0.82 (t, J = 7.4 Hz, 6 H, CH$_2$CH_3), 0.84 (t, J = 7.4 Hz, 6 H, CH$_2$CH_3), 1.02-1.23, 1.16-1.40 (2m, 2 × 4 H, CH_2CH$_3$), 1.54-1.89 (m, 8 H, CH_2CH), 3.06-3.15 (m, 2 H, OCH_2), 3.20-3.46 (overlapped with HDO, m, 16 H, OCH$_2$), 3.35 (s, 6 H, OCH_3), 3.46-3.56 (m, 2 H, OCH_2), 3.83 (s, 6 H, OCH_3), 4.35-4.45, 4.47-4.58 (2m, 2 × 2 H, CHCH$_2$), 5.21, 5.24 (AB, J = 12.8 Hz, 4 H, CH_2Ph), 6.03, 6.47, 6.72, 7.09 (4s, 4 × 2 H, ArH), 7.29-7.37, 7.39-7.46, 7.53-7.60 (3m, 2 H, 4 H, 4 H, ArH); ^{13}C NMR (CDCl$_3$) δ 14.4, 14.5 (CH$_2$$CH_3$), 21.3, 21.4 ($CH_2CH_3$), 35.1, 35.2 ($CHCH_2$), 37.48, 37.49 ($CH_2$CH), 55.5, 56.2 (O$CH_3$), 70.3, 70.55, 70.64, 70.80, 70.84 (OCH$_2$C), 71.2 (OCH$_2$Ph), 97.5, 101.7 (CH, Ar), 124.9, 125.1 (C, Ar), 125.8, 126.5, 127.3, 127.6, 128.5 (CH, Ar), 129.1, 129.4, 138.5, 154.4, 154.9, 156.3, 156.9 (C, Ar). Found: C, 74.51; H, 7.86; C$_{68}$H$_{86}$O$_{12}$; requires C, 74.56; H, 7.91%.

5.5.2.3 Dibenzyloxy crown-7 resorcinarene (55)

The general procedure for the synthesis of crown resorcinarenes was applied with **(46)** (0.502 g, 0.562 mmol), caesium carbonate (2.50 g, 7.67 mmol), anhydrous dimethylformamide (250 mL), and hexa(ethylene glycol) ditosylate **(52)** (0.568 mL, 0.697 g, 1.18 mmol). After the removal of the dimethylformamide, brine (100 mL) was added to the residue, and extracted with dichloromethane (2×50 mL). The combined organic extracts were dried (MgSO$_4$), filtered, and solvent removed under reduced pressure to give a solid (0.836 g) as crude product. The crude product was filtered through a plug of silica using dichloromethane (10 mL), then EtOAc (250 mL), and the solvent was removed under reduced pressure to give a yellow oil (0.547 g), which was left open to air overnight. The yellow oil was triturated with methanol to give the previously unreported product **(55)** (0.452 g, 70 %) as a white crystalline solid: mp 136°C (CHCl$_3$/MeOH); ^{1}H NMR (CDCl$_3$) δ 0.88 (t, $J = 7.4$ Hz, 6 H, CH$_2$C*H$_3$*), 0.91 (t, $J = 7.4$ Hz, 6 H, CH$_2$C*H$_3$*), 1.18-1.53 (m, 8 H, C*H$_2$*CH$_3$), 1.64-2.01 (m, 8 H, C*H$_2$*CH), 3.06-3.14, 3.14-3.22 (2m, 2×2 H, C*H$_2$*O), 3.35-3.44 (m, 2 H, C*H$_2$*O), 3.40 (s, 6 H, OC*H$_3$*), 3.44-3.70 (m, 18 H, C*H$_2$*O), 3.85 (s, 6 H, OC*H$_3$*), 4.47-4.54, 4.60-4.70 (2m, 2×2 H, C*H*CH$_2$), 5.18, 5.22 (AB, $J = 12.4$ Hz, 4 H, C*H$_2$*Ph), 6.11, 6.34, 6.52, 7.23 (4s, 4×2 H, Ar*H*), 7.29-7.36, 7.37-7.43, 7.54-7.60 (3m, 2 H, 4 H, 4 H, Ar*H*); ^{1}H NMR (DMSO-d$_6$) δ 0.81 (t, $J = 7.3$ Hz, 6 H, CH$_2$C*H$_3$*), 0.85 (t, $J = 7.3$ Hz, 6 H, CH$_2$C*H$_3$*), 1.05-1.22, 1.21-1.39 (2m, 2×4 H, C*H$_2$*CH$_3$), 1.53-1.68, 1.65-1.88 (2m, 2 H, 6 H, C*H$_2$*CH), 3.05-3.20 (m, 4 H, OC*H$_2$*), 3.23-3.33 (overlapped with HDO, m, 2 H, OC*H$_2$*), 3.35 (s, 6 H, OC*H$_3$*), 3.35-3.47, 3.47-3.58 (m, 15 H, 3 H, OC*H$_2$*), 3.84 (s, 6 H, OC*H$_3$*), 4.33-4.44, 4.47-4.58 (2m, 2×2 H, C*H*CH$_2$), 5.20, 5.24 (AB, $J = 12.3$ Hz, 4 H, C*H$_2$*Ph), 6.01, 6.40, 6.72 , 7.08 (4s, 4×2 H, Ar*H*), 7.30-7.37, 7.39-7.46, 7.53-7.60 (3m, 2 H, 4 H, 4 H, Ar*H*); ^{13}C NMR (CDCl$_3$) δ 14.4, 14.5 (CH$_2$*C*H$_3$), 21.3, 21.4 (*C*H$_2$CH$_3$), 35.2, 35.4 (*C*HCH$_2$), 37.3, 37.4 (*C*H$_2$CH), 55.6, 56.1 (O*C*H$_3$), 70.1, 70.4, 70.8, 70.86, 70.87, 71.0 (O*C*H$_2$C), 71.2 (O*C*H$_2$Ph), 97.3, 101.5 (*C*H, Ar), 124.9, 125.0 (*C*, Ar), 125.8, 126.5, 127.2, 127.6, 128.5 (*C*H, Ar), 129.1, 129.5, 138.4, 154.3, 154.9, 156.4, 156.7 (*C*, Ar). Found: C, 72.54; H, 7.72; C$_{70}$H$_{90}$O$_{13}$.H$_2$O; requires C, 72.64; H, 8.01%.

5.5.3 General procedure of the reduction of benzyl ethers

To a solution of benzyloxy crown resorcinarene dissolved in tetrahydrofuran was added anhydrous ammonia, which was condensed with EtOAc/liquid nitrogen. Sodium metal was then added to the colourless solution till a dark blue colour persisted throughout the solution for 30 minutes. The dark blue reaction mixture was then quenched with a spatula tip of ammonium chloride, and the solvents were allowed to evaporate to dryness. The residue was taken up in water, and the undissolved solids were collected by filteration. The solids were washed off the funnel with dichloromethane, and the solvent was removed under reduced pressure. The resultant residue was placed in an oven (140°C) for 5 minutes to remove water, and furnish the dihydroxy crown resorcinarene as a beige solid in good purity.

5.5.3.1 Dihydroxy crown-5 resorcinarene (56)

The general procedure was applied with **(53)** (0.342 g, 0.352 mmol), tetrahydrofuran (10 mL), and anhydrous ammonia (~50 mL), to give the pure, previously unreported product **(56)** (0.288 g, 100%) as a white solid: mp 259-260 °C (CHCl$_3$/MeOH); IR 3380 cm^{-1} (OH phenol); ^{1}H NMR (CDCl$_3$) δ 0.91 (t, J = 7.4 Hz, 6 H, CH$_2$CH_3), 0.96 (t, J = 7.4 Hz, 6 H, CH$_2$CH_3), 1.12-1.37 (m, 8 H, CH_2CH$_3$), 1.38-1.48 (m, 2 H, CH_2O), 1.81-1.97 (m, 4 + 2 H, CH_2CH + CH_2O), 1.97-2.04 (m, 2 H, CH_2O), 2.05-2.17 (m, 4 H, CH_2CH), 2.60-2.69, 2.87-2.97, 3.53-3.62 (3m, 3 × 2 H, CH_2O), 3.72, 3.84 (2s, 2 × 6 H, OCH_3), 3.86-3.93 (m, 2 H, CH_2O), 4.15 (t, J = 8.0 Hz, 2 H, CHCH$_2$), 4.26-4.36 (m, 2 H, CH_2O), 4.81 (t, J = 8.0 Hz, 2 H, CHCH$_2$), 6.37, 6.44, 6.84, 7.46 (4s, 4 × 2 H, ArH); ^{1}H NMR (DMSO-d$_6$) δ 0.83 (t, J = 7.2 Hz, 6 H), 0.85 (t, J = 7.2 Hz, 6 H), 1.03-1.25, 1.16-1.41 (2m, 2 × 4 H, CH_2CH$_3$), 1.54-1.81 (m, 8 H, CH_2CH), 3.06-3.21, 3.21-3.29, 3.33-3.45 (3m, 4 H, 2 H, 6 H, OCH_2), 3.38 (s, 6 H, OCH_3), 3.45-3.56 (m, 4 H, OCH_2), 3.78 (s, 6 H, OCH_3), 4.27-4.39 (m, 4 H, CHCH$_2$), 5.84, 6.44, 6.63, 6.99 (4s, 4 × 2 H, ArH), 8.88 (s, 2 H, OH); ^{13}C NMR (CDCl$_3$) δ 14.2, 14.4 (CH$_2$$CH_3$), 20.9, 20.9 (CH$_2$$CH_3$), 32.1, 33.9 ($CHCH_2$), 36.7, 39.1 ($CH_2$CH), 55.6, 55.7 (O$CH_3$), 68.7, 69.6, 69.8, 70.5 (OCH$_2$), 98.0, 99.4, 123.5 (CH, Ar), 123.7, 124.6 (C, Ar), 126.3 (CH, Ar), 127.4, 127.6, 152.0, 154.1, 155.1, 155.8 (C, Ar). Found: C, 71.79; H, 8.26; C$_{52}$H$_{70}$O$_{11}$; requires C, 71.70; H, 8.10%.

5.5.3.2 Dihydroxy crown-6 resorcinarene (57)

The general procedure was applied with **(54)** (0.393 g, 0.359 mmol), tetrahydrofuran (30 mL), and anhydrous ammonia (~90 mL), to give **(57)** good purity as a beige solid (0.340 g, 100%). For analysis, the beige solid was recrystallised from hot ethanol to give the pure previously unreported product **(57)** as white crystals: mp 250-251 °C (CHCl$_3$/MeOH); IR 3428 cm^{-1} (OH phenol); ^{1}H NMR (CDCl$_3$) δ 0.92 (t, J = 7.4 Hz, 6 H, CH$_2$CH_3), 0.96 (t, J = 7.4 Hz, 6 H, CH$_2$CH_3), 1.14-1.36 (m, 8 + 2 H, CH_2CH$_3$ + CH_2O), 1.80-1.87 (m, 2 H, CH_2O), 1.88-1.99 (m, 4 H, CH_2CH), 1.99-2.20 (m, 4 + 2 H, CH_2CH + CH_2O), 2.67-2.78, 2.96-3.07, 3.12-3.23, 3.52-3.60, 3.67-3.74 (5m, 5 × 2 H, CH_2O), 3.75, 3.84 (2s, 2 × 6 H, OCH_3), 3.89-3.99 (m, 2 H, CH_2O), 4.10-4.25 (m, 2 + 2 H, CHCH$_2$ + CH_2O), 4.86 (t, J = 8.1 Hz, 2 H, CHCH$_2$), 6.24, 6.40 (2s, 4 × 2 H, ArH), 6.74 (br s, 2 H, OH), 6.89, 7.50 (2s, 4 × 2 H, ArH); ^{1}H NMR (DMSO-d$_6$) δ 0.83 (t, J = 7.4 Hz, 6 H, CH$_2$CH_3), 0.85 (t, J = 7.4 Hz, 6 H, CH$_2$CH_3), 1.01-1.42 (m, 8 H, CH_2CH$_3$), 1.52-1.81 (m , 8 H, CH_2CH), 3.08-3.17, 3.17-3.25, 3.32-3.52 (3m, 2 H, 2 H, 16 H, CH_2O), 3.35, 3.77 (2s, 2 × 6 H, OCH_3), 4.28-4.39 (m, 4 H, CHCH$_2$), 5.9, 6.4, 6.5, 7.0 (4s, 4 × 2 H, ArH), 8.9 (s, 2 H, OH); ^{13}C NMR (CDCl$_3$) δ 14.2, 14.5 (CH$_2$CH_3), 20.9, 21.0 (CH_2CH$_3$), 31.9, 33.8 (CHCH$_2$), 36.9, 39.3 (CH_2CH), 55.5, 55.6 (OCH_3), 67.9, 69.4, 69.5, 69.9, 71.1 (OCH_2), 95.9, 99.3 (CH, Ar), 123.2, 123.92 (C, Ar), 123.93, 126.2 (CH, Ar), 127.2, 127.4, 151.9, 154.2, 155.2, 156.0. ^{13}C NMR (DMSO-d$_6$) δ 14.0, 14.2 (CH$_2$CH_3), 20.88, 20.90 (CH_2CH$_3$), 34.6, 34.9 (CHCH$_2$), 36.3, 36.8 (CH_2CH), 55.2, 55.5 (OCH_3), 69.4, 69.9, 70.0, 70.4 (OCH_2), 98.5, 101.9 (CH, Ar), 123.2, 123.4, 125.07 (C, Ar), 125.13, 125.3 (CH, Ar), 125.8 (C, Ar), 152.3, 154.1, 155.9, 156.4 (C, Ar) (note some signals are coincident). Found: C, 69.47; H, 8.27; C$_{54}$H$_{74}$O$_{12}$.H$_2$O; requires C, 69.50; H, 8.21%.

5.5.3.3 Dihydroxy crown-7 resorcinarene (58)

The general procedure was applied with (0.572 g, 0.502 mmol), tetrahydrofuran (30 mL), and anhydrous ammonia (~90 mL), to give **(58)** in good purity as an off-white solid (0.470 g, 98%). For analysis, the off-white solid was triturated with acetone to give the pure previously unreported product **(58)** as a white solid: mp 209-210 °C (MeCN); IR 3397 cm^{-1} (OH phenol); ^{1}H NMR (CDCl$_3$) δ 0.90 (t, J = 7.3 Hz, 6 H, CH$_2$CH_3), 0.96 (t, J = 7.4 Hz, 6 H, CH$_2$CH_3), 1.10-1.37 (m, 8 H, CH_2CH$_3$), 1.80-1.99, 2.01-2.19 (2m, 2 × 4 H, CH_2CH), 2.30-2.40, 2.40-2.50, 2.59-2.74, 2.86- 2.96, 2.99-3.10, 3.27-3.38, 3.55-3.73, (7m, 2 H, 4 H, 4 H, 2 H, 2 H, 2 H, 4 H, CH_2O), 3.76, 3.82 (2s, 2 × 6 H, OCH_3), 3.84-3.93 (m, 2 H, CH_2O), 4.10-4.23 (m, 2 + 2 H, CH_2O + CHCH$_2$), 4.86 (t, J = 8.1 Hz, 2 H, CHCH$_2$), 6.34, 6.40, 6.92, 7.47 (4s, 4 × 2 H, ArH); ^{1}H NMR (DMSO-d$_6$) δ 0.84 (t, J = 7.3 Hz, 6 H, CH_2CH$_3$), 0.85 (t, J = 7.3 Hz, 6 H, CH_2CH$_3$), 1.04-1.23, 1.19-1.39 (2m, 2 × 4 H, CH_2CH$_3$), 1.51-1.65, 1.61-1.81 (2m, 2 H, 6 H, CH_2CH), 3.05-3.17 (m, 4 H, OCH_2), 3.22-3.35 (overlapped with HDO, m, OCH_2), 3.35 (s, 6 H, OCH_3), 3.38-3.54 (m, 20 H, OCH_2), 3.77 (s, 6 H, OCH_3), 4.26-4.40 (m, 4 H, CHCH$_2$), 5.85, 6.39, 6.43, 7.02 (4s, 4 × 2 H, ArH), 8.88 (s, 2 H, OH). ^{13}C NMR (CDCl$_3$) δ 14.2, 14.4 (CH$_2$$CH_3$), 20.9, 21.0 ($CH_2CH_3$), 31.8, 33.8 ($CHCH_2$), 36.8, 39.5 ($CH_2$CH), 55.5, 55.7 (O$CH_3$), 67.7, 69.7, 70.1, 70.2, 70.4, 70.7 (OCH$_2$), 96.7, 99.3 (CH, Ar), 123.2 (C, Ar), 124.1 (CH, Ar), 124.2 (C, Ar), 126.1 (CH, Ar), 127.3 , 152.0, 154.2, 155.5, 155.8 (C, Ar) (note some signals are coincident). Found: C, 68.77; H, 8.59; C$_{56}$H$_{78}$O$_{13}$.H$_2$O; requires C, 68.83; H, 8.25%.
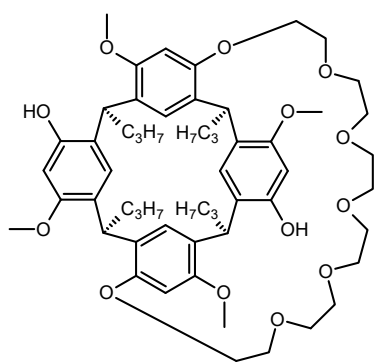
5.5.4 General procedure for the camphorsulfonylation of resorcinarenes

The synthetic procedure was adapted from that of **(48)** in **Section 4.3.4.1**. (1S)-(+)-camphorsulfonic acid (10 eq) and thionyl chloride were heated at reflux for 1 h. The thionyl chloride was evaporated under nitrogen to give a white crystalline solid, assumed to be (1S)-(+)-camphorsulfonyl chloride. To the freshly-prepared (1S)-(+)-camphorsulfonyl chloride was added resorcinarene (1 eq), dichloromethane and triethylamine (16 eq). The reaction mixture was stirred under nitrogen at room temperature for 1 h. The work up and purification is specific for each resorcinarene derivative.

5.5.4.1 Dicamphorsulfonate crown-5 resorcinarene (59a) and (59b)

The general procedure was applied with resorcinarene (1S)-(+)-camphorsulfonyl acid (57 mg, 0.245 mmol) and thionyl chloride (1 mL), crown-5 resorcinarene **(56)** (20 mg, 0.023 mmol), dichloromethane (3 mL) and triethylamine (0.052 mL, 0.072 mg, 0.709 mmol). The reaction mixture was stirred under nitrogen at room temperature for 40 minutes, then washed with dilute HCl (5 mL, 1 M). The layers separated, and the aqueous phase extracted with dichloromethane (5 mL). The combined yellow organic extracts were dried (CaCl$_2$) and solvent removed under reduced pressure to give an off-white solid (56 mg). The crude material was subjected to repeated preparative TLC (MeOH – DCM 2:98), with the same plate being developed two to three times, to give the previously unreported diastereomers **(59a)** (14 mg, 50%) and **(59b)** (13 mg, 48%).
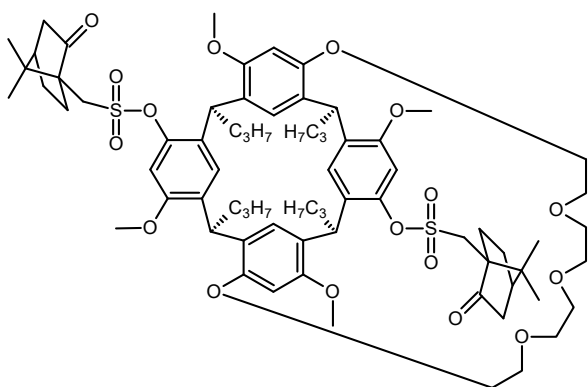
Crown-5 camphorsulfonate resorcinarene **(59a)**: IR 1749 cm^{-1} (C=O); ^{1}H NMR (CDCl$_3$) δ 0.90 (t, J = 7.3 Hz, 6 H, CH$_2$CH_3), 0.94 (s, 6 H, CH_3 camph), 0.96 (t, J = 7.3 Hz, 6 H, CH$_2$CH_3), 1.19-1.42 (m, 6 H, CH_2CH$_3$), 1.21 (s, 6 H, CH_3 camph), 1.42-1.55 (m, 2 + 2 H, CH_2CH$_3$ + CH_2 camph), 1.66-1.91 (m, 6 + 2 H, CH_2CH + CH_2 camph), 1.91-2.06 (m, 2 H, CH_2CH), 1.99 (d, J = 18.5 Hz, 2 H, CH_2 camph), 2.06-2.15 (m, 2 H, CH_2 camph), 2.13-2.19 (m, 2 H, CH camph), 2.44 (ddd, J = 18.5, 4.4, 3.4 Hz, 2 H, CH_2 camph), 2.57-2.72 (m, 2 H, CH_2 camph), 3.14-3.22, 3.22-3.33, 3.36-3.57 (3m, 2 H, 6 H, 8 H, CH_2O), 3.39 (s, 6 H, OCH_3), 3.41, 3.96 (AB, J = 14.9 Hz, 4 H, SCH_2), 3.91 (s, 6 H, OCH_3), 4.32-4.41, 4.51-4.59 (2m, 2 × 2 H, CHCH$_2$), 6.19, 6.56, 6.98, 7.19 (4s, 4 × 2 H, ArH); ^{13}C NMR (CDCl$_3$) δ 14.3, 14.5 (CH$_2$$CH_3$), 19.9, 20.2 (C$CH_3$, camph), 21.3, 21.4 ($CH_2CH_3$), 25.4, 27.1 ($CH_2$, camph), 35.2, 36.3 ($CHCH_2$), 37.07, 37.12 ($CH_2$CH), 42.7 ($CH_2$C=O, camph), 43.1 ($C$H, camph), 48.1 ($CCH_3$, camph), 49.1 (S$CH_2$, camph), 55.3, 56.2 (O$CH_3$), 58.4 ($C$C=O, camph), 70.5, 70.6, 71.1, 71.8 (OCH$_2$), 103.2, 103.6, (CH, Ar), 124.0, 124.7 (C, Ar), 125.3, 127.0 (CH, Ar), 131.1, 135.1, 145.4, 154.9, 156.5, 157.6 (C, Ar), 214.2 (C=O); [α]$_D$ +48.0 (c 1.02, CHCl$_3$); HRMS (ESI): calcd. for C$_{72}$H$_{102}$NO$_{17}$S$_2$ as [M + NH$_4$]$^+$ 1316.6584; found 1316.6527 (main peak); and calcd. for C$_{72}$H$_{99}$O$_{17}$S$_2$ as [M + H]$^+$ 1299.6318; found 1299.6270.

Crown-5 camphorsulfonate resorcinarene **(59b)**: IR 1748 cm^{-1} (C=O); ^{1}H NMR (CDCl$_3$) δ 0.90 (t, J = 7.3 Hz, 6 H, CH$_2$C*H*$_3$), 0.934 (s, 6 H, C*H*$_3$ camph), 0.95 (t, J = 7.3 Hz, 6 H, CH$_2$C*H*$_3$), 1.19-1.41 (m, 6 H, C*H*$_2$CH$_3$), 1.20 (s, 6 H, C*H*$_3$ camph), 1.41-1.54 (m, 2 + 2 H, C*H*$_2$CH$_3$ + C*H*$_2$ camph), 1.66-1.90 (m, 6 + 2 H, C*H*$_2$CH + C*H*$_2$ camph), 1.90-2.03 (m, 2 H, C*H*$_2$CH), 1.99 (d, J = 18.5 Hz, 2 H, C*H*$_2$ camph), 2.06-2.15 (m, 2 H, C*H*$_2$ camph), 2.13-2.19 (m, 2 H, C*H* camph), 2.43 (ddd, J = 18.5, 4.4, 3.4 Hz, 2 H, C*H*$_2$ camph), 2.60-2.71 (m, 2 H, C*H*$_2$ camph), 3.17-3.34 (m, 8 H, C*H*$_2$O), 3.35, 4.01 (AB, J = 14.9 Hz, 4 H, SC*H*$_2$), 3.36-3.43 (m, 2 H, C*H*$_2$O), 3.42 (s, 6 H, OC*H*$_3$), 3.43-3.58 (m, 6 H, C*H*$_2$O), 3.91 (s, 6 H, OC*H*$_3$), 4.32-4.40, 4.51-4.59 (2m, 2 × 2 H, C*H*CH$_2$), 6.17, 6.61, 7.00, 7.17 (4s, 4 × 2 H, Ar*H*); ^{13}C NMR (CDCl$_3$) δ 14.3, 14.5 (CH$_2$*C*H$_3$), 19.9, 20.2 (C*C*H$_3$, camph), 21.3, 21.4 (*C*H$_2$CH$_3$), 25.5, 27.1 (*C*H$_2$, camph), 35.4, 36.4 (*C*HCH$_2$), 36.9, 37.1 (*C*H$_2$CH), 42.7 (*C*H$_2$C=O, camph), 43.0 (*C*H, camph), 48.1 (*C*CH$_3$, camph), 48.8 (S*C*H$_2$, camph), 55.2, 56.2 (O*C*H$_3$), 58.4 (*C*C=O, camph), 70.5, 70.6, 71.2, 72.1 (O*C*H$_2$), 103.3, 103.7, (*C*H, Ar), 123.6, 124.7 (*C*, Ar), 125.4, 126.9 (*C*H, Ar), 130.9, 135.3, 145.5, 154.9, 156.6, 157.8 (*C*, Ar), 214.2 (C=O); [α]$_D$ -11.8 (*c* 1.02, CHCl$_3$); HRMS (ESI): calcd. for C$_{72}$H$_{102}$NO$_{17}$S$_2$ as [M + NH$_4$]$^+$ 1316.6584; found 1316.6526 (main peak); and calcd. for C$_{72}$H$_{99}$O$_{17}$S$_2$ as [M + H]$^+$ 1299.6318; found 1299.6258.

5.5.4.2 Dicamphorsulfonate crown-6 resorcinarene (60a) and (60b)

The general camphorsulonylation procedure was applied with (1*S*)-(+)-camphorsulfonyl acid (0.258 g, 1.11 mmol) and thionyl chloride (3 mL), crown-6 resorcinarene **(57)** (0.100 g, 0.109 mmol), dichloromethane (7 mL) and triethylamine (0.244 mL, 0.177 g, 1.75 mmol). The reaction mixture was stirred under nitrogen at room temperature for 50 minutes, then washed with dilute HCl (10 mL, 1 M). The layers separated, and the aqueous phase extracted with dichloromethane (5 mL). The combined yellow organic extracts were dried (CaCl$_2$) and solvent removed under reduced pressure to give an off-white solid (0.240 g). The crude material was subjected to column chromatography (silica: 23 × 25 mm). The impurity was first eluted with EtOAc – petroleum spirits (25 mL, 50:50), then the diastereomer mixture was eluted

with EtOAc (75 mL, 100%). The EtOAc was evaporated to give the diastereomer mixture as an off-white solid (0.143 g). This material was subjected to preparative TLC (MeOH – DCM 2:98), with the same plate being developed three times, to give the previously unreported diastereomers **(60a)** (0.058 g, 40%) and **(60b)** (0.057 g, 39%), along with unseparated diastereomer mixture (0.009 g, 6%).

Crown-6 camphorsulfonate resorcinarene **(60a)**: IR 1747 cm^{-1} (C=O); ^{1}H NMR (CDCl$_3$) δ 0.91 (t, J = 7.3 Hz, 6 H, CH$_2$CH_3), 0.94 (s, 6 H, CH_3 camph), 0.96 (t, J = 7.3 Hz, 6 H, CH$_2$CH_3), 1.21 (s, 6 H, CH_3 camph), 1.22-1.44 (m, 6 H, CH_2CH$_3$), 1.43-1.57 (m, 2 + 2 H, CH_2CH$_3$ + CH_2 camph), 1.66-1.92 (m, 6 + 2 H, CH_2CH + CH_2 camph), 1.92-2.05 (m, 2 H, CH_2CH), 1.99 (d, J = 18.4 Hz, 2 H, CH_2 camph), 2.06-2.16 (m, 2 H, CH_2 camph), 2.12-2.20 (m, 2 H, CH camph), 2.44 (ddd, J = 18.4, 4.4, 3.4 Hz, 2 H, CH_2 camph), 2.59-2.72 (m, 2 H, CH_2 camph), 3.14-3.46 (m, 10 H, CH_2O), 3.37 (s, 6 H, OCH_3), 3.42, 3.97 (AB, J = 14.9 Hz, 4 H, SCH_2), 3.46-3.59 (m, 10 H, CH_2O), 3.91 (s, 6 H, OCH_3), 4.31-4.40, 4.47-4.58 (2m, 2 × 2 H, CHCH$_2$), 6.16, 6.42, 6.95, 7.19 (4s, 4 × 2 H, ArH); ^{13}C NMR (CDCl$_3$) δ 14.4, 14.5 (CH$_2$$CH_3$), 19.9, 20.2 (C$CH_3$, camph), 21.2, 21.4 (C$H_2CH_3$), 25.4, 27.1 ($CH_2$, camph), 35.1, 36.3 ($CHCH_2$), 37.06, 37.11 ($CH_2$CH), 42.7 ($CH_2$C=O, camph), 43.1 ($C$H, camph), 48.1 ($CCH_3$, camph), 49.2 (S$CH_2$, camph), 55.5, 56.2 (O$CH_3$), 58.4 ($C$C=O, camph), 70.2, 70.4, 70.6, 70.8, 70.8 (OCH$_2$), 101.1, 103.5 (CH, Ar), 123.5, 124.0 (C, Ar), 125.2, 126.8 (CH, Ar), 131.2, 135.3, 145.4, 154.8, 156.6, 157.2 (C, Ar), 214.2 (C=O); $[\alpha]_D$ +46.5 (c 1.11, CHCl$_3$); HRMS (ESI): calcd. for C$_{74}$H$_{103}$O$_{18}$S$_2$ as [M + H]$^+$ 1343.6580; found 1343.6564.
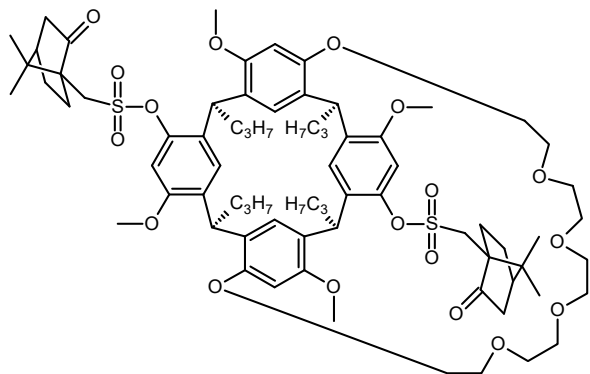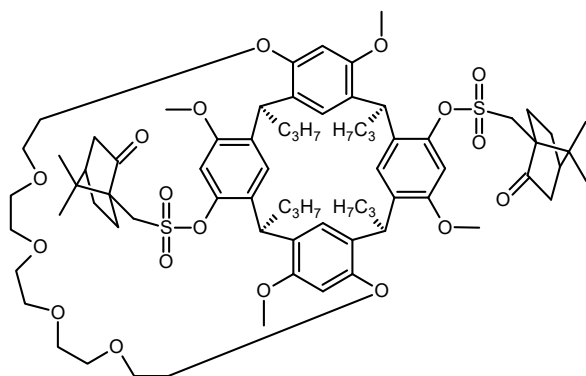
Crown-6 camphorsulfonate resorcinarene **(60b)**: IR 1748 cm^{-1} (C=O); ^{1}H NMR (CDCl$_3$) δ 0.90 (t, J = 7.3 Hz, 6 H, CH$_2$CH_3), 0.94 (s, 6 H, CH_3 camph), 0.95 (t, J = 7.3 Hz, 6 H, CH$_2$CH_3), 1.20 (s, 6 H, CH_3 camph), 1.21-1.43 (m, 6 H, CH_2CH$_3$), 1.43-1.57 (m, 2 + 2 H, CH_2CH$_3$ + CH_2 camph), 1.63-1.91 (m, 6 + 2 H, CH_2CH + CH_2 camph), 1.91-2.04 (m, 2 H, CH_2CH), 1.98 (d, J = 18.5 Hz, 2 H, CH_2 camph), 2.05-2.13 (m, 2 H, CH_2 camph), 2.13-2.19 (m, 2 H, CH camph), 2.43 (ddd, J = 18.5, 4.7, 3.4 Hz, 2 H, CH_2 camph), 2.59-2.71 (m, 2 H, CH_2 camph), 3.18-3.34 (m, 6 H, CH_2O), 3.36, 4.02 (AB, J = 14.9 Hz, 4 H, SCH_2), 3.39 (s, 6 H, OCH_3), 3.40-3.46, 3.46-3.60 (2m, 4 H, 10 H, CH_2O), 3.90 (s, 6 H, OCH_3), 4.31-4.40, 4.48-4.57 (2m, 2 × 2 H, CHCH$_2$), 6.14, 6.45, 6.97, 7.17 (4s, 4 × 2 H, ArH); ^{13}C NMR (CDCl$_3$) δ 14.4, 14.5 (CH$_2$CH_3), 19.9, 20.2 (CCH_3, camph), 21.3, 21.4 (CH_2CH$_3$), 25.5, 27.1 (CH_2, camph), 35.2, 36.3 (CHCH$_2$), 37.0, 37.1 (CH_2CH), 42.7 (CH_2C=O, camph), 43.1 (CH, camph), 48.1 (CCH$_3$, camph), 49.0 (SCH_2, camph), 55.4, 56.2 (OCH_3), 58.4 (CC=O, camph), 70.3, 70.58, 70.62, 70.7, 70.8 (OCH_2), 101.2, 103.6 (CH, Ar), 123.2, 123.9 (C, Ar), 125.2, 126.7 (CH, Ar), 131.1, 135.3, 145.4, 154.9, 156.6, 157.3 (C, Ar), 214.2 (C=O); $[\alpha]_D$ -16.5 (c 1.10, CHCl$_3$); HRMS (ESI): calcd. for C$_{74}$H$_{103}$O$_{18}$S$_2$ as [M + H]$^+$ 1343.6580; found 1343.6565.

5.5.4.3 Dicamphorsulfonate crown-7 resorcinarene (61a) and (61b)

The general procedure was applied with resorcinarene (1S)-(+)-camphorsulfonyl acid (0.050 g, 0.215 mmol) and thionyl chloride (1 mL), crown-7 resorcinarene **(58)** (0.020 g, 0.021 mmol), dichloromethane (3 mL) and triethylamine (0.047 mL, 0.034 g, 0.337 mmol). The reaction mixture was stirred under nitrogen at room temperature for 1 hour, then washed with dilute HCl (5 mL, 1 M). The layers separated, and the aqueous phase extracted with dichloromethane (5 mL). The combined yellow organic extracts were dried (CaCl$_2$) and solvent removed under reduced pressure to give an off-white solid (0.046 g). The crude material was subjected to column chromatography (silica: 23 × 25 mm). The impurity was first eluted with acetone – DCM (20 mL, 10:90), then the diastereomer mixture was eluted with acetone – DCM (60 mL, 30:70). The solvent was removed under reduced pressure to give the diastereomer mixture as a solid (0.027

206

g). This material was subjected to repeated preparative TLC (MeOH – DCM 2:98), with the same plate being developed two to three times, to give the previously unreported diastereomers **(61a)** (9.7 mg, 34%), **(61b)** (6.3 g, 22%), along with unseparated diastereomer mixture (4.2 mg, 15%).
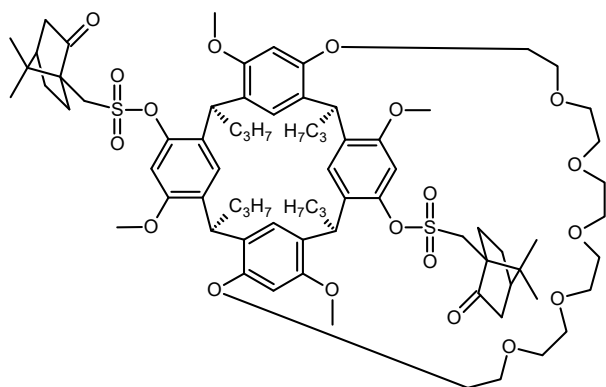
Crown-7 camphorsulfonate resorcinarene **(61a)**: IR 1748 cm^{-1} (C=O); ^{1}H NMR (CDCl$_3$) δ 0.92 (t, J = 7.3 Hz, 6 H, CH$_2$CH_3), 0.94 (s, 6 H, CH_3 camph), 0.95 (t, J = 7.3 Hz, 6 H, CH$_2$CH_3), 1.21 (s, 6 H, CH_3 camph), 1.22-1.43 (m, 6 H, CH_2CH$_3$), 1.43-1.56 (m, 2 + 2 H, CH_2CH$_3$ + CH_2 camph), 1.60-1.91 (m, 6 + 2 H, CH_2CH + CH_2 camph), 1.91-2.06 (m, 2 H, CH_2CH), 1.98 (d, J = 18.5 Hz, 2 H, CH_2 camph), 2.06-2.16 (m, 2 H, CH_2 camph), 2.12-2.20 (m, 2 H, CH camph), 2.44 (ddd, J = 18.5, 4.5, 3.4 Hz, 2 H, CH_2 camph), 2.59-2.71 (m, 2 H, CH_2 camph), 3.06-3.16, 3.17-3.27 (2m, 2 H, 2 H, CH_2O), 3.36 (s, 6 H, OCH_3), 3.37-3.46 (m, 2 H, CH_2O), 3.42, 3.97 (AB, J = 14.9 Hz, 4 H, SCH_2), 3.46-3.63 (2m, 4 H, 18 H, CH_2O), 3.91 (s, 6 H, OCH_3), 4.31-4.40, 4.48-4.57 (2m, 2 × 2 H, CHCH$_2$), 6.12, 6.31, 6.95, 7.18 (4s, 4 × 2 H, ArH); ^{13}C NMR (CDCl$_3$) δ 14.4, 14.5 (CH$_2$CH_3), 19.9, 20.1 (CCH$_3$, camph), 21.2, 21.4 (CH_2CH$_3$), 25.4, 27.1 (CH_2, camph), 35.2, 36.3 (CHCH$_2$), 37.0, 37.1 (CH_2CH), 42.7 (CH_2C=O, camph), 43.1 (CH, camph), 48.1 (CCH$_3$, camph), 49.2 (SCH_2, camph), 55.5, 56.1 (OCH_3), 58.4 (CC=O, camph), 70.0, 70.2, 70.8, 70.88, 70.95, 71.1 (OCH_2), 100.8, 103.5 (CH, Ar), 123.3, 124.3 (C, Ar), 125.3, 126.8 (CH, Ar), 131.2, 135.4, 145.3, 154.8, 156.7, 157.0 (C, Ar), 214.2 (C=O); [α]$_D$ +56.6 (c 0.99, CHCl$_3$); HRMS (ESI): calcd. for C$_{76}$H$_{110}$NO$_{19}$S$_2$ as [M + NH$_4$]$^+$ 1404.7108; found 1404.7069 (main peak); and calcd. for C$_{76}$H$_{107}$O$_{19}$S$_2$ as [M + H]$^+$ 1387.6842; found 1387.6809.
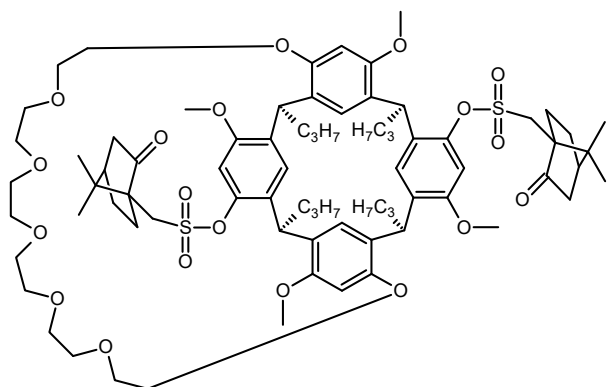
Crown-7 camphorsulfonate resorcinarene **(61b)**: IR 1748 cm^{-1} (C=O); ^{1}H NMR (CDCl$_3$) δ 0.91 (t, J = 7.3 Hz, 6 H, CH$_2$CH_3), 0.94 (s, 6 H, CH_3 camph), 0.94 (t, J = 7.3 Hz, 6 H, CH$_2$CH_3), 1.20 (s, 6 H, CH_3 camph), 1.22-1.44 (m, 6 H, CH_2CH$_3$), 1.44-1.56 (m, 2 + 2 H, CH_2CH$_3$ + CH_2 camph), 1.60-1.89 (m, 6 + 2 H, CH_2CH + CH_2 camph), 1.89-2.03 (m, 2 H, CH_2CH), 1.98 (d, J = 18.5 Hz, 2 H, CH_2 camph), 2.03-2.16 (m, 2 H, CH_2 camph), 2.12-2.20 (m, 2 H, CH camph), 2.44 (ddd, J = 18.5, 4.4, 3.4 Hz, 2 H, CH_2 camph), 2.59-2.71 (m, 2 H, CH_2 camph), 3.06-3.15, 3.19-3.27 (2m, 2 H, 2 H, CH_2O), 3.37, 4.01 (AB, J = 14.9 Hz, 4 H, SCH_2), 3.38 (s, 6 H, OCH_3), 3.39-3.47, 3.47-3.66 (2m, 2 H, 18 H, CH_2O), 3.90 (s, 6 H, OCH_3), 4.31-4.40, 4.48-4.57 (2m, 2 × 2 H, CHCH$_2$), 6.11, 6.33, 6.97, 7.17 (4s, 4 × 2 H, ArH); ^{13}C NMR (CDCl$_3$) δ 14.4, 14.5 (CH$_2$$CH_3$), 19.9, 20.1 ($CCH_3$, camph), 21.2, 21.4 ($CH_2CH_3$), 25.5, 27.1 ($CH_2$, camph), 35.3, 36.4 ($CHCH_2$), 36.9, 37.2 ($CH_2$CH), 42.7 ($CH_2$C=O, camph), 43.1 ($C$H, camph), 48.1 ($CCH_3$, camph), 49.1 (S$CH_2$, camph), 55.4, 56.1 (O$CH_3$), 58.4 ($C$C=O, camph), 70.1, 70.3, 70.8, 70.9, 71.0, 71.1 (OCH$_2$), 100.8, 103.6 (CH, Ar), 123.0, 124.2 (C, Ar), 125.4, 126.7 (CH, Ar), 131.0, 135.5, 145.3, 154.8, 156.6, 157.1 (C, Ar), 214.1 (C=O); [α]$_D$ -22.1 (c 0.99, CHCl$_3$); HRMS (ESI): calcd. for C$_{76}$H$_{110}$NO$_{19}$S$_2$ as [M + NH$_4$]$^+$ 1404.7108; found 1404.7064 (main peak); and calcd. for C$_{76}$H$_{107}$O$_{19}$S$_2$ as [M + H]$^+$ 1387.6842; found 1387.6790.

5.5.4.4 Dicamphorsulfonate diTBDMS resorcinarene diastereomeric mixture (62)

Diastereomeric mixture

The general camphorsulonylation procedure was applied with distal-TBDMS resorcinarene **(34)** (0.052 g, 0.0552 mmol), freshly-prepared (1*S*)-(+)-camphorsulfonyl chloride (0.226 g, 0.901 mmol), triethylamine (0.185 mL, 0.132 g, 1.33 mmol), and dichloromethane (6 mL). The clear, slightly yellow reaction mixture was stirred under nitrogen at room temperature for 1 h. The reaction mixture was then washed with dilute HCl (10 mL, 1 M), and the aqueous layer was extracted with dichloromethane (5 mL). The combined organic extracts were dried (MgSO4) and solvent removed under reduced pressure to give a glassy yellow solid (0.180 g) as crude product. A portion (0.119 g) of the crude product was subjected to preparative TLC (EtOAc – toluene 1:9) to give the purified diastereomic mixture **(62)** as a solid (0.025 g, 50%). The diastereomers could not be separated. ^{1}H NMR (only key signals quoted, CDCl3) δ -0.12, -0.11, 0.10, 0.11 (4s, 4 × 6 H, Si(C*H*3)2), 1.17, 1.19 (2s, 2 × 6 H, C*H*3 camph), 1.965 (d, *J* = 18.5 Hz, 2 H, C*H*2 camph), 1.968 (d, *J* = 18.5 Hz, 2 H, C*H*2 camph), 2.42 (apparent ddd, 4 H, C*H*2 camph), 2.54-2.66 (m, 4 H, C*H*2 camph), 3.27, 3.30, 3.84, 3.85 (2AB, *J* = 15.0 Hz, 2 × 4 H, SC*H*2), 3.94, 3.50, 3.71, 3.72 (4s, 4 × 6 H, OC*H*3), 4.36-4.47, 4.49-4.61 (2m, 2 × 4 H, C*H*CH2), 6.15, 6.17, 6.63, 6.67 (4s, 4 × 2 H, Ar*H*), 6.70-6.80 (m, 2 H, Ar*H*), 6.83, 6.85 (2s, 2 × 2 H, Ar*H*).

5.5.4.5 Attempted synthesis of dicamphorsulfonate resorcinarene

Crude resorcinarene diastreomer mixture **(62)** (0.196 g) was combined with caesium carbonate (0.068 g, 0.209 mmol) and non-anhydrous dimethylformamide (4 mL), then heated at 90°C open to air. After 45 minutes, the reaction was diluted with brine (20 mL) and extracted with diethyl ether till the organic extract was colourless and the aqueous layer was a slight yellow colour. The combined organic extracts were washed with brine, dried (MgSO4), filtered, and solvent removed under reduced pressure to give a brown oily residue (0.147 g). ^{1}H NMR spectroscopy indicated a complex mixture of resorcinarenes was obtained.

5.5.4.6 Dicamphorsulfonate dibenzyloxyresorcinarene diastereomeric mixture

The general camphorsulfonylation procedure was applied with distal-benzyloxyresorcinarene **(46)** (0.044 g, 0.0493 mmol), freshly-prepared (1*S*)-(+)-camphorsulfonyl chloride (0.122 g, 0.487 mmol), triethylamine (0.110 mL, 0.0798 g, 0.789 mmol), and dichloromethane (3 mL). The clear, slightly yellow reaction mixture was stirred under nitrogen at room temperature. After 1 hour 15 minutes, the reaction mixture was washed with dilute HCl (20 mL, 1 M). The layers were separated, and the aqueous phase was extracted with dichloromethane (5 mL). The combined yellow organic extracts were dried (MgSO$_4$) and solvent removed under reduced pressure to give a colourless glassy solid (0.112 g) as the crude product. The crude product was subjected to preparative TLC (THF – petroleum spirits 3:7) to give the purified diastereomers as a crystalline white solid (0.051 g, 78%). The diastereomers could not be separated. ^{1}H NMR (only key signals quoted, CDCl$_3$) δ 1.20, 1.22 (2s, 2 × 6 H, C*H*$_3$ camph), 1.98 (d, *J* = 18.5 Hz, 2 H, C*H*$_2$ camph), 1.99 (d, *J* = 18.5 Hz, 2 H, C*H*$_2$ camph), 2.44 (apparent ddd, 4 H, C*H*$_2$ camph), 2.60-2.72 (m, 4 H, C*H*$_2$ camph), 3.33, 3.34 (2s, 2 × 6 H, OC*H*$_3$), 3.38, 3.40, 3.97 , 4.01 (2AB, *J* = 14.9 Hz, 2 × 4 H, SC*H*$_2$), 3.559, 3.562 (2s, 2 × 6 H, OC*H*$_3$), 4.40-4.49, 4.49-4.58 (2m, 2 × 4 H, C*H*CH$_2$), 6.238, 6.244, 6.29, 6.34, 6.91, 6.93 (6s, 6 × 2 H, Ar*H*), 6.96-7.04 (m, 8 H, Ar*H*), 7.09, 7.10 (2s, 2 × 2 H, Ar*H*), 7.24-7.31 (m, 4 H, Ar*H*), 7.32-7.38 (m, 8 H, Ar*H*).

5.5.5 Bis-crown resorcinarenes

5.5.5.1 Bis-crown-5 resorcinarene (63)

The general procedure for the synthesis of crown resorcinarenes was applied with resorcinarene **(1)** (0.419 g, 0.588 mmol), caesium carbonate (1.84 g, 5.65 mmol), tetra(ethylene glycol) ditosylate **(50)** (0.595 mL, 0.739 g, 1.47 mmol), and anhydrous dimethylformamide (30 mL). After stirring at 90°C under nitrogen for 3 days, the solvent was removed under reduced pressure, and the

brown residue solid was taken up in water (50 mL) and filtered. The filtered solid was then purified by column chromatography (EtOAc 100%) to give the previously unreported product **(63)** as a white-yellow solid (0.138 g, 23%). For analysis, the white-yellow solid was recrystallised from CHCl₃/MeOH to give pure **(63)** as white crystals: mp 159-177 °C (CHCl₃/MeOH); ^{1}H NMR (CDCl₃) δ 0.89 (t, J = 7.3 Hz, 6 H, CH₂CH_3), 0.92 (t, J = 7.3 Hz, 6 H, CH₂CH_3), 1.16-1.52 (m, 8 H, CH_2CH₃), 1.65-1.97 (m, 8 H, CH_2CH), 3.08-3.18, 3.26-3.50 (m, 2 H, 6 H, CH_2O), 3.39 (s, 6 H, OCH_3), 3.50-3.79 (m, 12 H, CH_2O), 3.79 (t, J = 4.1 Hz, 4 H, CH_2O), 3.88-4.02 (m, 4 H, CH_2O), 3.92 (s, 6 H, OCH_3), 4.27 (dt, J = 12.0, 4.1 Hz, 2 H, CH_2O), 4.38-4.59 (m, 2 + 4 H, CH_2O + CHCH₂), 5.92, 6.08, 6.73, 7.18 (4s, 4 × 2 H, Ar); ^{13}C NMR (CDCl₃) δ 14.4, 14.5 (CH₂CH₃), 21.5 (CH₂CH₃), 35.7, 35.8 (CHCH₂), 36.7, 37.2 (CH₂CH), 55.7, 56.0 (OCH₃), 69.0, 69.5, 70.1, 70.8, 70.9, 71.1, 71.5, 71.7 (OCH₂), 97.8, 98.5 (CH, Ar), 123.0, 123.9 (C, Ar), 126.1, 126.8 (CH, Ar), 128.5, 129.2, 154.4, 155.0, 156.0, 156.5 (C, Ar) (note some signals are coincident); HRMS (ESI): calcd. for C₆₀H₈₈NO₁₄ as [M + NH₄]⁺ 1046.6199; found 1046.6178 (main peak); and calc. for C₆₀H₈₅O₁₄ as [M + H]⁺ 1029.5934; found 1029.5901.

5.5.5.2 Bis-crown-6 resorcinarene (64)

The general procedure for the synthesis of crown resorcinarenes was applied with resorcinarene **(1)** (0.451 g, 0.633 mmol), caesium carbonate (1.64 g, 5.03 mmol), penta(ethylene glycol) ditosylate **(51)** (0.686 mL, 0.864 g, 1.58 mmol), and anhydrous dimethylformamide (40 mL). After stirring at 90°C under nitrogen for 3 days, the solvent was removed under reduced pressure, and the brown residue solid was taken up in water (50 mL) and filtered. The filtered solid was then purified by column chromatography (acetone – DCM 40:60) to give the previously unreported product **(64)** as a glassy yellow solid (0.061 g, 8.6%). For analysis, the glassy yellow solid was recrystallised from CHCl₃/MeOH to give pure **(64)** as large colourless crystals: mp 125-126 °C (CHCl₃/MeOH); ^{1}H NMR (CDCl₃) δ 0.91 (t, J = 7.3 Hz, 6 H, CH₂CH_3), 0.92 (t, J = 7.3 Hz, 6 H, CH₂CH_3), 1.17-1.35, 1.35-1.51 (2m, 2 × 4 H, CH_2CH₃), 1.66-1.81, 1.81-1.95 (2m, 2 × 4 H, CH_2CH), 3.15-3.24, 3.25-3.39 (m, 2 H, 6 H, CH_2O), 3.40 (s, 6 H, OCH_3), 3.42-3.50 (m, 2 H, CH_2O), 3.56-3.61 (m, 4 H, CH_2O), 3.61-3.80 (m,

16 H, CH_2O), 3.91 (s, 6 H, OCH_3), 3.93-4.02 (m, 6 H, CH_2O), 4.22 (dt, J = 10.7, 3.9 Hz, 2 H, CH_2O), 4.32-4.40 (m, 2 H, CH_2O), 4.40-4.53 (m, 4 H, CHCH_2), 5.94, 6.09, 6.58, 7.18 (4s, 4 × 2 H, ArH); ^{13}C NMR (CDCl$_3$) δ 14.4, 14.5 (CH$_2$$CH_3$), 21.4 ($CH_2CH_3$), 35.6, 35.7 ($CHCH_2$), 36.6, 37.0 ($CH_2$CH), 55.7, 55.8 (O$CH_3$), 69.2, 69.9, 70.2, 70.4, 70.88, 70.89, 71.1, 71.3, 71.40, 71.43 (OCH$_2$), 97.0, 98.4 (CH, Ar), 123.0, 123.5 (C, Ar), 126.1, 126.5 (CH, Ar), 128.7, 129.2, 154.6, 155.0, 156.1, 156.6 (C, Ar) (note some signals are coincident); HRMS (ESI): calcd. for C$_{64}$H$_{92}$O$_{16}$ as [M]$^+$ 1116.6380; found 1116.6344; and calc. for C$_{64}$H$_{93}$O$_{16}$ as [M + H]$^+$ 1117.6458; found 1117.6406.

5.5.5.3 Bis-crown-7 resorcinarene (65)
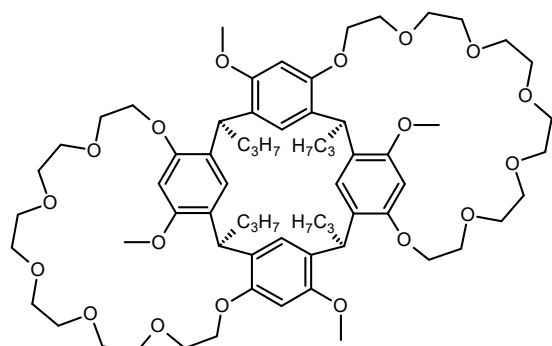
The general procedure for the synthesis of crown resorcinarenes was applied with resorcinarene **(1)** (0.310 g, 0.435 mmol), caesium carbonate (1.14 g, 3.49 mmol), hexa(ethylene glycol) ditosylate **(52)** (0.517 mL, 0.634 g, 1.07 mmol), and anhydrous dimethylformamide (30 mL).

After stirring at 90°C under nitrogen for 3 days, the solvent was removed under reduced pressure, and the brown residue solid was taken up in dichloromethane and filtered. The filtrate was then subjected to column chromatography (acetone – DCM 50:50), followed by preparative TLC (acetone – DCM 40:60). The mostly-pure product was then recrystallised from CHCl$_3$/MeOH to give the pure, previously unreported product **(65)** as off-white crystals (0.066 g). The mother liquor from the recrystallisation was subjected to preparative TLC (acetone – DCM 40:60) to recover more pure product (0.018 g), giving total **(65)** (0.084 g, 16%): mp 132 °C (CHCl$_3$/MeOH); ^{1}H NMR (CDCl$_3$) δ 0.90 (t, J = 7.3 Hz, 6 H, CH$_2$CH_3), 0.91 (t, J = 7.3 Hz, 6 H, CH$_2$CH_3), 1.18-1.35, 1.33-1.50 (2m, 2 × 4 H, CH_2CH$_3$), 1.64-1.80, 1.80-1.95 (2m, 2 × 4 H, CH_2CH), 3.11-3.24, 3.30-3.48 (m, 4 H, 6 H, CH_2O), 3.40 (s, 6 H, OCH_3), 3.56 (apparent t, 4 H, CH_2O), 3.59-3.81 (m, 25 H, CH_2O), 3.87-3.96 (m, 3 H, CH_2O), 3.89 (s, 6 H, OCH_3), 3.97-4.05 (m, 2 H, CH_2O), 4.15-4.24, 4.24-33 (2m, 2 H, 2 H, CH_2O), 4.39-4.46, 4.46-4.53 (2m, 2 × 2 H CHCH$_2$), 5.96, 6.09, 6.54, 7.16 (4s, 4 × 2 H, ArH); ^{13}C NMR (CDCl$_3$) δ 14.4, 14.5 (CH$_2$$CH_3$), 21.41, 21.44 ($CH_2CH_3$), 35.5, 35.6 ($CHCH_2$), 36.8, 37.1 ($CH_2$CH), 55.80, 55.84 (O$CH_3$), 69.0, 69.6, 69.9, 70.4, 70.7,

70.78, 70.81, 70.86, 70.95, 71.0, 71.08, 71.13 (OCH_2), 97.1, 98.5 (CH, Ar), 123.5, 123.8 (C, Ar), 126.1, 126.4 (CH, Ar), 128.8, 129.4, 154.6, 155.1, 156.1, 156.5 (C, Ar); HRMS (ESI): calcd. for $C_{88}H_{104}NO_{18}$ as $[M + NH_4]^+$ 1222.7248; found 1222.7235.

5.5.6 General procedure for the hydrolysis of camphorsulfonate resorcinarene diastereomers

The procedure by McIldowie and co-workers served as a guide.[66] Diastereomerically-pure camphorsulfonate resorcinarene (1 eq) was combined with sodium hydroxide (56 eq), ethanol, and water. The resultant clear solution was heated at reflux under nitrogen overnight. The ethanol was evaporated, and the white residue was acidified with dilute HCl (10 mL, 1 M), then extracted with dichloromethane (3 × 3 mL). The combined organic extracts were dried (MgSO$_4$) and solvent evaporated to give the enantio-pure resorcinarene.

5.5.6.1 Enantio-pure crown-6 resorcinarene (57a)

The general procedure was applied with resorcinarene **(60a)** (0.058 g, 0.0432 mmol), sodium hydroxide (0.097 g, 2.43 mmol), ethanol (5 mL) and water (2 mL) to give the previously unreported product **(57a)** (0.041 g, 100%) as an off-white solid: $[\alpha]_D$ -20.2 (*c* 1.10, CHCl$_3$); mp 251-252 °C (CHCl$_3$/MeOH). The ^{1}H NMR spectrum matched that of racemic crown-6 resorcinarene **(57)**.

5.5.6.2 Enantio-pure crown-6 resorcinarene (57b)

The general procedure was applied with resorcinarene **(60b)** (0.057 g, 0.0424 mmol), sodium hydroxide (0.010 g, 2.50 mmol), ethanol (5 mL) and water (2 mL) to give the previously unreported product **(57b)** (0.038 g, 98%) as a light-yellow solid: $[\alpha]_D$ +21.4 (*c* 1.08, CHCl$_3$); mp 252-253 °C (CHCl$_3$/MeOH). The ^{1}H NMR spectrum matched that of racemic crown-6 resorcinarene **(57)**.

5.5.7 General method for the NMR titration of resorcinarenes with salbutamol sulfate

Resorcinarene (5.2 μmol, ~ 5 mg) was weighed into an NMR tube, then DMSO-d$_6$ (0.5 mL) was added, followed by sonicating and heating with a heat gun to dissolve the resorcinarene. Resorcinarene **(53)** could not be entirely dissolved. After recording the ^{1}H NMR spectrum, the appropriate amount of salbutamol sulfate was weighed in a micro spatula and directly added to the NMR tube. The salbutamol sulfate was dissolved with heating with a heat gun, and the ^{1}H NMR spectrum recorded. The

process of adding salbutamol sulfate, dissolving and recording the ^{1}H NMR spectrum was repeated for the appropriate number of data points.

5.5.8   General method for membrane transport experiments

Membrane transport experiments were performed at ambient conditions in a glass U-tube with dimensions as shown in **Figure 5.22**. The source phase consisted of salbutamol sulfate (5 & 10 eq) dissolved in HCl (5 mL, 1 M) solution. MilliQ water (5 mL) was used for the receiving phase. The membrane consisted of the resorcinarene crown derivative (1 eq, **Table 5.6**) dissolved in dichloromethane (20 mL), and was mixed with a stirrer bar (1 × 0.7 cm). The stirrer bar was rotated at 500 RPM using a magnetic stirrer. The U-tubes were kept upright ontop of the stirrer plate by placing together in an appropriately-sized box.
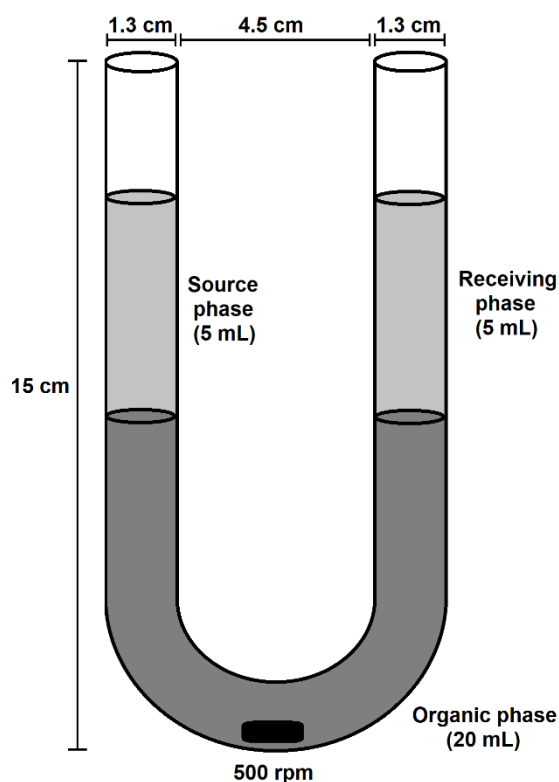
Figure 5.22   Schematic of the U-tube apparatus used for the membrane transport experiments.

Table 5.6 Masses of crown resorcinarene membrane carriers. Two sets of experiments were conducted with the salbutamol being in 5 and 10 equivalents with respect to the resorcinarene.

Resorcinarene crown	0.0277 mmol (mg)
diOBn crown-5 **(53)**	29
diOBn crown-6 **(54)**	31
diOBn crown-7 **(55)**	32
diOH crown-5 **(56)**	25
diOH crown-6 **(57)**	25
diOH crown-7 **(58)**	27
DicamphorSO$_2$ crown-5 **(59a)**	36
DicamphorSO$_2$ crown-5 **(59b)**	36
DicamphorSO$_2$ crown-6 **(60a)**	38
DicamphorSO$_2$ crown-6 **(60b)**	38
DicamphorSO$_2$ crown-7 **(61a)**	39
DicamphorSO$_2$ crown-7 **(61b)**	39
Bis-crown-5 **(63)** 17a	30
Bis-crown-6 **(64)** 17b	31
Bis-crown-7 **(65)** 17c	33
Parent resorcinarene **(1)**	20

The membrane transport of salbutamol was monitored by UV-vis spectrometry using a GBC UV/VIS 916 UV-vis spectrometer scanning from 200-400 nm at a speed of 480 nm/min and step size of 1 nm. The experimental procedure to monitor the membrane transport is illustrated in **Figure 5.23**. The receiving phase is first transferred to a vial using a Pasteur pipette to ensure thorough mixing of the receiving phase. Then the receiving phase is transferred to a cuvette that has been checked to have a zero UV-vis reading. The UV-vis spectrum of the receiving phase is recorded, then the receiving phase solutions are returned back to the U-tube, and the membrane transport experiment continued. The same procedure is repeated for the next analysis the following day. This procedure was carefully repeated for all membrane transport analyses to ensure best consistency and reproducibility of the results.
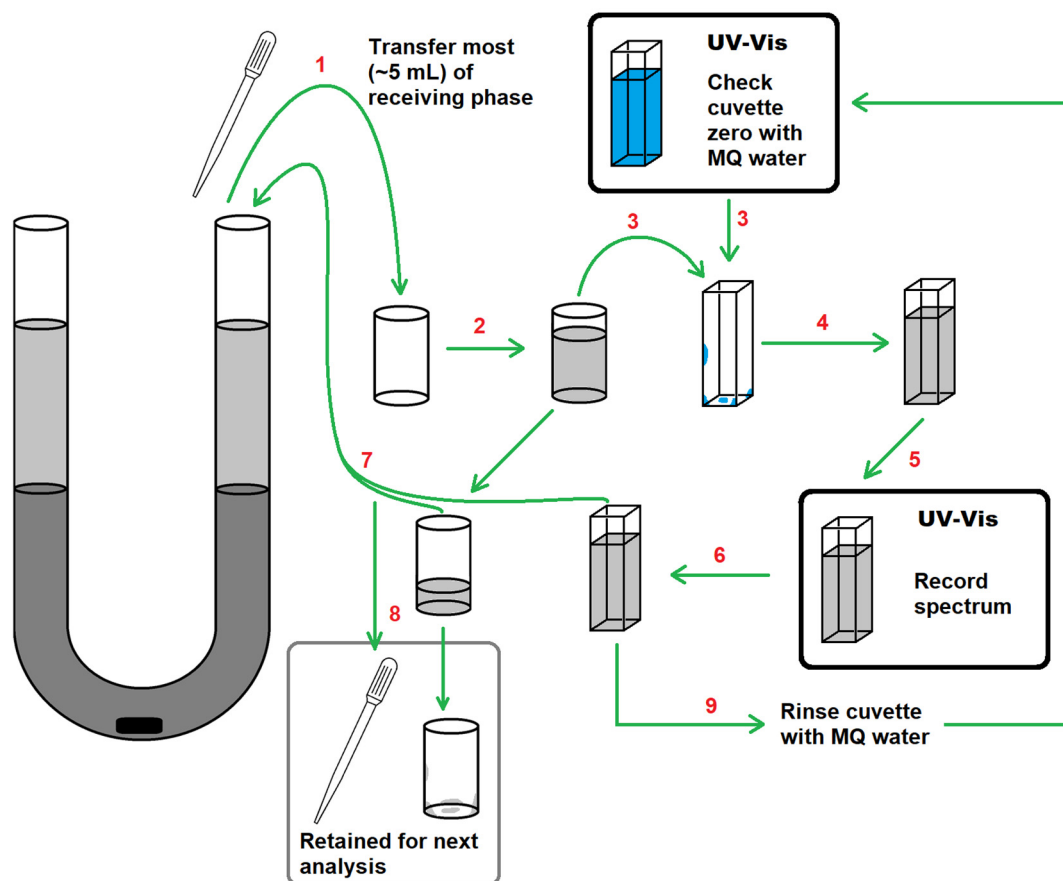
Figure 5.23 Analysis procedure for the membrane transport of salbutamol.

The membrane transport experiments were reset according to the following work up procedure. The bulk of the source and receiving aqueous phases were first removed by Pasteur pipette, then the remainder of the aqueous phase was removed via a separatory funnel. The organic phase was dried (CaCl$_2$), then the dichloromethane solvent was evaporated till the desired volume of 20 mL was achieved.

5.5.9 Investigation procedure of enantio-pure crown resorcinarenes as enantioselective membrane carriers for the chiral resolution of salbutmol

The receiving phase of membrane transport experiments with single enantiomer or diastereomer crown resoricnarenes was analysed by chiral HPLC by first transferring the receiving phase (~5 mL) from the U-tube into a vial (20 mL), then completely removing the water by freeze drying. The residue white solid was dissolved in a couple of drops of methanol, then filtered through a plug of PTFE filter paper, into a 300 µL Qsert vial for HPLC. The success of the salbutamol chiral resolution by the resorcinarene membrane carrier was determined using an Agilent 1200 series HPLC, equipped with an Astec® Chirobiotic-T® column under literature[181] conditions listed

in the following **Table 5.7**. This procedure was performed on a replicate membrane transport experiment for confirmation of the result.

Table 5.7   HPLC column conditions for the analysis of salbutamol enantioseparation.[181]

Column	Astec Chirobiotic-T, 25 cm × 4.6 mm I.D., 5 μm particles
Column temperature	Room temperature
Mobile phase	15 mM ammonium formate in methanol
Flow rate	1 mL/min
Injection	10 μL
Detector	UV, 220 nm

6 Conclusions and future work

In this project, three different strategies to synthesise a distally-functionalised tetramethoxyresorcinarene were explored. As summarised in **Scheme 6.1**, these were: calixarene rigid bridge, selective lithiation, and direct functionalisation of the resorcinarene phenols. The calixarene rigid bridge strategy yielded inconclusive results in the imine coupling of the resorcinarene to the calixarene. The strategy as a whole was realised to be impractical due to the many synthetic steps involved. The investigation into the selective lithiation of tetramethoxyresorcinarene indicated that the lithiation reaction was only applicable to a derivative of the resorcinarene with limited functionality.
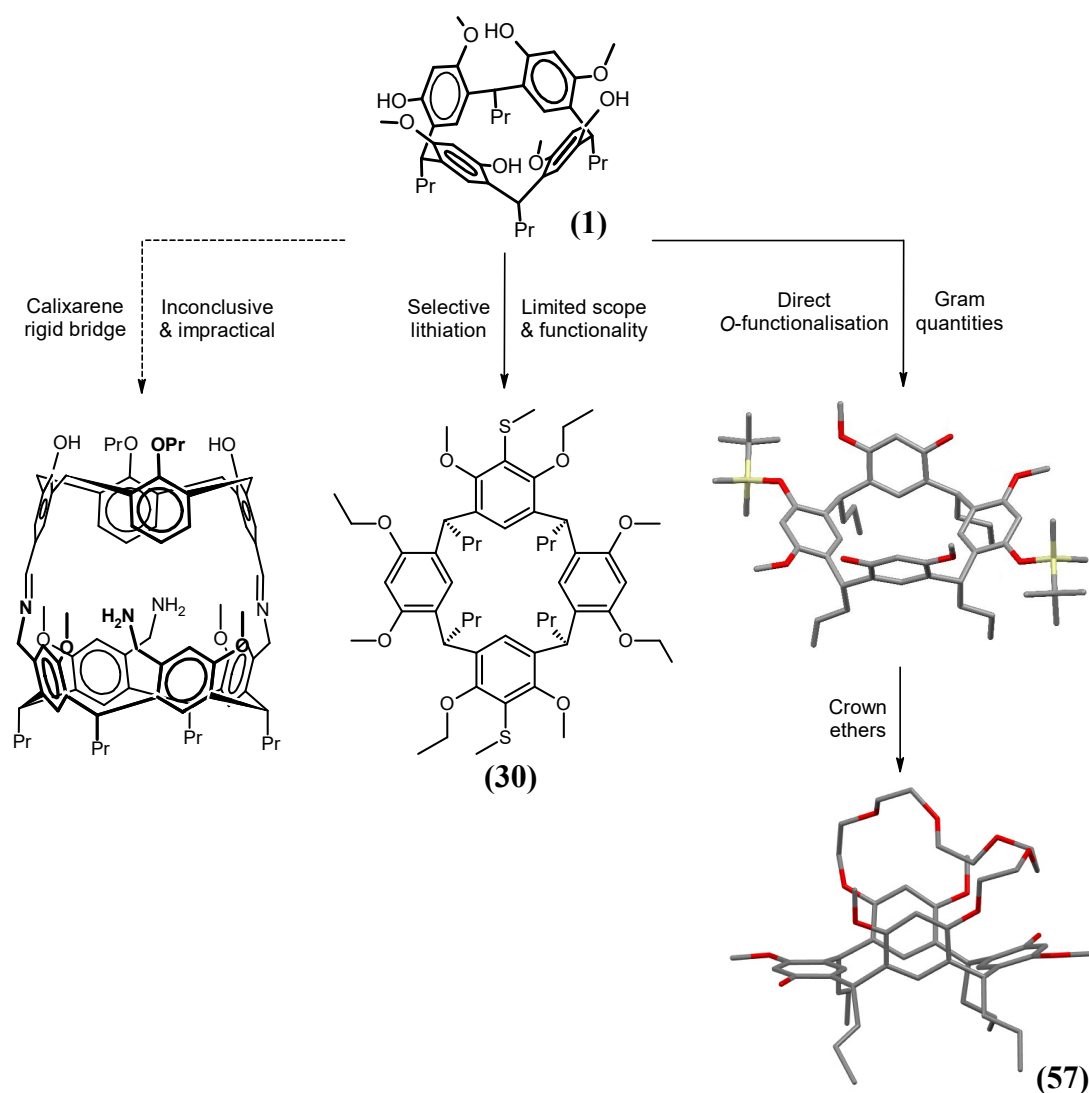
Scheme 6.1 Summary of the three different strategies to synthesise a distally-functionalised tetramethoxyresorcinarene.

Fortunately, the direct functionalisation of the resorcinarene phenols provided the breakthrough. Although all other partially-functionalised resorcinarene products were produced, the target distally-functionalised tetramethoxyresorcinarene was the major product and was isolated in gram-quantities through this simple, single-step reaction. This key intermediate enabled the distal-bridging of tetramethoxyresorcinarene which was accomplished with crown ethers of three different lengths. The interesting basket-shape architecture of these crown resorcinarenes, and their boat conformation, is evident in their crystal structures, which were obtained through X-ray diffraction on single crystals. The diastereomers of the crown 5-7 resorcinarenes were synthesised and separated, enabling the single enantiomers of the crown resorcinarenes to be obtained.

These distally-bridged crown resorcinarenes were investigated and were shown to be membrane carriers for salbutamol hydrochloride to various extents, albeit a very low transport yield. In spite of the low level of transport, the single enantiomers for one of the best membrane carriers were obtained from the hydrolysis of the corresponding separated diastereomers. These single enantiomers were examined for the potential to act as enantioselective membrane carriers for salbutamol. Analysis of the receiving phases by chiral HPLC unfortunately revealed no enantioseparation of the salbutamol by these single crown resorcinarene enantiomers. This was also the case for the separated crown resorcinarene diastereomers. Nevertheless, this work is a proof of concept and the first demonstration of a bulk liquid membrane carrier for salbutamol. With further investigation into the optimisation of the chiral resorcinarene and membrane transport conditions, the transport yield could be improved, and enantioselective transport may be a possibility.

6.1 Project refinement

6.1.1 Potential methods to enhance the enantioselectivity of the chiral resorcinarene

The lack of enantioselective transport by these enantio-pure chiral cavities may be caused by conformational flexibility, which would allow both crown resorcinarene enantiomers to flex and accommodate both enantiomers of salbutamol. Therefore, it is of interest to make the chiral cavity of the resorcinarene more rigid. This could be accomplished by adding some rigidity to the flexible crown ether bridge by incorporation of an aromatic spacer, as per the strategy by Sansone et al. (**Figure 1.13**).[92] In the literature, the synthesis of a crown ether moiety with an aromatic spacer has been accomplished in two steps in an overall yield of 55% (**Scheme 6.2**).[182]
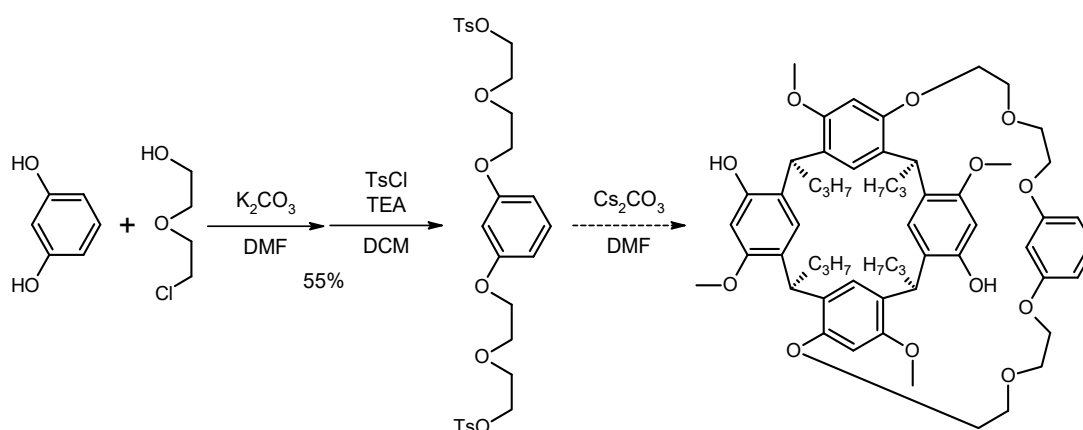
Scheme 6.2 Proposed synthesis of a crown resorcinarene with a rigid aromatic spacer.

Another method for making the cavity of the crown resorcinarene more rigid would be to connect the proximal aromatic rings with a short bridge, thereby converting the resorcinarene into a partial cavitand. This would not only rigidify the resorcinarene cavity, but also make it better defined as the aromatic rings would be prevented from bending out. It was for this reason of conformational rigidity that Duggan and co-workers utilised a cavitand as a scaffold for their boronic acid membrane carriers.[56] To bridge the proximal aromatic rings with a short bridge, complete demethylation of the resorcinarene is first required (**Scheme 6.3**). This should be possible through the procedure employed by Casnati et al.[48] for the demethylation of a crown calixarene.
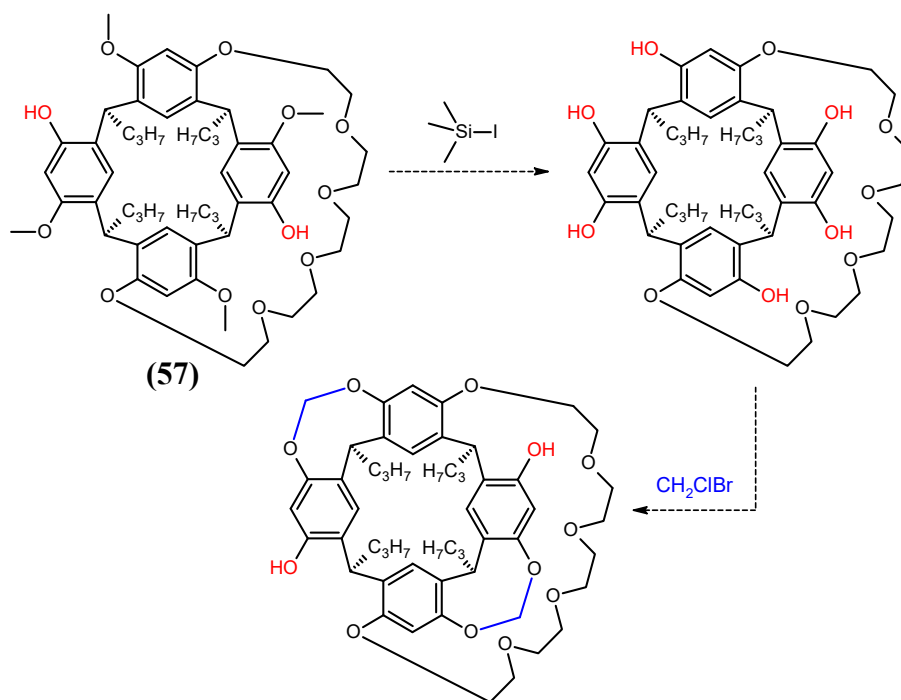
Scheme 6.3 Proposed synthesis of a chiral crown partial cavitand from a crown resorcinarene.

Other than making the cavity more rigid, another method to enhance the chirality of the cavity may be to increase the steric bulk of the methoxy substituents which endow the cavity with chirality. Substituents such as isobutyl groups may give a greater expression of the chirality of the resorcinarene cavity in terms of steric bulk. The notion is that a chirality of greater steric bulk would increase steric hindrance and hence would prevent the other enantiomer of a guest molecule from binding with the resorcinarene. Some literature precedence of this idea may be offered by the work by Heaney and co-workers in separating camphorsulfonate diastereomers of the chiral resorcinarene (**Scheme 5.3**). In their work, a better separation was found for camphorsulfonate diastereomers with bulkier alkoxy groups.[66] Perhaps the bulkier alkoxy groups increased the steric bulk of the resorcinarene chirality, which was responsible for the greater differences between their diastereomers.

There are two possible strategies to convert the methoxy groups to a bulkier alkoxy group. The first strategy would be to construct the resorcinarene macrocycle from a subunit with a bulky alkoxy group such as an isopropoxy or cyclopentyl group.[183] However, the different alkoxy group may impact the partial distal selectivity of the silylation reaction – this would be an interesting investigation in itself (**Scheme 6.6**).

The second strategy for obtaining a bulkier alkoxy group on the resorcinarene would be to alkylate the phenols of a dihydroxy crown resorcinarene with a bulky alkyl group (**Scheme 6.4**). The subsequent product could be demethylated to convert the four methoxy groups to phenols to increase functionality. However, if demethylation was required, the bulky alkoxy group needs to be unreactive under the harsh conditions for demethylation, which therefore excludes isopropoxy or cyclopentyl groups.
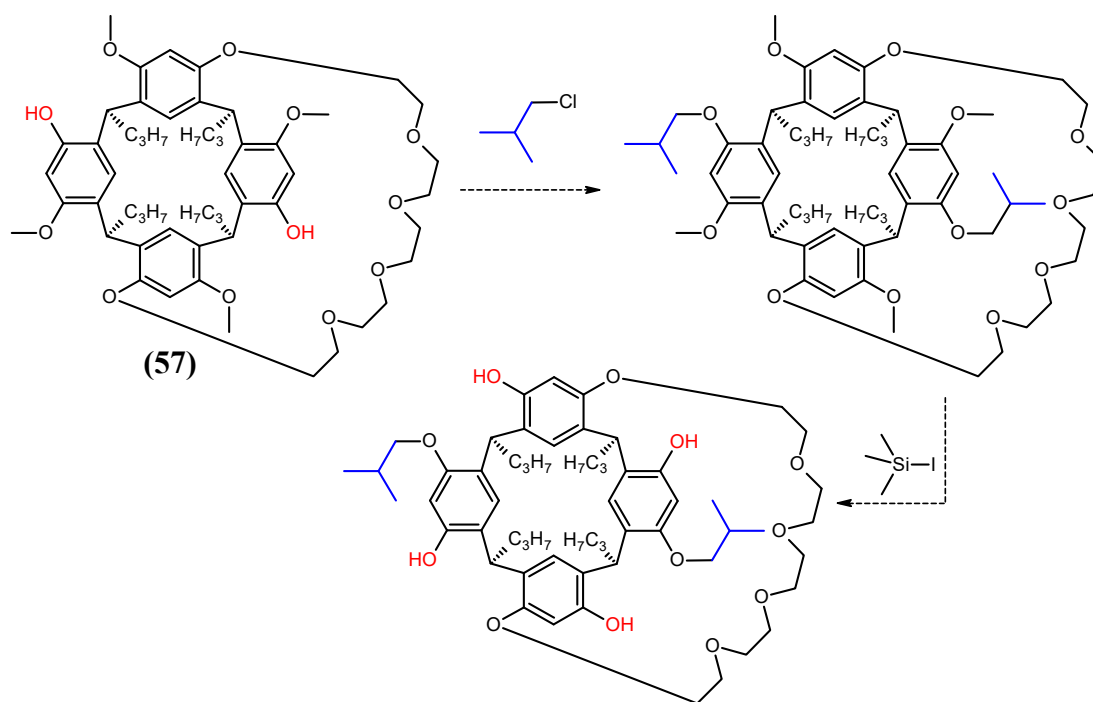
Scheme 6.4 A possible strategy for the synthesis of a crown resorcinarene with a bulkier alkoxy group.

6.1.2 The need for more informative studies for enantioselective binding

In this work, the combination of a crown resorcinarene host and salbutamol guest was investigated based on a general idea of the possible complimentary intermolecular interactions. However, there is a need for greater, more specific insight into how the chiral binding would occur. This knowledge would better enable the synthetic design of the resorcinarene membrane carrier, as well as enable more likely host-guest combinations to be investigated. Some knowledge of the binding could be provided by NMR titrations of the host and guest, as was briefly investigated with the crown resorcinarenes with salbutamol. However, more work is needed to develop this NMR titration technique to study salbutamol binding. In particular, the NMR solvent needs to be changed from dimethylsulfoxide, to a non-coordinating solvent like chloroform.

For the reason of solubility, changing the solvent to chloroform would necessitate changing the sulfate counter anion of salbutamol to something more hydrophobic.

Computational modelling of the binding would be of great assistance to predicting and understanding the binding between host and guest, as well as the influence of chirality. Since enantioselective binding is dependent on size and shape, computational modelling would be an ideal tool to visualise this event. In particular, the impact on enantioselective binding by the functional groups which endow the resorcinarene cavity with chirality could be better explored by a computational model. Factors such as the number, size, type and placement of these groups about the wider rim of the resorcinarene (as such in the resorcinarenes shown in **Scheme 6.3**) are of interest.

6.1.3   Further investigation of membrane transport

Regarding the membrane transport experiments, there remains much to be investigated. The membrane transport with these crown resorcinarenes could be performed on molecules other than salbutamol. Perhaps it would be helpful to study the transport of simple analogues of salbutamol, such as amino acids, to prove that something could be transported in substantial quantities by these crown resorcinarenes. This would enable establishment of the membrane transport procedures, as well as better understanding of the binding.

Regarding the investigation of crown resorcinarenes as potential membrane carriers for salbutamol, it would be of interest to conduct the membrane transport experiments using various sizes of crown ethers as membrane carriers. This would show if crown ethers alone could act as membrane carriers for salbutamol, and also provide a control experiment for the membrane transport mediated the crown resorcinarenes.

As discussed in this project, there are many variables and factors to be considered with the membrane transport experiments. There is still room for experimentation and improvement of the conditions for these experiments.

The ideal counter anion for minimising passive transport of the salbutamol through a blank membrane is the sulfate anion. However, the great hydrophilicity of the sulfate anion also prevents it from being carried across the membrane by a membrane carrier. This was the rationale for replacing the salbutamol anion from a sulfate to a chloride in the membrane transport experiments of this project. However, the trade off for

having a less hydrophilic counter anion was an increase in the passive transport of salbutamol, which is undesirable. This conundrum could be solved by installation of a counter anion onto the membrane carrier that would provide a counter anion for the salbutamol during transport through the organic membrane, while also assisting in the binding of the salbutamol to the membrane carrier via electrostatic interactions. Furthermore, a membrane carrier with a counter anion functionality would also enable an overall charge balance of the source and receiving phases through an exchange of H^+, as per the work by Adhikari et al.[28] (**Error! Reference source not found.**). Counter anion functional groups such as carboxylates could be installed on the chiral crown resorcinarene by a two-step procedure beginning with selective *O*-alkylation with ethyl bromoacetate, followed by hydrolysis of the ester (**Scheme 6.5**).
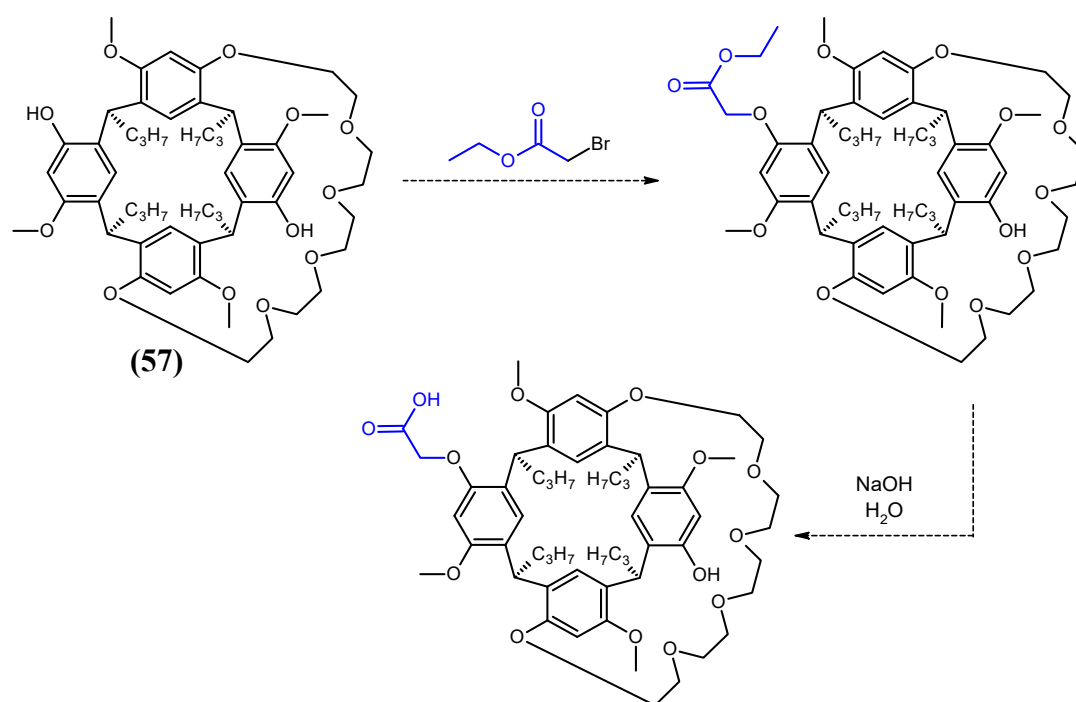
Scheme 6.5   The crown resorcinarene could be functionalised with a carboxylate to act as a counter anion for the membrane transport of salbutamol.

The passive transport of salbutamol could also be minimised by the choice of membrane solvent. Preliminary investigations in this project have suggested that less passive transport of salbutamol was occurring in dichloromethane than in chloroform. Perhaps this could be due to chloroform having a slightly stronger net dipole compared to dichloromethane. A more non-polar membrane solvent is desirable, since it should minimise passive transport, while still being able to dissolve the membrane carrier. Nevertheless, a membrane solvent which enables unambiguous results is sufficient,

since the ultimate goal would be to perform the membrane transport experiments with a solid supported membrane,[15, 26] which would make an organic solvent in a bulk liquid membrane redundant.

6.1.4 Further optimisation of resorcinarene distal functionalisation

In the silylation of resorcinarene **(1)**, the effect of the base, *O*-substituent, and reaction solvent was investigated. However, the potential impact of the reaction temperature, concentration and deprotonation time would be worth investigating. By adjusting these reaction conditions, it may be possible to increase the yield of the distally-functionalised resorcinarene.

Further experimentation of the distal functionalisation with other protecting groups may possibly give a better yield of the distally-functionalised product. In particular, protecting groups that are also stable under the Cs_2CO_3/DMF bridging conditions would be desirable to avoid the additional steps of replacing the TBDMS group. Potential candidates for this investigation could be a 2-(trimethylsilyl)ethoxymethyl ether, or an isopropyl ether, or a *tert*-butyl ether.

6.2 Project extention

In this work, the silylation was investigated on resorcinarenes with propyl and heptyl chains. It would be interesting to further investigate the impact of the resorcinarene alkyl chain on the proportions of the partially-functionalised products, particularly with a resorcinarene of short chain-length (**Scheme 6.6**). Additionally, the impact of the alkoxy group of the resorcinarene is completely unknown, since only tetramethoxyresorcinarenes were examined in this work. The silylation could be investigated on isopropoxy- and cyclopentyl- analogues of the chiral resorcinarene which are known in the literature.[183] Perhaps, for this investigation, a HPLC separation method could be employed for a rapid preliminary determination of the proportions of the partially-silylated resorcinarene products.
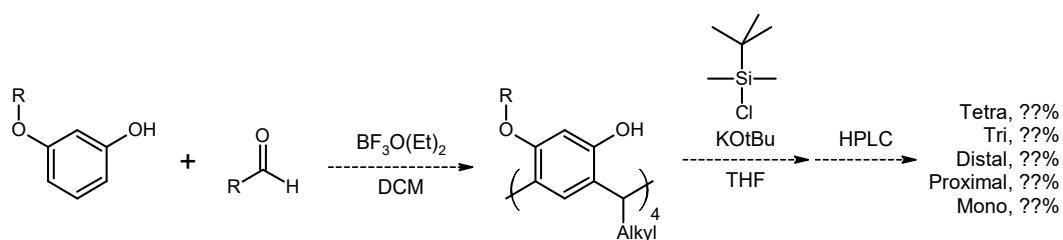
Scheme 6.6 Potential further investigation into the impact of the resorcinarene alkyl chain and alkoxy group on the proportions of partially-silylated products.

A different approach to modifying the chiral resorcinarene to be a potential membrane carrier would be to install a tri-armed bridge over the cavity of the resorcinarene (**Figure 6.1**). The synthesis of this product should be readily accomplished, since only one intramolecularly bridged product is possible.
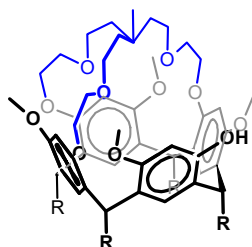
Figure 6.1 A tri-armed bridged resorcinarene may be a potential membrane carrier.

6.3 New directions

In this project, the groundwork for the synthesis of partially-functionalised chiral resorcinarenes has been laid. The optimisation of the yield of other partially-functionalised chiral resorcinarene products could be investigated with the goal of exploring a different avenue and application of the chiral resorcinarene. The ability to readily obtain practical amounts of partially-functionalised chiral resorcinarenes opens up new directions for research. The synthesis of chiral partial cavitands could be possible in the same manner as with the crown resorcinarene in **Scheme 6.3**. In this case, ethyl ethers could provide a more convenient group which is inert to the demethylation conditions (**Scheme 6.7**). In this strategy, the chirality of the resorcinarene cavity is preserved by *O*-alkylation of a partially-functionalised resorcinarene with ethoxy groups. Subsequent removal of all other *O*-substituents by hydrolysis and demethylation would furnish a chiral resorcinarene with neighbouring hydroxy groups that could accept a cavitand bridge. The synthesis of a chiral cavitand from an axially-chiral resorcinarene as such would be unprecedented, since most axially-chiral cavitands have been synthesised from octahydroxyresorcinarene. Chiral

cavitands are of current interest because of their ability for enantioselective complexation.[184, 185]
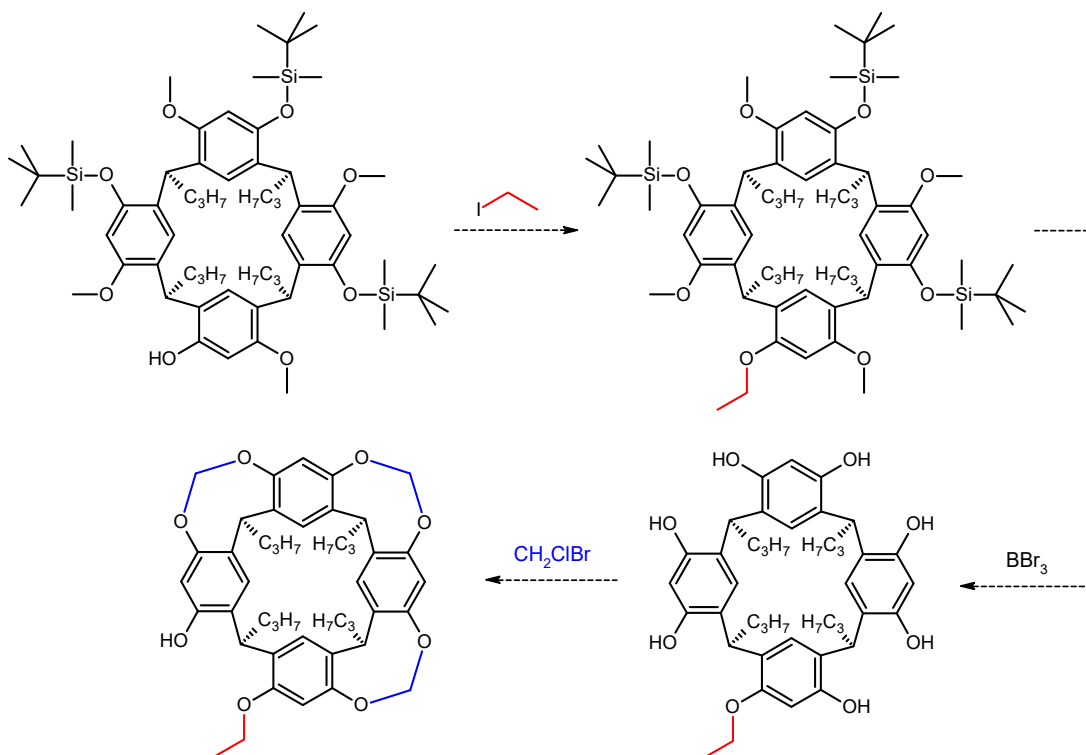
Scheme 6.7 Possible synthesis of a chiral partial cavitand from a partially-functionalised chiral resorcinarene.

Referring back to **Scheme 6.6**, a resorcinarene alkoxy group that would be of great synthetic utility would be one which is readily cleavable, such as a benzyloxy or isopropoxy group. A readily-cleavable group as such would not require the non-selective cleavage conditions as a methoxy group otherwise would. This would open up new synthetic opportunities such as the possibility for greater functionality in the potential partial cavitand synthesis (**Scheme 6.7**), through the use of alternative groups other than ethyl ethers.

The ability to obtain distal-benzyloxyresorcinarene **(46)** (**Figure 6.2**) in gram quantities opens up many possibilities for the installation of various other bridges and functionalities at the distal positions of the chiral resorcinarene. Other than increasing the rigidty of the bridge as in **Scheme 6.2**, different functionalisations could be incorporated into the bridge, depending on the target application. For instance, an amino crown ether could be installed as the bridge to target carboxylate guests. Other than the formation of an ether linkage, other bridging linkages, such as the formation of a triazole by 'click' chemistry, could be explored.
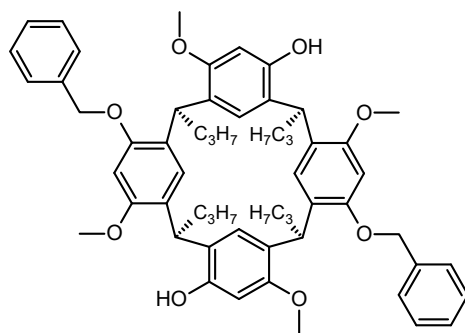
Figure 6.2 Distal-benzyloxyresorcinarene **(46)** provides the key intermediate that enables other distal bridging or functionalisations of the tetramethoxyresorcinarene.

A different avenue which could be explored for the chiral resorcinarene is its utilisation as a catalyst with potential enantioselectivity. In the literature, there are current investigations into calixarenes[186] and resorcinarenes[187] as potential catalysts.

7 References

1.   Sekhon, B. S., *Journal of Modern Medicinal Chemistry* **2013,** *1* (1), 10-36.

2.   Thall, E., *J. Chem. Educ.* **1996,** *73* (6), 481.

3.   Agranat, I.; Wainschtein, S. R.; Zusman, E. Z., *Nat Rev Drug Discov* **2012,** *11* (12), 972-973.

4.   Speirs, A. L., *The Lancet* **1962,** *279* (7224), 303-305.

5.   Budău, M.; Hancu, G.; Rusu, A.; Cârcu-Dobrin, M.; Muntean, D. L., *Advanced Pharmaceutical Bulletin* **2017,** *7* (4), 495-500.

6.   Calcaterra, A.; D'Acquarica, I., *J. Pharm. Biomed. Anal.* **2018,** *147*, 323-340.

7.   Mane, S., *Analytical Methods* **2016,** *8* (42), 7567-7586.

8.   Templeton, A. G. B.; Chapman, I. D.; Chilvers, E. R.; Morley, J.; Handley, D. A., *Pulmonary Pharmacology & Therapeutics* **1998,** *11* (1), 1-6.

9.   Mitra, S.; Ugur, M.; Ugur, O.; Goodman, H. M.; McCullough, J. R.; Yamaguchi, H., *Mol. Pharmacol.* **1998,** *53* (3), 347-54.

10.   Agrawal, D. K.; Ariyarathna, K.; Kelbe, P. W., *Journal of Allergy and Clinical Immunology* **2004,** *113* (3), 503-510.

11.   Nguyen, L. A.; He, H.; Pham-Huy, C., *International Journal of Biomedical Science : IJBS* **2006,** *2* (2), 85-100.

12.   Thalomid (thalidomide) Approval Letter. U.S. Food and Drug Administration: 1998. http://www.accessdata.fda.gov/drugsatfda_docs/appletter/1998/20785ltr.pdf (accessed 16 July 2018).

13.   Blaser, H.-U.; Schmidt, E., in *Asymmetric Catalysis on Industrial Scale*, Wiley-VCH Verlag GmbH & Co. KGaA: 2004; pp 1-19.

14.   Humphrey, C. E.; Ahmed, M.; Ghanem, A.; Turner, N. J., in *Separation of Enantiomers: Synthetic Methods*, Todd, M., Ed. Wiley: Somerset, NJ, USA, 2014; pp 123-160.

15.   Xie, R.; Chu, L.-Y.; Deng, J.-G., *Chem. Soc. Rev.* **2008,** *37* (6), 1243-1263.

16.   Harrington, P. J.; Lodewijk, E., *Organic Process Research & Development* **1997,** *1* (1), 72-76.

17.   Pasteur, L., *Ann Chim Phys* **1848,** (24), 442-458.

18.   Crosby, J., *Tetrahedron* **1991,** *47* (27), 4789-4846.

19.   Pellisier, H., in *Separation of Enantiomers: Synthetic Methods*, Todd, M., Ed. Wiley: Somerset, NJ, USA, 2014; pp 75-122.

20.   Schoemaker, H. E.; Mink, D.; Wubbolts, M. G., *Science* **2003,** *299* (5613), 1694-1697.

21.   Rajendran, A.; Paredes, G.; Mazzotti, M., *J. Chromatogr. A* **2009,** *1216* (4), 709-738.

22.   West, C., *Current Analytical Chemistry* **2014,** *10* (1), 99-120.

23.   Speybrouck, D.; Lipka, E., *J. Chromatogr. A* **2016,** *1467*, 33-55.

24.   Johannsen, M.; Brunner, G., *The Journal of Supercritical Fluids* **2018,** *134*, 61-70.

25.   Ward, T. J.; Ward, K. D., *Anal. Chem.* **2012,** *84* (2), 626-635.

26.   Gössi, A.; Riedl, W.; Schuur, B., *Journal of Chemical Technology & Biotechnology* **2018,** *93* (3), 629-644.

27.   Zhang, F.; He, L.; Sun, W.; Cheng, Y.; Liu, J.; Ren, Z., *RSC Advances* **2015,** *5* (52), 41729-41735.

28.   Adhikari, B. B.; Fujii, A.; Schramm, M. P., *Eur. J. Org. Chem.* **2014,** *2014* (14,), 2972–2979.

29.   Tan, D. A. Chemical Research Methods 362, Undergraduate Research Report, Curtin University, **2012**.

30.   Biwer, A.; Antranikian, G.; Heinzle, E., *Appl. Microbiol. Biotechnol.* **2002,** *59* (6), 609-617.

31.   Buschmann, H. J.; Cleve, E.; Mutihac, L.; Schollmeyer, E., *Microchem. J.* **2000,** *64* (1), 99-103.

32.   Connors, K. A., *Chem. Rev.* **1997,** *97* (5), 1325-1358.

33.   Diacu, E.; Mutihac, L.; Ruse, E.; Ceausescu, M., *J Incl Phenom Macrocycl Chem* **2011,** *71* (3-4), 339-342.

34.   Loftsson, T.; Brewster, M. E., *J. Pharm. Sci.* **1996,** *85* (10), 1017-1025.

35.   Mutihac, R.-C.; Riegler, H., *Langmuir* **2009,** *26* (9), 6394-6399.

36.   Szejtli, J., *Chem. Rev.* **1998,** *98* (5), 1743-1754.

37.   Wang, Z.; Takashima, Y.; Yamaguchi, H.; Harada, A., *Org. Lett.* **2011,** *13* (16), 4356-4359.

38.   Zhou, J.; Ritter, H., *Polymer Chemistry* **2010,** *1* (10), 1552-1559.

39.   Wang, X.; Bun Ching, C., *Chem. Eng. Sci.* **2005,** *60* (5), 1337-1347.

40. Zhang, X.; Zhang, C.; Sun, G.; Xu, X.; Tan, Y.; Wu, H.; Cao, R.; Liu, J.; Wu, J., *Instrumentation Science & Technology* **2012,** *40* (2-3), 194-215.

41. Ward, T. J., *Anal. Chem.* **2002,** *74* (12), 2863-2872.

42. Li, L.; Li, X.; Luo, Q.; You, T., *Talanta* **2015,** *142* (0), 28-34.

43. Stancu, A.-D.; Hillebrand, M.; Tablet, C.; Mutihac, L., *J Incl Phenom Macrocycl Chem* **2014,** *78* (1-4), 71-76.

44. Steffeck, R. J.; Zelechonok, Y.; Gahm, K. H., *J. Chromatogr. A* **2002,** *947* (2), 301-305.

45. Breccia, P.; Van Gool, M.; Pérez-Fernández, R.; Martín-Santamaría, S.; Gago, F.; Prados, P.; de Mendoza, J., *J. Am. Chem. Soc.* **2003,** *125* (27), 8270-8284.

46. Tero, T.-R.; Nissinen, M., *Tetrahedron* **2014,** *70* (6), 1111-1123.

47. Bozkurt, S.; Durmaz, M.; Yilmaz, M.; Sirit, A., *Tetrahedron: Asymmetry* **2008,** *19* (5), 618-623.

48. Casnati, A.; Pochini, A.; Ungaro, R.; Ugozzoli, F.; Arnaud, F.; Fanni, S.; Schwing, M.-J.; Egberink, R. J. M.; de Jong, F.; Reinhoudt, D. N., *J. Am. Chem. Soc.* **1995,** *117* (10), 2767-2777.

49. Durmaz, M., *J Incl Phenom Macrocycl Chem* **2012,** *74* (1-4), 361-368.

50. Durmaz, M.; Bozkurt, S.; Naziroglu, H. N.; Yilmaz, M.; Sirit, A., *Tetrahedron: Asymmetry* **2011,** *22* (7), 791-796.

51. Gong, S.-L.; Zhong, Z.-L.; Chen, Y.-Y., *Reactive & Functional Polymers* **2002,** *51* (2-3), 111-116.

52. Adhikari, B. B.; Roshandel, S.; Fujii, A.; Schramm, M. P., *Eur. J. Org. Chem.* **2015,** *2015* (12), 2683-2690.

53. Gutsche, C. D.; Bauer, L. J., *J. Am. Chem. Soc.* **1985,** *107* (21), 6052-6059.

54. Gutsche, C. D., *Calixarenes Revisited*. Royal Society of Chemistry: United Kingdom, 1998; p 51.

55. Timmerman, P.; Verboom, W.; Reinhoudt, D. N., *Tetrahedron* **1996,** *52* (8), 2663-2704.

56. Altamore, T. M.; Barrett, E. S.; Duggan, P. J.; Sherburn, M. S.; Szydzik, M. L., *Org. Lett.* **2002,** *4* (20), 3489-3491.

57. Oshima, T.; Inoue, K.; Furusaki, S.; Goto, M., *Journal of Membrane Science* **2003,** *217* (1), 87-97.

58. Bozkurt, S.; Yilmaz, M.; Sirit, A., *Chirality* **2012,** *24* (2), 129-136.

59. Shirakawa, S.; Moriyama, A.; Shimizu, S., *Eur. J. Org. Chem.* **2008,** *2008* (35), 5957-5964.

60. Shirakawa, S.; Shimizu, S., *Eur. J. Org. Chem.* **2009,** *2009* (12), 1916-1924.

61. McIldowie, M. J.; Mocerino, M.; Ogden, M. I., *Supramol. Chem.* **2010,** *22* (1), 13-39.

62. Arnott, G. E., *Chemistry – A European Journal* **2018,** *24* (8), 1744-1754.

63. Page, P. C. B.; Heaney, H.; Sampler, E. P., *J. Am. Chem. Soc.* **1999,** *121* (28), 6751-6752.

64. El Gihani, M. T.; Heaney, H.; Slawin, A. M. Z., *Tetrahedron Lett.* **1995,** *36* (27), 4905-4908.

65. McIldowie, M. J.; Mocerino, M.; Skelton, B. W.; White, A. H., *Org. Lett.* **2000,** *2* (24), 3869-3871.

66. Buckley, B. R.; Page, P. C. B.; Chan, Y.; Heaney, H.; Klaes, M.; McIldowie, M. J.; McKee, V.; Mattay, J.; Mocerino, M.; Moreno, E.; Skelton, B. W.; White, A. H., *Eur. J. Org. Chem.* **2006,** *2006* (22), 5135-5151.

67. Yang, Y.; Cao, X.; Surowiec, M.; Bartsch, R. A., *Tetrahedron* **2010,** *66* (2), 447-454.

68. He, Y.; Xiao, Y.; Meng, L.; Zeng, Z.; Wu, X.; Wu, C.-T., *Tetrahedron Lett.* **2002,** *43* (35), 6249-6253.

69. Arduini, A.; Fabbi, M.; Mantovani, M.; Mirone, L.; Pochini, A.; Secchi, A.; Ungaro, R., *J. Org. Chem.* **1995,** *60* (5), 1454-1457.

70. Joseph, R.; Rao, C. P., *Chem. Rev.* **2011,** *111* (8), 4658-4702.

71. Asfari, Z.; Wenger, S.; Vicens, J., *Supramol. Sci.* **1994,** *1* (2), 103-110.

72. Casnati, A., *Chem. Commun.* **2013,** *49* (61), 6827-6830.

73. Duncan, N. C.; Roach, B. D.; Williams, N. J.; Bonnesen, P. V.; Rajbanshi, A.; Moyer, B. A., *Sep. Sci. Technol.* **2012,** *47* (14-15), 2074-2087.

74. Van Loon, J. D.; Arduini, A.; Coppi, L.; Verboom, W.; Pochini, A.; Ungaro, R.; Harkema, S.; Reinhoudt, D. N., *J. Org. Chem.* **1990,** *55* (21), 5639-5646.

75. Zajícová, M.; Eigner, V.; Budka, J.; Lhoták, P., *Tetrahedron Lett.* **2015,** *56* (41), 5529-5532.

76. Kanamathareddy, S.; Gutsche, C. D., *J. Org. Chem.* **1995,** *60* (19), 6070-6075.

77. Goldmann, H.; Vogt, W.; Paulus, E.; Böhmer, V., *J. Am. Chem. Soc.* **1988,** *110* (20), 6811-6817.

78. Zeng, C.-C.; Yuan, H.-S.; Huang, Z.-T., *Chin. J. Chem .* **2002,** *20* (8), 795-802.

79. Cacciapaglia, R.; Di Stefano, S.; Mandolini, L., *J. Phys. Org. Chem.* **2008,** *21* (7-8), 688-693.

80. Arduini, A.; Fanni, S.; Manfredi, G.; Pochini, A.; Ungaro, R.; Sicuri, A. R.; Ugozzoli, F., *J. Org. Chem.* **1995,** *60* (5), 1448-1453.

81. Arduini, A.; Fanni, S.; Pochini, A.; Sicuri, A. R.; Ungaro, R., *Tetrahedron* **1995,** *51* (29), 7951-7958.

82. Lhoták, P.; Shinkai, S., *Tetrahedron Lett.* **1996,** *37* (5), 645-648.

83. Hudrlik, P. F.; Hudrlik, A. M.; Zhang, L.; Arasho, W. D.; Cho, J., *J. Org. Chem.* **2007,** *72* (21), 7858-7862.

84. Larsen, M.; Jørgensen, M., *J. Org. Chem.* **1996,** *61* (19), 6651-6655.

85. Barton, O. G. Doctor of Philosophy Dissertation, Universität Bielefeld, **2008**. http://pub.uni-bielefeld.de/publication/2302017 (accessed 16 May 2016).

86. Hüggenberg, W.; Seper, A.; Oppel, I. M.; Dyker, G., *Eur. J. Org. Chem.* **2010,** *2010* (35), 6786-6797.

87. Liu, F.-Q.; Harder, G.; Tilley, T. D., *J. Am. Chem. Soc.* **1998,** *120* (13), 3271-3272.

88. Struck, O.; van Duynhoven, J. P. M.; Verboom, W.; Harkema, S.; Reinhoudt, D. N., *Chem. Commun.* **1996,** (13), 1517-1518.

89. Düker, M. H.; Kutter, F.; Dülcks, T.; Azov, V. A., *Supramol. Chem.* **2014,** *26* (7-8), 552-560.

90. Casnati, A.; Fabbi, M.; Pelizzi, N.; Pochini, A.; Sansone, F.; Ungaro, R.; Di Modugno, E.; Tarzia, G., *Bioorg. Med. Chem. Lett.* **1996,** *6* (22), 2699-2704.

91. Casnati, A.; Sansone, F.; Ungaro, R., *Acc. Chem. Res.* **2003,** *36* (4), 246-254.

92. Sansone, F.; Baldini, L.; Casnati, A.; Lazzarotto, M.; Ugozzoli, F.; Ungaro, R., *PNAS* **2002,** *99* (8), 4842-4847.

93. Morikawa, O.; Nakanishi, K.; Miyashiro, M.; Kobayashi, K.; Konishi, H., *Synthesis* **2000,** *2000* (02), 233-236.

94. Konishi, H.; Nakamaru, H.; Nakatani, H.; Ueyama, T.; Kobayashi, K.; Morikawa, O., *Chem. Lett.* **1997,** *26* (2), 185-186.

95. Shivanyuk, A.; Paulus, E. F.; Böhmer, V.; Vogt, W., *J. Org. Chem.* **1998,** *63* (19), 6448-6449.

96. Lukin, O.; Shivanyuk, A.; Pirozhenko, V. V.; Tsymbal, I. F.; Kalchenko, V. I., *J. Org. Chem.* **1998,** *63* (25), 9510-9516.

97. Shivanyuk, A.; Schmidt, C.; Böhmer, V.; Paulus, E. F.; Lukin, O.; Vogt, W., *J. Am. Chem. Soc.* **1998,** *120* (18), 4319-4326.

98. Arnott, G. E.; Bulman Page, P. C.; Heaney, H.; Hunter, R.; Sampler, E. P., *Synlett* **2001,** *2001* (03), 0412-0414.

99. Arnott, G. E.; Heaney, H.; Hunter, R.; Page, Philip C. B., *Eur. J. Org. Chem.* **2004,** *2004* (24), 5126-5134.

100. Arnott, G. E.; Hunter, R., *Tetrahedron* **2006,** *62* (5), 992-1000.

101. Higler, I.; Boerrigter, H.; Verboom, W.; Kooijman, H.; Spek, A. L.; Reinhoudt, D. N., *Eur. J. Org. Chem.* **1998,** *1998* (8), 1597-1607.

102. Salorinne, K.; Nissinen, M., *Org. Lett.* **2006,** *8* (24), 5473-5476.

103. Salorinne, K.; Tero, T.-R.; Riikonen, K.; Nissinen, M., *Org. Biomol. Chem.* **2009,** *7* (20), 4211-4217.

104. Salorinne, K.; Nissinen, M., *Tetrahedron* **2008,** *64* (8), 1798-1807.

105. Helttunen, K.; Moridi, N.; Shahgaldian, P.; Nissinen, M., *Org. Biomol. Chem.* **2012,** *10* (10), 2019-2025.

106. Helttunen, K.; Salorinne, K.; Barboza, T.; Barbosa, H. C.; Suhonen, A.; Nissinen, M., *New J. Chem.* **2012,** *36* (3), 789-795.

107. Tan, D. A. Chemistry Honours Disseratation, Curtin University, **2014**.

108. Barrett, E. S.; Irwin, J. L.; Turner, P.; Sherburn, M. S., *J. Org. Chem.* **2001,** *66* (24), 8227-8229.

109. Irwin, J. L.; Sherburn, M. S., *J. Org. Chem.* **2000,** *65* (2), 602-605.

110. Irwin, J. L.; Sherburn, M. S., *J. Org. Chem.* **2000,** *65* (18), 5846-5848.

111. Ngodwana, L.; Kleinhans, D. J.; Smuts, A.-J.; van Otterlo, W. A. L.; Arnott, G. E., *RSC Advances* **2013,** *3* (12), 3873-3876.

112. Tan, D. A.; Mocerino, M., in *Calixarenes and Beyond*, Neri, P.; Sessler, J. L.; Wang, M.-X., Eds. Springer International Publishing: Cham, 2016; pp 235-253.

113. Struck, O.; Chrisstoffels, L. A. J.; Lugtenberg, R. J. W.; Verboom, W.; van Hummel, G. J.; Harkema, S.; Reinhoudt, D. N., *J. Org. Chem.* **1997,** *62* (8), 2487-2493.

114. Iwamoto, H.; Niimi, K.; Haino, T.; Fukazawa, Y., *Tetrahedron* **2009,** *65* (35), 7259-7267.

115. Cram, D. J.; Blanda, M. T.; Paek, K.; Knobler, C. B., *J. Am. Chem. Soc.* **1992,** *114* (20), 7765-7773.

116. Cram, D. J.; Jaeger, R.; Deshayes, K., *J. Am. Chem. Soc.* **1993,** *115* (22), 10111-10116.

117. Cram, D. J.; Karbach, S.; Kim, Y. H.; Baczynskyj, L.; Marti, K.; Sampson, R. M.; Kalleymeyn, G. W., *J. Am. Chem. Soc.* **1988,** *110* (8), 2554-2560.

118. Sherman, J. C.; Cram, D. J., *J. Am. Chem. Soc.* **1989,** *111* (12), 4527-4528.

119. Stastny, V.; Lhoták, P.; Michlová, V.; Stibor, I.; Sykora, J., *Tetrahedron* **2002,** *58* (36), 7207-7211.

120. van Wageningen, A. M. A.; Timmerman, P.; van Duynhoven, J. P. M.; Verboom, W.; van Veggel, F. C. J. M.; Reinhoudt, D. N., *Chemistry – A European Journal* **1997,** *3* (4), 639-654.

121. Beyeh, N. K.; Valkonen, A.; Rissanen, K., *Org. Lett.* **2010,** *12* (7), 1392-1395.

122. Chapman, R. G.; Chopra, N.; Cochien, E. D.; Sherman, J. C., *J. Am. Chem. Soc.* **1994,** *116* (1), 369-370.

123. Misztal, K.; Sartori, A.; Pinalli, R.; Massera, C.; Dalcanale, E., *Supramol. Chem.* **2014,** *26* (3-4), 151-156.

124. Jean-Marc, B.; Helen, S. E., *Helv. Chim. Acta* **2005,** *88* (10), 2722-2730.

125. Beyeh, N. K.; Rissanen, K., *Tetrahedron Lett.* **2009,** *50* (52), 7369-7373.

126. Tapia, R.; Torres, G.; Valderrama, J. A., *Synth. Commun.* **1986,** *16* (6), 681-687.

127. Ghirga, F.; D'Acquarica, I.; Delle Monache, G.; Mannina, L.; Molinaro, C.; Nevola, L.; Sobolev, A. P.; Pierini, M.; Botta, B., *J. Org. Chem.* **2013,** *78* (14), 6935-6946.

128. Bonini, C.; Chiummiento, L.; Funicello, M.; Lopardo, M. T.; Lupattelli, P.; Laurita, A.; Cornia, A., *J. Org. Chem.* **2008,** *73* (11), 4233-4236.

129. Pasquale, S.; Sattin, S.; Escudero-Adán, E. C.; Martínez-Belmonte, M.; de Mendoza, J., **2012,** *3*, 785.

130. Grajda, M.; Wierzbicki, M.; Cmoch, P.; Szumna, A., *J. Org. Chem.* **2013,** *78* (22), 11597-11601.

131. Buckley, B. R.; Boxhall, J. Y.; Page, P. C. B.; Chan, Y.; Elsegood, M. R. J.; Heaney, H.; Holmes, K. E.; McIldowie, M. J.; McKee, V.; McGrath, M. J.; Mocerino, M.; Poulton, A. M.; Sampler, E. P.; Skelton, B. W.; White, A. H., *Eur. J. Org. Chem.* **2006,** *2006* (22), 5117-5134.

132. Gutsche, C. D.; Nam, K. C., *J. Am. Chem. Soc.* **1988,** *110* (18), 6153-6162.

133. Wiegmann, S.; Neumann, B.; Stammler, H.-G.; Mattay, J., *Eur. J. Org. Chem.* **2012,** *2012* (21), 3955-3961.

134. Page, P. C. B.; Bygrave, T. R.; Chan, Y.; Heaney, H.; McKee, V., *Eur. J. Org. Chem.* **2011,** *2011* (16), 3016-3025.

135. Smith, J. N.; Lucas, N. T., *Chem. Commun.* **2018,** *54* (37), 4716-4719.

136. Mićović, V.; Mihailović, M., *J. Org. Chem.* **1953,** *18* (9), 1190-1200.

137. Fieser, L. F.; Fieser, M., *Reagents for Organic Synthesis*. John Wiley & Sons, INC.: United States of America, 1967; Vol. 1, p 584.

138. Casnati, A.; Pirondini, L.; Pelizzi, N.; Ungaro, R., *Supramol. Chem.* **2000,** *12* (1), 53-65.

139. Iwamoto, K.; Araki, K.; Shinkai, S., *J. Org. Chem.* **1991,** *56* (16), 4955-4962.

140. Liang, Z.; Liu, Z.; Gao, Y., *Tetrahedron Lett.* **2007,** *48* (20), 3587-3590.

141. Zeng, C. C.; Zheng, Q. Y.; Tang, Y. L.; Huang, Z. T., *Tetrahedron* **2003,** *59* (14), 2539-2548.

142. Sharma, S. K.; Gutsche, C. D., *J. Org. Chem.* **1996,** *61* (7), 2564-2568.

143. Timmerman, P.; Boerrigter, H.; Verboom, W.; Reinhoudt, D. N., *Recl. Trav. Chim. Pays-Bas* **1995,** *114* (3), 103-111.

144. Kelderman, E.; Verboom, W.; Engbersen, J. F. J.; Reinhoudt, D. N.; Heesink, G. J. T.; van Hulst, N. F.; Derhaeg, L.; Persoons, A., *Angewandte Chemie International Edition in English* **1992,** *31* (8), 1075-1077.

145. Stibor, I.; Budka, J.; Michlova, V.; Tkadlecova, M.; Pojarova, M.; Curinova, P.; Lhotak, P., *New J. Chem.* **2008,** *32* (9), 1597-1607.

146. Regayeg, M.; Vocanson, F.; Duport, A.; Blondeau, B.; Perrin, M.; Fort, A.; Lamartine, R., *Materials Science and Engineering: C* **2002,** *21* (1–2), 131-135.

147. Casnati, A.; Bonetti, F.; Sansone, F.; Ugozzoli, F.; Ungaro, R., *Collect. Czech. Chem. Commun.* **2004,** *69* (5), 1063-1079.

148. Curinova, P.; Stibor, I.; Budka, J.; Sykora, J.; Lang, K.; Lhotak, P., *New J. Chem.* **2009,** *33* (3), 612-619.

149. Iwamoto, K.; Fujimoto, K.; Matsuda, T.; Shinkai, S., *Tetrahedron Lett.* **1990,** *31* (49), 7169-7172.

150. Danila, C.; Bolte, M.; Bohmer, V., *Org. Biomol. Chem.* **2005,** *3* (1), 172-184.

151. Mendez-Arroyo, J.; Barroso-Flores, J.; Lifschitz, A. M.; Sarjeant, A. A.; Stern, C. L.; Mirkin, C. A., *J. Am. Chem. Soc.* **2014,** *136* (29), 10340-10348.

152. Verboom, W.; Durie, A.; Egberink, R. J. M.; Asfari, Z.; Reinhoudt, D. N., *J. Org. Chem.* **1992,** *57* (4), 1313-1316.

153. Sansone, F.; Dudič, M.; Donofrio, G.; Rivetti, C.; Baldini, L.; Casnati, A.; Cellai, S.; Ungaro, R., *J. Am. Chem. Soc.* **2006,** *128* (45), 14528-14536.

154. Kumar, S.; Varadarajan, R.; Chawla, H. M.; Hundal, G.; Hundal, M. S., *Tetrahedron* **2004,** *60* (4), 1001-1005.

155. Gigante, B.; Prazeres, A. O.; Marcelo-Curto, M. J.; Cornelis, A.; Laszlo, P., *J. Org. Chem.* **1995,** *60* (11), 3445-3447.

156. Gottlieb, H. E.; Kotlyar, V.; Nudelman, A., *J. Org. Chem.* **1997,** *62* (21), 7512-7515.

157. Strobel, M.; Kita-Tokarczyk, K.; Taubert, A.; Vebert, C.; Heiney, P. A.; Chami, M.; Meier, W., *Adv. Funct. Mater.* **2006,** *16* (2), 252-259.

158. Ikeda, A.; Nagasaki, T.; Araki, K.; Shinkai, S., *Tetrahedron* **1992,** *48* (6), 1059-1070.

159. Snieckus, V., *Chem. Rev.* **1990,** *90* (6), 879-933.

160. Townsend, C. A.; Bloom, L. M., *Tetrahedron Lett.* **1981,** *22* (40), 3923-3924.

161. Blair, A.; Kazerouni, N., *Cancer Causes & Control* **1997,** *8* (3), 473-490.

162. Li, X.; Gibb, B. C., *Supramol. Chem.* **2003,** *15* (7-8), 495-503.

163. Bonger, K. M.; van den Berg, R. J. B. H. N.; Heitman, L. H.; Ijzerman, A. P.; Oosterom, J.; Timmers, C. M.; Overkleeft, H. S.; van der Marel, G. A., *Biorg. Med. Chem.* **2007,** *15* (14), 4841-4856.

164. Jiang, Z.-Y.; Wang, Y.-G., *Tetrahedron Lett.* **2003,** *44* (19), 3859-3861.

165. Davies, J. S.; Higginbotham, C. L.; Tremeer, E. J.; Brown, C.; Treadgold, R. C., *J. Chem. Soc., Perkin Trans. 1* **1992,** (22), 3043-3048.

166. Goff, C. M.; Matchette, M. A.; Shabestary, N.; Khazaeli, S., *Polyhedron* **1996,** *15* (21), 3897-3903.

167. Alfonsov, V. A.; Bredikhin, A. A.; Bredikhina, Z. A.; Eliseenkova, R. M.; Kataeva, O. N.; Litvinov, I. A.; Pudovik, M. A., *Struct. Chem.* **2008,** *19* (6), 873-878.

168. Talotta, C.; Gaeta, C.; Neri, P., *J. Org. Chem.* **2014,** *79* (20), 9842-9846.

169. Talotta, C.; Gaeta, C.; Troisi, F.; Monaco, G.; Zanasi, R.; Mazzeo, G.; Rosini, C.; Neri, P., *Org. Lett.* **2010,** *12* (13), 2912-2915.

170. Jat, K. R.; Khairwa, A., *Pulmonary Pharmacology & Therapeutics* **2013,** *26* (2), 239-248.

171. Brunetti, L.; Poiani, G.; Dhanaliwala, F.; Poppiti, K.; Haenam, K.; Dong-Churl, S., *American Journal of Health-System Pharmacy* **2015,** *72* (12), 1026-1035.

172. Nowak, R. M.; Emerman, C. L.; Schaefer, K.; DiSantostefano, R. L.; Vaickus, L.; Roach, J. M., *The American Journal of Emergency Medicine* **2004,** *22* (1), 29-36.

173. Donohue, J. F.; Hanania, N. A.; Ciubotaru, R. L.; Noe, L.; Pasta, D. J.; Schaefer, K.; Claus, R.; Andrews, W. T.; Roach, J., *Clinical Therapeutics* **2008,** *30*, 989-1002.

174. Bakale, R. P.; Wald, S. A.; Butler, H. T.; Gao, Y.; Hong, Y.; Nie, X.; Zepp, C. M., *Clinical Reviews in Allergy & Immunology* **1996,** *14* (1), 7-35.

175. Bannon, Y. B.; Corish, J.; Corrigan, O. I.; Masterson, J. G., *Drug Dev. Ind. Pharm.* **1988,** *14* (15-17), 2151-2166.

176. Rodriguez Bayon, A. M.; Corish, J.; Corrigan, O. I., *Drug Dev. Ind. Pharm.* **1993,** *19* (10), 1169-1181.

177. Patel, A.; Page, C. P.; Brown, M. B.; Jones, S. A., *J. Pharm. Pharmacol.* **2010,** *62* (10), 1283.

178. Qi, A.; Friend, J. R.; Yeo, L. Y.; Morton, D. A. V.; McIntosh, M. P.; Spiccia, L., *Lab on a Chip* **2009,** *9* (15), 2184-2193.

179. Thordarson, P., *Chem. Soc. Rev.* **2011,** *40* (3), 1305-1323.

180. Ouchi, M.; Inoue, Y.; Liu, Y.; Nagamune, S.; Nakamura, S.; Wada, K.; Hakushi, T., *Bull. Chem. Soc. Jpn.* **1990,** *63* (4), 1260-1262.

181. Sigma-Aldrich® HPLC Analysis of Salbutamol Enantiomers on Astec® CHIROBIOTIC® T. https://www.sigmaaldrich.com/technical-documents/articles/analytical-applications/hplc/hplc-analysis-of-salbutamol-enantiomers-g004512.html (accessed 27/11/2017).

182. Dasgupta, S.; Wu, J., *Org. Biomol. Chem.* **2011,** *9* (9), 3504-3515.

183. Boxhall, J. Y.; Page, P. C. B.; Elsegood, M. R. J.; Chan, Y.; Heaney, H.; Holmes, K. E.; McGrath, M. J., *Synlett* **2003,** *2003* (07), 1002-1006.

184. Gropp, C.; Quigley, B. L.; Diederich, F., *J. Am. Chem. Soc.* **2018,** *140* (8), 2705-2717.

185. Maffei, F.; Brancatelli, G.; Barboza, T.; Dalcanale, E.; Geremia, S.; Pinalli, R., *Supramol. Chem.* **2018,** *30* (7), 600-609.

186. De Simone, N. A.; Meninno, S.; Talotta, C.; Gaeta, C.; Neri, P.; Lattanzi, A., *J. Org. Chem.* **2018**.

187. Ngodwana, L.; Bose, S.; Smith, V. J.; Otterlo, W. A. L. v.; Arnott, G. E., *Eur. J. Inorg. Chem.* **2017,** *2017* (13), 1923-1929.

Appendix A

NMR and IR Spectra

Table of Contents

Appendix A

Appendix A

Appendix A

2 Distal functionalisation of resorcinarene by a calixarene rigid bridge

Synthesis of tetraamino- and tetraformyl- resorcinarenes via the *ortho* position

(1) $1^4,3^6,5^6,7^6$-tetrahydroxy-$1^6,3^4,5^4,7^4$-tetramethoxy-2,4,6,8-tetrapropylresorcin[4]arene
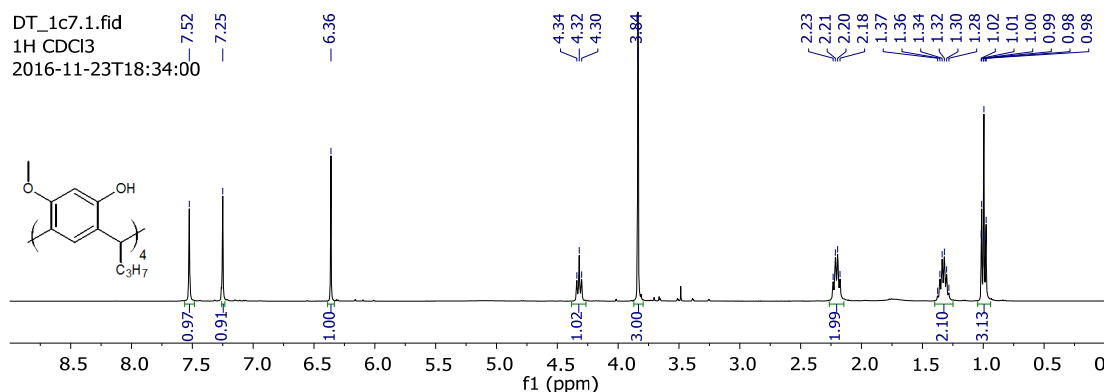
Appendix A1.1 (1) ^{1}H NMR spectrum recorded in CDCl$_3$.

(2) $1^4,3^6,5^6,7^6$-tetrahydroxy-$1^6,3^4,5^4,7^4$-tetramethoxy-$1^5,3^5,5^5,7^5$-tetra(dimethylaminomethylene)-2,4,6,8-tetrapropylresorcin[4]arene
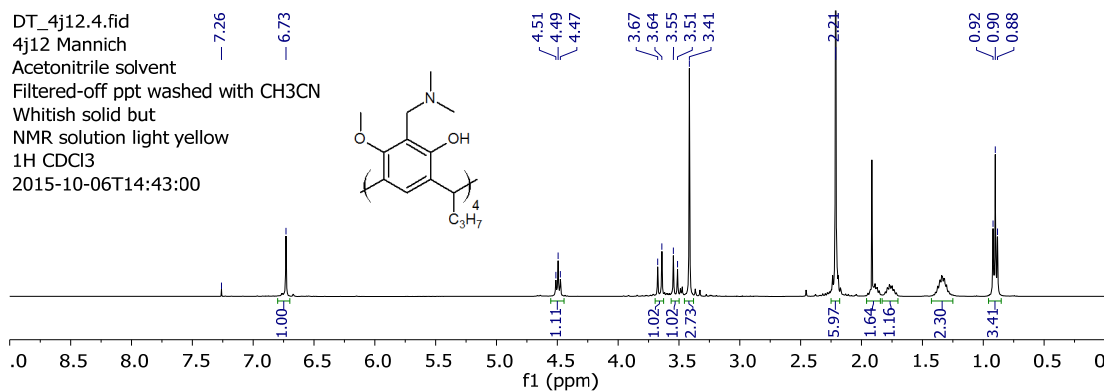
Appendix A2.1 (2) ^{1}H NMR spectrum recorded in CDCl$_3$.
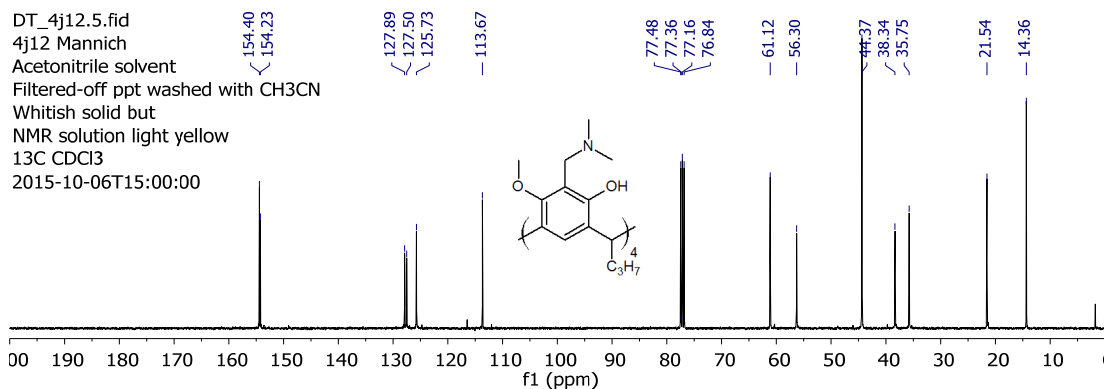
Appendix A2.2 (2) ^{13}C NMR spectrum recorded in CDCl$_3$.
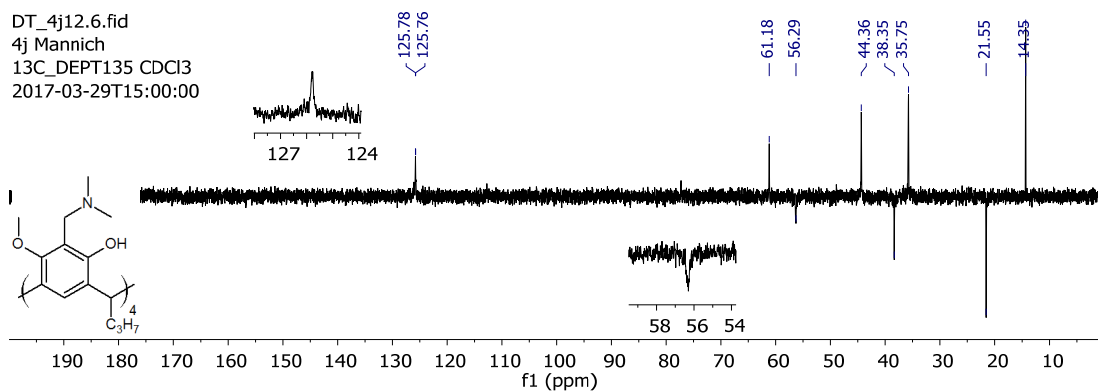
Appendix A - 1

Appendix A2.3 **(2)** DEPT-135 NMR spectrum recorded in CDCl₃.
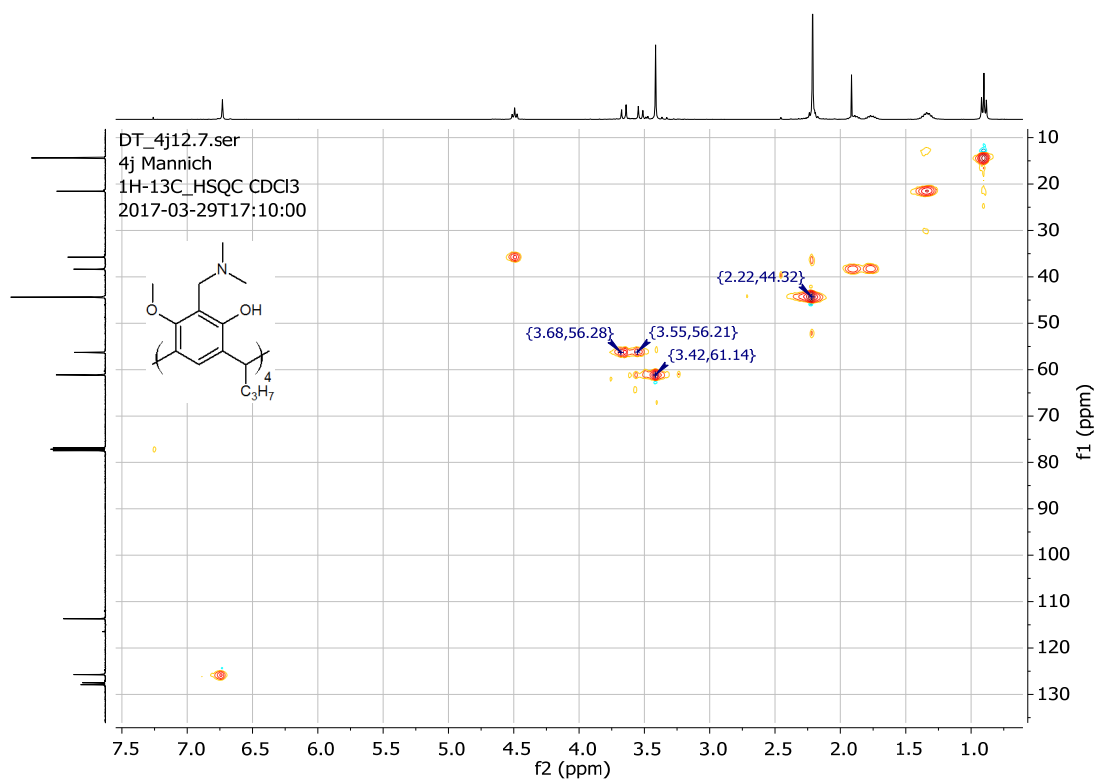
Appendix A2.4 **(2)** HSQC NMR spectrum recorded in CDCl₃.

Analyst
Date

Analyst
Friday, 15 April 2016 2:56 PM

PEIR2002325_1   DT_4j Mannich Me2N
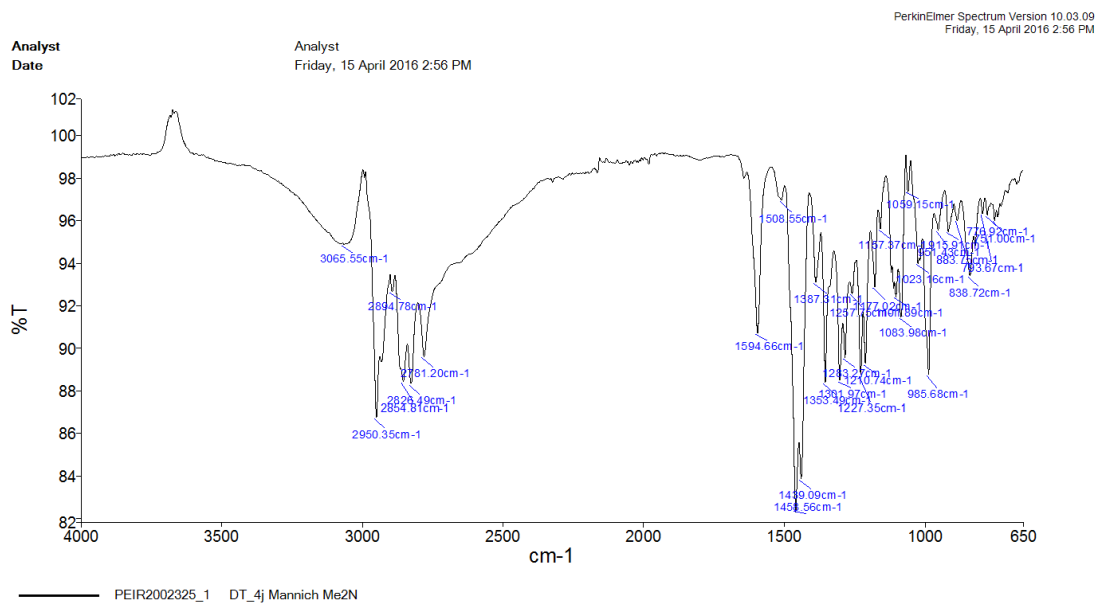
Appendix A2.5 (2) IR spectrum.

Synthesis of tetraamino- and tetraformyl- resorcinarenes via phenols

(3) $1^4,3^6,5^6,7^6$-tetratrifluoromethanesulfonyl-$1^6,3^4,5^4,7^4$-tetramethoxy-2,4,6,8-tetrapropylresorcin[4]arene

DT_2f9.1.fid
2f9 OTf
recrys 2x
Elemental analysis sample
1H CDCl3
2016-01-28T11:57:00
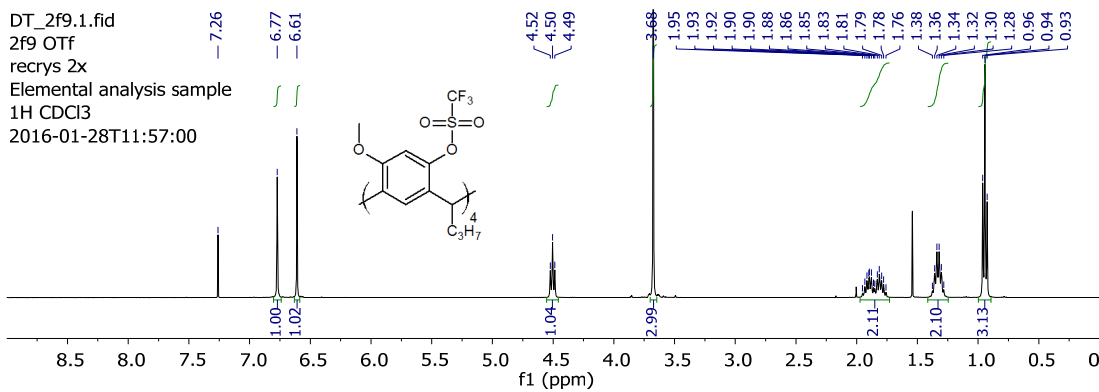
Appendix A3.1 (3) ^{13}C NMR spectrum recorded in CDCl$_3$.

DT_2f9.5.fid
2f9 resorcinarene OTf
13C CDCl3
2016-02-08T13:55:00
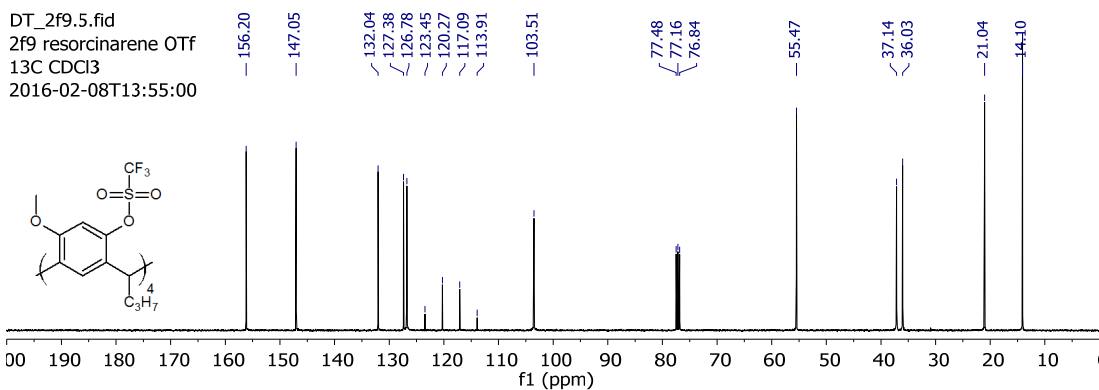
Appendix A3.2 (3) ^{13}C NMR spectrum recorded in CDCl$_3$.
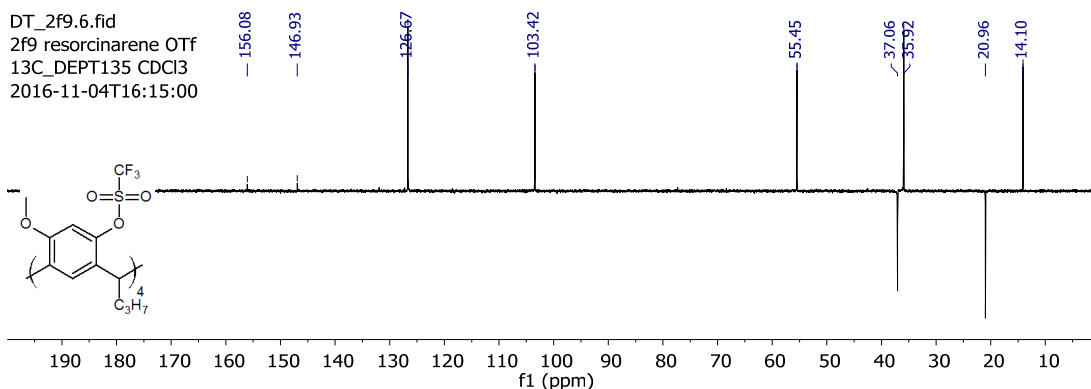
Appendix A3.3 **(3)** DEPT-135 NMR spectrum recorded in CDCl₃.

(4) 1⁴,3⁶,5⁶,7⁶- tetramethoxy-1⁶,3⁴,5⁴,7⁴-tetranitrile -2,4,6,8-tetrapropylresorcin[4]arene
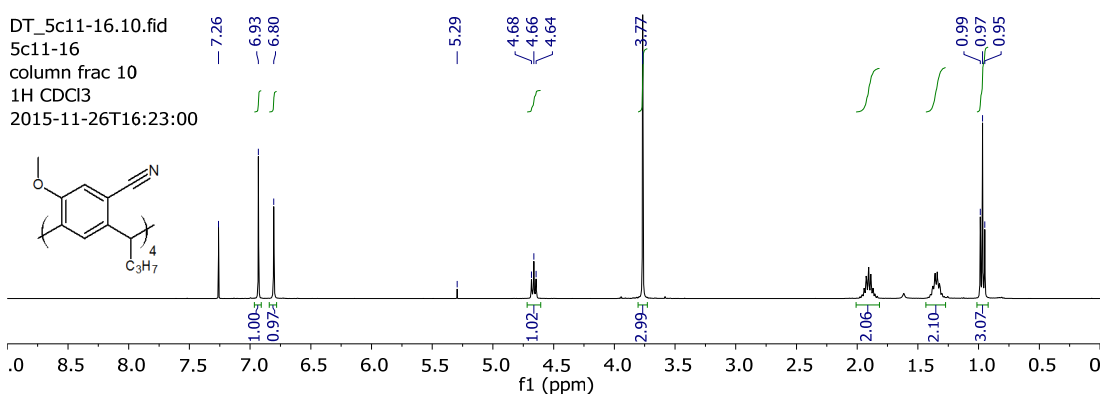
Appendix A4.1 **(4)** ^{1}H NMR spectrum recorded in CDCl₃.
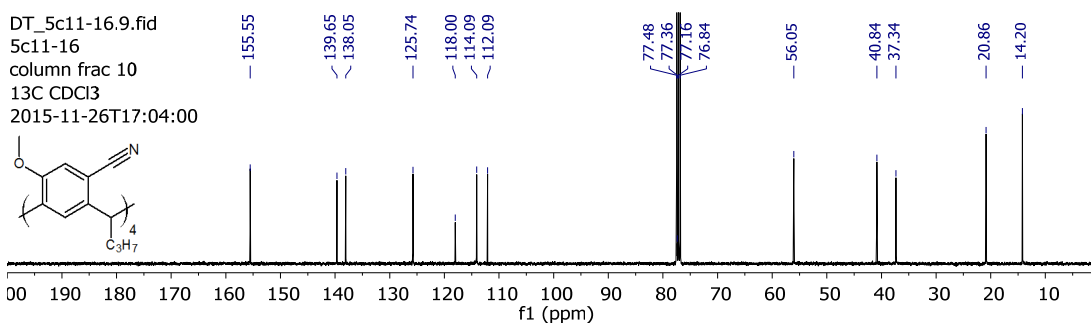
Appendix A4.2 **(4)** ^{13}C NMR spectrum in CDCl₃.
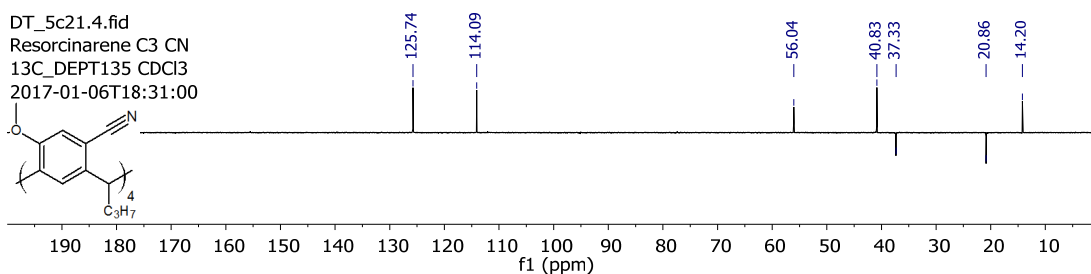
Appendix A4.3 **(4)** DEPT-135 NMR spectrum recorded in CDCl₃.
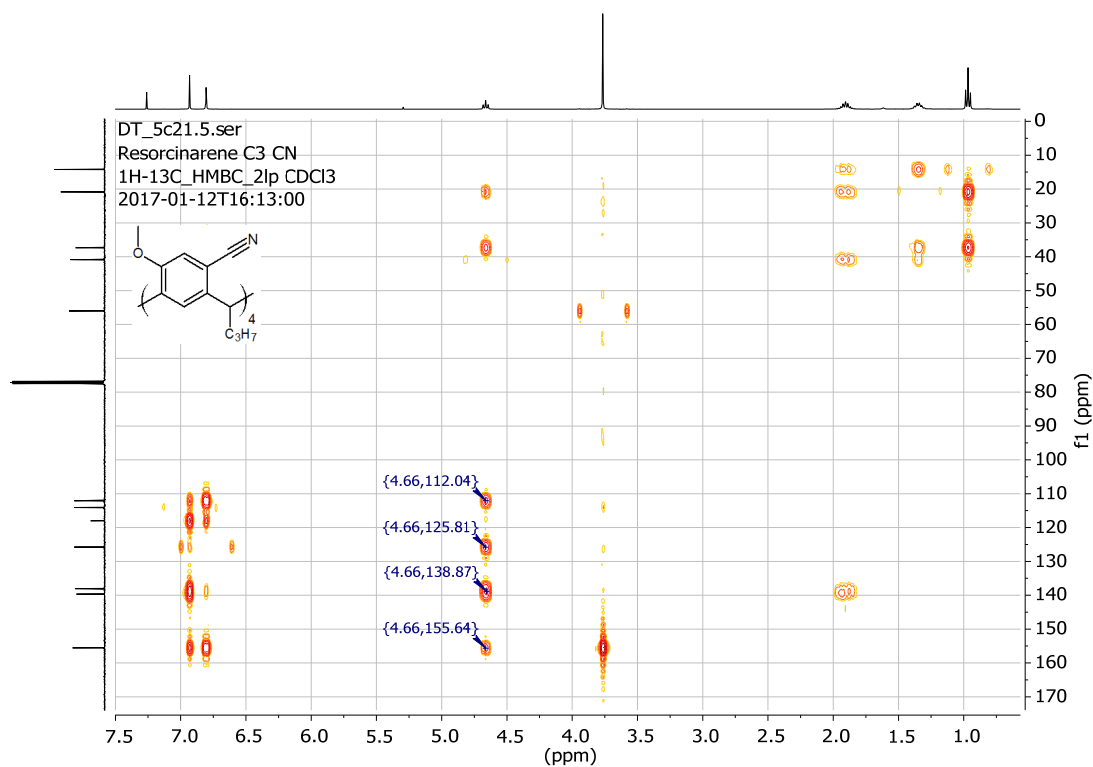
Appendix A4.4 **(4)** HMBC NMR spectrum recorded in CDCl₃.
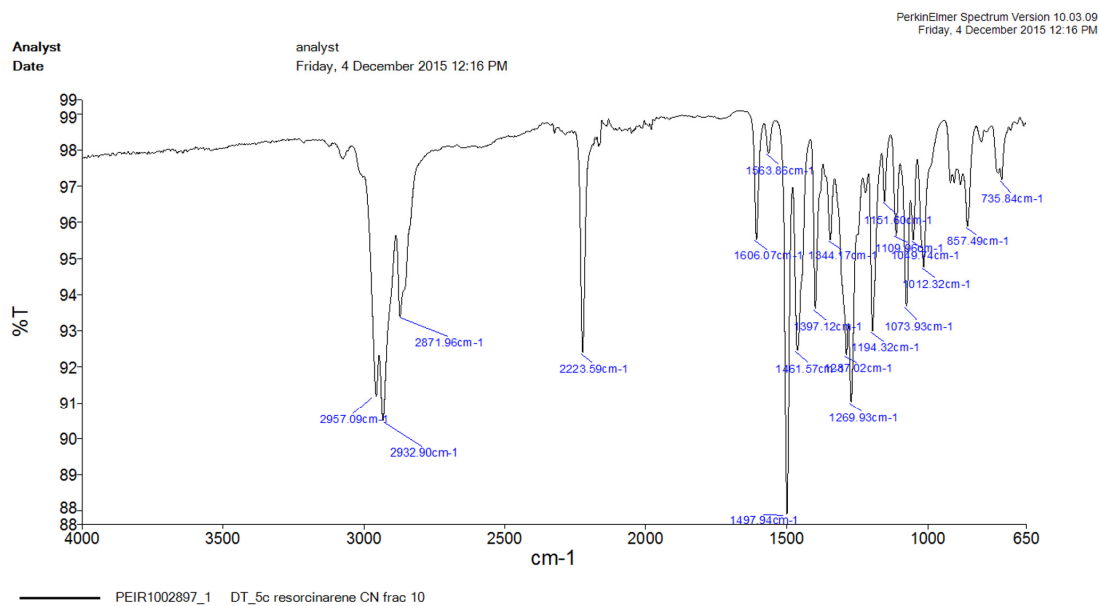
Appendix A4.5 **(4)** IR spectrum.

(5) $1^4,3^6,5^6,7^6$-tetraformyl-$1^6,3^4,5^4,7^4$-tetramethoxy-2,4,6,8-tetrapropylresorcin[4]arene

7.26 7.22 6.95   5.13 5.11 5.09   3.71   0.99 0.97 0.95

1.00   1.04 1.00   1.08   3.14   2.06 2.27 3.26
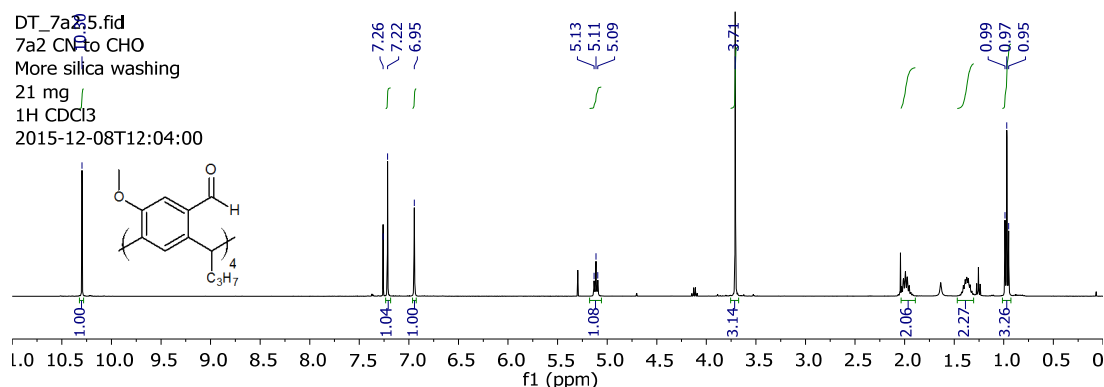
Appendix A5.1 (5) ^{1}H NMR spectrum recorded in CDCl$_3$.

154.86   140.07 139.61 132.85 126.75   109.60   77.48 77.16 76.84   55.66   37.74 36.85   21.15   14.33
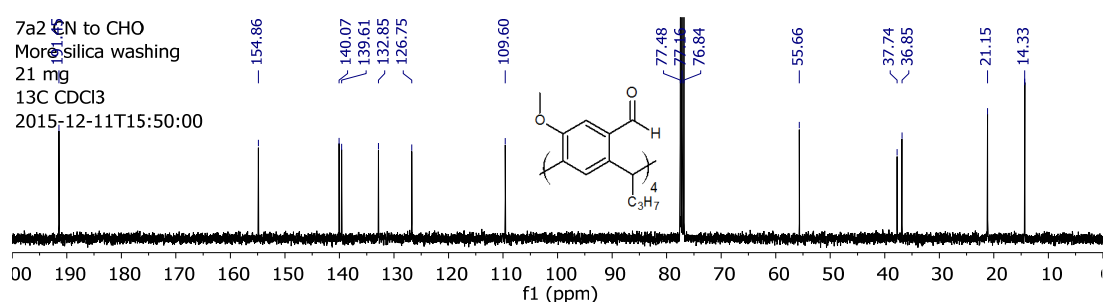
Appendix A5.2 (5) ^{13}C NMR spectrum.

191.44   126.75   109.60   55.66   37.74 36.85   29.84   21.15   14.33
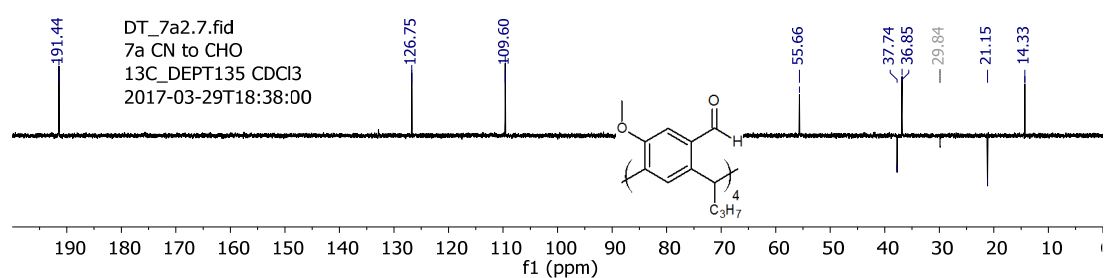
Appendix A5.3 (5) DEPT-135 NMR spectrum recorded in CDCl$_3$.

(6) $1^4,3^6,5^6,7^6$-tetra(amminomethyl)-$1^6,3^4,5^4,7^4$-tetramethoxy-2,4,6,8-tetrapropylresorcin[4]arene

7.26   6.74 6.68   4.39 4.37 4.35 3.81 3.77 3.68 3.56 3.53 1.97 1.95 1.93 1.91 1.90 1.88 1.86 1.84 1.83 1.82 1.81 1.79 1.77 1.43 1.39 1.37 1.35 1.33 0.96 0.94 0.92

0.95 1.00   1.05   1.12 2.98 1.12   1.17 1.21   2.68   3.71
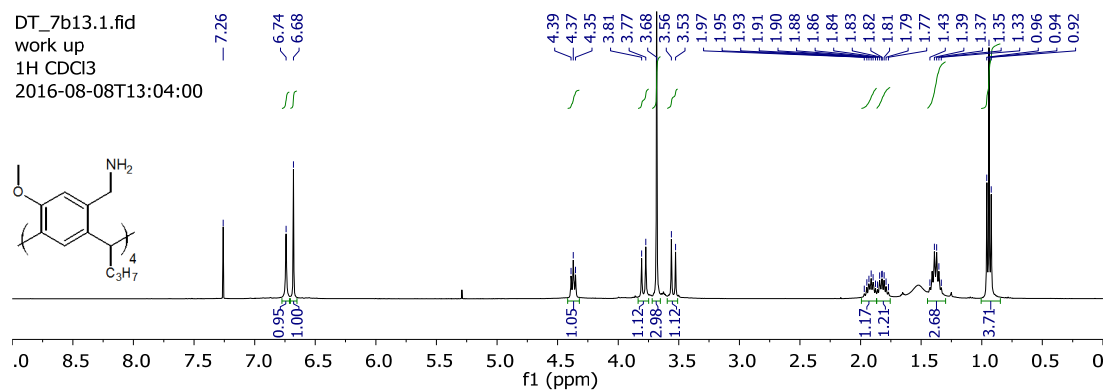
Appendix A6.1 (6) ^{1}H NMR spectrum recorded in CDCl$_3$.

154.73
140.05
134.76
131.73
126.35
110.73
77.48
76.84
55.36
43.79
38.08
37.95
21.41
14.46

f1 (ppm)
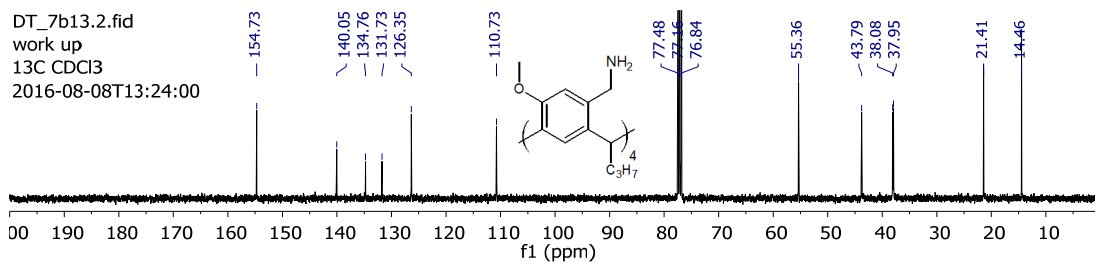
Appendix A6.2 **(6)** ^{13}C NMR spectrum in CDCl$_3$.

126.34
110.75
55.36
43.78
38.08
37.94
21.41
14.46

CH2NH2

f1 (ppm)
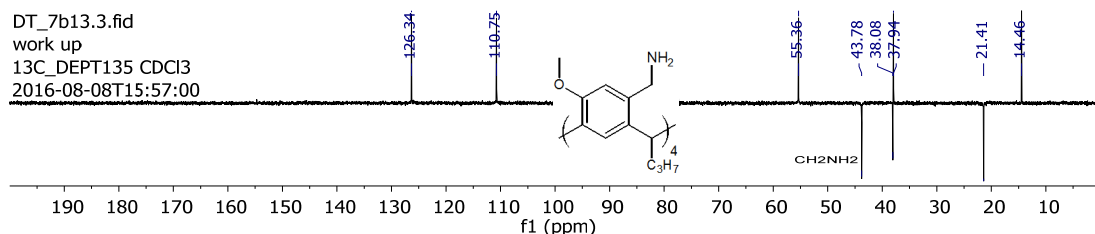
Appendix A6.3 **(6)** DEPT-135 NMR spectrum recorded in CDCl$_3$.

%T

1610.7
1570
3280.7
3375.36cm-1
1088.63cm-1
1404.73cm-1
1193.85cm-1
1455.66cm-1
1262.30cm-1
1497.54cm-1
2929.46cm-1

cm-1

PEIR1003431_1   DT_7b13 resorcinarene tetra NH2
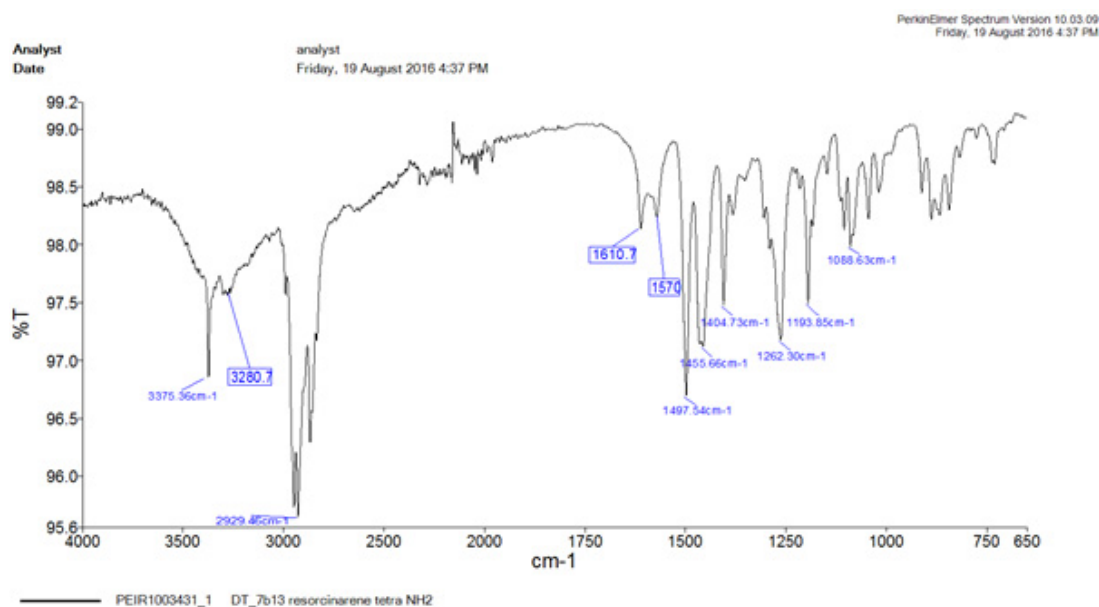
Appendix A6.4 **(6)** IR spectrum.

Synthesis of a calixarene as a rigid bridge

(8) 25,27-Dihydroxy-26,28-di-*n*-propoxycalixarene

8.29
7.26
7.07
7.05
6.94
6.92
6.77
6.75
6.73
6.67
6.65
6.63
4.35
4.32
4.00
3.99
3.97
3.40
3.37
2.12
2.11
2.09
2.07
2.06
2.04
1.34
1.32
1.31

OH PrO OPr HO

1.78
4.04
4.00
1.97
1.90
3.91
3.97
3.83
4.01
5.92

f1 (ppm)
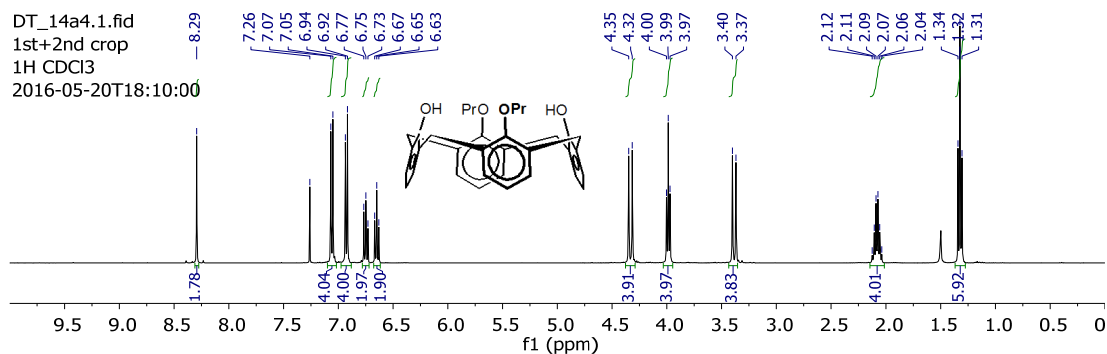
Appendix A7.1 **(8)** ^{1}H NMR spectrum recorded in CDCl$_3$.
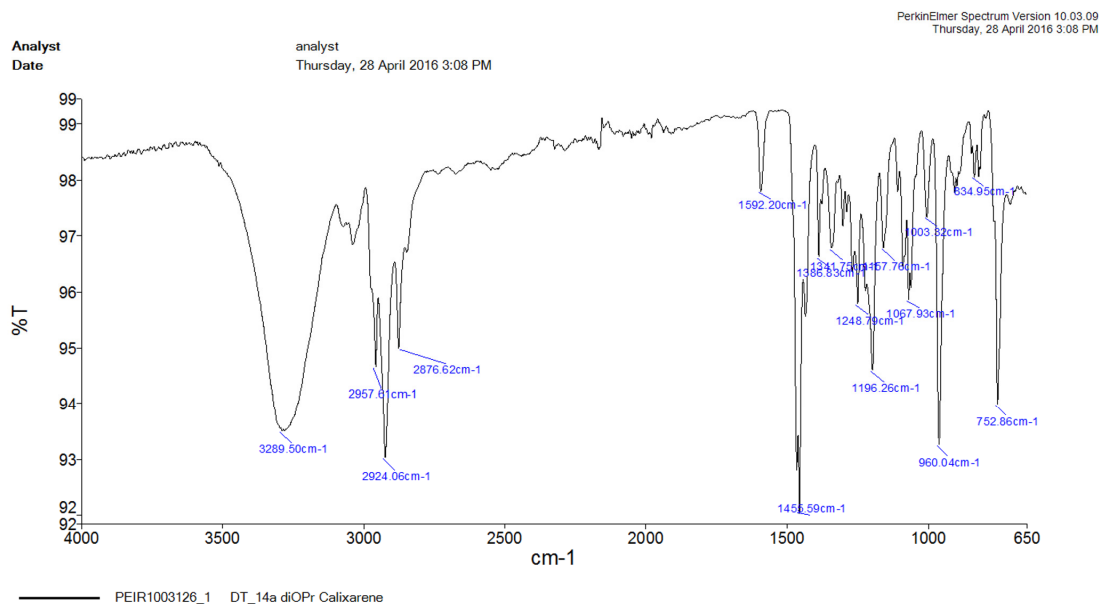
Appendix A - 7

Appendix A7.2 **(8)** IR spectrum.

(9) 5,17-Diformyl-25,27-dihydroxy-26,28-di-*n*-propoxycalixarene
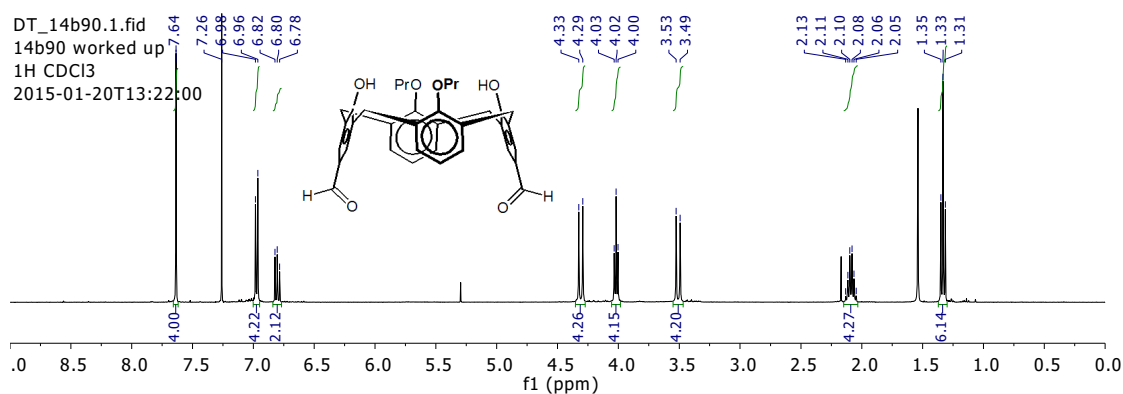
Appendix A8.1 **(9)** ^{1}H NMR spectrum recorded in CDCl$_3$.
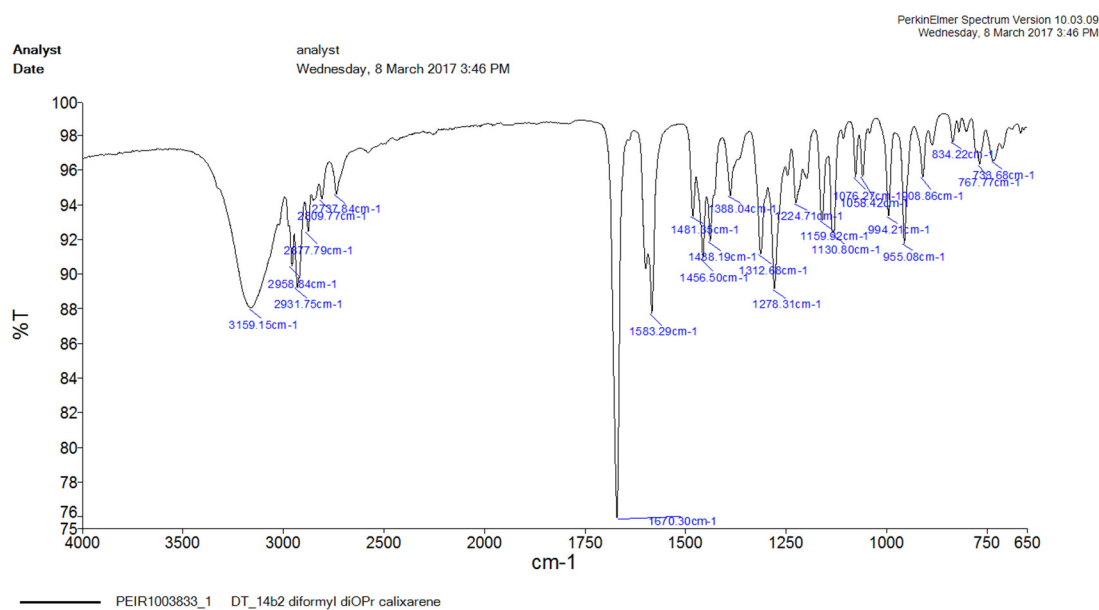
Appendix A8.2 **(9)** IR spectrum.

Appendix A - 8

(10) 5,17-Dinitro-26,28-dipropoxycalixarene
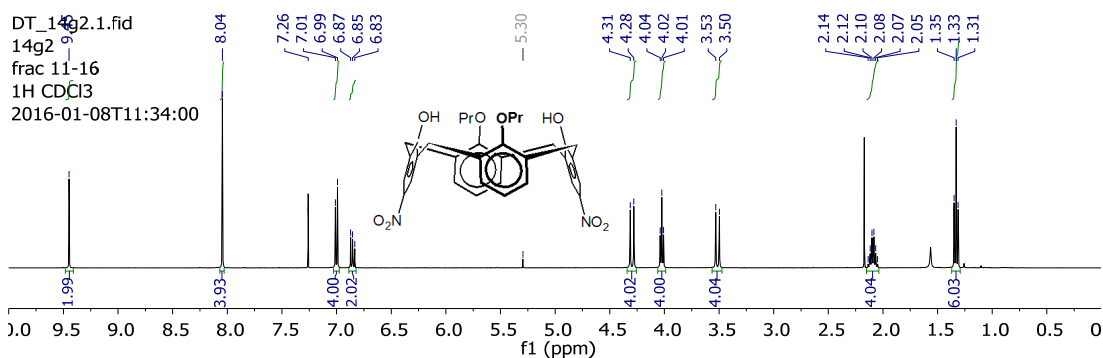
Appendix A9.1 **(10)** ^{1}H NMR spectrum recorded in CDCl$_3$.

(11) 5,17-Diamino-26,28-dipropoxycalixarene
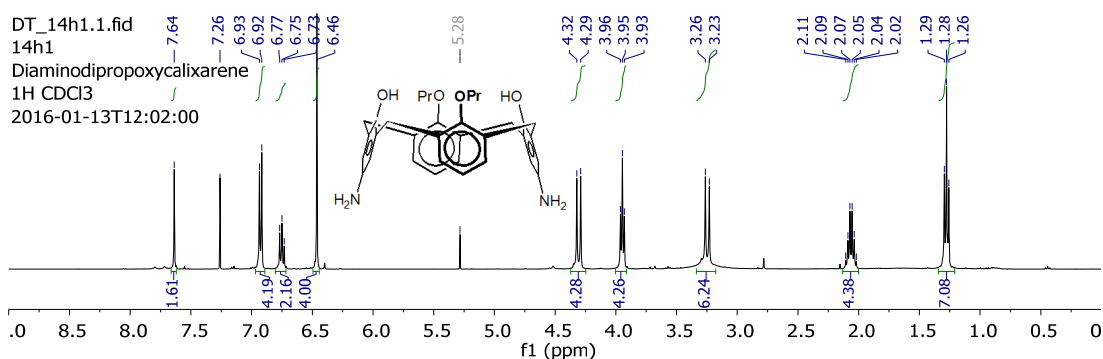
Appendix A10.1 (11) ^{1}H NMR spectrum recorded in CDCl$_3$.

(12) di((ethoxycarbonyl)methoxy) calixarene cone
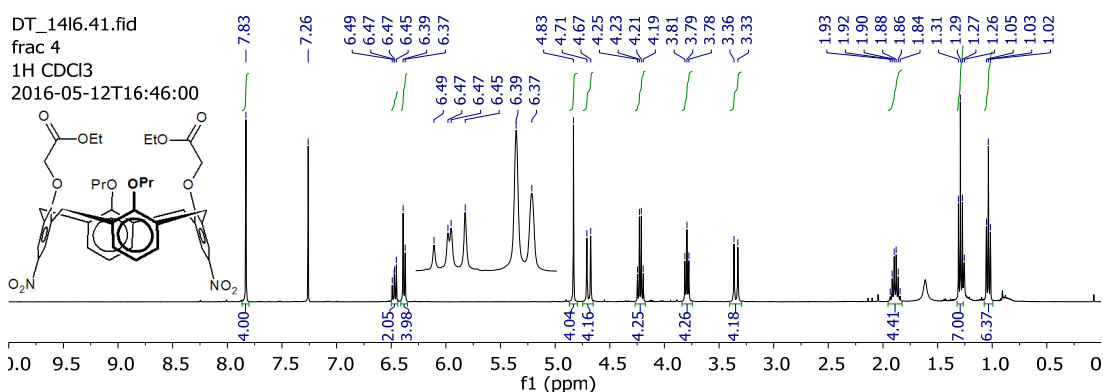
Appendix A11.1 (12) ^{1}H NMR spectrum recorded in CDCl$_3$.
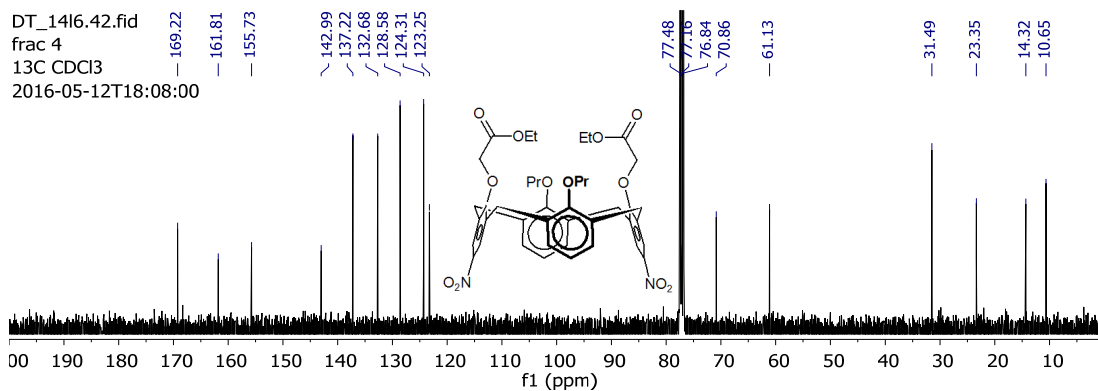
Appendix A11.2 (12) ^{13}C NMR spectrum recorded in CDCl$_3$.
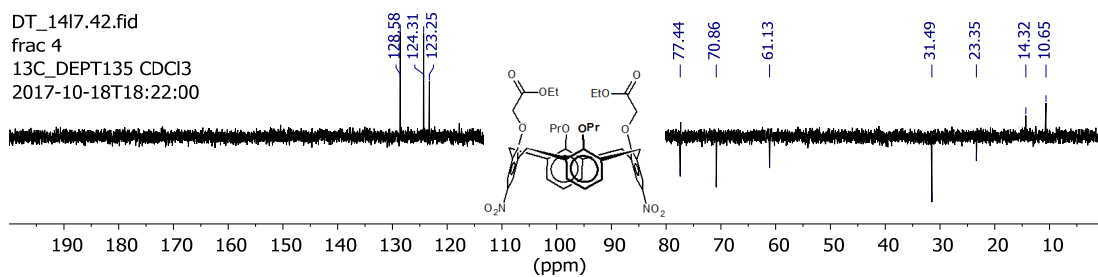
Appendix A11.3 (12) DEPT-135 NMR spectrum recorded in CDCl$_3$.
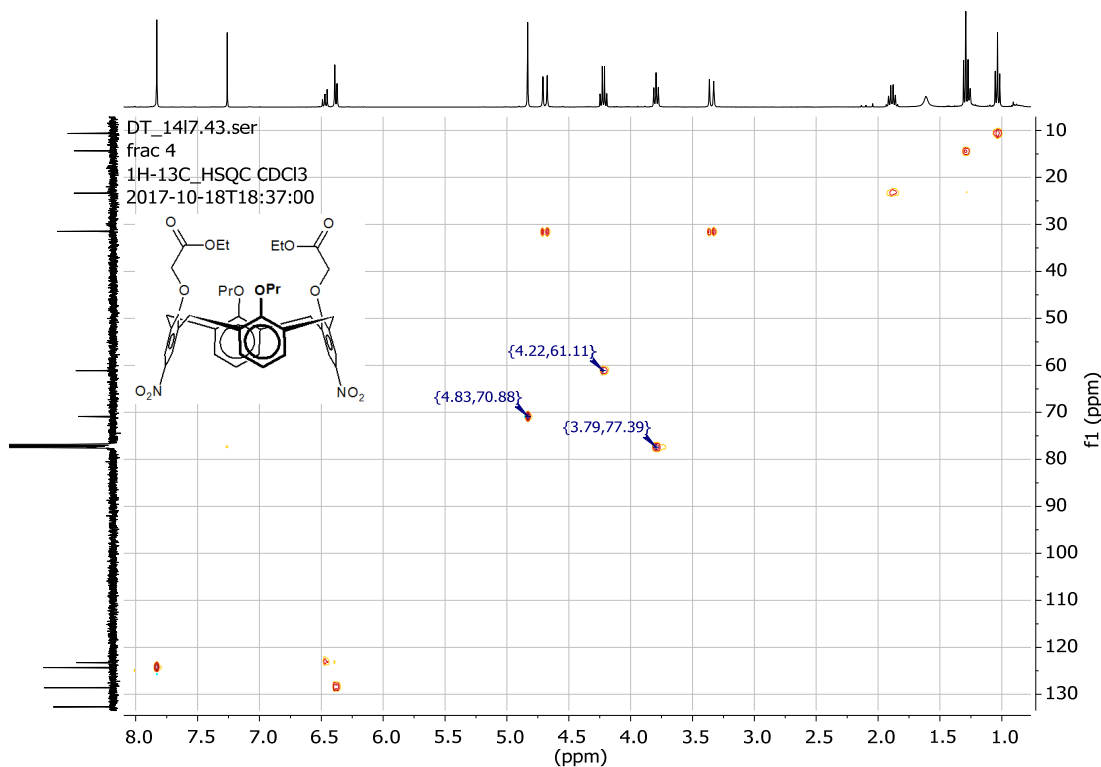
Appendix A11.4 (12) HSQC NMR spectrum recorded in CDCl$_3$.
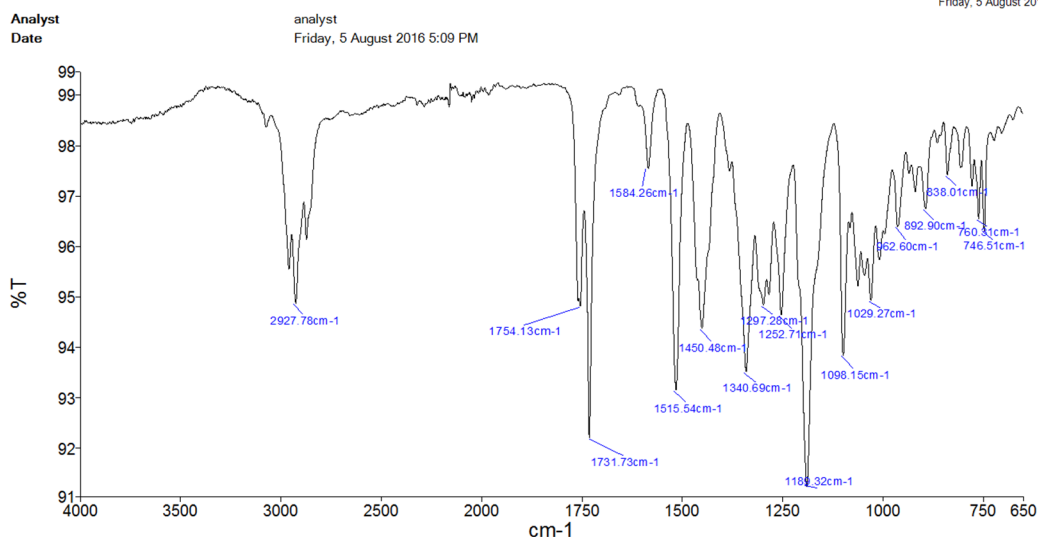
Appendix A11.5 (12) IR spectrum.

(13) di((ethoxycarbonyl)methoxy) calixarene partial cone
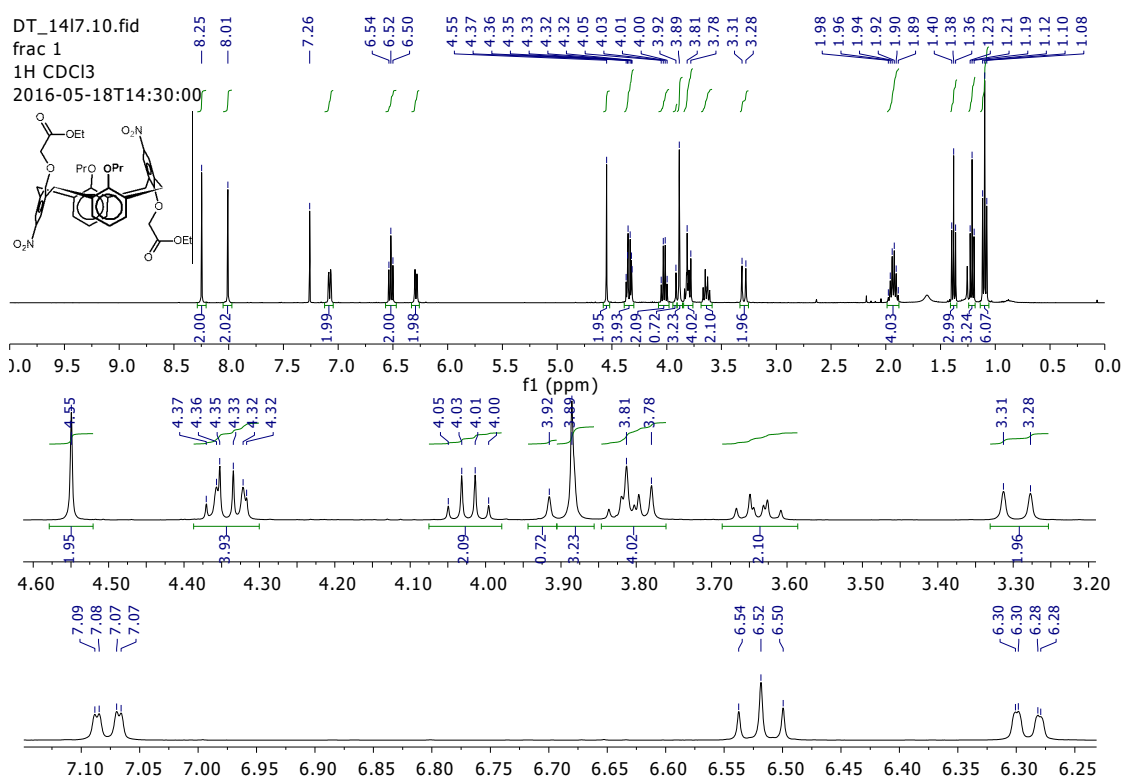
Appendix A12.1 (13) ^{1}H NMR spectrum recorded in CDCl$_3$.
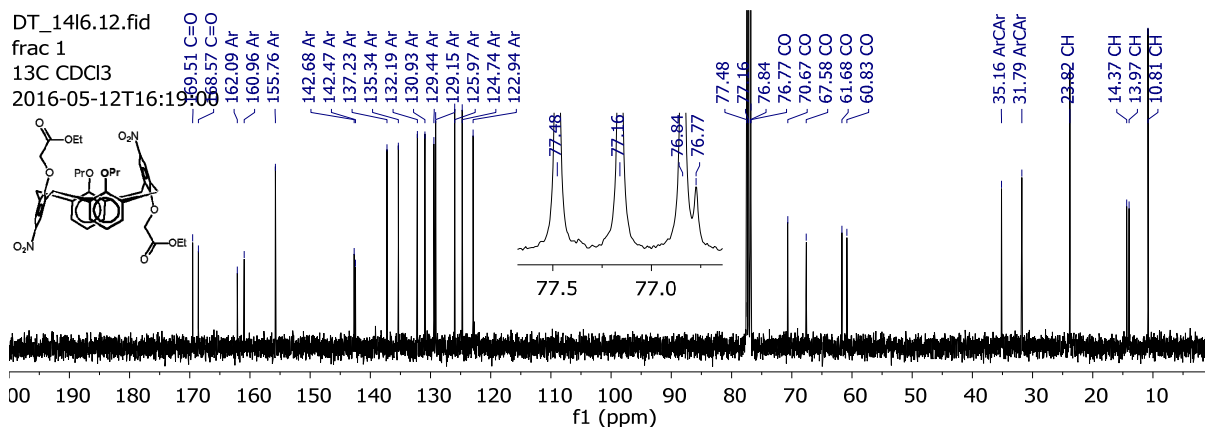
Appendix A12.2 (13) ^{13}C NMR spectrum.
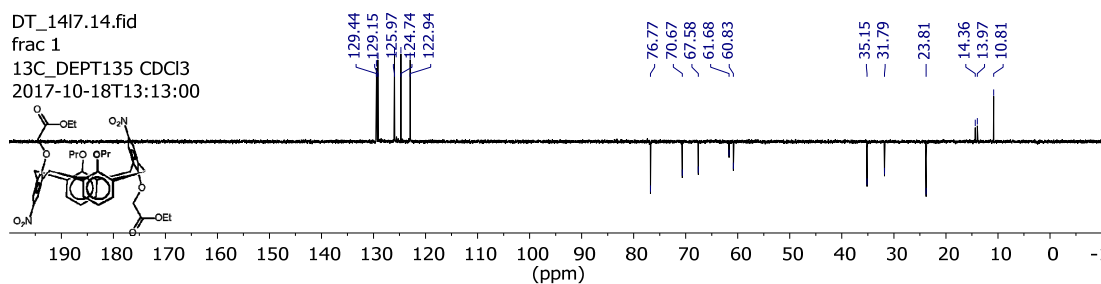
Appendix A12.3 (13) DEPT-135 NMR spectrum recorded in CDCl$_3$.
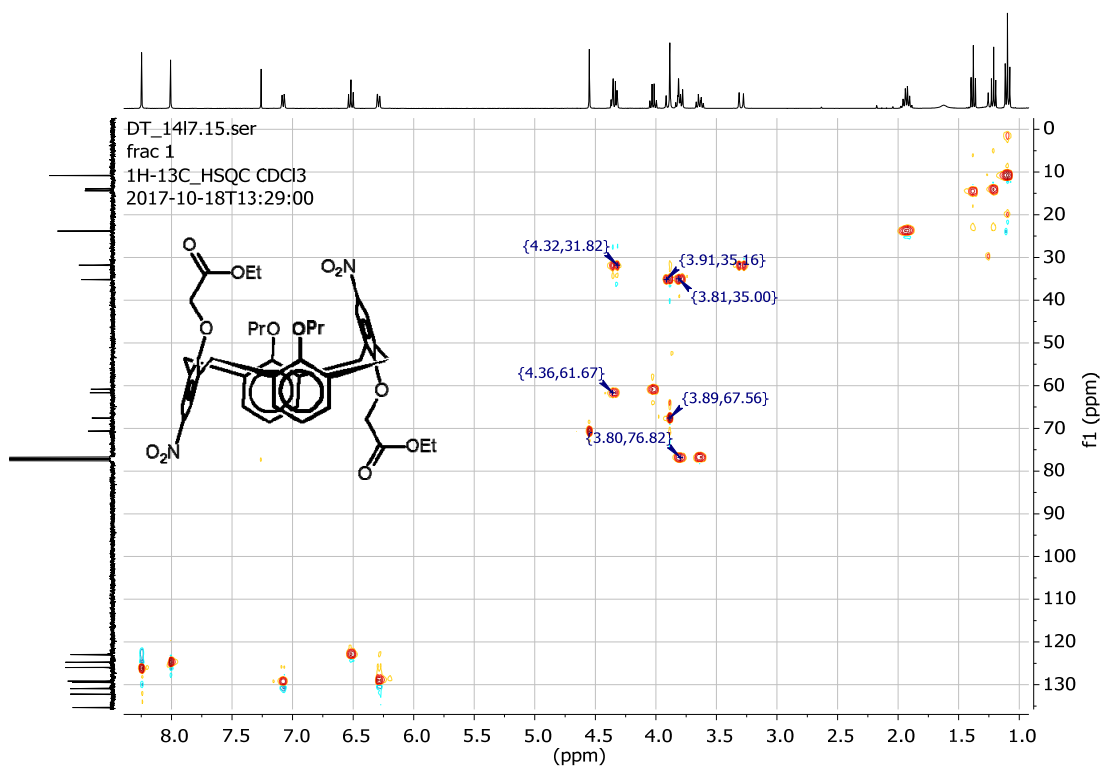
Appendix A12.4 (13) HSQC NMR spectrum recorded in CDCl$_3$.
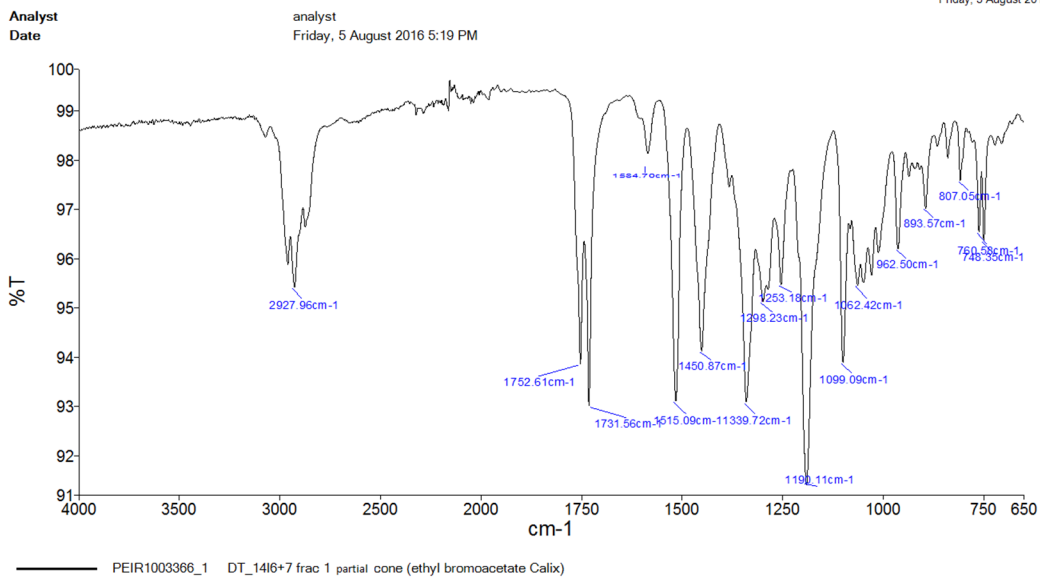
Appendix A - 12

Appendix A12.5 (13) IR spectrum.

(14) Allyl calixarene cone
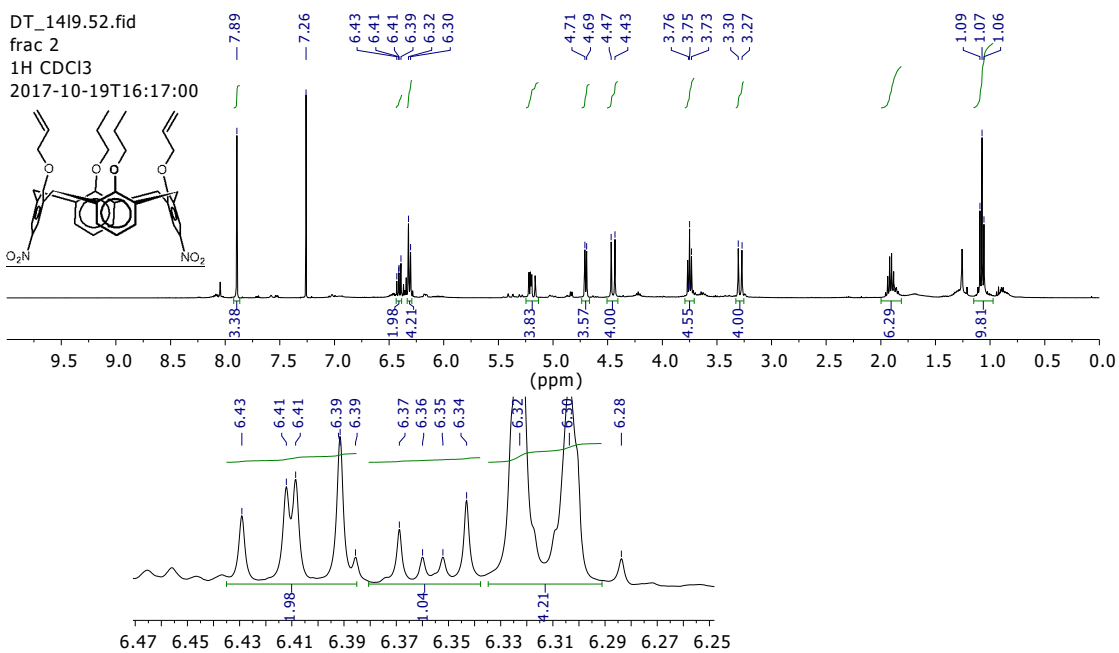
Appendix A13.1 (14) ^{1}H NMR spectrum recorded in CDCl$_3$.
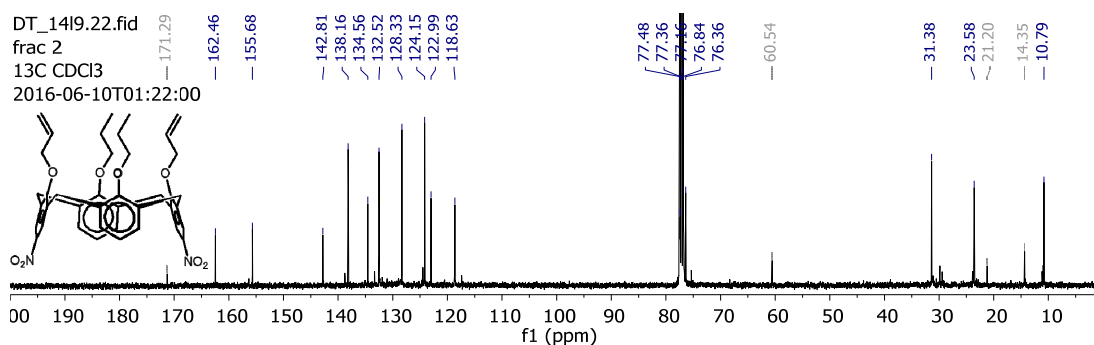
Appendix A13.2 (14) ^{13}C NMR spectrum recorded in CDCl$_3$.
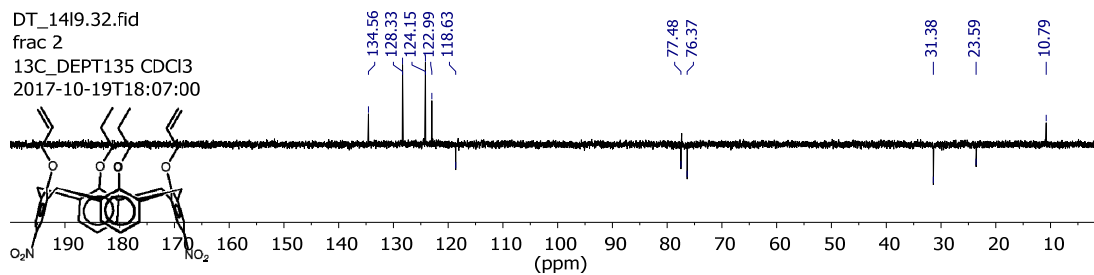
Appendix A13.3 (14) DEPT-135 NMR spectrum recorded in CDCl$_3$.
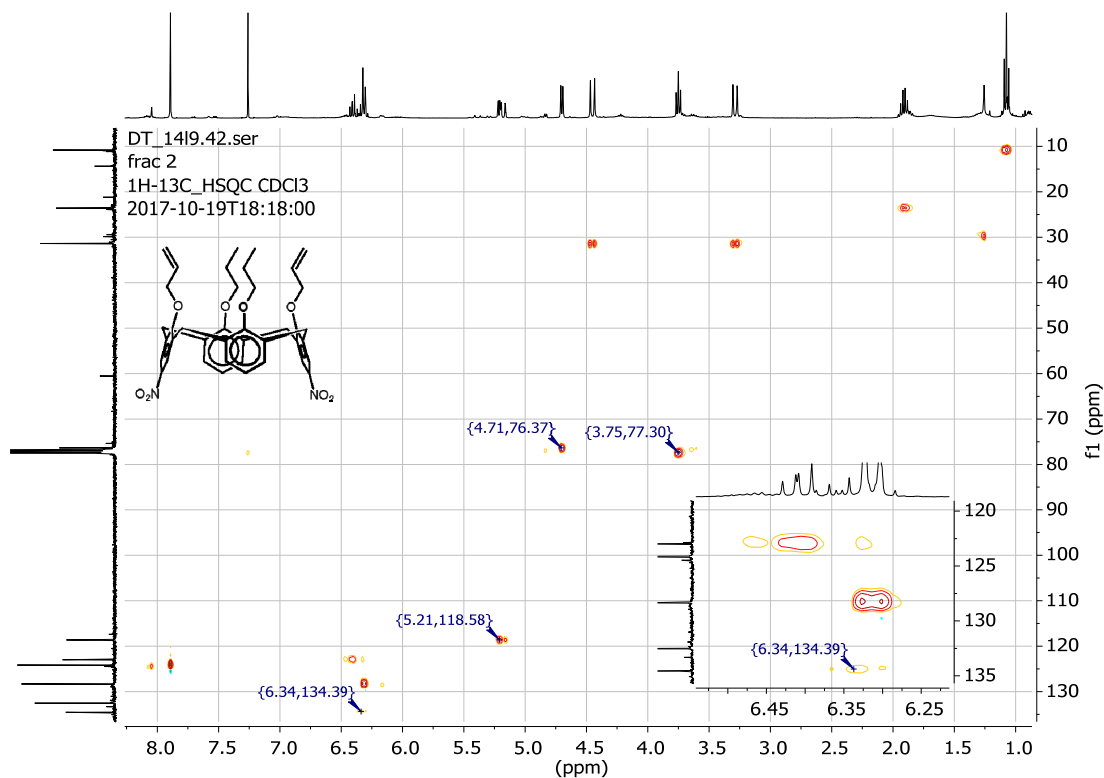
Appendix A13.4 (14) HSQC NMR spectrum recorded in CDCl$_3$.
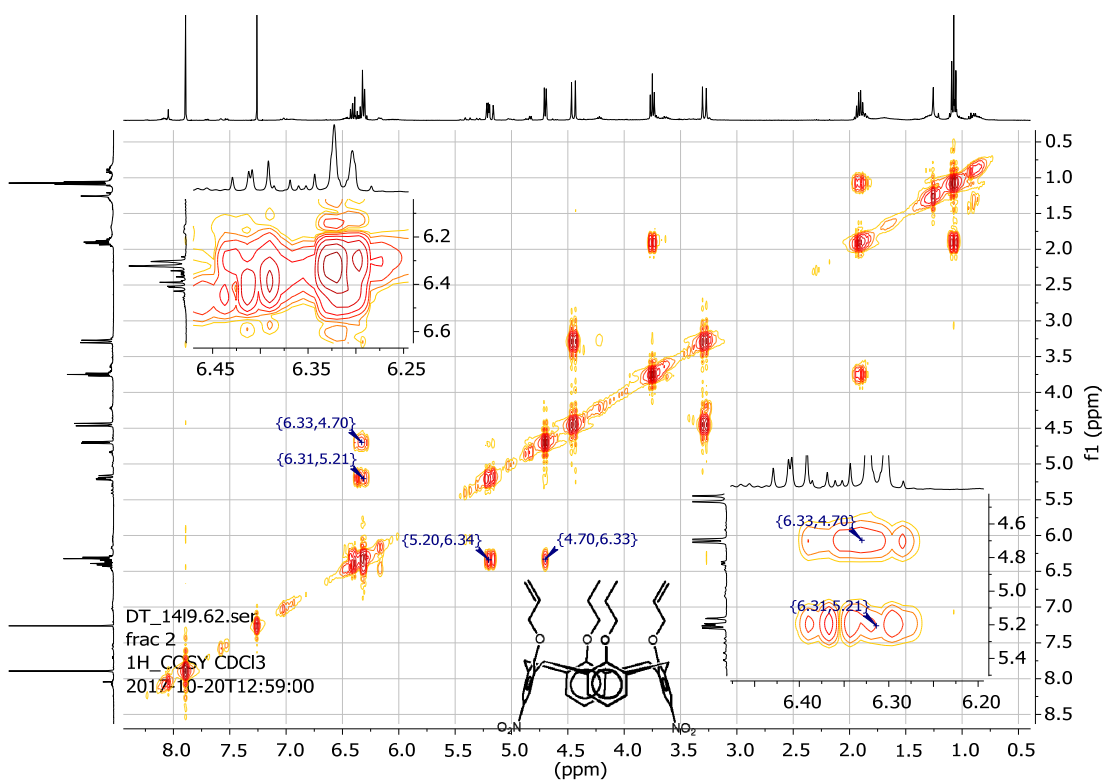
Appendix A13.5 (14) COSY NMR spectrum recorded in CDCl₃.

(15) Allyl calixarene partial cone
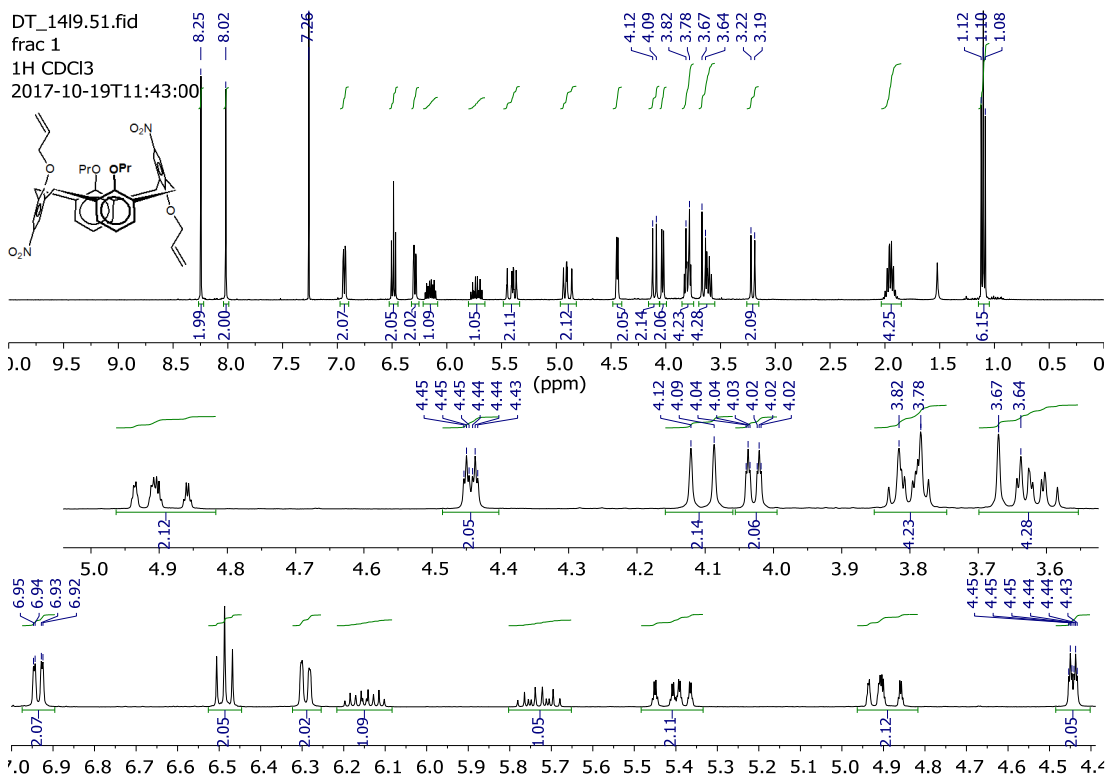
Appendix A14.1 (15) ¹H NMR spectrum recorded in CDCl₃.
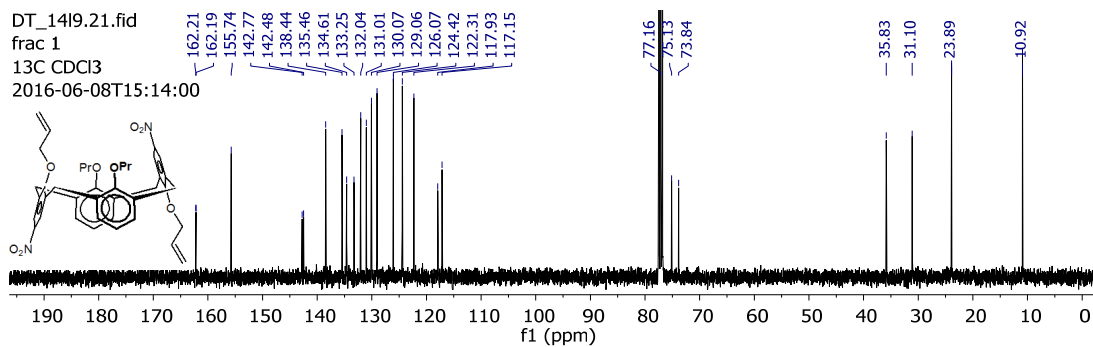
Appendix A14.2 (15) ^{13}C NMR spectrum recorded in CDCl$_3$.
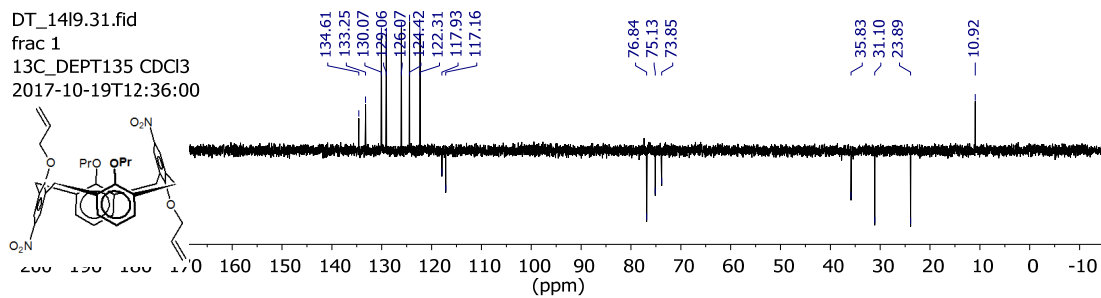
Appendix A14.3 (15) DEPT-135 NMR spectrum recorded in CDCl$_3$.
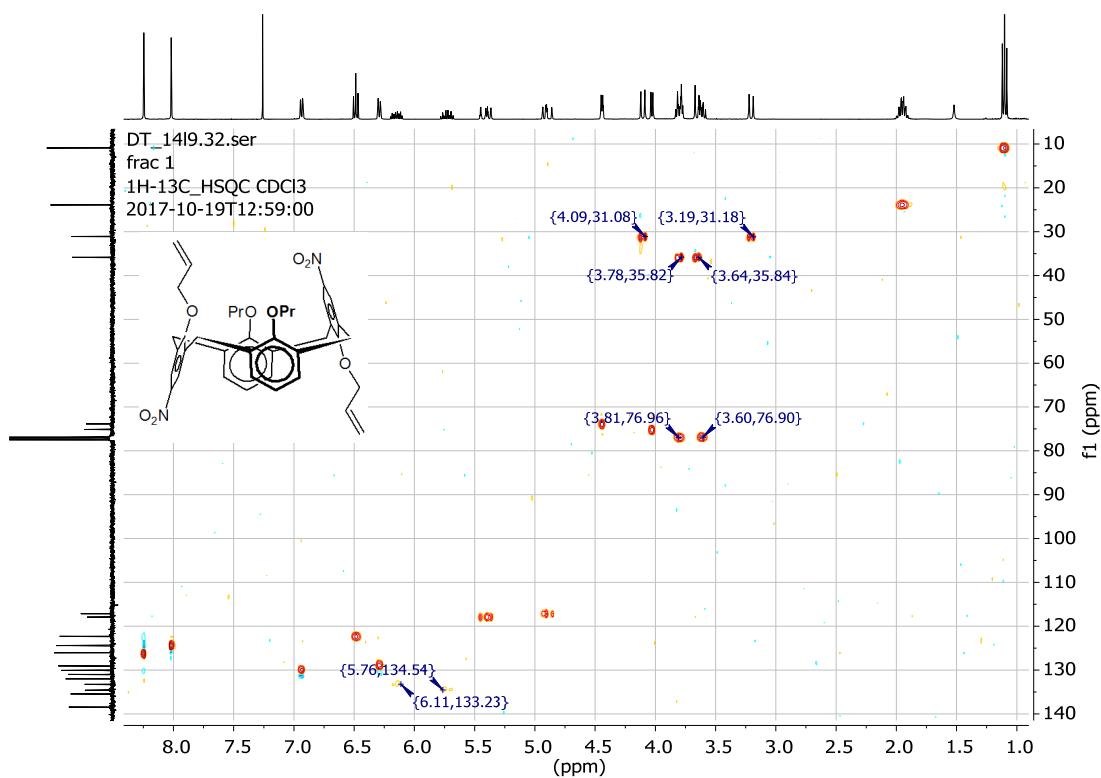
Appendix A14.4 (15) HSQC NMR spectrum recorded in CDCl$_3$.

(16) Allyl calixarene 1,3-alternate
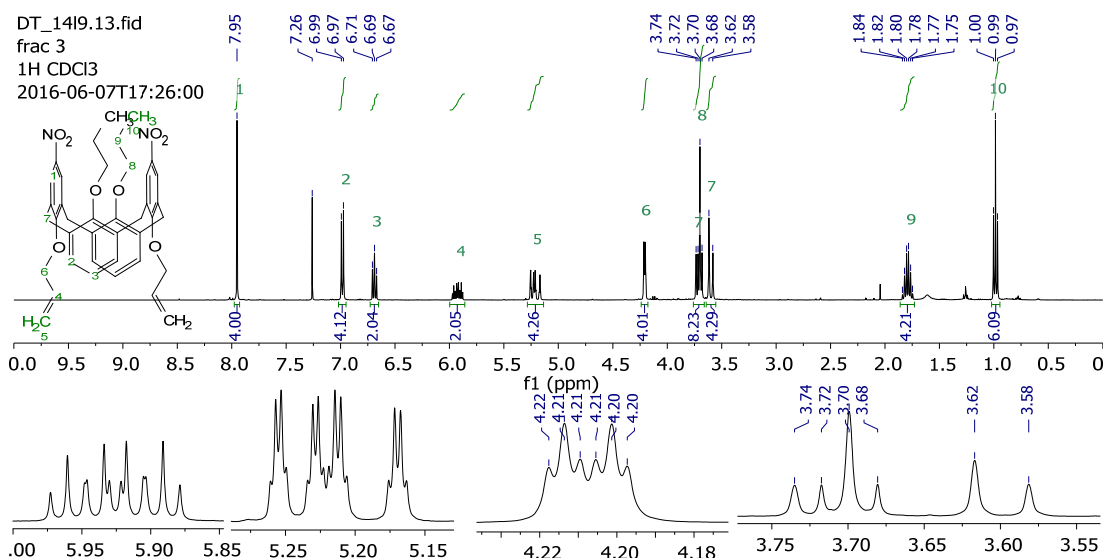
Appendix A15.1 (16) ^{1}H NMR spectrum recorded in CDCl$_3$.
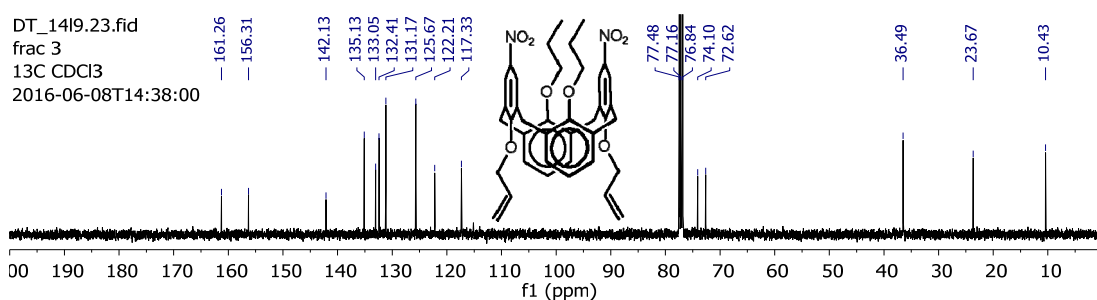
Appendix A15.2 (16) ^{13}C NMR spectrum recorded in CDCl$_3$.
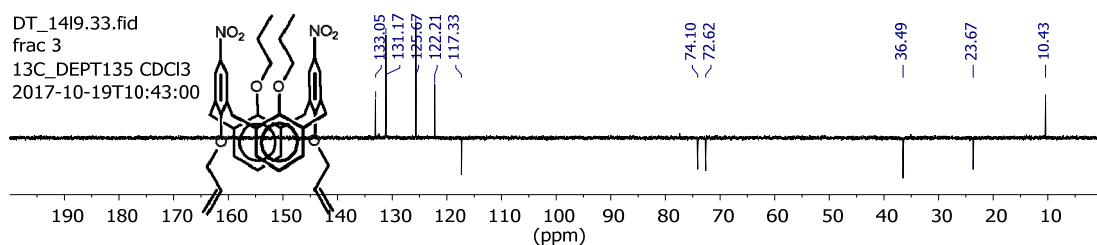
Appendix A15.3 (16) DEPT-135 NMR spectrum recorded in CDCl$_3$.
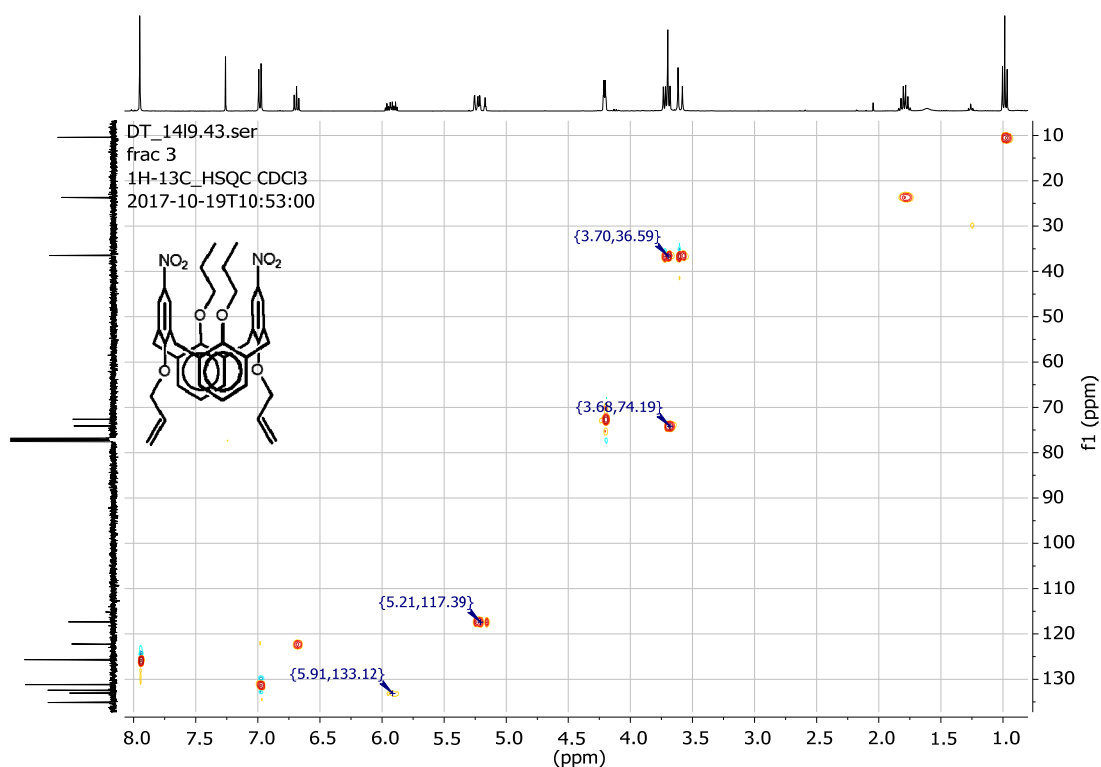
Appendix A15.4 (16) HSQC NMR spectrum recorded in CDCl₃.

(17) 25,26,27,28-Tetrapropoxycalixarene
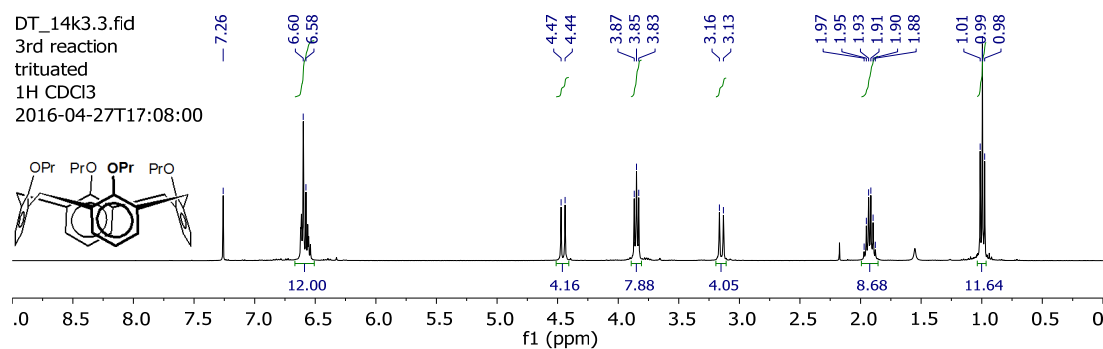
Appendix A16.1 (17) ¹H NMR spectrum recorded in CDCl₃.

(18) 5,11,17,23-Tetrabromo-25,26,27,28-tetrapropoxycalixarene
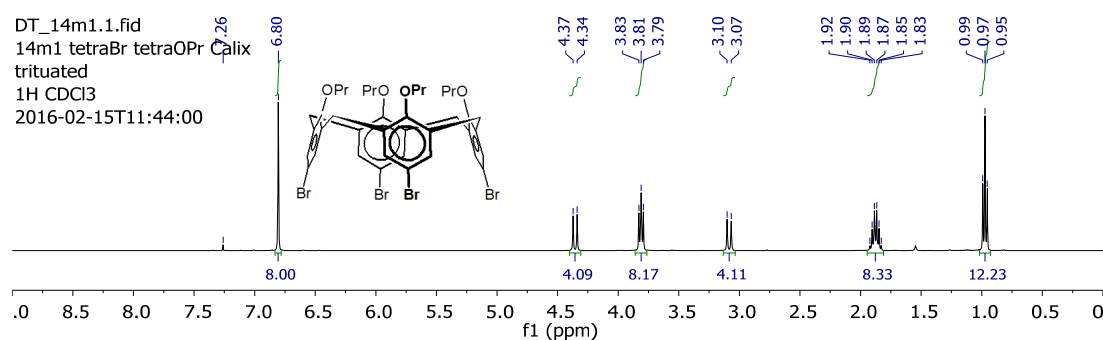
Appendix A17.1 (18) ¹H NMR spectrum recorded in CDCl₃.

(19) 5,17-Dibromo-25,26,27,28-tetrapropoxycalixarene
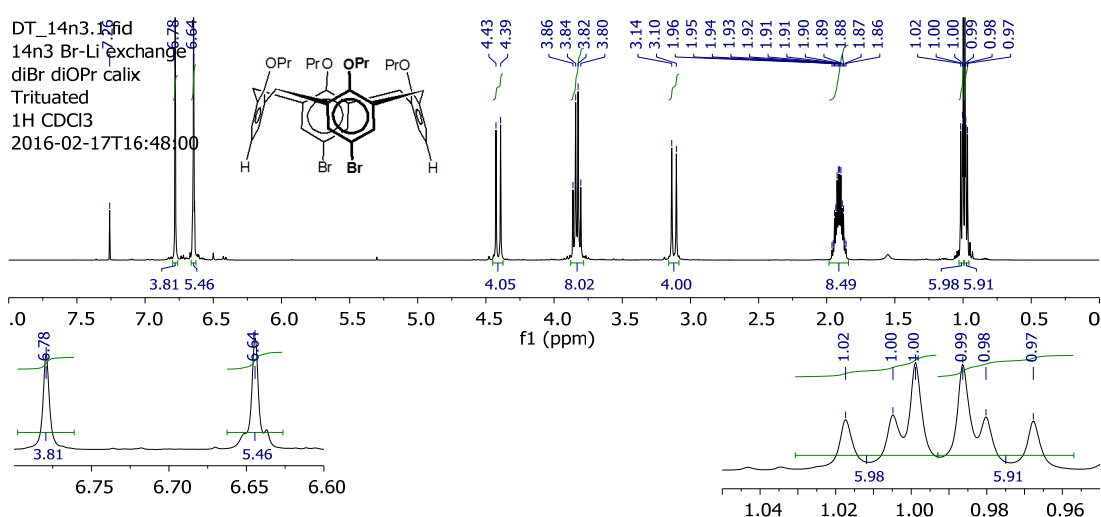
Appendix A18.1 (19) ^{1}H NMR spectrum recorded in CDCl3.

(20) 5,17-Dibromo-22,23-dinitro-25,26,27,28-tetrapropoxycalixarene
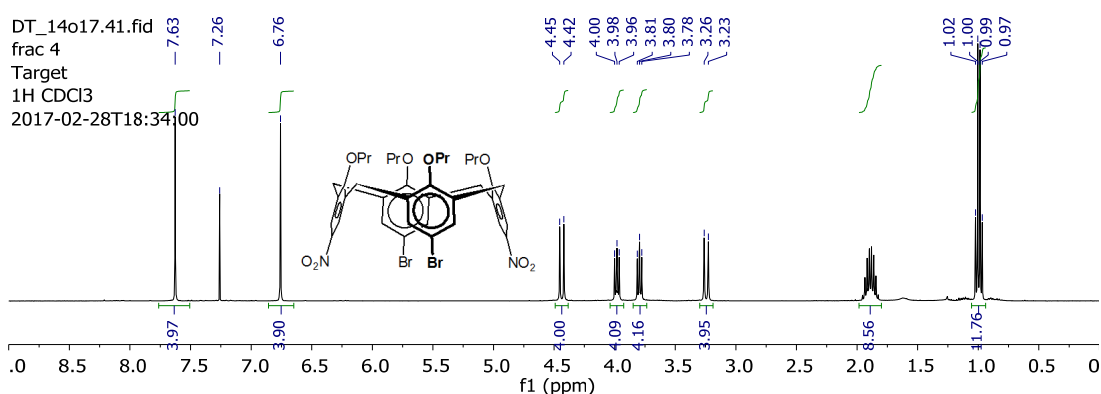
Appendix A19.1 (20) ^{1}H NMR spectrum recorded in CDCl3.
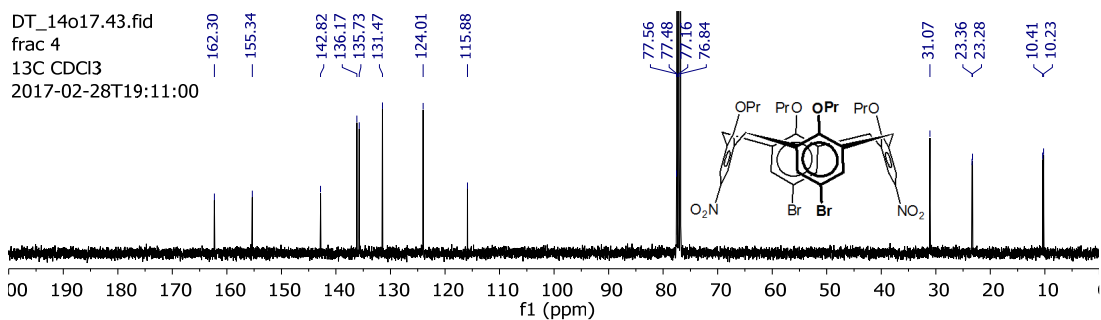
Appendix A19.2 (20) ^{13}C NMR spectrum.
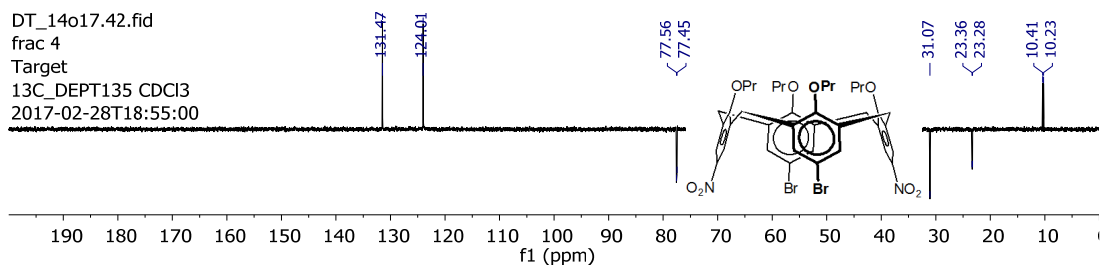
Appendix A19.3 (20) DEPT-135 NMR spectrum recorded in CDCl3.

(21) 5,17-Diamino-22,23-dibromo-25,26,27,28-tetrapropoxycalixarene
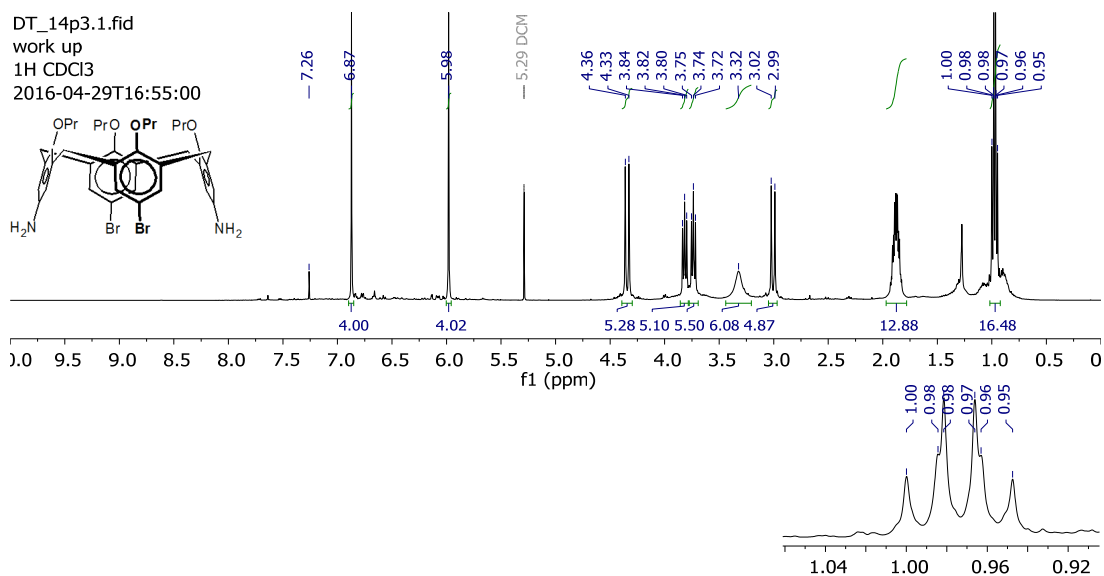
Appendix A20.1 (21) ^{1}H NMR spectrum recorded in CDCl$_3$.
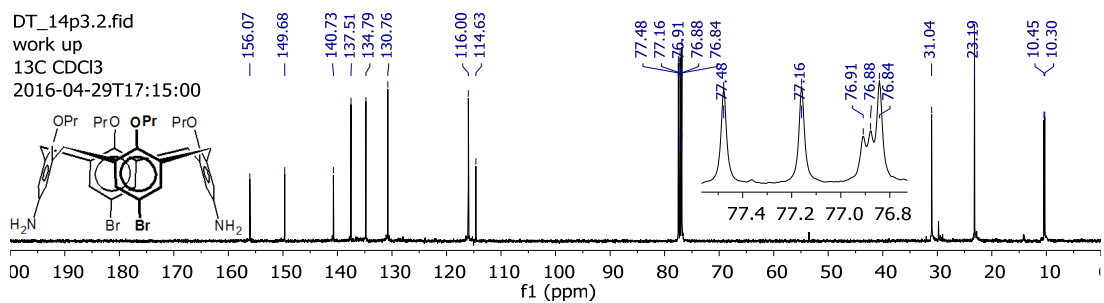
Appendix A20.2 (21) ^{13}C NMR spectrum recorded in CDCl$_3$.

3 Distal functionalisation of resorcinarene by selective lithiation

(22) 14,3⁶,5⁶,7⁶-tetrabenzyloxy-1⁶,3⁴,5⁴,7⁴-tetramethoxy-2,4,6,8-tetrapropylresorcin[4]arene
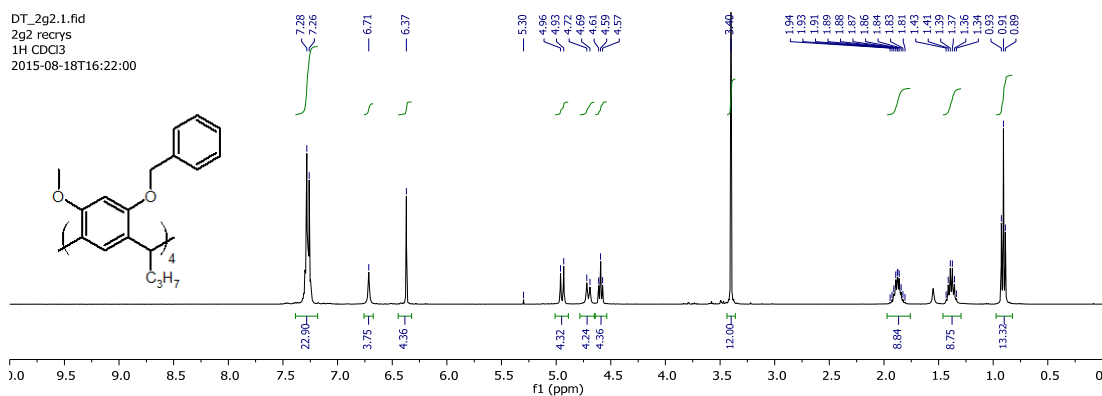
Appendix A21.1 (22) ^{1}H NMR spectrum recorded in CDCl$_3$.
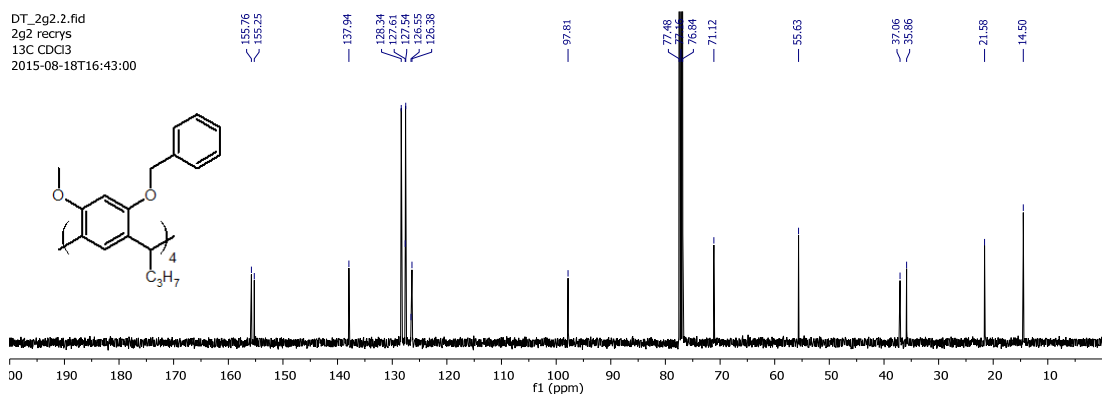
Appendix A21.2 (22) ^{13}C NMR spectrum recorded in CDCl$_3$.
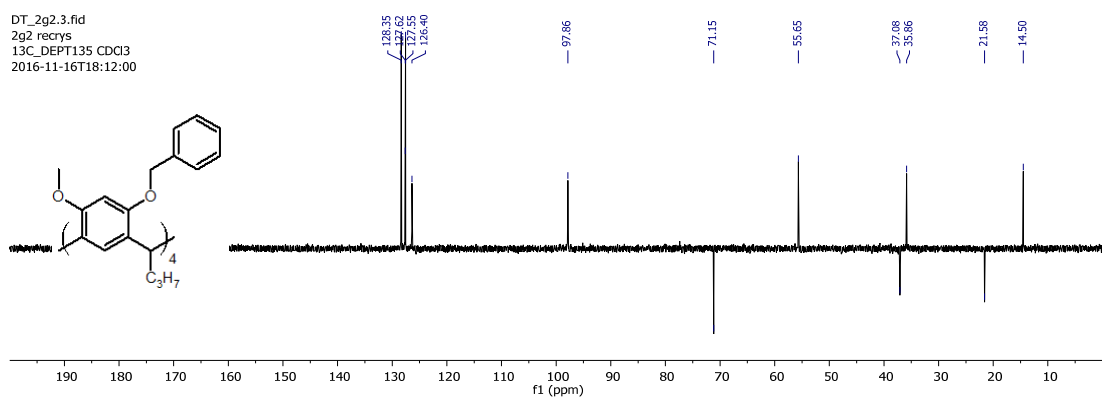
Appendix A21.3 (22) DEPT-135 NMR spectrum recorded in CDCl$_3$.

(23) $1^4,3^6,5^6,7^6$-tetramethoxymethyl-$1^6,3^4,5^4,7^4$-tetramethoxy-2,4,6,8-tetrapropylresorcin[4]arene
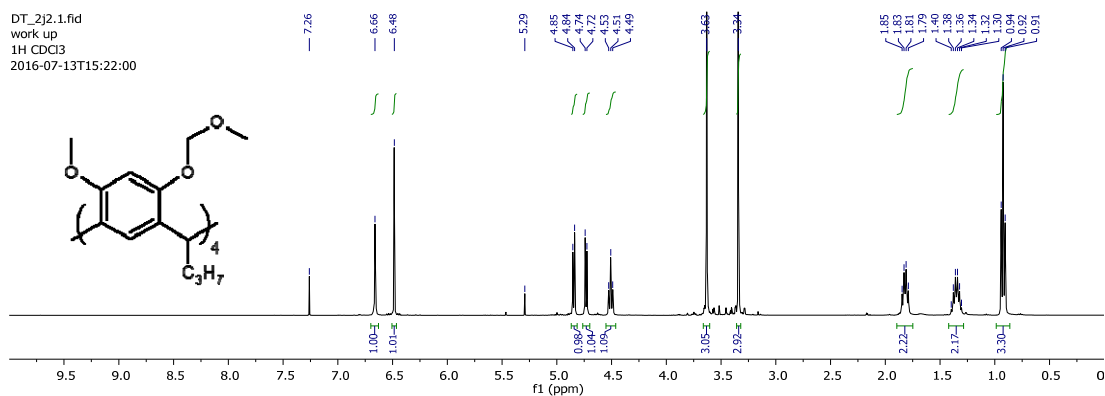
Appendix A22.1 (23) ^{1}H NMR spectrum recorded in CDCl₃.
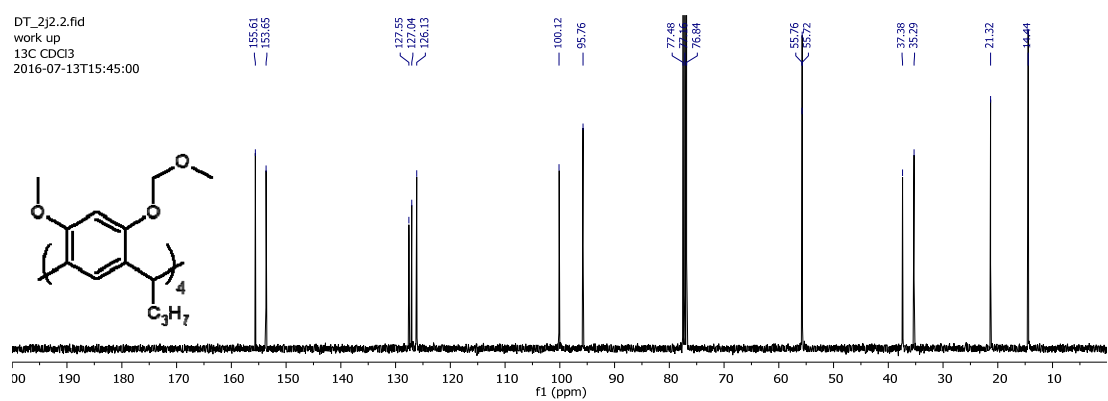
Appendix A22.2 (23) ^{13}C NMR spectrum recorded in CDCl₃.
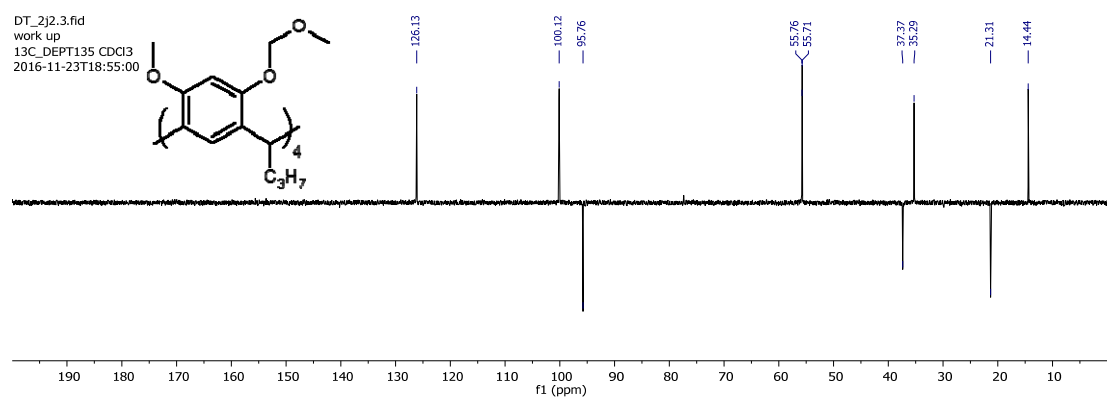
Appendix A22.3 (23) DEPT-135 NMR spectrum recorded in CDCl₃.

(24) - (28) Lithiation of $1^4,3^6,5^6,7^6$-tetramethoxymethyl-$1^6,3^4,5^4,7^4$-tetramethoxy-2,4,6,8-tetrapropylresorcin[4]arene (23)
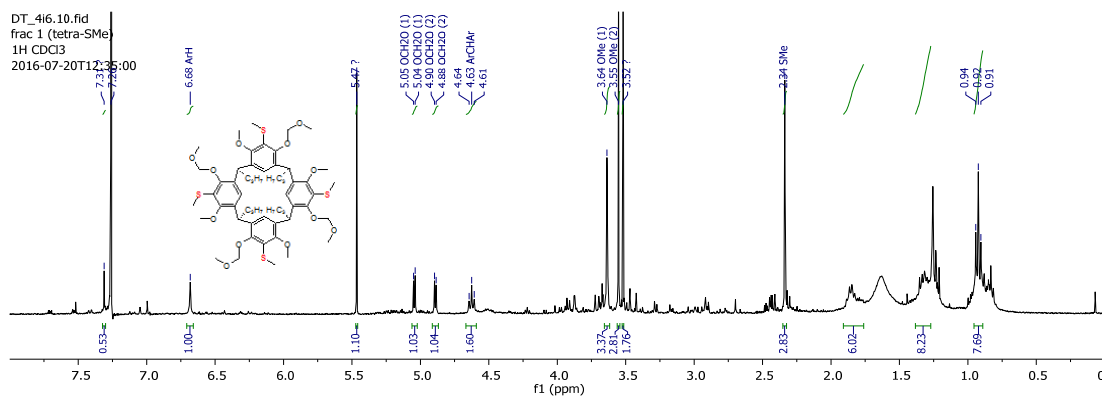
Appendix A23.1 (28) ^{1}H NMR spectrum recorded in CDCl$_3$.
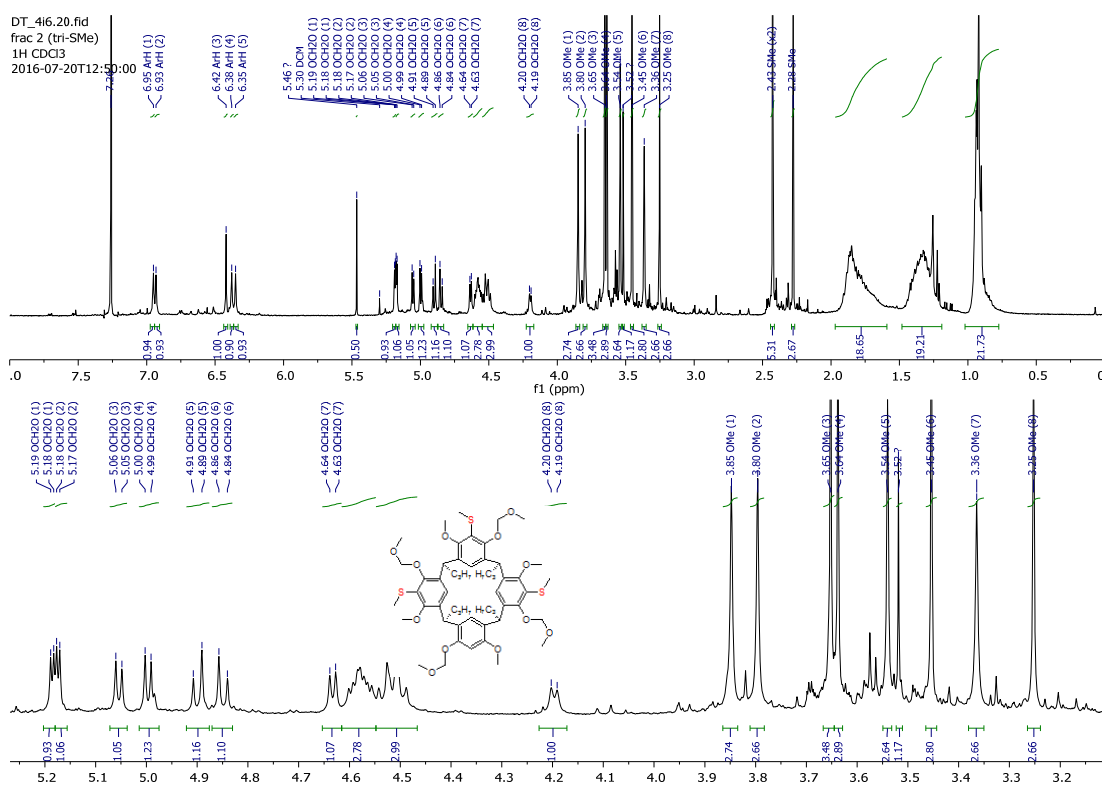
Appendix A23.2 (27) ^{1}H NMR spectrum recorded in CDCl$_3$.
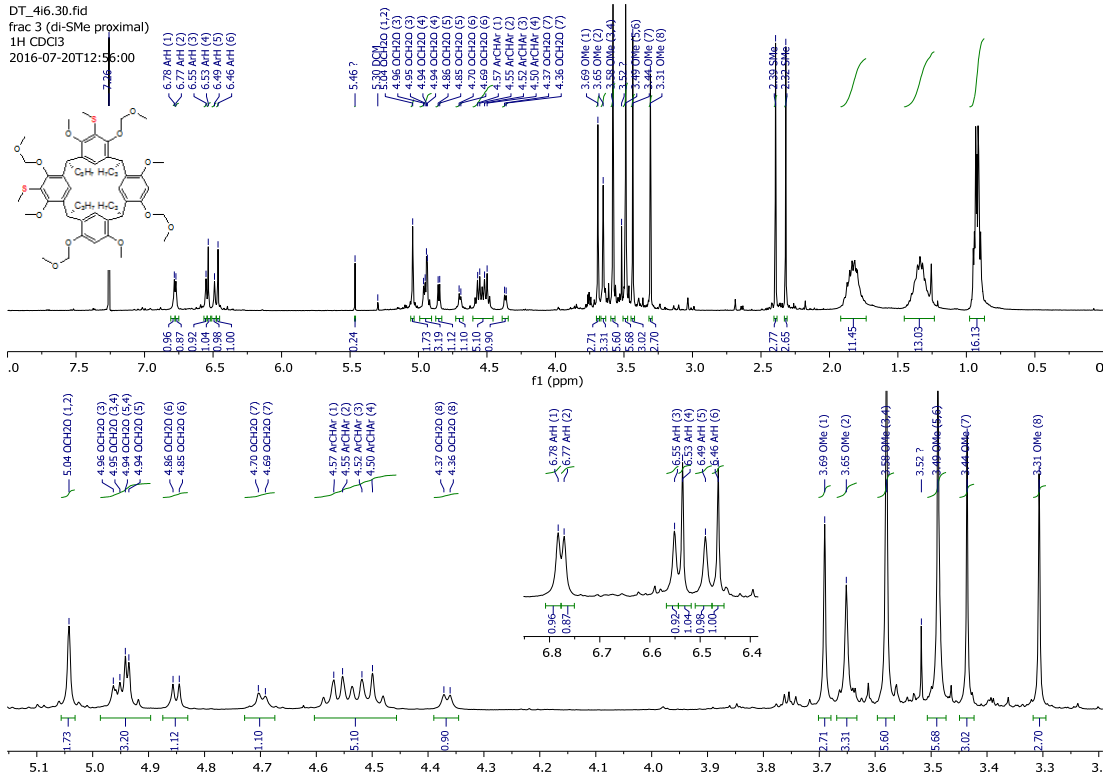
Appendix A23.3 (26) ^{1}H NMR spectrum recorded in CDCl$_3$.
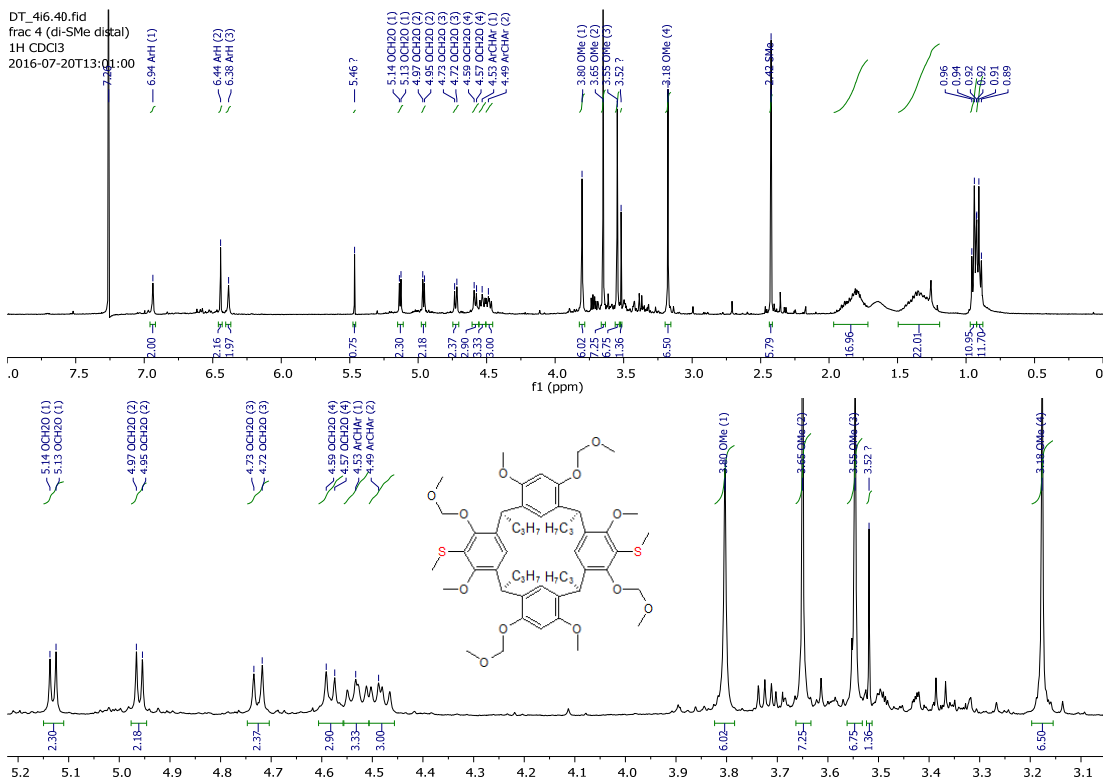
Appendix A23.4 (25) ^{1}H NMR spectrum recorded in CDCl$_3$.
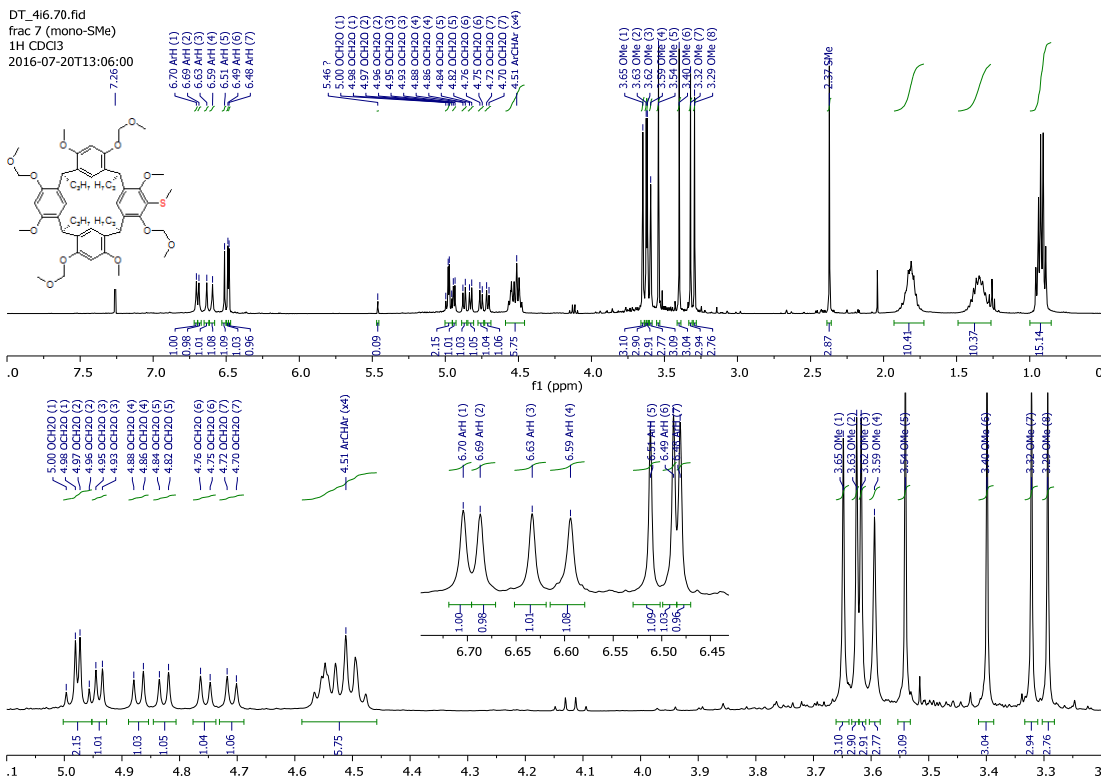
Appendix A23.5 (24) ^{1}H NMR spectrum recorded in CDCl$_3$.

(29) $1^4,3^6,5^6,7^6$-tetraethoxy-$1^6,3^4,5^4,7^4$-tetramethoxy-2,4,6,8-tetrapropylresorcin[4]arene
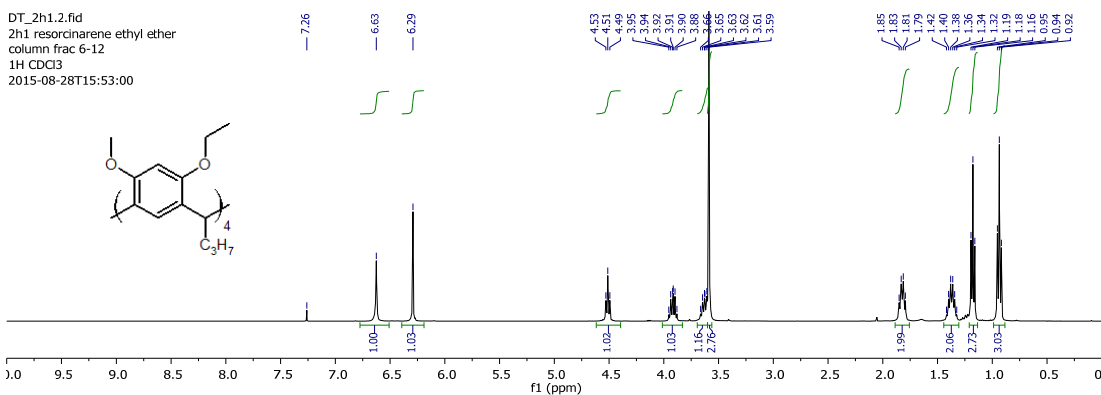
Appendix A1.1 (29) ^{1}H NMR spectrum recorded in CDCl$_3$.
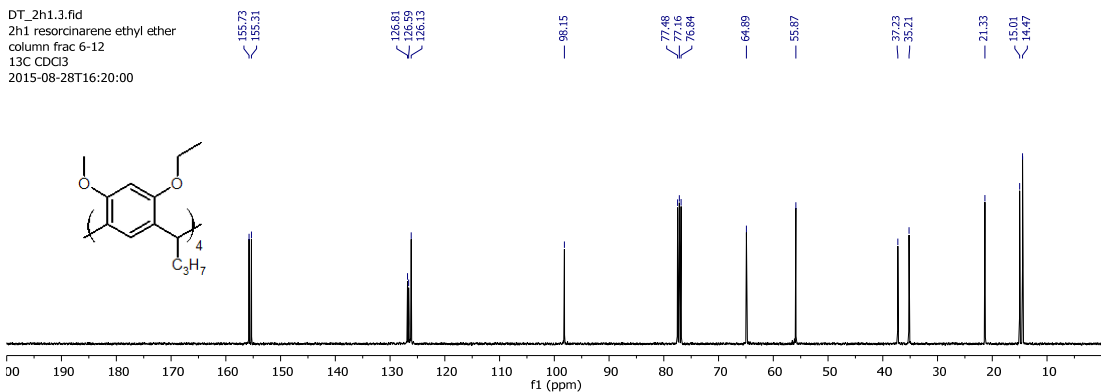
Appendix A1.2 (29) ^{13}C NMR spectrum recorded in CDCl$_3$.
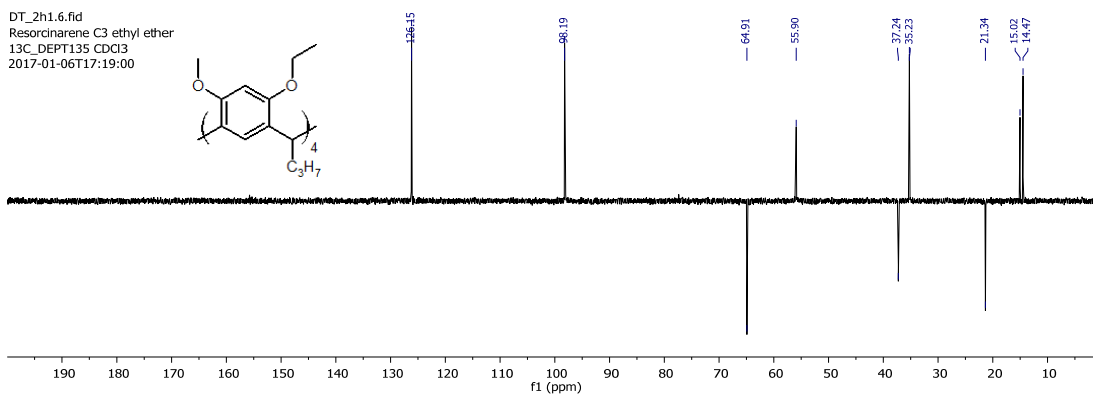
Appendix A1.3 (29) DEPT-135 NMR spectrum recorded in CDCl₃.

(30) Synthesis of 1⁴,3⁶,5⁶,7⁶-tetraethoxy-1⁶,3⁴,5⁴,7⁴-tetramethoxy-1⁵,5⁵-di(methylthio)-2,4,6,8-tetrapropylresorcin[4]arene
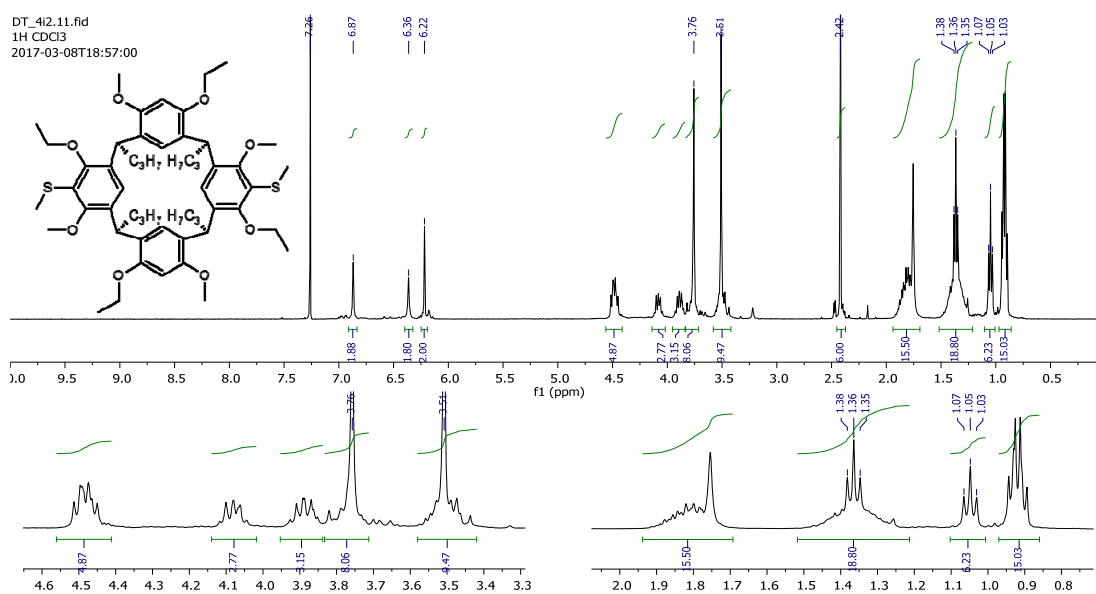
Appendix A2.1 (30) ¹H NMR spectrum recorded in CDCl₃.
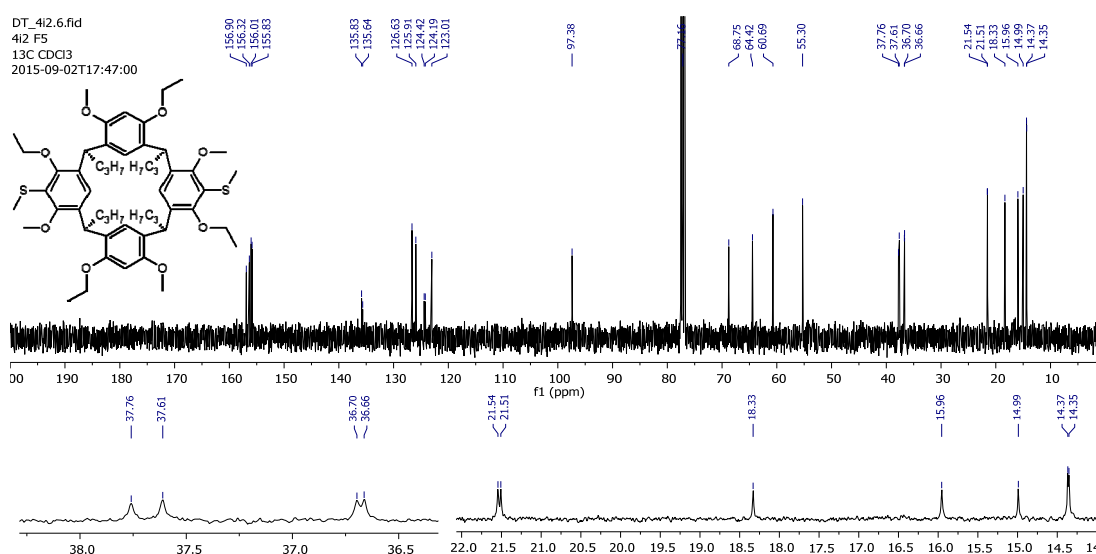
Appendix A2.2 (30) ¹³C NMR spectrum recorded in CDCl₃.
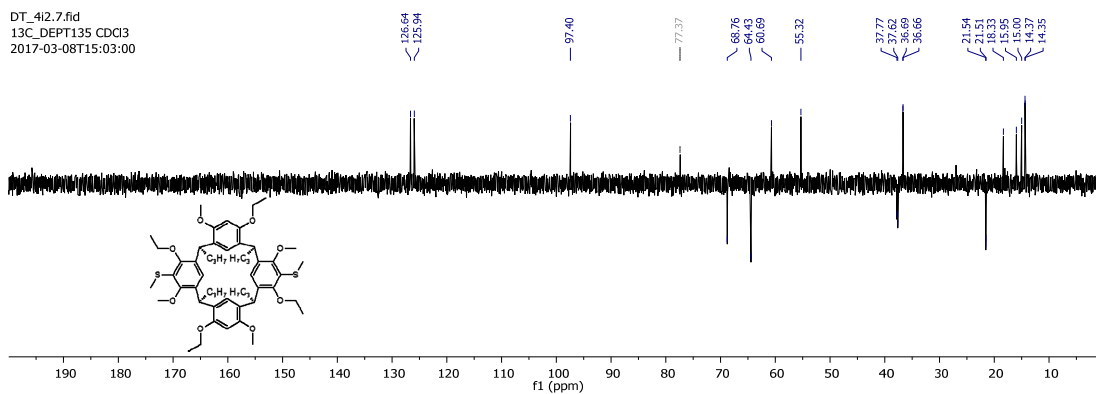
Appendix A2.3 (30) DEPT-135 NMR spectrum recorded in CDCl₃.
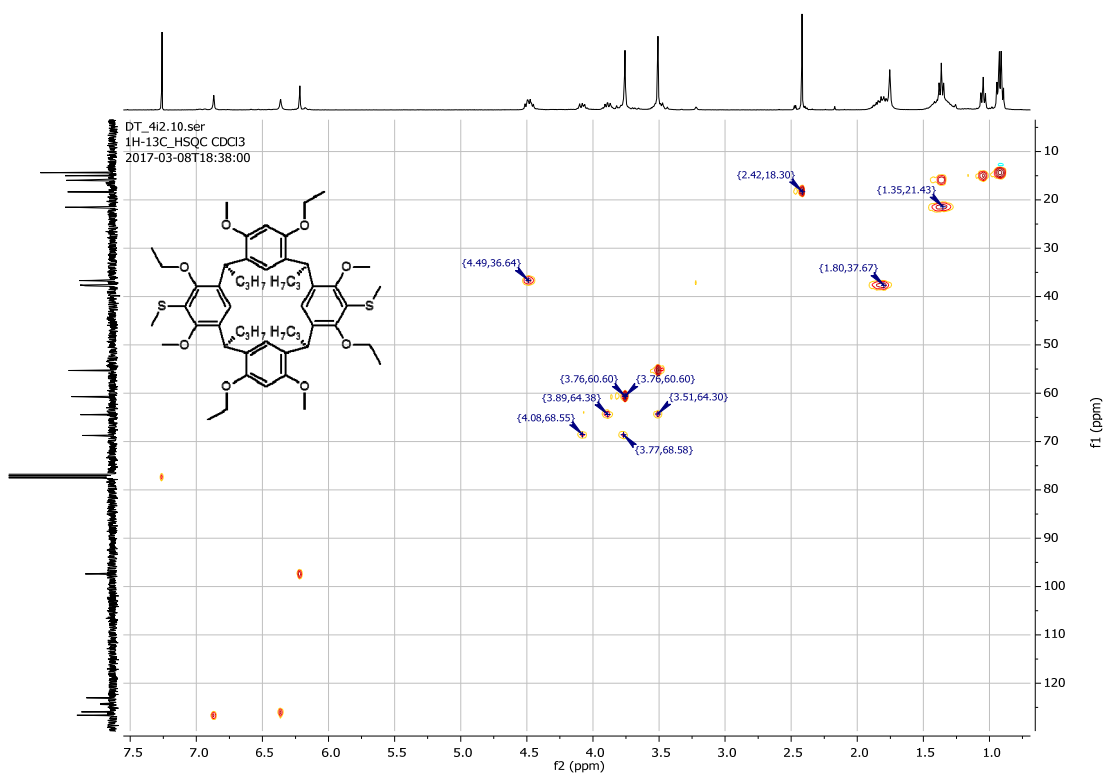
Appendix A2.4 (30) HSQC NMR spectrum recorded in CDCl₃.

4   Direct distal functionalisation of resorcinarene phenols

TBDMS

(32) Mono TBDMS
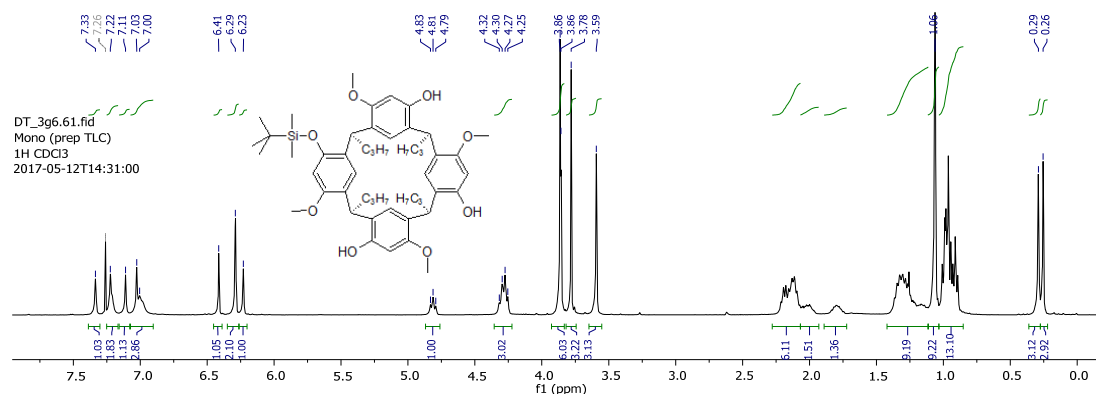
Appendix A3.1   (32) ^{1}H NMR spectrum recorded in CDCl$_3$.
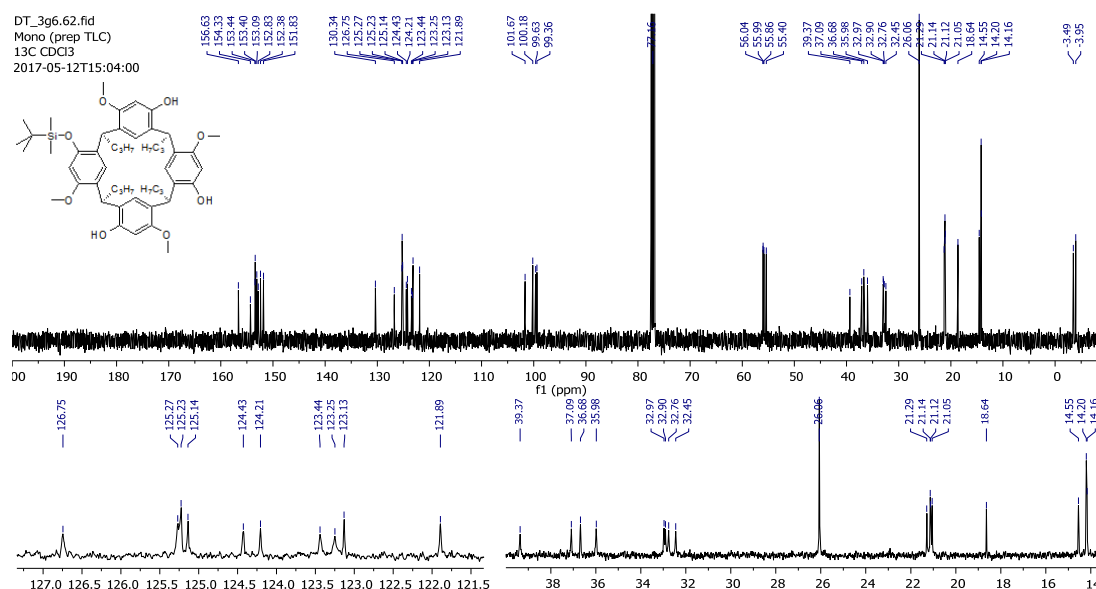
Appendix A3.2   (32) ^{13}C NMR spectrum recorded in CDCl$_3$.
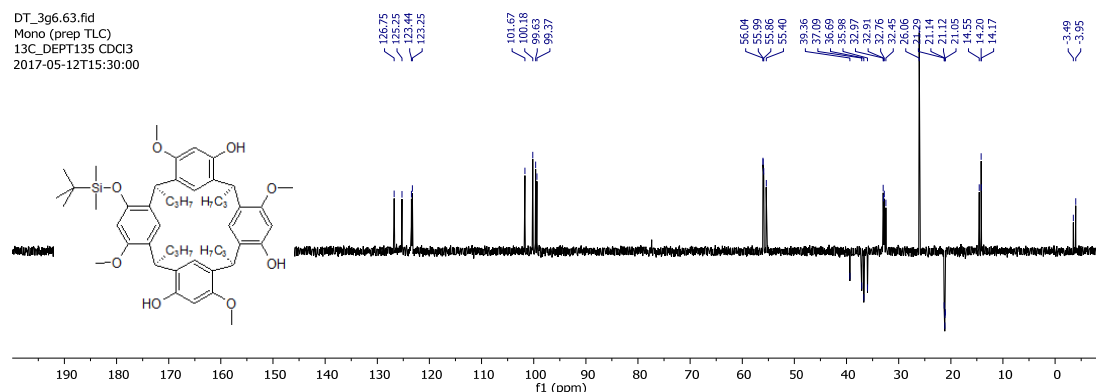
Appendix A3.3   (32) DEPT-135 NMR spectrum recorded in CDCl$_3$.

Appendix A3.4 **(32)** HSQC NMR spectrum recorded in CDCl$_3$.
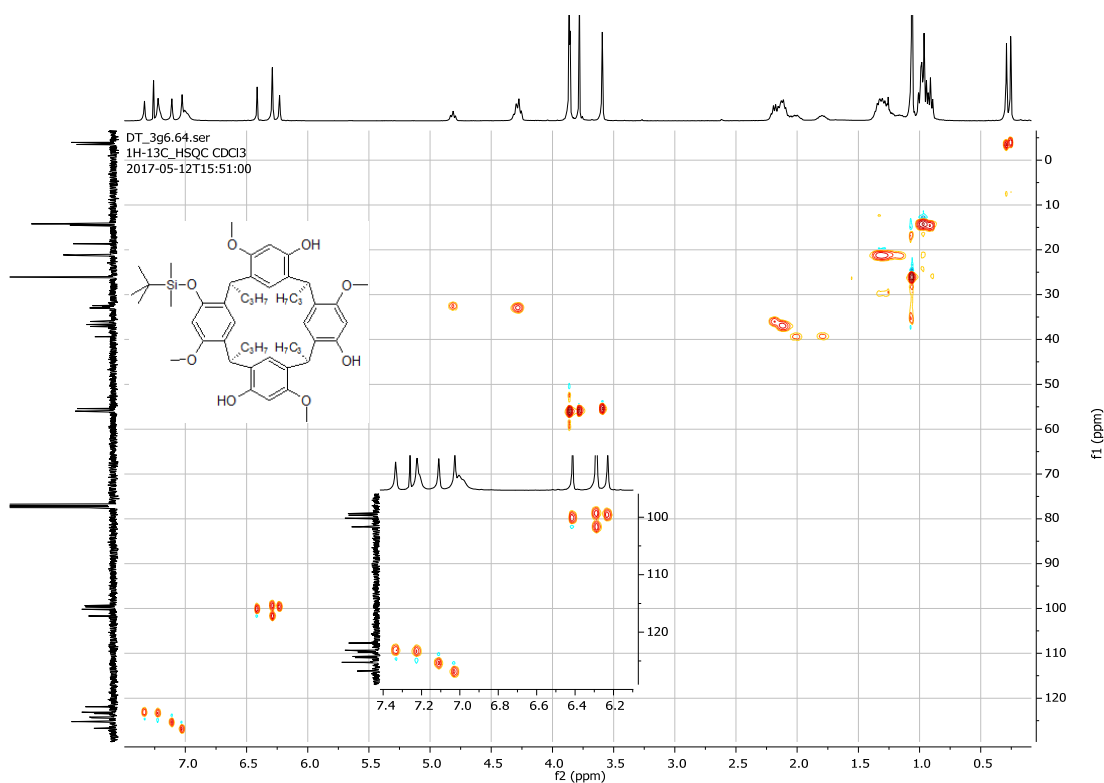
(33) Proximal TBDMS

Appendix A4.1 **(33)** ^{1}H NMR spectrum recorded in CDCl$_3$.
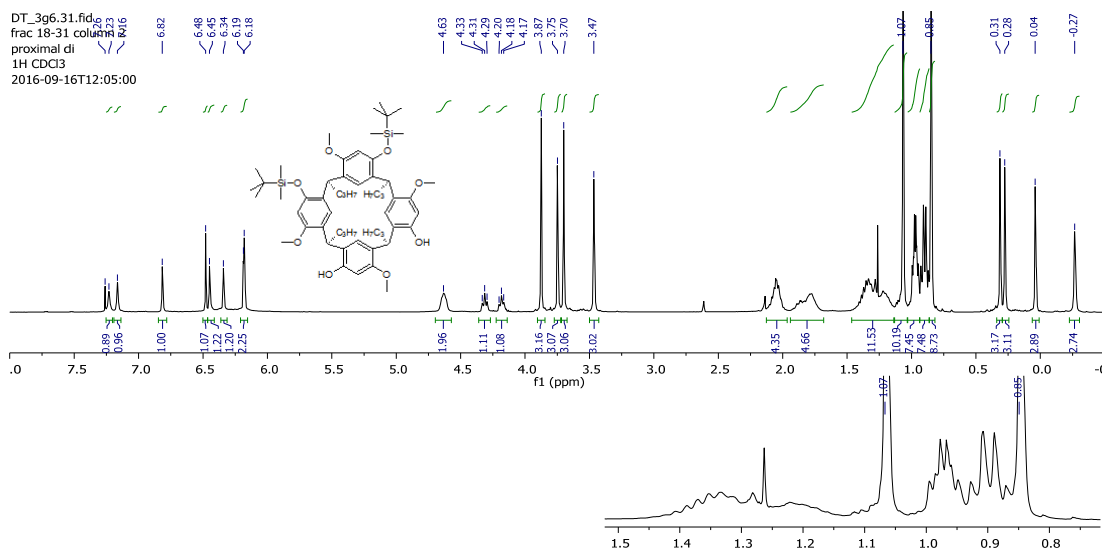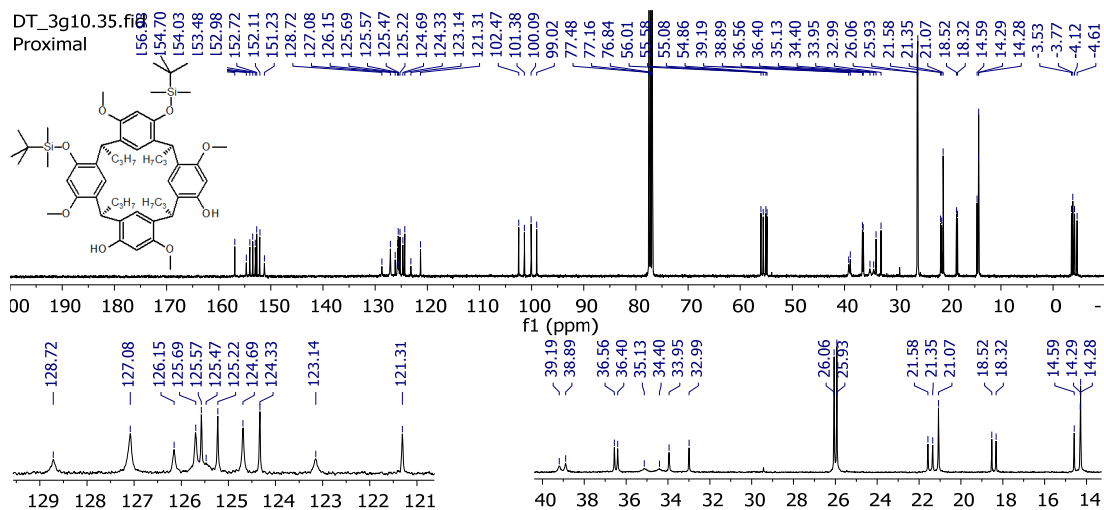
Appendix A4.2 (33) ^{13}C NMR spectrum recorded in CDCl$_3$.
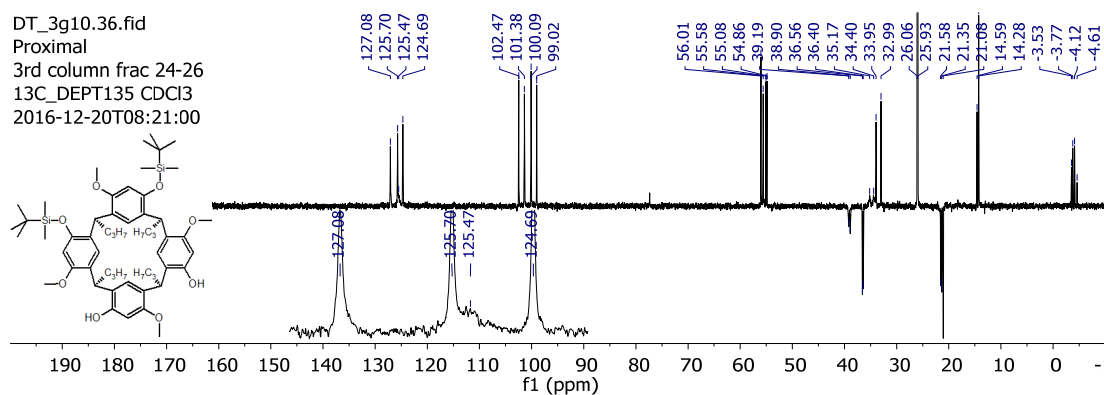
Appendix A4.3 (33) DEPT-135 NMR spectrum recorded in CDCl$_3$.
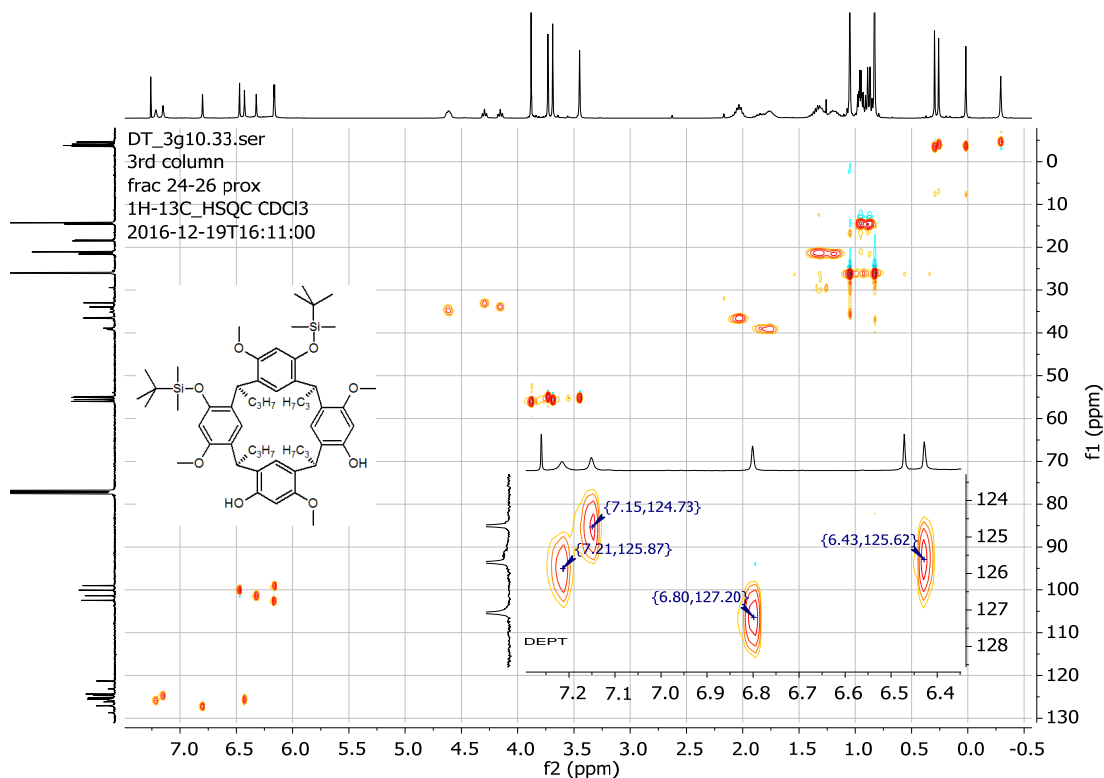
Appendix A4.4 (33) HSQC NMR spectrum recorded in CDCl$_3$.

(34) Distal TBDMS
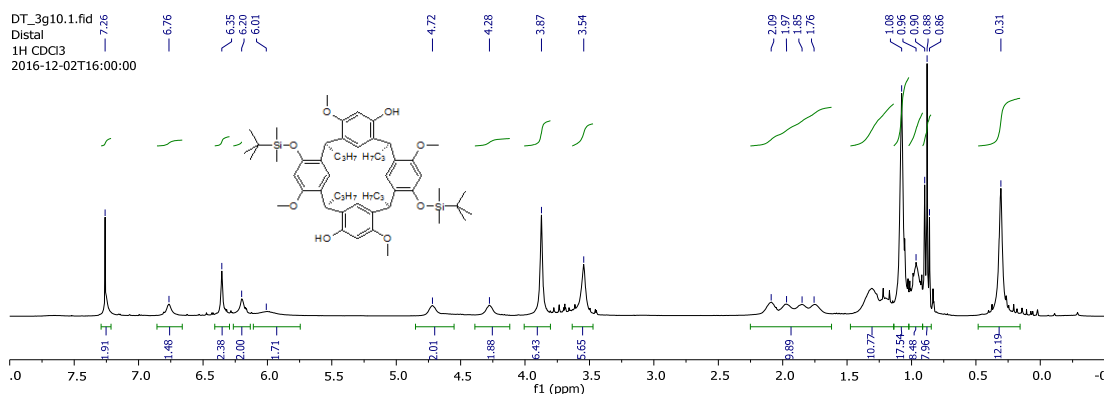
Appendix A5.1 **(34)** ^{1}H NMR spectrum recorded in CDCl$_3$.
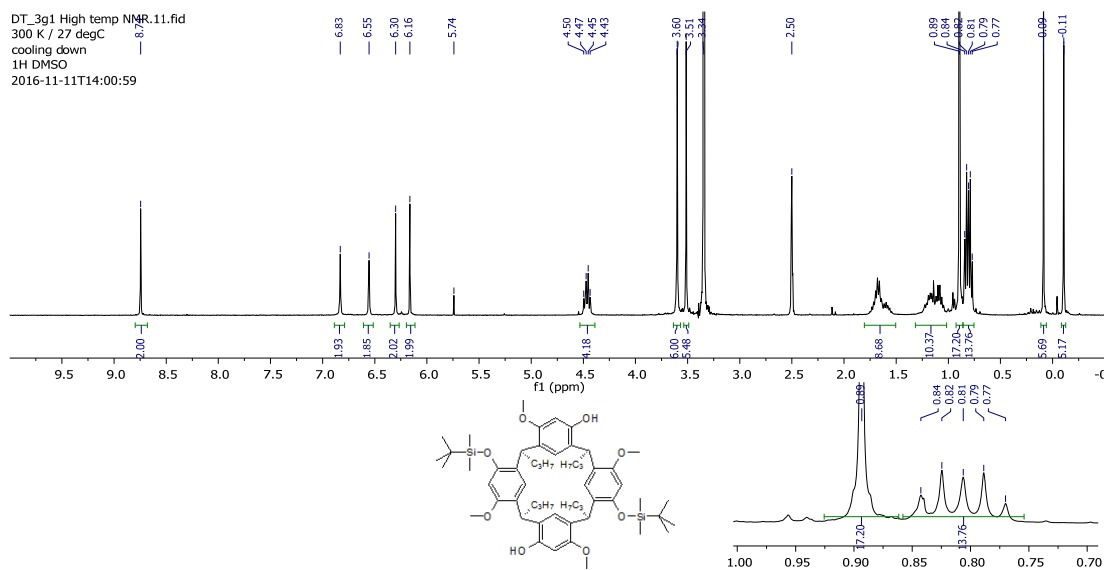
Appendix A5.2 **(34)** ^{1}H NMR spectrum recorded in DMSO-d$_6$.
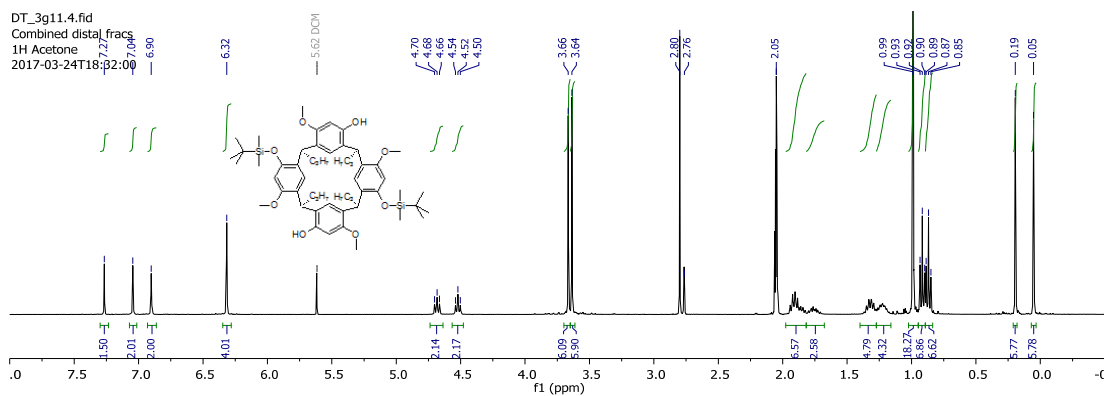
Appendix A5.3 **(34)** ^{1}H NMR spectrum recorded in acetone-d$_6$.
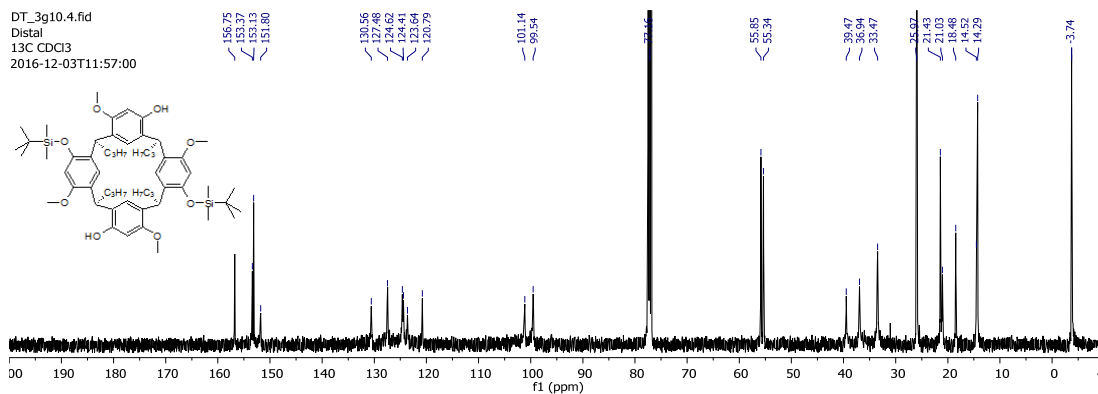
Appendix A5.4 **(34)** ^{13}C NMR spectrum recorded in CDCl$_3$.
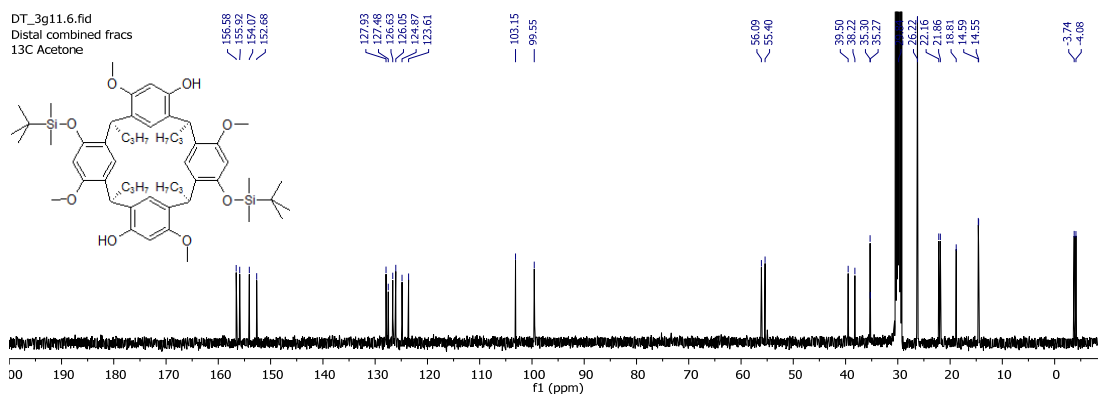
Appendix A5.5 **(34)** ^{13}C NMR spectrum recorded in acetone-d$_6$.
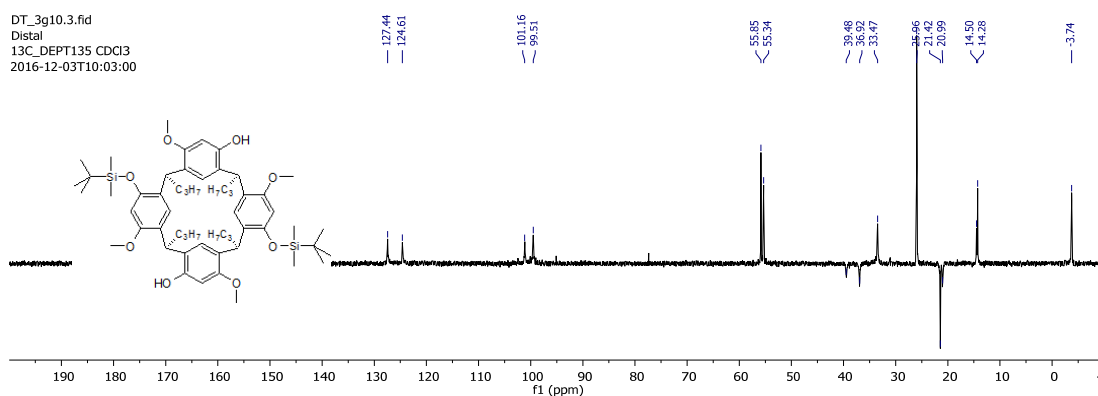
Appendix A5.6 **(34)** DEPT-135 NMR spectrum recorded in CDCl$_3$.
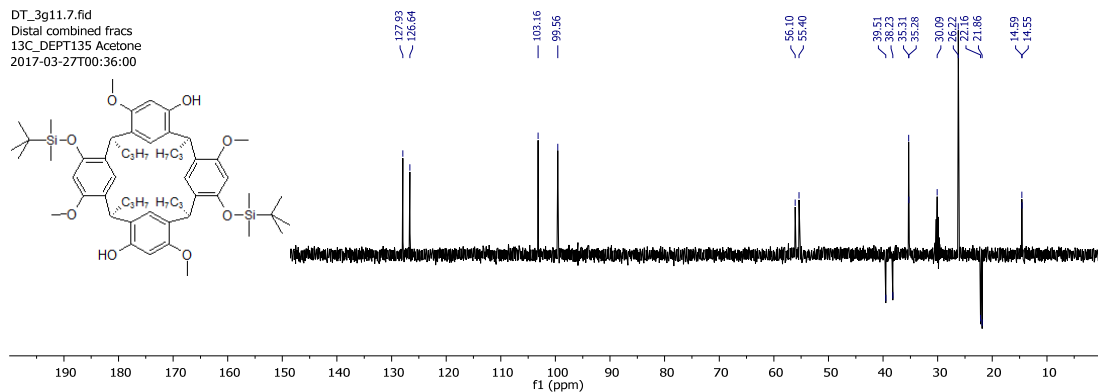
Appendix A5.7 **(34)** DEPT-135 NMR spectrum in recorded acetone-d$_6$.
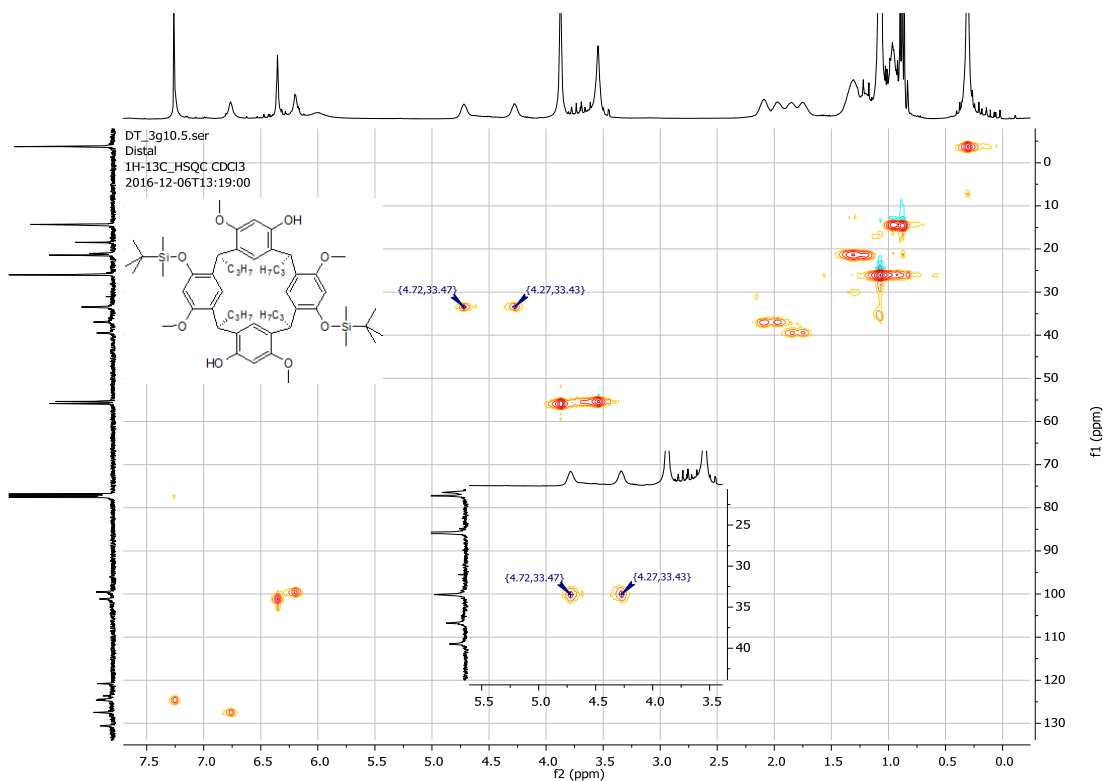
Appendix A5.8 **(34)** HSQC NMR spectrum recorded in CDCl$_3$.

(35) Tri TBDMS
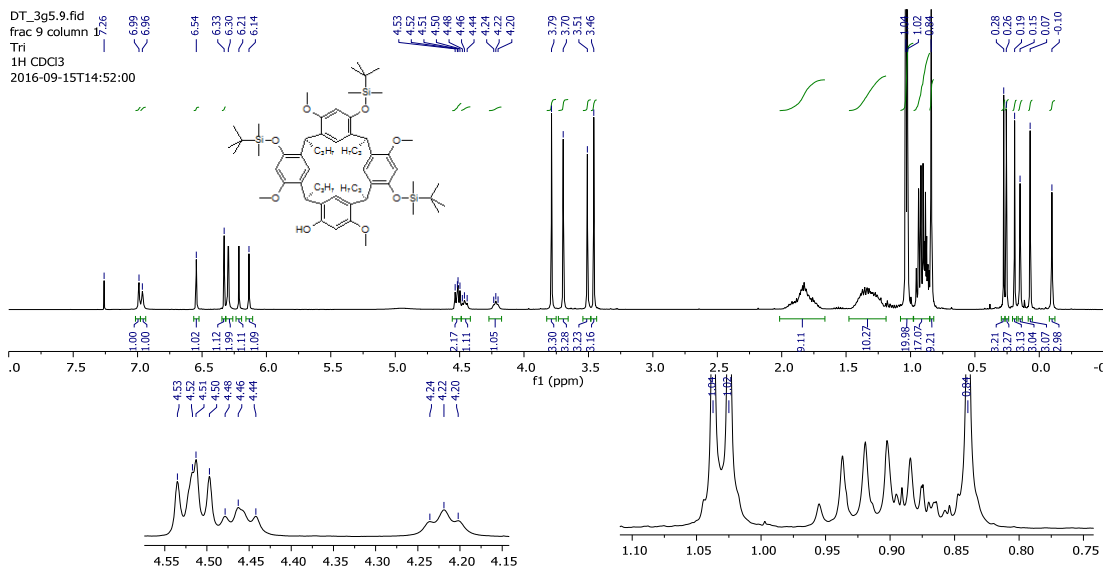
Appendix A6.1 **(35)** ^{1}H NMR spectrum recorded in CDCl$_3$.
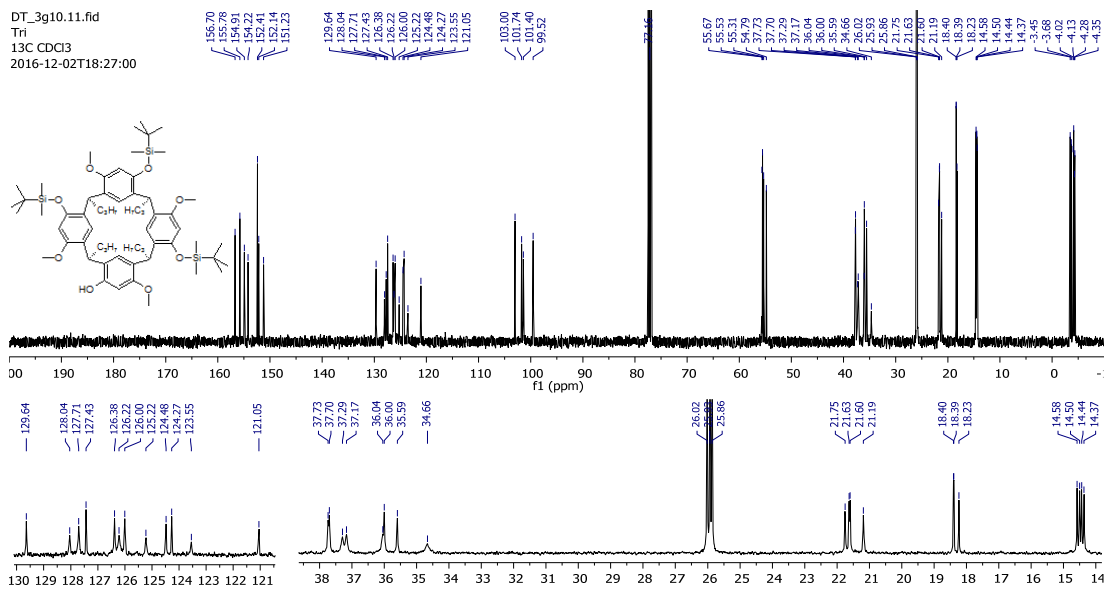
Appendix A6.2 **(35)** ^{13}C NMR spectrum recorded in CDCl$_3$.
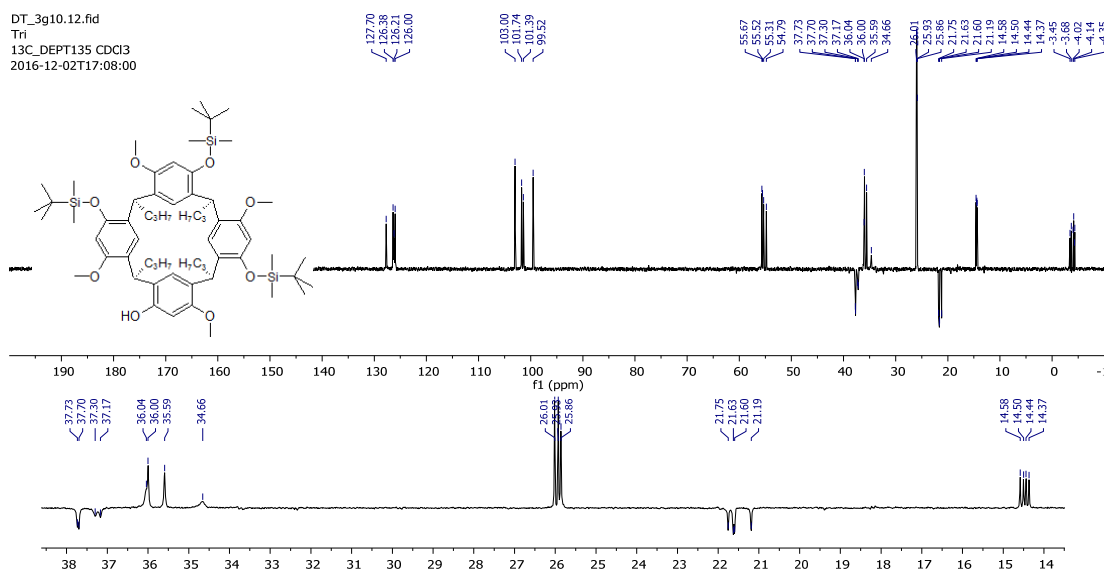
Appendix A6.3 **(35)** DEPT-135 NMR spectrum recorded in CDCl$_3$.

TBDMS heptyl

(36) Mono TBDMS heptyl
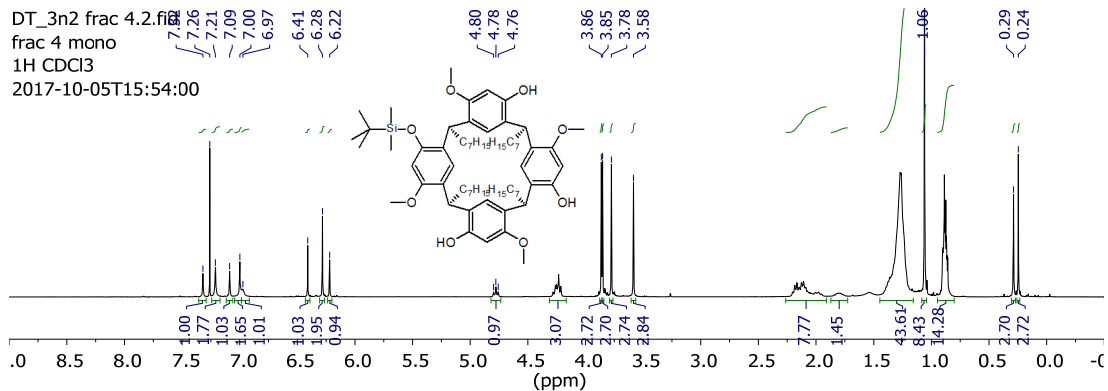
Appendix A7.1 **(36)** ^{1}H NMR spectrum recorded in CDCl$_3$.
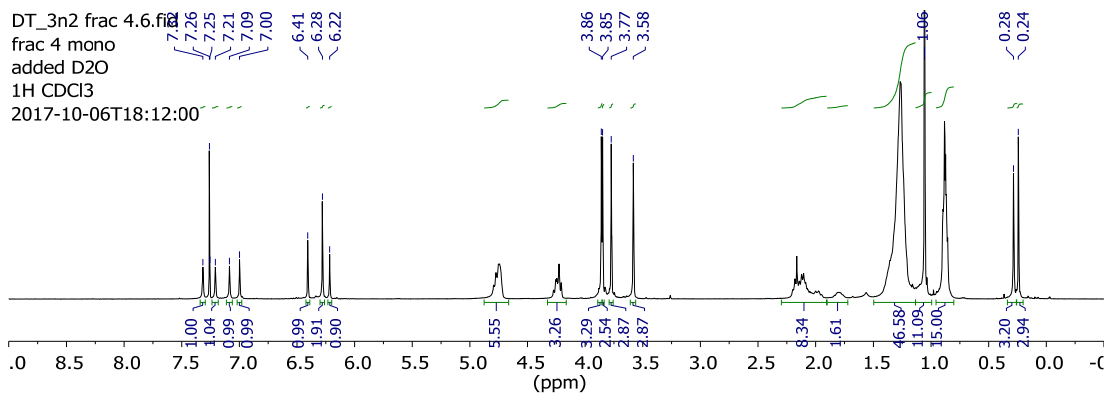
Appendix A7.2 (36) ^1H NMR spectrum recorded in $CDCl_3$ with D_2O exchange.
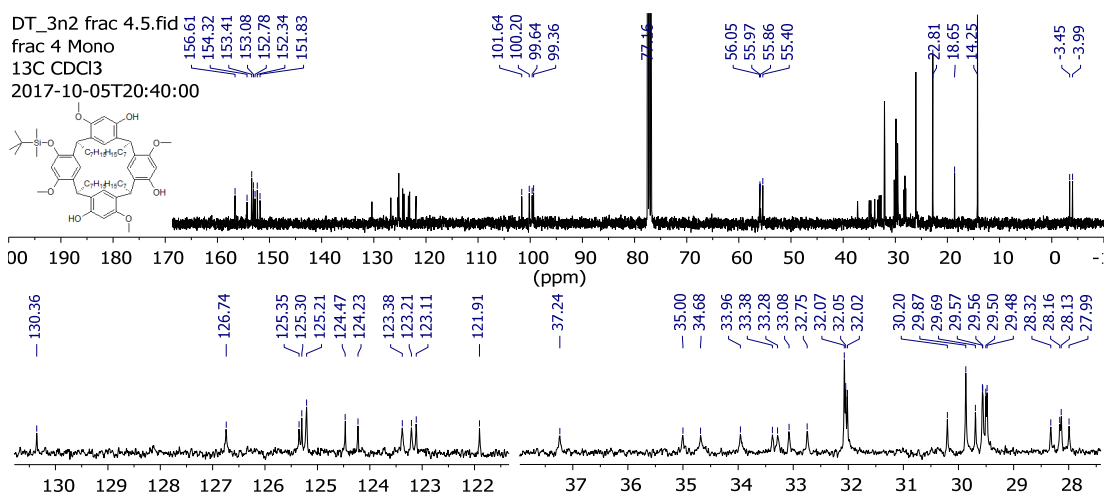
Appendix A7.3 (36) ^{13}C NMR spectrum recorded in $CDCl_3$.
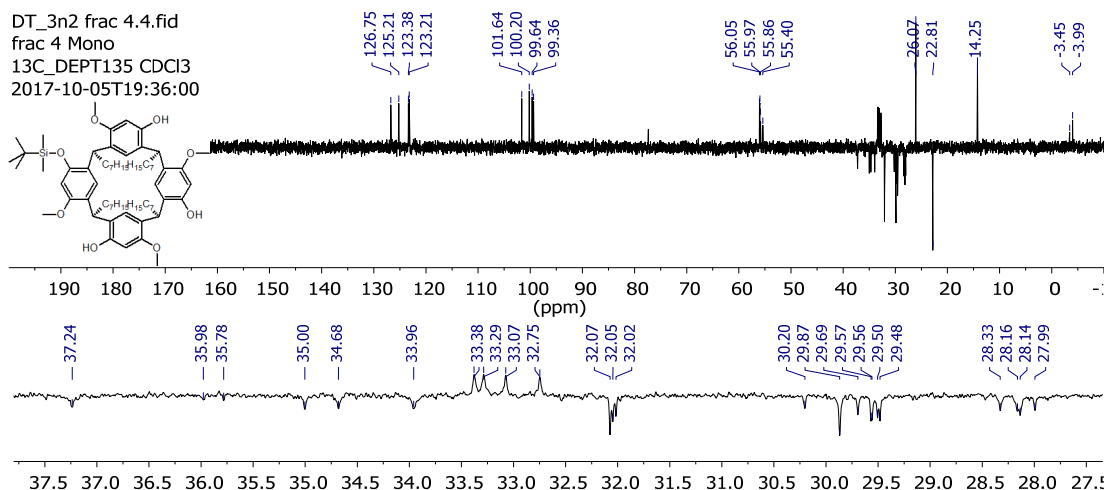
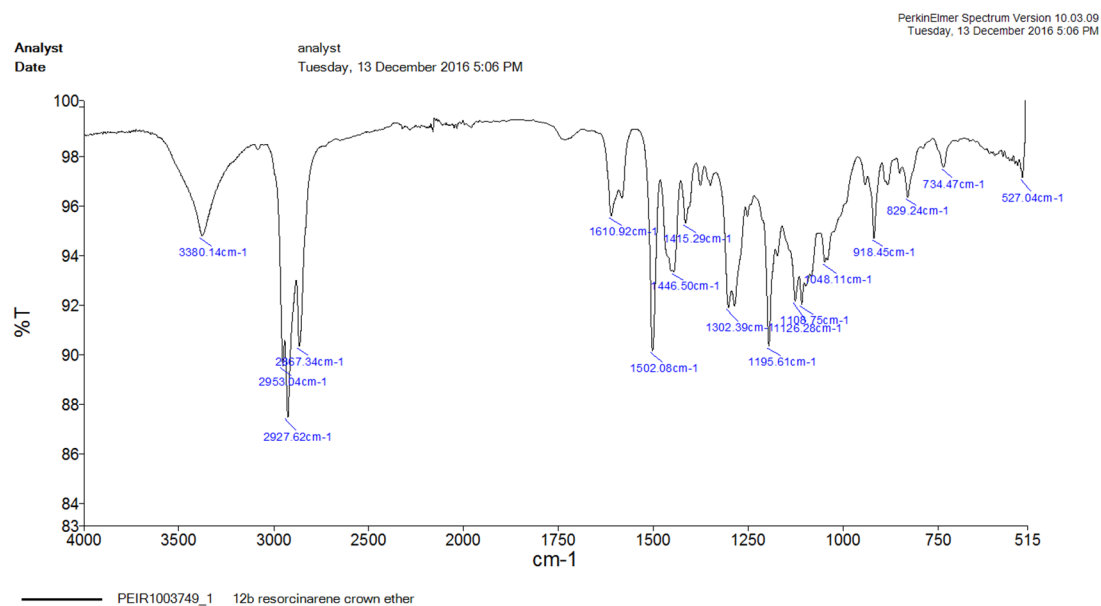**Appendix A7.4 (36)** DEPT-135 NMR spectrum recorded in $CDCl_3$.

Appendix A - 35

(37) Proximal TBDMS heptyl

DT_3n2 frac 3.1.fid
frac 3 Prox
1H CDCl3
2017-10-05T11:34:00
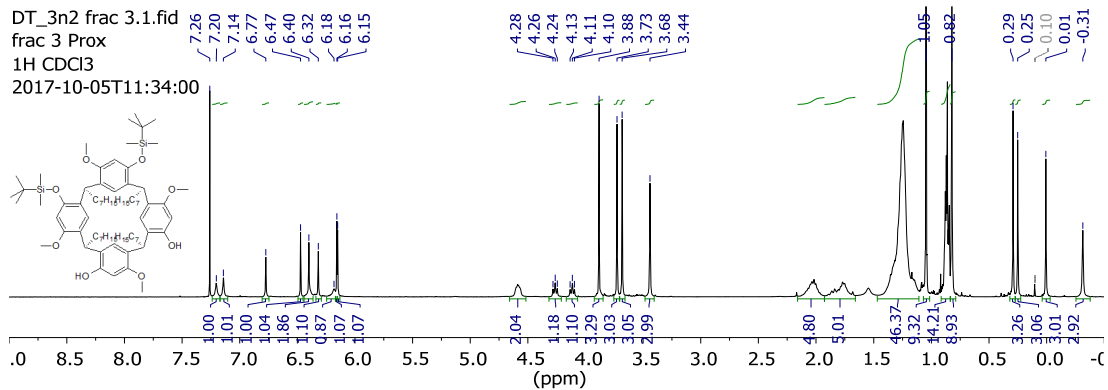
Appendix A8.1 **(37)** ^{1}H NMR spectrum recorded in CDCl$_3$.

DT_3n4.33.fid
frac 3
NMR solution after 7 h
13C CDCl3
2017-10-18T01:14:00
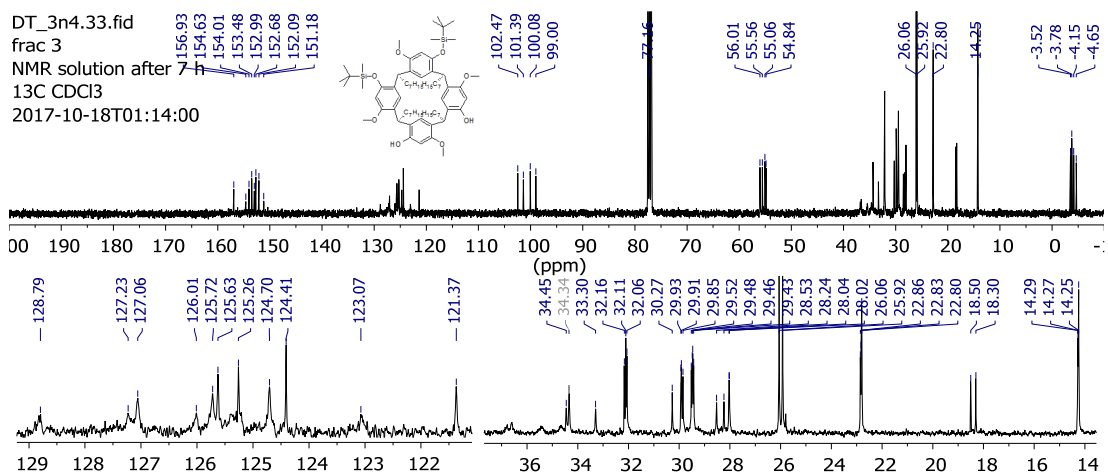
Appendix A8.2 **(37)** ^{13}C NMR spectrum recorded in CDCl$_3$.

DT_3n4.31.fid
frac 3
13C_DEPT135 CDCl3
2017-10-17T18:37:00
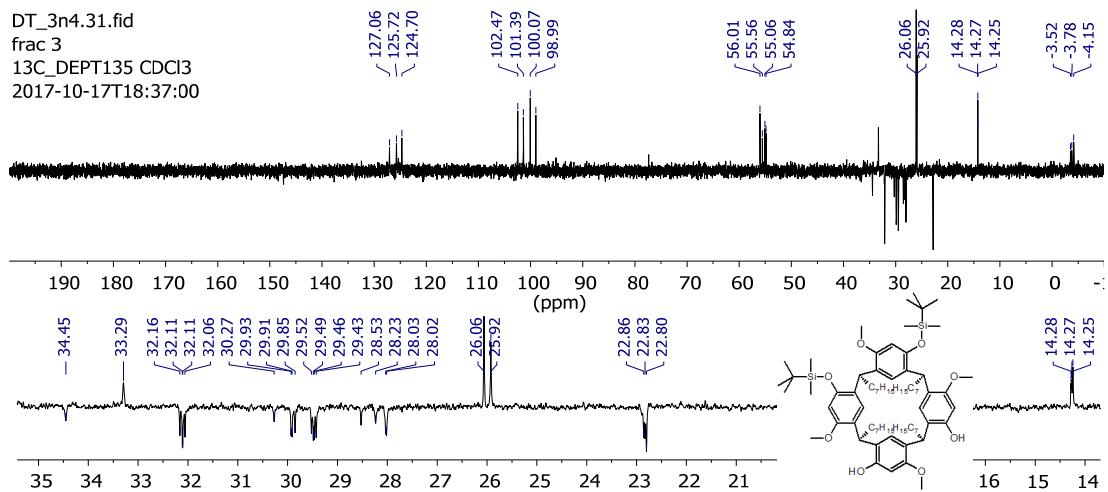
Appendix A8.3 **(37)** DEPT-135 NMR spectrum recorded in CDCl$_3$.

(38) Distal TBDMS heptyl

DT_3n2 frac 2.3.fid
frac 2 Distal
After evap with MeOH
1H CDCl3
2017-10-06T12:03:00
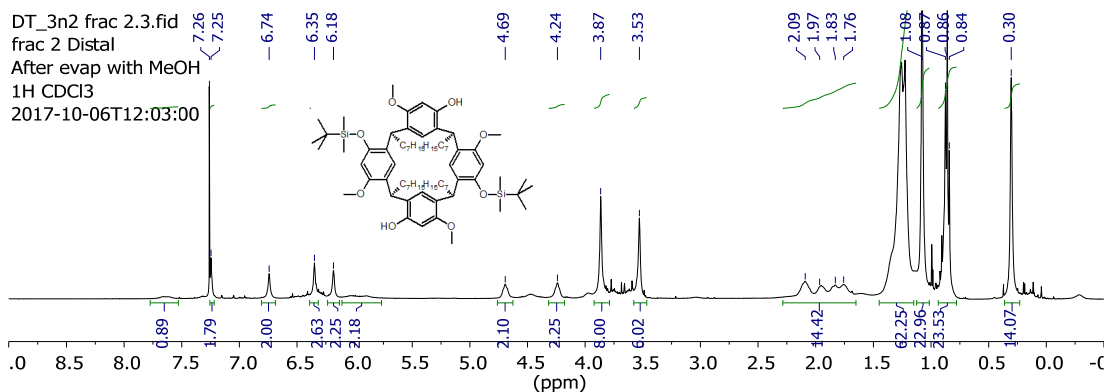
Appendix A9.1 **(38)** ^{1}H NMR spectrum recorded in CDCl$_3$.

DT_3n2 frac 2.7.fid
frac 2 Distal
1H Acetone
2017-10-09T17:08:00
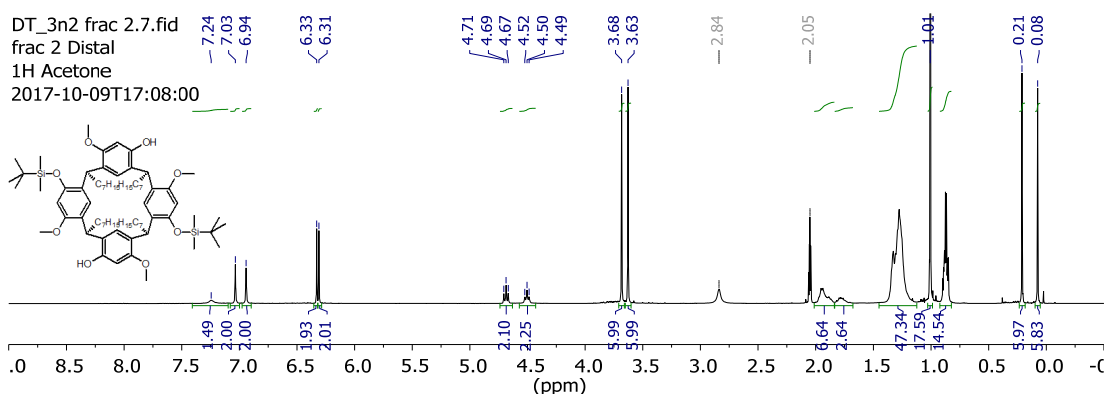
Appendix A9.2 **(38)** ^{1}H NMR spectrum recorded in acetone-d$_6$.

DT_3n2 frac 2.6.fid
frac 2 Distal
13C CDCl3
2017-10-08T05:08:00
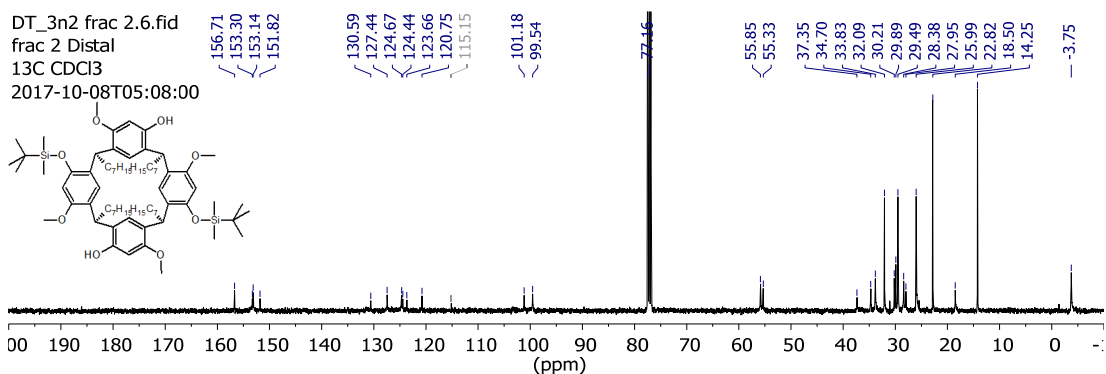
Appendix A9.3 **(38)** ^{13}C NMR spectrum recorded in CDCl$_3$.

DT_3n2 frac 2.9.fid
frac 2 Distal
13C Acetone
2017-10-09T18:26:00
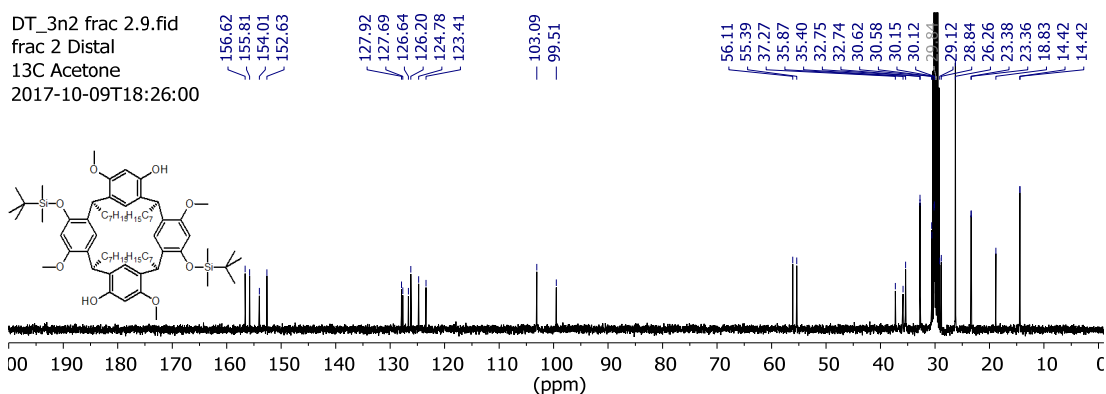
Appendix A9.4 **(38)** ^{13}C NMR spectrum recorded in acetone-d$_6$.

DT_3n2 frac 2.4.fid
frac 2 Distal
13C_DEPT135 CDCl3
2017-10-06T12:28:00

127.43 124.67 101.16 99.54 55.85 55.33 37.34 34.72 33.82 32.10 30.22 29.90 29.49 28.38 27.95 26.00 22.83 14.26 -3.75

37.34 34.72 33.82 32.10 30.16 29.9 28.38 27.95 26.00 22.83
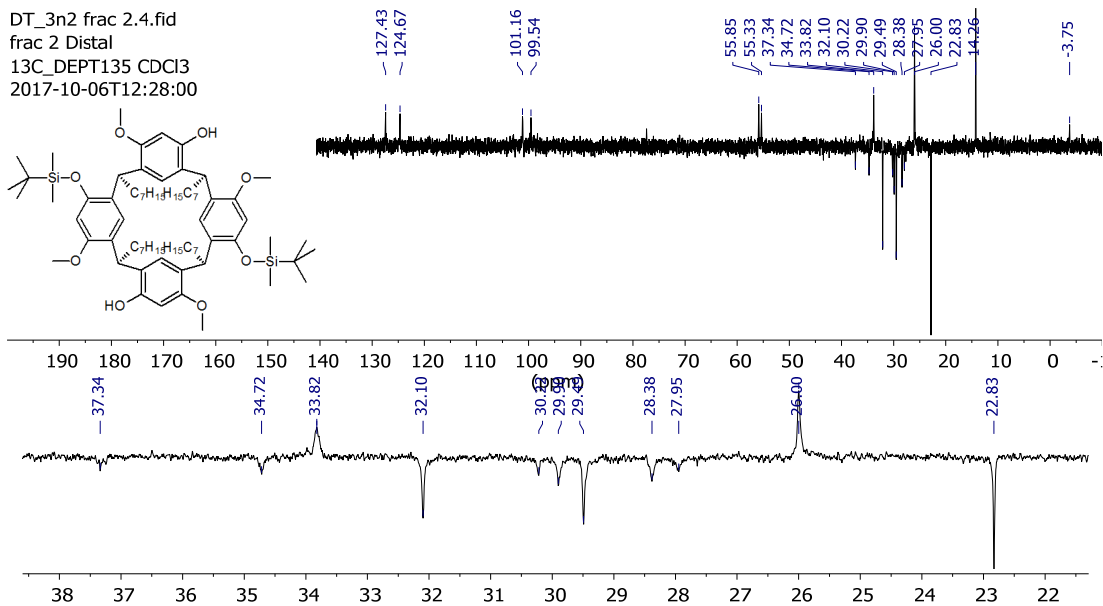
Appendix A9.5 (38) DEPT-135 NMR spectrum recorded in CDCl$_3$.

DT_3n2 frac 2.8.fid
frac 2 Distal
13C_DEPT135 Acetone
2017-10-09T18:09:00

127.92 126.64 103.09 99.52 56.11 55.39 37.27 35.87 35.40 32.76 32.74 30.62 30.58 30.16 30.12 29.12 28.84 26.26 23.38 23.36 14.42 14.42 -3.72 4.04

37.27 35.87 35.40 32.76 32.74 30.62 30.58 30.12 29.12 28.84 26.7 23.38 23.36 14.42 14.42
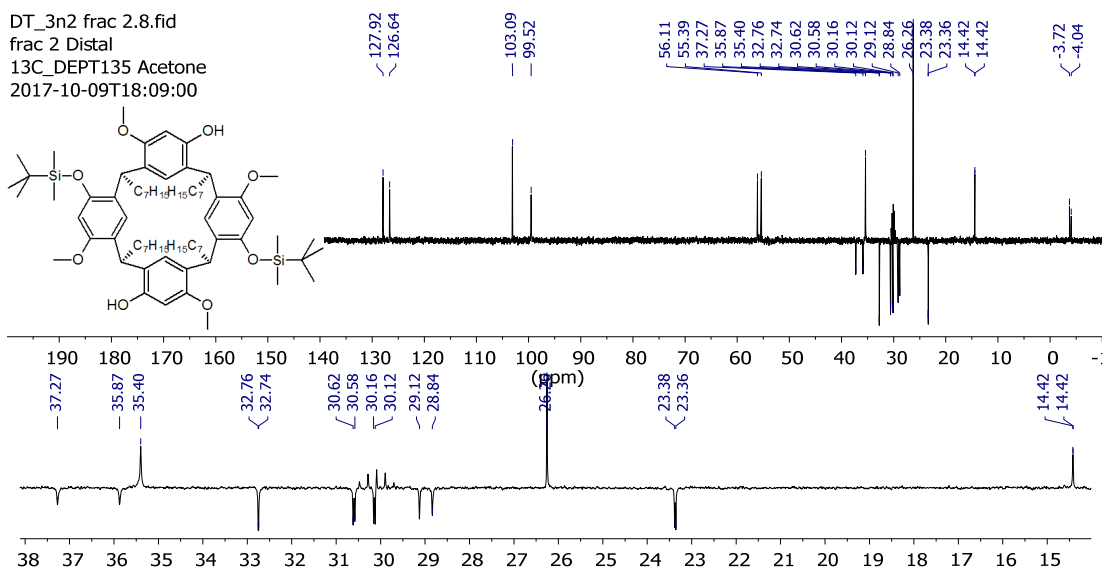
Appendix A9.6 (38) DEPT-135 NMR spectrum recorded in acetone.

(39) Tri TBDMS heptyl

DT_3n3 frac 1.1.fid
frac 1 Tri
1H CDCl3
2017-10-11T15:00:00

7.26 6.98 6.95 6.50 6.31 6.28 6.25 6.19 6.11 4.49 4.47 4.46 3.78 3.68 3.49 3.43 1.03 1.01 0.82 0.37 0.27 0.24 0.18 0.13 0.05 -0.12

1.00 0.99 1.01 1.07 1.08 0.91 1.02 1.01 2.20 2.09 1.10 3.17 3.10 2.98 3.08 9.55 47.36 8.67 8.31 15.22 7.87 3.03 2.86 2.98 2.86 3.02 2.70
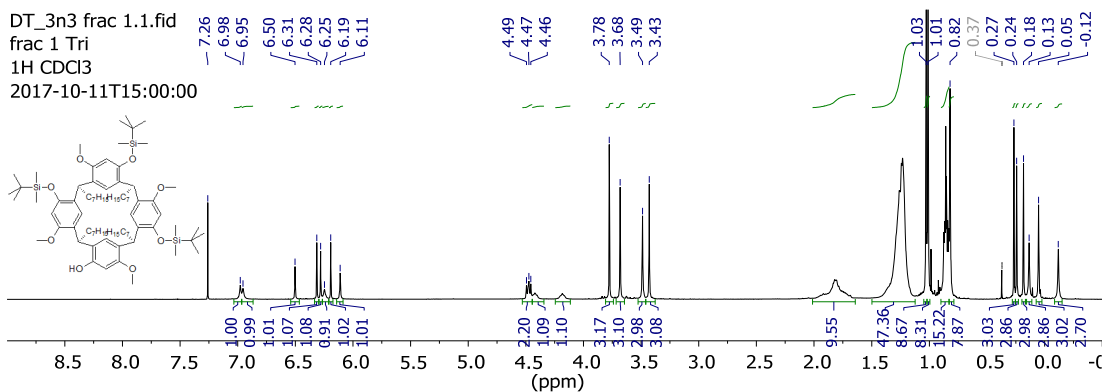
Appendix A10.1 (36) ^{1}H NMR spectrum recorded in CDCl$_3$.
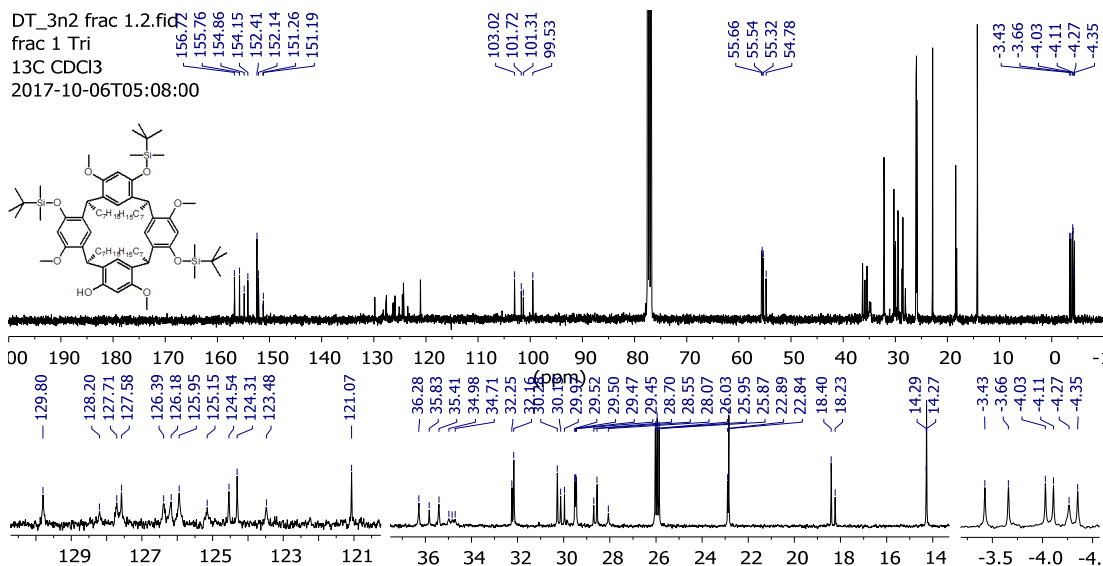
Appendix A10.2 (36) ^{13}C NMR spectrum recorded in CDCl$_3$.
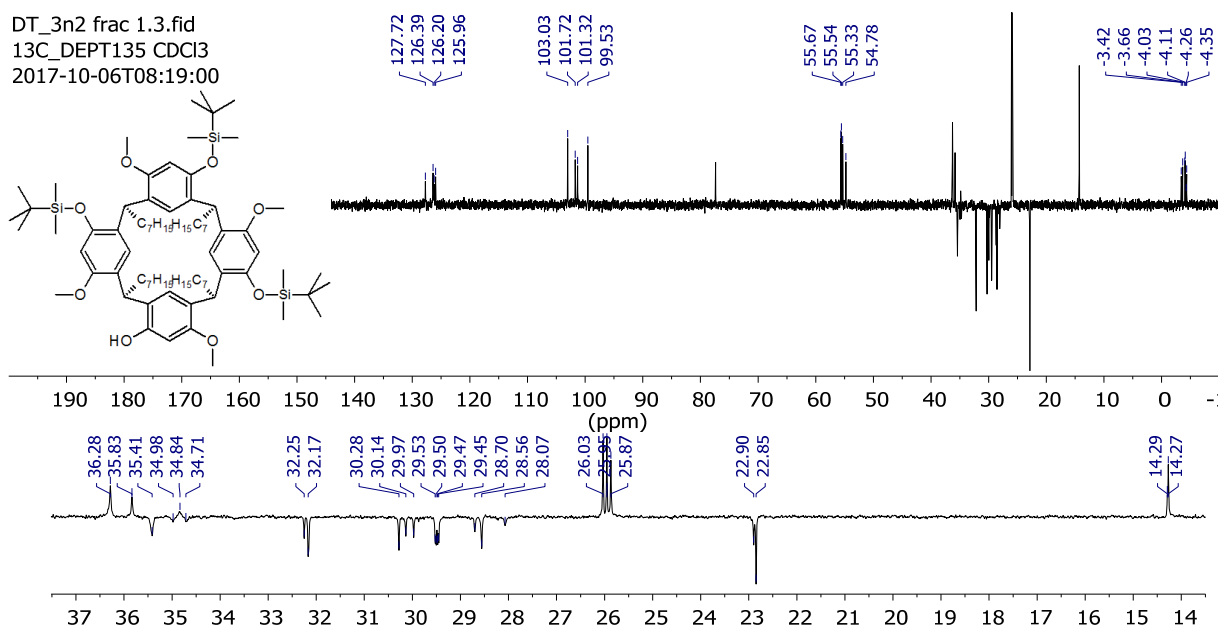
Appendix A10.3 (36) DEPT-135 NMR spectrum recorded in CDCl$_3$.

TBDPS

(40) Mono TBDPS
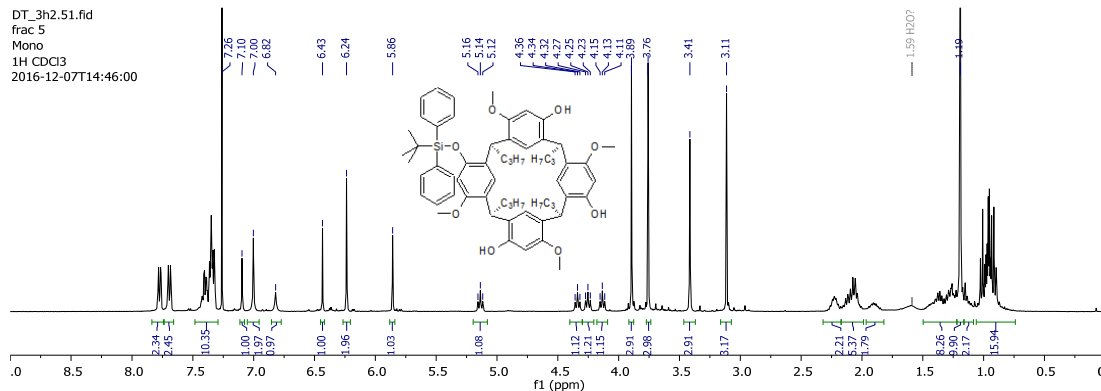
Appendix A11.1 (40) ^{1}H NMR spectrum.
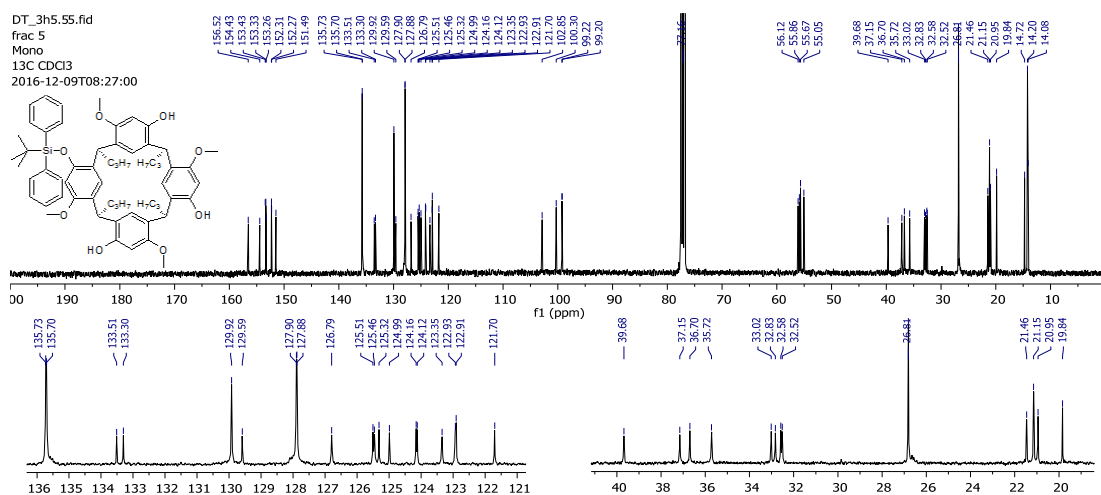
Appendix A11.2 (40) ^{13}C NMR spectrum.
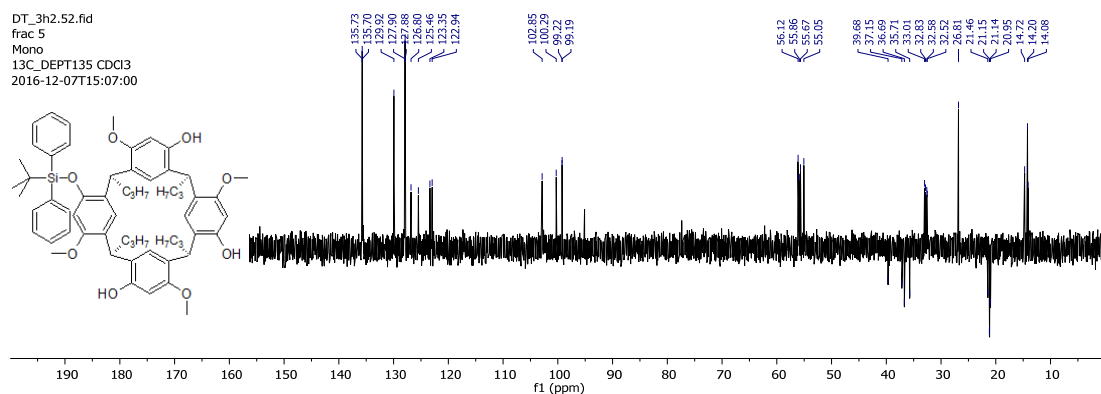
Appendix A11.3 (40) DPET-135 NMR spectrum.
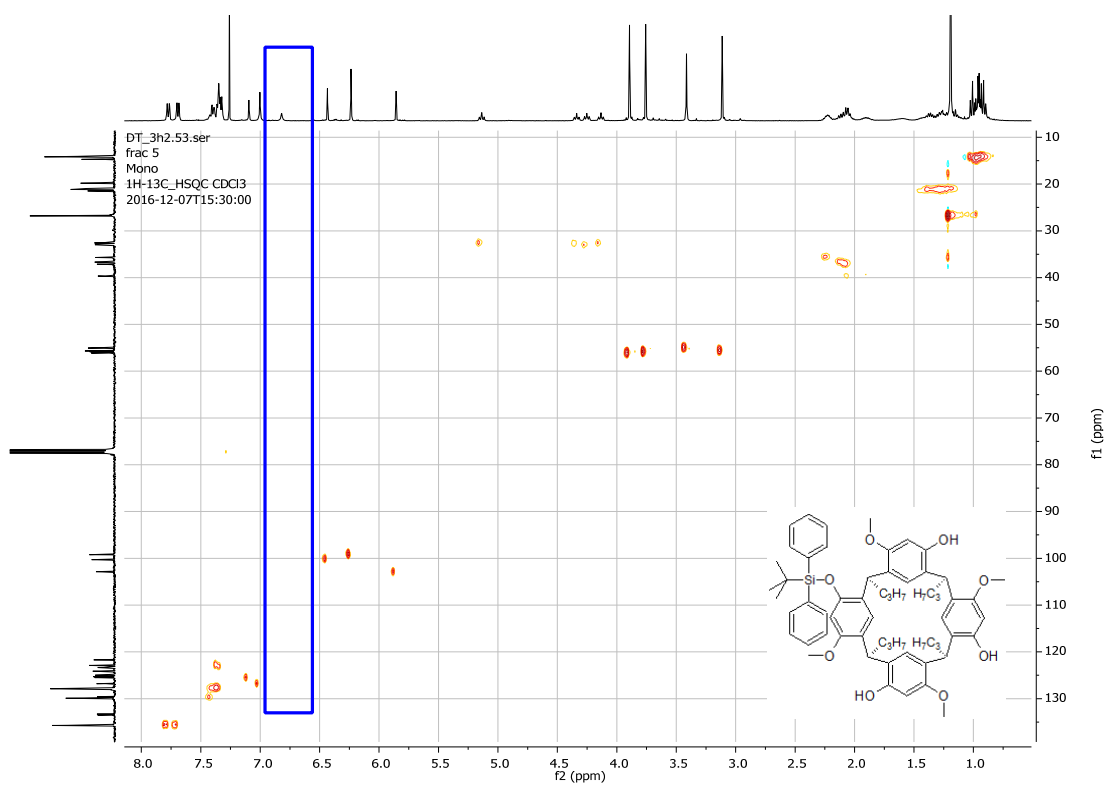
Appendix A11.4 (40) HSQC NMR spectrum.

(41) Proximal TBDPS
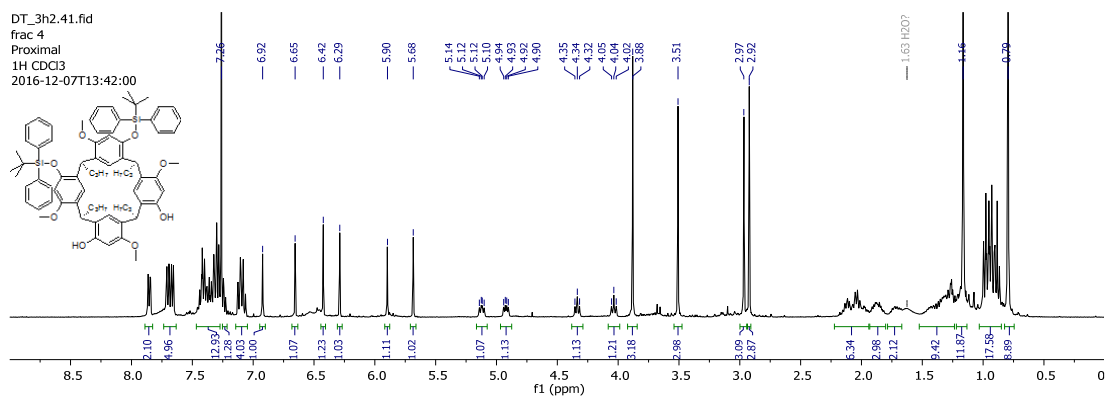
Appendix A12.1 (41) ^{1}H NMR spectrum.
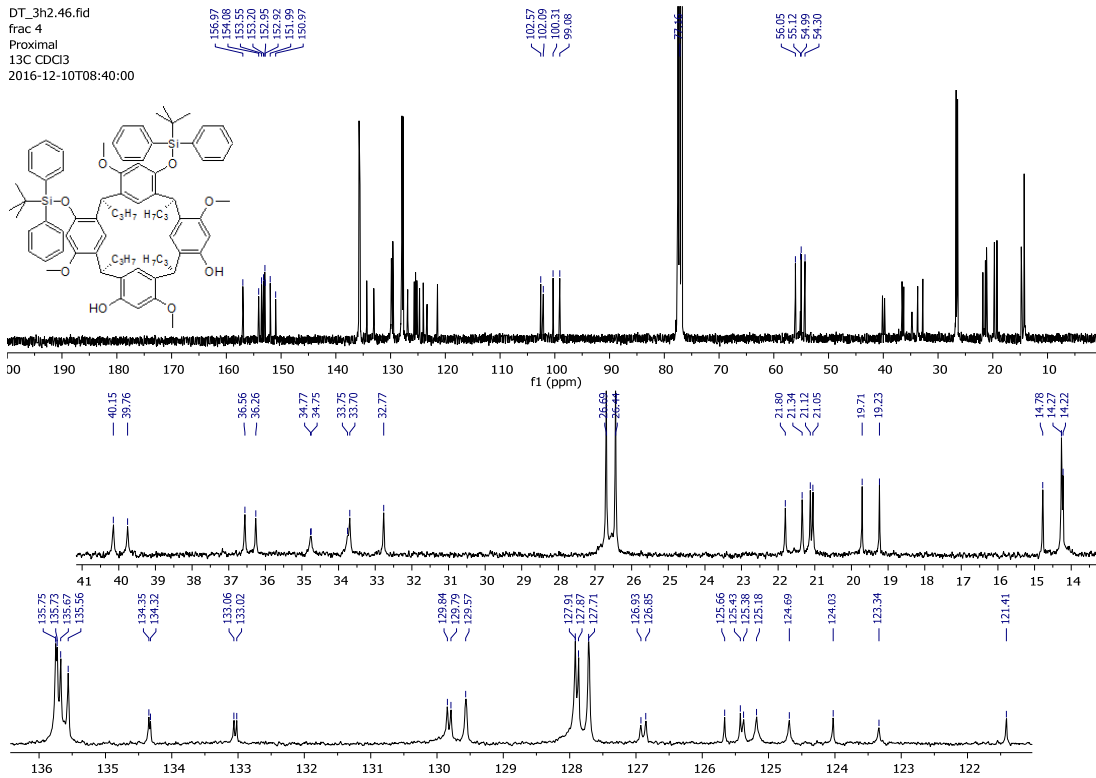
Appendix A12.2 (41) ^{13}C NMR spectrum.
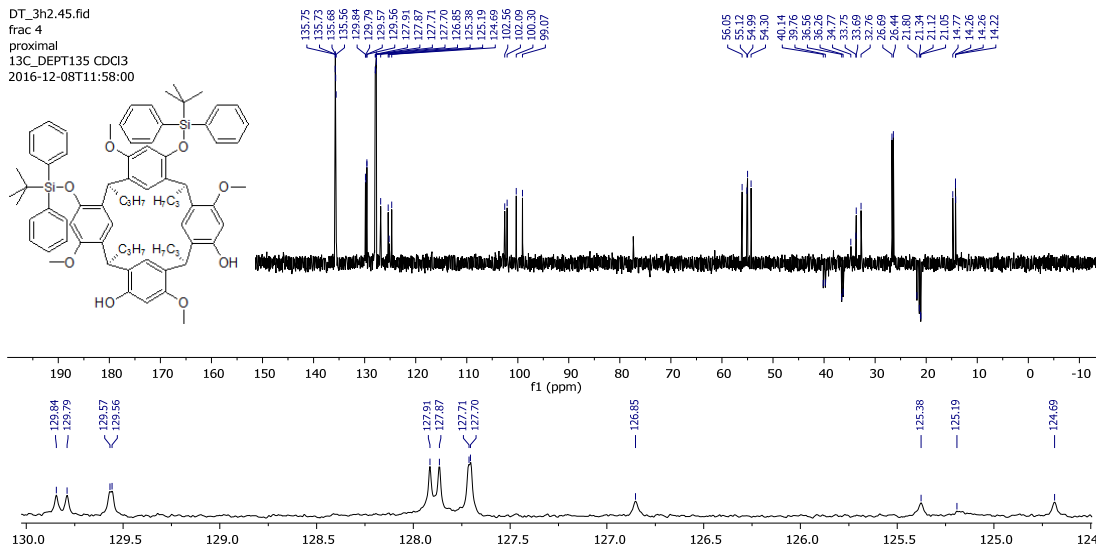
Appendix A12.3 (41) DEPT-135 NMR spectrum.

(42) Distal TBDPS
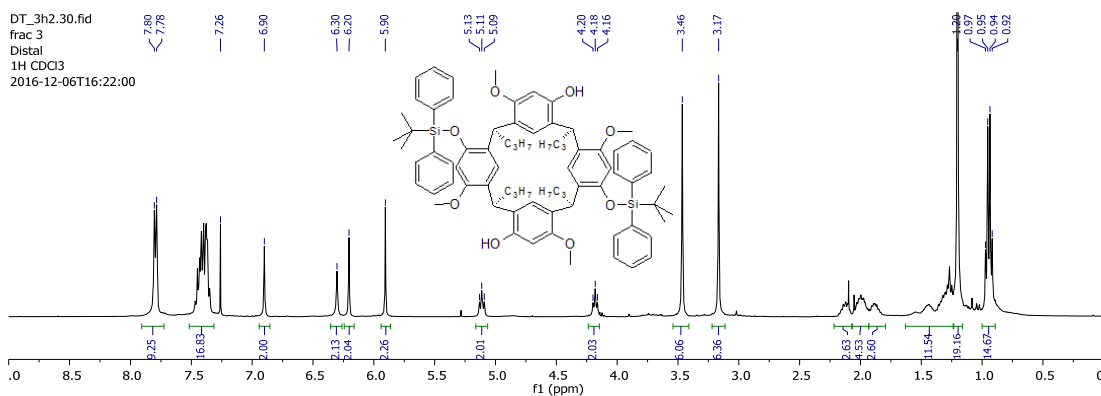
Appendix A13.1 (42) ^{1}H NMR spectrum.
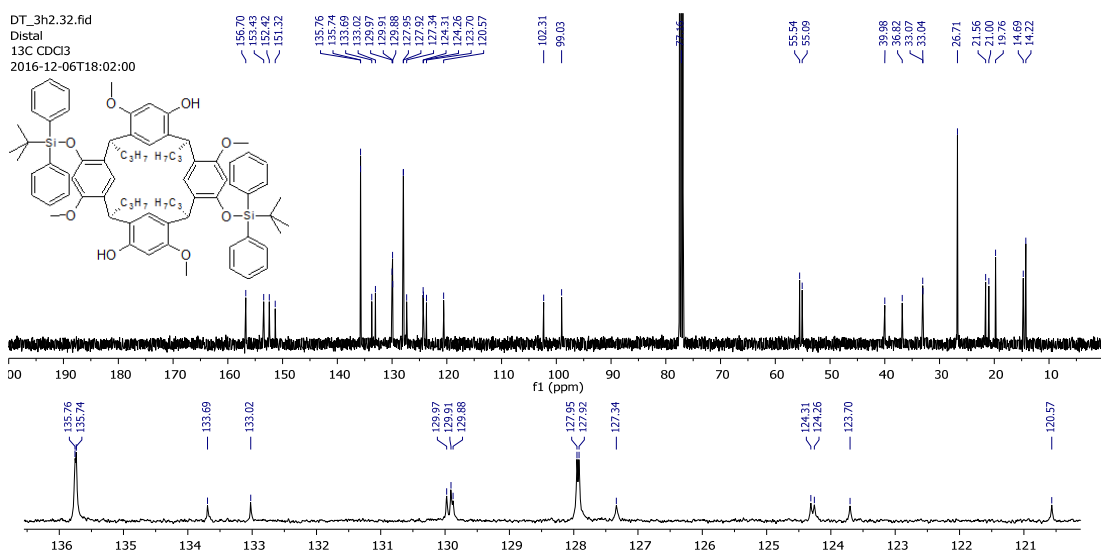
Appendix A13.2 (42) ^{13}C NMR spectrum.
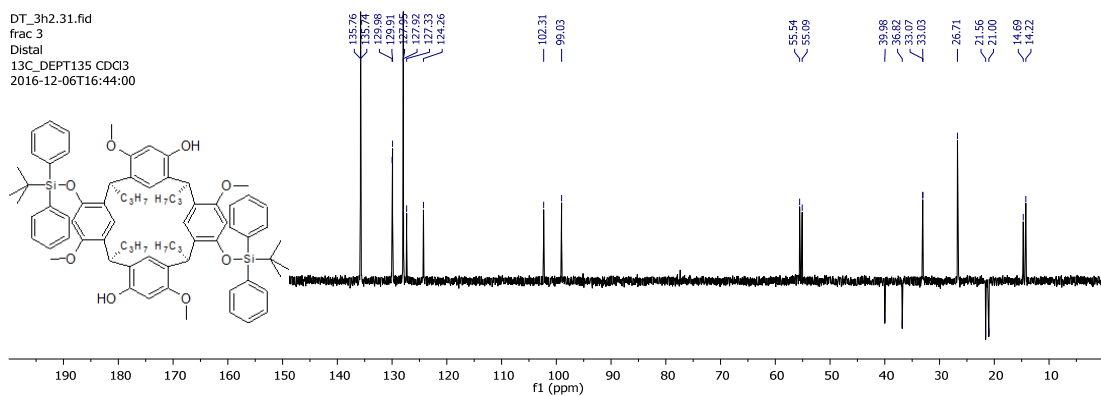
Appendix A13.3 (42) DEPT-135 NMR spectrum.

(43) Tri TBDPS

DT_3h2.20.fid
frac 2
Tri + TBDPS-OH
1H CDCl3
2016-12-06T16:07:00
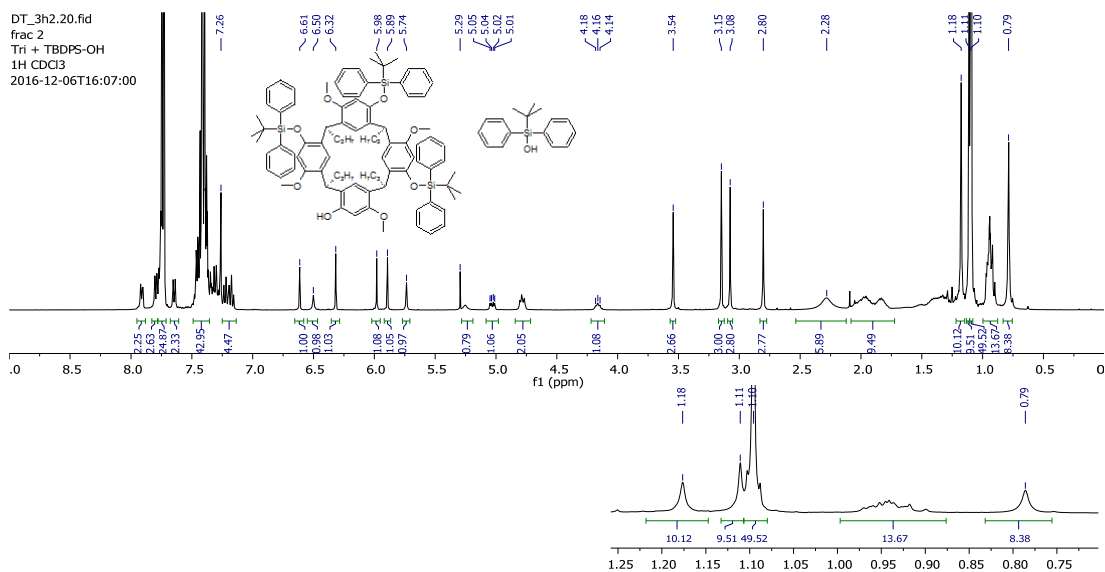
Appendix A14.1 (43) ^{1}H NMR spectrum.

Benzyl ether

(44) Mono benzyl ether

DT_3i2.84.fid
frac 1 MeOH recrys
trace of SM
1H CDCl3
2017-01-09T18:14:00

DT_3i3.54.fid
Mono
1H CDCl3 +D2O
2017-02-13T15:24:00
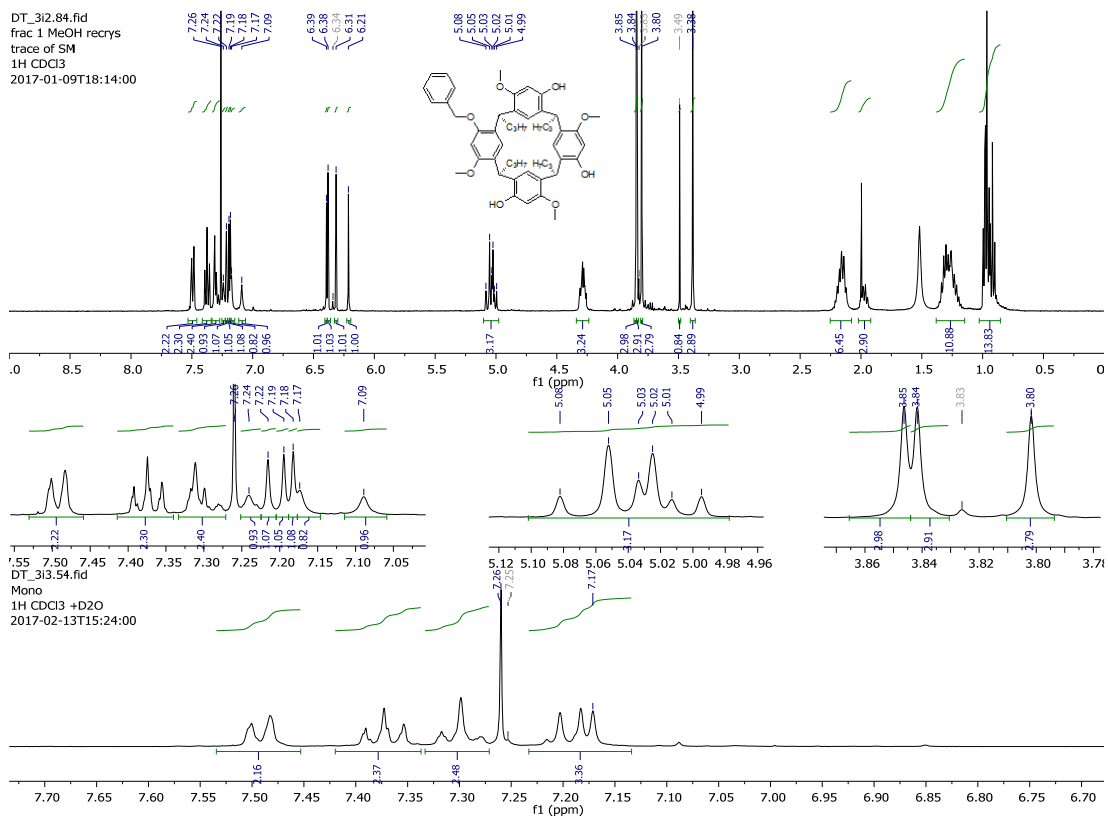
Appendix A15.1 (44) ^{1}H NMR spectrum recorded in CDCl₃.
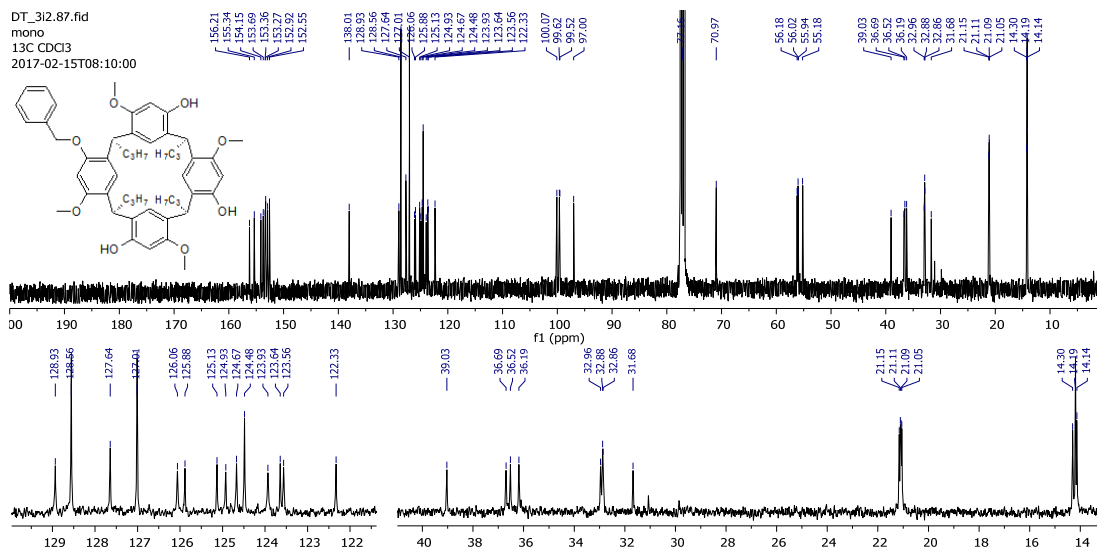
Appendix A15.2 (44) ^{13}C NMR spectrum recorded in CDCl$_3$.
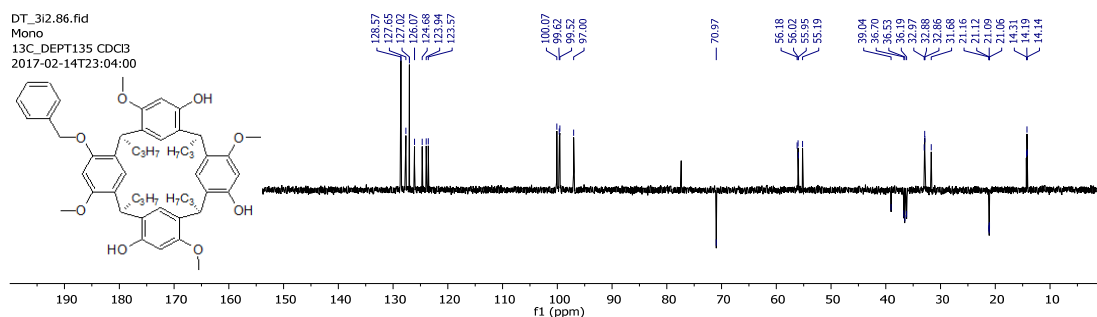
Appendix A15.3 (44) DEPT-135 NMR spectrum recorded in CDCl$_3$.

(45) Proximal benzyl ether
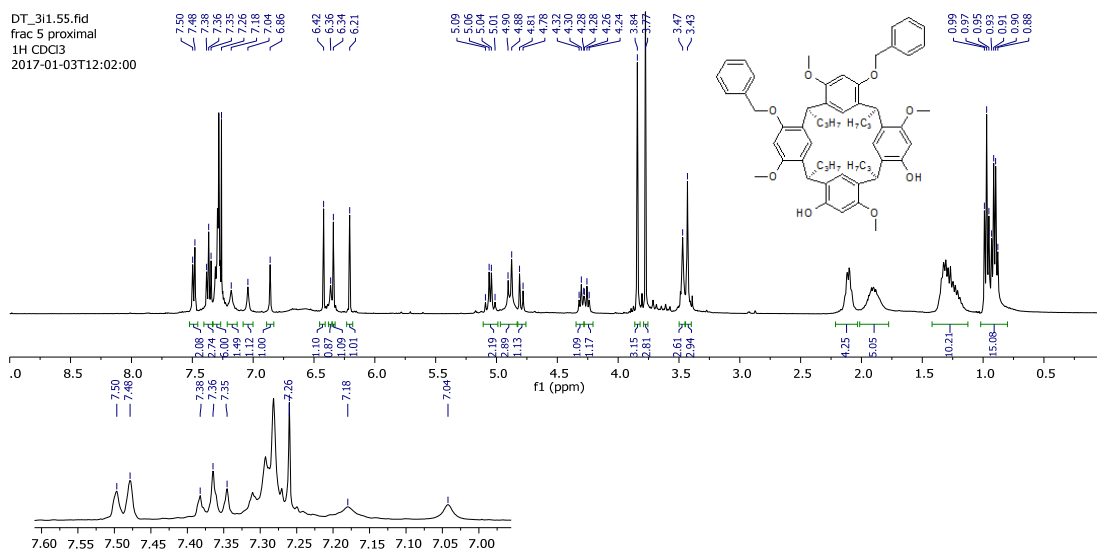
Appendix A16.1 (45) ^{1}H NMR spectrum recorded in CDCl$_3$.
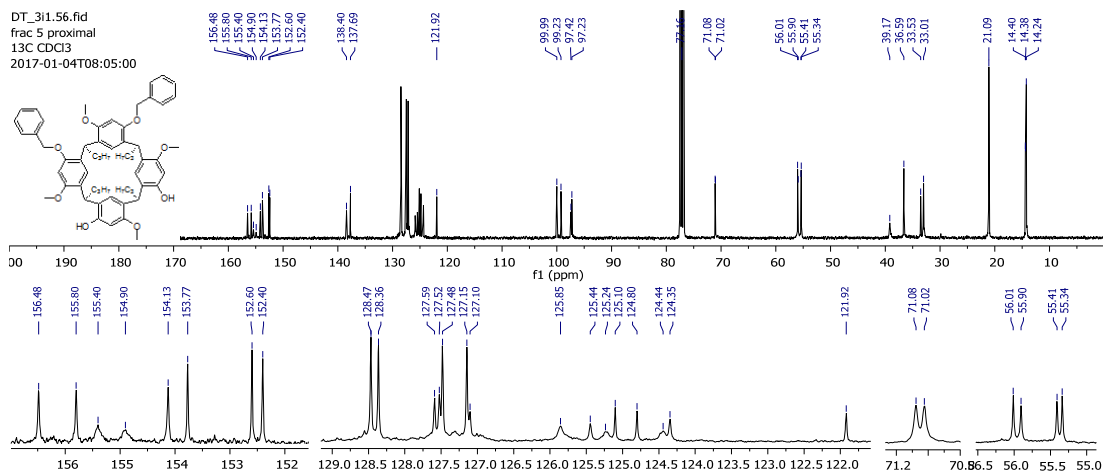
Appendix A16.2 (45) ^{13}C NMR spectrum recorded in CDCl$_3$.
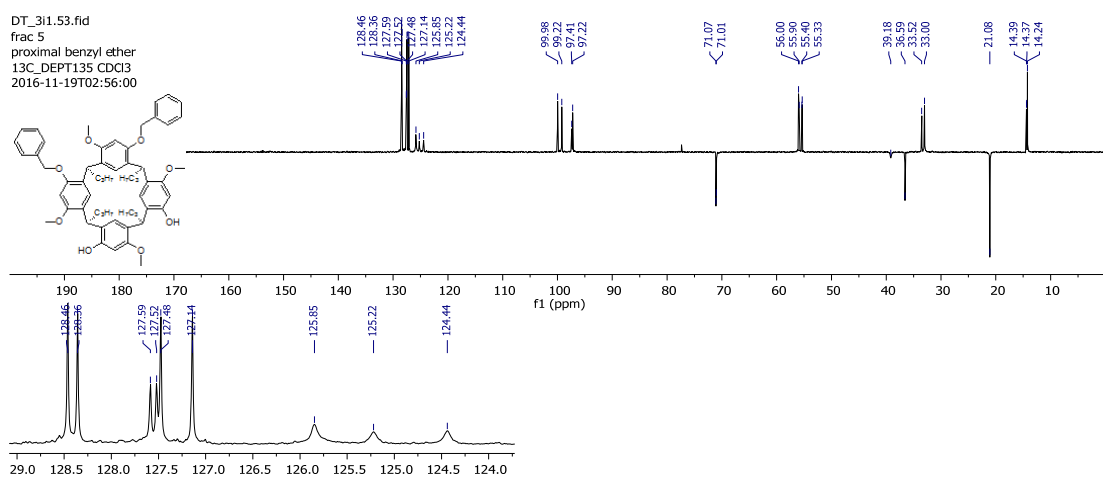
Appendix A16.3 (45) DEPT-135 NMR spectrum recorded in CDCl$_3$.
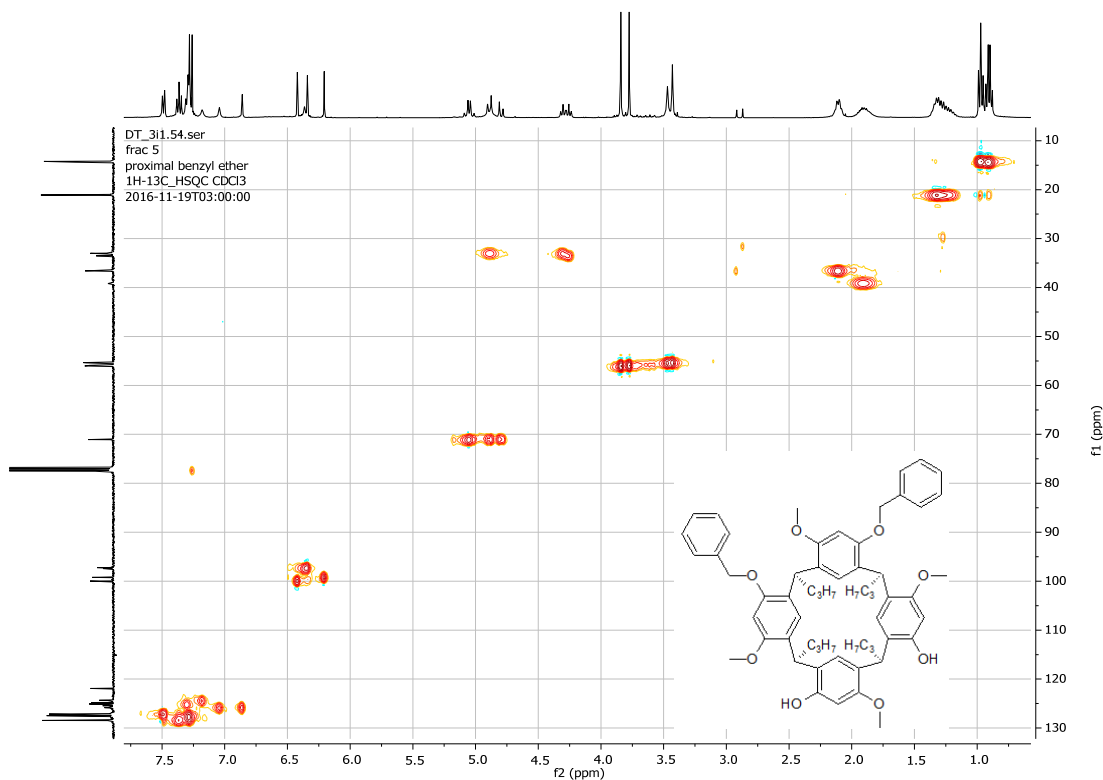
Appendix A16.4 (45) HSQC NMR spectrum recorded in CDCl$_3$.

(46) Distal benzyl ether
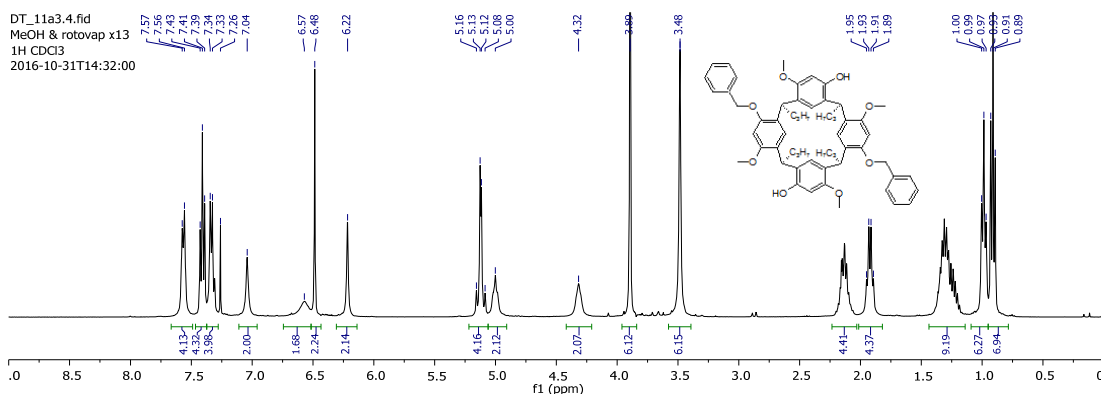
Appendix A17.1 (46) ^{1}H NMR spectrum recorded in CDCl$_3$.
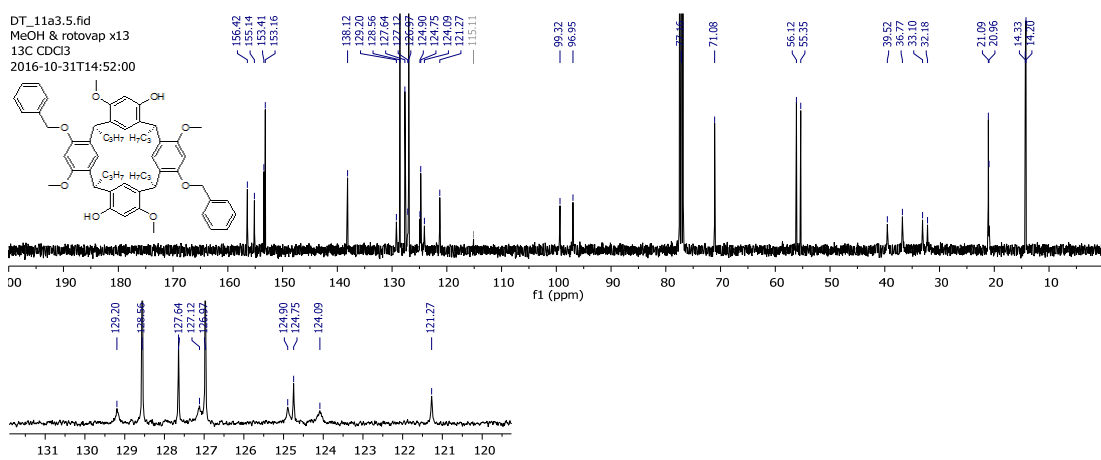
Appendix A17.2 (46) ^{13}C NMR spectrum recorded in CDCl$_3$.
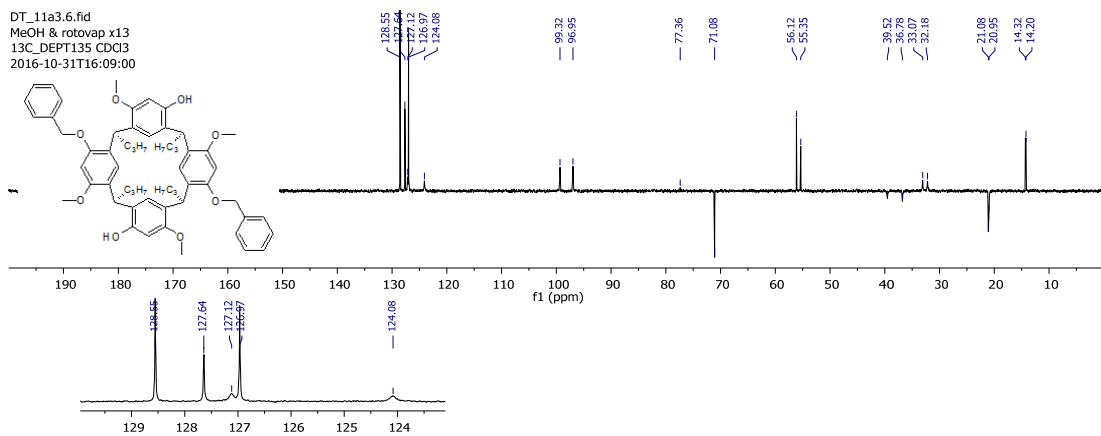
Appendix A17.3 (46) DEPT-135 NMR spectrum recorded in CDCl$_3$.
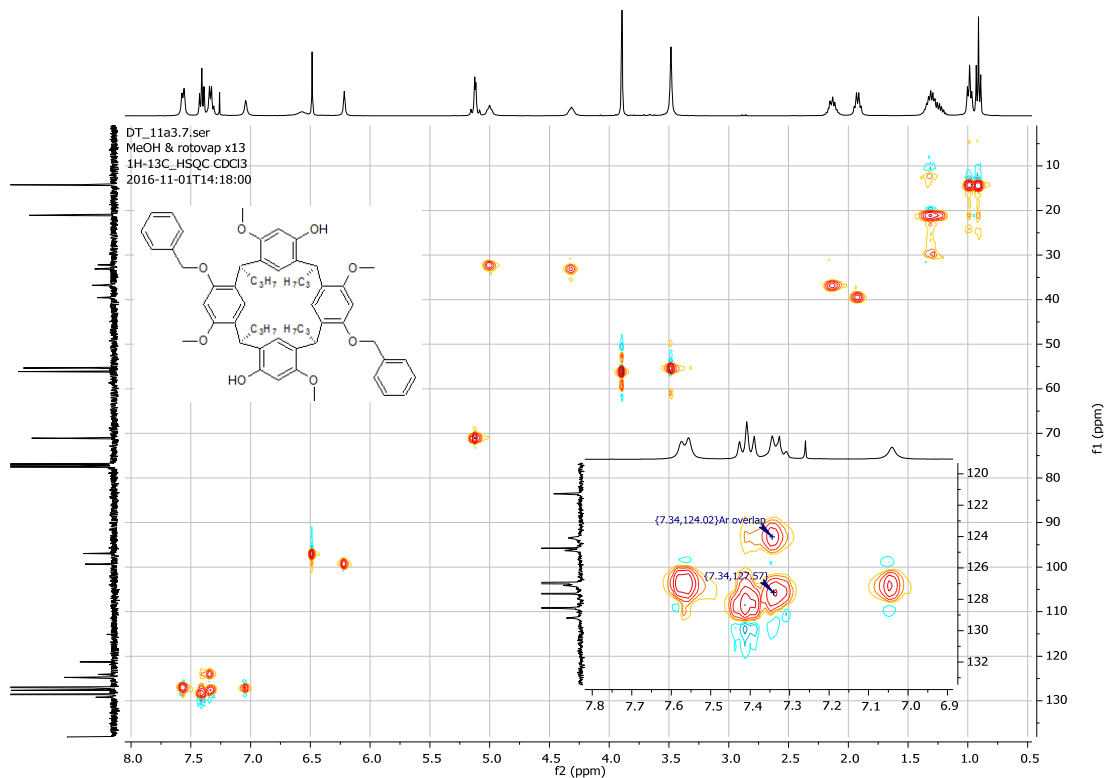
Appendix A17.4 (46) HSQC NMR spectrum recorded in CDCl₃.

(47) Tri benzyl ether
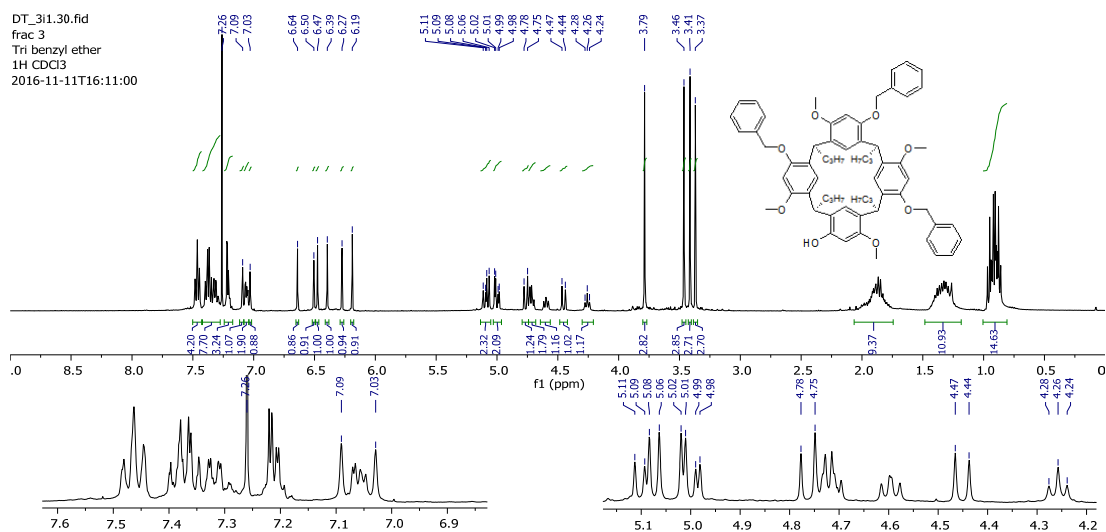
Appendix A18.1 (47) ¹H NMR spectrum recorded in CDCl₃.
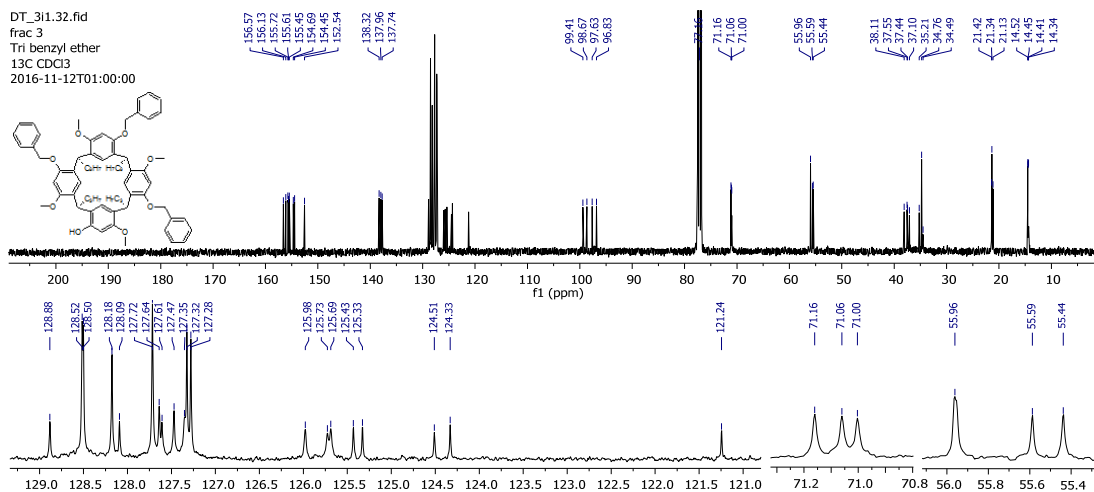
Appendix A18.2 (47) ^{13}C NMR spectrum recorded in CDCl$_3$.
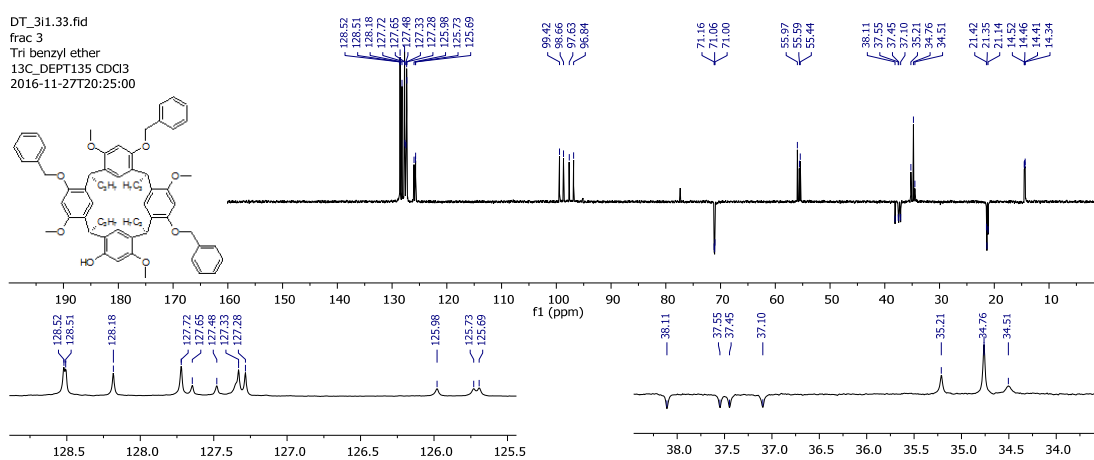
Appendix A18.3 (47) DEPT-135 NMR spectrum recorded in CDCl$_3$.
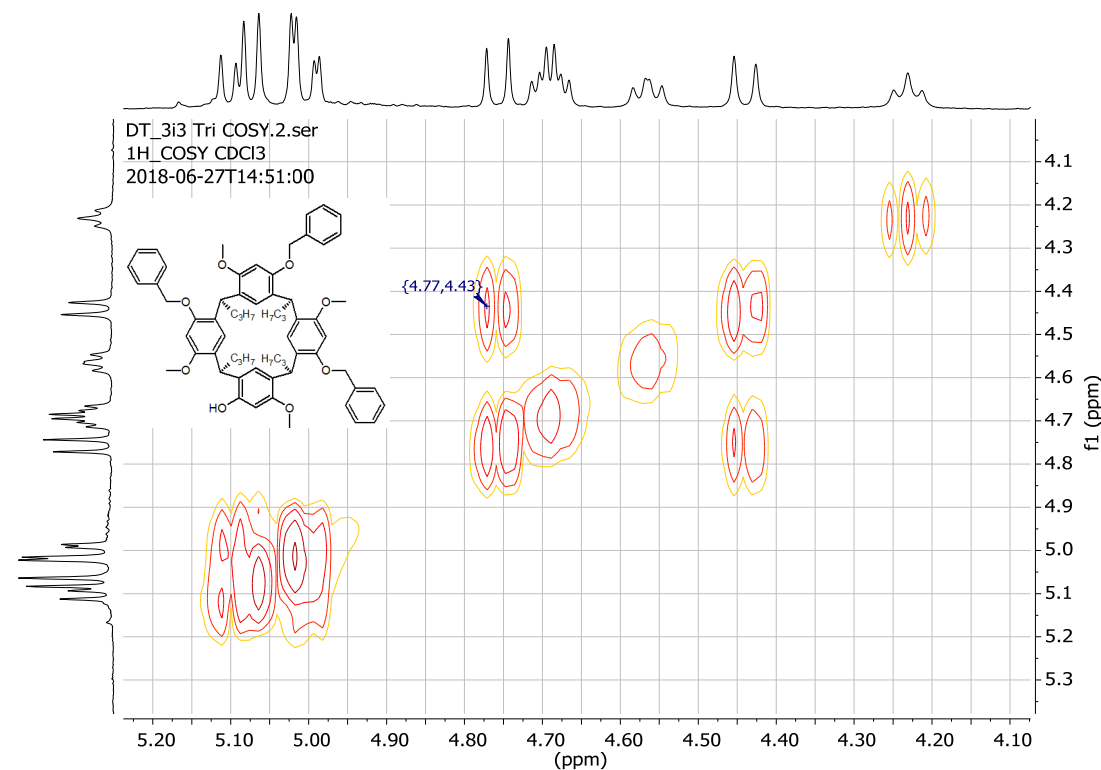
Appendix A18.4 (47) COSY NMR spectrum recorded in CDCl$_3$.
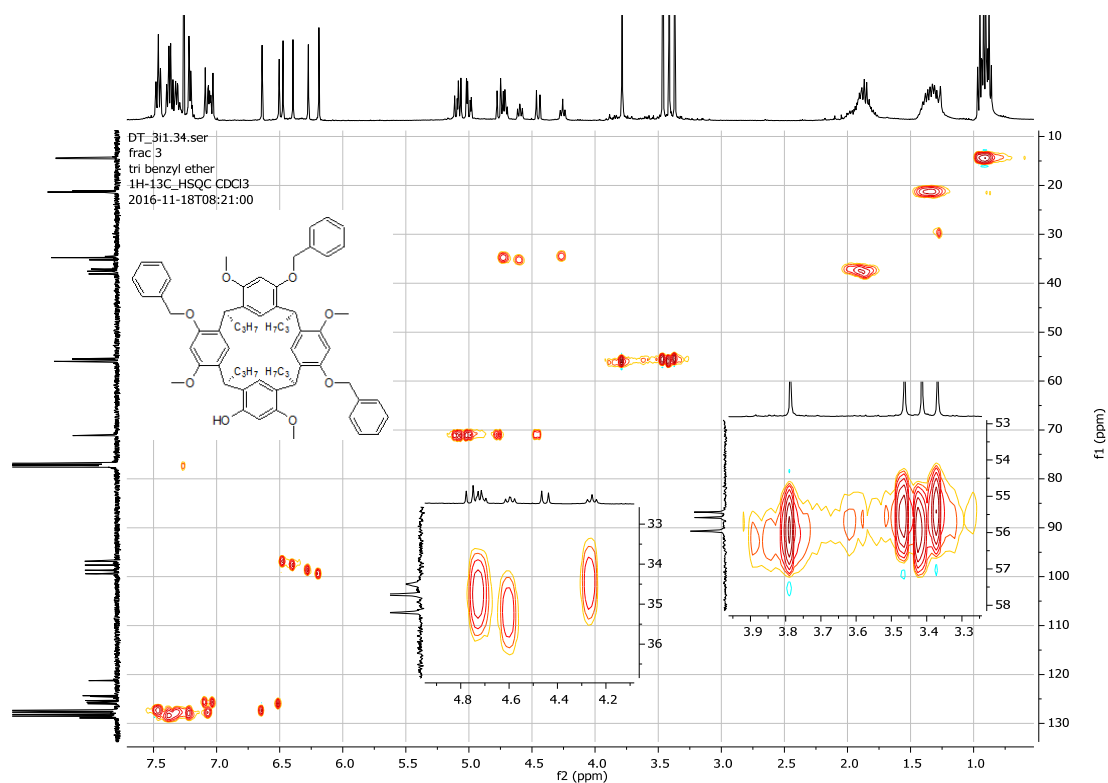
Appendix A18.5 (47) HSQC NMR spectrum recorded in CDCl$_3$.

Replacement of TBDMS protecting groups

(48) 1^4,5^6-di-*tert*-butyldimethylsilylether-3^6,7^6-dimethanesulfonyl-1^6,3^4,5^4,7^4-tetramethoxy-2,4,6,8-tetrapropylresorcin[4]arene
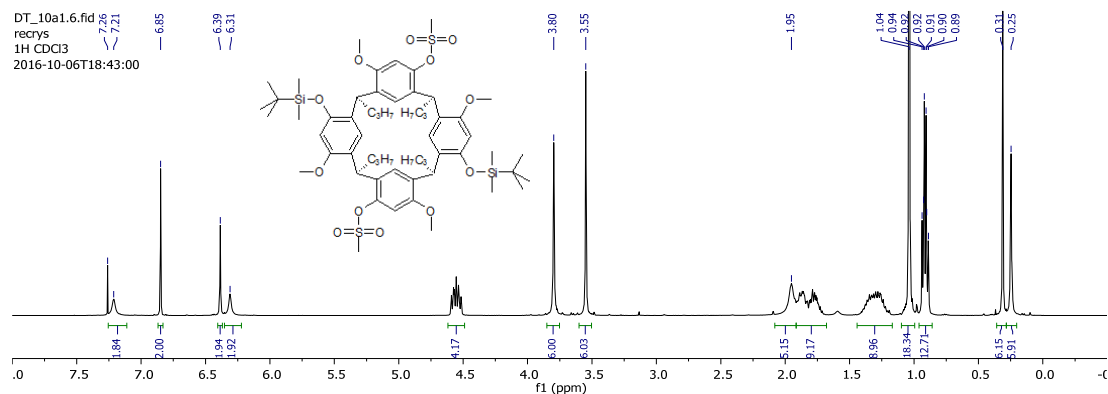
Appendix A19.1 (48) ^{1}H NMR spectrum recorded in CDCl$_3$.
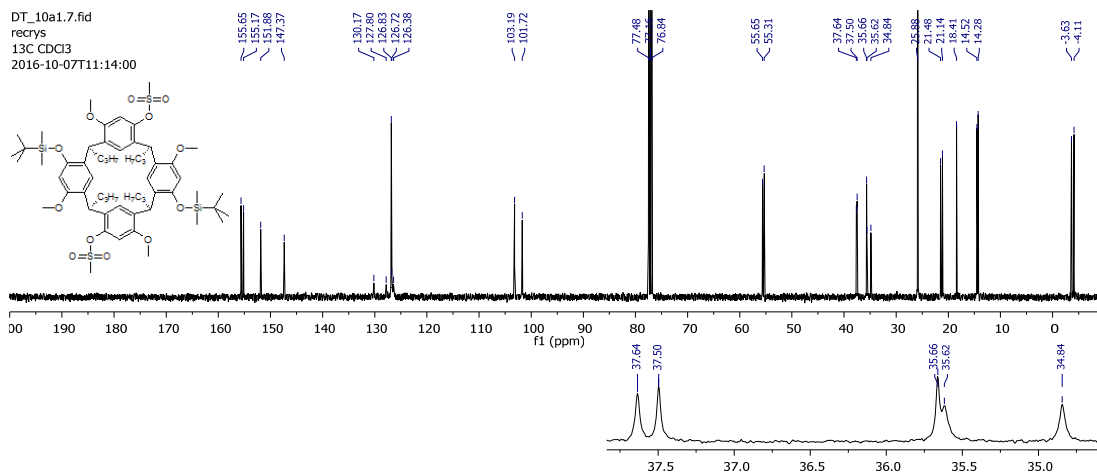
Appendix A19.2 (48) ^{13}C NMR spectrum recorded in CDCl$_3$.
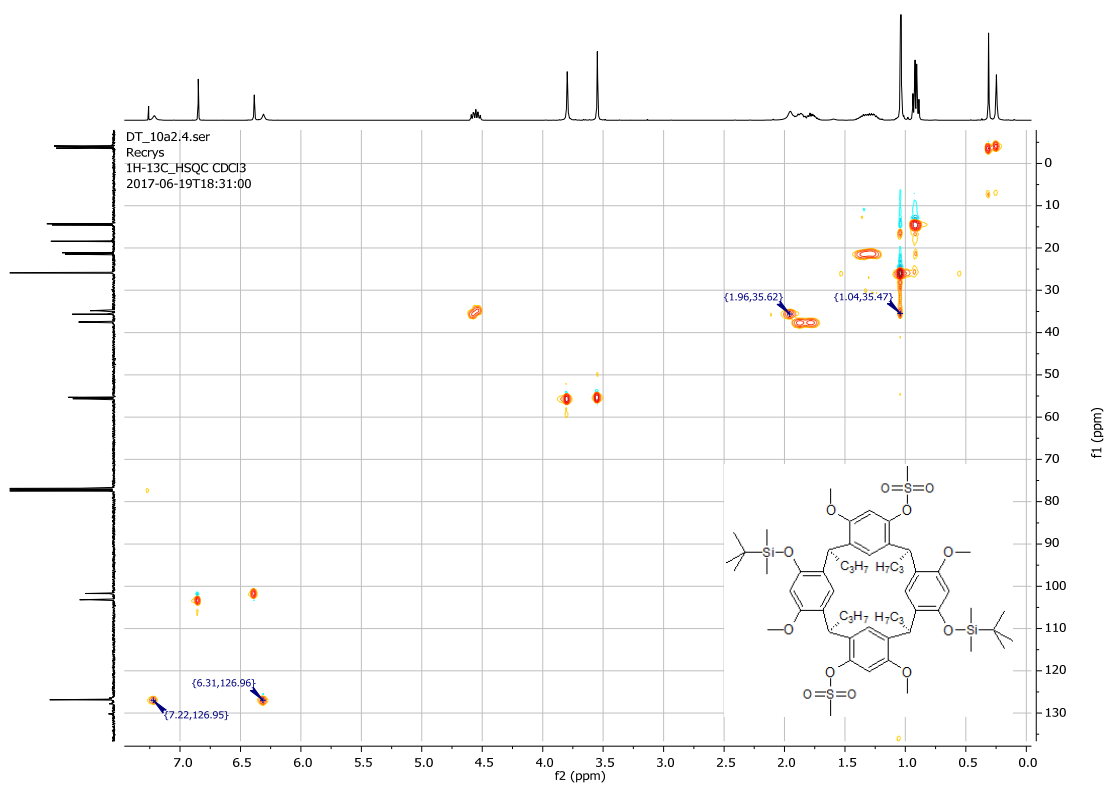
Appendix A19.3 (48) HSQC NMR spectrum recorded in CDCl$_3$.

(49) $1^4,5^6$-dibenzyloxy-$3^6,7^6$-di-*tert*-butyldimethylsilylether-$1^6,3^4,5^4,7^4$-tetramethoxy-2,4,6,8-tetrapropylresorcin[4]arene

DT_10b5.1.fid
columned
1H CDCl3
2016-10-26T18:55:00
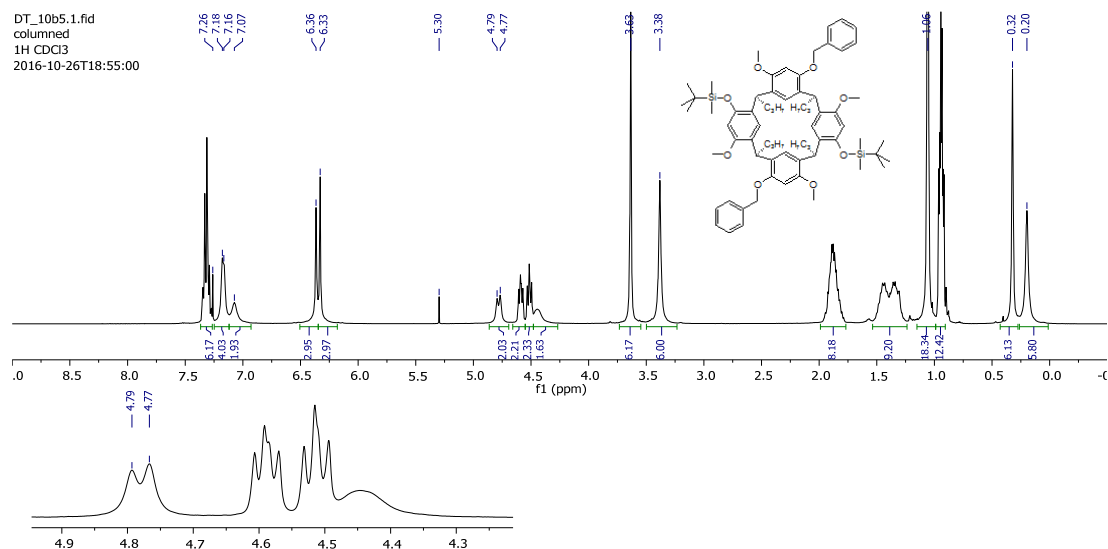
Appendix A20.1 (49) ^{1}H NMR spectrum recorded in CDCl$_3$.

DT_10b5.2.fid
columned
13C CDCl3
2016-10-26T19:16:00
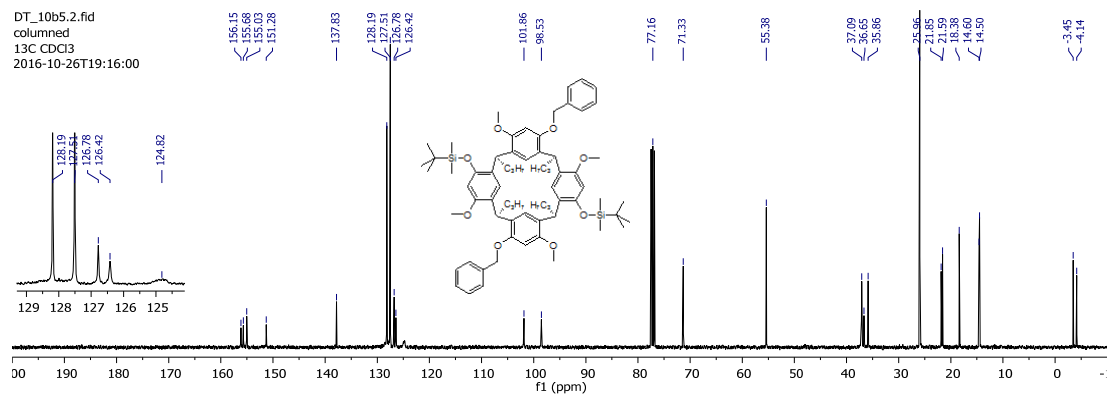
Appendix A20.2 (49) ^{13}C NMR spectrum recorded in CDCl$_3$.

DT_10b5.3.fid
columned
13C_DEPT135 CDCl3
2016-10-26T19:34:00
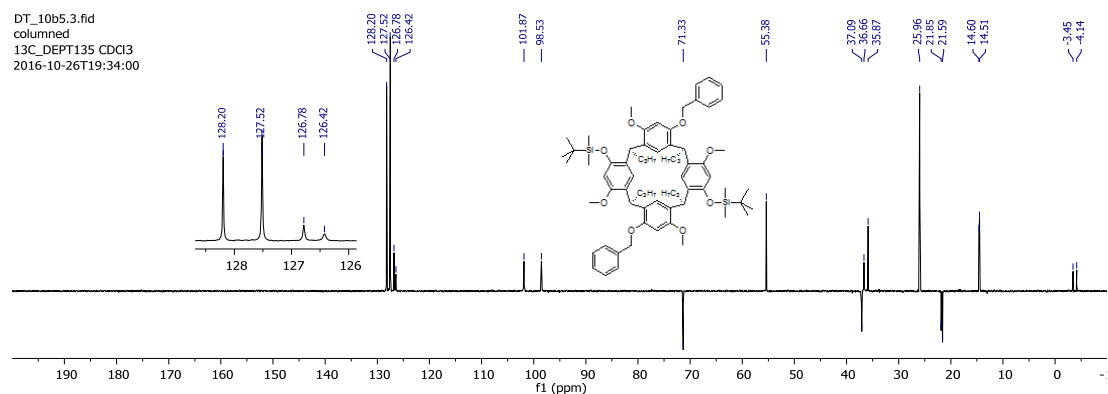
Appendix A20.3 (49) DEPT-135 NMR spectrum recorded in CDCl$_3$.
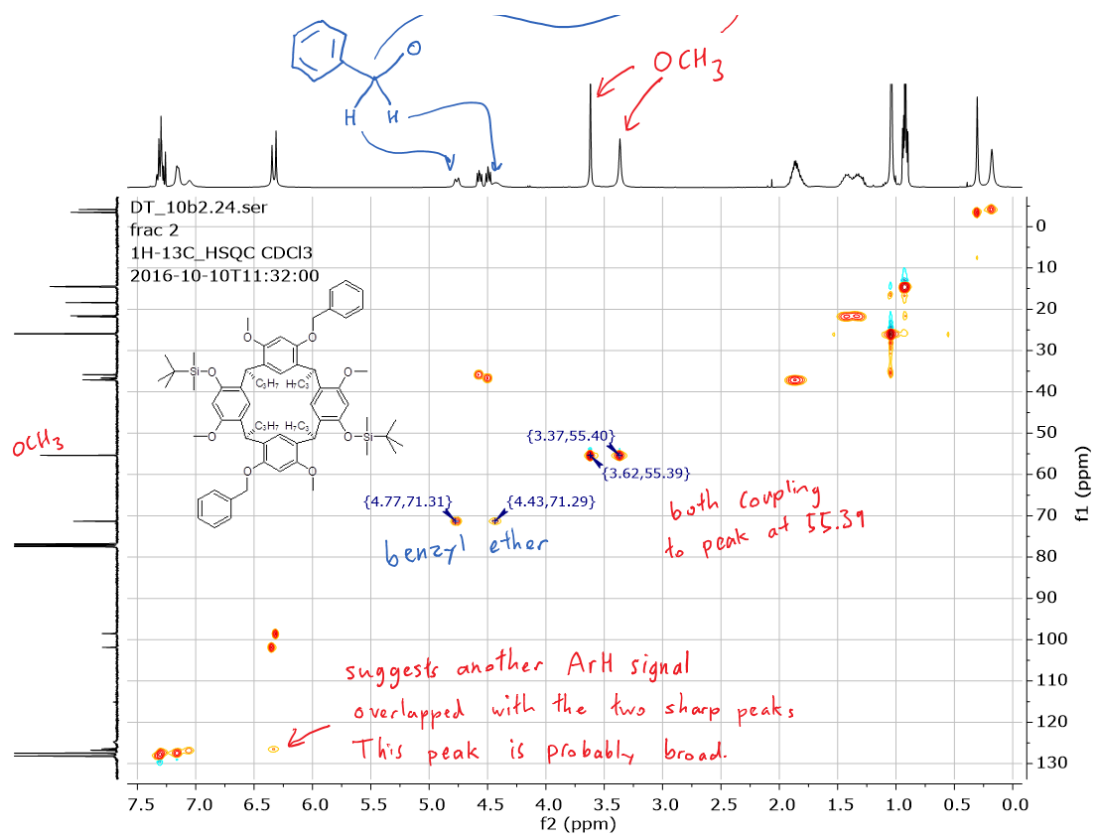
Appendix A20.4 (49) HSQC NMR spectrum recorded in CDCl$_3$.

5 Synthesis of crown resorcinarenes

Poly(ethylene glycol)ditoluenesulfonate

(50) Tetra(ethylene glycol)ditoluenesulfonate
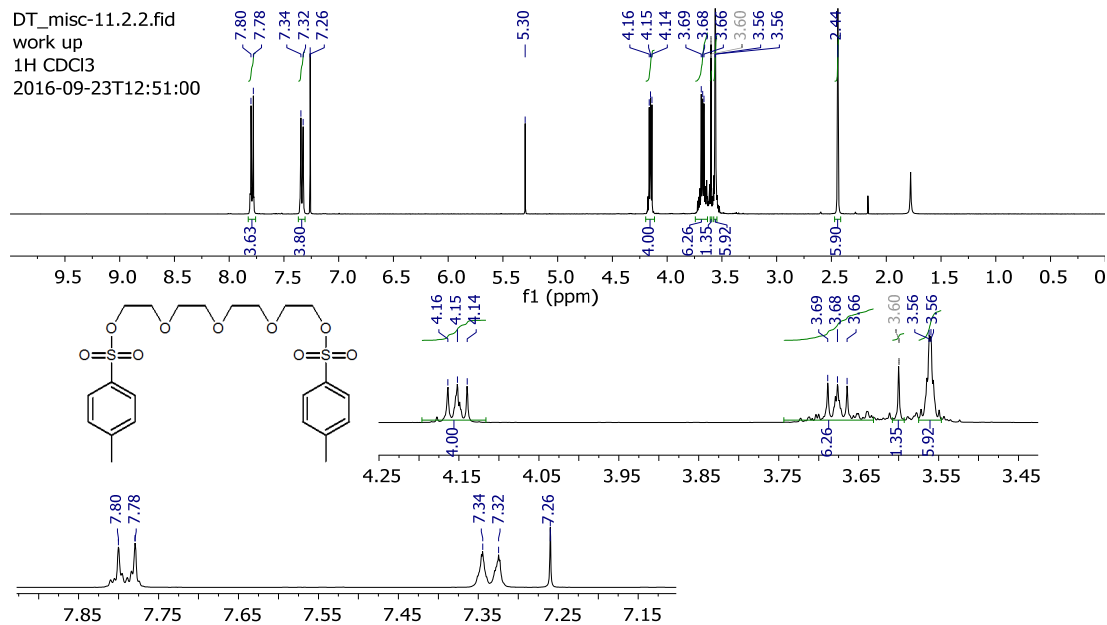
Appendix A21.1 (50) [superscript 1]H NMR spectrum recorded in CDCl[subscript 3].

(51) Penta(ethylene glycol)ditoluenesulfonate
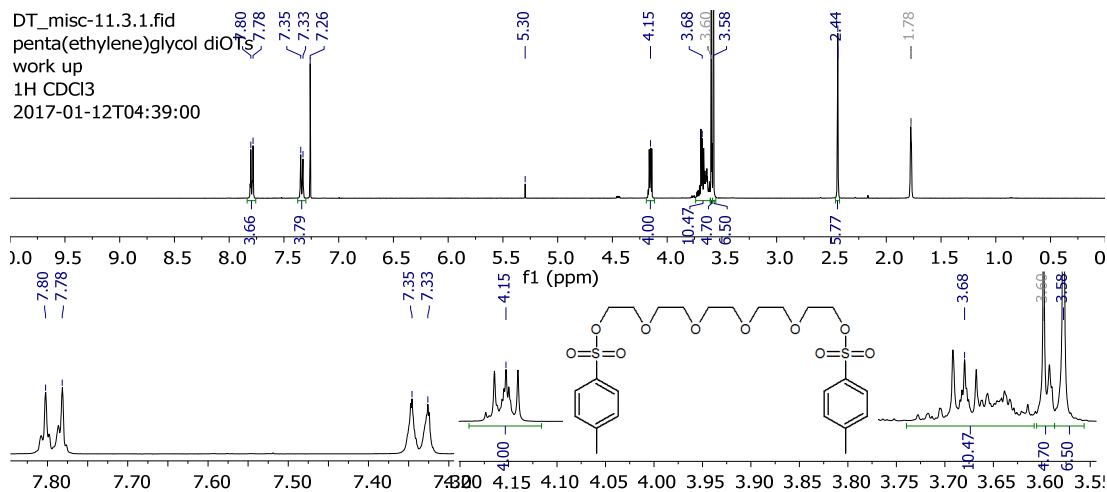
Appendix A22.1 (51) [superscript 1]H NMR spectrum recorded in CDCl[subscript 3].
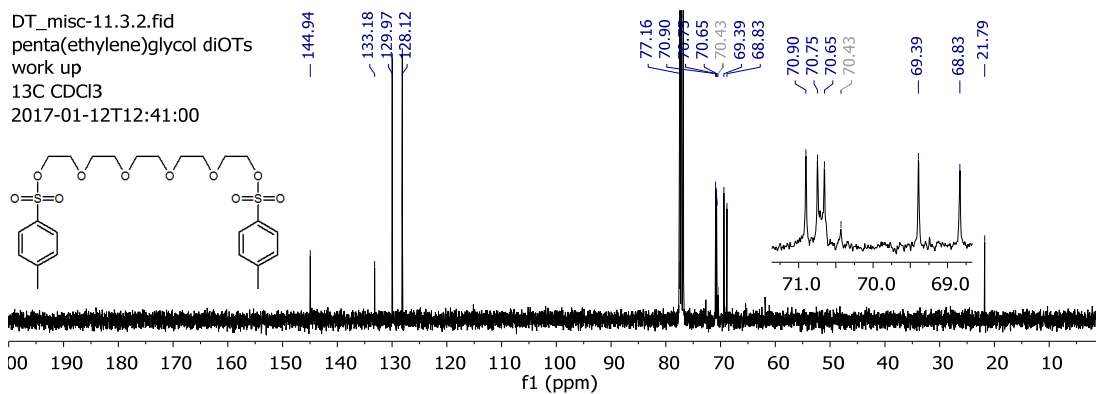
Appendix A22.2 (51) ^{13}C NMR spectrum recorded in CDCl₃.

(52) Hexa(ethylene glycol)ditoluenesulfonate
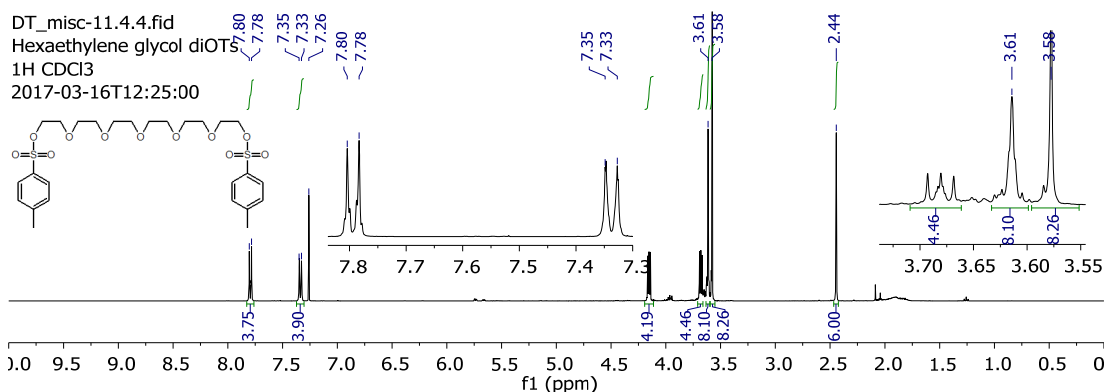
Appendix A23.1 (52) ^{1}H NMR spectrum recorded in CDCl₃.
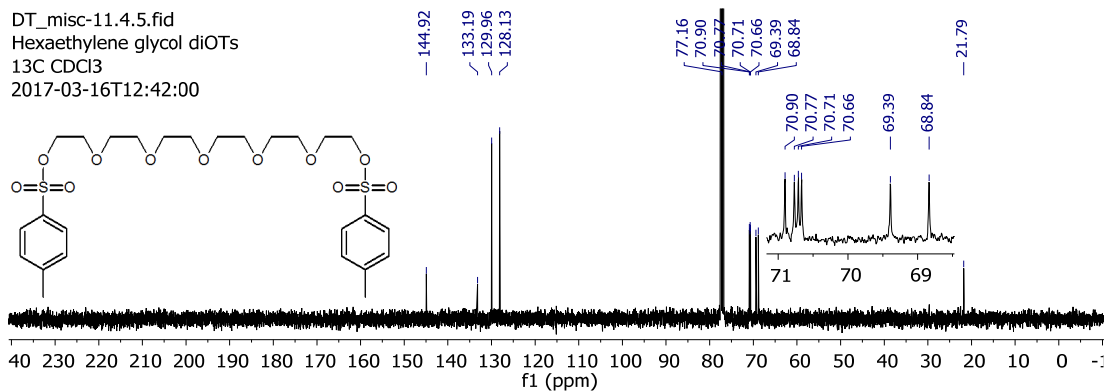
Appendix A23.2 (52) ^{13}C NMR spectrum recorded in CDCl₃.

Dibenzyloxy crown resorcinarenes

(53) Dibenzyloxy crown-5 resorcinarene
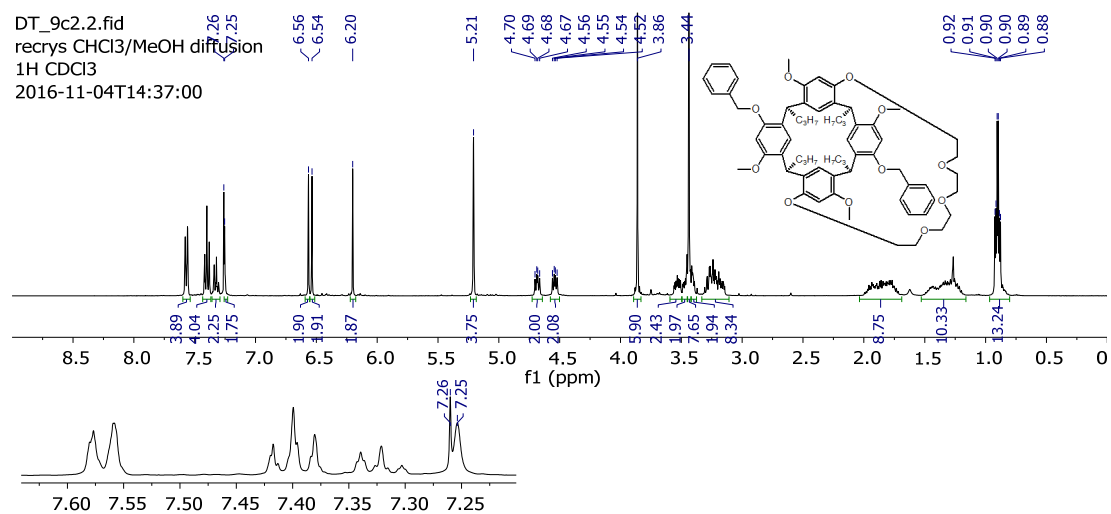
Appendix A24.1 (53) ^{1}H NMR spectrum recorded in CDCl$_3$.
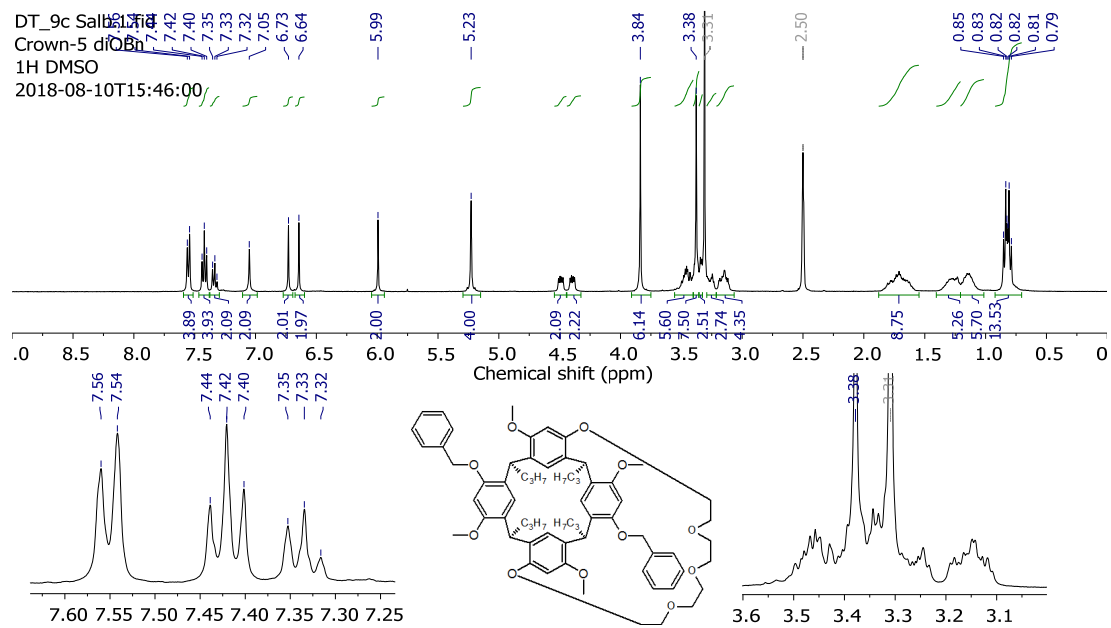
Appendix A24.2 (53) ^{1}H NMR spectrum recorded in DMSO-d$_6$.
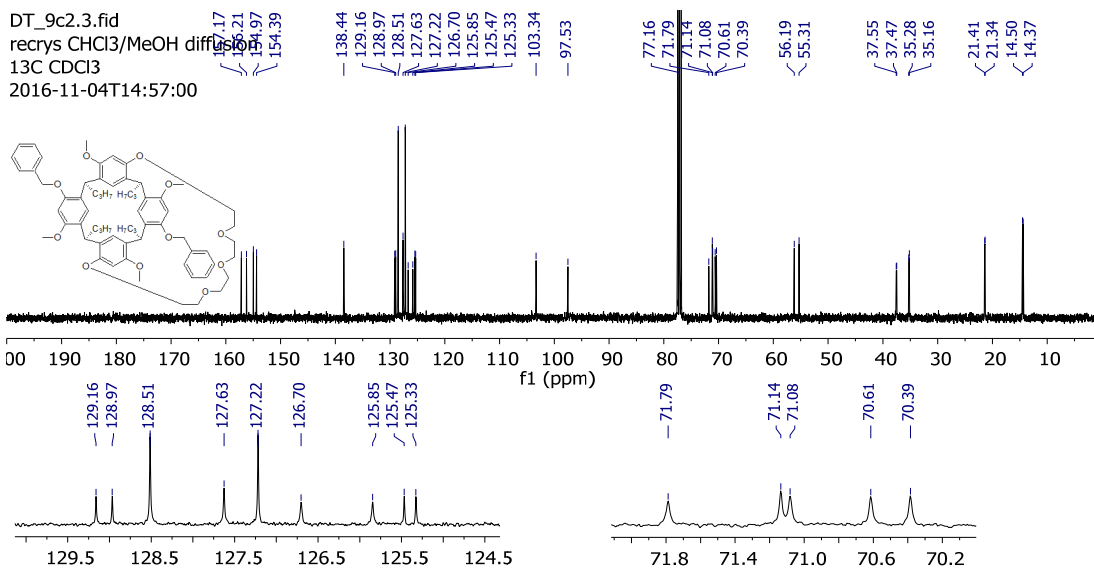
Appendix A24.3 (53) ^{13}C NMR spectrum recorded in CDCl$_3$.
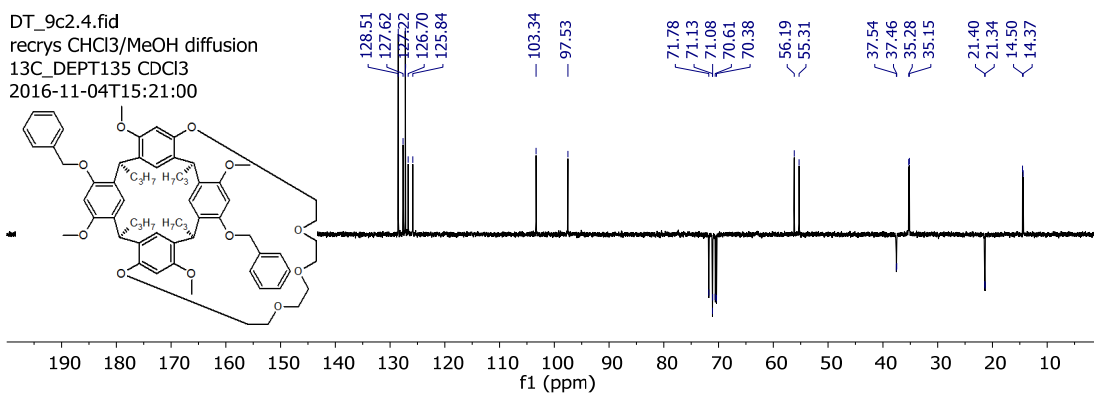
Appendix A24.4 (53) DEPT-135 NMR spectrum recorded in CDCl$_3$.
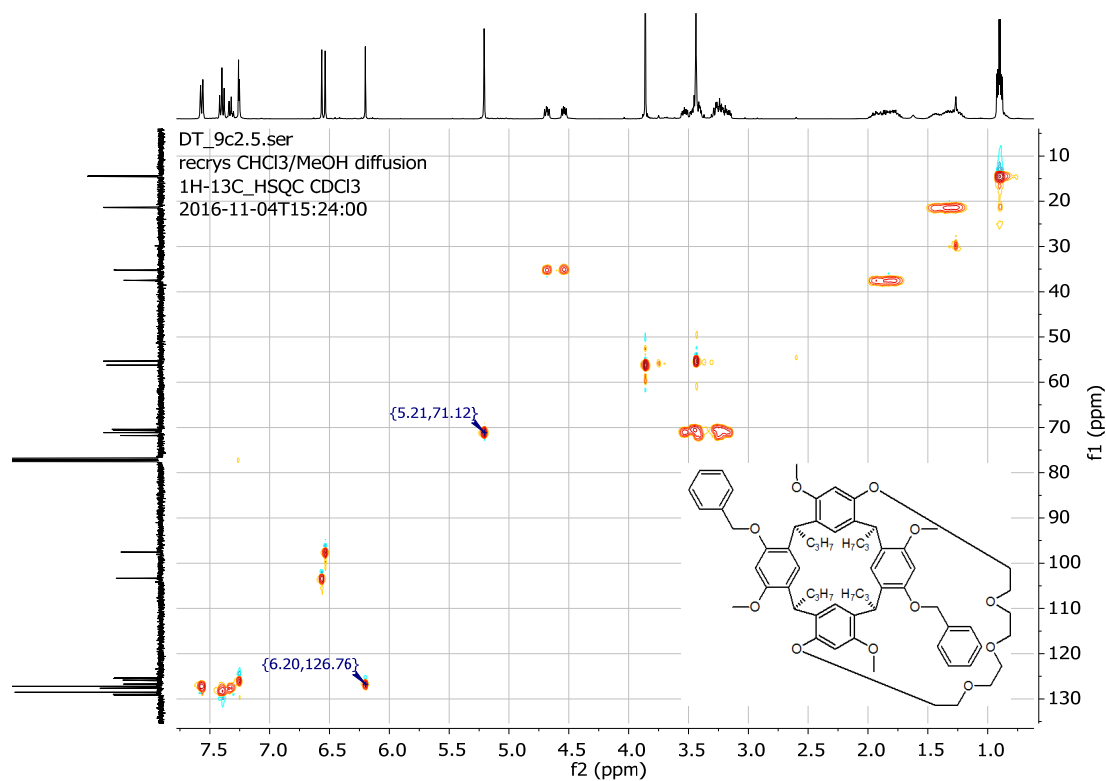
Appendix A24.5 (53) HSQC NMR spectrum recorded in CDCl₃.
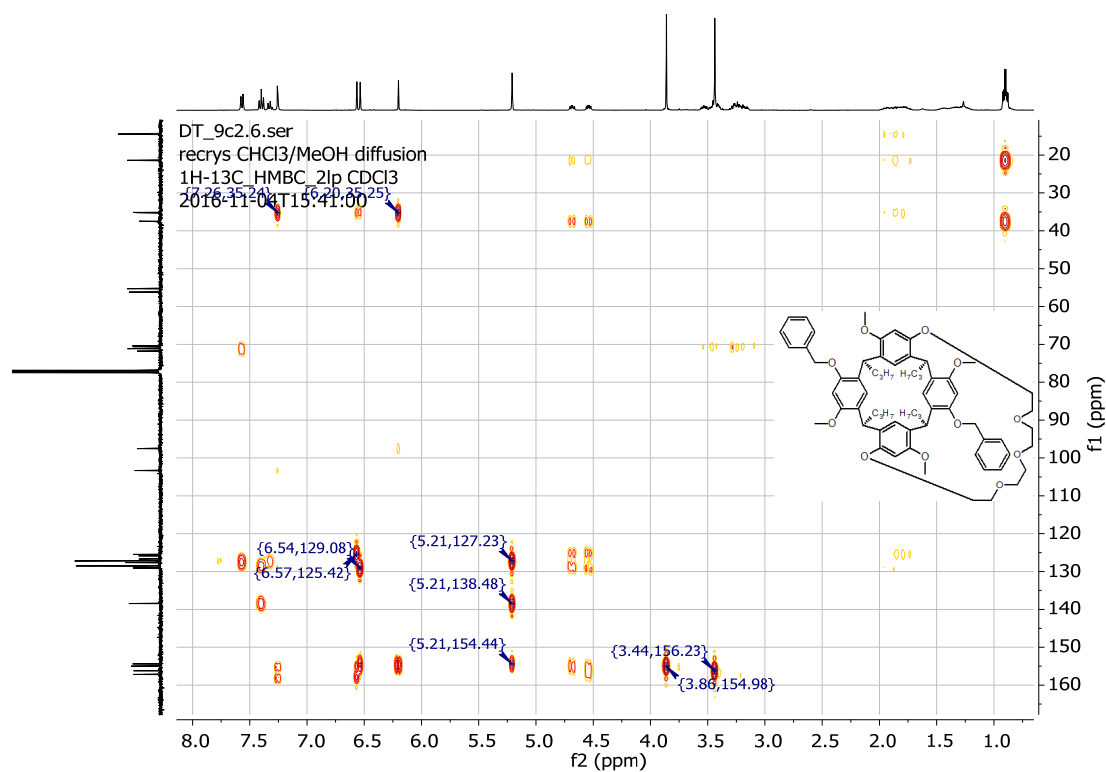
Appendix A24.6 (53) HMBC NMR spectrum recorded in CDCl₃.

(54) Dibenzyloxy crown-6 resorcinarene
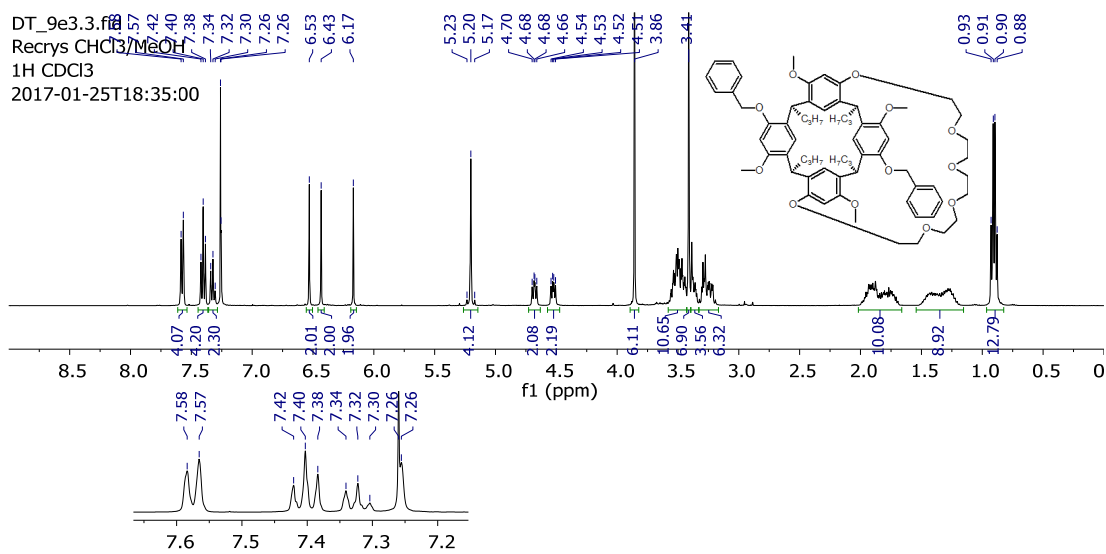
Appendix A25.1 (54) ^{1}H NMR spectrum recorded in CDCl$_3$.
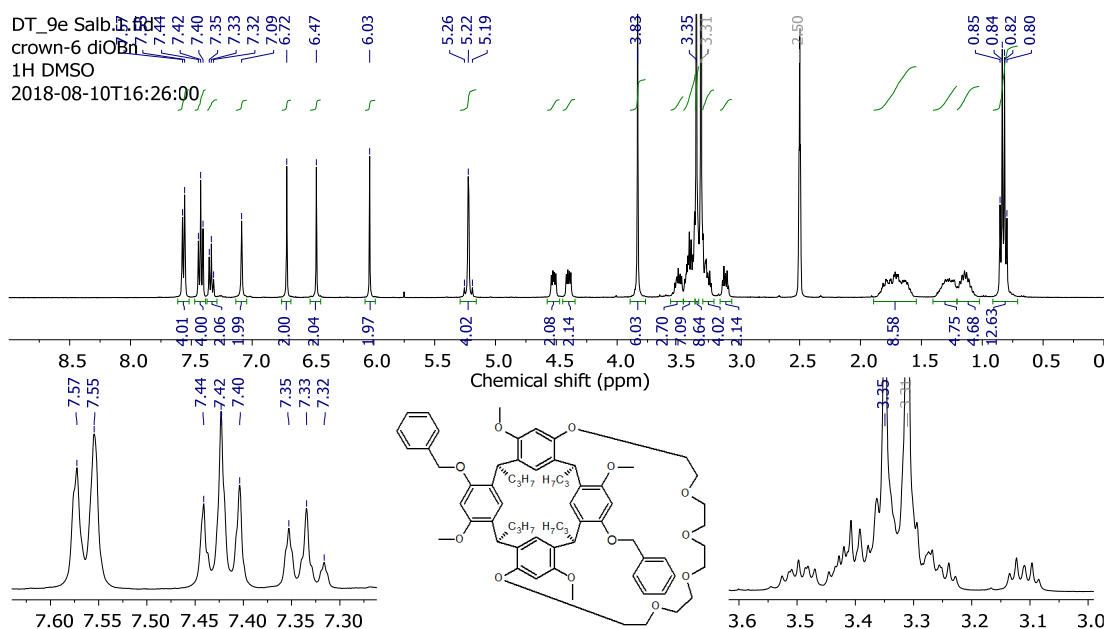
Appendix A25.2 (54) ^{1}H NMR spectrum recorded in DMSO-d$_6$.
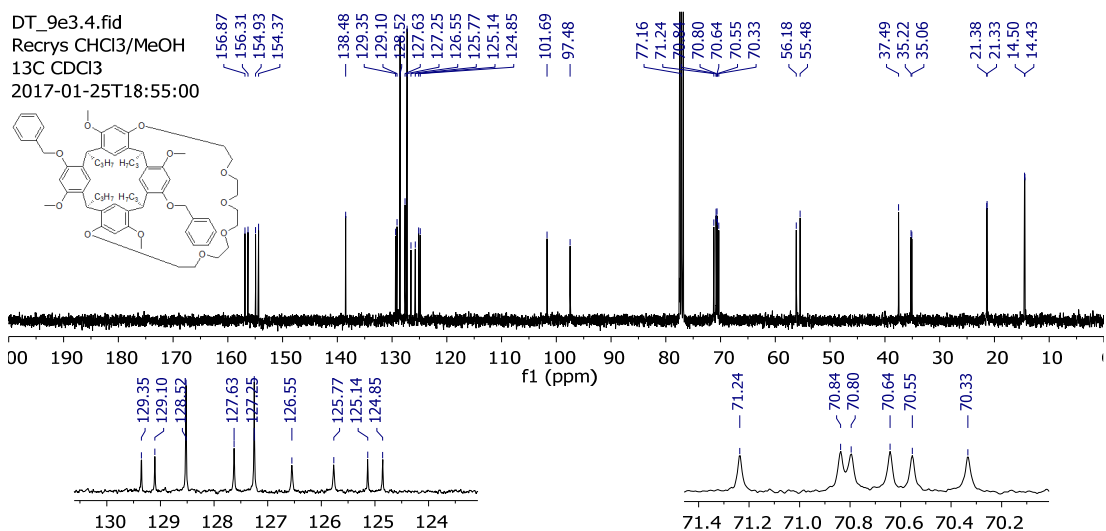
Appendix A25.3 (54) ^{13}C NMR spectrum recorded in CDCl3.

DT_9e3.5.fid
Recrys CHCl3/MeOH
13C_DEPT135 CDCl3
2017-01-26T17:48:00

128.53 127.63 127.25 126.55 125.77 101.70 97.48 71.24 70.84 70.81 70.64 70.55 70.34 56.18 55.48 37.49 37.48 35.23 35.07 21.38 21.33 14.51 14.43

190 180 170 160 150 140 130 120 110 100 90 80 70 60 50 40 30 20 10

f1 (ppm)

128.53 127.63 127.25 126.55 125.77

128.5 127.5 126.5 125.5

37.49 37.48

37.60 37.50 37.40
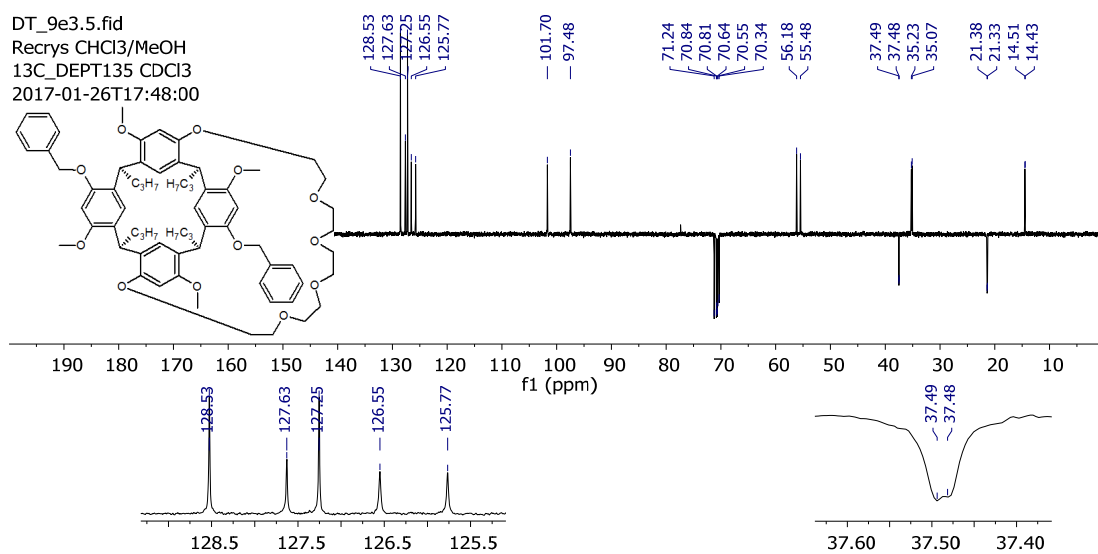
Appendix A25.4 (54) DEPT-135 spectrum recorded in CDCl3.

DT_9e3.6.ser
Recrys CHCl3/MeOH
1H-13C_HSQC CDCl3
2017-01-26T17:51:00

{5.20,71.27}

{6.17,126.67}

10 20 30 40 50 60 70 80 90 100 110 120 130

f1 (ppm)

7.5 7.0 6.5 6.0 5.5 5.0 4.5 4.0 3.5 3.0 2.5 2.0 1.5 1.0

f2 (ppm)
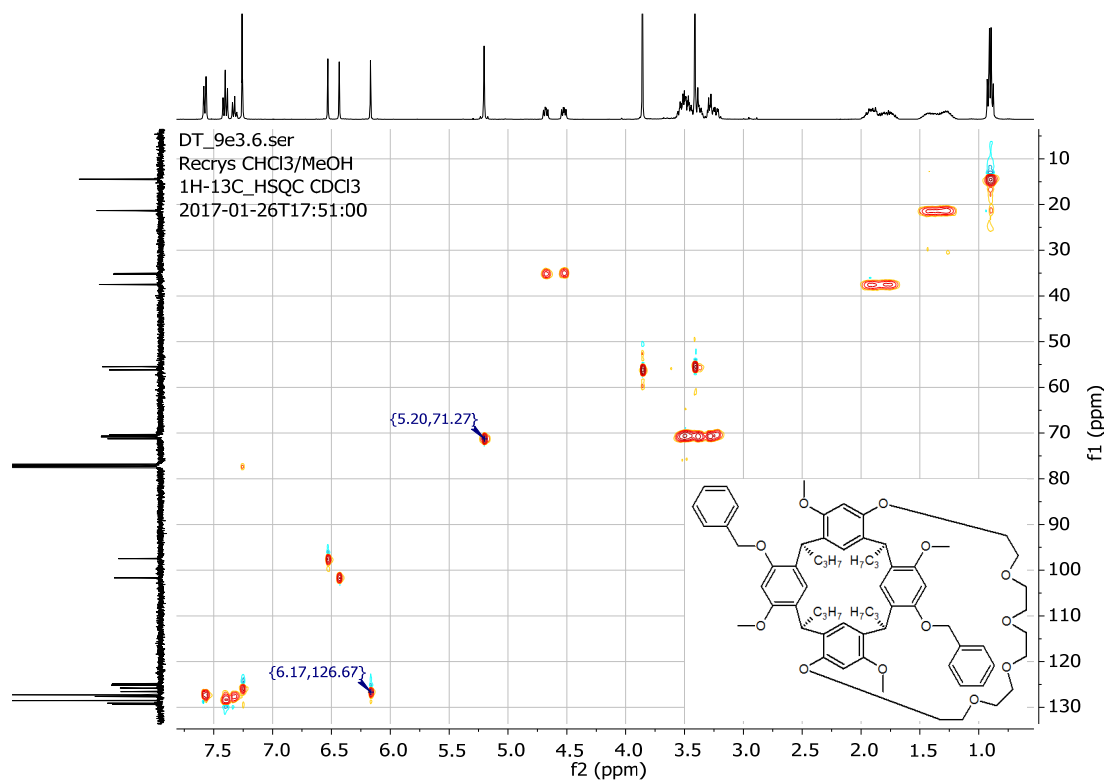
Appendix A25.5 (54) HSQC NMR spectrum recorded in CDCl3.

(55) Dibenzyloxy crown-7 resorcinarene
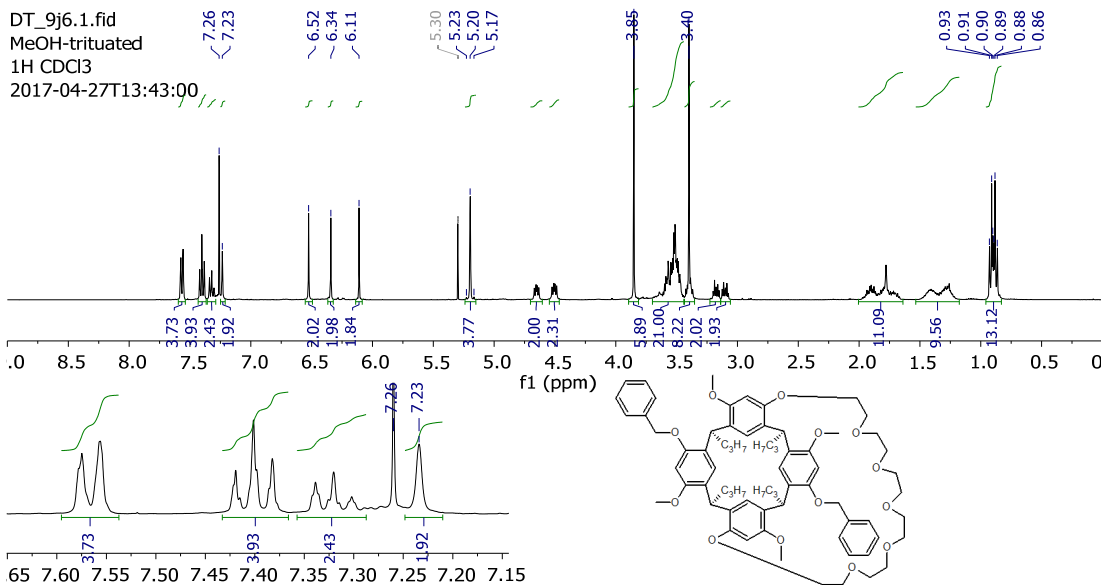
Appendix A26.1 (55) ^{1}H NMR spectrum recorded in CDCl$_3$.
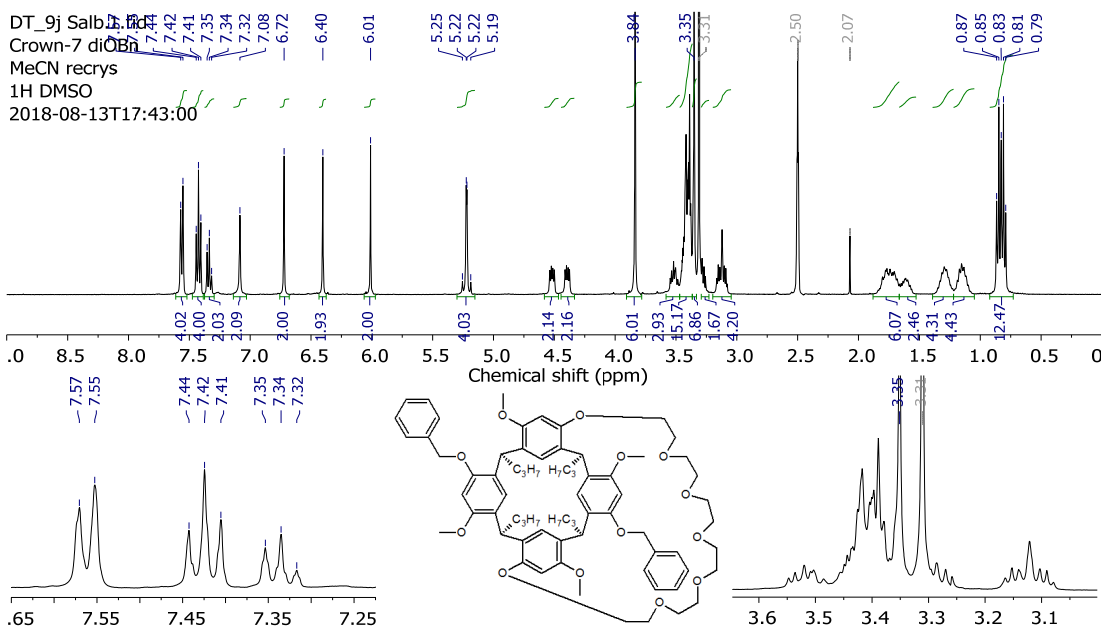
Appendix A26.2 (55) ^{1}H NMR spectrum recorded in DMSO-d$_6$.
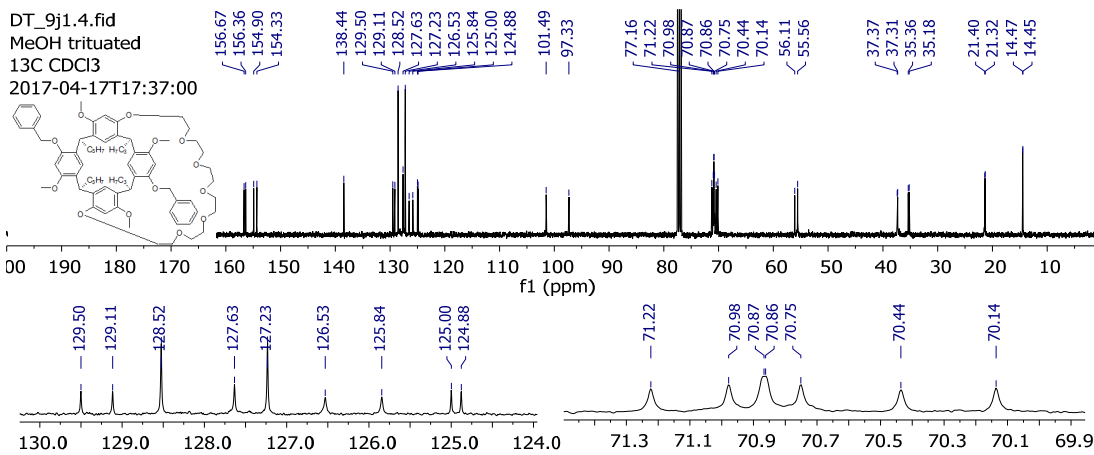
Appendix A26.3 (55) ^{13}C NMR spectrum recorded in CDCl$_3$.
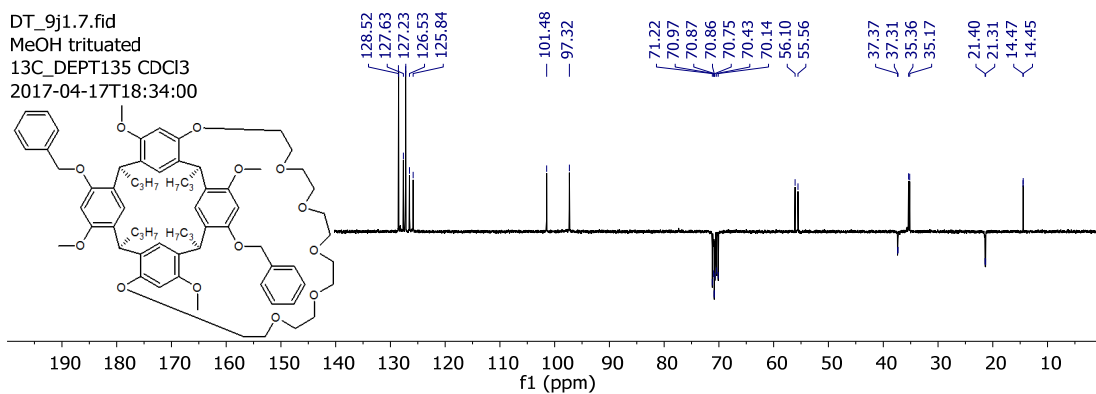
Appendix A26.4 (55) DEPT-135 spectrum recorded in CDCl$_3$.
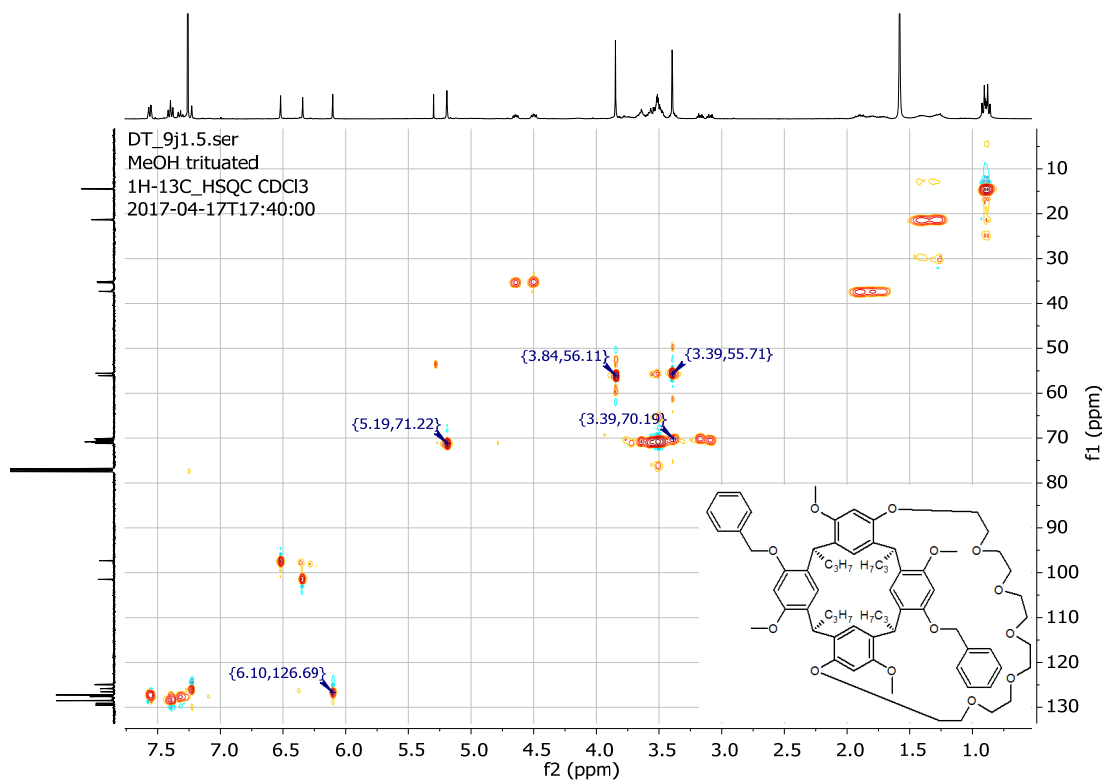
Appendix A26.5 (55) HSQC NMR spectrum recorded in CDCl$_3$.

Dihydroxy crown resorcinarenes

(56) Dihydroxy crown-5 resorcinarene
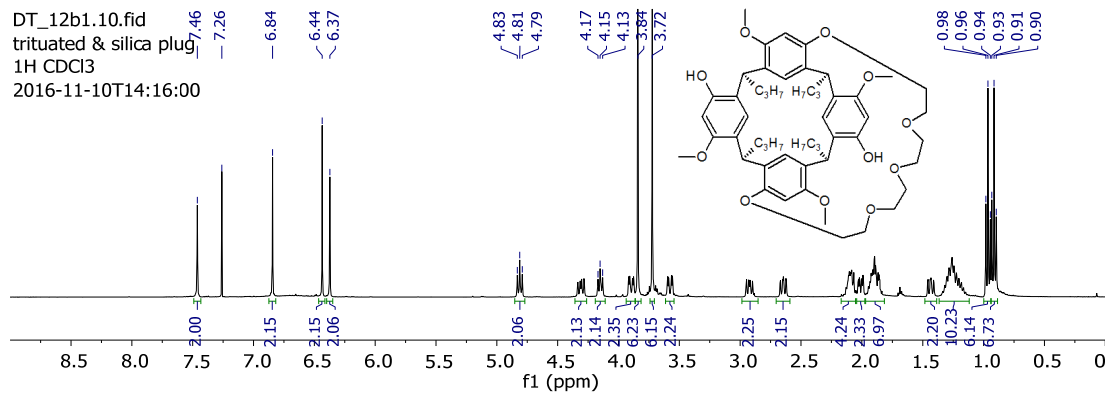
Appendix A27.1 (56) ^{1}H NMR spectrum recorded in CDCl₃.
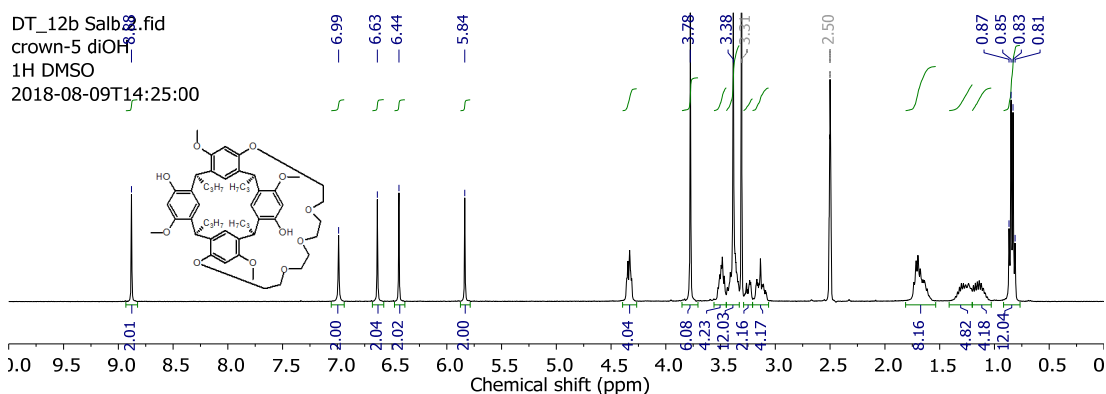
Appendix A27.2 (56) ^{1}H NMR spectrum recorded in DMSO-d₆.
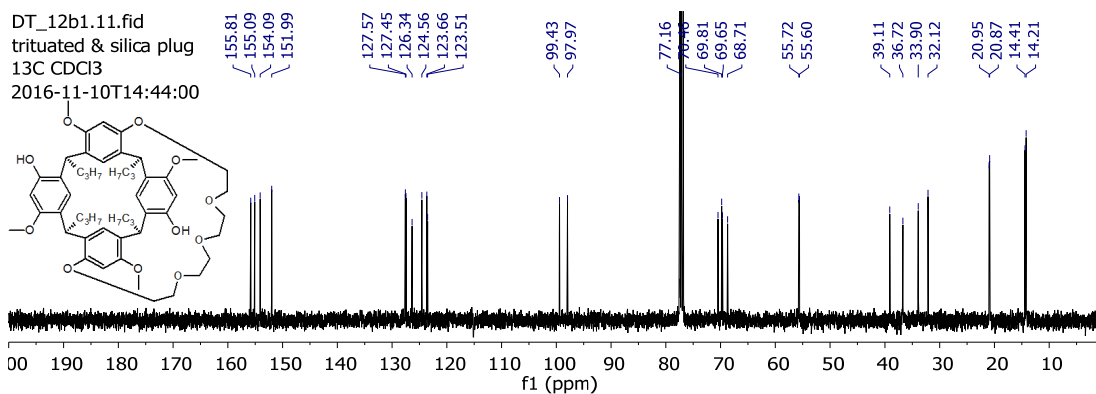
Appendix A27.3 (56) ^{13}C NMR spectrum recorded in CDCl₃.
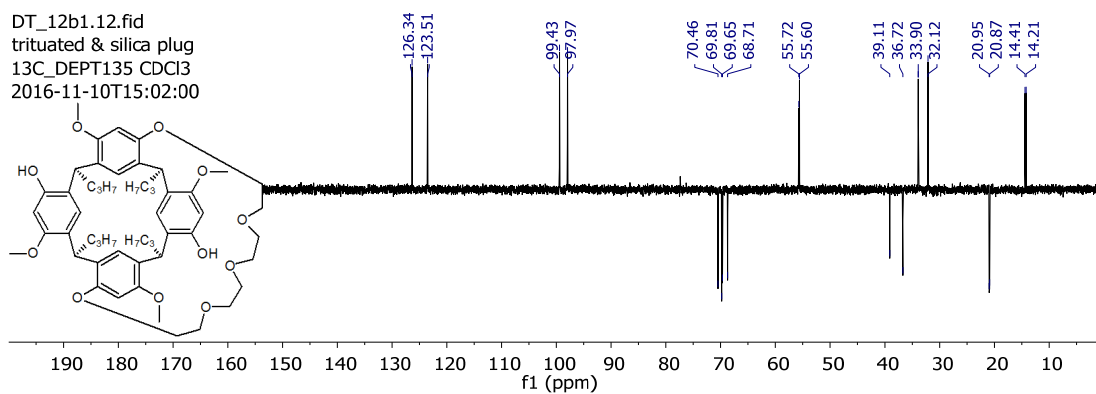
Appendix A27.4 (56) DEPT-135 spectrum recorded in CDCl₃.
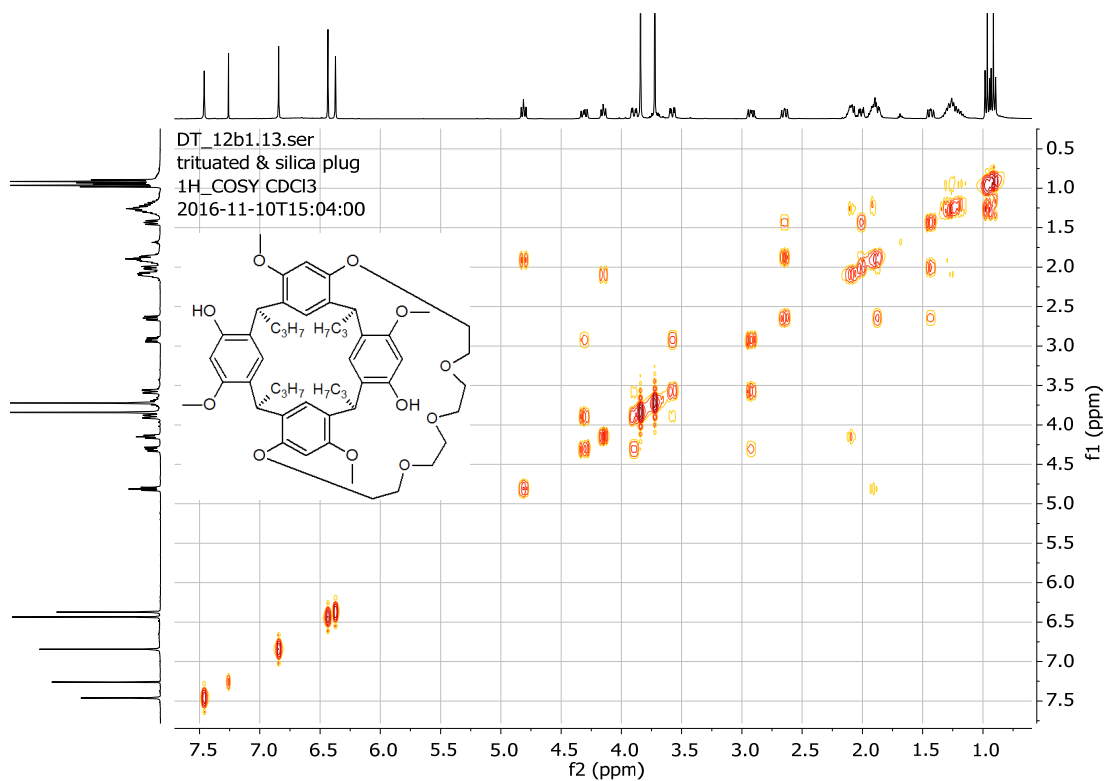
Appendix A27.5 (56) COSY spectrum recorded in CDCl₃.
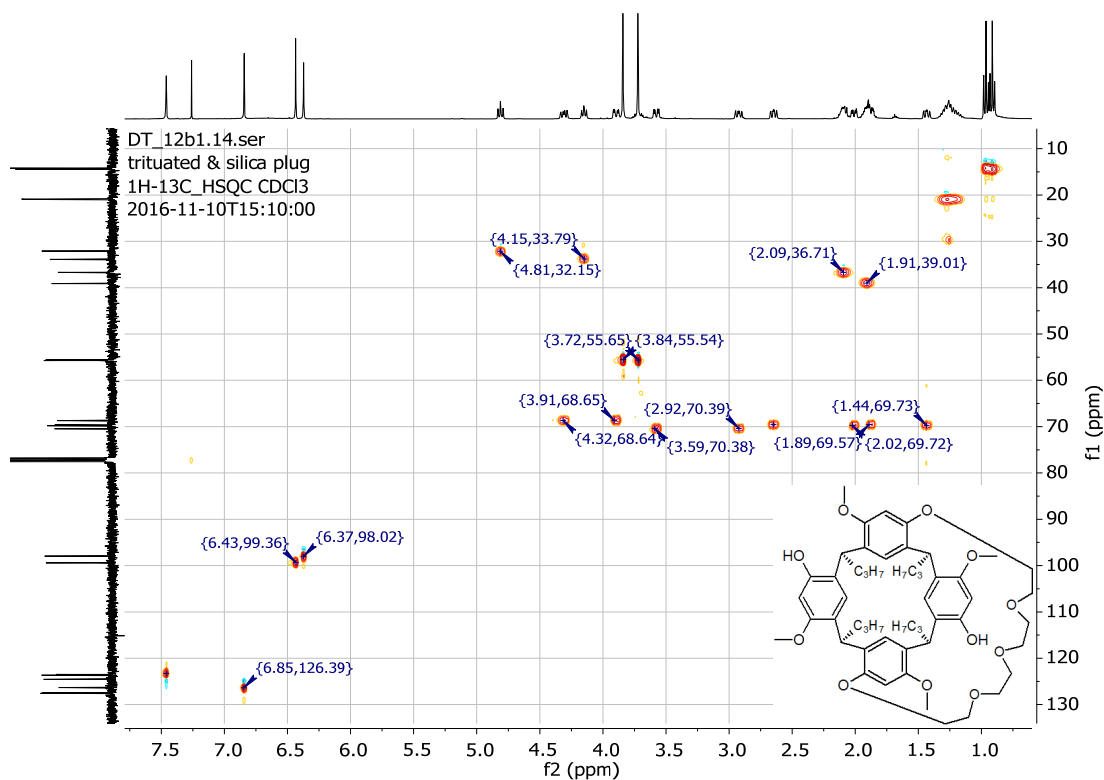
Appendix A27.6 (56) HSQC NMR spectrum recorded in CDCl₃.
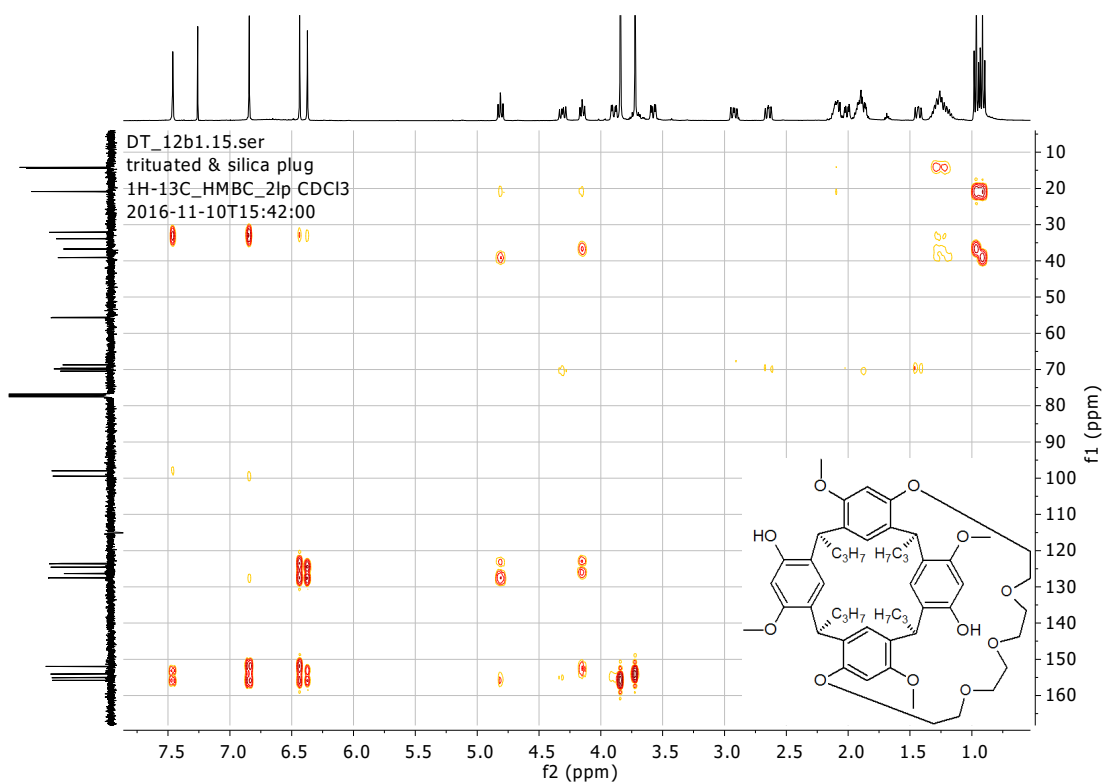
Appendix A - 64

Appendix A27.7 (56) HMBC NMR spectrum recorded in CDCl$_3$.

Appendix A27.8 (56) IR spectrum.

(57) Dihydroxy crown-6 resorcinarene
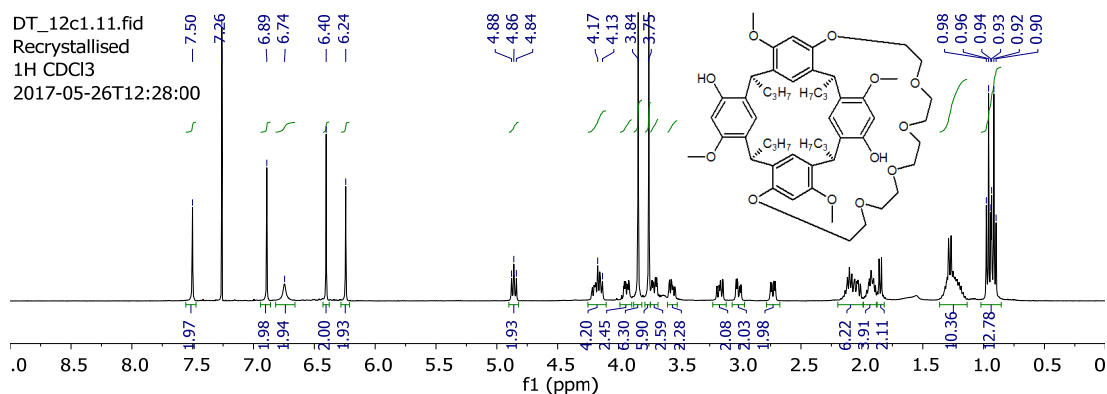
Appendix A28.1 (57) ^{1}H NMR spectrum recorded in CDCl$_3$.
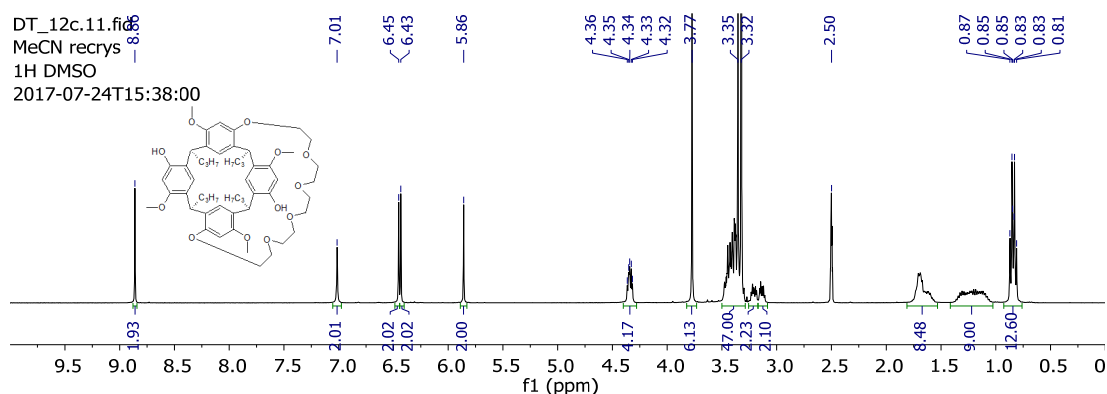
Appendix A28.2 (57) ^{1}H NMR spectrum recorded in DMSO-d$_6$.
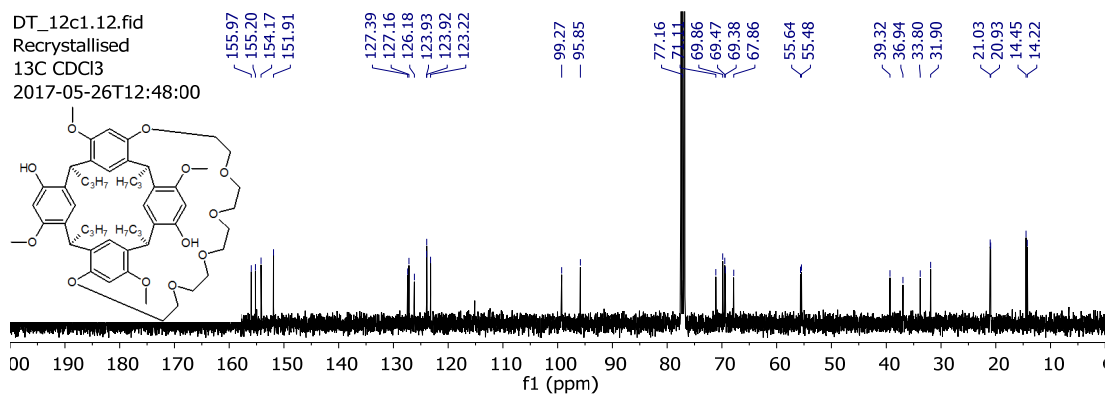
Appendix A28.3 (57) ^{13}C NMR spectrum recorded in CDCl$_3$.
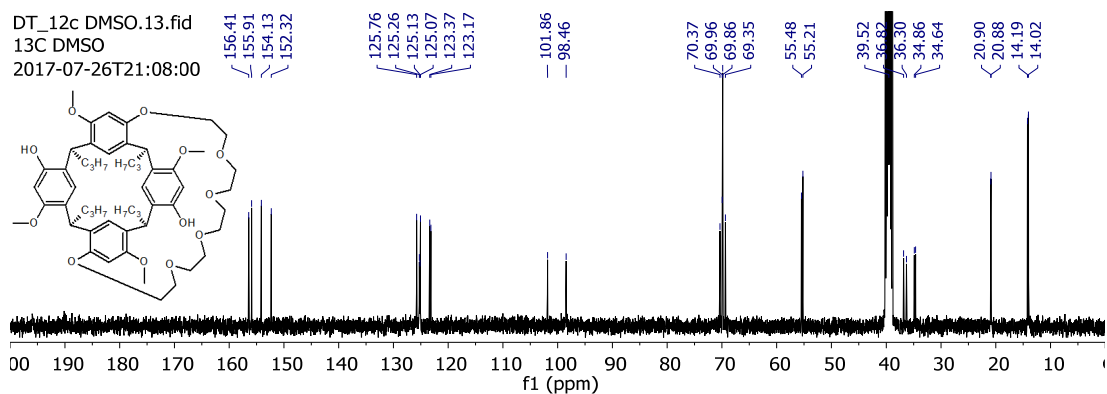
Appendix A28.4 (57) ^{13}C NMR spectrum recorded in DMSO-d$_6$.
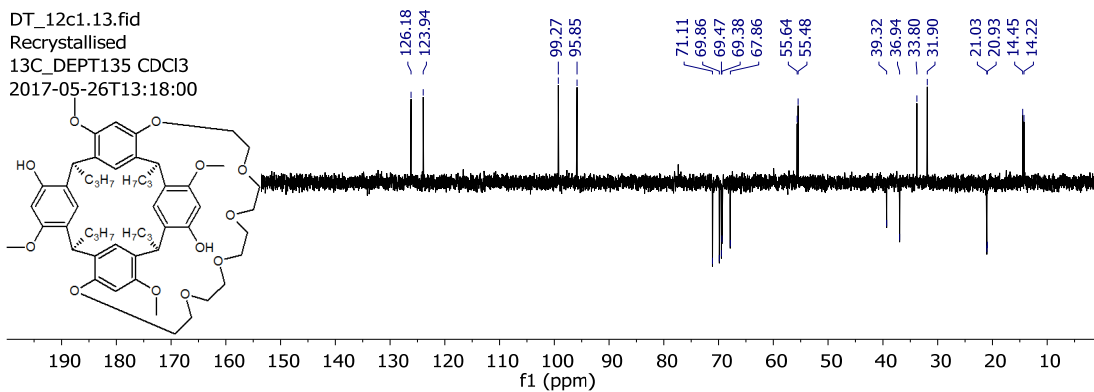
Appendix A28.5 (57) DEPT-135 spectrum recorded in CDCl₃.
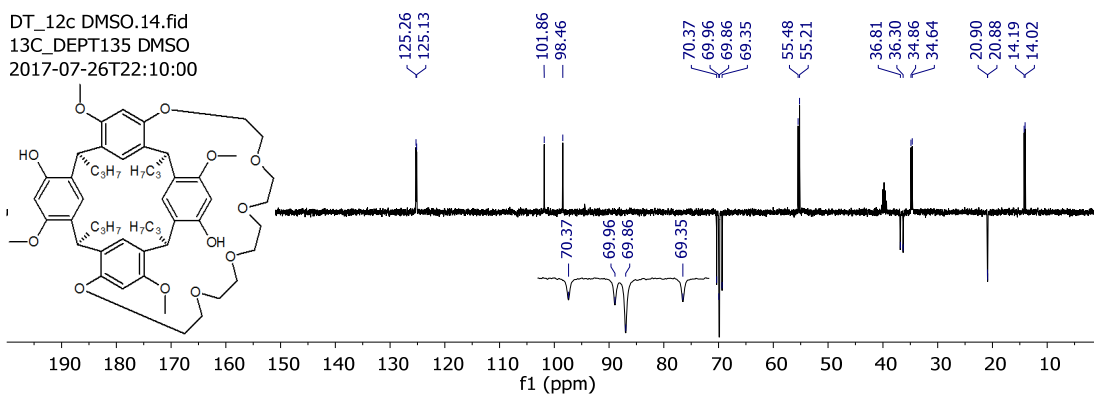
Appendix A28.6 (57) DEPT-135 spectrum recorded in DMSO-d₆.
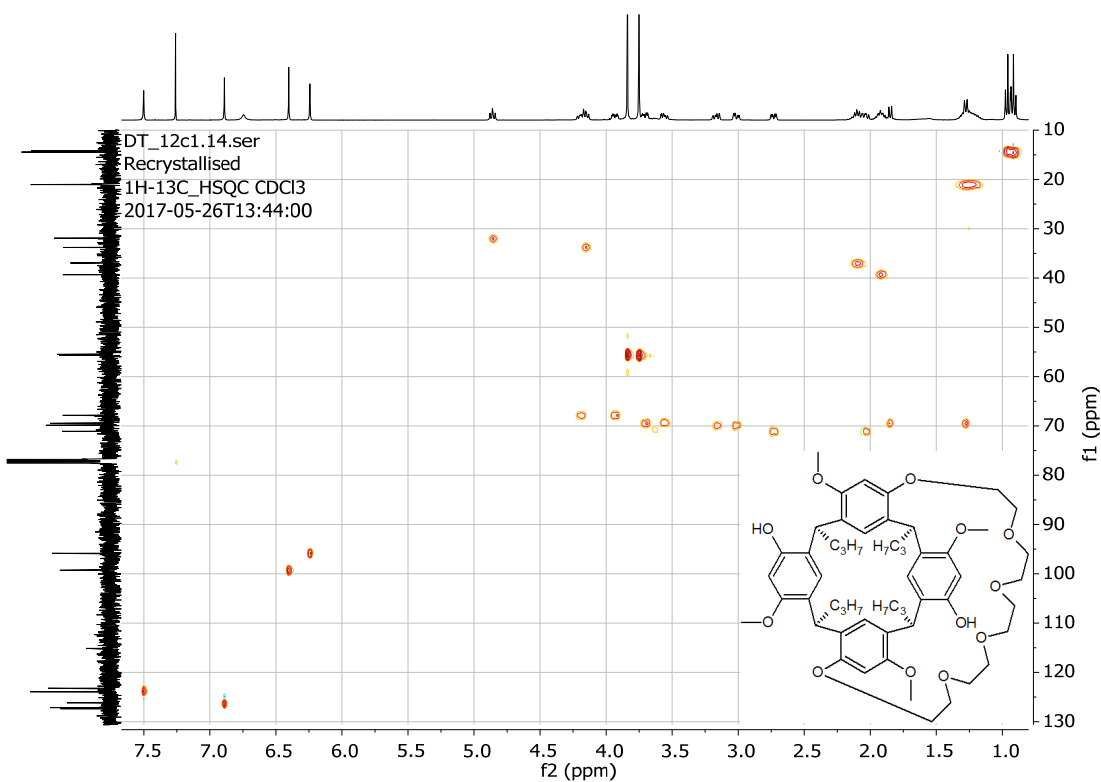
Appendix A28.7 (57) HSQC NMR spectrum recorded in CDCl₃.
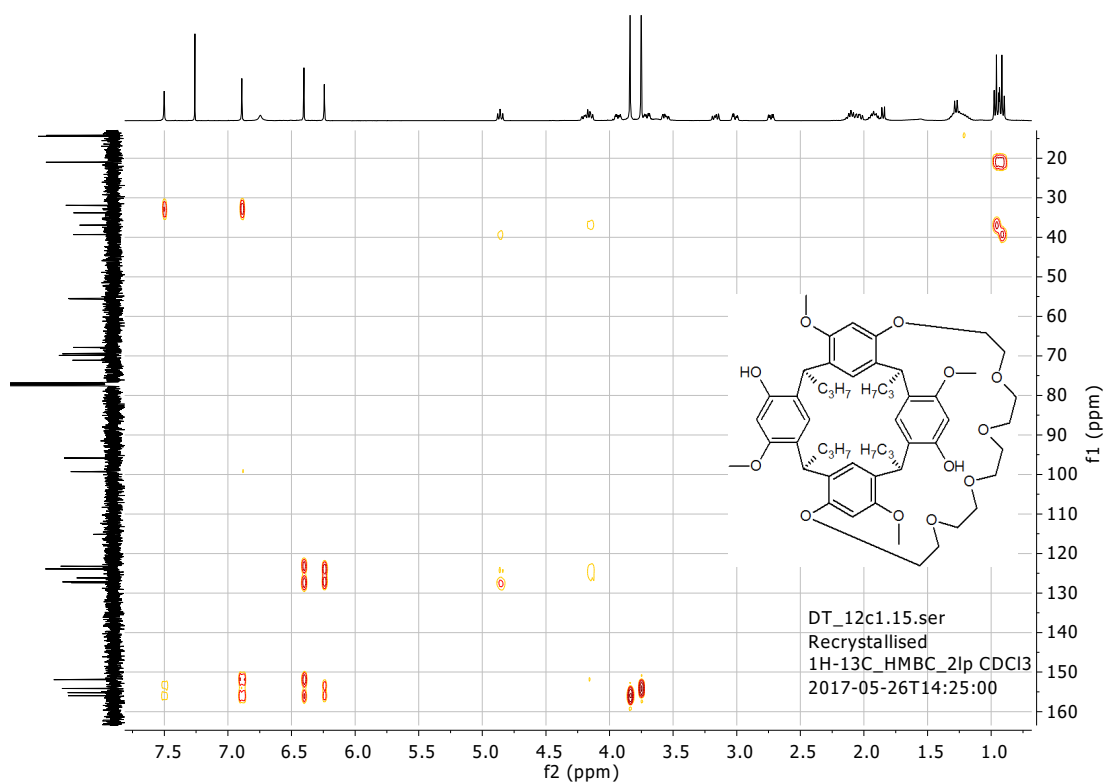
Appendix A28.8 (57) HMBC NMR spectrum recorded in CDCl$_3$.
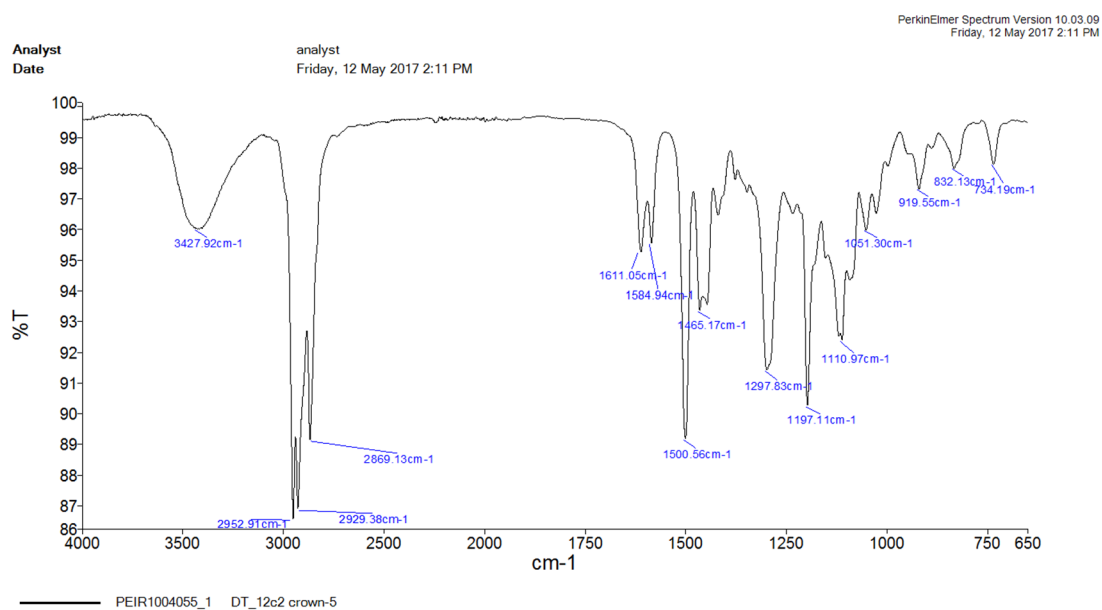
Appendix A28.9 (57) IR spectrum.

(58) Dihydroxy crown-7 resorcinarene
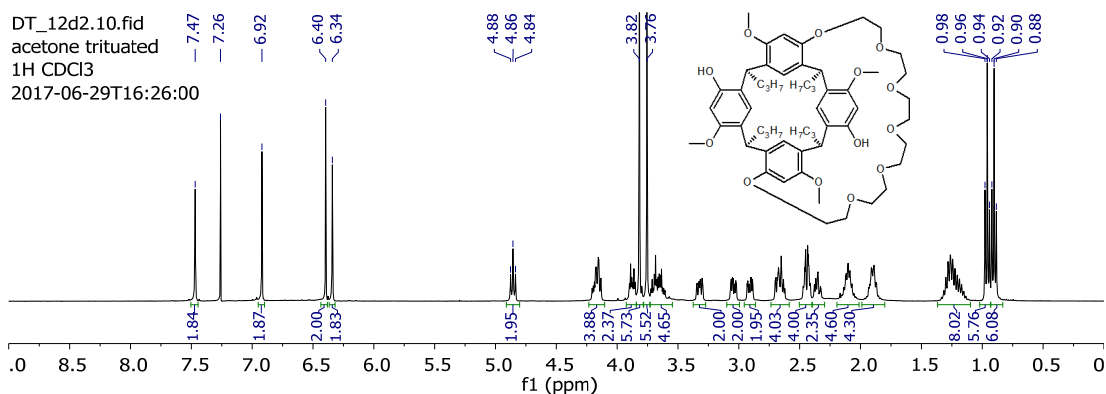
Appendix A29.1 (58) ^{1}H NMR spectrum recorded in CDCl₃.
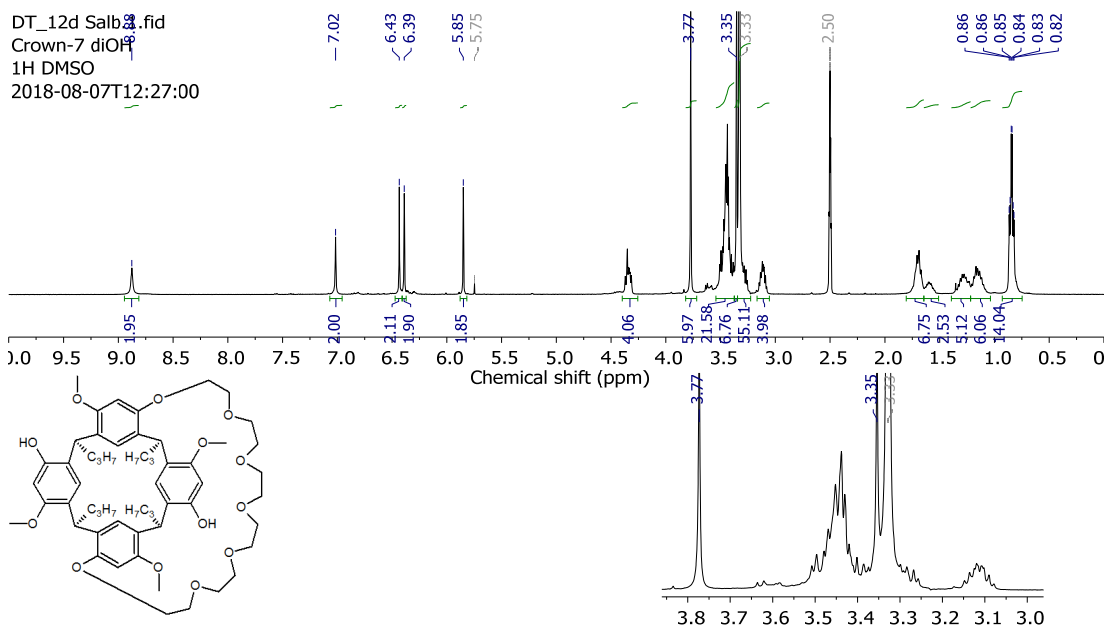
Appendix A29.2 (58) ^{1}H NMR spectrum recorded in DMSO-d₆.
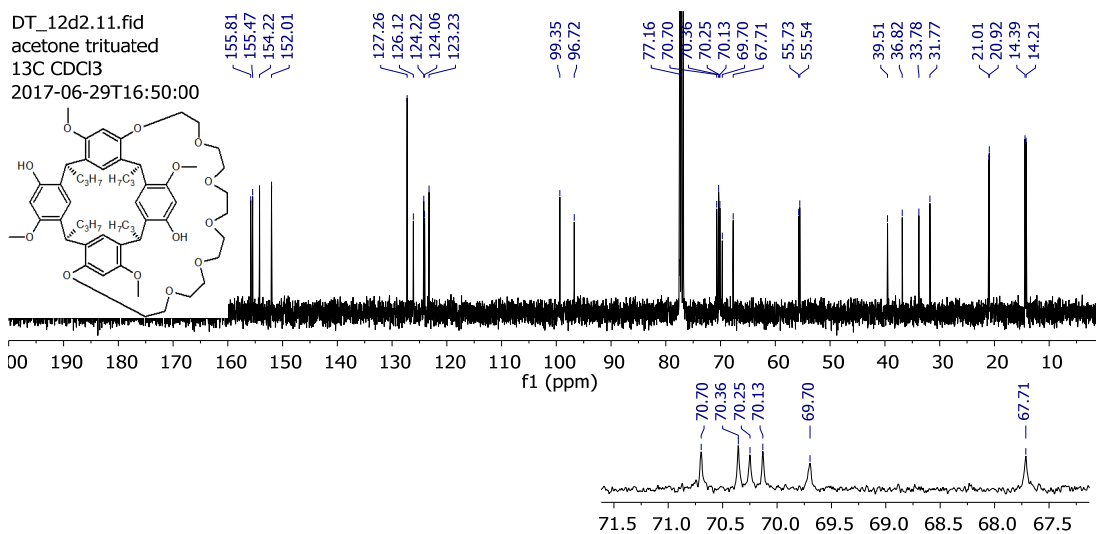
Appendix A29.3 (58) ^{13}C NMR spectrum recorded in CDCl₃.
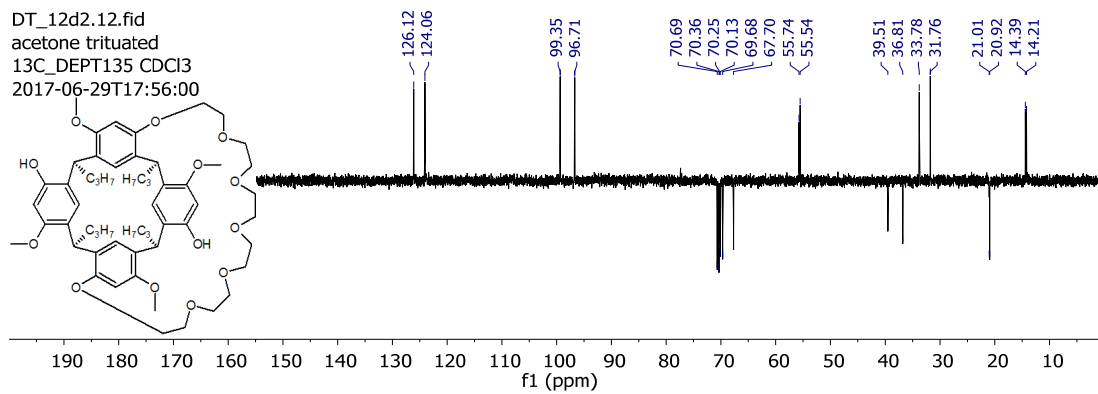
Appendix A29.4 (58) DEPT-135 spectrum recorded in CDCl$_3$.
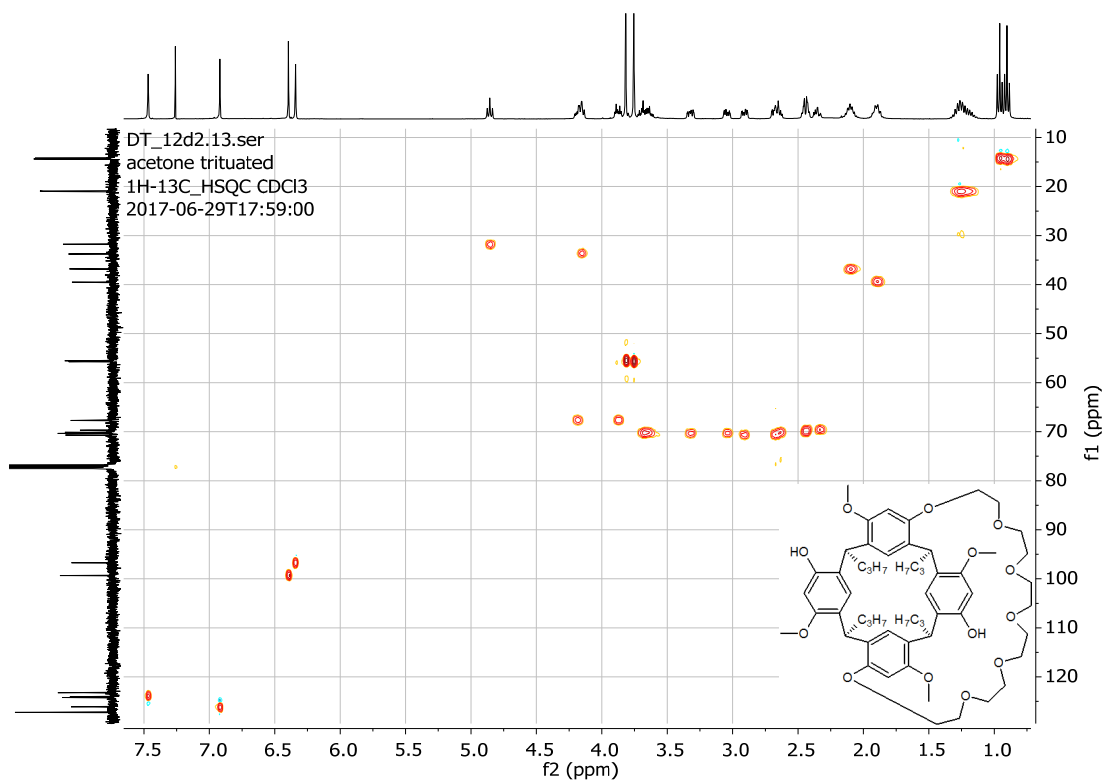
Appendix A29.5 (58) HSQC NMR spectrum recorded in CDCl$_3$.
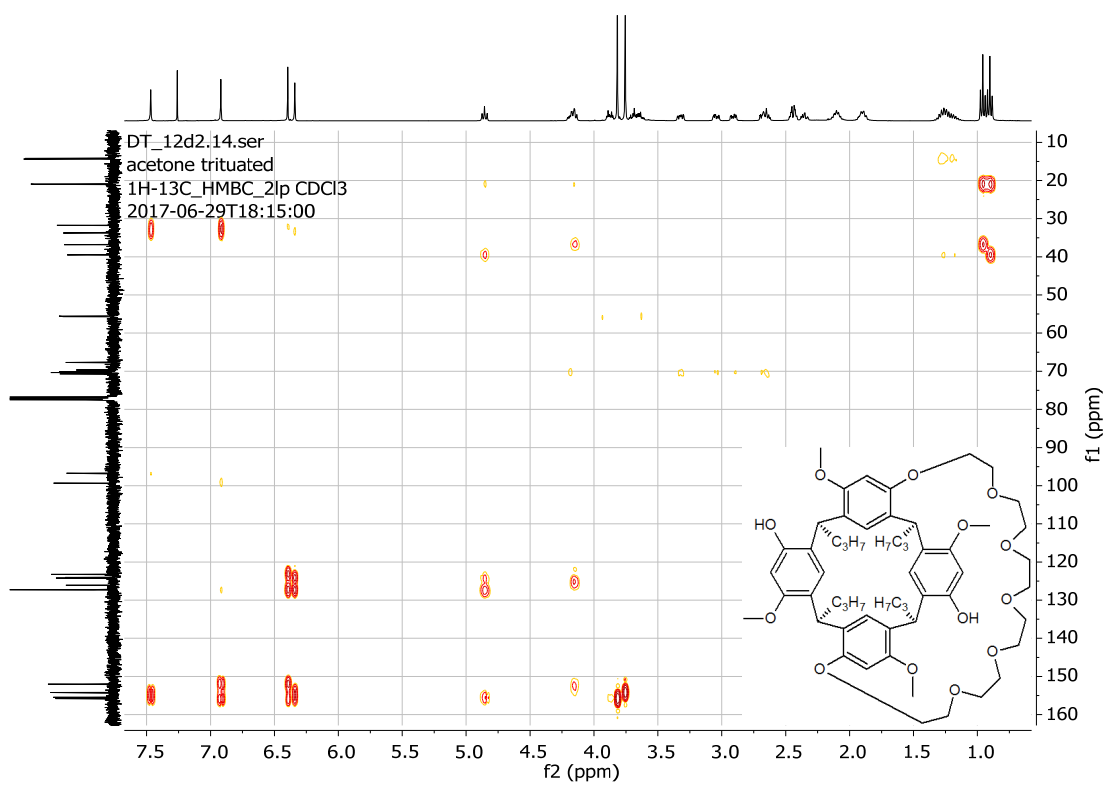
Appendix A29.6 (58) HMBC NMR spectrum recorded in CDCl$_3$.

Camphorsulfonate crown resorcinarene diastereomers

(59a) Dicamphorsulfonate crown-5 resorcinarene

DT_13e2.4.fid
pTLC F1
1H CDCl3
2018-04-03T18:52:00
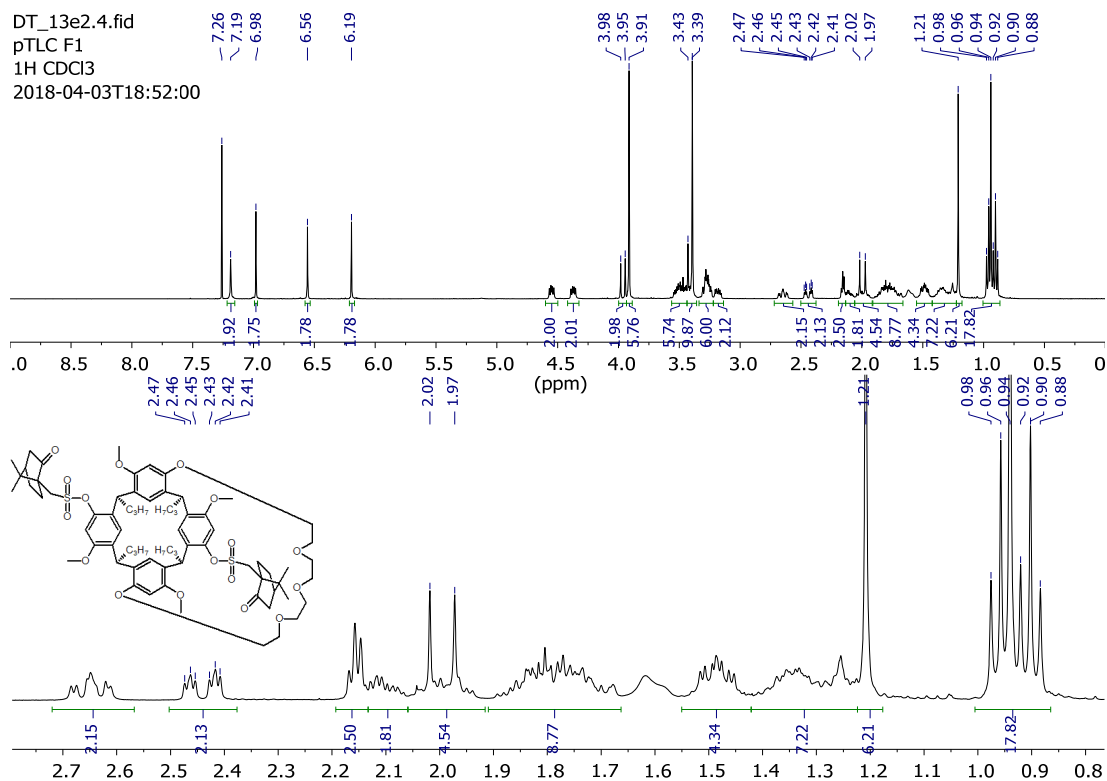
Appendix A30.1 (59a) ^{1}H NMR spectrum recorded in CDCl$_3$.

DT_13e2.7.fid
pTLC F1
13C CDCl3
2018-04-03
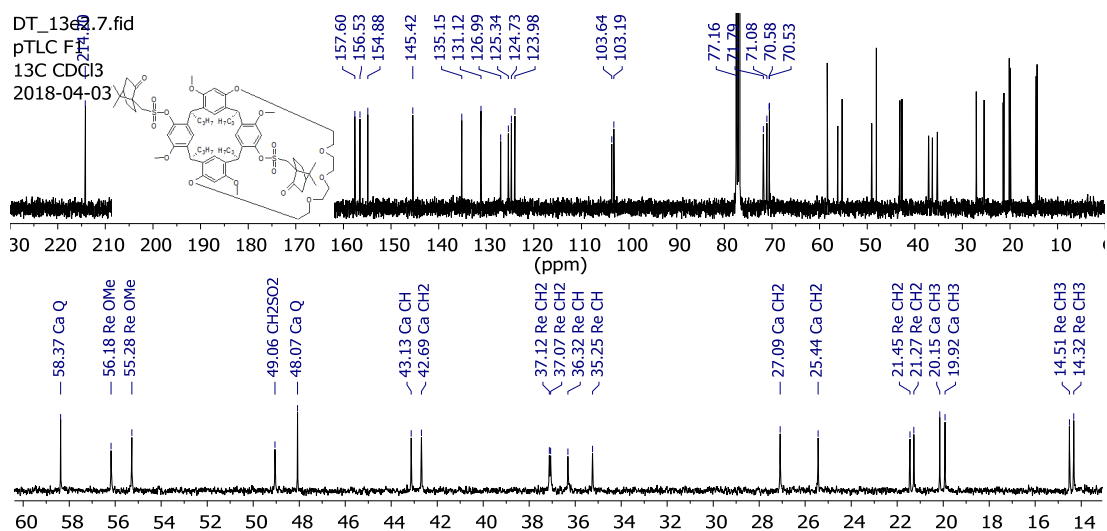
Appendix A30.2 (59a) ^{13}C NMR spectrum recorded in CDCl$_3$.
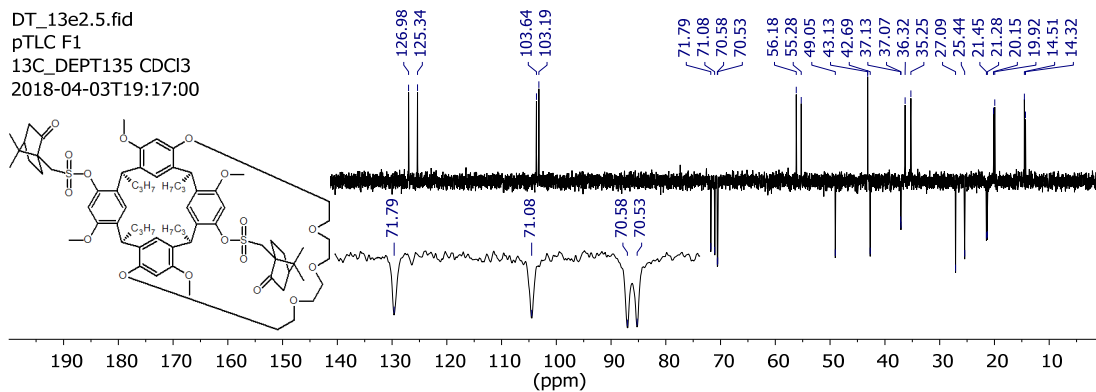
Appendix A30.3 (59a) DEPT-135 spectrum recorded in CDCl₃.
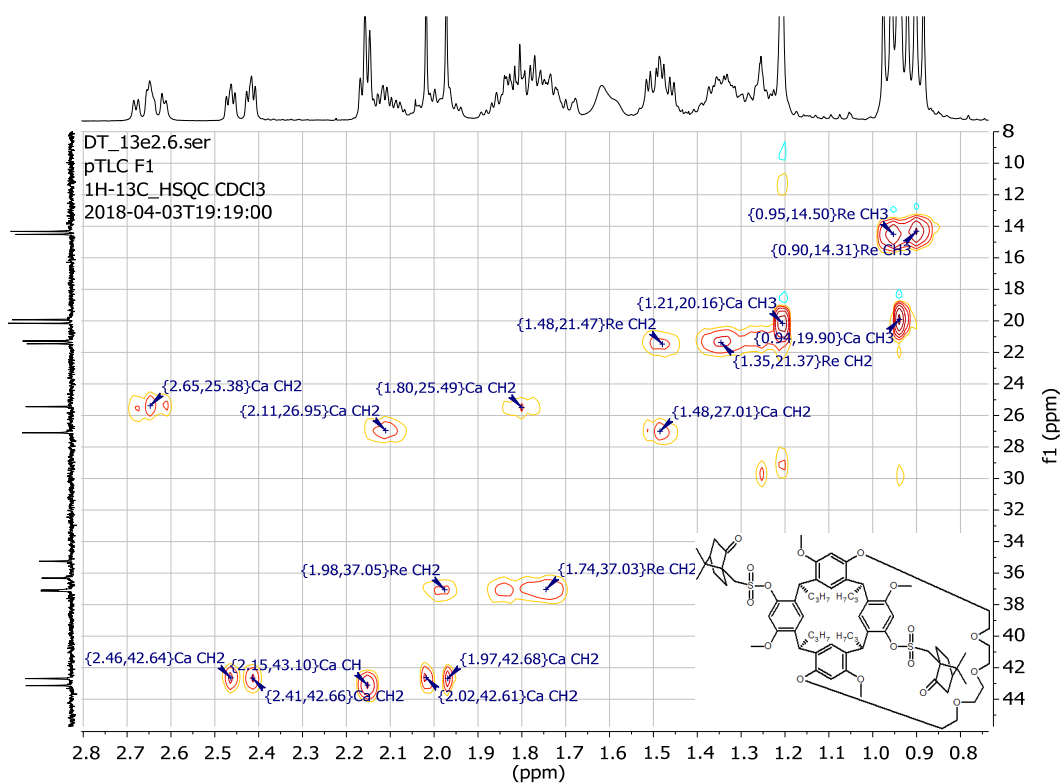
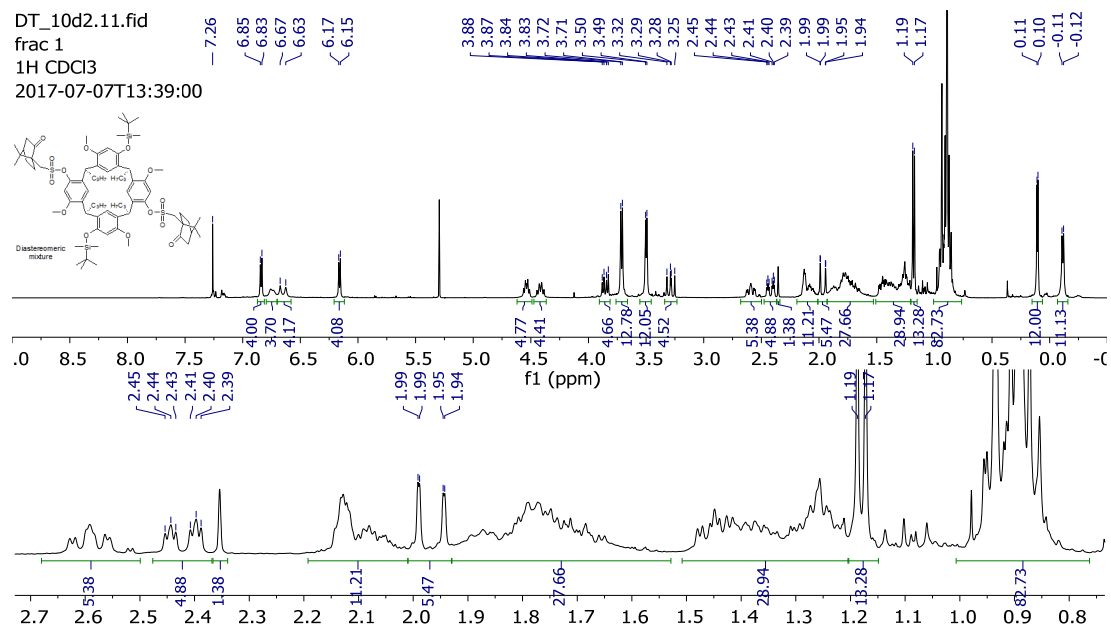**Appendix A30.4 (59a)** HSQC NMR spectrum (expansion) recorded in CDCl₃.

Appendix A30.5 (59a) HSQC NMR spectrum recorded in CDCl₃.

(59b) Dicamphorsulfonate crown-5 resorcinarene
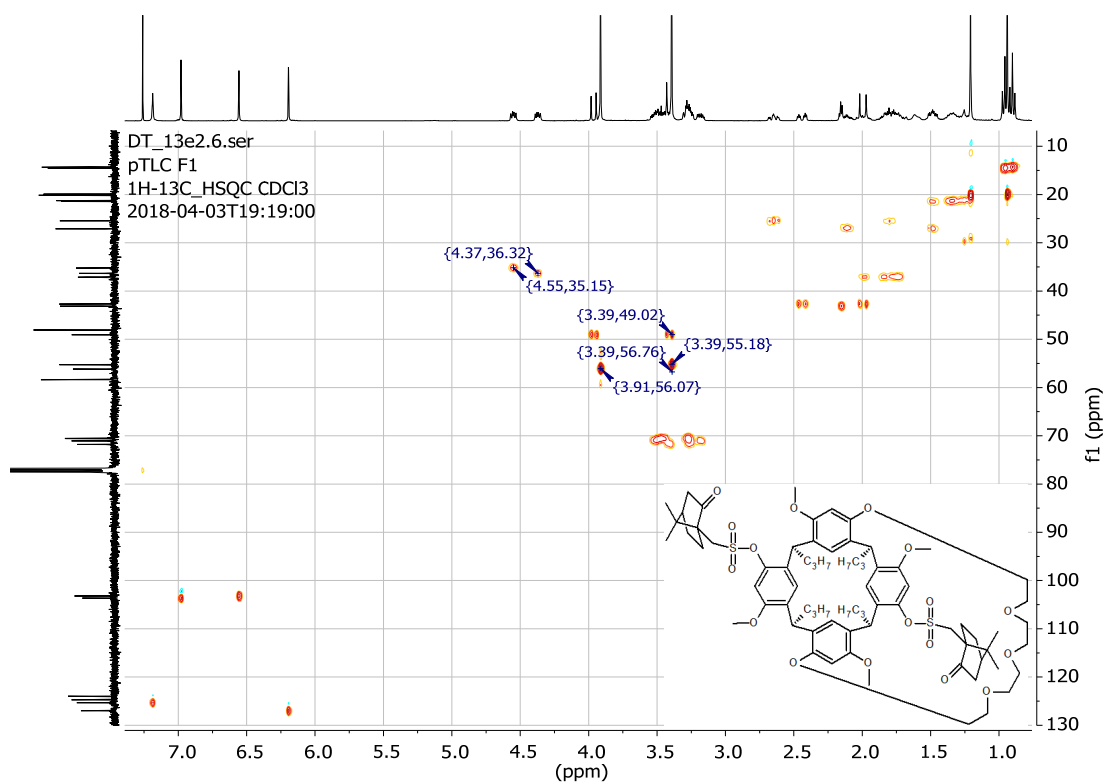
Appendix A31.1 (59b) ¹H NMR spectrum recorded in CDCl₃.
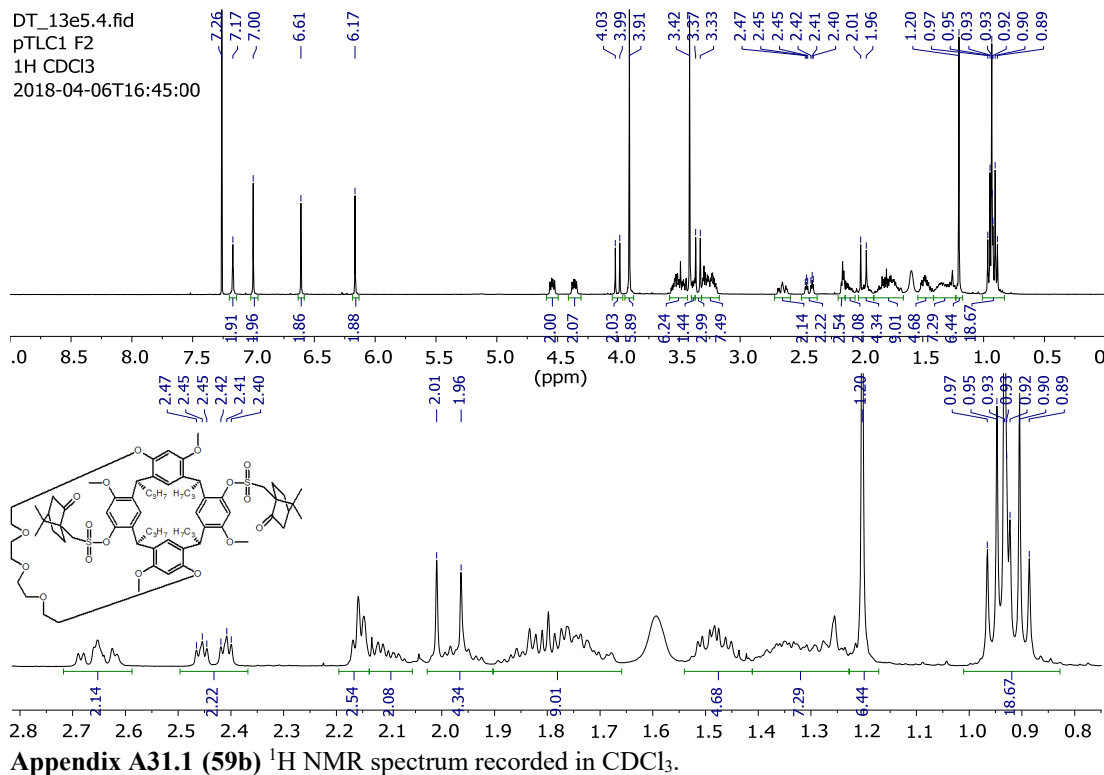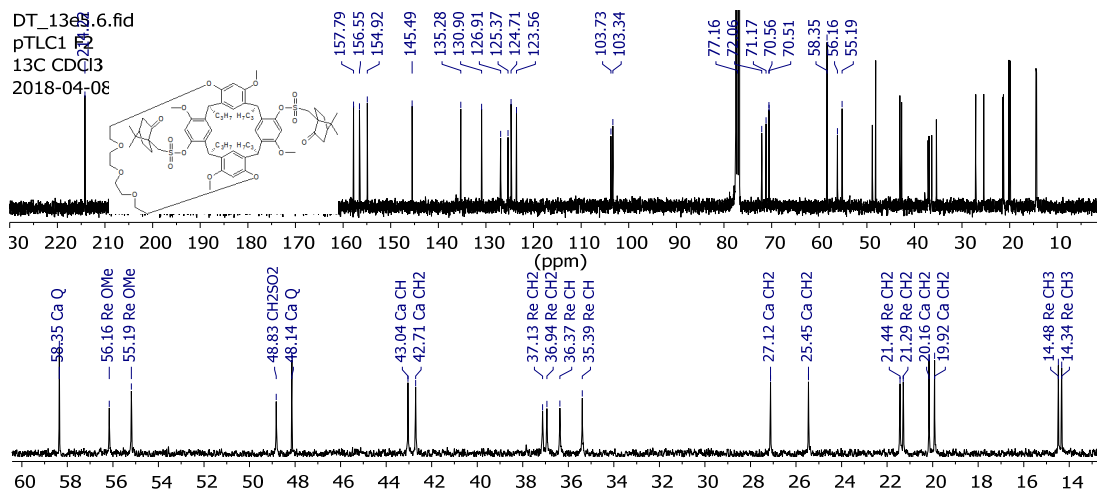
Appendix A31.2 (59b) ^{13}C NMR spectrum recorded in CDCl$_3$.
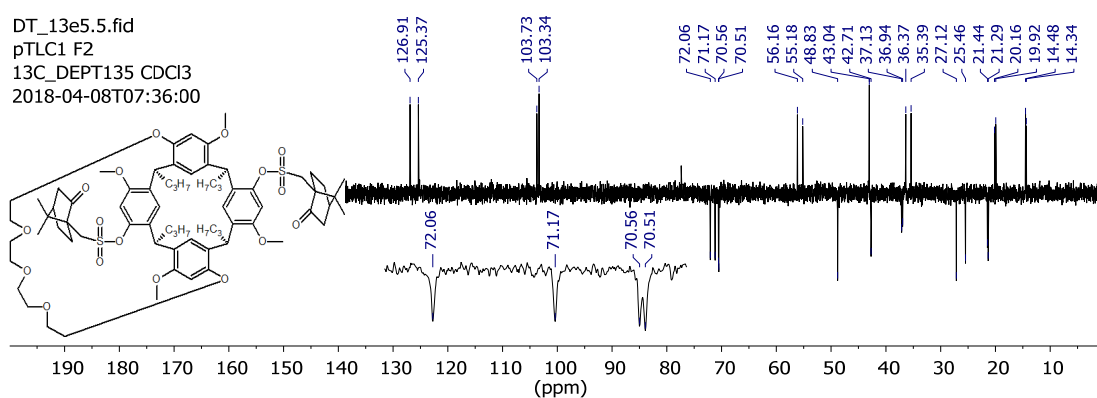
Appendix A31.3 (59b) DEPT-135 spectrum recorded in CDCl$_3$.
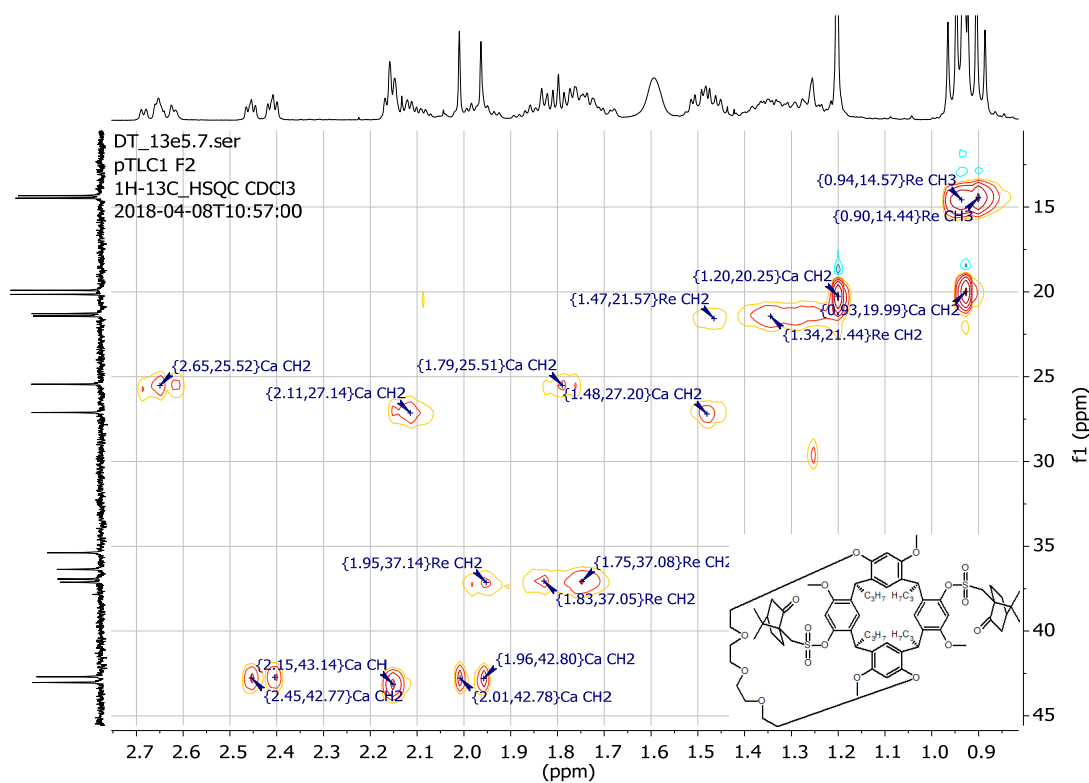
Appendix A31.4 (59b) HSQC NMR spectrum (expansion) recorded in CDCl$_3$.
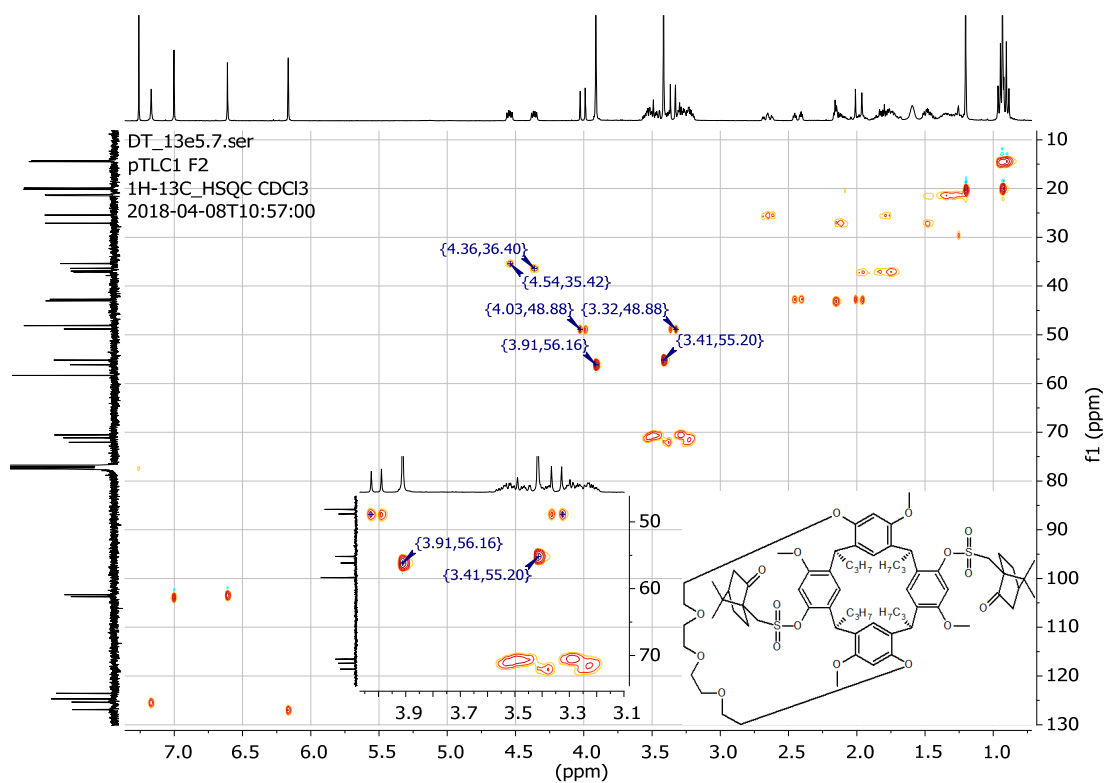
Appendix A31.5 (59b) HSQC NMR spectrum recorded in CDCl$_3$.

(60a) Dicamphorsulfonate crown-6 resorcinarene
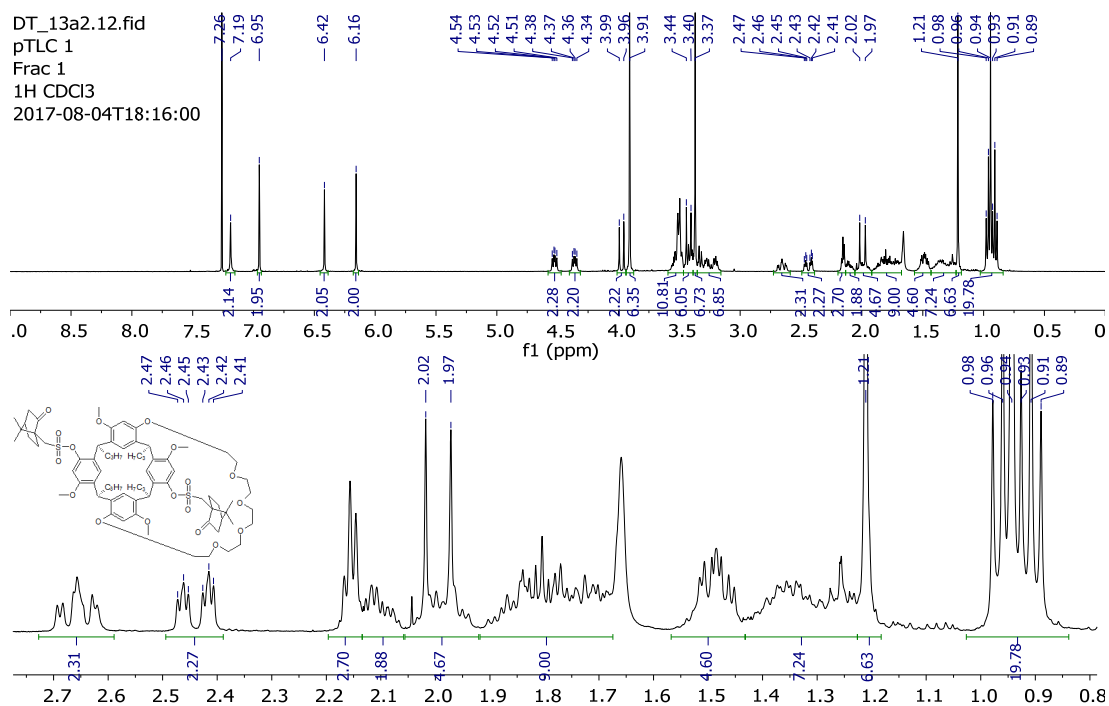
Appendix A32.1 (60a) ^{1}H NMR spectrum recorded in CDCl$_3$.
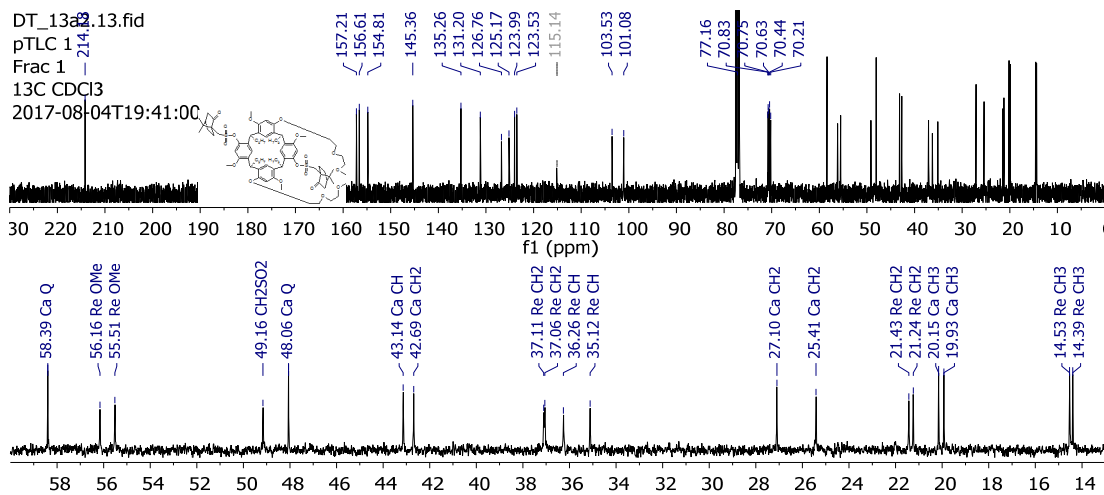
Appendix A32.2 (60a) ^{13}C NMR spectrum recorded in CDCl$_3$.
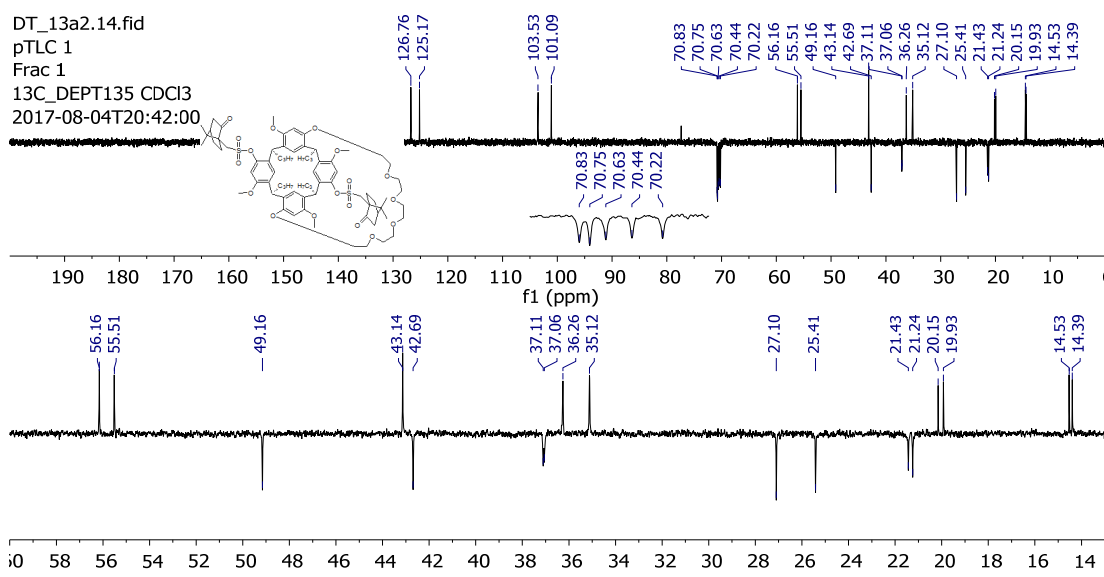
Appendix A32.3 (60a) DEPT-135 spectrum recorded in CDCl$_3$.
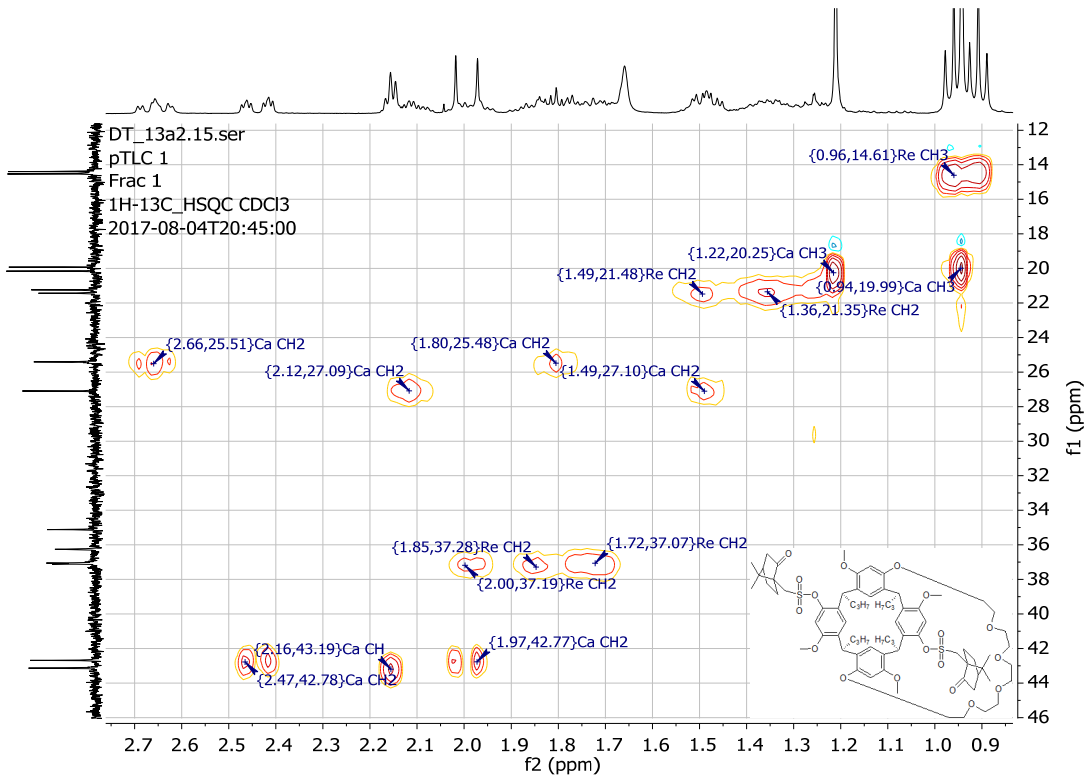
Appendix A32.4 (60a) HSQC NMR spectrum (expansion) recorded in CDCl$_3$.
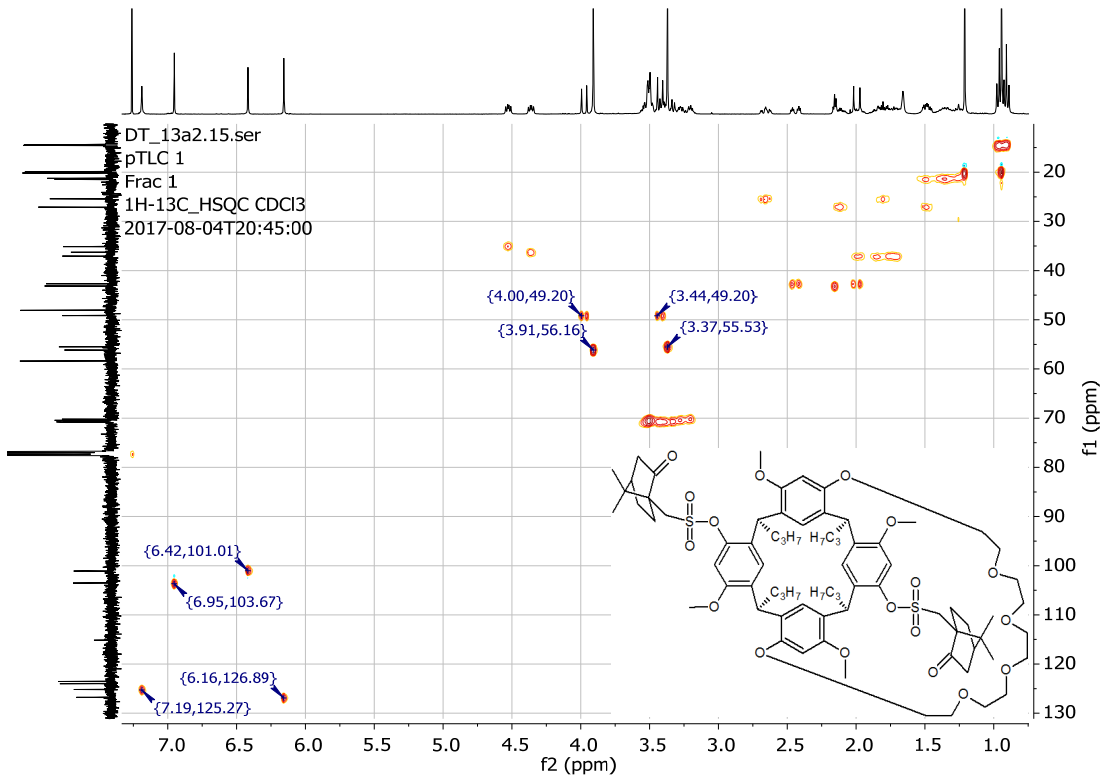
Appendix A32.5 (60a) HSQC NMR spectrum recorded in CDCl$_3$.

Analyst
Date

Analyst
Thursday, 1 February 2018 4:45 PM
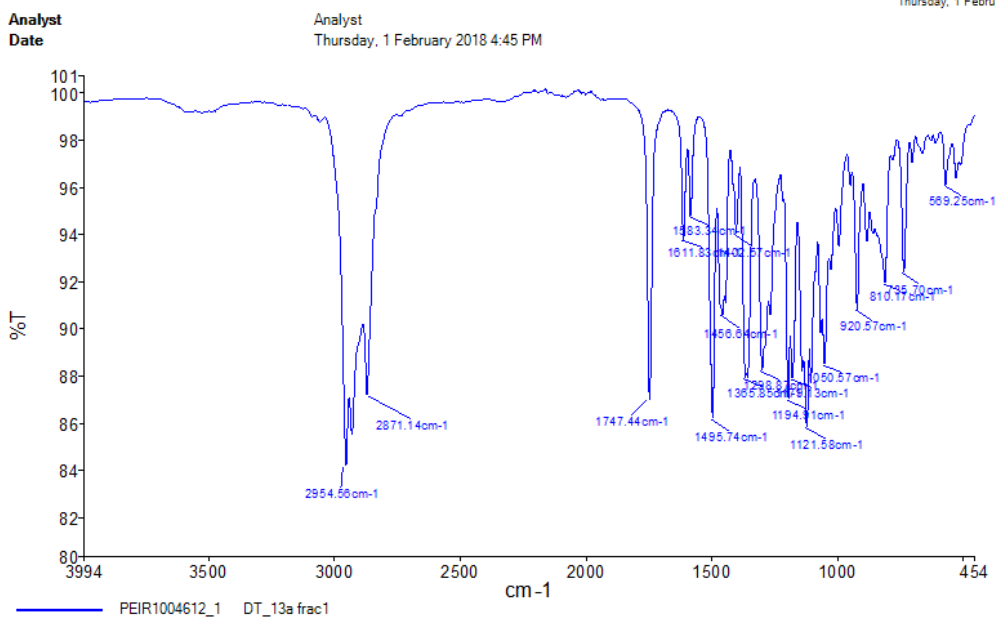
Appendix A32.6 (60a) IR spectrum.

(60b) Dicamphorsulfonate crown-6 resorcinarene

DT_13a4.20.fid
frac 2 pTLC2a
1H CDCl3
2018-01-08T11:56:00
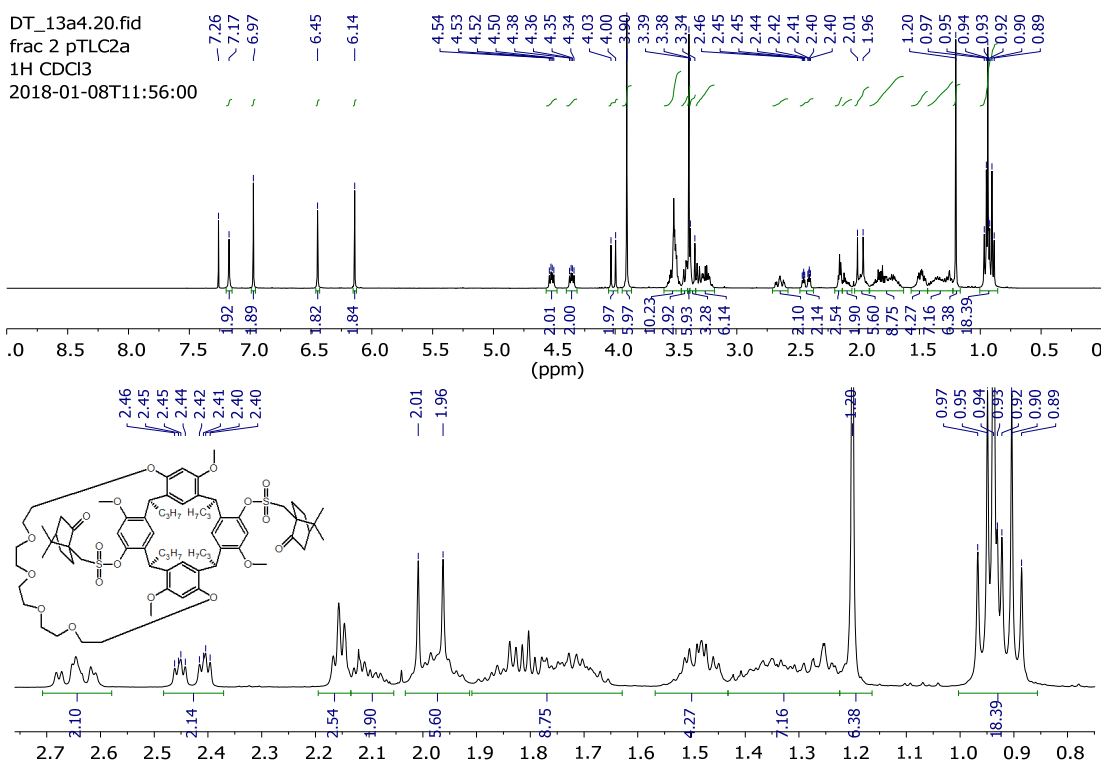
Appendix A33.1 (60b) ^{1}H NMR spectrum recorded in CDCl$_3$.
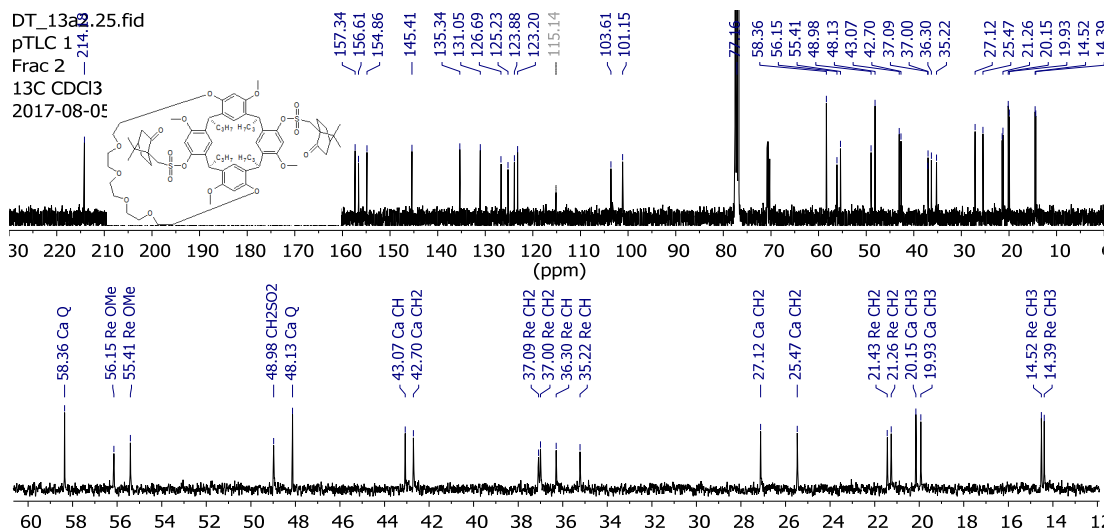
Appendix A33.2 (60b) ^{13}C NMR spectrum recorded in CDCl$_3$.
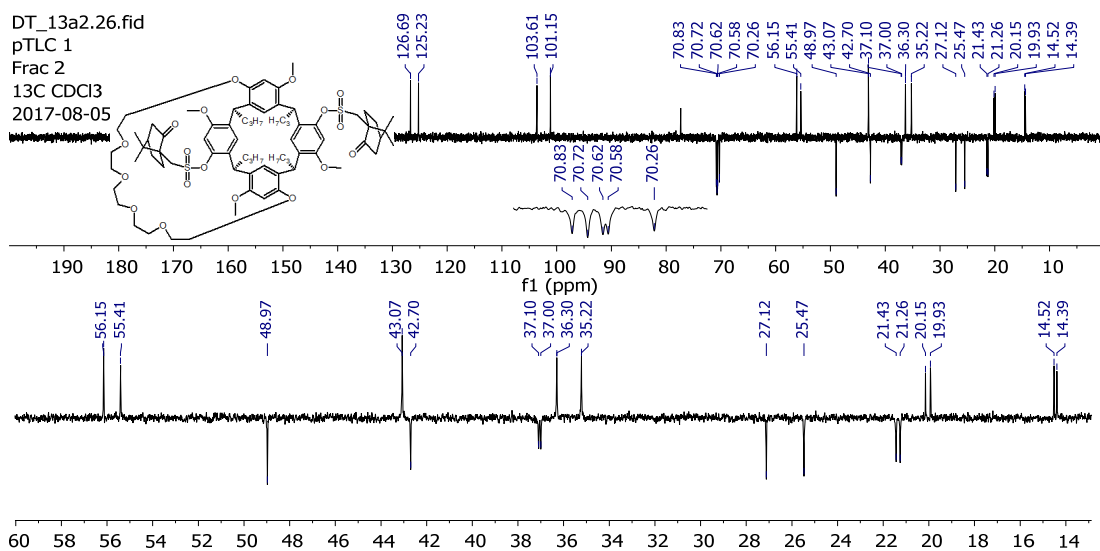
Appendix A33.3 (60b) DEPT-135 spectrum recorded in CDCl$_3$.
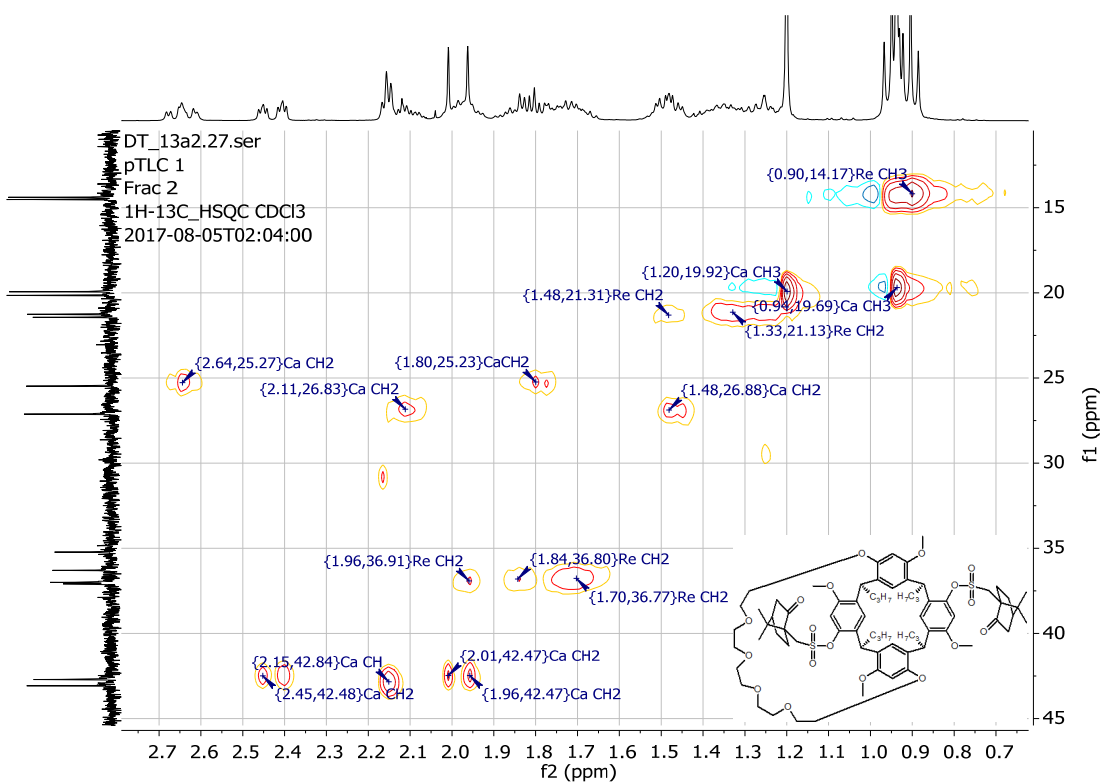
Appendix A33.4 (60b) HSQC NMR spectrum (expansion) recorded in CDCl$_3$.
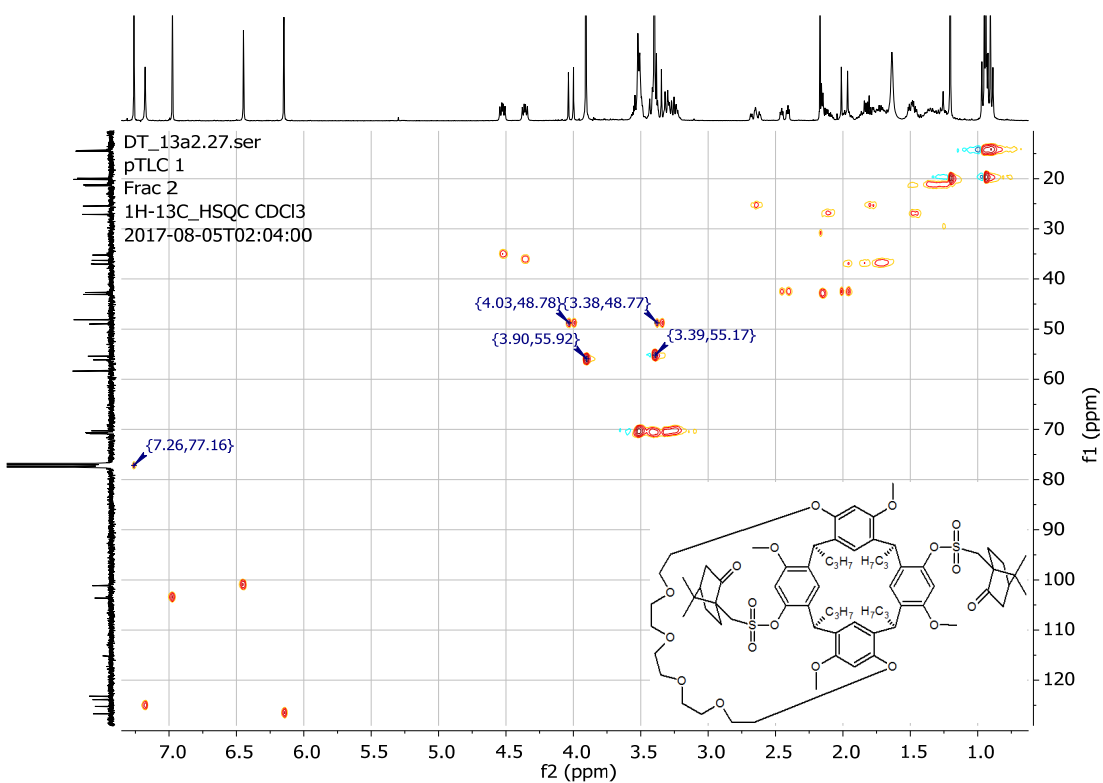
Appendix A33.5 (60b) HSQC NMR spectrum recorded in CDCl$_3$.
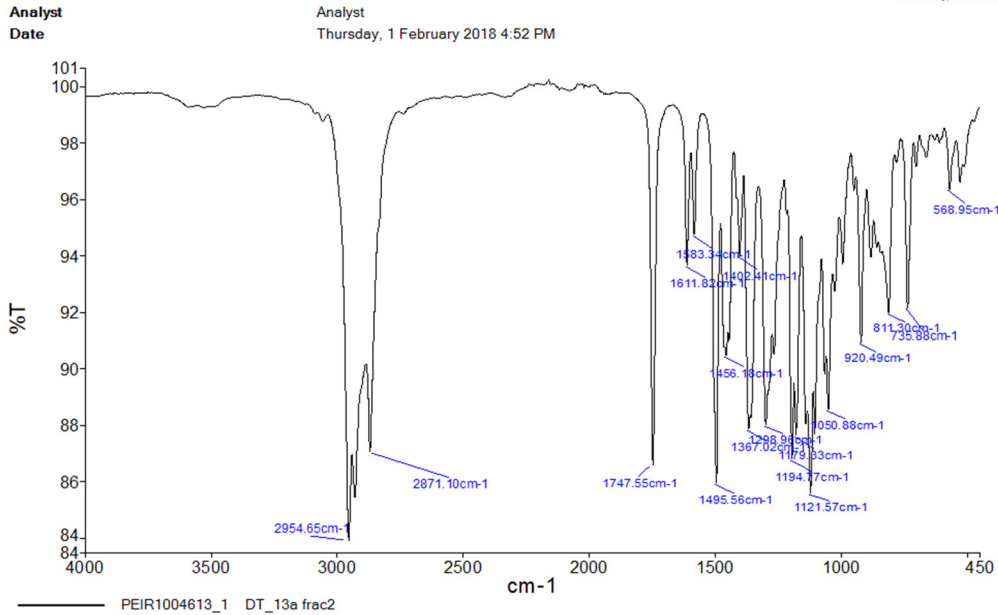
Appendix A33.6 (60b) IR spectrum.

(61a) Dicamphorsulfonate crown-7 resorcinarene

DT_13d1.14.fid
pTLC4a F1
1H CDCl3
2018-03-16T18:33:00
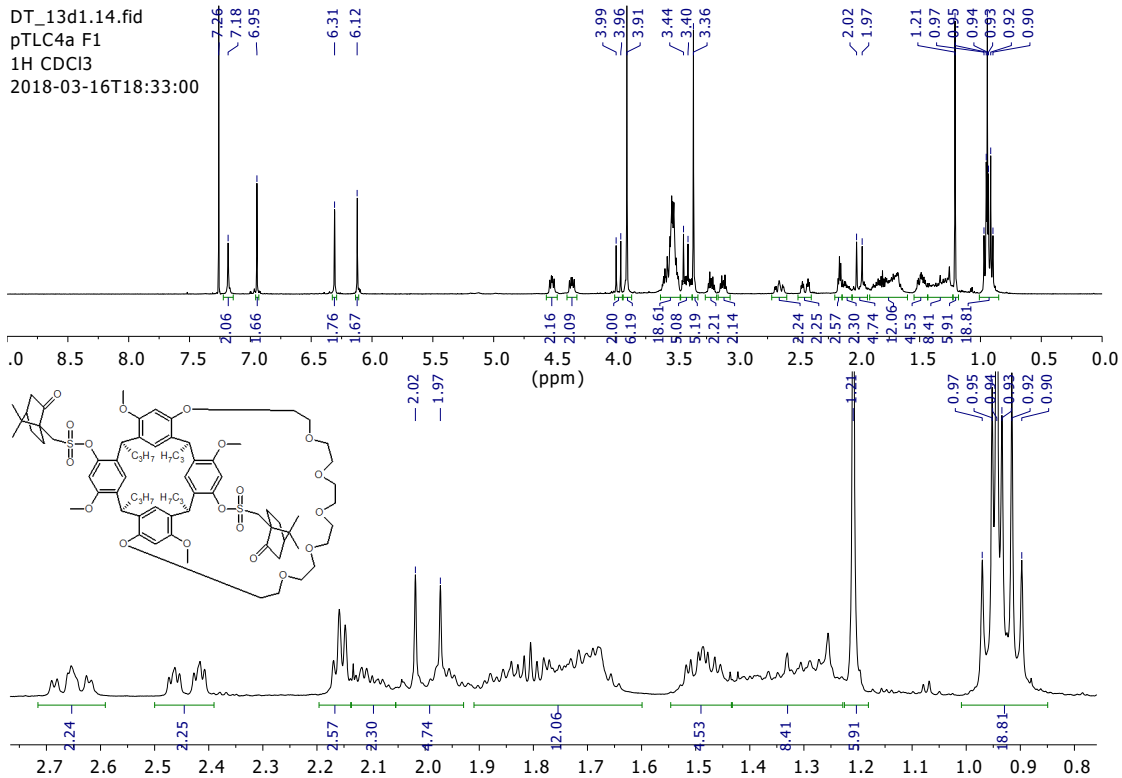
Appendix A34.1 (61a) ^{1}H NMR spectrum recorded in CDCl$_3$.
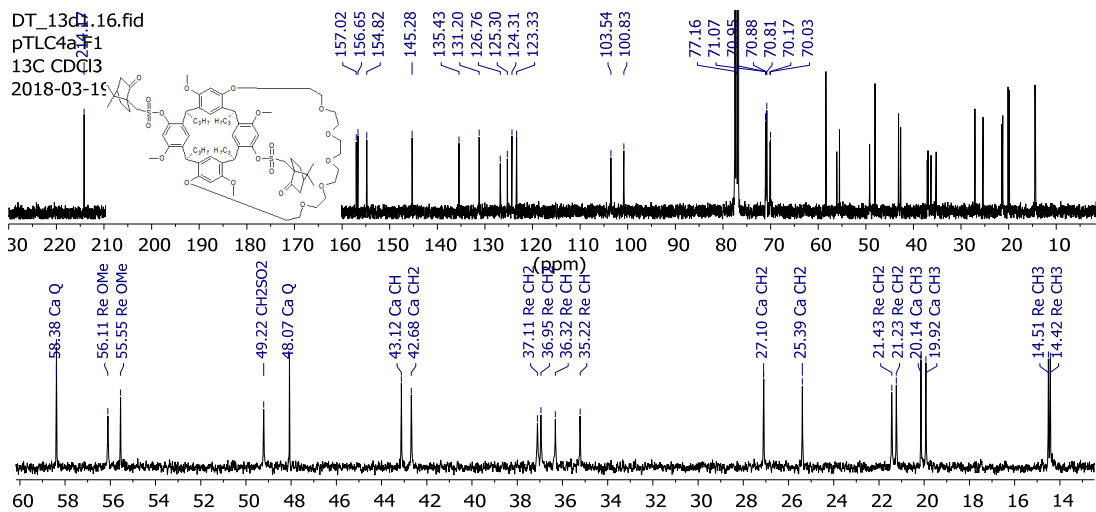
Appendix A34.2 (61a) ^{13}C NMR spectrum recorded in CDCl$_3$.
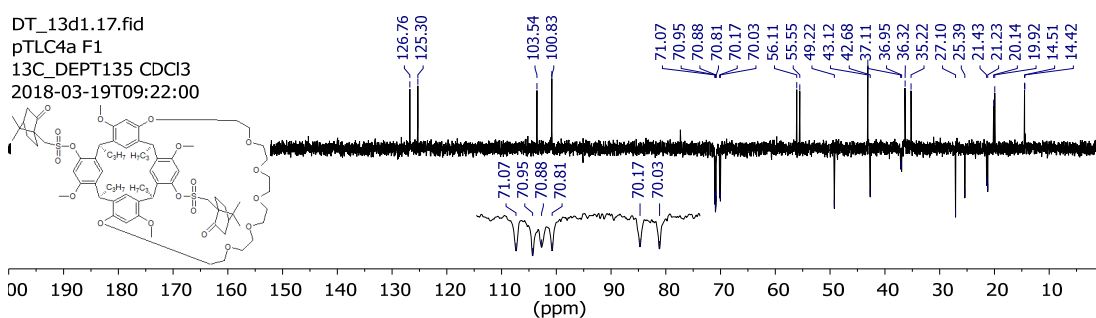
Appendix A34.3 (61a) DEPT-135 spectrum recorded in CDCl$_3$.
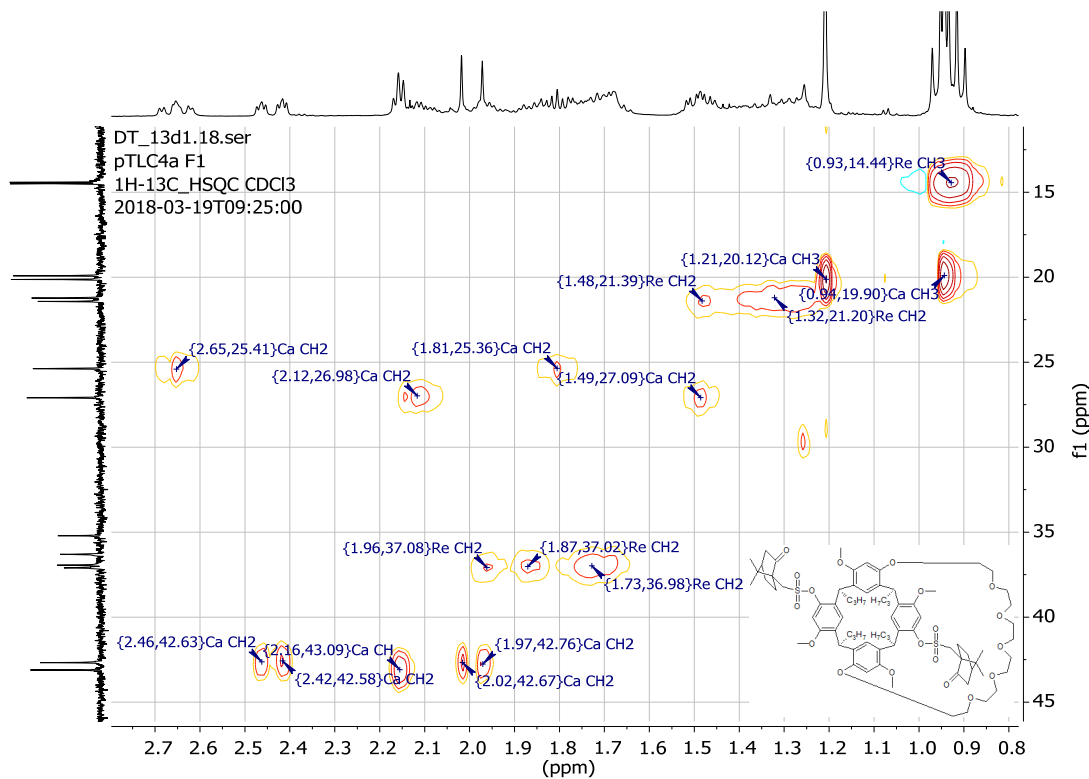
Appendix A34.4 (61a) HSQC NMR spectrum (expansion) recorded in CDCl$_3$.
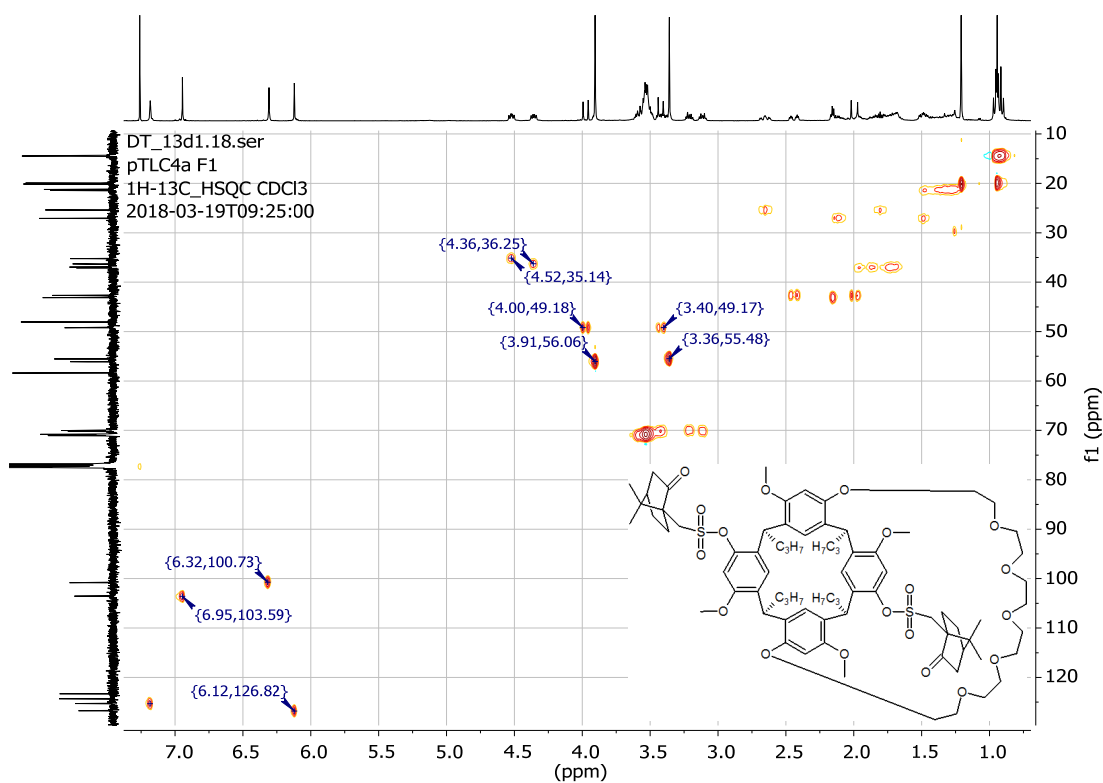
Appendix A34.5 (61a) HSQC NMR spectrum recorded in CDCl₃.

(61b) Dicamphorsulfonate crown-7 resorcinarene
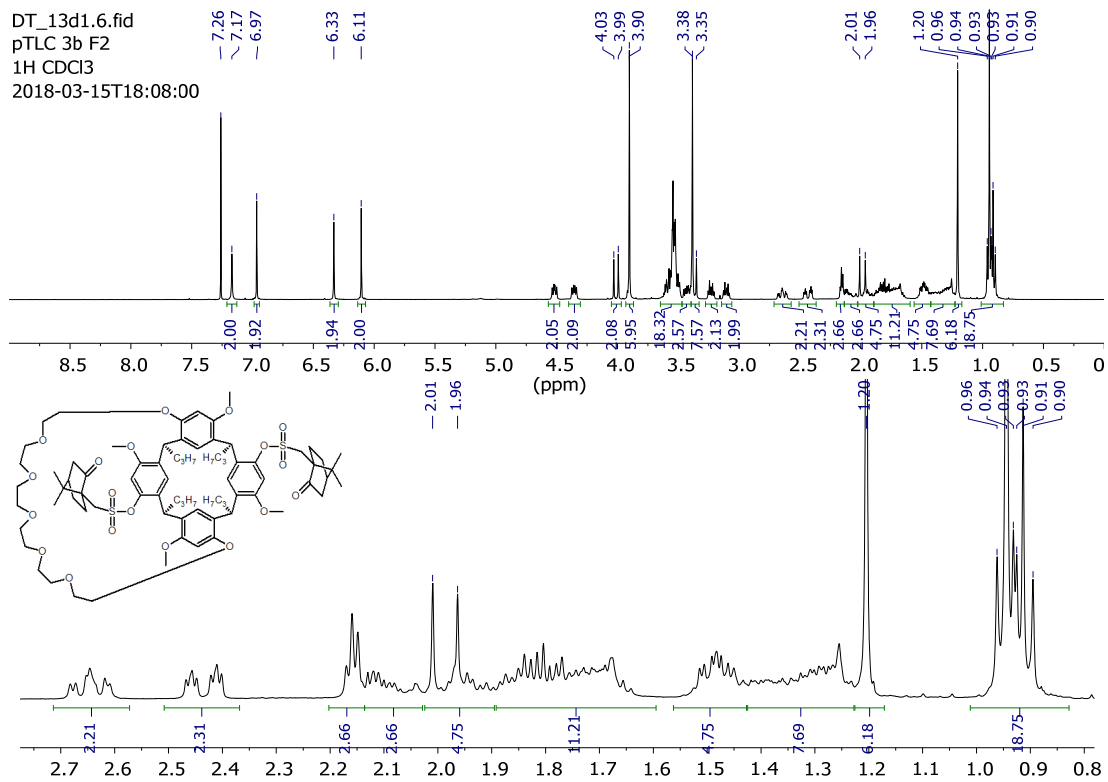
Appendix A35.1 (61b) ¹H NMR spectrum recorded in CDCl₃.
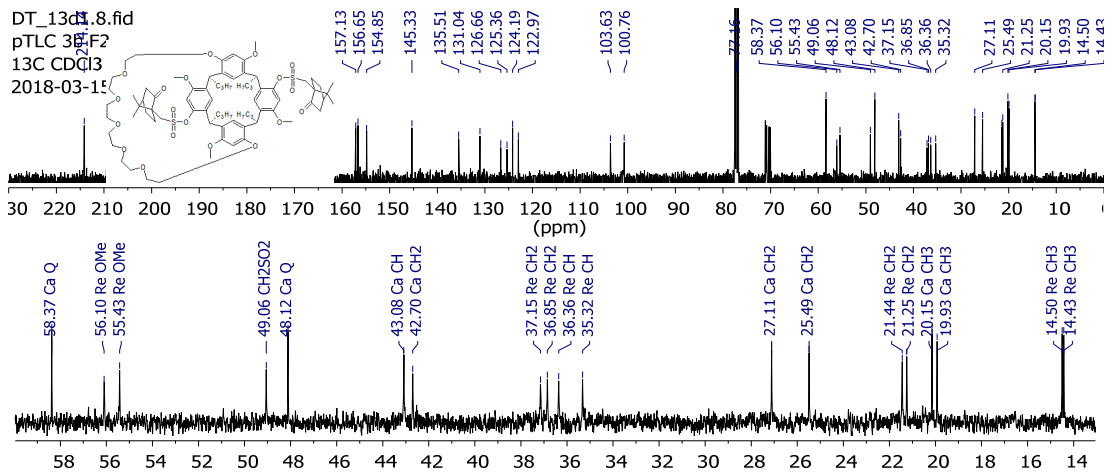
Appendix A35.2 (61b) ^{13}C NMR spectrum recorded in CDCl$_3$.
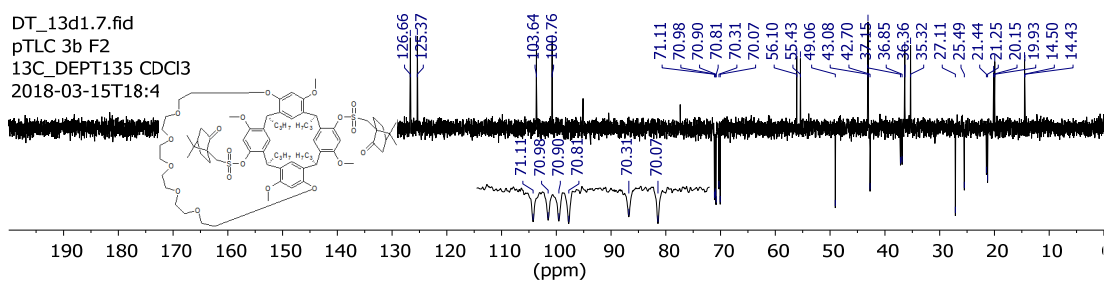
Appendix A35.3 (61b) DEPT-135 spectrum recorded in CDCl$_3$.
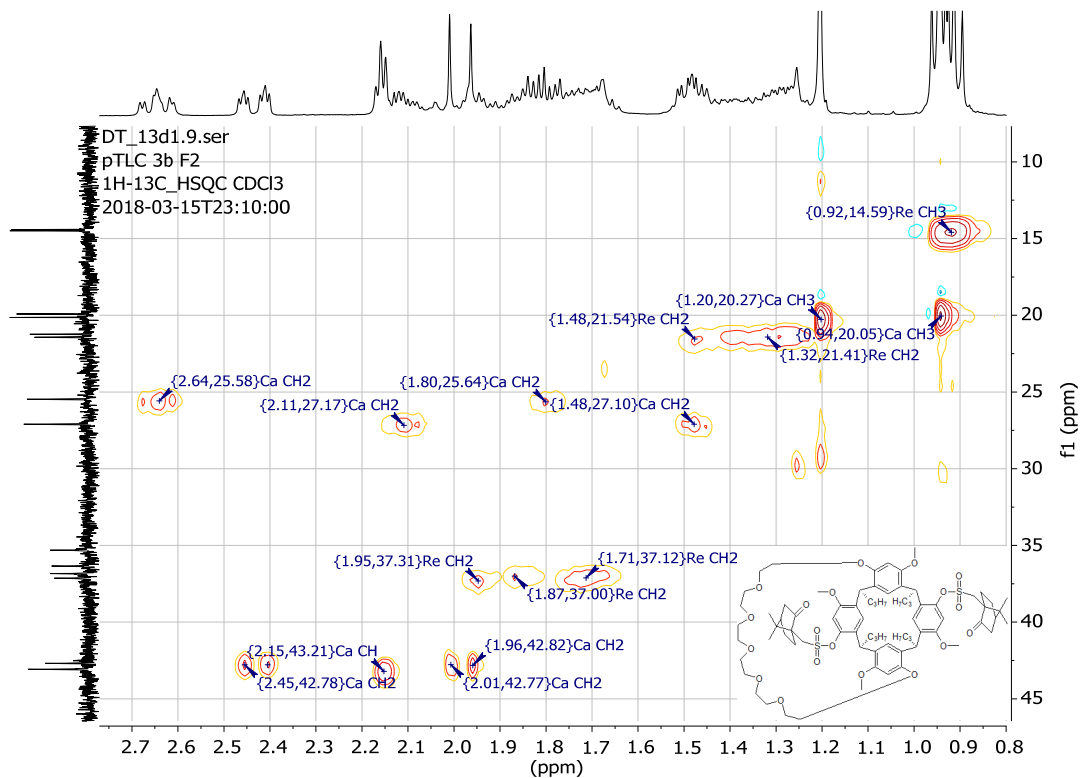
Appendix A35.4 (61b) HSQC NMR spectrum (expansion) recorded in CDCl$_3$.
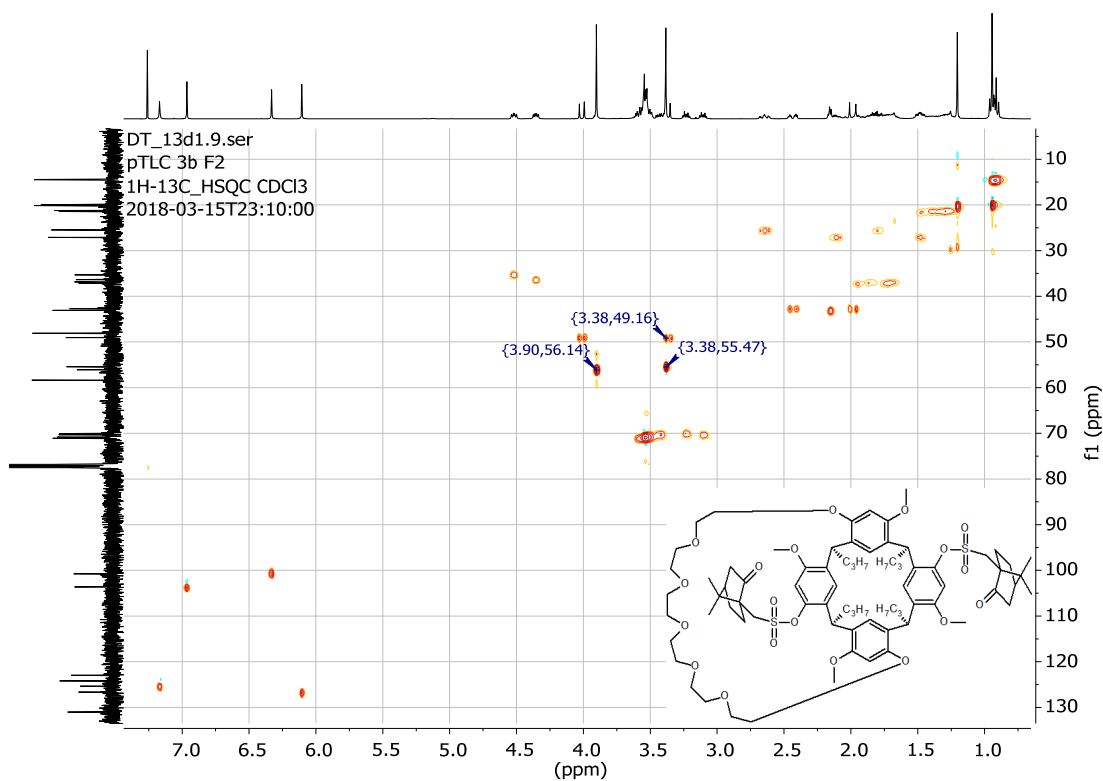
Appendix A35.5 (61b) HSQC NMR spectrum recorded in CDCl$_3$.

(62) Diastereomeric mixture of dicamphorsulfonate diTBDMS resorcinarene

Appendix A36.1 Diastereomeric mixture **(62)** ^{1}H NMR spectrum recorded in CDCl$_3$.

Diasteromeric mixture of dicamphorsulfonate dibenzyloxy resorcinarene
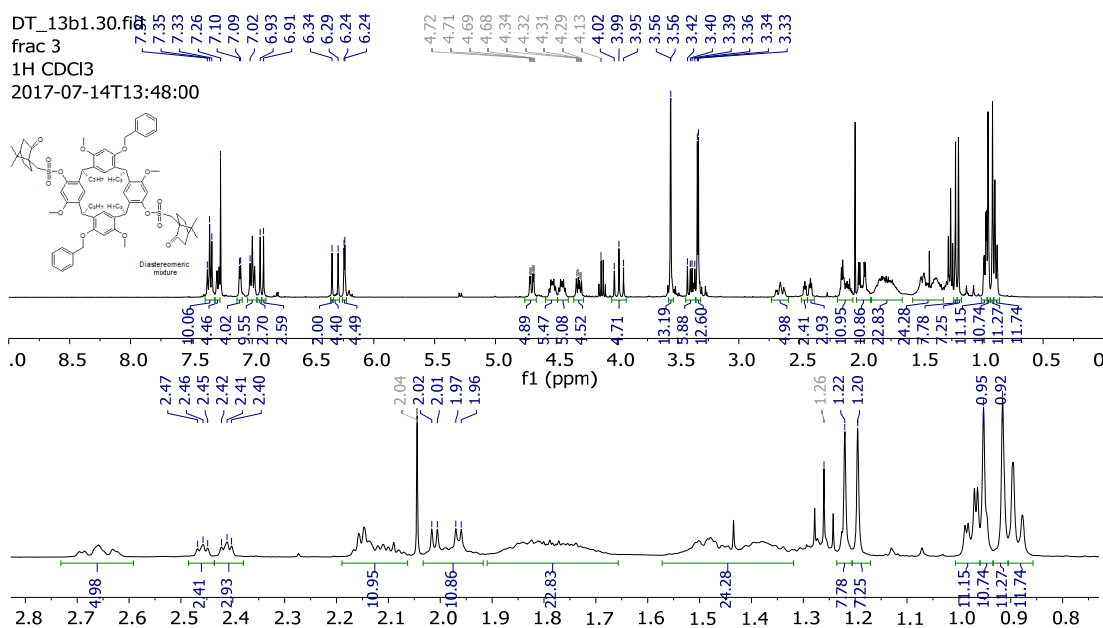
Appendix A37.1 Diastereomeric mixture dicamphorsulfonate dibenzyloxy resorcinarene ^{1}H NMR spectrum recorded in CDCl$_3$.

Bis-crown resorcinarenes

(63) Bis-crown-5 resorcinarene
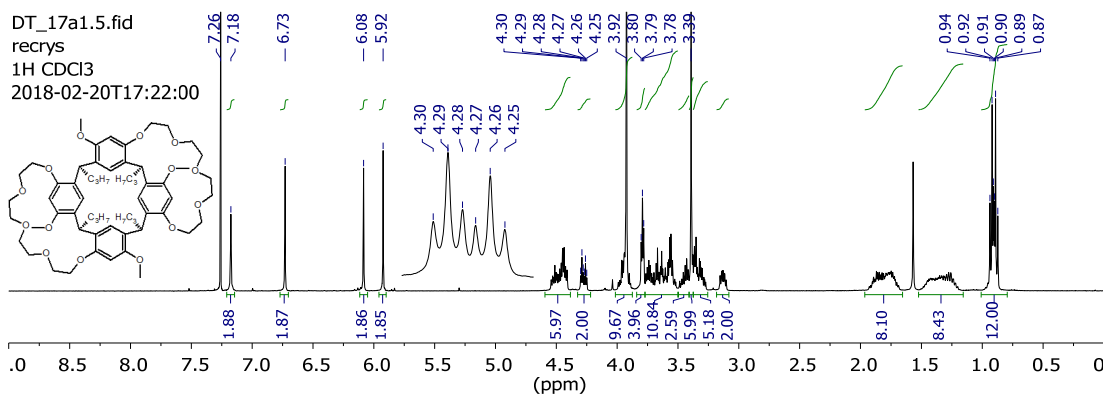
Appendix A38.1 (63) ^{1}H NMR spectrum recorded in CDCl$_3$.
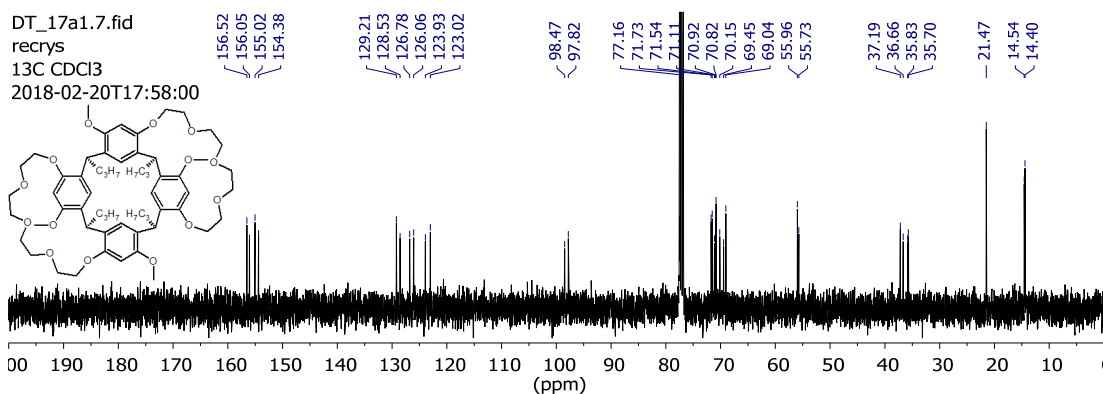
Appendix A38.2 (63) ^{13}C NMR spectrum recorded in CDCl$_3$.
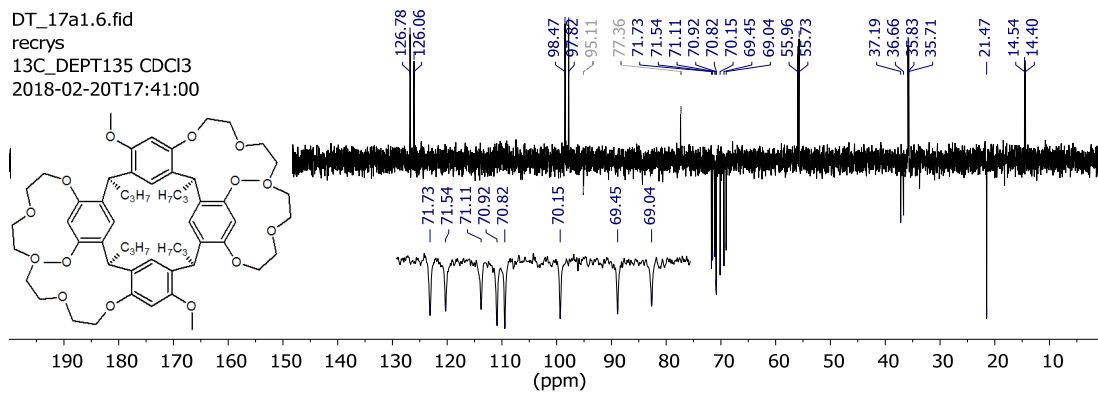
Appendix A38.3 (63) ^{13}C NMR spectrum recorded in CDCl$_3$.
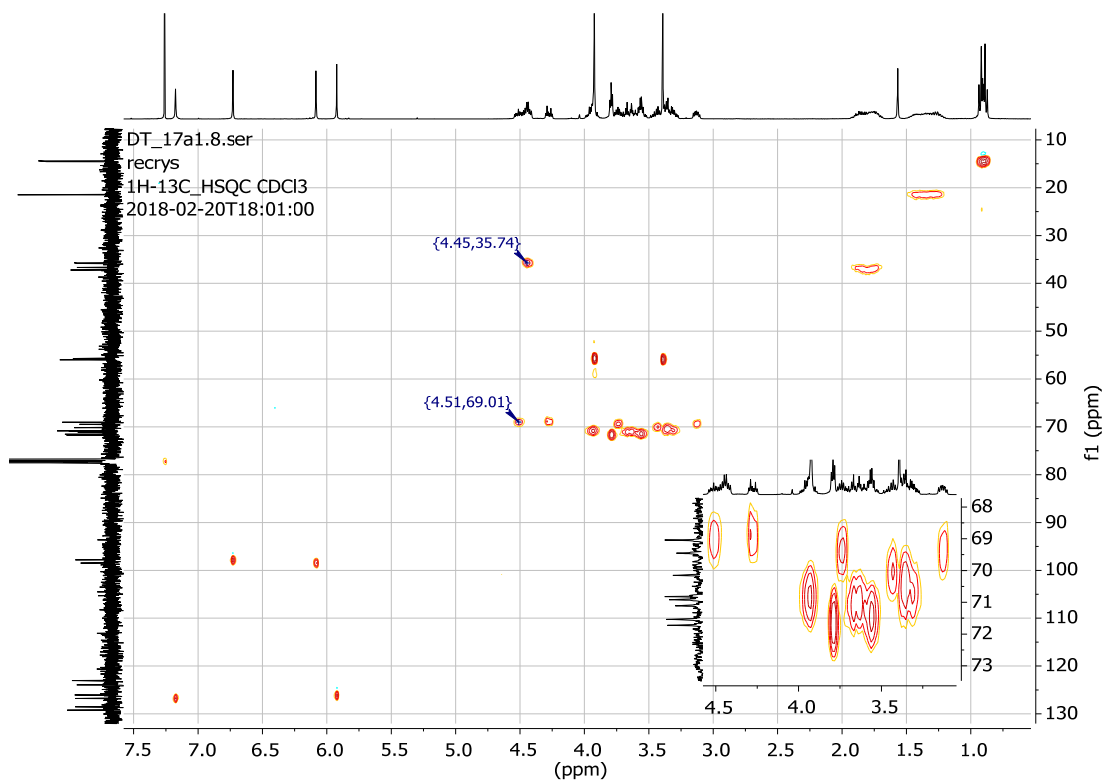
Appendix A38.4 (63) HSQC NMR spectrum recorded in CDCl$_3$.

(64) Bis-crown-6 resorcinarene

DT_17b2.3.fid
columned/recrys
1H CDCl3
2018-04-11T15:41:00
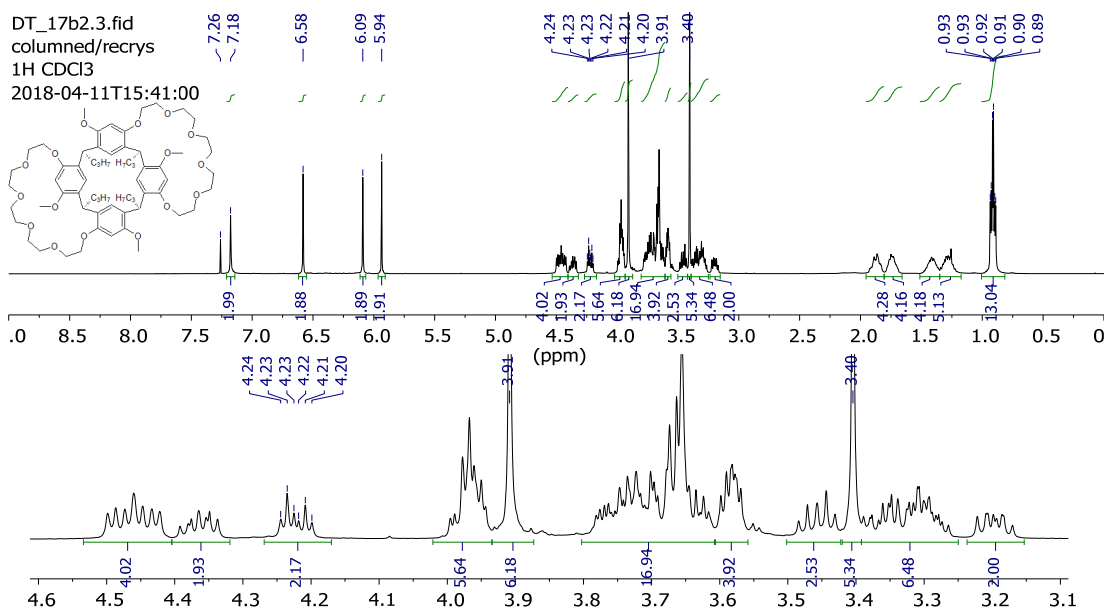
Appendix A39.1 (64) ^{1}H NMR spectrum recorded in CDCl$_3$.

DT_17b2.5.fid
columned/recrys
13C CDCl3
2018-04-11T16:29:00
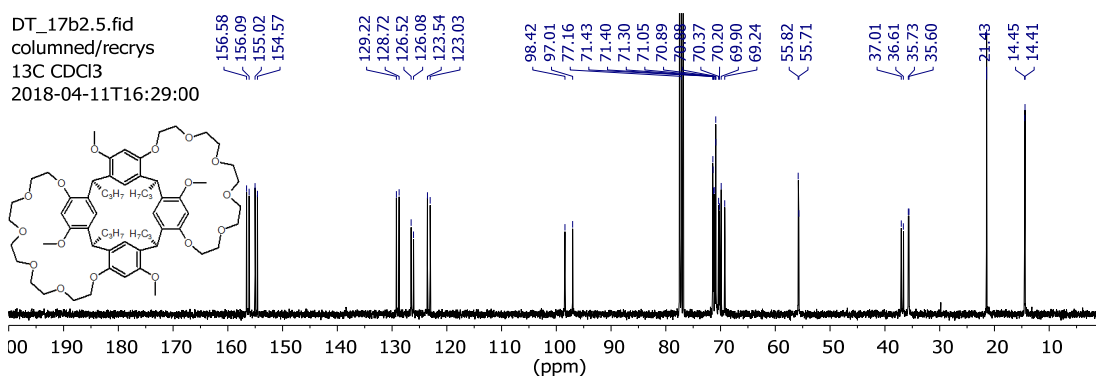
Appendix A39.2 (64) ^{13}C NMR spectrum recorded in CDCl$_3$.

DT_17b2.4.fid
columned/recrys
13C_DEPT135 CDCl3
2018-04-11T16:01:00
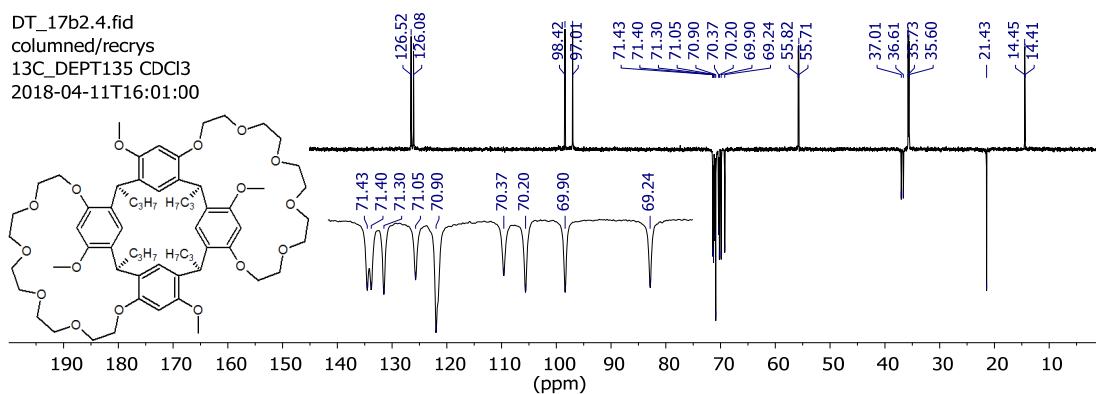
Appendix A39.3 (64) DEPT-135 NMR spectrum recorded in CDCl$_3$.
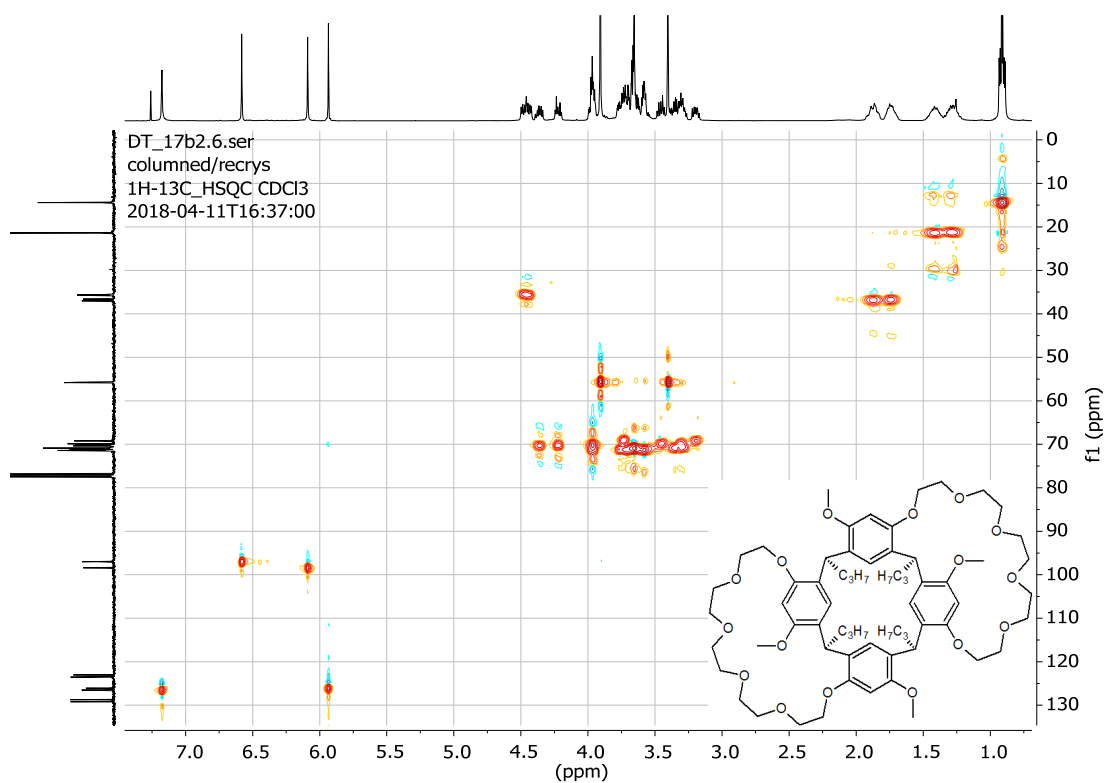
Appendix A39.4 (64) HSQC NMR spectrum recorded in CDCl$_3$.

(65) Bis-crown-7 resorcinarene
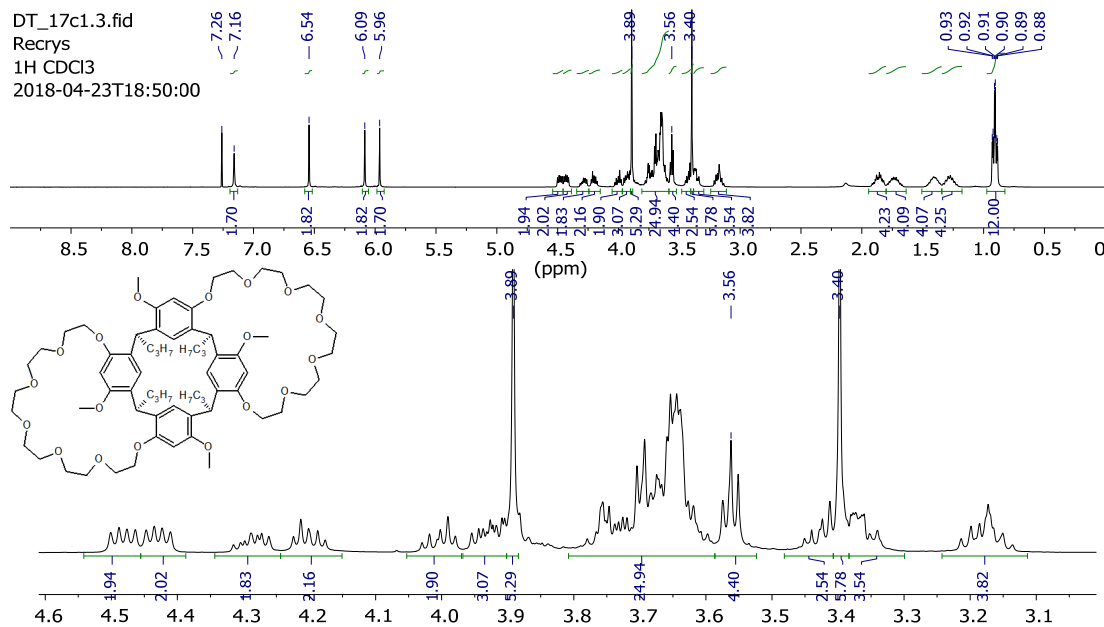
Appendix A40.1 (65) ^{1}H NMR spectrum recorded in CDCl$_3$.
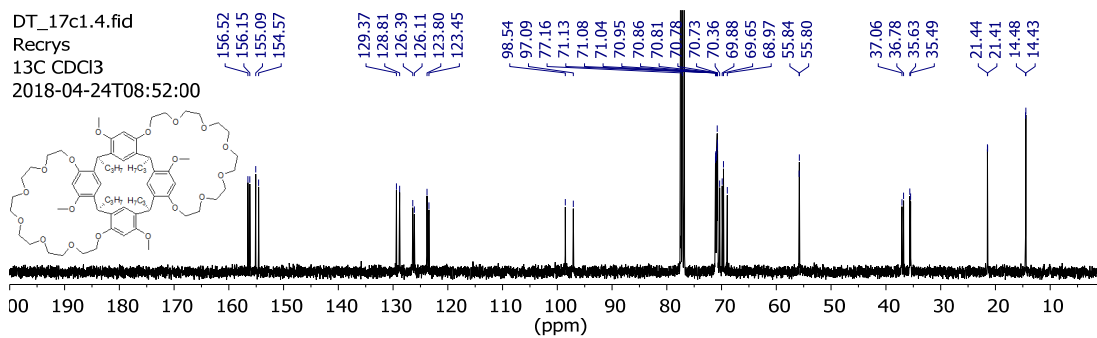
Appendix A40.2 (65) ^{13}C NMR spectrum recorded in CDCl$_3$.
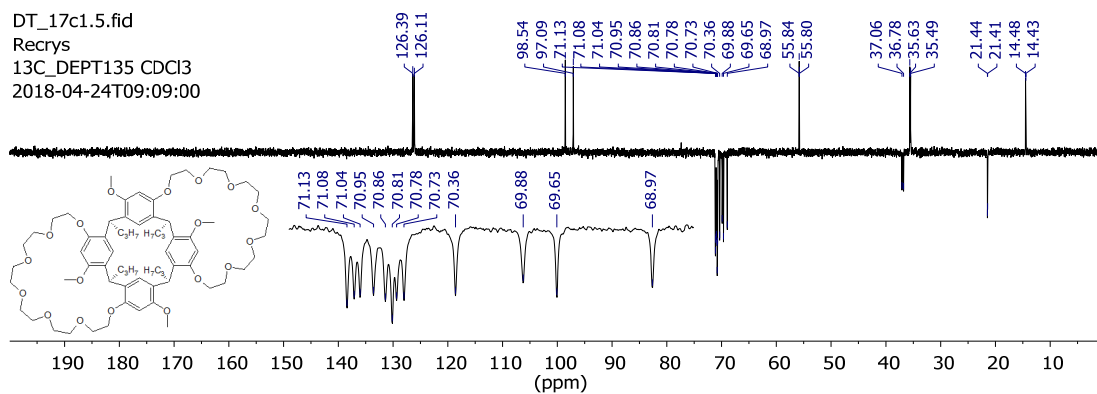
Appendix A40.3 (65) DEPT-135 NMR spectrum recorded in CDCl$_3$.
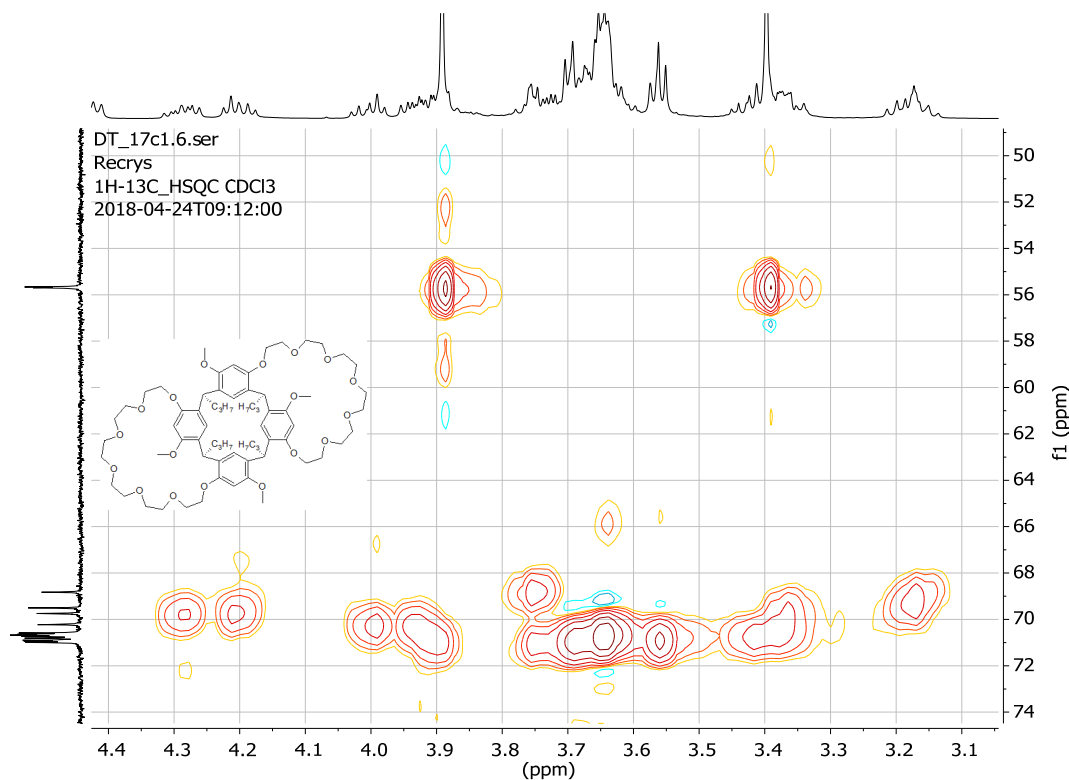
Appendix A40.4 (65) HSQC NMR spectrum recorded in CDCl$_3$.

Appendix B

X-ray Data Collection and Crystal Structure Determinations

Contents

Appendix B

General experimental information

Crystal structures of the compounds were determined by X-ray diffraction methods by A/Prof. Chiara Massera from the University of Parma, Italy.

For the samples Mono-TBDMS **(32)**, Prox-TBDMS **(33)**, Distal-TBDMS **(34)**, Mono-TBDPS **(40)**, Distal-TBDPS **(42)**, Distal-OBn **(46)**, Distal-TBDMS **(38)**, diOBn diTBDMS **(49)**, diOBn crown-6 **(54)**, diOBn crown-7 **(55)** and diOH crown-6 **(57)** intensity data and cell parameters were recorded at 190(2) K on a Bruker ApexII diffractometer (MoKα radiation λ = 0.71073 Å) equipped with a CCD area detector and a graphite monochromator.

For diMeSO$_2$ diTBDMS **(48)** intensity data and cell parameters were recorded at 298(2) K on a Bruker Smart Breeze.

For dicamphorsulfonate crown-6 **(60)** intensity data and cell parameters were recorded at 190(2) K on a Bruker D8 Venture PhotonII diffractometer (CuKα radiation λ = 1.54178 Å).

All raw frame data acquired on Bruker instruments were processed using the programs SAINT and SADABS to yield the reflection data files.[1-3]

For Tri-TBDMS **(35)** and for diOBn crown-5 **(53)**, intensity data and cell parameters were recorded at 100(2) K at the ELETTRA Synchrotron Light Source (CNR Trieste, strada statale 14, Area Science Park, 34149, Basovizza, Trieste, Italy), and the raw frame data were processed using the program package CrysAlisPro 1.171.38.41.[4]

All structures were solved by Direct Methods using the SIR97 program[5] and refined on F_o^2 by full-matrix least-squares procedures, using the SHELXL-2014/7 program[6] in the WinGX suite v.2014.1.[7]

The crystals of Tri-TBDMS **(35)**, Mono-TBDPS **(40)** and Distal-TBDPS **(42)** diffracted poorly, but the data were good enough to establish the crystal and molecular structure of the products.

All non-hydrogen atoms were refined with anisotropic atomic displacements, unless in cases where disorder was present (solvent, alkyl chains, etc.). The hydrogen atoms were included in the refinement at idealized geometry (C-H 0.96, 0.93 and 0.98 Å for methyl, aromatic and methylenic H atoms, respectively) and refined "riding" on the corresponding parent atoms. The weighting schemes used in the last cycle of refinement were $w = 1/[\sigma^2 F_o^2 + (0.0391P)^2]$, $w = 1/[\sigma^2 F_o^2 + (0.0672P)^2 + 0.6860P]$, $w = 1/[\sigma^2 F_o^2 + (0.0764P)^2 + 2.4161P]$, $w = 1/[\sigma^2 F_o^2 + (0.4203P)^2]$, $w = 1/[\sigma^2 F_o^2 + (0.1289P)^2]$, $w = 1/[\sigma^2 F_o^2 + (0.0P)^2]$, $w = 1/[\sigma^2 F_o^2 + (0.0897P)^2 + 0.9194P]$, $w = 1/[\sigma^2 F_o^2 + (0.1210P)^2 + 2.9812P]$, $w = 1/[\sigma^2 F_o^2 + (+1.4916P)^2 + 1.4759P]$, $w = 1/[\sigma^2 F_o^2 + (0.0948\ P)^2 + 2.2146P]$, $w = 1/[\sigma^2 F_o^2 + (0.1816\ P)^2 + 4.6366\ P]$, $w = 1/[\sigma^2 F_o^2 + (0.4158P)^2]$, $w = 1/[\sigma^2 F_o^2 + (0.0721P)^2 + 1.4916P]$, $w = 1/[\sigma^2 F_o^2 + (0.3255P)^2]$ and $w = 1/[\sigma^2 F_o^2 + (0.1593P)^2 + 0.2094P]$, where $P = (F_o^2 + 2F_c^2)/3$, for Mono-TBDMS **(32)**, Prox-TBDMS **(33)**, Distal-TBDMS **(34)**, Tri-TBDMS **(35),** Mono-TBDPS **(40)**, Distal-TBDPS **(42)**, Distal-OBn **(46)**, Distal-TBDMS **(38)**, diMeSO₂ diTBDMS **(48)**, diOBn diTBDMS **(49)**, diOBn crown-5 **(53)**, diOBn crown-6 **(54)**, diOBn crown-7 **(55)**, diOH crown-6 **(57)** and dicamphSO₂ crown-6 **(60)** respectively.

For diOBn crown-6 **(54)** the calculated molar mass, density and absorption coefficient include two disordered water molecules per cell which do not appear in the final files because of the refinements carried out with data subjected to SQUEEZE.[8]

Crystal data and experimental details for data collection and structure refinement are reported in the following **Table B1** to **Table B7**.

Crystal data and structure refinement

Table B1   Crystal data and structure refinement information for compounds Mono-TBDMS **(32)** and Prox-TBDMS **(33)**.

Compound	Mono-TBDMS **(32)**	Prox-TBDMS **(33)**
empirical formula	$C_{50}H_{70}O_8Si$	$C_{56}H_{84}O_8Si_2$
M	827.15	941.41
crys syst	Triclinic	Triclinic
space group	*P-1*	*P-1*
a/Å	11.467(3)	13.582(1)
b/Å	14.222(4)	14.896(1)
c/Å	16.757(5)	16.117(2)
α/°	103.940(5)	109.063(2)
β/°	109.484(6)	99.137(2)
γ/°	98.901(6)	111.256(2)
V/Å^3	2416.5(12)	2726.3(4)
Z	2	2
ρ /g cm^{-3}	1.137	1.147
μ /mm^{-1}	0.098	0.116
F(000)	896	1024
total reflections	13171	39382
unique reflections (R_{int})	8088 (0.0547)	13777 (0.0810)
observed reflections *[$F_o>4\sigma(F_o)$]*	4083	8068
GOF on F^{2a}	1.013	1.007
R indices *[$F_o>4\sigma(F_o)$]*[b]R_1, wR_2	0.0611, 0.1108	0.0606, 0.1403
largest diff. peak and hole (eÅ^{-3})	0.291, -0.338	1.182, -0.723

[a]Goodness-of-fit $S = [\Sigma w(F_o^2-F_c^2)^2/ (n-p)]1/2$, where n is the number of reflections and p the number of parameters. [b]$R_1 = \Sigma \| F_o | - | F_c \| / \Sigma | F_o |$, $wR_2 = [\Sigma[w(F_o^2-F_c^2)^2]/\Sigma[w(F_o^2)^2]]^{1/2}$.

Table B2   Crystal data and structure refinement information for compounds Distal-TBDMS **(34)** and Tri-TBDMS **(35)**.

Compound	Distal-TBDMS **(34)**	Tri-TBDMS **(35)**
empirical formula	$C_{56}H_{84}O_8Si_2$	$C_{62}H_{98}O_8Si_3$
M	941.41	1055.67
crys syst	monoclinic	Monoclinic
space group	$P21/n$	$P21/n$
a/Å	14.039(2)	29.220(5
b/Å	26.618(3)	10.963(2)
c/Å	14.620(2)	41.528(8)
α/°	-	-
β/°	93.690(2)	103.399(9)
γ/°	-	-
V/Å^3	5452.0(12)	12941(4)
Z	4	8
ρ /g cm^{-3}	1.147	1.084
μ /mm^{-1}	0.116	0.089
$F(000)$	2048	4608
total reflections	58411	195561
unique reflections (R_{int})	9328 (0.1197)	41455 (0.0581)
observed reflections $[F_o>4\sigma(F_o)]$	4915	27378
GOF on F^{2a}	1.002	1.024
R indices $[F_o>4\sigma(F_o)]^bR_1$, wR_2	0.0610, 0.1431	0.1497, 0.4188
largest diff. peak and hole (eÅ^{-3})	0.712, -0.316	5.387, -1.175

[a]Goodness-of-fit $S = [\Sigma w(F_o^2-F_c^2)^2/ (n-p)]1/2$, where n is the number of reflections and p the number of parameters. [b]$R_1 = \Sigma \|F_o\| - \|F_c\| / \Sigma |F_o|$, $wR_2 = [\Sigma[w(F_o^2 - F_c^2)^2]/\Sigma[w(F_o^2)^2]]^{1/2}$.

Table B3   Crystal data and structure refinement information for compounds Mono-TBDPS **(40)** and Distal-TBDPS **(42)**.

Compound	Mono-TBDPS **(40)**	Distal-TBDPS **(42)**
empirical formula	$C_{60}H_{74}O_8Si \cdot 2H_2O$	$C_{76}H_{91}O_8Si_2 \cdot \frac{1}{2} H_2O$
M	987.31	1198.68
crys syst	Monoclinic	Triclinic
space group	$C\ 2/c$	$P\text{-}1$
$a/\text{Å}$	26.098(9)	14.161(6)
$b/\text{Å}$	18.207(9)	14.414(6)
$c/\text{Å}$	25.589(9)	18.256(7)
$\alpha/°$	-	104.816(9)
$\beta/°$	99.641(7)	95.977(9)
$\gamma/°$	-	98.881(9)
$V/\text{Å}^3$	11987(8)	3519(2)
Z	8	2
$\rho\ /\text{g cm}^{-3}$	1.094	1.131
$\mu\ /\text{mm}^{-1}$	0.092	0.104
$F(000)$	4256	1290
total reflections	24615	28261
unique reflections (R_{int})	8716 (0.2574)	8541 (0.3872)
observed reflections $[F_o > 4\sigma(F_o)]$	2934	2587
GOF on F^{2a}	1.001	0.826
R indices $[F_o > 4\sigma(F_o)]^{b}R_1,\ wR_2$	0.1049, 0.2409	0.00950, 0.2160
largest diff. peak and hole ($e\text{Å}^{-3}$)	1.038, -0.347	0.952, -0.293

[a]Goodness-of-fit $S = [\Sigma w(F_o^2 - F_c^2)^2/ (n\text{-}p)]1/2$, where n is the number of reflections and p the number of parameters. [b]$R_1 = \Sigma \|F_o| - |F_c\|/\Sigma |F_o|$, $wR_2 = [\Sigma[w(F_o^2 - F_c^2)^2]/\Sigma[w(F_o^2)^2]]^{1/2}$.

Table B4 Crystal data and structure refinement information for compounds Distal-OBn **(46)** and Distal-TBDMS **(38)**.

Compound	Distal-OBn **(46)**	Distal-TBDMS **(38)**
empirical formula	$C_{58}H_{68}O_8$	$C_{58}H_{68}O_8$
M	893.12	1165.82
crys syst	Triclinic	Triclinic
space group	*P-1*	*P-1*
a/Å	15.559(2)	12.635(1)
b/Å	16.121(2)	14.113(1)
c/Å	21.417(2)	20.164(2)
α/°	77.881(2)	90.250(1)
β/°	71.290(2)	95.111(1)
γ/°	80.371(2)	96.340(1)
V/Å^3	4945.6(10)	3559.0(5)
Z	4	2
ρ /g cm^{-3}	1.199	1.088
μ /mm^{-1}	0.078	0.100
$F(000)$	1920	1280
total reflections	70215	36741
unique reflections (R_{int})	24690 (0.0372)	11379 (0.0494)
observed reflections *[$F_o>4\sigma(F_o)$]*	16183	7897
GOF on F^{2a}	1.005	1.001
R indices *[$F_o>4\sigma(F_o)$]*[b]R_1, wR_2	0.0555, 0.1495	0.0682, 0.1892
largest diff. peak and hole (eÅ^{-3})	0.745, -0.475	0.979, -0.563

[a]Goodness-of-fit $S = [\Sigma w(F_o^2-F_c^2)^2/ (n-p)]^{1/2}$, where n is the number of reflections and p the number of parameters. [b]$R_1 = \Sigma \|F_o| - |F_c\|/\Sigma |F_o|$, $wR_2 = [\Sigma[w(F_o^2-F_c^2)^2]/\Sigma[w(F_o^2)^2]]^{1/2}$.

Table B5   Crystal data and structure refinement information for compounds diMeSO$_2$ diTBDMS **(48)** and diOBn diTBDMS **(49)**.

Compound	diMeSO$_2$ diTBDMS **(48)**	diOBn diTBDMS **(49)**
empirical formula	C$_{58}$H$_{88}$O$_{12}$S$_2$Si$_2$	C$_{70}$H$_{96}$O$_8$Si$_2$
M	1097.58	1121.64
crys syst	Triclinic	Triclinic
space group	P-1	P-1
a/Å	12.490(2)	14.0561(6)
b/Å	13.875(3)	14.2020(6)
c/Å	19.606(2)	17.9849(8)
a/°	77.472(2)	87.243(1)
b/°	86.473(2)	69.162(1)
g/°	74.004(2)	81.920(1)
V/Å^3	3188.4(9)	3322.1(2)
Z	2	2
ρ /g cm^{-3}	1.143	1.121
m /mm^{-1}	0.175	0.105
F(000)	1184	1216
total reflections	39204	41481
unique reflections (R_{int})	13119 (0.0441)	13880 (0.0335)
observed reflections $[F_o>4\sigma(F_o)]$	8350	10354
GOF on F^{2a}	1.008	1.006
R indices $[F_o>4\sigma(F_o)]^b$$R_1$, wR_2	0.0755, 0.2159	0.0597, 0.1627
largest diff. peak and hole (eÅ^{-3})	1.333, -0.492	2.060, -0.739

[a]Goodness-of-fit S = $[\Sigma w(F_o{}^2\text{-}F_c{}^2)^2/ (n\text{-}p)]1/2$, where n is the number of reflections and p the number of parameters. [b]$R_1 = \Sigma\|\,|F_o|\text{-}|F_c|\,\|/\Sigma\,|F_o|$, $wR_2 = [\Sigma[w(F_o{}^2\text{-}F_c{}^2)^2]/\Sigma[w(F_o{}^2)^2]]^{1/2}$.

Table B6   Crystal data and structure refinement information for compounds diOBn crown-5 **(53)** and diOBn crown-6 **(54)**.

| Compound	diOBn crown-5 **(53)**	diOBn crown-6 **(54)**.
empirical formula	$C_{66}H_{82}O_{11}$	$C_{68}H_{88}O_{13}$
M	1051.31	1113.38
crys syst	Monoclinic	Triclinic
space group	*P21/n*	*P-1*
a/Å	19.1720(2)	12.1540(4)
b/Å	24.7360(3)	14.4487(5)
c/Å	24.7452(3)	19.1555(6)
α/°		77.867(2)
β/°	104.106(1)	79.263(2)
γ/°		88.568(2)
V/Å^3	11381.3(2)	3230.8(2)
Z	8	2
ρ /g cm^{-3}	1.227	1.144
μ /mm^{-1}	0.053	0.078
F(000)	4528	1200
total reflections	221915	33942
unique reflections (R_{int})	39506 (0.0739)	13197 (0.0393)
observed reflections $[F_o>4\sigma(F_o)]$	34102	7513
GOF on F^{2a}	1.004	1.027
R indices $[F_o>4\sigma(F_o)]^bR_1$, wR_2	0.0838, 0.2400	0.1316, 0.4296
largest diff. peak and hole (eÅ^{-3})	2.364, -0.965	1.429, -0.932

[a]Goodness-of-fit $S = [\Sigma w(F_o^2 - F_c^2)^2 / (n-p)]1/2$, where n is the number of reflections and p the number of parameters. [b]$R_1 = \Sigma ||F_o| - |F_c|| / \Sigma |F_o|$, $wR_2 = [\Sigma[w(F_o^2 - F_c^2)^2] / \Sigma[w(F_o^2)^2]]^{1/2}$.

Table B7 Crystal data and structure refinement information for compounds diOBn crown-7 **(55)**, and diOH crown-6 **(57)**.

Compound	diOBn crown-7 **(55)**	diOH crown-6 **(57)**
empirical formula	$C_{71}H_{92}O_{13}Cl_2$	$C_{54}H_{76}O_{13}$
M	1224.34	933.14
crys syst	Monoclinic	Triclinic
space group	*P21/n*	*P-1*
a/Å	12.155(1)	10.9616(5)
b/Å	50.046(5)	14.3251(7)
c/Å	12.350(1)	16.7964(7)
α/°		97.860(3)
β/°	119.407(2)	99.661(3)
γ/°		100.439(3)
V/Å^3	6544.6(10)	2518.7(2)
Z	4	2
ρ /g cm^{-3}	1.243	1.230
μ /mm^{-1}	0.162	0.087
$F(000)$	2624	1008
total reflections	33428	27939
unique reflections (R_{int})	10277 (0.0743)	12502 (0.0459)
observed reflections *[$F_o>4\sigma(F_o)$]*	5958	5588
GOF on F^{2a}	1.008	1.016
R indices *[$F_o>4\sigma(F_o)$]*[b]R_1, wR_2	0.0563, 0.1326	0.1295, 0.3990
largest diff. peak and hole (eÅ^{-3})	0.233, -0.407	1.506, -0.656

[a]Goodness-of-fit $S = [\Sigma w(F_o^2-F_c^2)^2/ (n-p)]^{1/2}$, where n is the number of reflections and p the number of parameters. [b]$R_1 = \Sigma\|F_o| - |F_c\|/\Sigma|F_o|$, $wR_2 = [\Sigma[w(F_o^2-F_c^2)^2]/\Sigma[w(F_o^2)^2]]^{1/2}$.

Table B8   Crystal data and structure refinement information for compound dicamphSO$_2$ crown-6 **(60)**.

Compound	dicamphSO$_2$ crown-6 **(60)**
empirical formula	C$_{78}$H$_{112}$O$_{19}$.Si$_2$· ½ H$_2$O
M	1426.80
crys syst	Triclinic
space group	$P\ 1$
a/Å	15.4379(8)
b/Å	15.8165(8)
c/Å	17.7024(8)
α/°	70.226(2)
β/°	72.490(2)
γ/°	84.648(2)
V/Å^3	3878.9(3)
Z	2
ρ /g cm^{-3}	1.222
μ /mm^{-1}	1.184
F(000)	1538
total reflections	65317
unique reflections (R$_{int}$)	27089 (0.0399)
observed reflections *[F$_o$>4σ(F$_o$)]*	25856
GOF on F^{2a}	1.006
R indices *[F$_o$>4σ(F$_o$)]*^{b}R$_1$, wR$_2$	0.0642, 0.1834
largest diff. peak and hole (eÅ^{-3})	0.690, -0.477

[a]Goodness-of-fit $S = [\Sigma w(F_o^2-F_c^2)^2/ (n-p)]1/2$, where n is the number of reflections and p the number of parameters. [b]$R_1 = \Sigma \| F_o | - | F_c \| /\Sigma | F_o |$, $wR_2 = [\Sigma[w(F_o^2-F_c^2)^2]/\Sigma[w(F_o^2)^2]]^{1/2}$.

ORTEP view of crystal structures

For all crystal structures, the hydrogen atoms of the alkyl chains have been omitted for clarity.
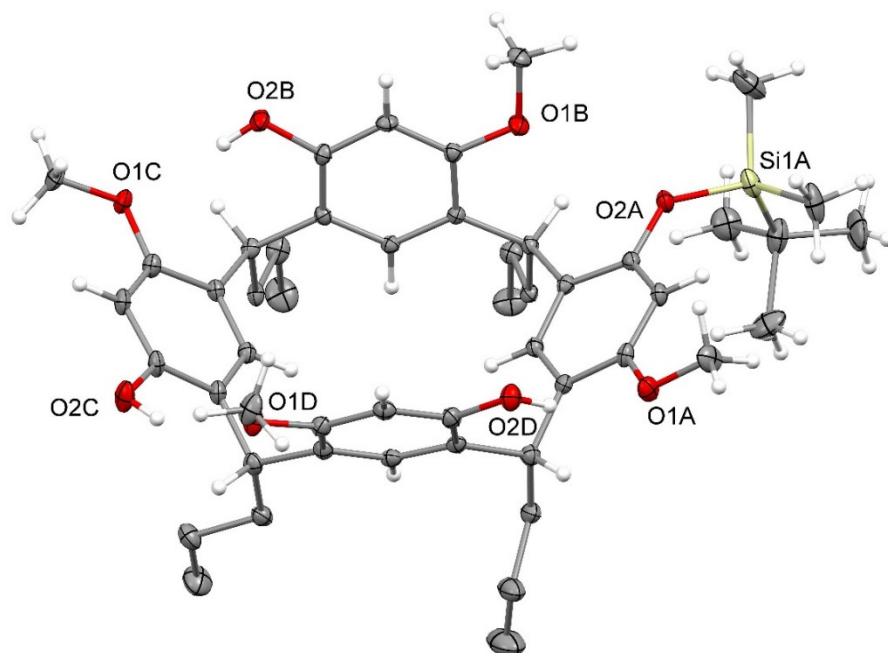
Figure B1   ORTEP view (20% probability level) of Mono-TBDMS resorcinarene **(32)**.
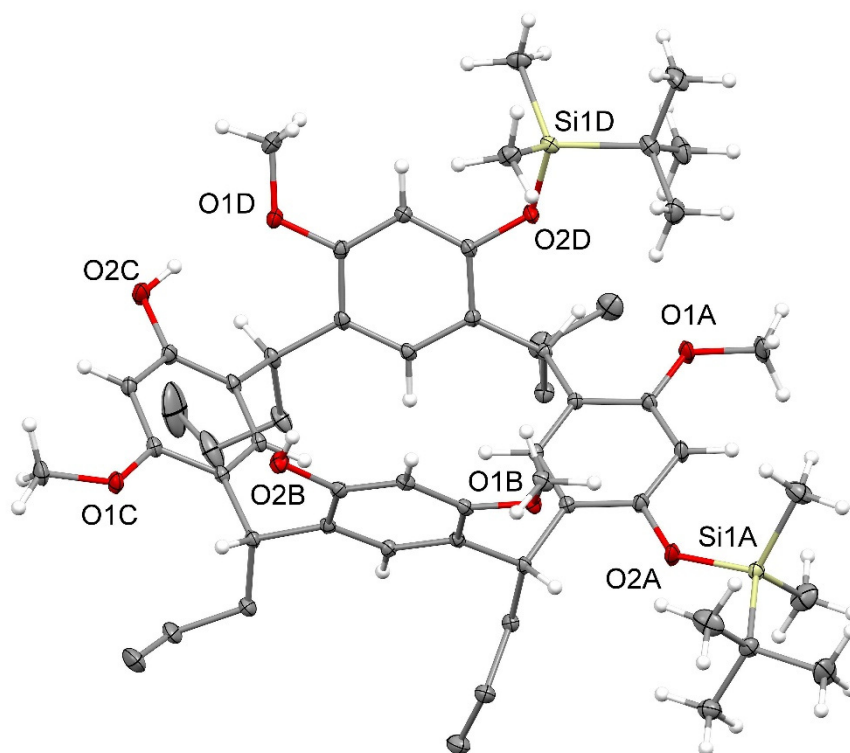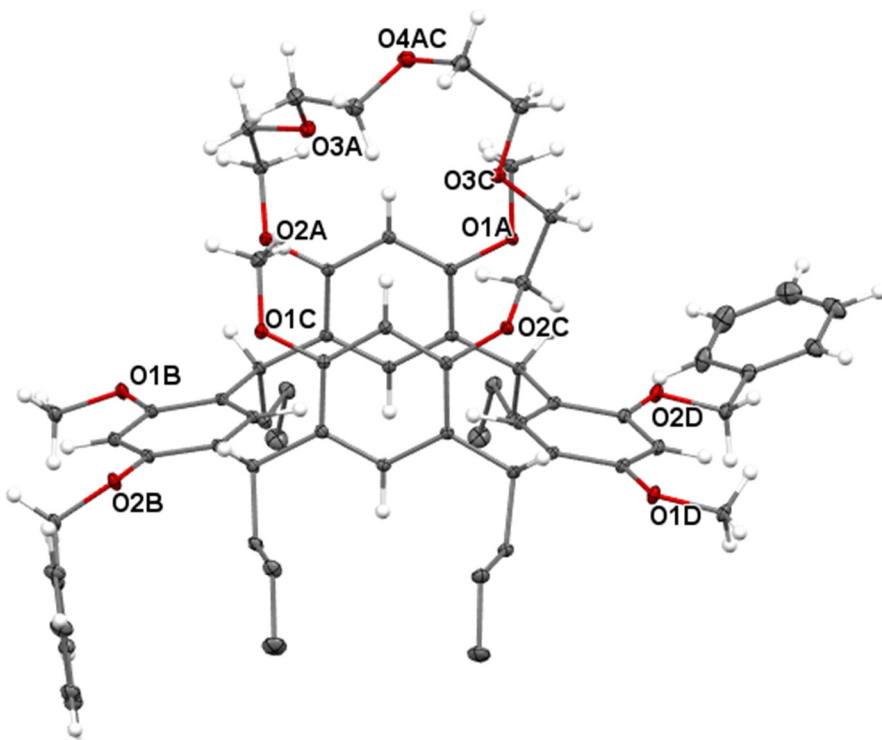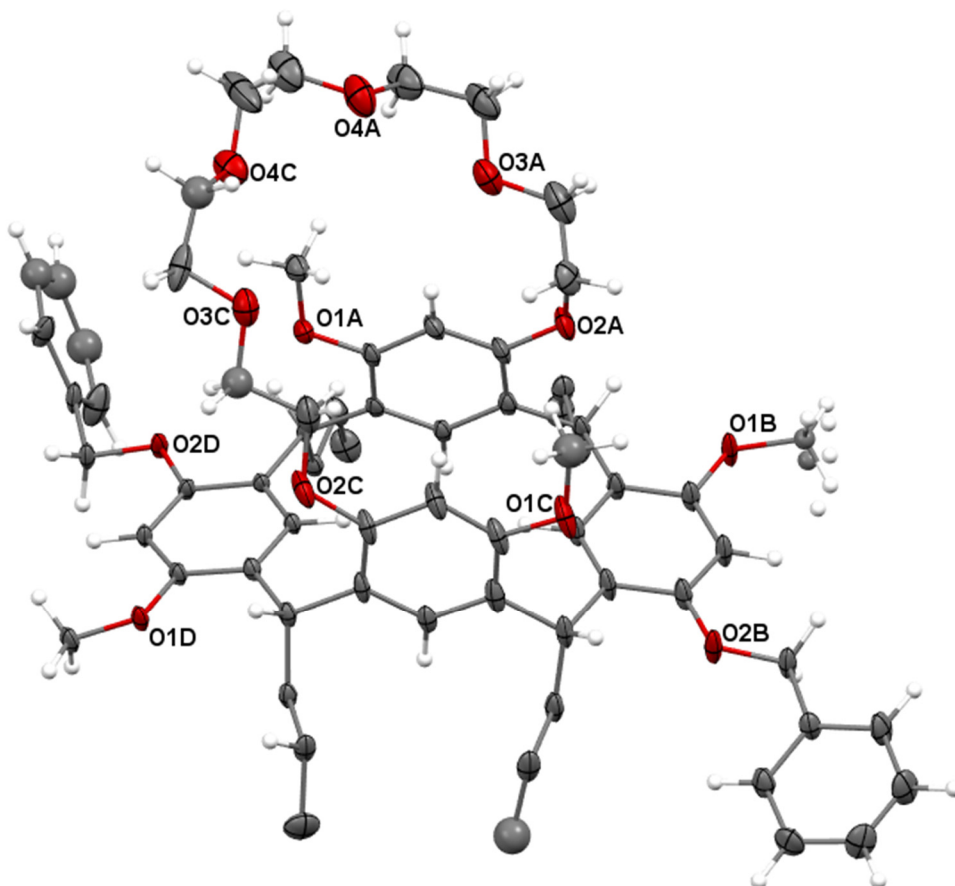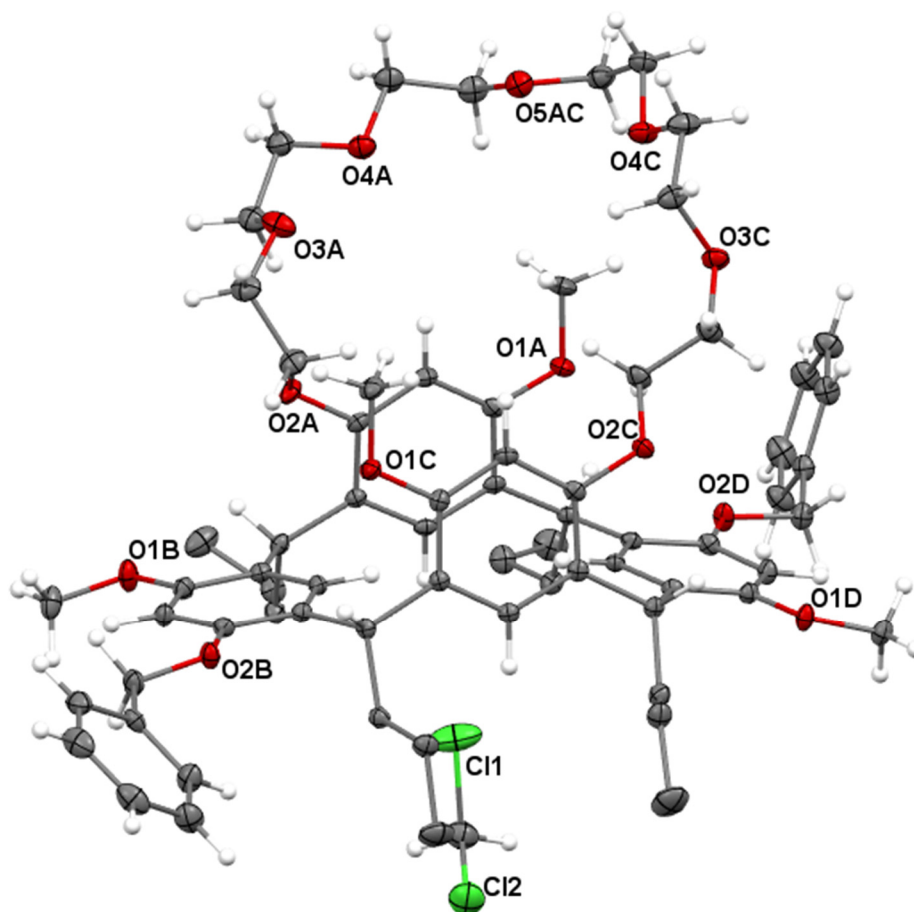

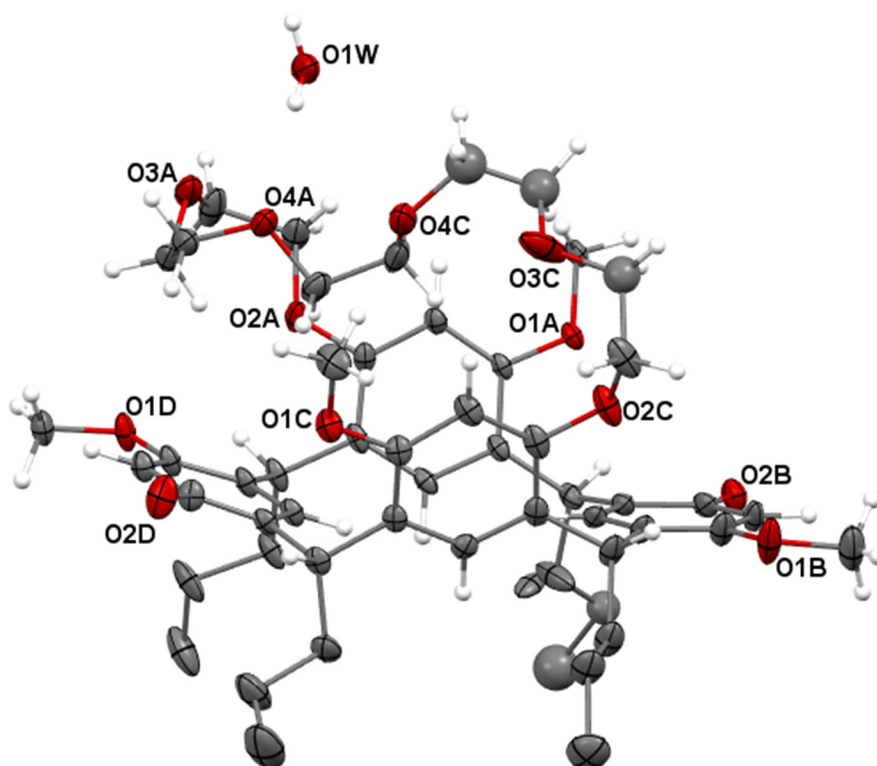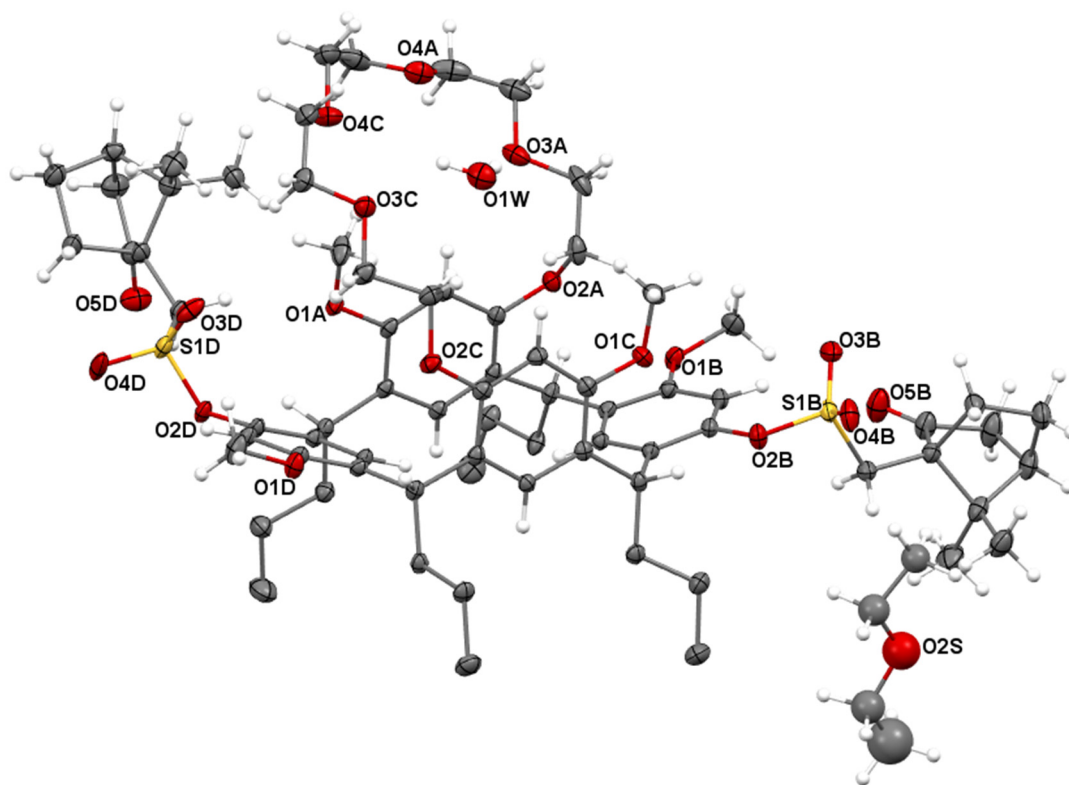**Figure B2**   ORTEP view (20% probability level) of Prox-TBDMS resorcinarene **(33)**.
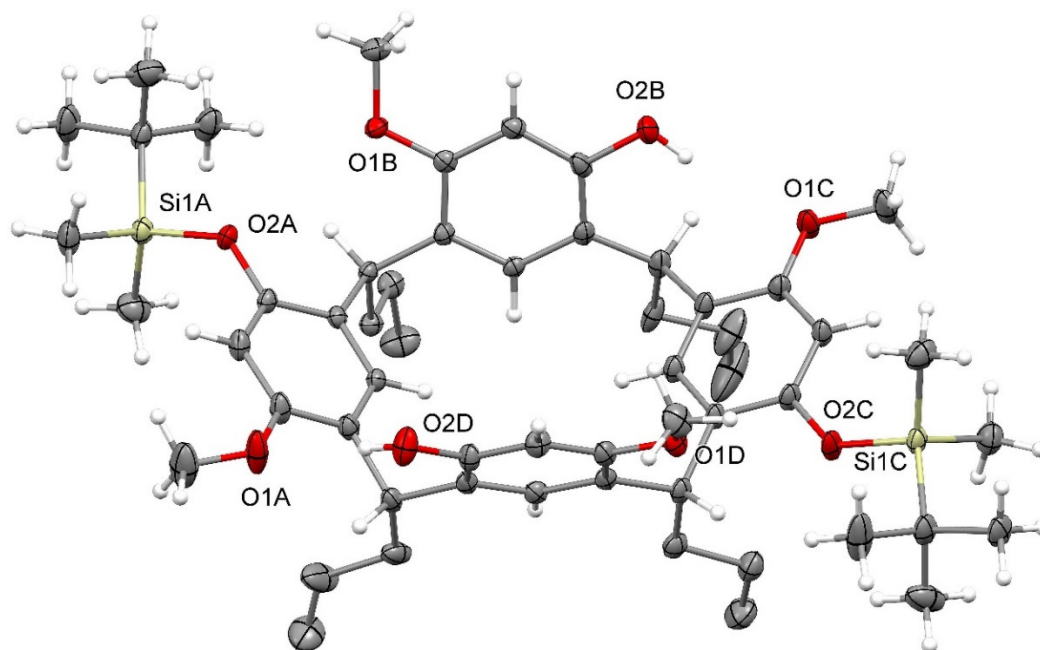
Figure B3   ORTEP view (20% probability level) of Distal-TBDMS resorcinarene **(34)**.
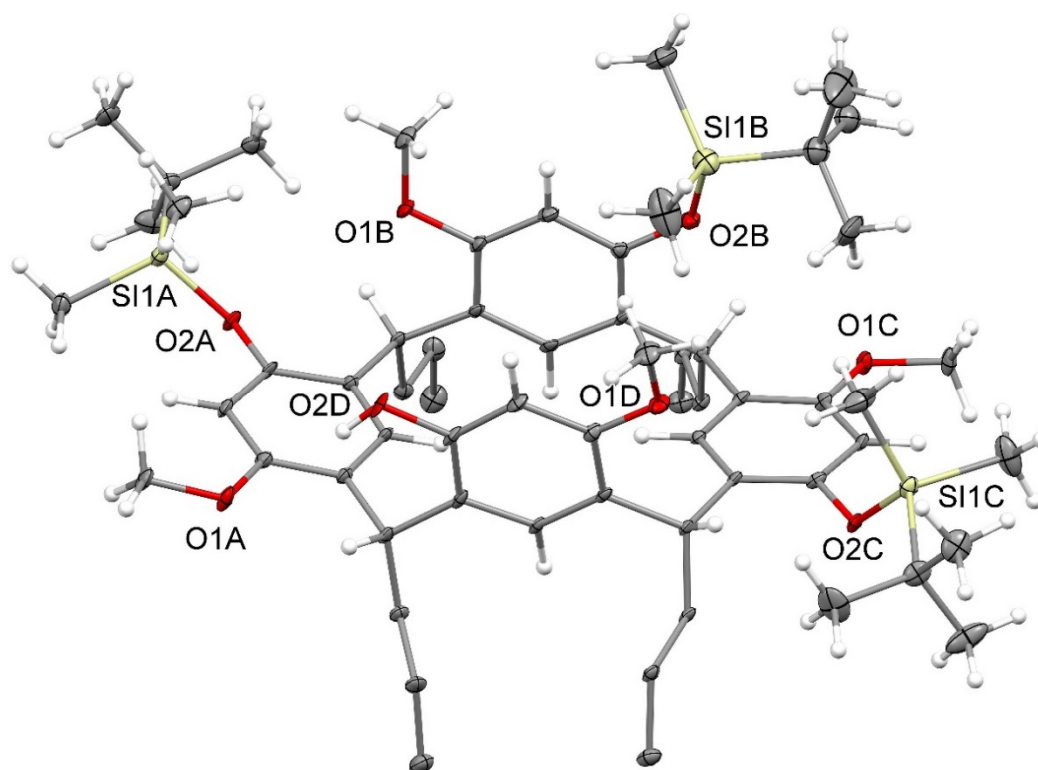
Figure B4   ORTEP view (20% probability level) of Tri-TBDMS resorcinarene **(35)**. One of two independent molecules.
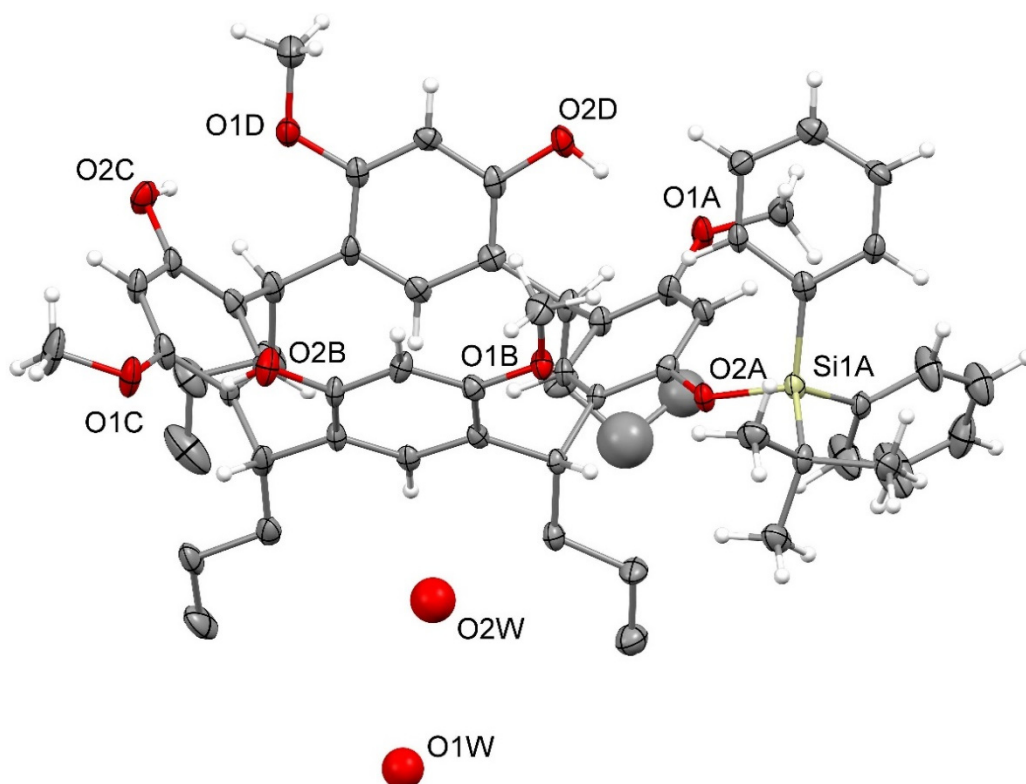
Figure B5 ORTEP view (20% probability level) of Mono-TBDPS resorcinarene **(40)**. The hydrogen atoms of the water molecules could not be located in the difference Fourier map.
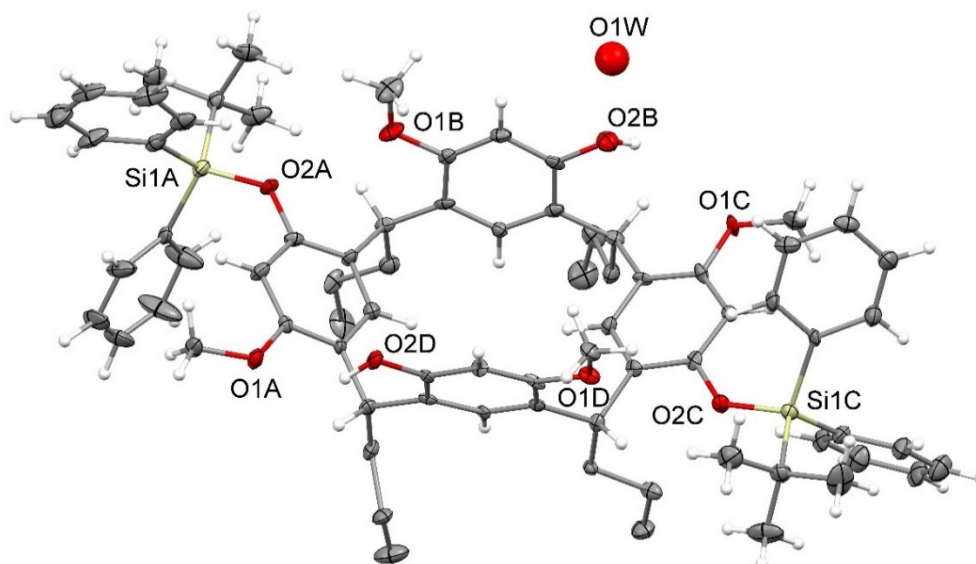
Figure B6 ORTEP view (20% probability level) of Distal-TBDPS resorcinarene **(42)**. The hydrogen atoms of the water molecules could not be located in the difference Fourier map.
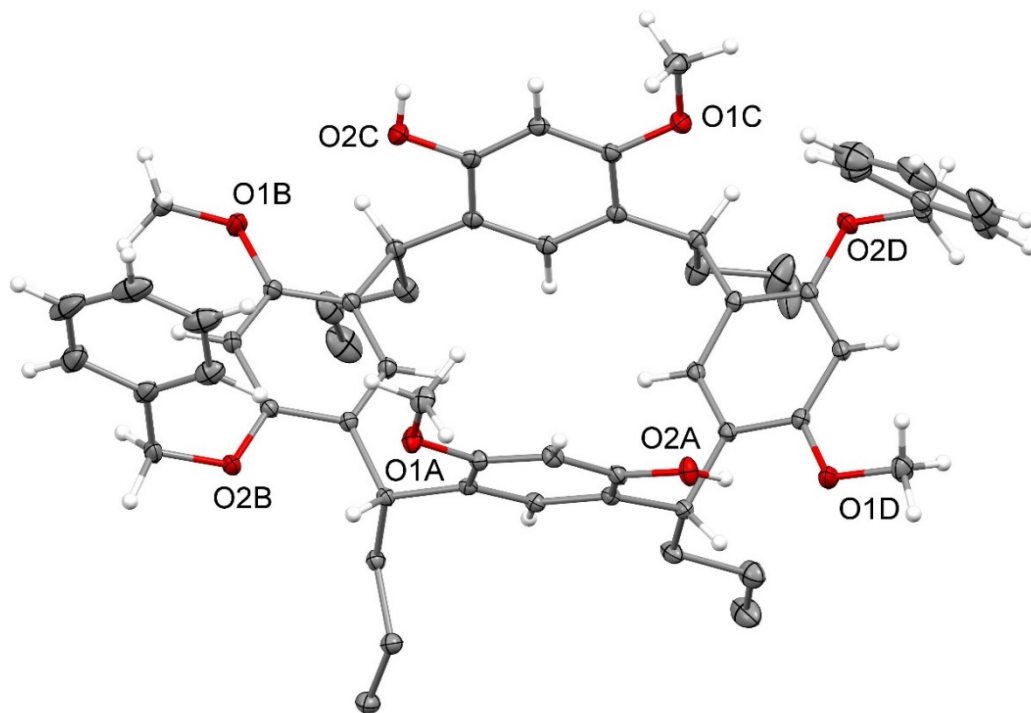
Figure B7   ORTEP view (20% probability level) of Distal-OBn resorcinarene **(46)**. One of two independent molecules.
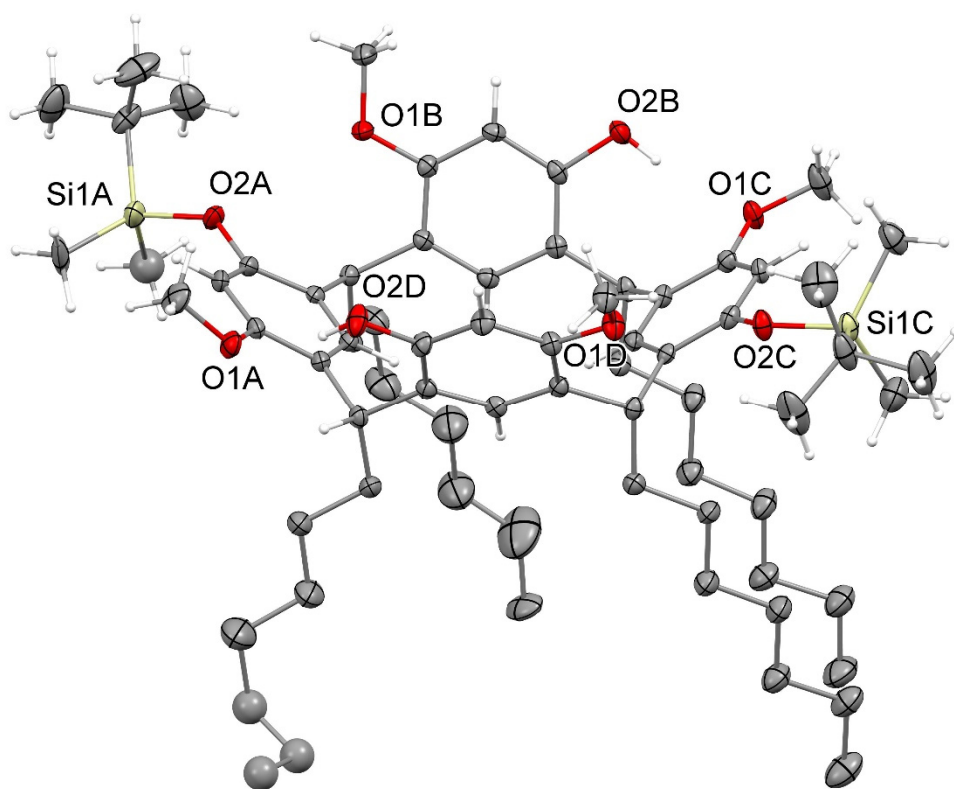
Figure B8   ORTEP view (20% probability level) of Distal-TBDMS resorcinarene **(38)**.
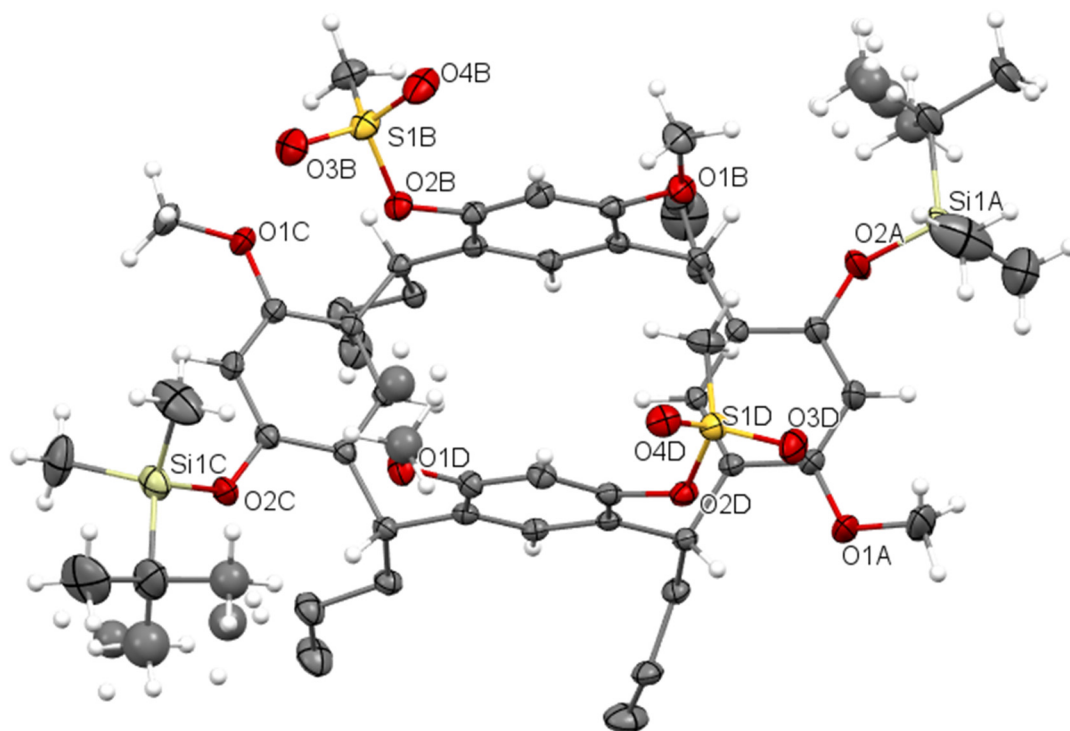
Figure B9 ORTEP view (20% probability level) of DiMeSO$_2$ diTBDMS resorcinarene **(48)**.
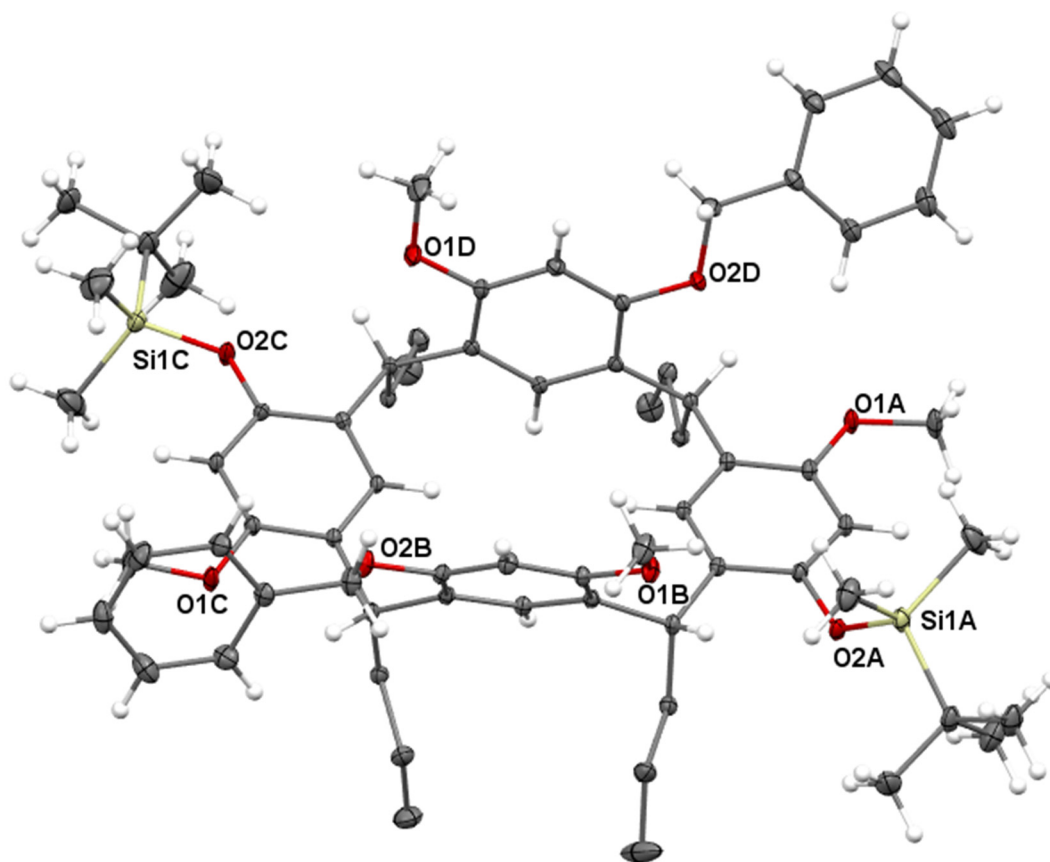
Figure B10 ORTEP view (20% probability level) of DiOBn diTBDMS resorcinarene **(49)**.

Figure B11 ORTEP view (20% probability level) of DiOBn crown-5 resorcinarene **(53)**.

Figure B12 ORTEP view (20% probability level) of DiOBn crown-6 resorcinarene **(54)**.

Figure B13 ORTEP view (20% probability level) of DiOBn crown-7 resorcinarene **(55)**.

Figure B14 ORTEP view (20% probability level) of DiOH crown-6 resorcinarene **(57)**.

Figure B15 ORTEP view (20% probability level) of Dicamphorsulfonate crown-6 resorcinarene **(60)** diastereomeric mixture crystallised from diethyl ether. One of two independent molecules.

References

1.   *SADABS* Bruker Analytical X-ray Systems: Madison, Wisconsin, USA, **2004**.

2.   Sheldrick, G. M. *SADABS v2.03: Area-Detector Absorption Correction*, University of Göttingen: Germany, **1999**.

3.   *SAINT Software Users Guide, Version 6.0*, Bruker Analytical X-ray Systems: Madison, Wisconsin, USA, **1999**.

4.   *CrysAlisPro 1.171.38.41*, Rigaku Oxford Diffraction: **2015**.

5.   Altomare, A.; Burla, M. C.; Camalli, M.; Cascarano, G. L.; Giacovazzo, C.; Guagliardi, A.; Moliterni, A. G. G.; Polidori, G.; Spagna, R., *J. Appl. Cryst* **1999,** *32*, 115-119.

6.   Sheldrick, G., *Acta Crystallographica Section A* **2008,** *64* (1), 112-122.

7.   Farrugia, L., *J. Appl. Crystallogr.* **2012,** *45* (4), 849-854.

8.   van der Sluis, P.; Spek, A. L., *Acta Crystallographica Section A* **1990,** *46* (3), 194-201.

Appendix C

Membrane Transport

UV-Vis Data

The membrane transport of salbutamol was monitored by UV-vis spectrometry using a GBC UV/VIS 916 UV-vis spectrometer scanning from 200-400 nm at a speed of 480 nm/min and step size of 1 nm. Each experiment was repeated in multiple runs for consistency.

An example of the UV-vis spectra from one run is given on page 1.

For each spectrum, the absorbance at 224 nm was plotted against time to give the amount of salbutamol present in the receiving phase over the course of the run. This data for every run is presented in a graph for each experiment. For some experiments, the consistent runs without outliers, were selected for the average to be calculated – these selected runs are presented in a second graph.

The experiments were conducted using salbutamol in 5 equivalents (pages 2-16) and 10 equivalents (pages 17-27).

Appendix C

(61) diOH crown-6 - salbutamol 10 eq - 21/5 - 28/5

Appendix C - 1

DCM blank - salbutamol 5 eq

DCM blank - salbutamol 5 eq - selected
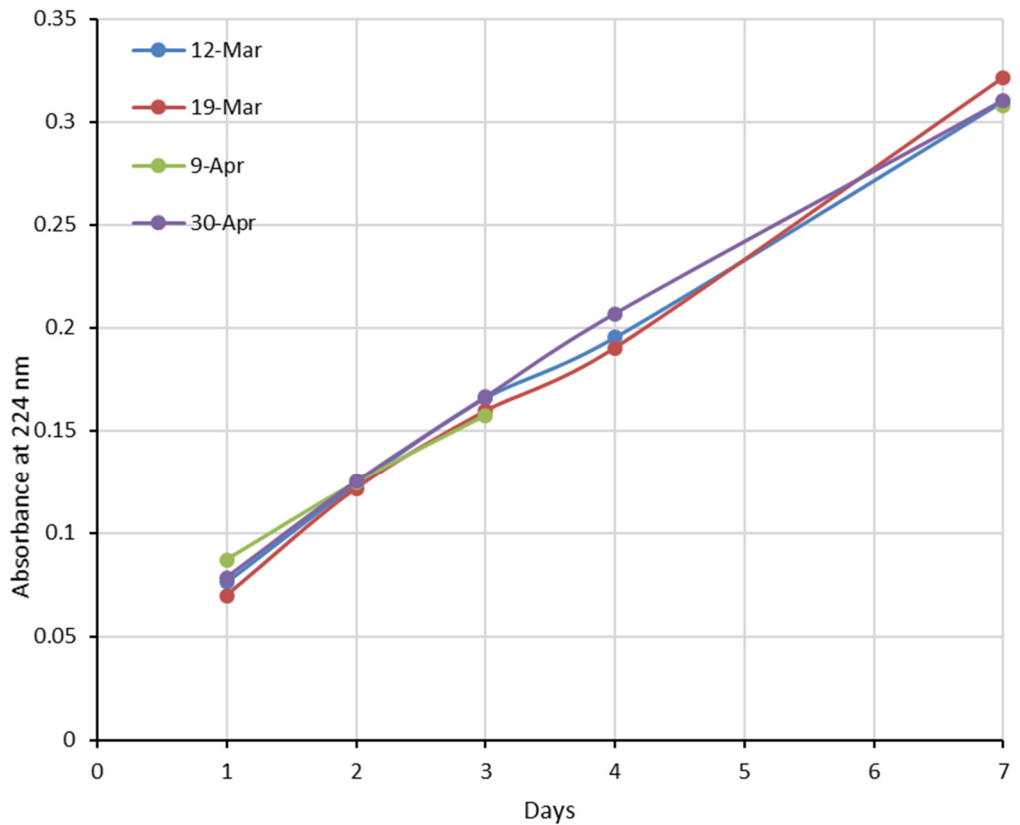
Appendix C - 2
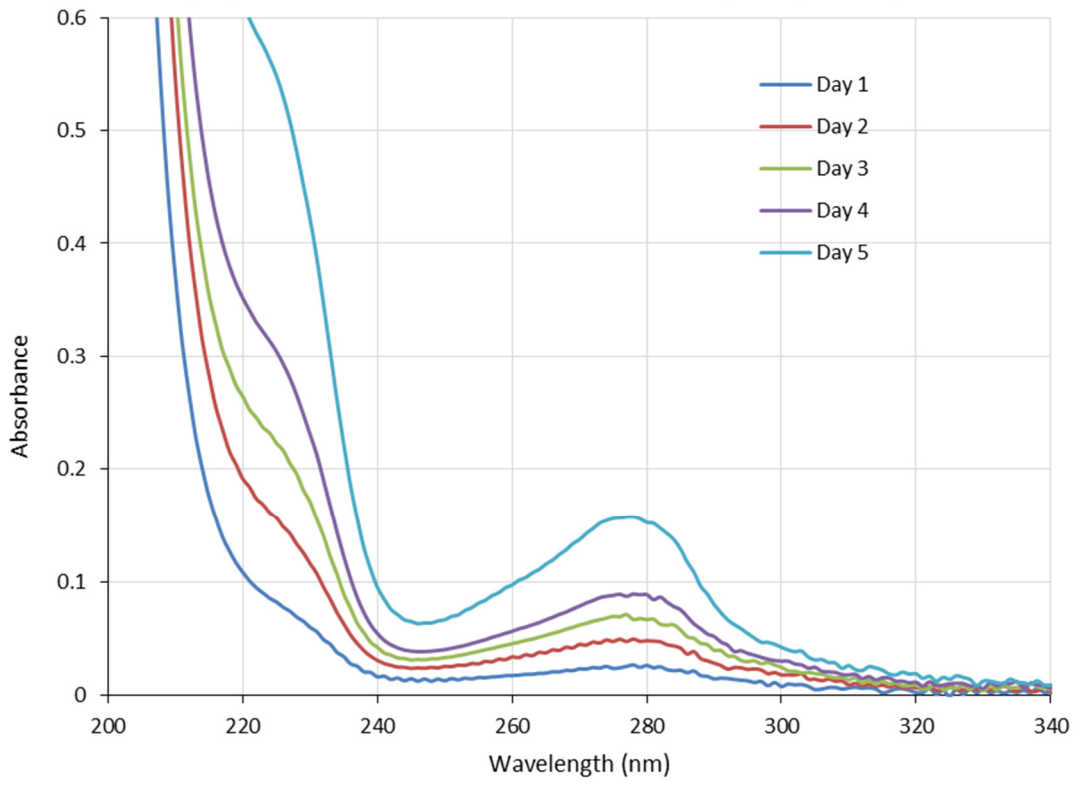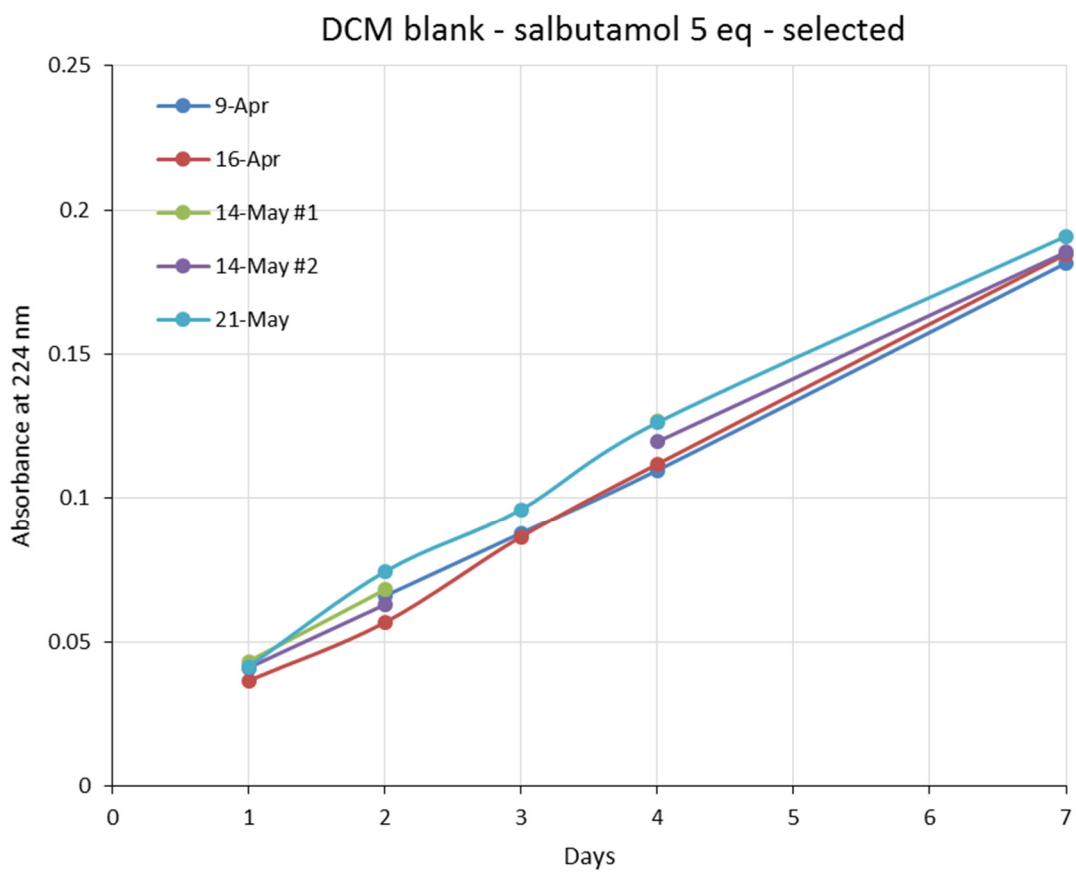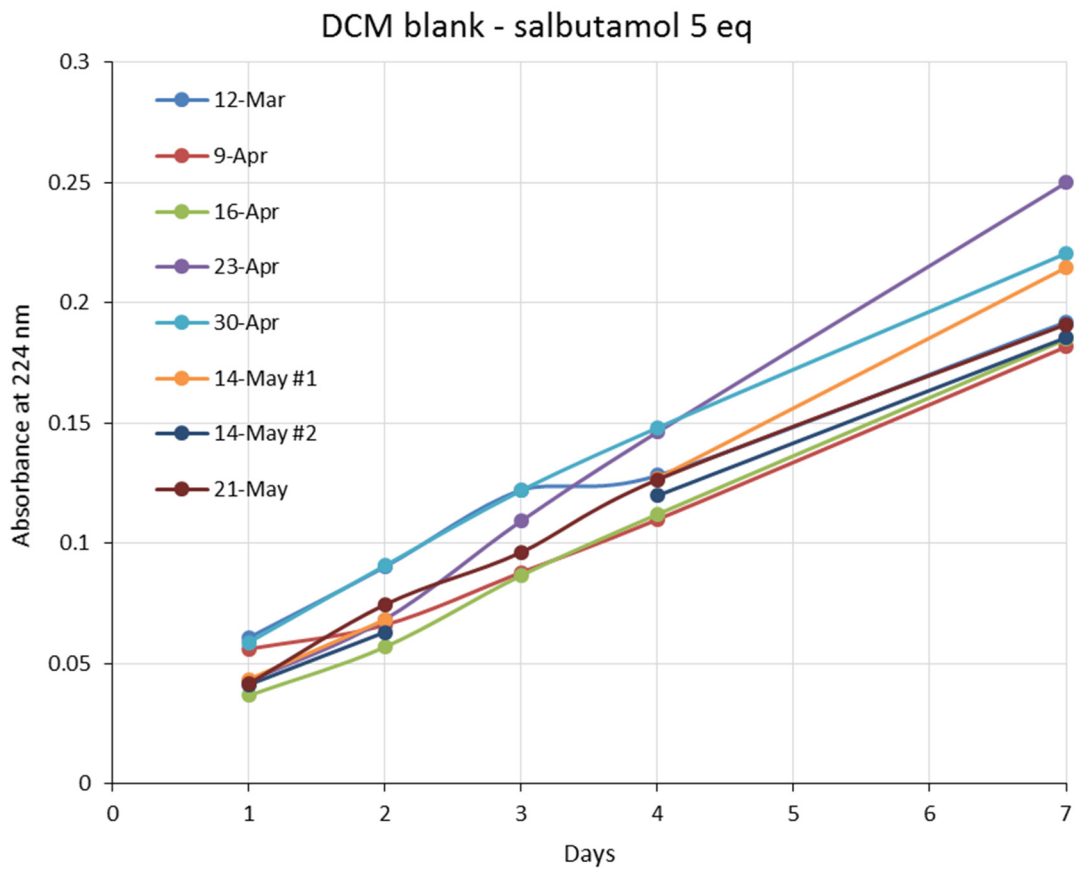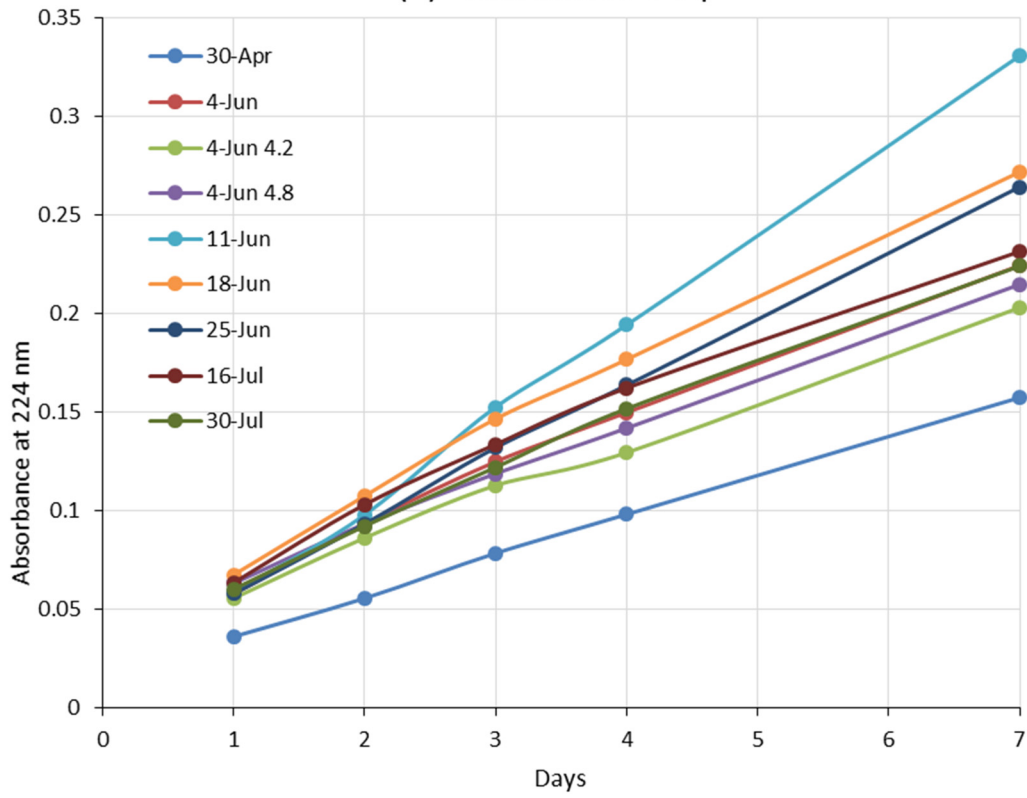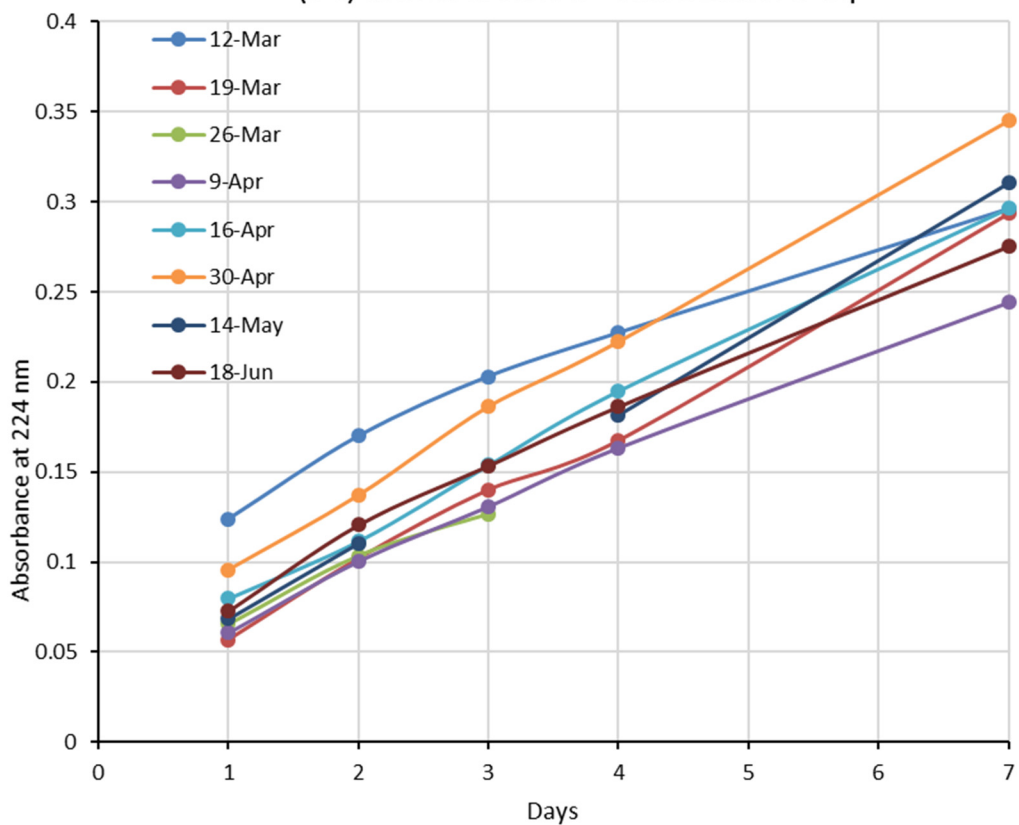
(1) - salbutamol 5 eq

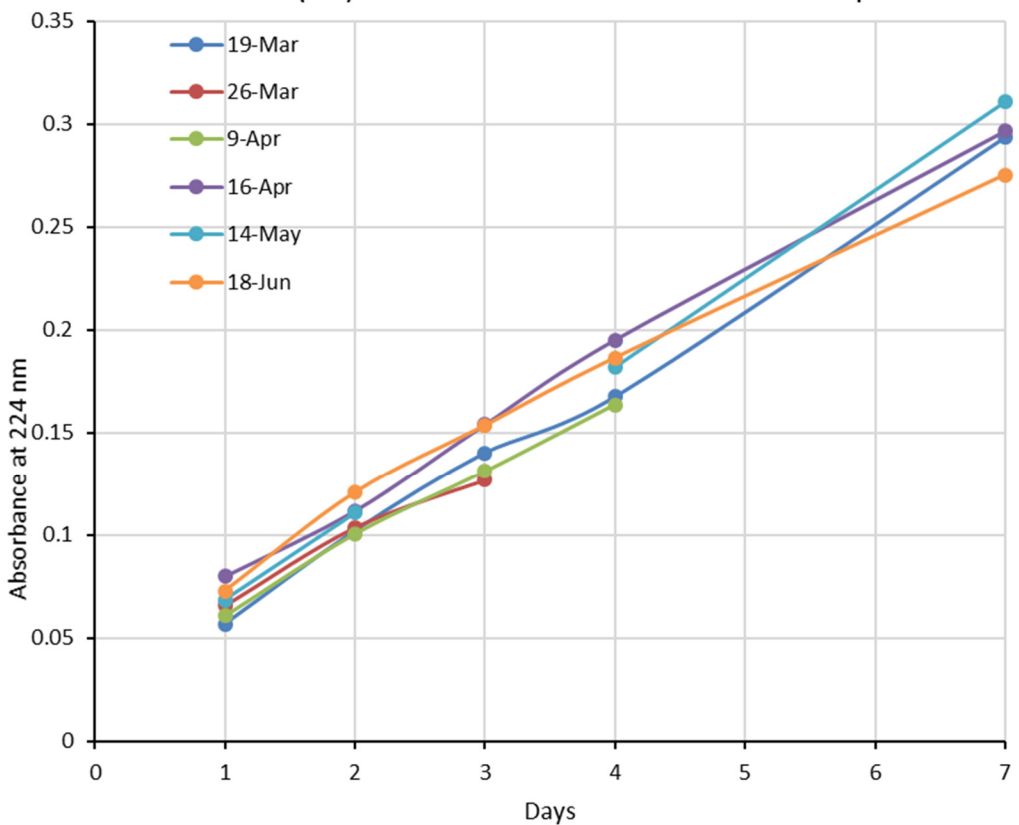(1) - salbutamol 5 eq - selected
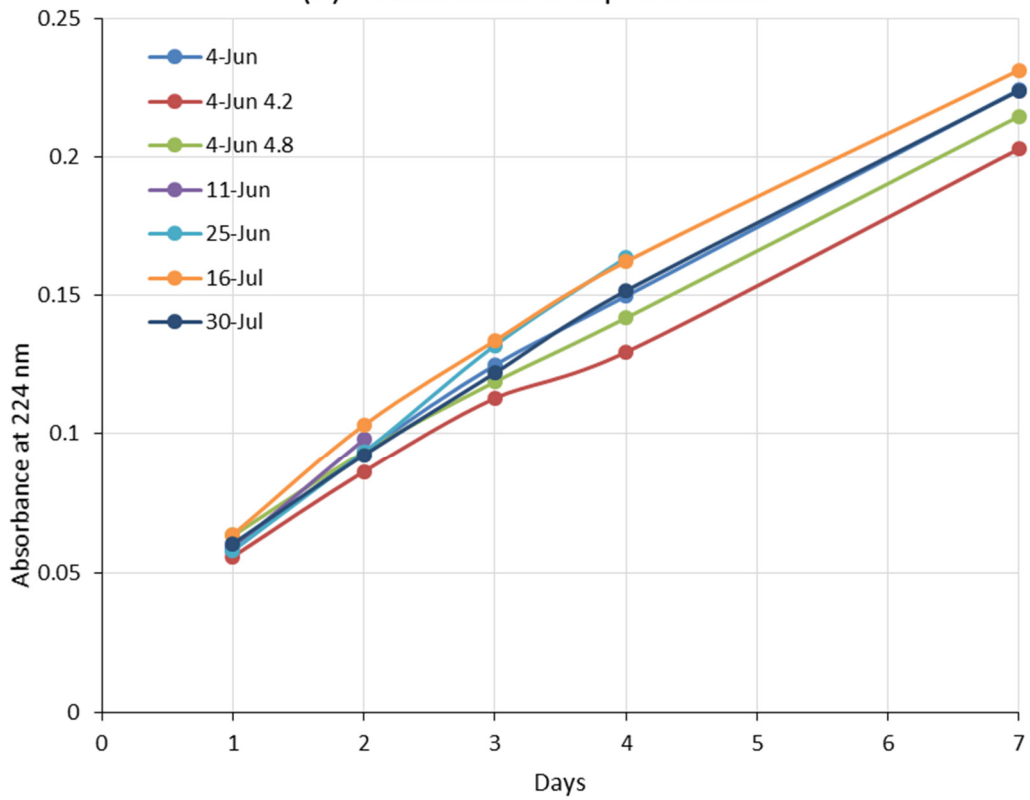
(53) diOBn crown-5 - salbutamol 5 eq

(53) diOBn crown-5 - salbutamol 5 eq - selected

Appendix C - 4
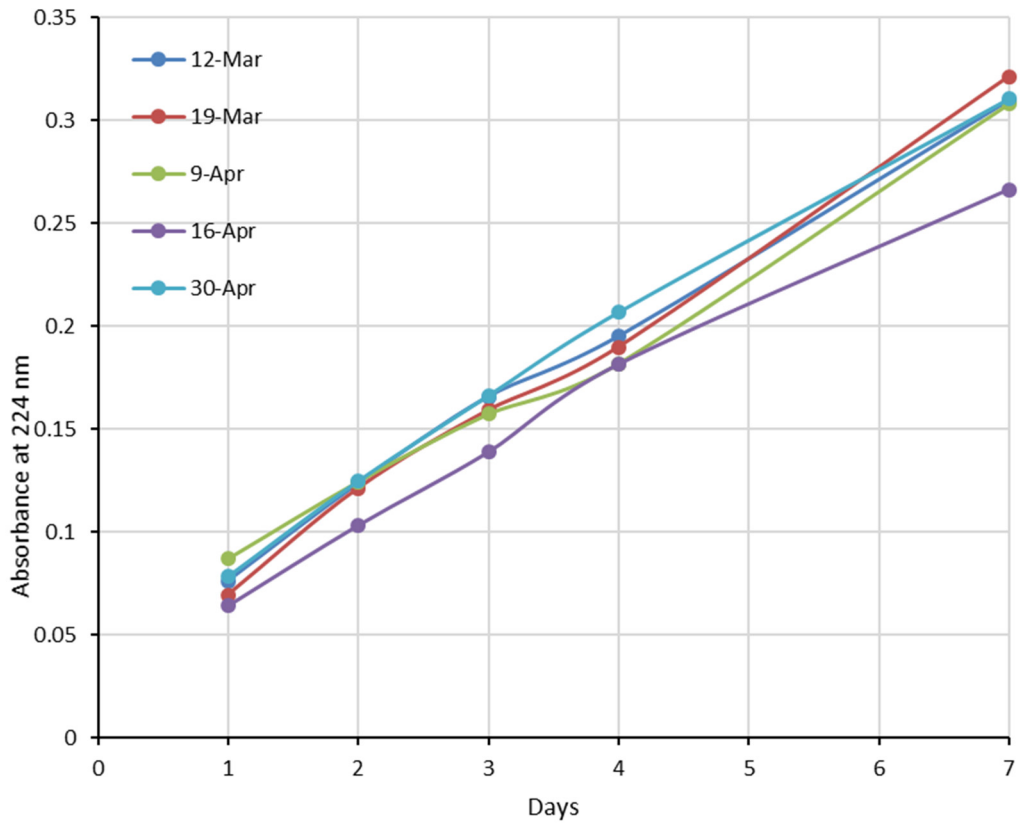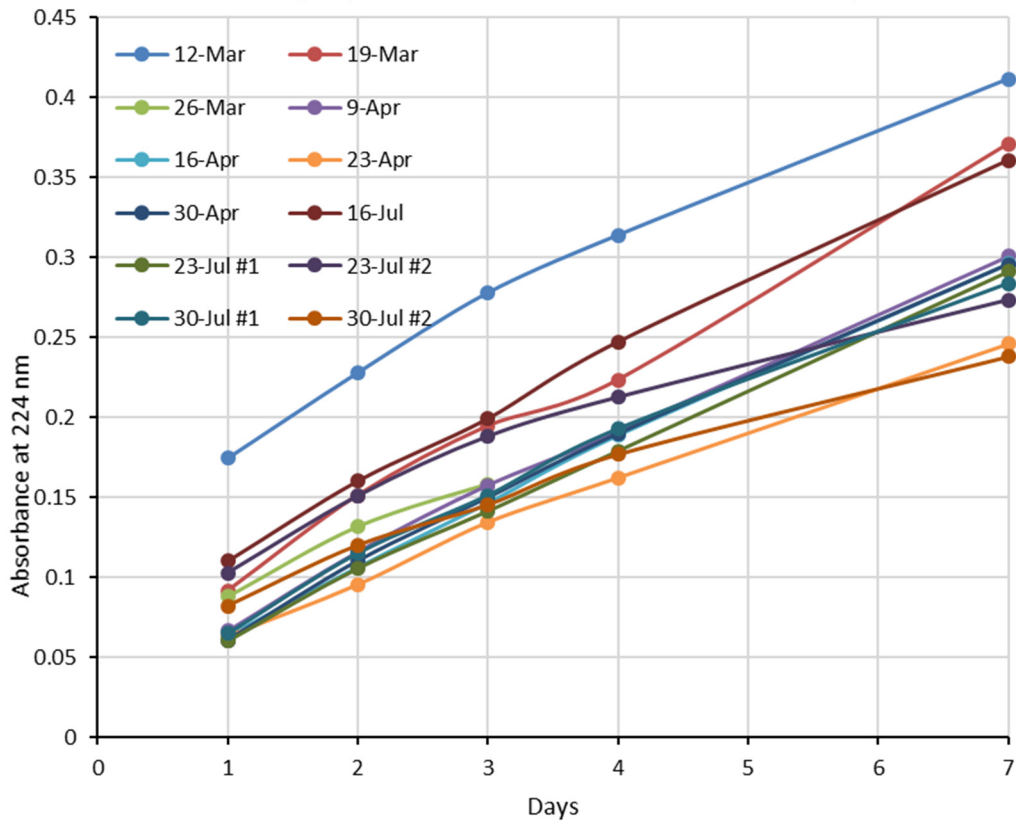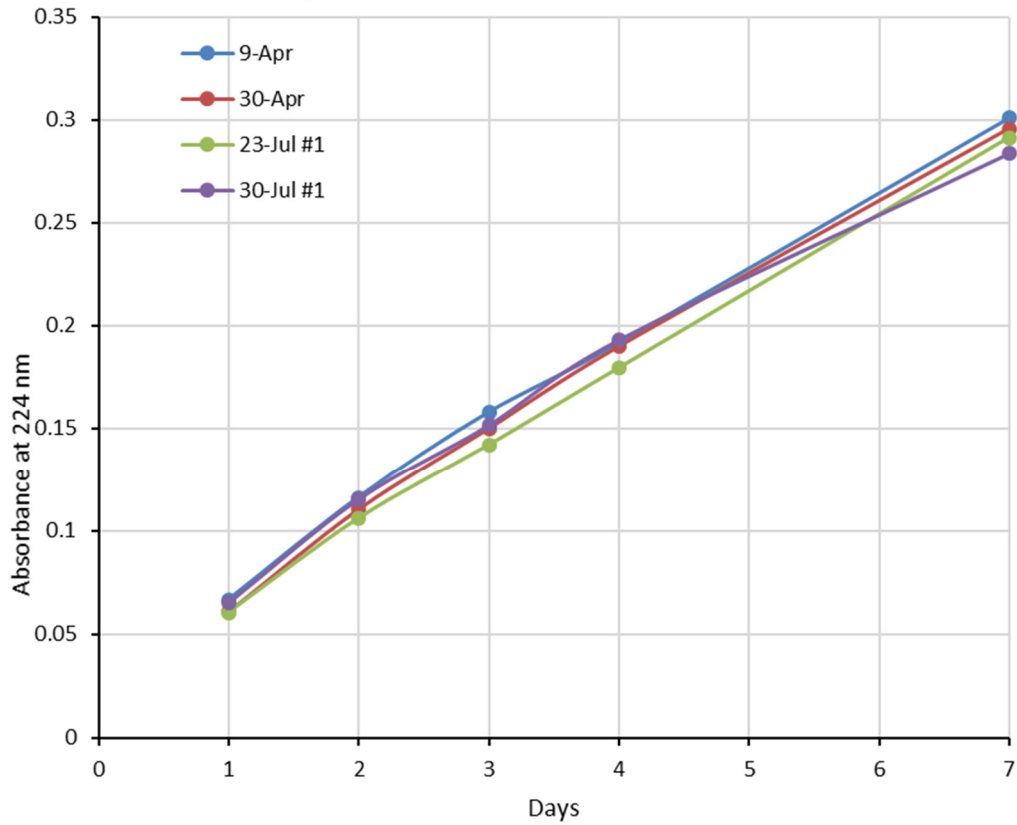
(54) diOBn crown-6 - salbutamol 5 eq
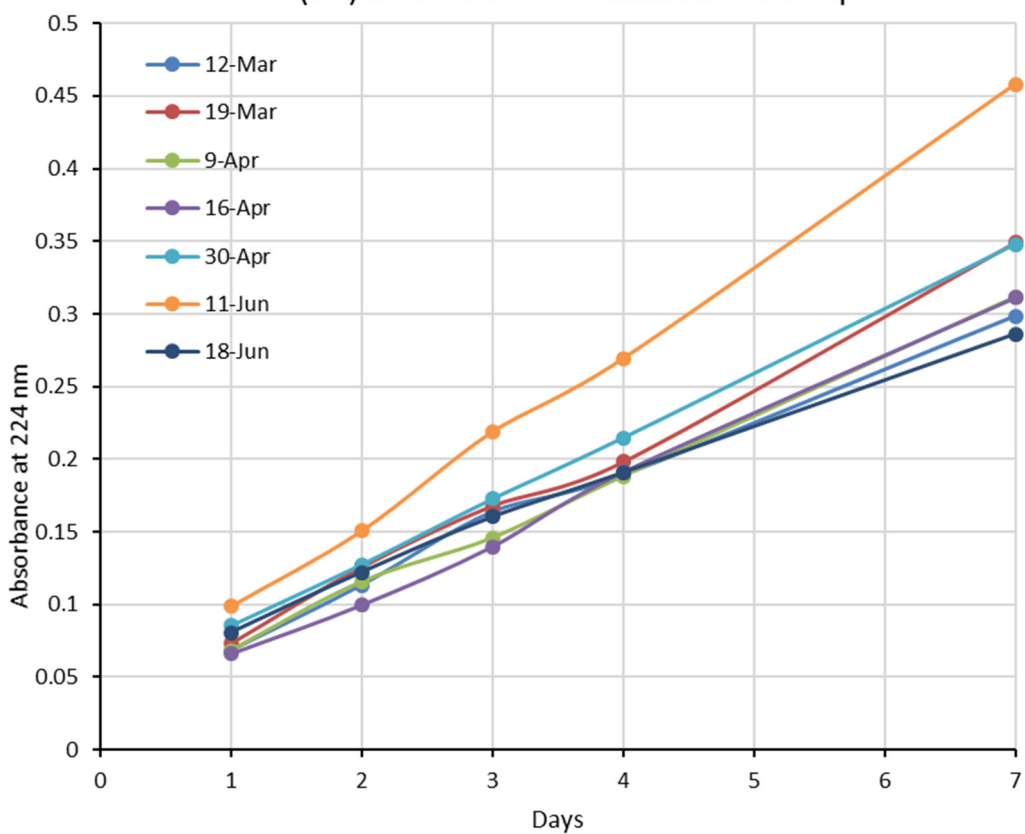

(54) diOBn crown-6 - salbutamol 5 eq - selected

Appendix C - 5

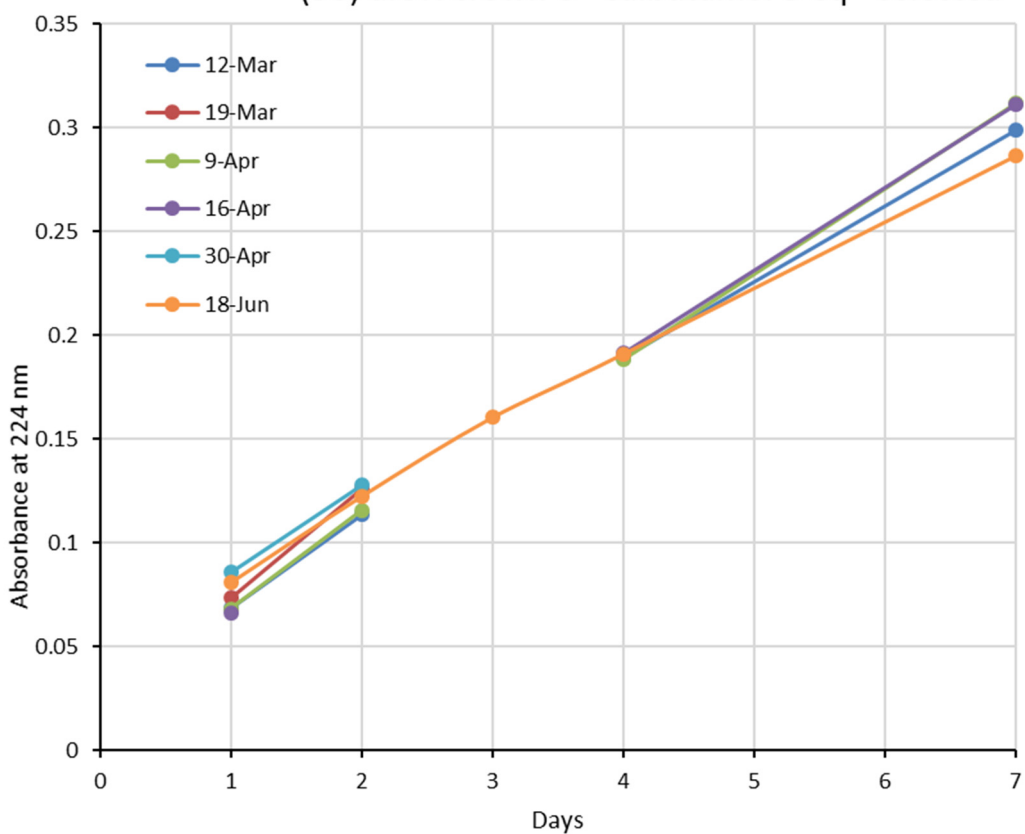(55) diOBn crown-7 - salbutamol 5 eq

(55) diOBn crown-7 - salbutamol - selected
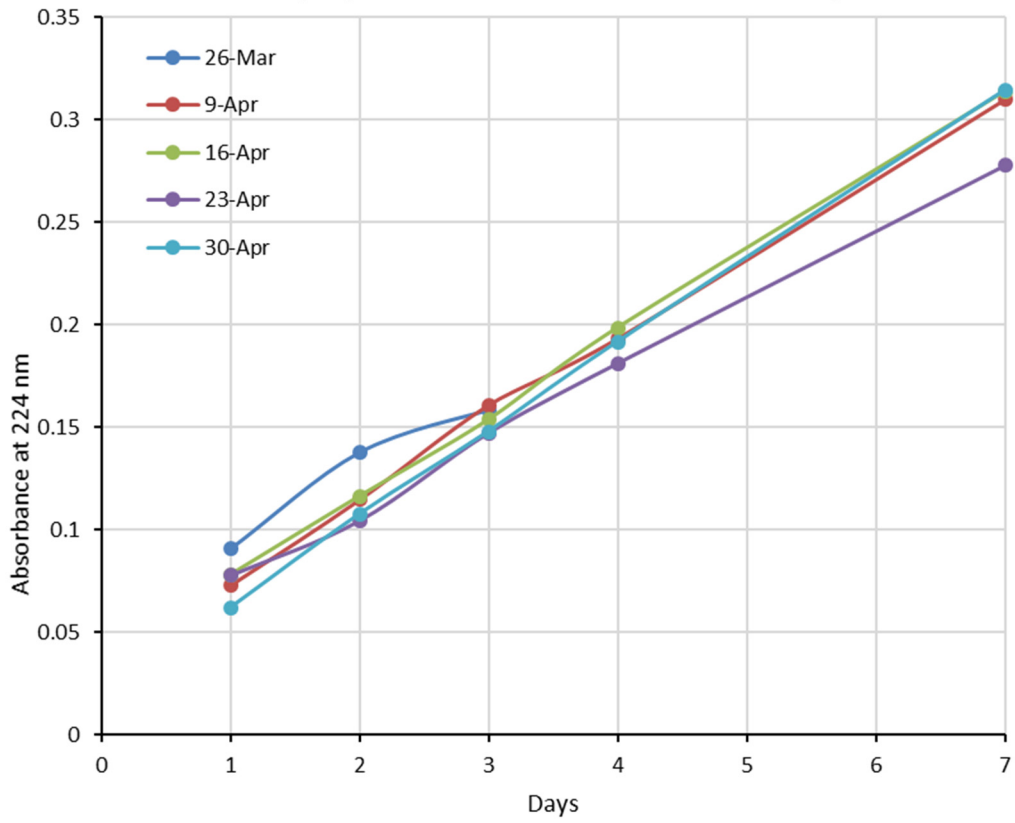
Appendix C - 6
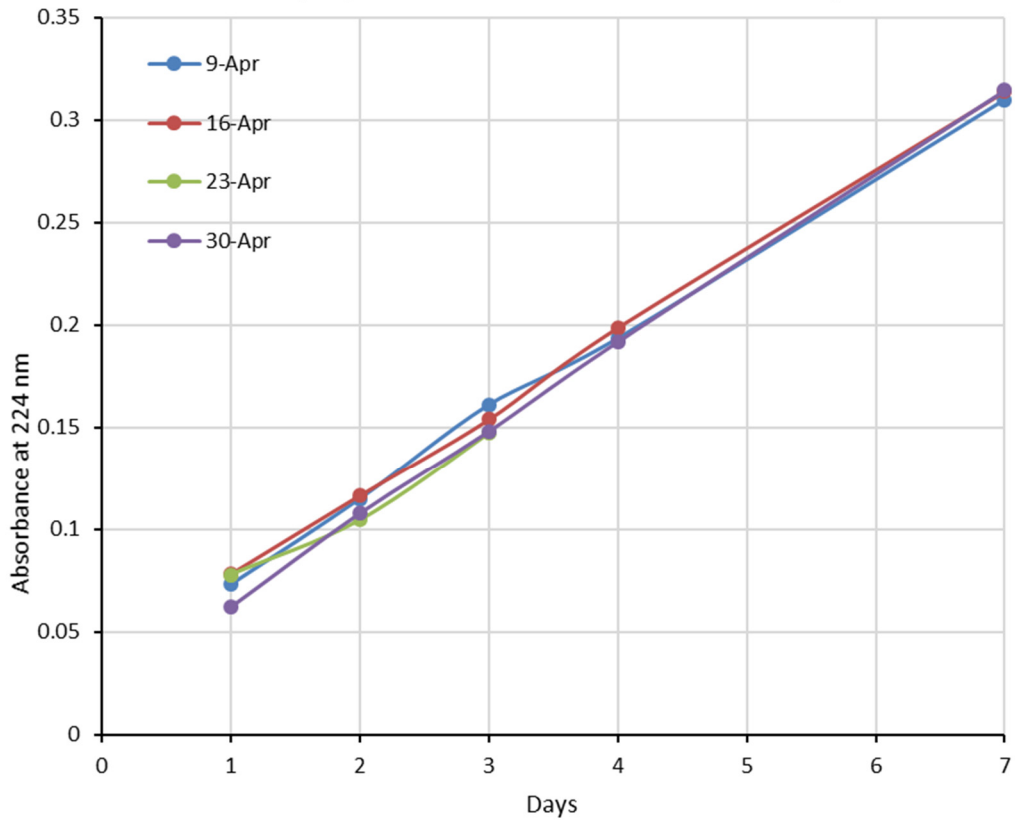
(56) diOH crown-5 - salbutamol 5 eq

(56) diOH crown-5 - salbutamol 5 eq - selected
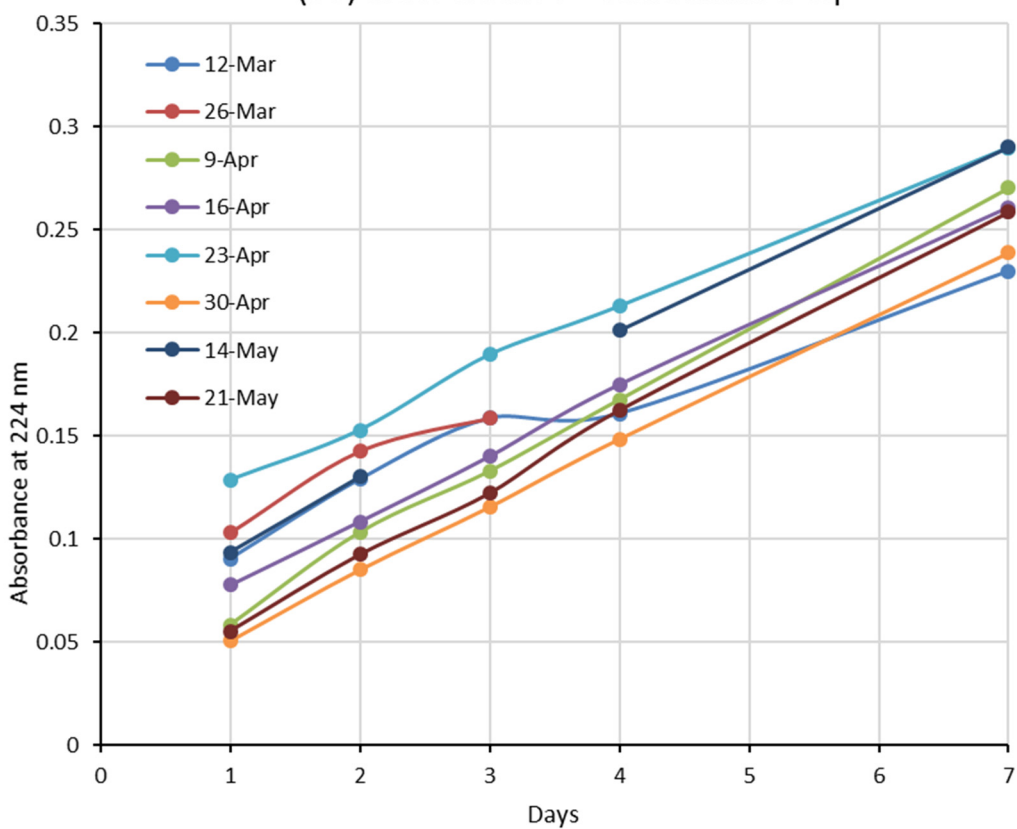
Appendix C - 7

(57) diOH crown-6 - salbutamol 5 eq

(57) diOH crown-6 - salbutamol 5 eq - selected

Appendix C - 8

(58) diOH crown-7 - salbutamol 5 eq

(58) diOH crown-7 - salbutamol 5 eq - selected

Appendix C - 9
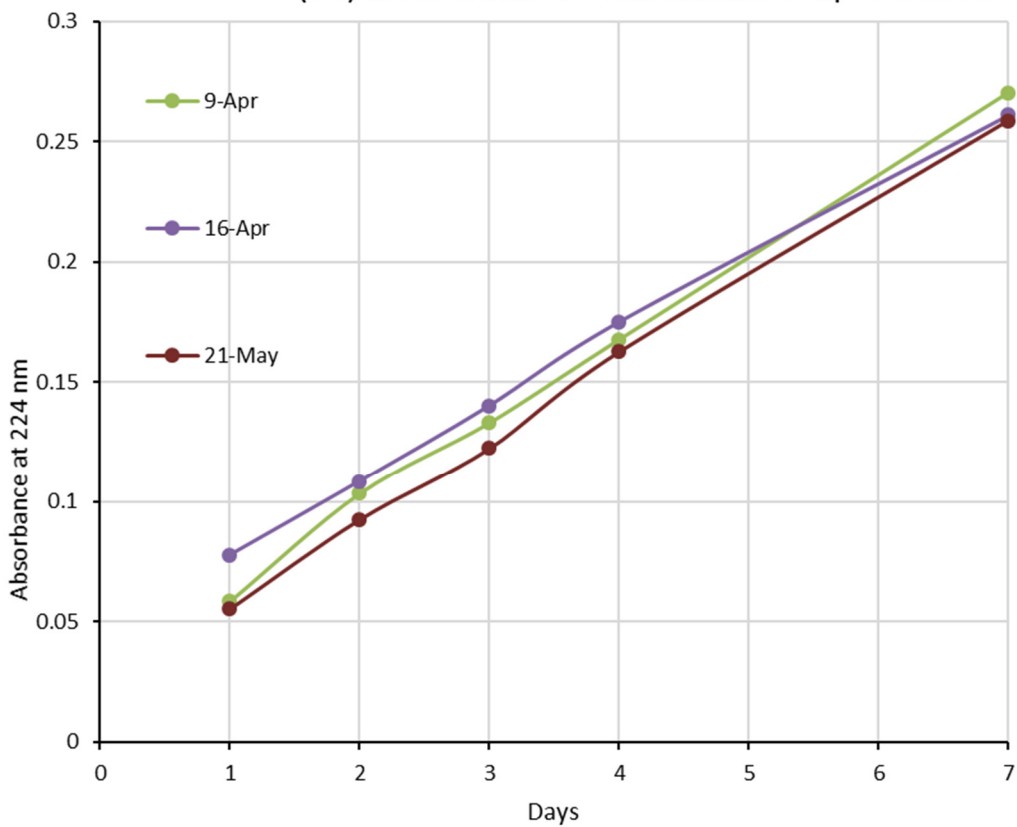
(59a) dicamphSO2 crown-5 - salbutamol 5 eq

(59a) dicamphSO2 crown-5 - salbutamol 5 eq - selected

(59b) dicamphSO2 crown-5 - salbutamol 5 eq

(60a) dicamphSO2 crown-6 - salbutamol 5 eq

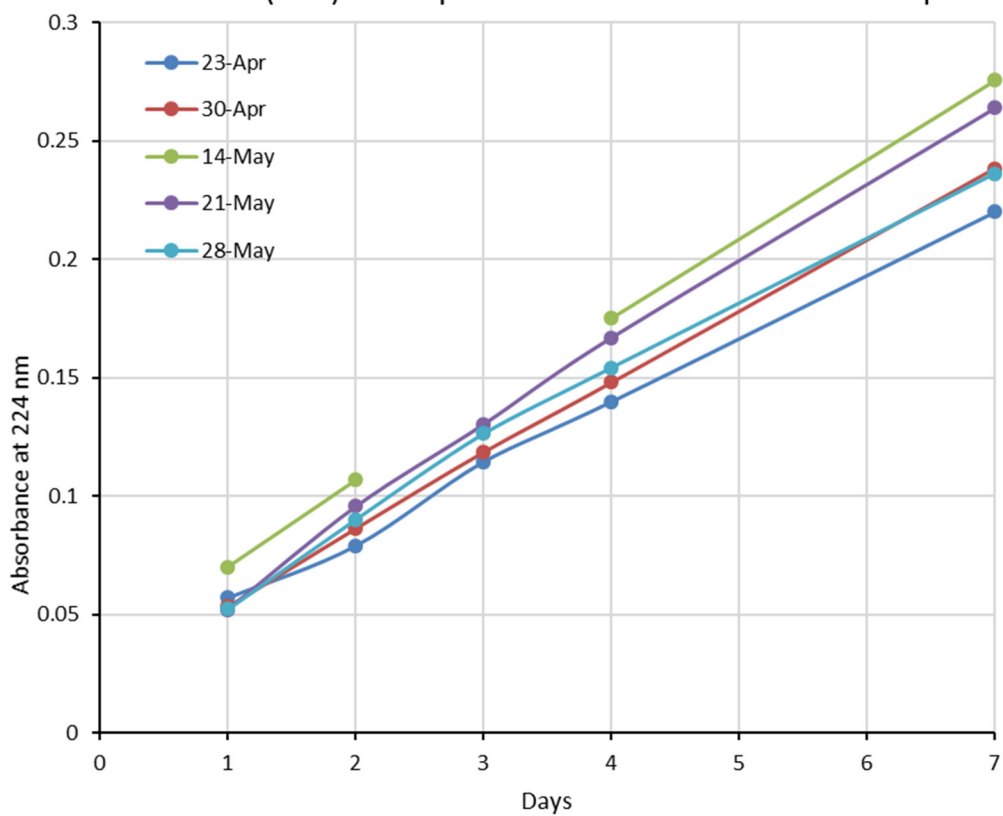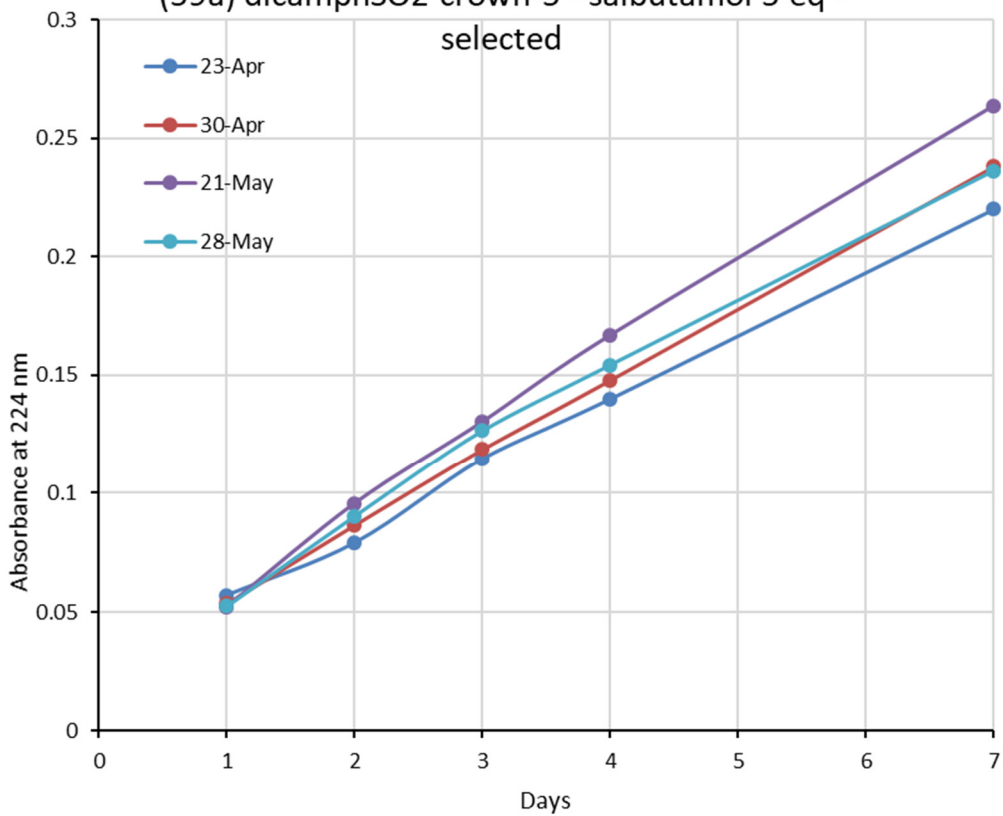(60a) dicamphSO2 crown-6 - salbutamol 5 eq - selected

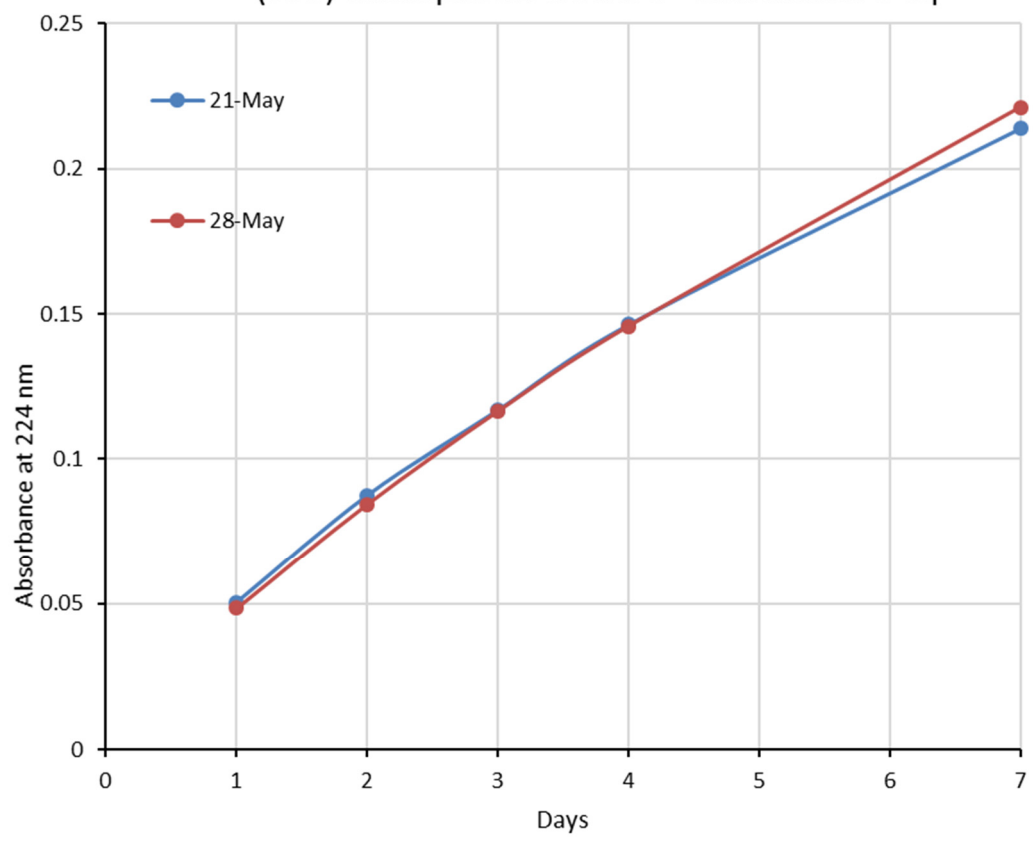(60b) dicamphSO2 crown-6 - salbutamol 5 eq

(60b) dicamphSO2 crown-6 - salbutamol 5 eq - selected

(61a) dicamphSO2 crown-7 - salbutamol 5 eq

(61b) dicamphSO2 crown-7 - salbutamol 5 eq

Appendix C - 14

(63) bis-crown-5 - salbutamol

(63) bis-crown-5 - salbutamol 5 eq - selected

Appendix C - 15

(64) bis-crown-6 - salbutamol 5 eq

(65) bis-crown-7 - salbutamol 5 eq

Appendix C - 16

DCM blank - salbutamol 10 eq

DCM blank - salbutamol 10 eq - selected

Appendix C - 17
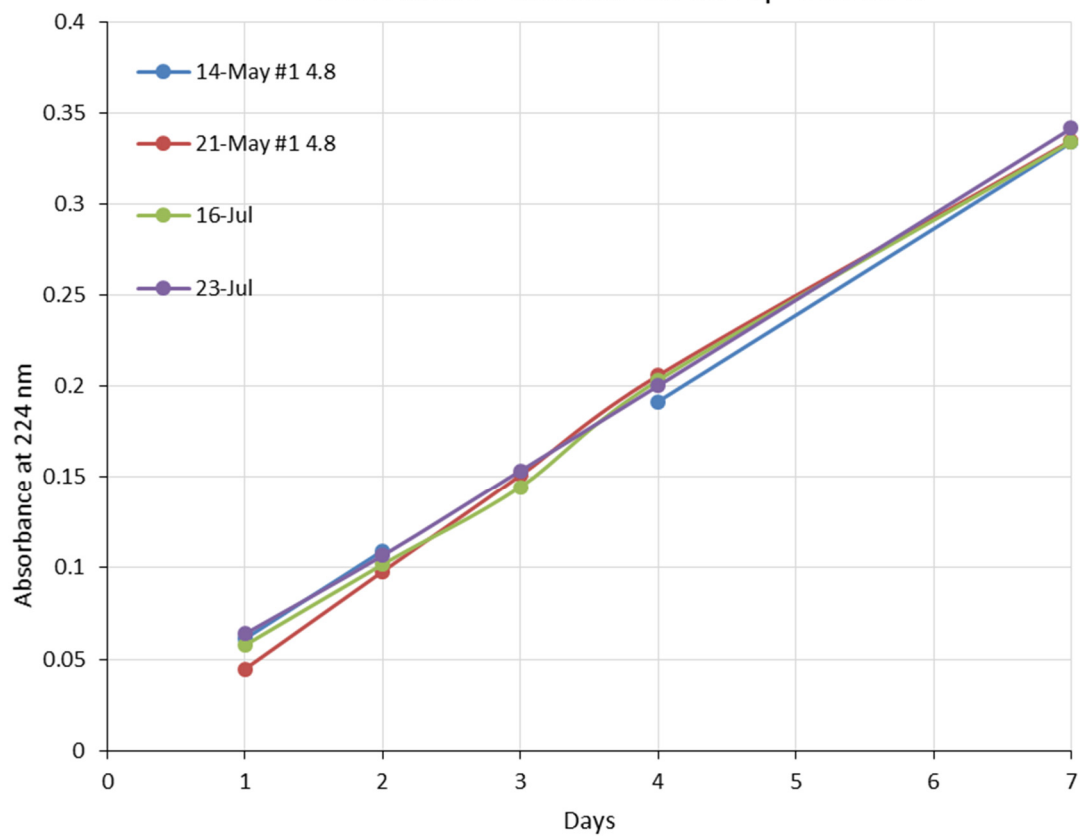
(1) - salbutamol - 10 eq

(1) - salbutamol 10 eq - selected
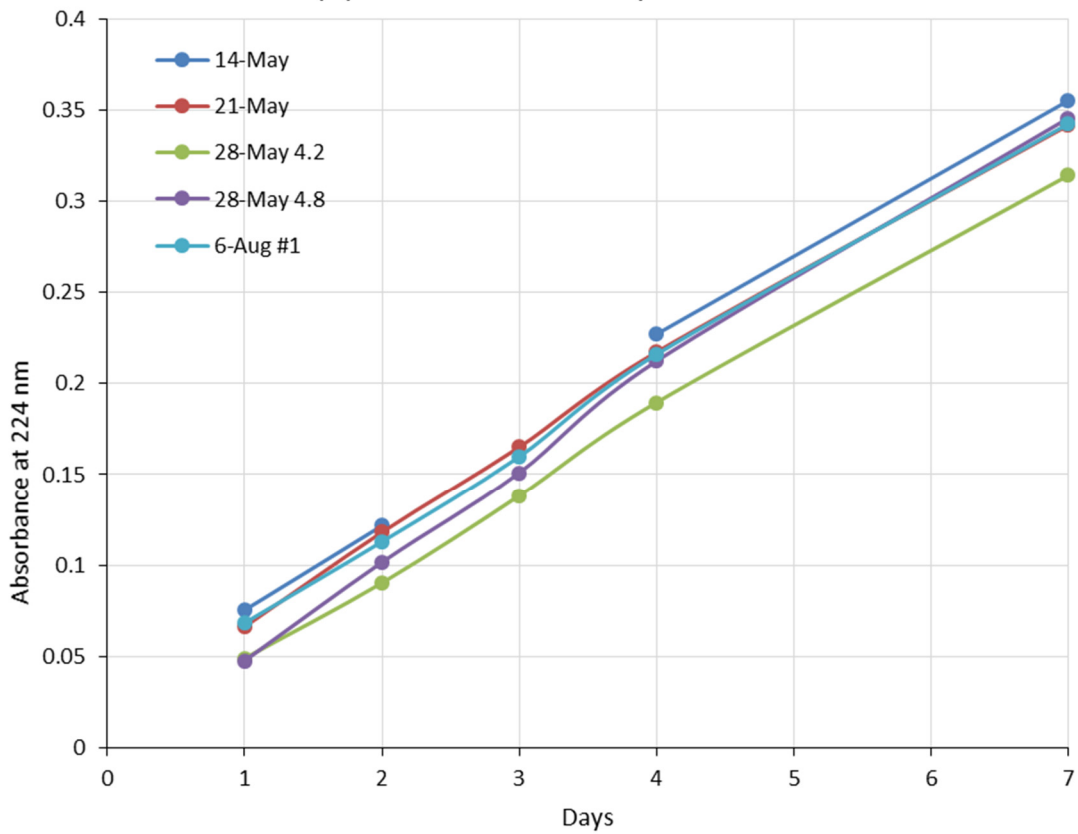
Appendix C - 18

(53) diOBn crown-5 - salbutamol 10 eq

Legend:
- 25-Jun (blue)
- 2-Jul (red)
- 9-Jul (green)

Y-axis: Absorbance at 224 nm
X-axis: Days

(54) diOBn crown-6 - salbutamol 10 eq

Legend:
- 25-Jun (blue)
- 2-Jul (red)

Y-axis: Absorbance at 224 nm
X-axis: Days

Appendix C - 19

(55) diOBn crown-7 - salbutamol 10 eq

(56) diOH crown-5 - salbutamol 10 eq
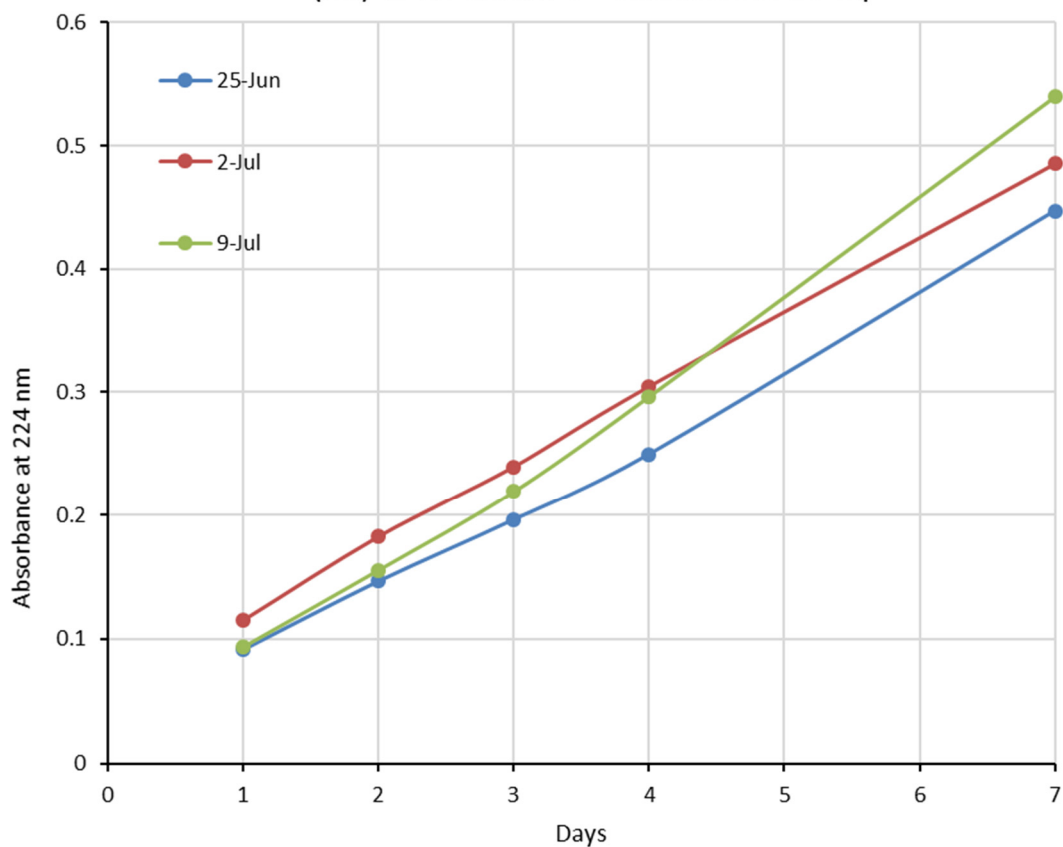
(57) diOH crown-6 - salbutamol 10 eq
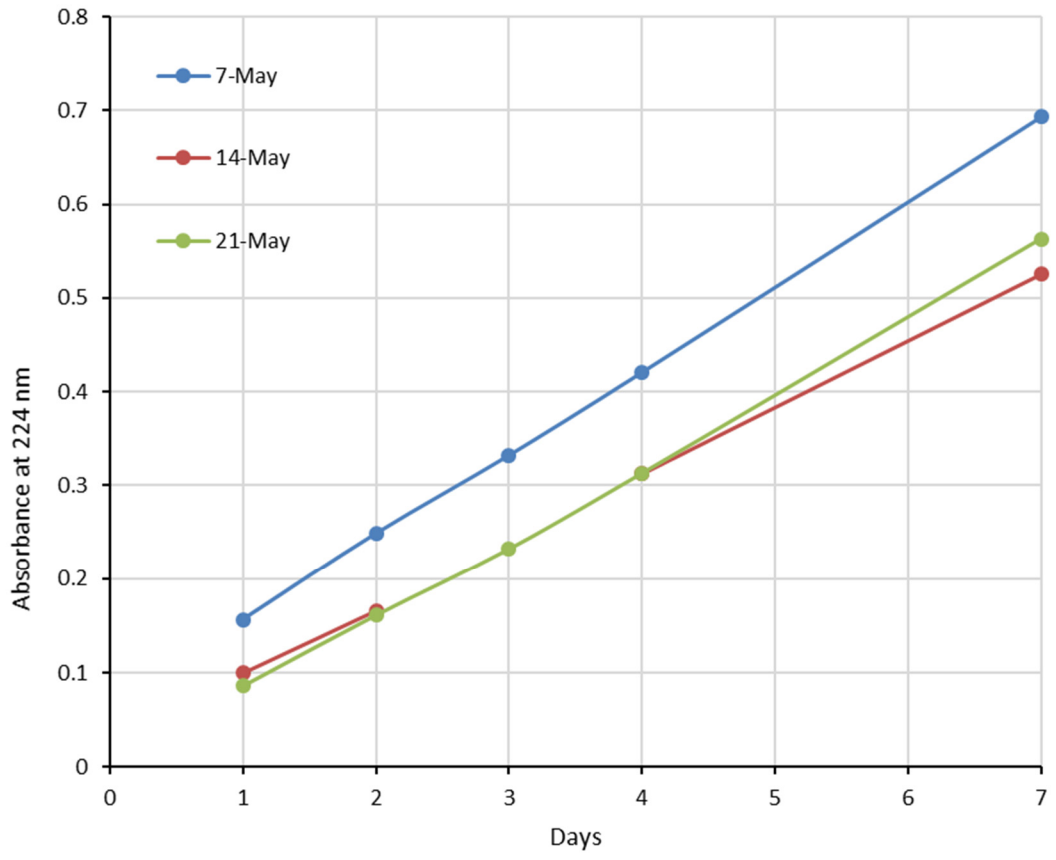
(58) diOH crown-7 - salbutamol 10 eq

(58) diOH crown-7 - salbutamol 10 eq - selected

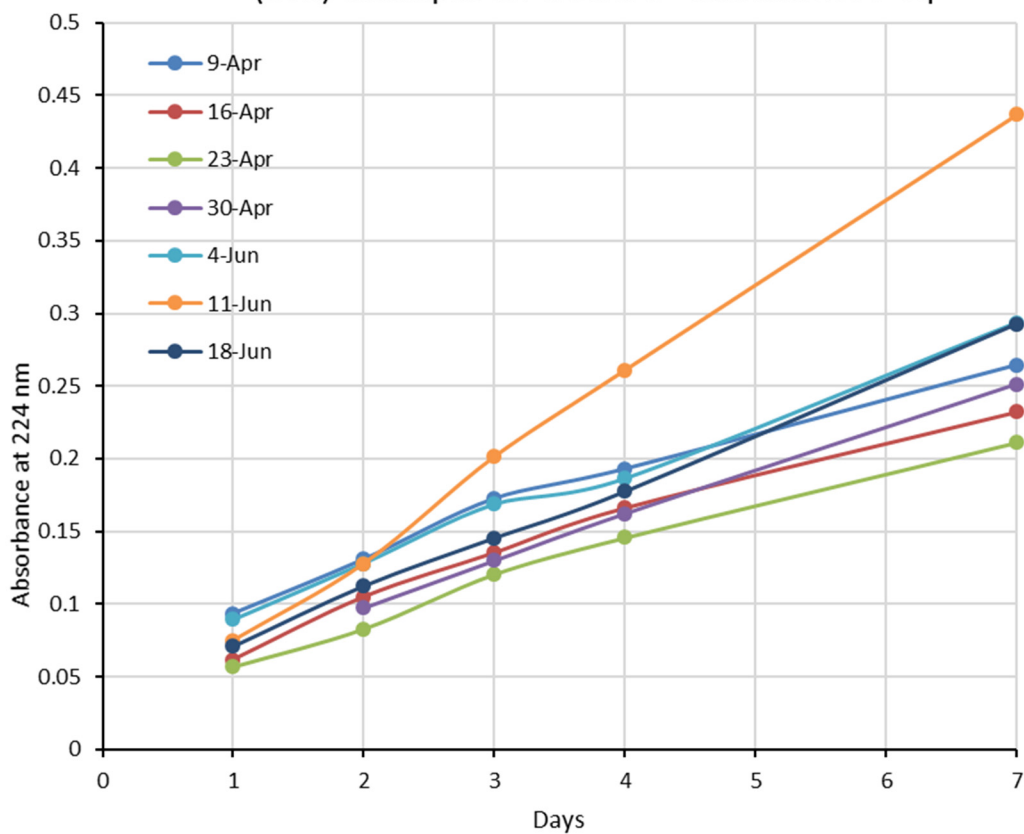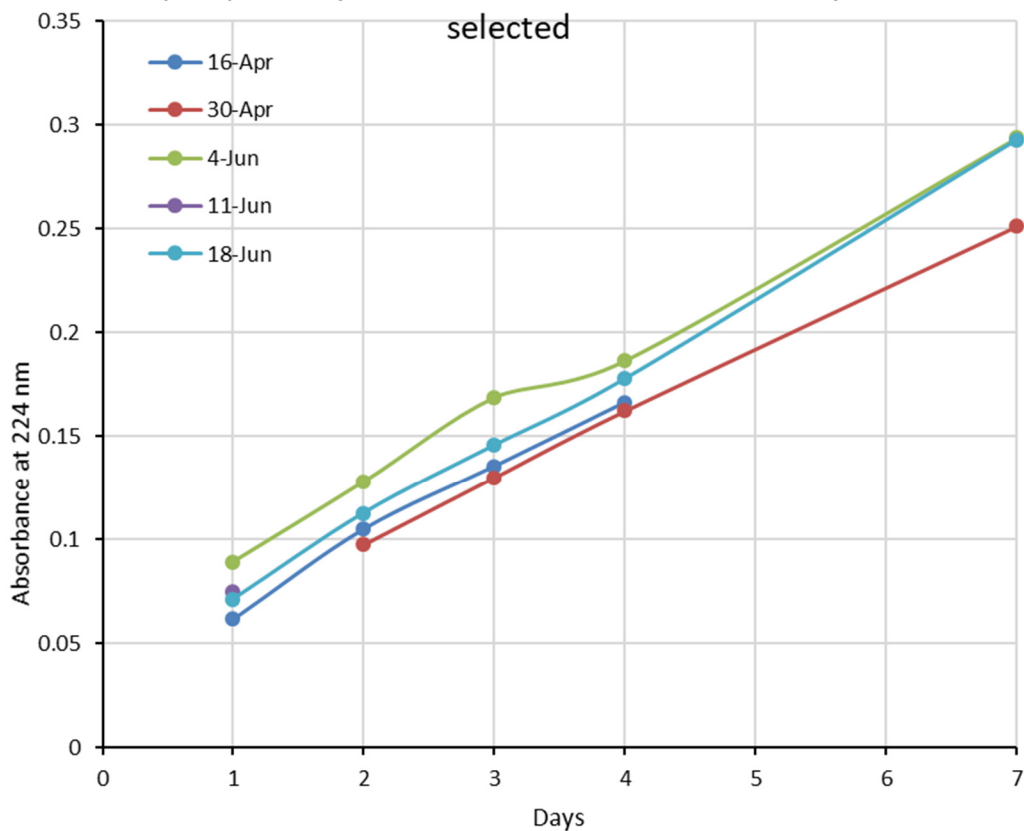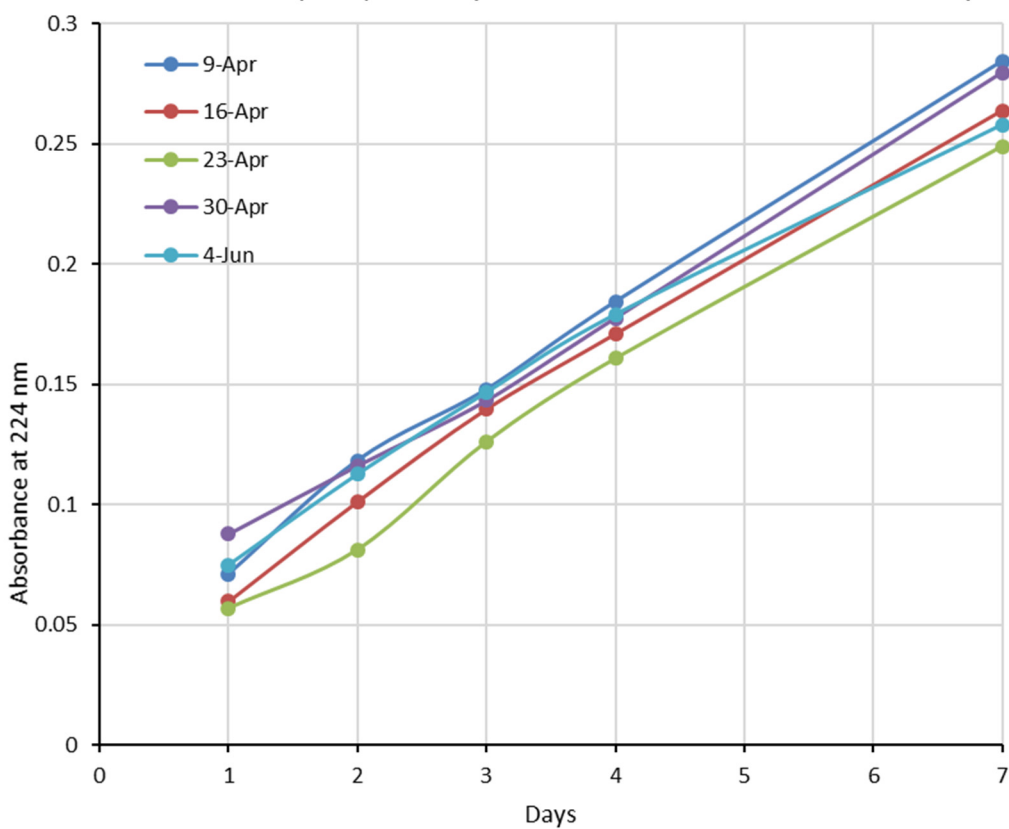*Appendix C - 22*
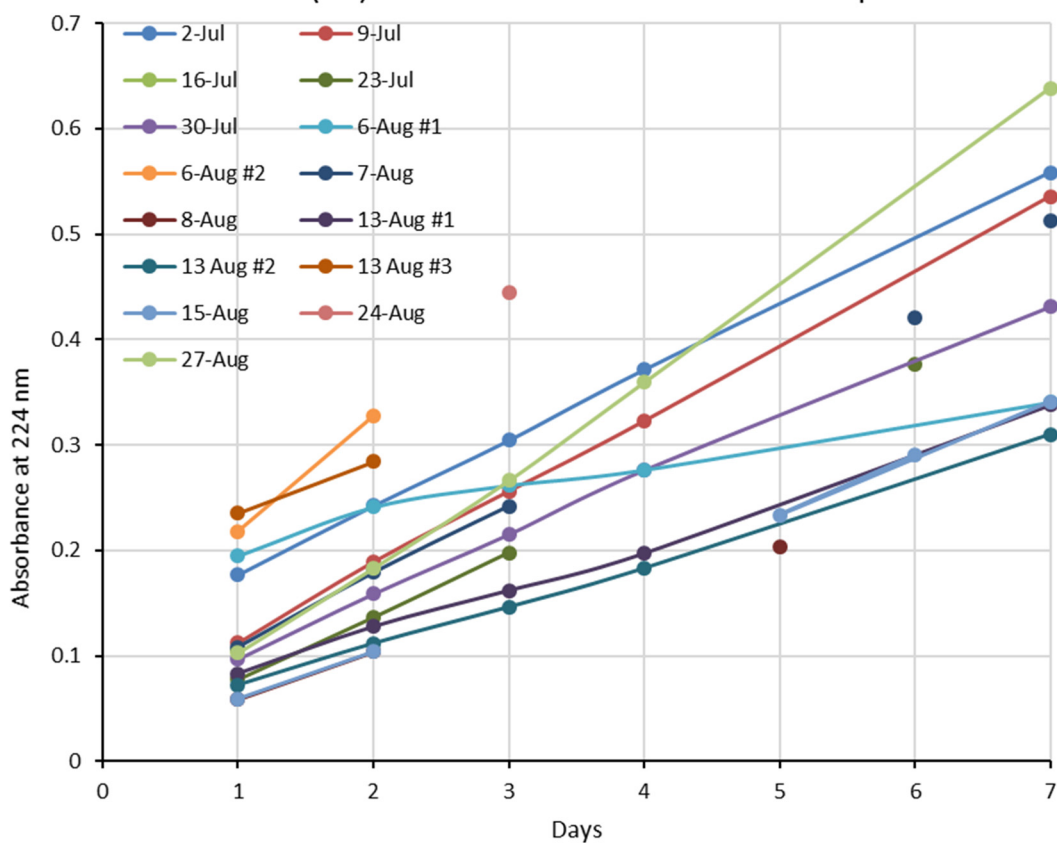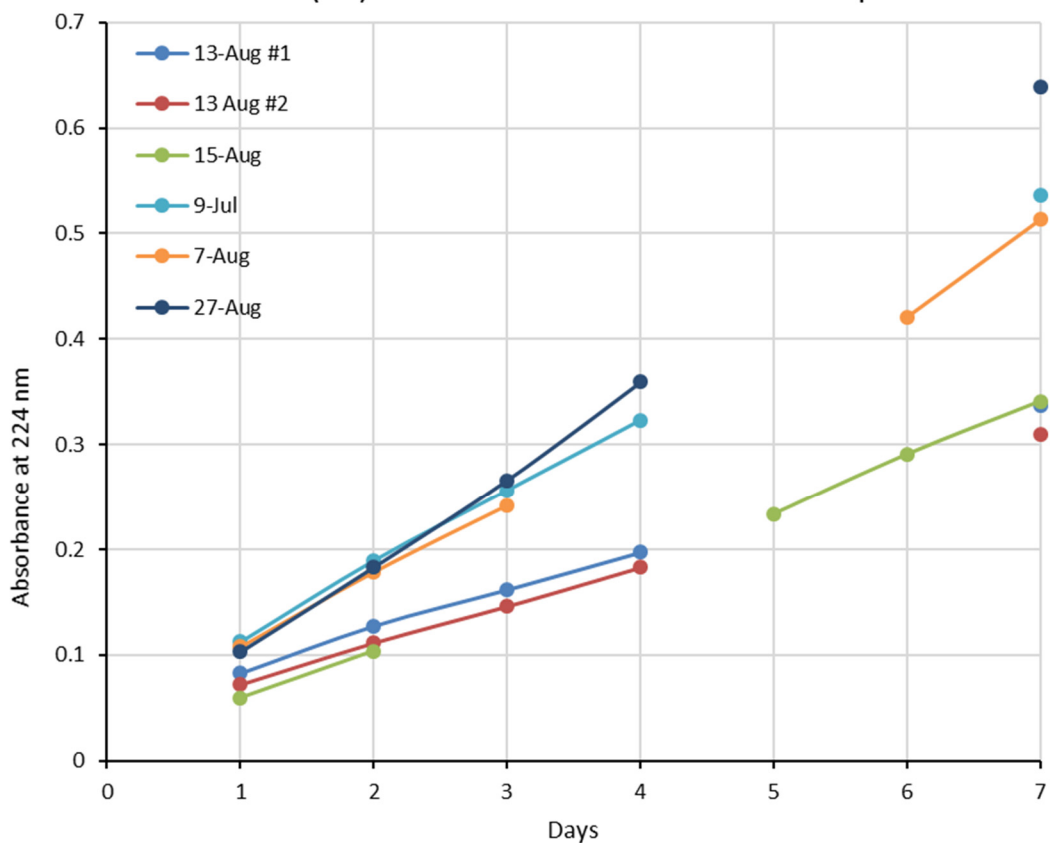
(59a) dicamphSO2 crown-5 - salbutamol 10 eq
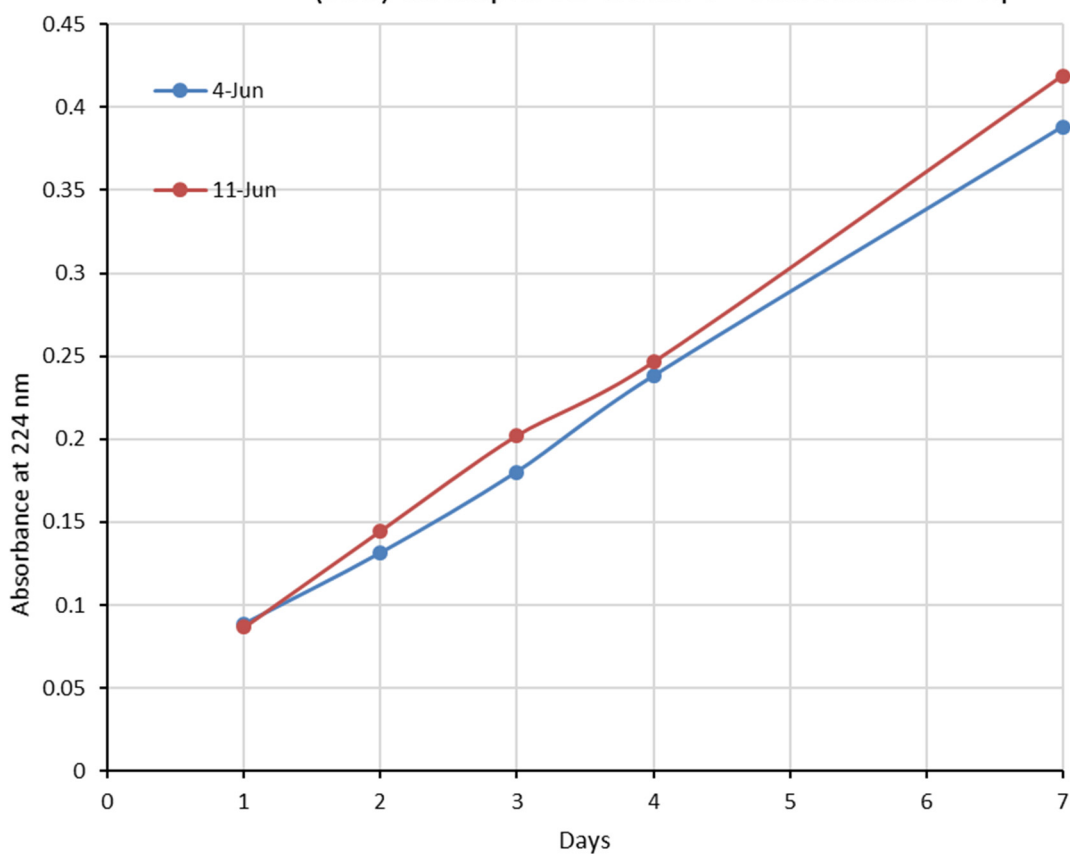
(59b) dicamphSO2 crown-5 - salbutamol 10 eq
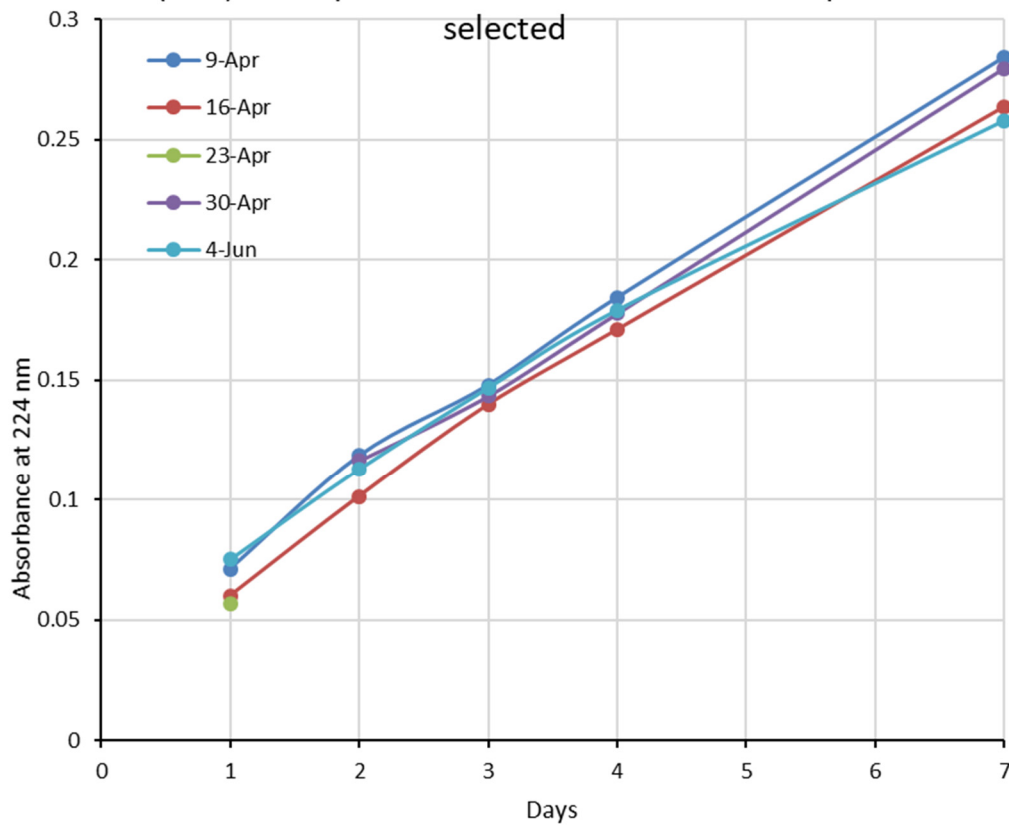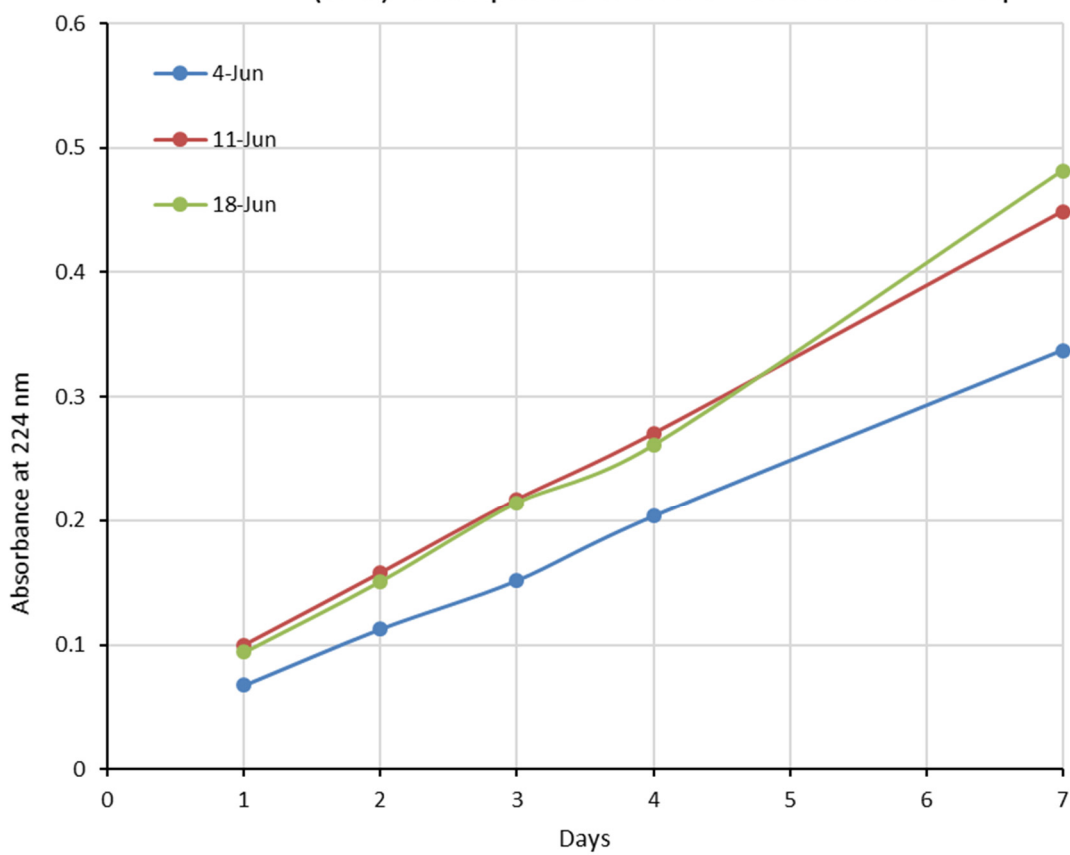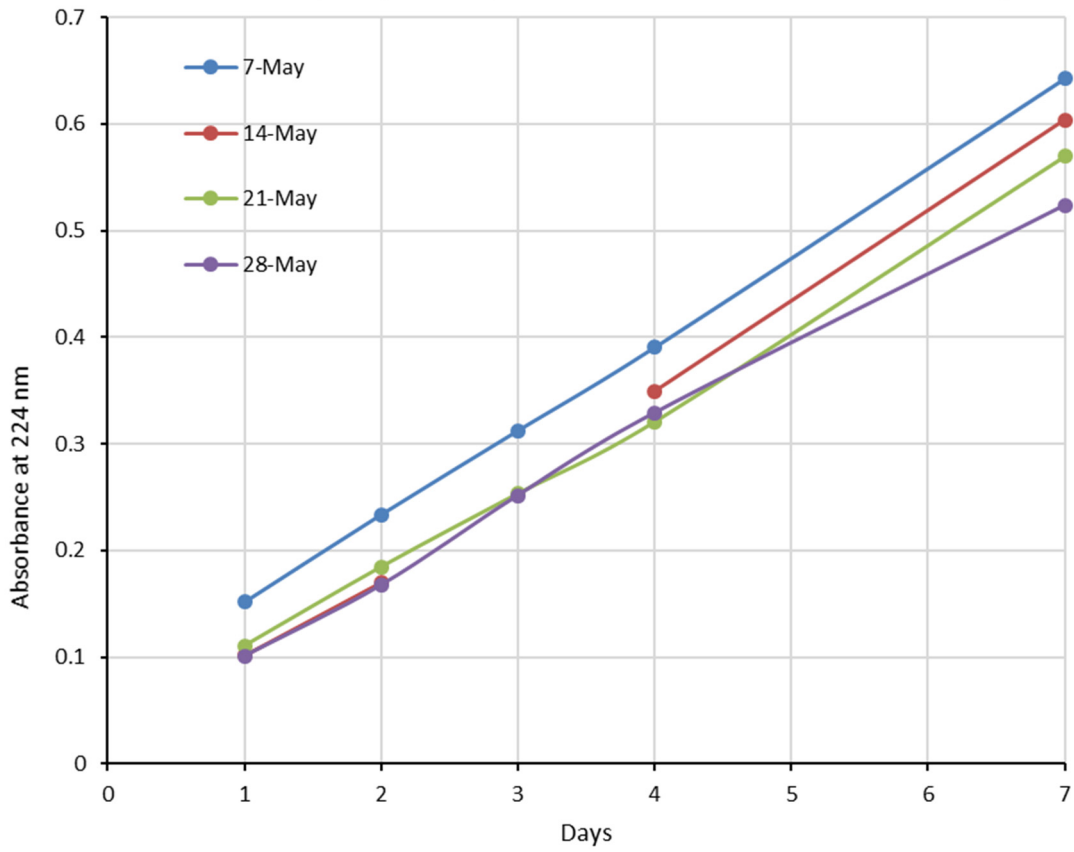
(60a) dicamphSO2 crown-6 - salbutamol 10 eq

(60b) dicamphSO2 crown-6 - salbutamol 10 eq
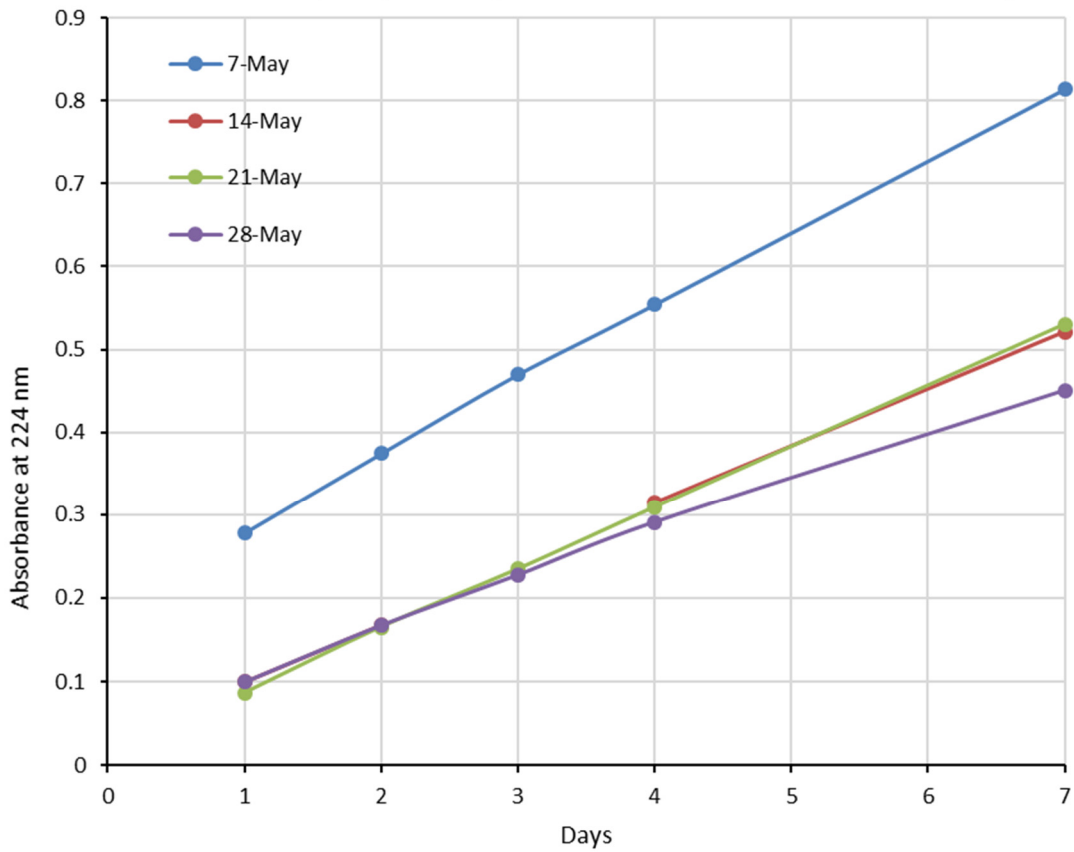
Appendix C - 24
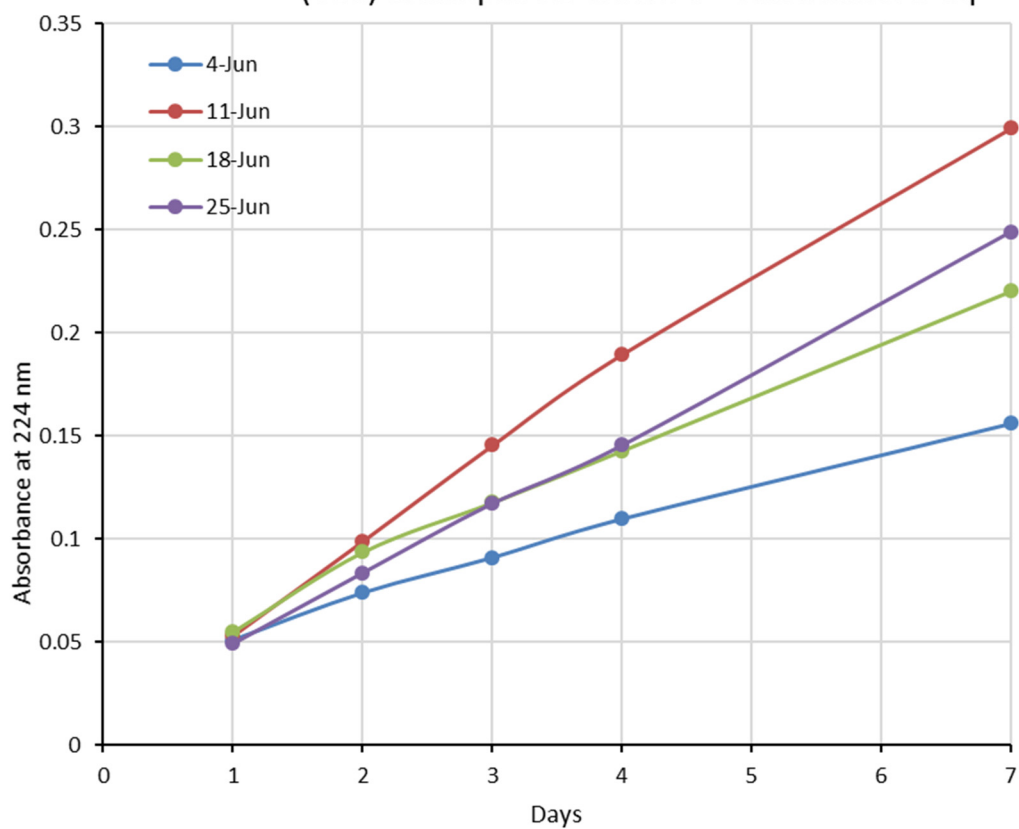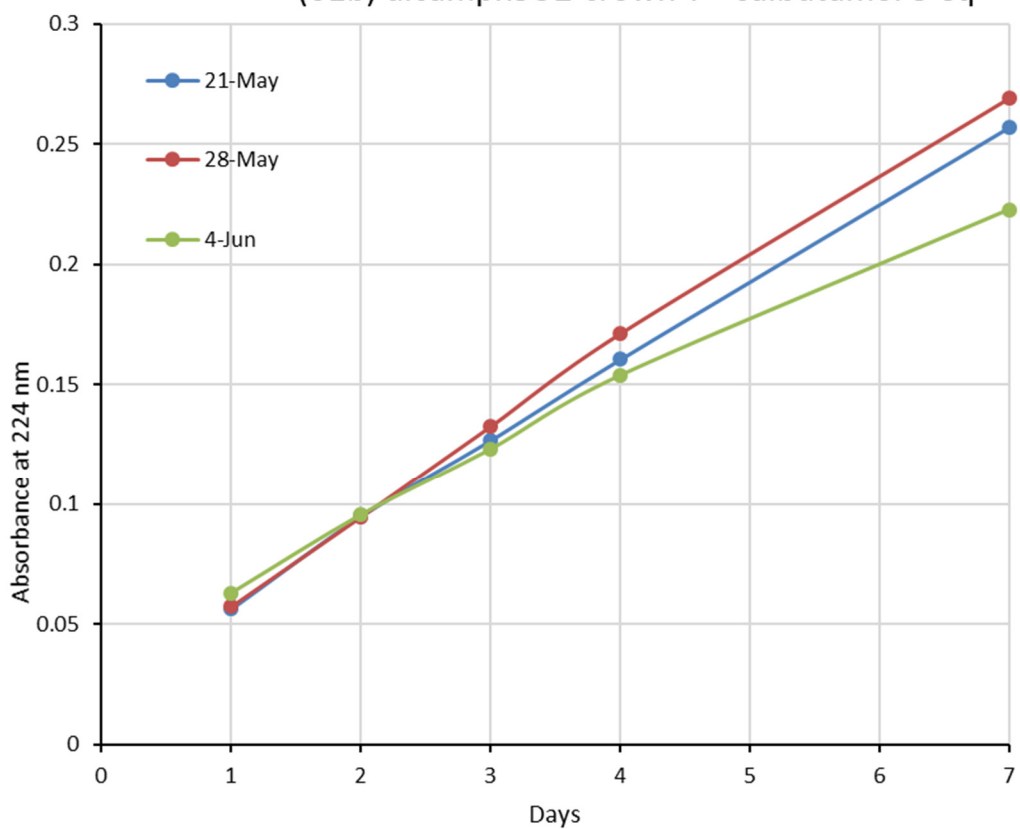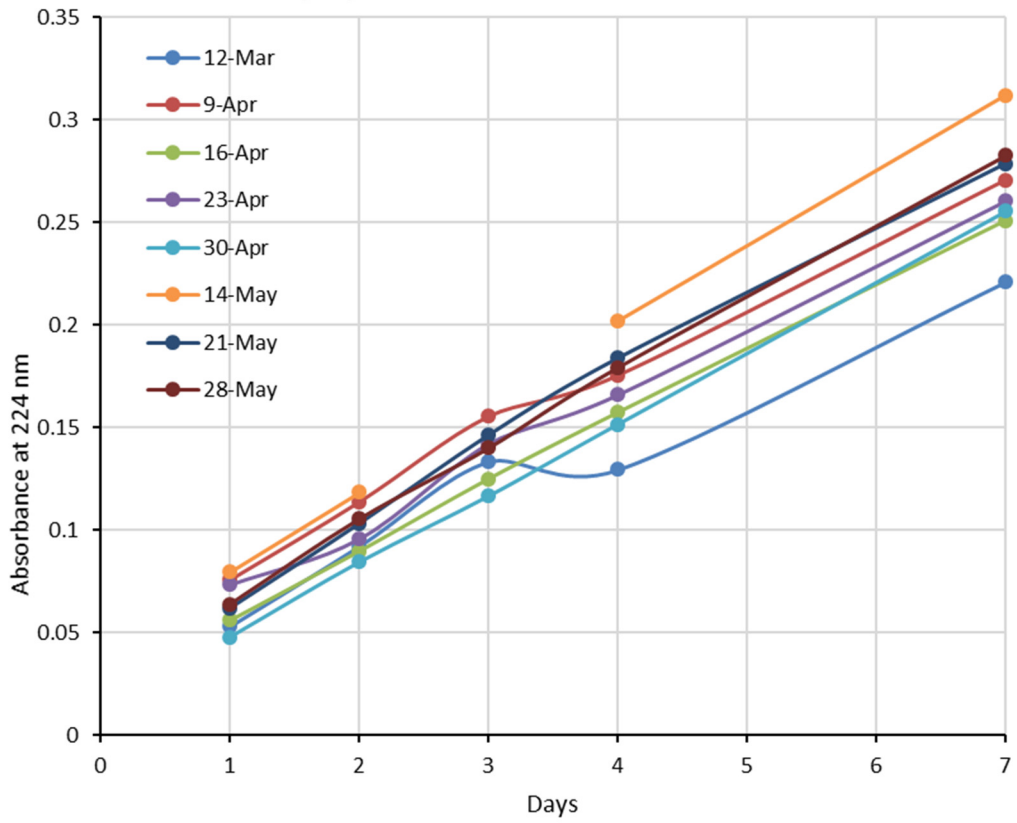
(61a) dicamphSO2 crown-7 - salbutamol 10 eq
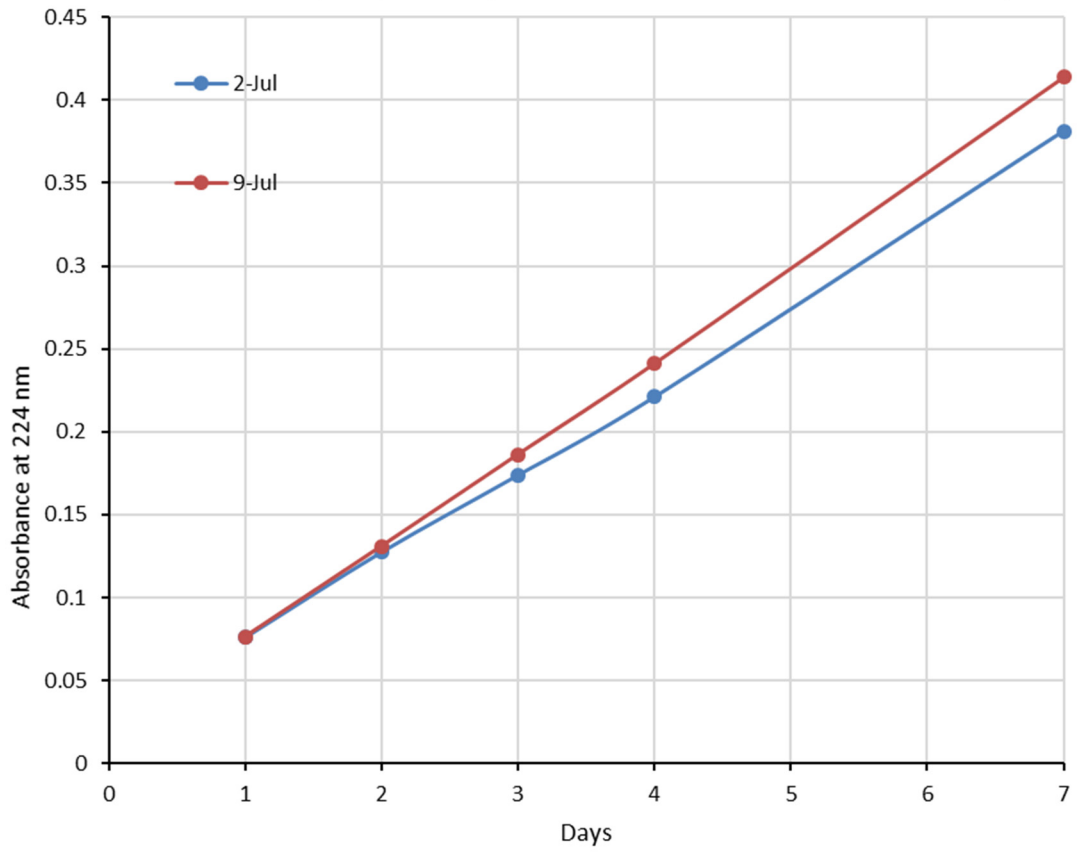
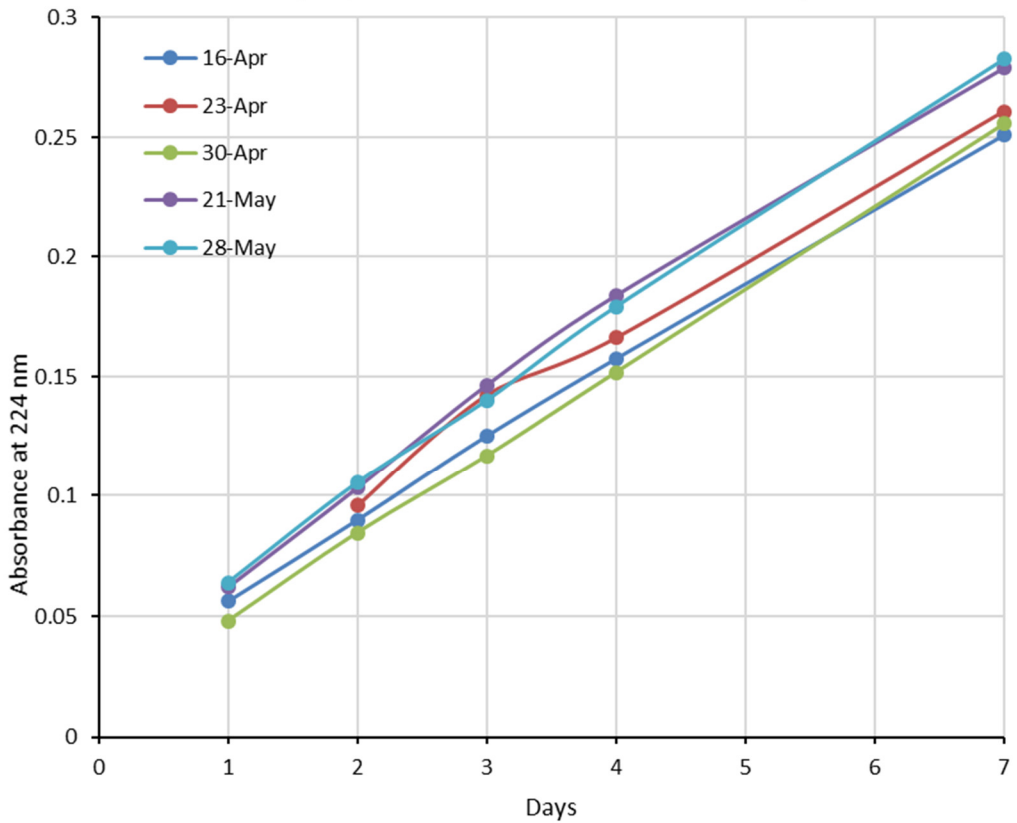(61b) dicamphSO2 crown-7 - salbutamol 10 eq
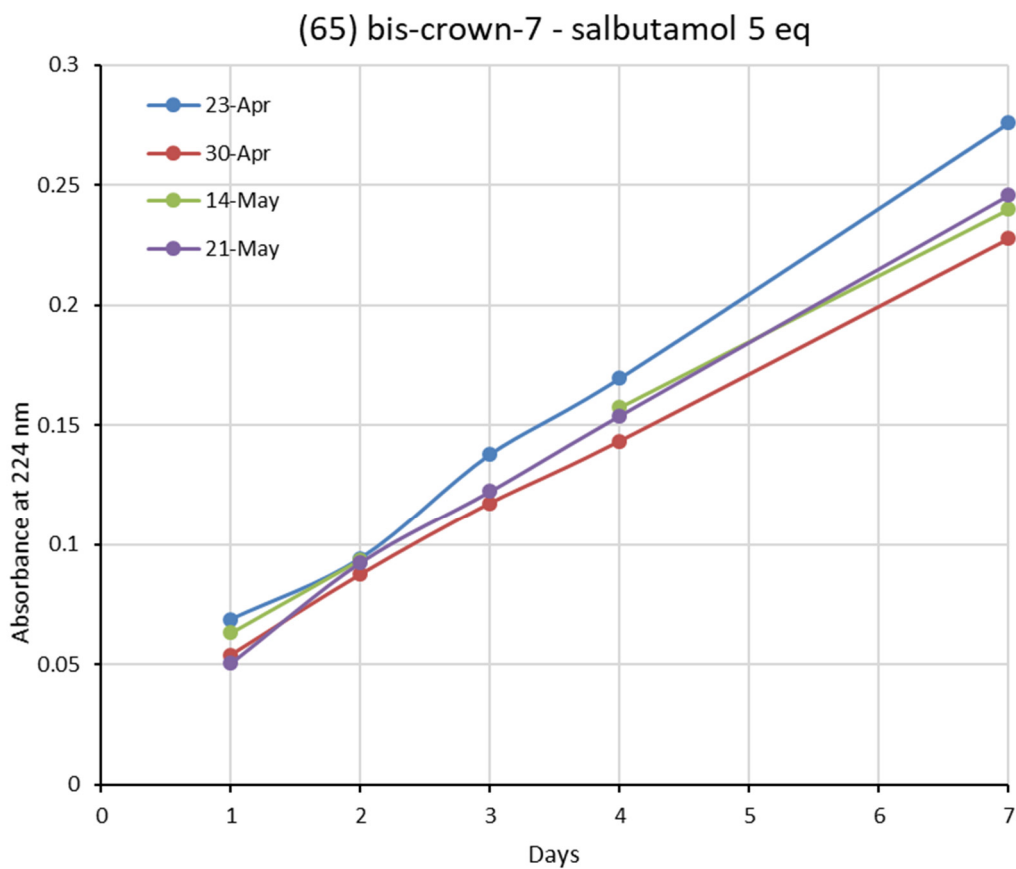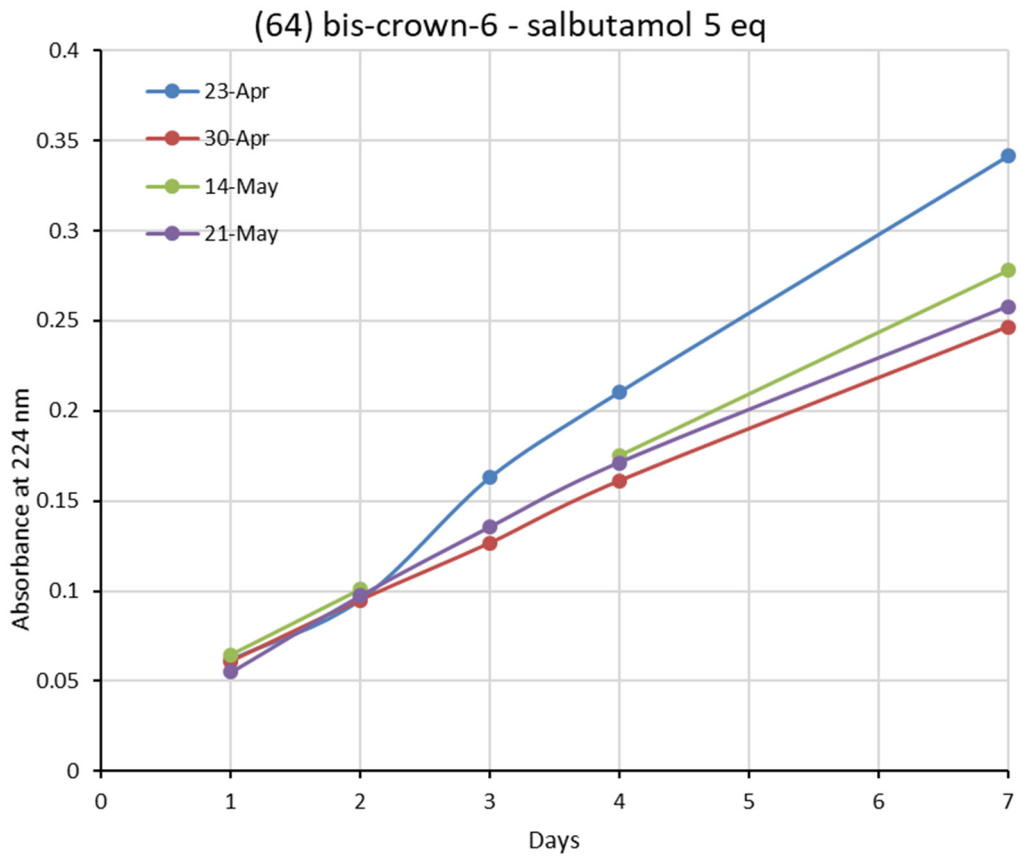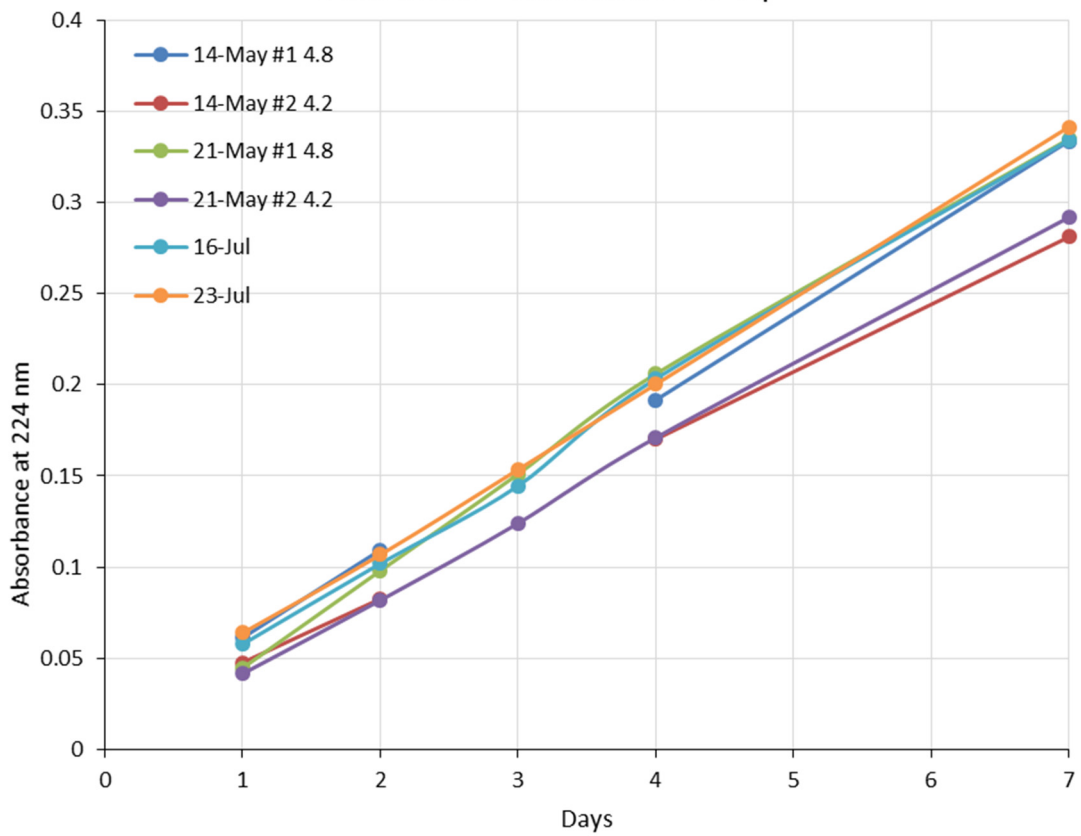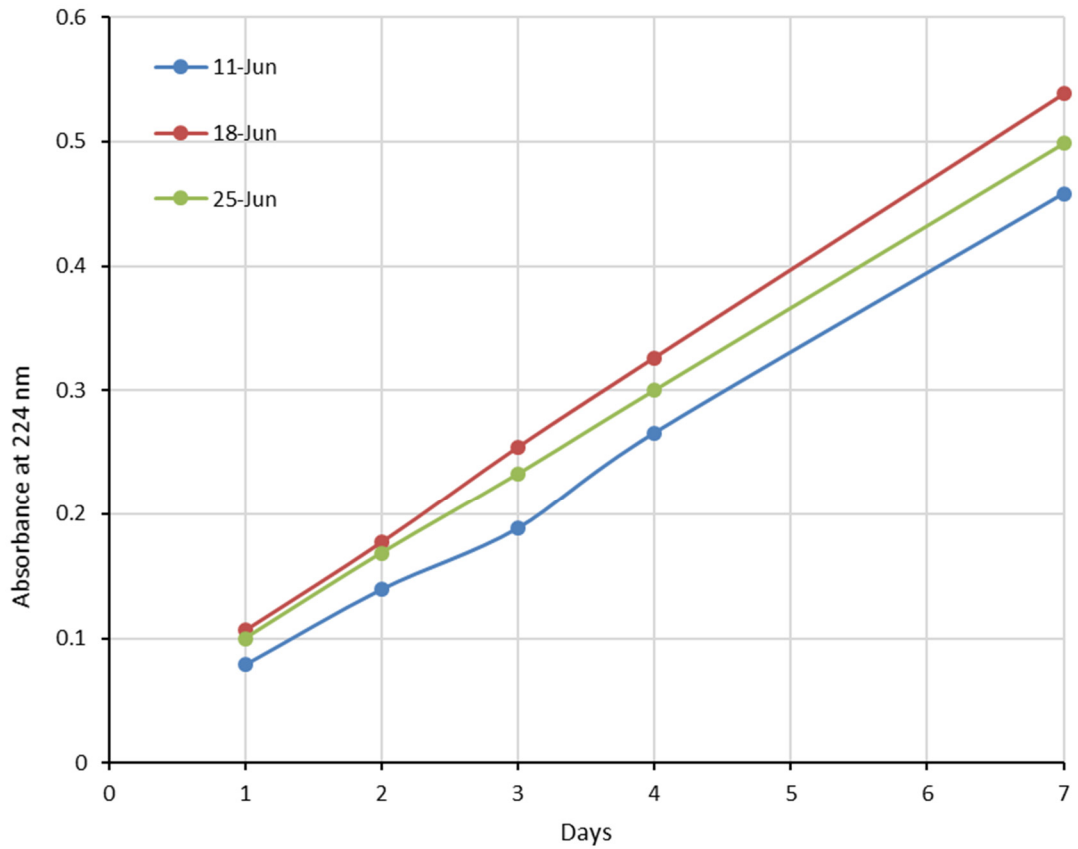
(63) bis-crown-5 - salbutamol 10 eq

(64) bis-crown-6 - salbutamol 10 eq
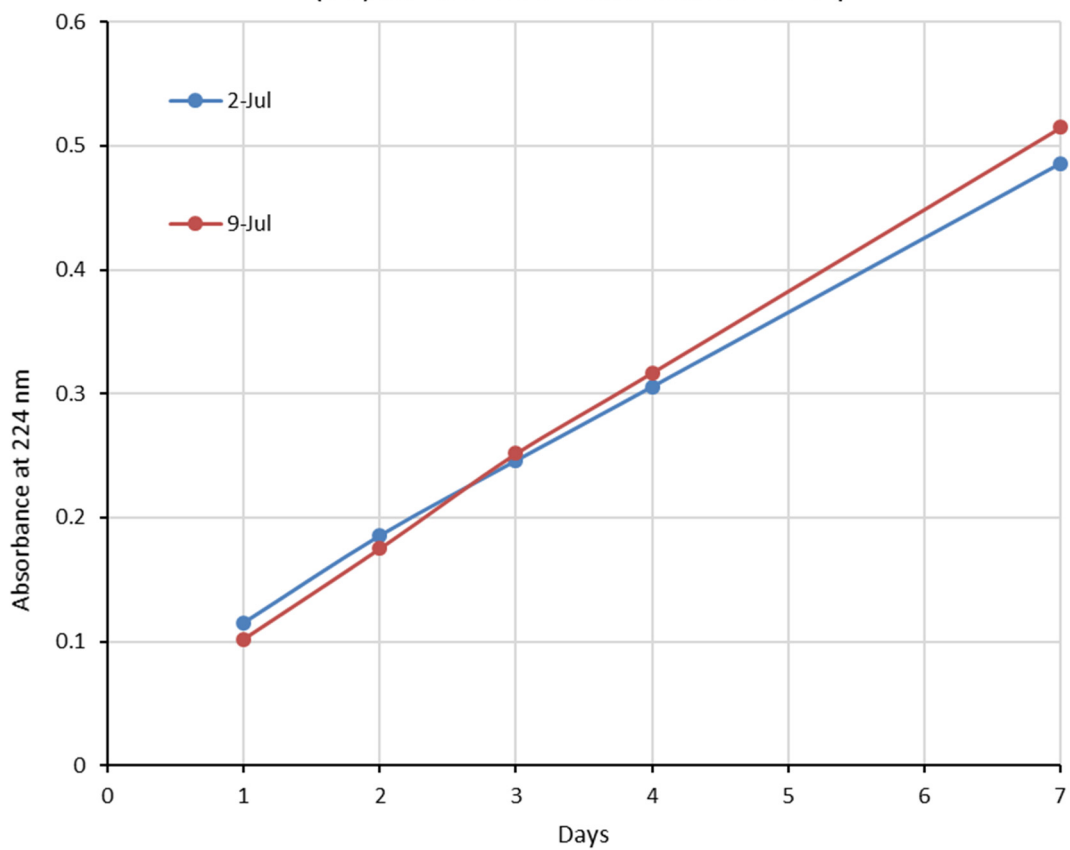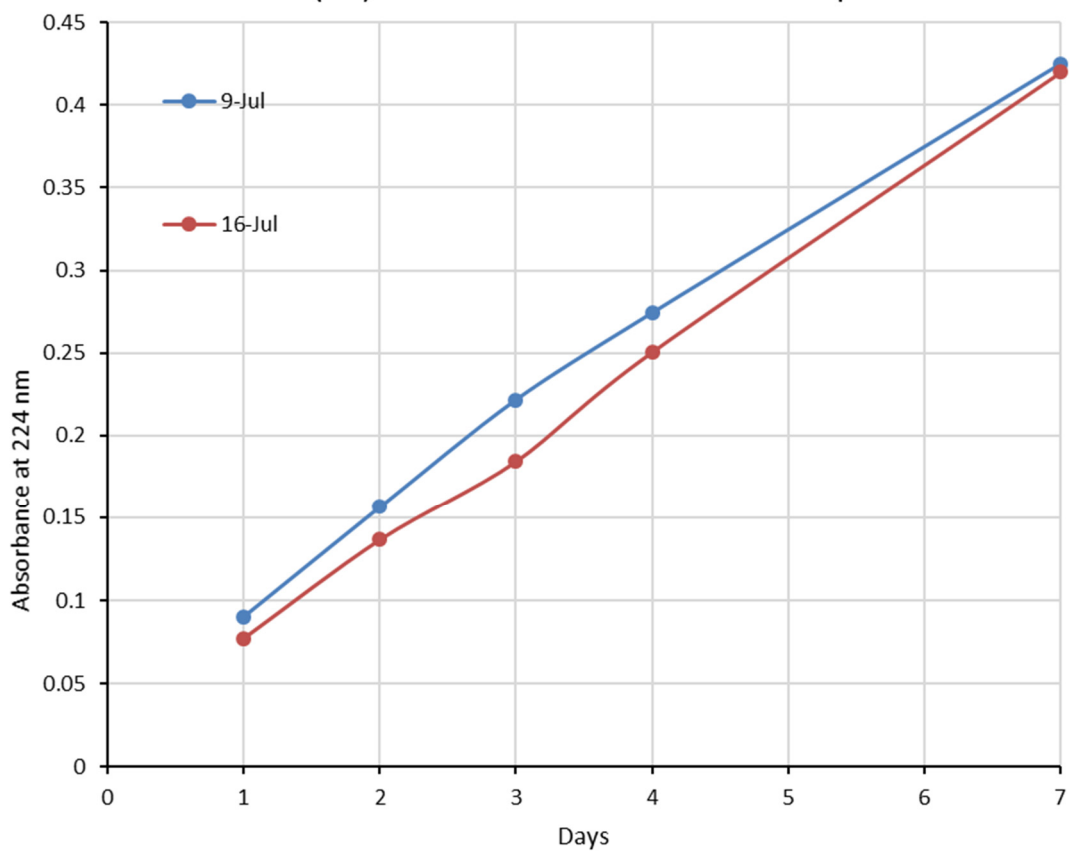
Appendix C - 26

(65) bis-crown-7 - salbutamol 10 eq
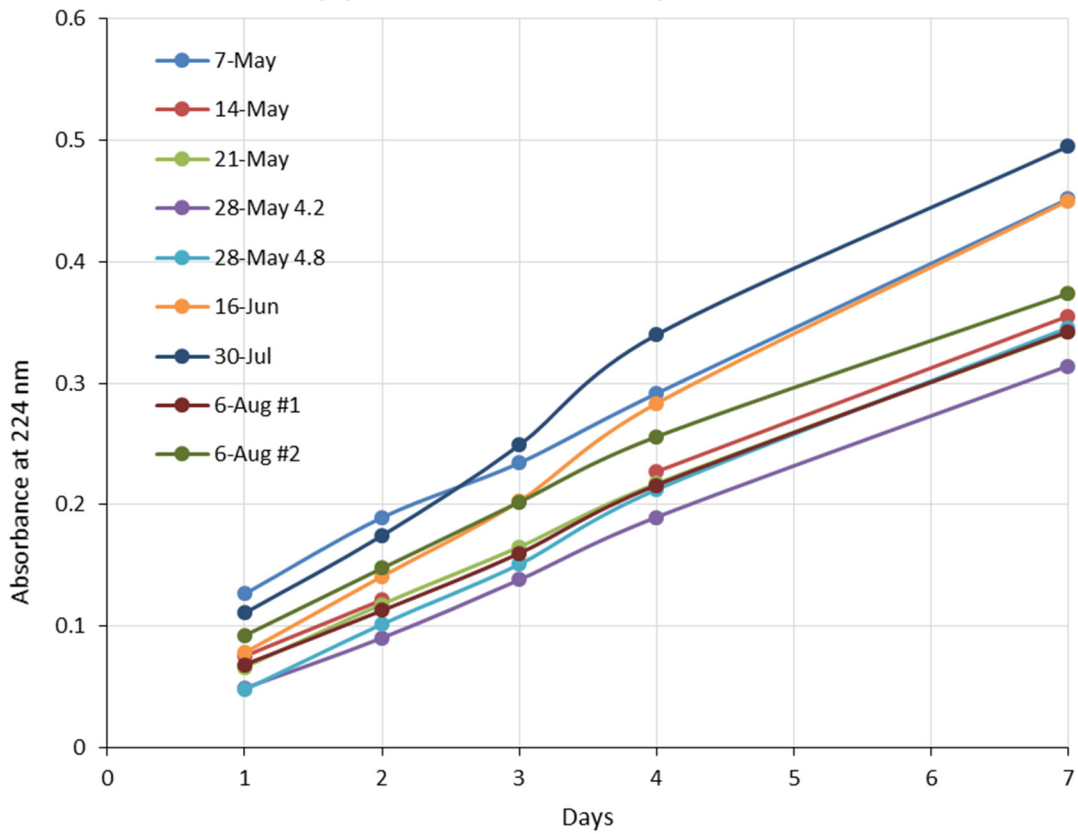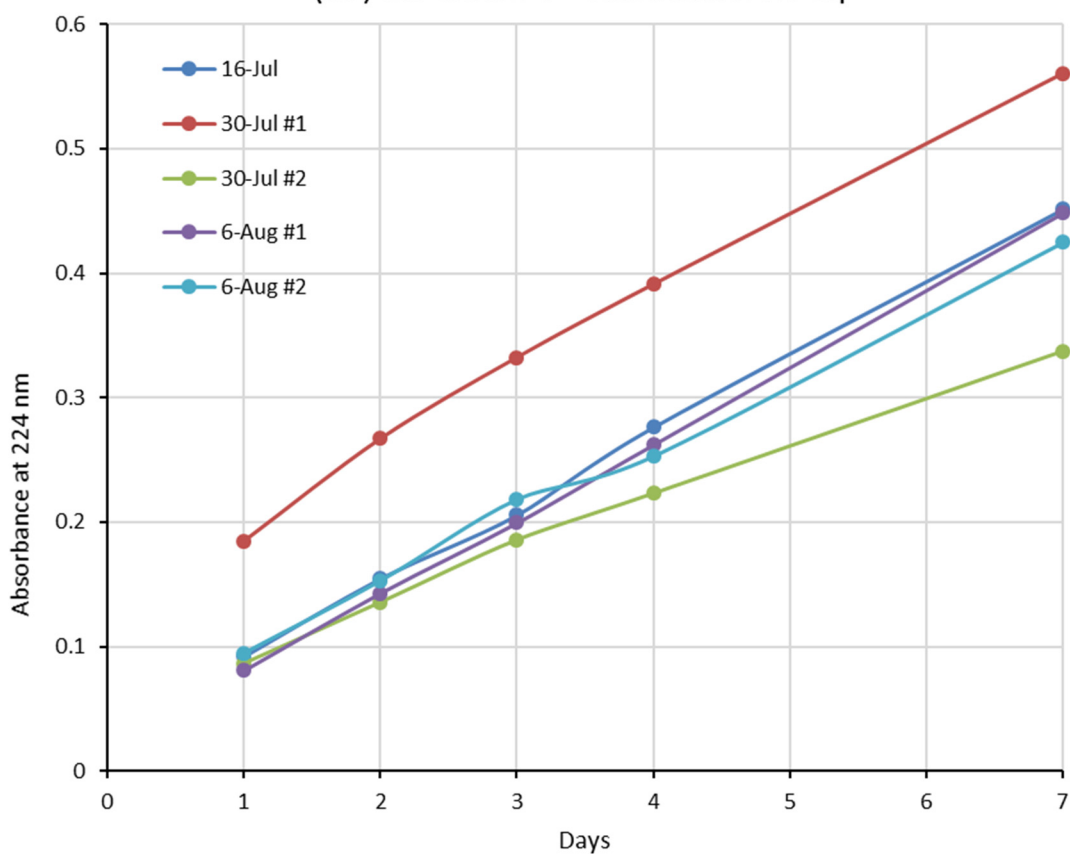

(65) bis-crown-7 - salbutamol 10 eq - selected
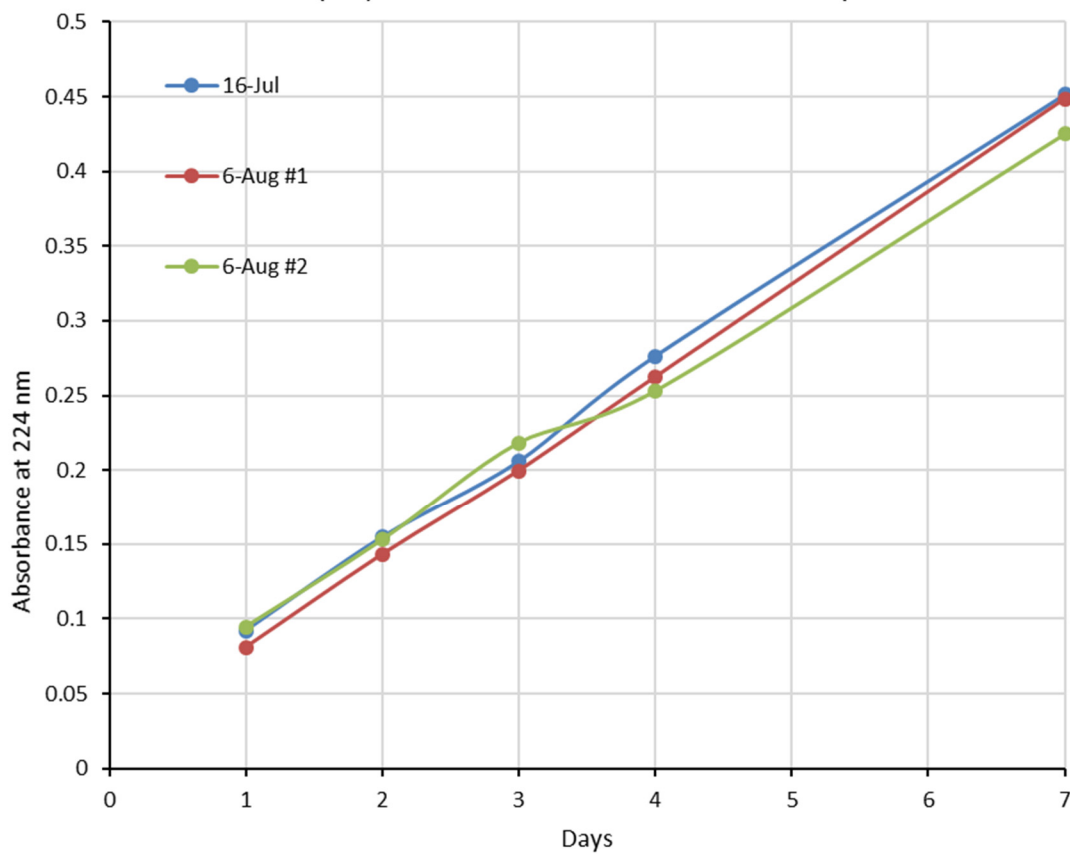
Appendix D

Copyright Permission

Statements

This Agreement between Curtin University -- Daniel Tan ("You") and John Wiley and Sons ("John Wiley and Sons") consists of your license details and the terms and conditions provided by John Wiley and Sons and Copyright Clearance Center.

License Number	4425700118601
License date	Sep 10, 2018
Licensed Content Publisher	John Wiley and Sons
Licensed Content Publication	European Journal of Organic Chemistry
Licensed Content Title	Calixarene-Mediated Liquid-Membrane Transport of Choline Conjugates
Licensed Content Author	Birendra Babu Adhikari, Ayu Fujii, Michael P. Schramm
Licensed Content Date	Mar 26, 2014
Licensed Content Volume	2014
Licensed Content Issue	14
Licensed Content Pages	8
Type of use	Dissertation/Thesis
Requestor type	University/Academic
Format	Print and electronic
Portion	Abstract
Will you be translating?	No
Title of your thesis / dissertation	Synthesis and Application of Distally-Bridged Chiral Resorcinarenes as Enantioselective Membrane Carriers
Expected completion date	Sep 2018
Expected size (number of pages)	250
Requestor Location	Curtin University Kent Street, Bentley Perth, WA 6102 Australia Attn: Curtin University
Publisher Tax ID	EU826007151
Total	0.00 AUD
Terms and Conditions	

TERMS AND CONDITIONS

Terms and Conditions

- The materials you have requested permission to reproduce or reuse (the "Wiley Materials") are protected by copyright.

- You are hereby granted a personal, non-exclusive, non-sub licensable (on a stand-alone basis), non-transferable, worldwide, limited license to reproduce the Wiley Materials for the purpose specified in the licensing process. This license, **and any CONTENT (PDF or image file) purchased as part of your order,** is for a one-time use only and limited to any maximum distribution number specified in the license. The first instance of republication or reuse granted by this license must be completed within two years of the date of the grant of this license (although copies prepared before the end date may be distributed thereafter). The Wiley Materials shall not be used in any other manner or for any other purpose, beyond what is granted in the license. Permission is granted subject to an appropriate acknowledgement given to the author, title of the material/book/journal and the publisher. You shall also duplicate the copyright notice that appears in the Wiley publication in your use of the Wiley Material. Permission is also granted on the understanding that nowhere in the text is a previously published source acknowledged for all or part of this Wiley Material. Any third party content is expressly excluded from this permission.

- With respect to the Wiley Materials, all rights are reserved. Except as expressly granted by the terms of the license, no part of the Wiley Materials may be copied, modified, adapted (except for minor reformatting required by the new Publication), translated, reproduced, transferred or distributed, in any form or by any means, and no derivative works may be made based on the Wiley Materials without the prior permission of the respective copyright owner.**For STM Signatory Publishers clearing permission under the terms of the STM Permissions Guidelines only, the terms of the license are extended to include subsequent editions and for editions in other languages, provided such editions are for the work as a whole in situ and does not involve the separate exploitation of the permitted figures or extracts,** You may not alter, remove or suppress in any manner any copyright, trademark or other notices displayed by the Wiley Materials. You may not license, rent, sell, loan, lease, pledge, offer as security, transfer or assign the Wiley Materials on a stand-alone basis, or any of the rights granted to you hereunder to any other person.

- The Wiley Materials and all of the intellectual property rights therein shall at all times remain the exclusive property of John Wiley & Sons Inc, the Wiley Companies, or their respective licensors, and your interest therein is only that of having possession of and the right to reproduce the Wiley Materials pursuant to Section 2 herein during the continuance of this Agreement. You agree that you own no right, title or interest in or to the Wiley Materials or any of the intellectual property rights therein. You shall have no rights hereunder other than the license as provided for above in Section 2. No right, license or interest to any trademark, trade name, service mark or other branding ("Marks") of WILEY or its licensors is granted hereunder, and you agree that you shall not assert any such right, license or interest with respect thereto

- NEITHER WILEY NOR ITS LICENSORS MAKES ANY WARRANTY OR REPRESENTATION OF ANY KIND TO YOU OR ANY THIRD PARTY, EXPRESS, IMPLIED OR STATUTORY, WITH RESPECT TO THE MATERIALS OR THE ACCURACY OF ANY INFORMATION CONTAINED IN THE MATERIALS, INCLUDING, WITHOUT LIMITATION, ANY IMPLIED WARRANTY OF MERCHANTABILITY, ACCURACY, SATISFACTORY QUALITY, FITNESS FOR A PARTICULAR PURPOSE, USABILITY, INTEGRATION OR NON-INFRINGEMENT AND ALL SUCH WARRANTIES ARE HEREBY EXCLUDED BY WILEY AND ITS LICENSORS AND WAIVED

BY YOU.

- WILEY shall have the right to terminate this Agreement immediately upon breach of this Agreement by you.

- You shall indemnify, defend and hold harmless WILEY, its Licensors and their respective directors, officers, agents and employees, from and against any actual or threatened claims, demands, causes of action or proceedings arising from any breach of this Agreement by you.

- IN NO EVENT SHALL WILEY OR ITS LICENSORS BE LIABLE TO YOU OR ANY OTHER PARTY OR ANY OTHER PERSON OR ENTITY FOR ANY SPECIAL, CONSEQUENTIAL, INCIDENTAL, INDIRECT, EXEMPLARY OR PUNITIVE DAMAGES, HOWEVER CAUSED, ARISING OUT OF OR IN CONNECTION WITH THE DOWNLOADING, PROVISIONING, VIEWING OR USE OF THE MATERIALS REGARDLESS OF THE FORM OF ACTION, WHETHER FOR BREACH OF CONTRACT, BREACH OF WARRANTY, TORT, NEGLIGENCE, INFRINGEMENT OR OTHERWISE (INCLUDING, WITHOUT LIMITATION, DAMAGES BASED ON LOSS OF PROFITS, DATA, FILES, USE, BUSINESS OPPORTUNITY OR CLAIMS OF THIRD PARTIES), AND WHETHER OR NOT THE PARTY HAS BEEN ADVISED OF THE POSSIBILITY OF SUCH DAMAGES. THIS LIMITATION SHALL APPLY NOTWITHSTANDING ANY FAILURE OF ESSENTIAL PURPOSE OF ANY LIMITED REMEDY PROVIDED HEREIN.

- Should any provision of this Agreement be held by a court of competent jurisdiction to be illegal, invalid, or unenforceable, that provision shall be deemed amended to achieve as nearly as possible the same economic effect as the original provision, and the legality, validity and enforceability of the remaining provisions of this Agreement shall not be affected or impaired thereby.

- The failure of either party to enforce any term or condition of this Agreement shall not constitute a waiver of either party's right to enforce each and every term and condition of this Agreement. No breach under this agreement shall be deemed waived or excused by either party unless such waiver or consent is in writing signed by the party granting such waiver or consent. The waiver by or consent of a party to a breach of any provision of this Agreement shall not operate or be construed as a waiver of or consent to any other or subsequent breach by such other party.

- This Agreement may not be assigned (including by operation of law or otherwise) by you without WILEY's prior written consent.

- Any fee required for this permission shall be non-refundable after thirty (30) days from receipt by the CCC.

- These terms and conditions together with CCC's Billing and Payment terms and conditions (which are incorporated herein) form the entire agreement between you and WILEY concerning this licensing transaction and (in the absence of fraud) supersedes all prior agreements and representations of the parties, oral or written. This Agreement may not be amended except in writing signed by both parties. This Agreement shall be binding upon and inure to the benefit of the parties' successors, legal representatives, and authorized assigns.

- In the event of any conflict between your obligations established by these terms and conditions and those established by CCC's Billing and Payment terms and conditions, these terms and conditions shall prevail.

- WILEY expressly reserves all rights not specifically granted in the combination of (i) the license details provided by you and accepted in the course of this licensing transaction, (ii) these terms and conditions and (iii) CCC's Billing and Payment terms and conditions.

- This Agreement will be void if the Type of Use, Format, Circulation, or Requestor Type was misrepresented during the licensing process.

- This Agreement shall be governed by and construed in accordance with the laws of the State of New York, USA, without regards to such state's conflict of law rules. Any legal action, suit or proceeding arising out of or relating to these Terms and Conditions or the breach thereof shall be instituted in a court of competent jurisdiction in New York County in the State of New York in the United States of America and each party hereby consents and submits to the personal jurisdiction of such court, waives any objection to venue in such court and consents to service of process by registered or certified mail, return receipt requested, at the last known address of such party.

WILEY OPEN ACCESS TERMS AND CONDITIONS
Wiley Publishes Open Access Articles in fully Open Access Journals and in Subscription journals offering Online Open. Although most of the fully Open Access journals publish open access articles under the terms of the Creative Commons Attribution (CC BY) License only, the subscription journals and a few of the Open Access Journals offer a choice of Creative Commons Licenses. The license type is clearly identified on the article.
The Creative Commons Attribution License
The Creative Commons Attribution License (CC-BY) allows users to copy, distribute and transmit an article, adapt the article and make commercial use of the article. The CC-BY license permits commercial and non-
Creative Commons Attribution Non-Commercial License
The Creative Commons Attribution Non-Commercial (CC-BY-NC)License permits use, distribution and reproduction in any medium, provided the original work is properly cited and is not used for commercial purposes.(see below)

Creative Commons Attribution-Non-Commercial-NoDerivs License
The Creative Commons Attribution Non-Commercial-NoDerivs License (CC-BY-NC-ND) permits use, distribution and reproduction in any medium, provided the original work is properly cited, is not used for commercial purposes and no modifications or adaptations are made. (see below)
Use by commercial "for-profit" organizations
Use of Wiley Open Access articles for commercial, promotional, or marketing purposes requires further explicit permission from Wiley and will be subject to a fee.
Further details can be found on Wiley Online Library
http://olabout.wiley.com/WileyCDA/Section/id-410895.html

Other Terms and Conditions:

v1.10 Last updated September 2015

Questions? customercare@copyright.com or +1-855-239-3415 (toll free in the US) or +1-978-646-2777.

Copyright Clearance Center

RightsLink®

Home | Create Account | Help | Chat

ACS Publications
Most Trusted. Most Cited. Most Read.

Title: Peptido- and Glycocalixarenes: Playing with Hydrogen Bonds around Hydrophobic Cavities

Author: Alessandro Casnati, Francesco Sansone, Rocco Ungaro

Publication: Accounts of Chemical Research

Publisher: American Chemical Society

Date: Apr 1, 2003

Copyright © 2003, American Chemical Society

PERMISSION/LICENSE IS GRANTED FOR YOUR ORDER AT NO CHARGE

This type of permission/license, instead of the standard Terms & Conditions, is sent to you because no fee is being charged for your order. Please note the following:

- Permission is granted for your request in both print and electronic formats, and translations.
- If figures and/or tables were requested, they may be adapted or used in part.
- Please print this page for your records and send a copy of it to your publisher/graduate school.
- Appropriate credit for the requested material should be given as follows: "Reprinted (adapted) with permission from (COMPLETE REFERENCE CITATION). Copyright (YEAR) American Chemical Society." Insert appropriate information in place of the capitalized words.
- One-time permission is granted only for the use specified in your request. No additional uses are granted (such as derivative works or other editions). For any other uses, please submit a new request.

If credit is given to another source for the material you requested, permission must be obtained from that source.

BACK | CLOSE WINDOW

Appendix D - 5

This Agreement between Curtin University -- Daniel Tan ("You") and Springer Nature ("Springer Nature") consists of your license details and the terms and conditions provided by Springer Nature and Copyright Clearance Center.

License Number	4431871499037
License date	Sep 18, 2018
Licensed Content Publisher	Springer Nature
Licensed Content Publication	Springer eBook
Licensed Content Title	Calix[4]arenes and Resorcinarenes Bridged at the Wider Rim
Licensed Content Author	Daniel A. Tan, Mauro Mocerino
Licensed Content Date	Jan 1, 2016
Type of Use	Thesis/Dissertation
Requestor type	academic/university or research institute
Format	print and electronic
Portion	full article/chapter
Will you be translating?	no
Circulation/distribution	<501
Author of this Springer Nature content	yes
Title	Synthesis and Application of Distally-Bridged Chiral Resorcinarenes as Enantioselective Membrane Carriers
Instructor name	n/a
Institution name	n/a
Expected presentation date	Sep 2018
Requestor Location	Curtin University Kent Street, Bentley

Perth, WA 6102 Australia Attn: Curtin University |
| Billing Type | Invoice |
| Billing Address | Curtin University Kent Street, Bentley

Perth, Australia 6102 Attn: Curtin University |
| Total | 0.00 AUD |

Terms and Conditions

Springer Nature Terms and Conditions for RightsLink Permissions
Springer Nature Customer Service Centre GmbH (the Licensor) hereby grants you a non-exclusive, world-wide licence to reproduce the material and for the purpose and requirements specified in the attached copy of your order form, and for no other use, subject to the conditions below:

1. The Licensor warrants that it has, to the best of its knowledge, the rights to license reuse of this material. However, you should ensure that the material you are requesting is original to the Licensor and does not carry the copyright of another entity (as credited in the published version).

   If the credit line on any part of the material you have requested indicates that it was reprinted or adapted with permission from another source, then you should also seek permission from that source to reuse the material.

2. Where **print only** permission has been granted for a fee, separate permission must be obtained for any additional electronic re-use.

3. Permission granted **free of charge** for material in print is also usually granted for any electronic version of that work, provided that the material is incidental to your work as a whole and that the electronic version is essentially equivalent to, or substitutes for, the print version.

4. A licence for 'post on a website' is valid for 12 months from the licence date. This licence does not cover use of full text articles on websites.

5. Where **'reuse in a dissertation/thesis'** has been selected the following terms apply: Print rights of the final author's accepted manuscript (for clarity, NOT the published version) for up to 100 copies, electronic rights for use only on a personal website or institutional repository as defined by the Sherpa guideline (www.sherpa.ac.uk/romeo/).

6. Permission granted for books and journals is granted for the lifetime of the first edition and does not apply to second and subsequent editions (except where the first edition permission was granted free of charge or for signatories to the STM Permissions Guidelines http://www.stm-assoc.org/copyright-legal-affairs/permissions/permissions-guidelines/), and does not apply for editions in other languages unless additional translation rights have been granted separately in the licence.

7. Rights for additional components such as custom editions and derivatives require additional permission and may be subject to an additional fee. Please apply to Journalpermissions@springernature.com/bookpermissions@springernature.com for these rights.

8. The Licensor's permission must be acknowledged next to the licensed material in print. In electronic form, this acknowledgement must be visible at the same time as the figures/tables/illustrations or abstract, and must be hyperlinked to the journal/book's homepage. Our required acknowledgement format is in the Appendix below.

9. Use of the material for incidental promotional use, minor editing privileges (this does not include cropping, adapting, omitting material or any other changes that affect the meaning, intention or moral rights of the author) and copies for the disabled are permitted under this licence.

10. Minor adaptations of single figures (changes of format, colour and style) do not require the Licensor's approval. However, the adaptation should be credited as shown in Appendix below.

Appendix — Acknowledgements:

For Journal Content:
Reprinted by permission from [**the Licensor**]: [**Journal Publisher** (e.g. Nature/Springer/Palgrave)] [**JOURNAL NAME**] [**REFERENCE CITATION** (Article name, Author(s) Name), [**COPYRIGHT**] (year of publication)

For **Advance Online Publication papers:**
Reprinted by permission from [**the Licensor**]: [**Journal Publisher** (e.g. Nature/Springer/Palgrave)] [**JOURNAL NAME**] [**REFERENCE CITATION** (Article name, Author(s) Name), [**COPYRIGHT**] (year of publication), advance online publication, day month year (doi: 10.1038/sj.[JOURNAL ACRONYM].)

For Adaptations/Translations:
Adapted/Translated by permission from [**the Licensor**]: [**Journal Publisher** (e.g. Nature/Springer/Palgrave)] [**JOURNAL NAME**] [**REFERENCE CITATION** (Article name, Author(s) Name), [**COPYRIGHT**] (year of publication)

Note: For any republication from the British Journal of Cancer, the following credit line style applies:

Reprinted/adapted/translated by permission from [**the Licensor**]: on behalf of Cancer Research UK: : [**Journal Publisher** (e.g. Nature/Springer/Palgrave)] [**JOURNAL NAME**] [**REFERENCE CITATION** (Article name, Author(s) Name), [**COPYRIGHT**] (year of publication)

For **Advance Online Publication** papers:
Reprinted by permission from The [**the Licensor**]: on behalf of Cancer Research UK: [**Journal Publisher** (e.g. Nature/Springer/Palgrave)] [**JOURNAL NAME**] [**REFERENCE CITATION** (Article name, Author(s) Name), [**COPYRIGHT**] (year of publication), advance online publication, day month year (doi: 10.1038/sj. [JOURNAL ACRONYM])

For Book content:
Reprinted/adapted by permission from [**the Licensor**]: [**Book Publisher** (e.g. Palgrave Macmillan, Springer etc) [**Book Title**] by [**Book author**(s)] [**COPYRIGHT**] (year of publication)

Other Conditions:

Version 1.1

This Agreement between Curtin University -- Daniel Tan ("You") and Springer Nature ("Springer Nature") consists of your license details and the terms and conditions provided by Springer Nature and Copyright Clearance Center.

License Number	4431870932581
License date	Sep 18, 2018
Licensed Content Publisher	Springer Nature
Licensed Content Publication	Journal of Inclusion Phenomena and Macrocyclic Chemistry
Licensed Content Title	Distal functionalisation of C4 symmetric tetramethoxyresorcinarene by selective lithiation
Licensed Content Author	Daniel A. Tan, Mauro Mocerino
Licensed Content Date	Jan 1, 2018
Licensed Content Volume	91
Licensed Content Issue	1
Type of Use	Thesis/Dissertation
Requestor type	academic/university or research institute
Format	print and electronic
Portion	full article/chapter
Will you be translating?	no
Circulation/distribution	<501
Author of this Springer Nature content	yes
Title	Synthesis and Application of Distally-Bridged Chiral Resorcinarenes as Enantioselective Membrane Carriers
Instructor name	n/a
Institution name	n/a
Expected presentation date	Sep 2018
Requestor Location	Curtin University Kent Street, Bentley Perth, WA 6102 Australia Attn: Curtin University
Billing Type	Invoice
Billing Address	Curtin University Kent Street, Bentley Perth, Australia 6102 Attn: Curtin University
Total	0.00 AUD

Terms and Conditions

Springer Nature Terms and Conditions for RightsLink Permissions
Springer Nature Customer Service Centre GmbH (the Licensor) hereby grants you a non-exclusive, world-wide licence to reproduce the material and for the purpose and

requirements specified in the attached copy of your order form, and for no other use, subject to the conditions below:

1. The Licensor warrants that it has, to the best of its knowledge, the rights to license reuse of this material. However, you should ensure that the material you are requesting is original to the Licensor and does not carry the copyright of another entity (as credited in the published version).

   If the credit line on any part of the material you have requested indicates that it was reprinted or adapted with permission from another source, then you should also seek permission from that source to reuse the material.

2. Where **print only** permission has been granted for a fee, separate permission must be obtained for any additional electronic re-use.

3. Permission granted **free of charge** for material in print is also usually granted for any electronic version of that work, provided that the material is incidental to your work as a whole and that the electronic version is essentially equivalent to, or substitutes for, the print version.

4. A licence for 'post on a website' is valid for 12 months from the licence date. This licence does not cover use of full text articles on websites.

5. Where **'reuse in a dissertation/thesis'** has been selected the following terms apply: Print rights of the final author's accepted manuscript (for clarity, NOT the published version) for up to 100 copies, electronic rights for use only on a personal website or institutional repository as defined by the Sherpa guideline (www.sherpa.ac.uk/romeo/).

6. Permission granted for books and journals is granted for the lifetime of the first edition and does not apply to second and subsequent editions (except where the first edition permission was granted free of charge or for signatories to the STM Permissions Guidelines http://www.stm-assoc.org/copyright-legal-affairs/permissions/permissions-guidelines/), and does not apply for editions in other languages unless additional translation rights have been granted separately in the licence.

7. Rights for additional components such as custom editions and derivatives require additional permission and may be subject to an additional fee. Please apply to Journalpermissions@springernature.com/bookpermissions@springernature.com for these rights.

8. The Licensor's permission must be acknowledged next to the licensed material in print. In electronic form, this acknowledgement must be visible at the same time as the figures/tables/illustrations or abstract, and must be hyperlinked to the journal/book's homepage. Our required acknowledgement format is in the Appendix below.

9. Use of the material for incidental promotional use, minor editing privileges (this does not include cropping, adapting, omitting material or any other changes that affect the meaning, intention or moral rights of the author) and copies for the disabled are permitted under this licence.

10. Minor adaptations of single figures (changes of format, colour and style) do not require the Licensor's approval. However, the adaptation should be credited as shown in Appendix below.

Appendix — Acknowledgements:

For Journal Content:
Reprinted by permission from [**the Licensor**]: [**Journal Publisher** (e.g. Nature/Springer/Palgrave)] [**JOURNAL NAME**] [**REFERENCE CITATION** (Article name, Author(s) Name), [**COPYRIGHT**] (year of publication)

For **Advance Online Publication papers:**
Reprinted by permission from [**the Licensor**]: [**Journal Publisher** (e.g. Nature/Springer/Palgrave)] [**JOURNAL NAME**] [**REFERENCE CITATION**

(Article name, Author(s) Name), **[COPYRIGHT]** (year of publication), advance online publication, day month year (doi: 10.1038/sj.[JOURNAL ACRONYM].)

For Adaptations/Translations:
Adapted/Translated by permission from **[the Licensor]**: **[Journal Publisher** (e.g. Nature/Springer/Palgrave)**] [JOURNAL NAME] [REFERENCE CITATION** (Article name, Author(s) Name), **[COPYRIGHT]** (year of publication)

<u>**Note: For any republication from the British Journal of Cancer, the following credit line style applies:**</u>

Reprinted/adapted/translated by permission from **[the Licensor]**: on behalf of Cancer Research UK: : **[Journal Publisher** (e.g. Nature/Springer/Palgrave)**] [JOURNAL NAME] [REFERENCE CITATION** (Article name, Author(s) Name), **[COPYRIGHT]** (year of publication)

For **Advance Online Publication** papers:
Reprinted by permission from The **[the Licensor]**: on behalf of Cancer Research UK: **[Journal Publisher** (e.g. Nature/Springer/Palgrave)**] [JOURNAL NAME] [REFERENCE CITATION** (Article name, Author(s) Name), **[COPYRIGHT]** (year of publication), advance online publication, day month year (doi: 10.1038/sj. [JOURNAL ACRONYM])

For Book content:
Reprinted/adapted by permission from **[the Licensor]**: **[Book Publisher** (e.g. Palgrave Macmillan, Springer etc) **[Book Title]** by **[Book author**(s)**] [COPYRIGHT]** (year of publication)

Other Conditions:

Version 1.1